

Sand and gravel transport through a riffle-pool sequence

Submitted in candidature for the degree of
Doctor of Philosophy
to the University of Newcastle upon Tyne

by

David John Milan

NEWCASTLE UNIVERSITY LIBRARY

201 11466 5

Thesis L7005

November 2000

"If you stood on the bottom rail of a bridge, and leant over, and watched the river slipping slowly away beneath you, you would suddenly know everything that there is to be known."

Winnie-the-Pooh

Abstract

Sand and gravel transport through a riffle-pool sequence

This study focuses upon flow hydraulics, sediment transport and riffle-pool maintenance on the River Rede, Northumberland, UK. Analysis of bed structure indicate pools to be coarser than riffles, suggesting these to be zones of maximum tractive force at high flow. Tractive force reversal can be demonstrated using a combination of velocity, shear stress and gravel tracer data, and is therefore advocated as a mechanism for maintaining the riffle-pool form. Three dimensional flow structures are likely to increase the likelihood of reversal in pools situated on bends, which may not always be detected using one-dimensional measures of flow hydraulics.

Magnetic tracing and basket trapping techniques were used to provide an insight into rates of movement, accumulation, initial motion criteria and routing, of sand. Sand is transported selectively and is mobilised at between $11-22 \text{ Nm}^{-2}$. Deposition of sub 2mm material is prevalent on morphological high points (bars / riffle margins), although greatest quantities were routed through morphological lows. Freeze core evidence shows limited intragravel storage.

Gravel tracer movements showed evidence of size selective entrainment overall, however hiding effects were also found to be evident at two scales; 30-50mm and 110-140mm (for riffles) and 20-90mm and 110-140mm for pool. Slope exponents for log-log relations between scaled grain size (D/D_{50}) versus dimensionless shear stress (θ_c) of ≈ 0.9 suggest that hiding strongly influences sediment transport. Stream power estimates from $\rho g Q_s$ demonstrate a higher threshold for motion for gravel in pools (132 Wm^{-2}) compared with riffles (127 Wm^{-2}). Differences in initial motion criteria (θ_c) between riffles and pools were found to be significant ($p < 0.05$), indicating pool sediments to be less mobile than riffle, despite pool sediments being less compact. Reduced mobility of pool bedload sediment results from clasts being sheltered by immobile lag gravel found in the pool. It appears therefore that mobility differences between riffles and pools, related to bed structure, does not explain riffle-pool maintenance on the Rede.

Scaled travel distance (L/L_{50s}) for tracers in the reach as a whole showed a convex-up relationship with scaled grain size (D/D_{50s}), demonstrating that for tracer grains progressively coarser than the surrounding D_{50} surface grains, travel distance drops off rapidly, whereas grains progressively finer than the surrounding clasts, travel further but at a less rapid rate. Furthermore, virtual velocity (V^*) of tracer grains showed a positive dependence upon D/D_{50s} .

Gravel tracer movement provided important insights into riffle-pool maintenance. Transfer of material through the Rede riffle-pool sequence appeared to be influenced by flow magnitude and duration. For low magnitude high frequency flows below 25% bankfull, intra-unit movement was found to predominate. Medium magnitude and frequency flows (up to 50% bankfull) appeared capable of inter-unit transport; scour from pool troughs and deposition on pool exit slopes / riffle heads, movement of material from riffles to bar edges and from bar to bar. For higher magnitude low frequency flows up to bankfull, there was less scour from pools, and a dominance of bar-to-bar sediment transfer. Limited evidence of sediment routing and deposition in pools suggest these to be scour / sediment source zones only, with supply originating from the bed and outer bank. These data demonstrate the importance of different flow magnitude and frequency in creating / maintaining different areas of the riffle-pool structure.

Acknowledgements

There are so many people to thank that it is difficult to know where to start. Please forgive me if I have missed you out – thanks anyway. A good place to start would be to thank my supervisor Dr Andy Large, who somehow has put up with my time-consuming write-up and stubborn views on how bits of sediment move in flowing water. Thanks for all your help in the field, digging mouldy sand, pushing wheel-barrows, freeze-coring, for proof-reading my hieroglyphics and the input to the papers. I may forget your curry evenings but I will never forget all the help and encouragement you have given me – I am eternally grateful. Talking of flowing water, this time of the amber variety, I am also indebted to Dr George Heritage for his continuous encouragement and belief in the Rede research. I fully appreciate the 'unofficial-supervision', not to mention the help on the papers, in the field, and giving me access to your great mind! Still on the theme of things liquid, thanks is also extended Martin Charlton for help with all things spatial (particularly on the *Catena* paper), encouragement and thought-provoking (but often slurred) conversations in the pub. Thanks also must be extended to Dr Chris Brunsdon for his help with statistical analysis in Chapter 5, and for help in the *Sedimentary Geology* paper.

I must also thank Ernie Rice at Lemington glass works, and 'Moustache Man' (Jeff Winters?) at Redland Bricks for letting me use their Kilns free of charge. Thanks to John Batey Northumbrian Water Plc, for letting me gain access to the Rede field sites, and for the use of their tractor. I am also very grateful to Dr Allan Stephenson and the Department of Physics at Newcastle University for letting me use their magnetic susceptibility meter, and for providing technical advice on mineral magnetics. I am grateful to Lancaster University Geography Department for allowing me to use their laser particle sizer, and am grateful to Andy Quin for assistance in its operation. The archaeology practice at Newcastle University also allowed us to use their wheel barrows and shovels for the sand tracing experiment. Anne Rooke is thanked for her cartographic assistance on Figure 4.1.

A number of people also helped in the field and in shifting six tonnes of sand. I am extremely grateful to those who lent a hand. In particular I must thank Dr Rachel Suckling, Dr Andy Moores (for bearing his cheeks), Dr Basil Davies (for his amazingly clean boiler suit), Mark Wild (for his camera technique), Dr Clive Waddington (sorry about your caravan Clive!). Peter Donnelly and Richard Pawson helped out with the freeze-coring. Watts Stelling deserves a mention for being Watts Stelling (that's two mentions!). Dr Ian Boomer, Dr Ian Fuller, Harry 'the heel', Annie, Jacqui and Dr Cath Newson, have all provided encouragement a long the way. My house mates at 21, Forsyth Rd, particularly Deryck and Gillian are also thanked for helping to keep my sanity.

Thanks also to my parents Alf and Eleanor, who have given me moral and financial support, not only through the period of the PhD, but throughout my education. I quite literally wouldn't have got here without them!

Last but by no means least, I must thank Claire for being patient and being there for me. I know it has been a nightmare for you at times. As Martin Charlton says "Writing a PhD is the male equivalent of giving birth". I feel like I have just had sextuplets! It was a long time coming, but I finally made it! All (good?) things must come to an end I guess. Now I can start the next chapter of my life rather than the PhD!

David Milan, Newcastle upon Tyne, November, 2000.

Table of Contents

Title page	(i)	
Abstract	(ii)	
Acknowledgements	(iii)	
Table of contents	(iv)	
Chapter One	Study aims and background to sediment transport through riffle-pool morphology	Page
1.1	Introduction : significance of riffle-pool morphology	1
1.2	Study objectives and thesis structure	2
1.3.1	The riffle-pool unit	5
1.3.2	Quantitative identification of riffles and pools	5
1.3.3	Theories of riffle-pool formation	6
1.3.4	Riffle-pool hydraulics and maintenance	9
1.4	Gravel-bed sediment structure	12
1.4.1	Surface layer texture	13
1.4.2	Variations in surface structure and implications for mobility	14
1.4.3	Subsurface sediments	14
1.5	Incipient motion	15
1.5.1	Size -selective entrainment and static armouring	17
1.5.2	Relative mobility of grains in mixed-sized sediments	18
1.5.3	Equal mobility hypothesis and mobile armouring	19
1.5.4	Mobility of sediments through riffles and pools	20
1.6	Sediment sorting in the riffle-pool sequence	20
1.6.1	Routing of gravel (Phase 2 bedload) through the riffle-pool sequence	23
1.6.2	Routing and sorting of fines (Phase 1 bedload)	24
1.6.3	Size sorting	26
1.7	Vertical sorting mechanisms – development of fines	26
1.8	Study objectives, experimental design and controlling variables	27
Chapter Two	Study site and methodology	
2.1	Introduction	35
2.2	Background to the Rede study area	37
2.2.1	Catchment lithology	37
2.2.2	The study reach background and character	39
2.2.3	Channel morphology	41
2.2.4	Catchment climate and hydrology	41
2.3	Calculation of discharge	43
2.4	Sediment tracing	43
2.4.2	Tracing gravel (Phase 2 bedload)	45
2.4.3	Tracing sand (Phase 1 bedload)	48
2.4.4	Magnetic Tracing of fluvial sediments	49
2.4.5	Magnetic measures and detection	49
2.4.6	Magnetic tracer manufacture	52

2.4.7	Effects of grain size	55
2.4.8	Background magnetic signature	55
2.4.9	Seeding of magnetic tracer	57
2.5	Sediment sampling methods	60
2.5.1	Surface sediments	60
2.5.2	Subsurface sediments and the application of freeze-coring techniques	61
2.5.3	Fine bedload transport and trapping	64
2.5.4	Strategy to detect fine-tracer development	66
2.5.5	Laboratory procedures and grain-size analysis	66
2.6	Approaches to estimating hydraulics through a riffle-pool sequence	67
2.6.1	Past Approaches and associated problems	67
2.6.2	Determination of velocity	70
2.6.3	Determination of boundary shear stresses	71
2.6.4	Mean and point boundary shear stress	72
2.7	Spatial analysis	73
2.8	Summary and conclusions	74

Chapter Three Sedimentology of the Rede riffle-pool sequence

3.1	Introduction	75
3.2	Sampling strategy	76
3.2.1	Sediment sampling	76
3.3	Results	78
3.3.1	Surface layer: general characteristics	78
3.3.2	Surface layer: grain-size characteristics	79
3.3.3	Surface layer: grain shape characteristics	83
3.3.4	The Substrate: characteristics of freeze cores	83
3.3.5	Sub-surface grain-size characteristics	85
3.3.6	The matrix	86
3.3.7	Riffle-pool scale vertical variability	90
3.3.8	Bed compaction / strength	95
3.4	Discussion and conclusions	96
3.5	Summary	105

Chapter Four Hydraulic characteristics of the Rede riffle-pool sequence

4.1	Introduction	106
4.2	Methods and extent of the Rede hydraulic data set	106
4.3	Results	107
4.3.1	Cross-section averaged velocity	107
4.3.2	Bed and profile-averaged velocity	110
4.3.3	Boundary shear stress distribution	114
4.3.4	Prediction of boundary shear stress	126
4.4	Discussion and conclusions	128
4.4.1	Tractive force variation through pools and riffles	128
4.4.2	Problems with cross-sectional measures	129
4.4.3	Problems with velocity profiling	129
4.4.4	Problems with Du Boys	131

4.5	Summary	132
Chapter Five	Mobility of bed sediments through a riffle-pool sequence 1: fine bedload	
5.1	Introduction	133
5.2	Experimental design - trapping	134
5.3	Results	136
5.3.1	Hydrograph character and sampling periods	136
5.3.2	Transport distance	138
5.3.3	Grain size characteristics of sand entering traps	141
5.3.4	Mobility	143
5.3.5	Size effects	151
5.4	Discussion and conclusions	162
5.5	Summary	166
Chapter Six	Mobility of bed sediments through a riffle-pool sequence 2: coarse bedload	
6.1	Introduction	168
6.2	Experimental design	169
6.2.1	Virtual velocity	169
6.3	Results	172
6.3.1	Recovery rate	172
6.3.2	Transport distance	172
6.3.3	Shape factors	176
6.3.4	Tracer movement and stream power	178
6.3.5	Thresholds for transport for tracer grains in riffles and pools	180
6.3.6	Mobility and size selectivity for riffles and pools and a comparison with other published data	183
6.3.7	Virtual velocity of tracers – dependence upon scaled tracer size and dimensionless shields entrainment function	186
6.4	Discussion and conclusions	190
6.4.1	Size selectivity and travel distance	191
6.4.2	Grain mobility	193
6.4.3	Virtual velocity, shear stress and grain size	195
6.5	Summary	196
Chapter Seven	Phase 1 sediment routing through a riffle-pool sequence	
7.1	Introduction	198
7.2	Approach	198
7.3	Results I: Basket traps – temporal and spatial variability in accumulation and grain size	199
7.3.1	Temporal variation in accumulation rate	199
7.3.2	Temporal variation in the grain-size of accumulating sediments	202
7.3.3	Influence of relative form (morphology) and surface grain size	205
7.4	Results II: Magnetics – routing and sorting	207
7.4.1	Dimensionless surface susceptibility	207

7.4.2	Mass susceptibility of sand in basket traps (χ)	212
7.4.3	Vertical sorting of tracer (Phase 1 material)	216
7.5	Discussion and conclusions	217
7.5.1	Accumulation of fines within traps	217
7.5.2	Fine bedload routing	217
7.5.3	Movement and storage of tracer	220
7.5.4	Fine sediment storage in gravel interstices	222
7.6	Summary	223
Chapter Eight	Phase 2 sediment routing through a riffle-pool sequence	
8.1	Introduction	225
8.2	Approach	226
8.3	Results	227
8.3.1	Tracer paths and morphology	227
8.3.2	Grain size attributes of depositing tracers	235
8.4	Discussion and conclusions	243
8.4.1	Sorting patterns	243
8.4.2	Influence of flow character upon tracer movements and implications for morphological change	250
8.5	Summary	254
Chapter Nine	Discussion and conclusions: Sand and gravel transport and the maintenance of the riffle-pool sequence	
9.1	Tractive force reversal	256
9.1.1	Support for reversal from tracer data, and limitations with cross-section average measures	256
9.1.2	Further support for reversal using point measures	257
9.2	Implications of tractive force distribution for channel changes and sediment transport	258
9.2.1	Predicted areas of potential morphological change	259
9.2.2	Observed morphological changes May 1996-January 1998	261
9.3	Sediment sorting patterns and tractive force reversal	264
9.3.1	Competing views of reversal model	266
9.3.2	Modification of reversal model	277
9.4	Influence of sediment structure upon riffle-pool maintenance	284
9.4.1	Sediment structure and turbulent flow	287
9.5	Site specificity of riffle-pool sequences and riffle-pool maintenance	288
9.5.1	Sinuosity	288
9.5.2	Sediment supply and source	291
9.5.3	Mode of pool formation / influence of channel obstructions	292
9.6	Riffle-pool maintenance; the Rede and other sites	292
9.7	Summary and fulfilment of study objectives	295
9.8	Macro-scale turbulent flow structures and riffle-pool maintenance: future and ongoing research	297
	References	299

List of Tables

1.1	Summary of a range of studies documenting textural differences between the bed sediments of riffles and pools	21
1.2	Study objectives, experimental design and controlling variables on the Rede study reach	29
2.1	Major stratigraphic sub-divisions in the Rede catchment	39
2.2	Summary of size and shape characteristics of tracer clasts	48
2.3	Sampling guidelines previously recommended when using freeze-coring techniques	64
2.4	Range of parameters used to quantify riffle-pool hydraulics	68
3.1	Summary surface layer characteristics of individual geomorphic units	79
3.2	Summary substrate grain-size characteristics	86
3.3	Summary of matrix size distribution of individual geomorphic units	89
3.4	Structure of matrix sediments in isolation	90
4.1	Summary of changes in boundary shear stress with increasing discharge	124
4.2	Mean changes in relative k_r , grain roughness (D_{84}/d) for the Rede with discharge	131
5.1	A flood-by-flood account of tracer position though the Rede riffle-pool sequence	139
5.2	Percentage by weight composition of sediments entering basket traps	142
5.3	Log-log regressions for accumulation rate versus shear stress for $<2000\mu\text{m}$ material	145
5.4	Trap rating relations of the form $A = a_i \tau^{b_i}$ for material $<2000\mu\text{m}$	152
5.5	Size-specific rating relations of the form $A_i = a_i \tau^{b_i}$ for individual traps and material $< 2000 \mu\text{m}$, for riffle A	155
5.6	Size-specific rating relations of the form $A_i = a_i \tau^{b_i}$ for individual traps and material $< 2000 \mu\text{m}$, for riffle B	156
5.7	Size-specific rating relations of the form $A_i = a_i \tau^{b_i}$ for individual traps and material $< 2000 \mu\text{m}$, for riffle C	157
5.8	Anova table demonstrating the significance of grain size effects upon the relationship between sediment accumulation and shear stress	162
6.1	Anova table for distance of travel of different clast shapes, a) Pools, b) Riffles	177
6.2	Size-specific rating relations of the form $L = a \Omega^b$, where d is the mean distance of transport for tracer data taken from riffles and pools, Ω is stream power and a and b are regression coefficients	178
6.3	Anova table, comparing Shields dimensionless entrainment function data for riffles and pools	183
7.1	Documented field studies describing accumulation rates of fines in gravel-bed rivers	218

8.1	Number and percentage of deposited tracers and percentage total area for each morphological sub-unit	241
8.2	Comparison of the sizes of tracers mobilised in pools compared with the largest bed particle measured in the pool	249
9.1	Studies on different riffle-pool sequences: site specific characteristics	
		269-276

List of Figures

1.1	Structure of thesis	4
2.1	Roles of the processes investigated in the formation and maintenance of riffle-pool sequences	36
2.2	The Rede study catchment; (a) catchment map, (b) study reach location showing the position of the stage recorder (SR)	38
2.3	Study reach details, (a) position of cross-sections, (b) position of basket traps and cell-based survey shown by squares, (c) contour map of riffle-pool morphology	40
2.4	Mean monthly rainfall characteristics at Catcleugh Nursery, full record for 1 Feb 1963 to 1 May 1998, (b) rainfall characteristics for the study period 1 January 1995 to 1 st May 1998	42
2.5	Stage discharge relationship for the River Rede study site, a) log-log regression, b) linear regression	44
2.6	Emplacement positions of gravel tracers in the Rede riffle-pool sequence	47
2.7	Grain size distribution of gravel tracers emplaced throughout the Rede riffle-pool sequence	47
2.8	Calibration curve for estimating the percentage by weight tracer material within a sample of a given magnetic susceptibility	51
2.9	Comparison of enhanced tracer sands and background samples taken from the Rede site	53
2.10	Results of laboratory trials into the optimum conditions for magnetic enhancement, a) influence of heating duration at 700°C, b) influence of reducing agent concentration, c) effect of temperature	54
2.11	Grain size factors, for Phase 1 tracer; a) grain size distribution of un-enhanced and enhanced Greensand tracer material, b) variation in χ with grain size, c) contribution factor of χ by each grain size fraction	56
2.12	The natural background χ distribution, assessed from freeze-core samples taken from the Rede channel bed	58

2.13	Variation in the mean background χ_t for riffle sub-units and pools	58
2.14	Emplacement location for tracer sands	59
2.15	Sediment sampling techniques, (a) freeze-coring, (b) basket trap sampling	62
2.16	Bed long profile of the Rede riffle pool sequence and water surface profiles surveyed over five flows of varying magnitude	72
3.1	Cell-based sediment sampling scheme	77
3.2	Variation in median grain-size for surface (armour) layer sediments for morphological sub-units	80
3.3	Downstream pattern in surface grain size from cell-based data; (a) right-bank, (b) mid-channel, (c) left-bank	81
3.4	Lateral variability of armour layer sediments	82
3.5	Grain-size distribution for sub-surface sediments obtained using freeze-coring	85
3.6	Variation in median grain size of sub-surface sediments for morphological sub-units for (i) 0-15cm (A), (ii) 15-30cm (B), 30-45cm (iii) (C), (iv) 45-60cm (D)	87
3.7	Variation in the percentage by weight of matrix (<2mm) sediments morphological sub-units for (i) 0-15cm (A), (ii) 15-30cm (B), (iii) 30-45cm (C), (iv) 45-60cm	88
3.8	Variation in median grain size of matrix sediments for morphological sub-units for (i) 0-15cm (A), (ii) 15-30cm (B), (iii) 30-45cm (C), (iv) 45-60cm	91
3.9	Grain-size distributions for the River Rede study reach for (a) Riffle and (b) pools	92
3.10	Vertical variation in median grain size for a) riffle heads, b) riffle crests, c) riffle tails, d) pools, and sub 2mm concentrations for e) riffle heads, f) riffle crests, g) riffle tails, h) pools	93
3.11	Vertical variation in median grain size for a) left-bank, b) mid-channel, c) right-bank, d) pools, and sub 2mm concentrations for e) left-bank, f) mid-channel, g) right-bank, h) pools	94

3.12	Variation in bed strength / compaction for different morphological sub-units	95
3.13	Contour plot of bed compaction for the upstream section of the study site	97
3.14	Contour plot of bed compaction for the middle section of the study site	98
3.15	Contour plot of bed compaction for the downstream section of the study site	99
4.1	Cross-section averaged velocity pattern with increasing discharge for six riffle-pool units throughout the study reach, a) Pool 1 and Riffle 1, b) Riffle 1 and Pool 2, c) Pool 2 and Riffle 2, d) Riffle 2 and Pool 3, e) Pool 3 and Riffle 3, f) Riffle 3 and Pool 4	109
4.2	Spatial pattern in profile averaged and bed velocity for study reach A for flows $0.3-3.6 \text{ m}^3\text{s}^{-1}$, a) Profile average $0.3 \text{ m}^3\text{s}^{-1}$, b) Profile average $1 \text{ m}^3\text{s}^{-1}$, c) Profile average $3.6 \text{ m}^3\text{s}^{-1}$, d) Bed $0.3 \text{ m}^3\text{s}^{-1}$, e) Bed $1 \text{ m}^3\text{s}^{-1}$, f) Bed $3.6 \text{ m}^3\text{s}^{-1}$	111
4.3	Morphological variation in profile averaged velocity (0.6 depth) for a) $0.3 \text{ m}^3\text{s}^{-1}$, b) $1 \text{ m}^3\text{s}^{-1}$ and c) $3.6 \text{ m}^3\text{s}^{-1}$	112
4.4	Morphological variation in near-bed velocity for a) $0.3 \text{ m}^3\text{s}^{-1}$, b) $1 \text{ m}^3\text{s}^{-1}$ and c) $3.6 \text{ m}^3\text{s}^{-1}$. No pool data available for $3.6 \text{ m}^3\text{s}^{-1}$	113
4.5	Spatial pattern of point shear stress estimated from velocity profiles for study at flows of a) $0.3 \text{ m}^3\text{s}^{-1}$, b) $1 \text{ m}^3\text{s}^{-1}$, c) $3.6 \text{ m}^3\text{s}^{-1}$	115
4.6	Morphological variation in shear stress calculated from velocity profiling and equation 2.3 a) $0.3 \text{ m}^3\text{s}^{-1}$, b) $1 \text{ m}^3\text{s}^{-1}$ and c) $3.6 \text{ m}^3\text{s}^{-1}$. No pool data available for $3.6 \text{ m}^3\text{s}^{-1}$	116
4.7	Spatial variability of cross-section average shear stress estimated using the Du Boys equation for flows of a) $0.1 \text{ m}^3\text{s}^{-1}$, b) $2 \text{ m}^3\text{s}^{-1}$, c) $5.44 \text{ m}^3\text{s}^{-1}$, d) $7.26 \text{ m}^3\text{s}^{-1}$, e) $8.52 \text{ m}^3\text{s}^{-1}$	118
4.8	Spatial variability of point shear stress estimated using the Du Boys equation for a) $0.1 \text{ m}^3\text{s}^{-1}$, b) $2 \text{ m}^3\text{s}^{-1}$, c) $5.44 \text{ m}^3\text{s}^{-1}$, d) $7.26 \text{ m}^3\text{s}^{-1}$, e) $8.52 \text{ m}^3\text{s}^{-1}$	120
4.9	Stage-dependent morphological variation in τ calculated using ρgds for a) $0.1 \text{ m}^3\text{s}^{-1}$, b) $2 \text{ m}^3\text{s}^{-1}$, c) $5.44 \text{ m}^3\text{s}^{-1}$, d) $7.26 \text{ m}^3\text{s}^{-1}$, e) $8.52 \text{ m}^3\text{s}^{-1}$	121-122

4.10	Change in cross-section wetted area for cross-sections taken in the trough of the pools and crests of the riffles throughout the Rede study reach	130
5.1	Flow hydrograph for the study period 15 th March 1996-11 th March 1997. The dotted lines represent the accumulation time between sampling	137
5.2	Relationship between mobilisation index (Q_t) and travel distance of tracer centroid calculated using equation 5.1	139
5.3	Temporal patterns of grain size accumulation in traps. (a) flow, (b) time series of mean percentage by weight of (b) accumulation for different grain size fractions	142
5.4	Trap rating relations for material <2mm based on period-averaged samples. The fitted equations are log-log regressions through all of the data for a) riffle A, b) riffle B, and c) riffle C	144
5.5	Trap rating relations for material <2mm for riffle A. The fitted relations are the log-log regressions presented in Table 5.8. a) Traps located at the riffle head, b) traps located at the b) riffle crest, c) traps located at the riffle tail	146
5.6	Trap rating relations for material <2mm for riffle B. The fitted relations are the log-log regressions presented in Table 5.8. a) Traps located at the riffle head, b) traps located at the b) crest, c) traps located at the riffle tail	147
5.7	Trap rating relations for material <2mm for riffle C. The fitted relations are the log-log regressions presented in Table 5.8. a) Traps located at the riffle head, b) traps located at the riffle crest, c) traps located at the riffle tail	148
5.8	Size-specific rating relations for different grain size fractions for all traps, a) 1000-2000 μm , b) 500-1000 μm , c) 250-500 μm and d) 125-250 μm	153
5.9	Log-log graph representation of size-specific rating relations based on all 9 traps located on riffle A. The fitted relations are the regression equations in Table 5.6 for 'All data' riffle A	159
5.10	Behaviour of p_i/f_i over the thirteen month study period for the weighted average load for all traps located on riffle A. Departure from 1.0 indicates size-selective transport.	161

6.1	Discharge hydrographs for periods in between tracer re-surveys, a) 21/01/98-22/03/98, b) 22/03/98-08/04/98, c) 08/04/98-08/06/98, d) 08/06/98-05/11/98, e) 05/11/98-28/02/99	170
6.2	Percentage recovery of different size fractions of tracer clasts for each successive surveys for a) riffles, and b) pools	173
6.3	Distance of travel a) versus particle size for pools and riffles, b) cumulative distribution of travel distance for pools and riffles demonstrating that around 10% of the pool tracers were transported further than riffle tracers	174
6.4	Travel distance versus particle size fraction for a) riffles and b) pools	175
6.5	Log-log rating curves for size-specific mean transport distance versus stream power ($\rho g Q_s$) for a) Riffles and c) Pools. The size specific rating relations are presented in Table 6.2	179
6.6	Decrease in critical dimensionless shear stress for entrainment with increasing grain size relative to the bed, as inferred from individual tracer clast movement ($>0.5\text{m}$), transported at different shear stresses in riffles and pools	181
6.7	Relative travel distance of each size fraction for the Rede reach as a whole, and riffles and pools separately	184
6.8	Nondimensional velocity V^* of each tracer size fraction of relative grain size D^* for the reach as a whole, riffles and pools	186
6.9	Alternative plot of nondimensional velocity V^* as a function of Shields stress θ_c	188
6.10	Comparison of observed nondimensional velocities V^* for different size fractions for riffles and pools with values predicted from relative grain size D^* and Shields stress θ_c using equations 6.14, 6.15 and 6.16	190
7.1	Temporal and spatial variability in infiltration rates, a) Discharge, b) between riffle, c) cross-channel b) variability, d) longitudinal variability	200
7.2	Longitudinal temporal variability in grain size of accumulating fines for the head, crest and tail of each study riffle. b) riffle A, c) riffle B, d) riffle C	203

7.3	Cross-channel temporal variability of grain size for each study riffle. b) riffle A, c) riffle B, d) riffle C	204
7.4	Plots indicating the relationship between accumulation rate and variation in relative roughness a) all data b) down riffle and c) cross-riffle	206
7.5	Plot indicating the relationship between relative grain roughness and rate of accumulation of fines in traps a) all data b) down riffle and c) cross riffle	208
7.6	Spatial distribution in surface magnetic susceptibility χ , a) background before any emplacement of tracer, b) 1 week after emplacement 30/4/96, c) post flood 22/5/96	209
7.7	Temporal and spatial variation in χ ($\times 10^6$), a) Discharge, b) between riffle, c) cross-channel variability, d) longitudinal (down riffle) variability	213
7.8	A morphologically-based summary of fine bedload storage through the Rede riffle-pool sequence	221
8.1	Tracer paths after a peak flow of $2.71 \text{ m}^3 \text{s}^{-1}$, a) 20-40mm, b) 40-70mm, c) >70mm	228
8.2	Tracer paths after a peak flow of $5.95 \text{ m}^3 \text{s}^{-1}$, a) 20-40mm, b) 40-70mm, c) >70mm	229
8.3	Tracer paths after a peak flow of $7.44 \text{ m}^3 \text{s}^{-1}$, a) 20-40mm, b) 40-70mm, c) >70mm	230
8.4	Tracer paths after a peak flow of $9.92 \text{ m}^3 \text{s}^{-1}$, a) 20-40mm, b) 40-70mm, c) >70mm	231
8.5	Tracer paths after a peak flow of $6.94 \text{ m}^3 \text{s}^{-1}$, a) 20-40mm, b) 40-70mm, c) >70mm	232
8.6	Comparison of grain size of deposited tracer clasts with surrounding morphological sub-unit, a) Riffle head, c) riffle crest, c) riffle tail	236-238
8.7	Summary of tracer grain-sizes deposited on different morphological a) units, b) sub-units	240
8.8	Comparison of cumulative grain size distributions for tracer clasts (all 288 grains) against riffle, pool and bar surface sediments sampled using a Wolman grid technique	242

8.9	Change in the grain size distribution of tracer clasts located in a) riffles and b) pools	244
8.10	Grain size differences between riffles and pools after each recorded flood	245
8.11	Phase 2 sediment budget through the Rede riffle pool sequence, indicating the percentage of tracer particles deposited in each morphological sub-unit	246
8.12	Duration curves for the River Rede, a) flow, b) percentage bankfull discharge	251
8.13	Number of events capable of morphological change / sediment transport between 23/11/96 to 22.11.97	252
9.1	Grey-scale plots indicating the spatial pattern of scour ($\tau_0 - \tau_c$) at (a) $0.07\text{m}^3\text{s}^{-1}$, (b) $2.17\text{m}^3\text{s}^{-1}$, (c), $5.4\text{m}^3\text{s}^{-1}$ (d), $7.3\text{m}^3\text{s}^{-1}$ (e) $8.5\text{m}^3\text{s}^{-1}$	260
9.2	Morphological changes to the Rede riffle-pool sequence between (a) June 1996 and July 1997, and (b) July 1997 and January 1998	262
9.3	Coarse lag development in pools	265
9.4	Positive feedback mechanism for Rede pools	266
9.5	Reversal model where pools are finer than riffles	267-268
9.6	Reversal model where pools are coarser than riffles	278-279
9.7	Modification of reversal model, detailing sediment transport routing through the Rede riffle-pool sequence	281-282
9.8	Cartoon demonstrating the patchy nature of the sediment surface of riffles on the river Rede, which is suggested as being responsible for the bimodal pattern in mean transport distance for tracers versus grain size	285
9.9	Factors supporting mode of riffle-pool maintenance for the Rede	293

Appendices

2.1	Cross-section profiles for the study reach for June 1996 and 1997	314-317
2.2	Suspended sediment rating curve for the Rede study site	318
4.1	Velocity-discharge relationships for cross-sections	319
4.2	Discharge-water surface elevation (<i>d</i>) rating curves for 30 cross-sections in Rede study reach	320-323
4.3	Discharge-slope rating curves	324
5.1	Size characteristics of sediments entering basket traps	325
5.2	Correlation coefficient between sediment sample sequences at different traps for 1-2mm, River Rede	326
5.3	Correlation coefficient between sediment sample sequences at different traps for 500-1000 μ m, River Rede	327
5.4	Correlation coefficient between sediment sample sequences at different traps for 250-500 μ m, River Rede	328
5.5	Correlation coefficient between sediment sample sequences at different traps for 125-250 μ m, River Rede	329
7.1	Spatial variability in magnetic susceptibility of Phase 1 bedload accumulating in basket traps; a) background 20.4.96, b) 3.2 $m^3 s^{-1}$ 22.5.95, c) 0.54 $m^3 s^{-1}$ 6.6.96, 2.08 $m^3 s^{-1}$ 10.9.96, e) 3.39 $m^3 s^{-1}$ 14.10.96, f) 5.44 $m^3 s^{-1}$ 2.11.96, g) 7.12 $m^3 s^{-1}$ 17.11.96, h) 4.13 $m^3 s^{-1}$ 10.12.96, 4.09 $m^3 s^{-1}$ 22.12.96, j) 1.23 $m^3 s^{-1}$ 15.1.97, k) 3.81 $m^3 s^{-1}$ 31.1.97, l) 3.99 $m^3 s^{-1}$ 8.2.97, m) 8.62 $m^3 s^{-1}$ 11.3.97	330-332
7.2	Depth variation in magnetic susceptibility of matrix sediments sampled using freeze-coring.	336-336
8.1	Tracer clast positions after flood 1 ($2.71 m^3 s^{-1}$)	337
8.2	Tracer clast positions after flood 1 ($5.95 m^3 s^{-1}$)	338
8.3	Tracer clast positions after flood 1 ($7.44 m^3 s^{-1}$)	339

8.4	Tracer clast positions after flood 1 ($9.92 \text{ m}^3\text{s}^{-1}$)	340
8.5	Tracer clast positions after flood 1 ($6.44 \text{ m}^3\text{s}^{-1}$)	341

List of plates

2.1	Seeding of magnetic tracer	59
3.1	Bed surface of the Rede channel demonstrating the patchy surface structure	78
3.2	Freeze-core demonstrating large clast in the upper 0-15cm of substrate	84
3.3	Lag deposits in Pool 1, River Rede	101
4.1	The Rede riffle-pool sequence at a) low flow ($\approx 0.1 \text{m}^3 \text{s}^{-1}$) August 1995, (b) high flow ($\approx 5 \text{m}^3 \text{s}^{-1}$) May 1996	108
7.1	Deposition of magnetic sand on bar surfaces	211

Chapter One

Study aims and background to sediment transport and mobility through riffle-pool morphology

1.1 Introduction: significance of riffle-pool morphology

The importance of moderate slope gravel bed rivers characterised by riffle-pool bedforms is becoming increasingly apparent. Riffle-pool sequences have been shown to be of importance in maintaining the quasi-equilibrium of the stream system (Leopold *et al.*, 1964; Dolling, 1968; Keller and Melhorn, 1978), by either minimising the potential energy loss per unit mass of water (Yang, 1971) or minimising total power expenditure (Cherkauer, 1973). The riffle-pool unit is the fundamental morphologic control on bed scour, sediment transfer and deposition (Carling, 1991), and may be a primary determinant in bank erosion and meander initiation (Leopold and Wolman, 1960; Langbein and Leopold, 1966; Richards, 1976a, 1978; Ashworth, 1987), bar growth (Clifford, 1993a) and channel planform instability (Richards, 1982).

Riffles and pools have also been shown to provide a valuable ecological resource to aquatic systems. By creating a diverse range of hydraulic and morphological niches riffles and pools are critical in sustaining habitats (Greenwood and Richardot-Coulet, 1996). It is now recognised that river engineering and rehabilitation projects should understand both the formation and maintenance of these bedforms (Keller, 1978a; Brookes, 1990 and 1992; Newbury, 1995; Kondolf and Micheli, 1995). Riffles provide appropriate hydraulic conditions for spawning, particularly for salmonids, and also some cyprinid species (Burner, 1951; Stuart, 1953; Milan and Petts, 1998; Milan *et al.*, 2000). Furthermore, pools provide important 'holding' habitat for adult fish (Bjornn *et al.*, 1977). Riffles and pools provide a diverse range of macroinvertebrate fauna, which are utilised by fish as a food resource (Scullion, 1982; Minshall and Minshall, 1977).

There is a growing need for research to focus upon inputs, storages and outputs of sediment within riffle-pool units, and their morphological response to changing sediment supply and hydrology – itself characteristic of climate change or

anthropogenic influences such as land-use change. An understanding of the buffering capacity of the riffle-pool sequence could be important in regulating the stability of the channel further downstream (Keller, 1978; Sear, 1994). Bearing in mind the importance of riffle-pool morphology it is disturbing that Fox (in press) has estimated that a total of 174,000 riffles have been lost as a result of engineering practices along 25,500 km of channel in the UK. Significant advances have been made in England and Wales during the last decade to address river management issues such as the loss of riffle-pool morphology using geomorphological principles, for example the River Habitat Survey, and National Rivers Authority / Environment Agency research and development programmes (Newson *et al.*, 2000). Moves towards environmentally sensitive river engineering and river restoration / rehabilitation, have generated a need for further information concerning flow and sediment dynamics through riffle-pool sequences.

An improved understanding of sediment mobility through riffle pool sequences is also essential for a range of geomorphological, engineering, sediment transport, paleohydraulic and ecological problems (Andrews, 1983). For example information on flows required for maintaining good gravel quality for fish spawning and morphology for fish habitat is an important objective for river managers (e.g. Milhous, 1996). In particular data are required on the flows required to produce a shear stress for partial gravel movement (framework dilation) to flush out harmful accumulations of fines from interstitial voids, without scouring away too much gravel and destroying channel morphology. From a review of the literature, Milan *et al.* (2000) have demonstrated that concentrations of sub-1mm sediments in excess of 14% result in increased mortality of fish embryos. Many lowland streams in Britain which support Brown Trout have concentrations well in excess this figure, which may reflect reduction in flushing capacity due to flow regulation, increased siltation due to changing land-use, and loss of riffle-pool morphology due to engineering practices (Milan and Petts, 1998).

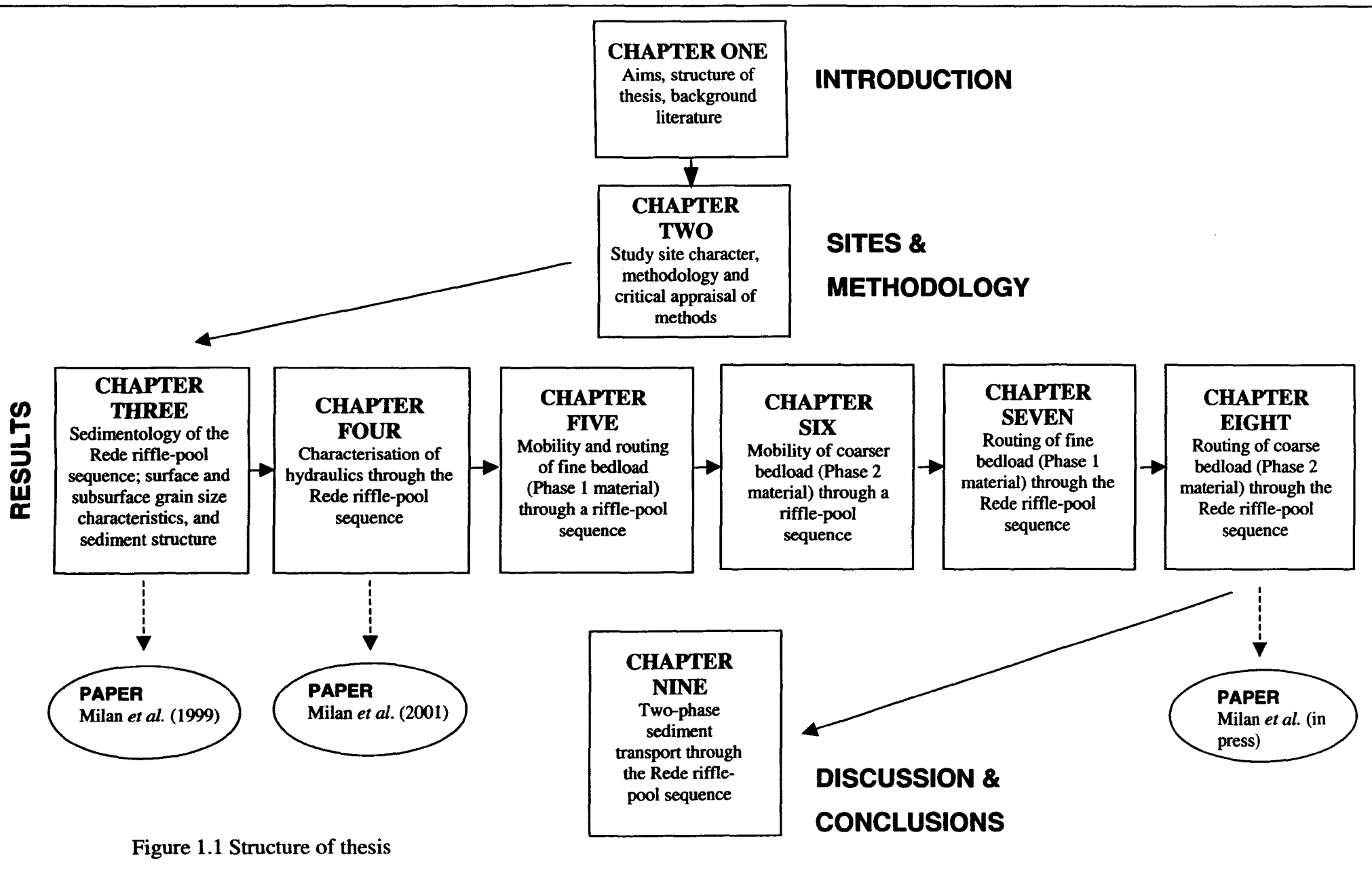
1.2 Study aims and thesis structure

With these research needs in mind, the principle aim of this thesis is to investigate riffle-pool maintenance through field analysis of hydraulic character and associated sediment movement through an upland riffle-pool sequence. Analysis of coarse and

fine-grained sorting processes will lead to an improved understanding of the maintenance of these bedforms and initial motion criteria for both gravel and sand modes. In particular this thesis aims to;

- (i) Improve current understanding of sediment sorting mechanisms in upland gravel bed rivers displaying riffle-pool topography, through identification of grain size variability and sediment routing,
- (ii) Test the hydraulic and sediment transport models of Keller (1971) and Jackson and Beschta (1982),
- (iii) Examine the mobility and initial motion criterion of gravel and sand in riffles and pools,
- (iv) Consider the implications of flow hydraulics and sediment transport processes upon the maintenance of riffle-pool morphology.

To fulfil these aims the thesis follows the pathway outlined in Figure 1.1. Chapter One will review the background literature to riffle pool maintenance, hydraulics, sediment transport, sorting and mobility. Chapter Two introduces the field site and the methods used throughout the investigation. Chapter Three focuses upon the sedimentology displayed through riffle-pool morphology at the study site, whilst Chapter Four identifies the spatial variation in stage-dependent hydraulics and discusses implications for sediment transport and riffle-pool maintenance, whilst testing Keller's reversal hypothesis (see section 1.3.4). Chapters Five and Six investigate the mobility of sand (Phase 1) and gravel bedload (Phase 2) respectively, whilst Chapters Seven and Eight examine the routing and sorting of fine and coarse bedload. Chapter Nine discusses the findings in the light of previous work, and highlights the major advances made by this investigation, and concludes by providing a summary of the main findings of the investigation commenting on how successfully the study has fulfilled the initial aims.



1.3.1 The riffle-pool unit

Clifford (1993a) refers to riffle-pool sequences as quasi-regular alterations of shallows and deeps which are characteristic of moderate slope gravel-bed rivers (below an upper limit of 1%). Riffles (topographic highs) and pools (intervening lows) are marked by stage-dependent contrasts in flow velocity, water surface slope, channel morphology and bed sedimentology. Over most of the flow range, riffles are shallower, faster zones, of steeper water surface, with coarser, better-sorted and more interlocked bed material than intervening pools. Riffles tend to be stable features, as shown by Dury's (1970) resurvey of the Hawkesbury River after 100 years. Pools on bends show less stability laterally, typically showing bank scour which is usually balanced by accretion on an inner point bar (Hooke, 1977).

1.3.2 Quantitative identification of riffles and pools

A range of different methods has been used to differentiate between riffles and pools. These include bed material size (Leopold *et al.*, 1964, p. 206-208), water surface slope (Yang, 1971), and the index v^2/d , where v and d are the mean velocity and mean depth of flow, respectively (Wolman, 1955). However, Richards (1976a) claims that these methods are of little value because their discriminating power changes with discharge and / or with the previous history of discharge events. Carling and Orr (2000) in a review of over 50 scientific articles found only three definitions to be precise and reliable. The three robust, objective methods were the *control point method* (Yang, 1971), the *zero-crossing method* (Dury, 1970; Nordin, 1971; Richards, 1976a; Shen and Cheong, 1977; Sidorchuk, 1996), and *power spectral analysis* (Box and Jenkins, 1976; Bloomfield, 1976). This study utilises the zero-crossing method; details on the other two techniques are summarised in Carling and Orr (2000). The zero-crossing method provides an objective means of delimiting riffles and pools based purely on the undulations in bed topography. The technique involves survey of the long profile of the bed through a sequence of riffles and pools, and the fitting of a regression equation to the plot of bed elevation versus downstream distance. For short reaches, Richards (1976a) has claimed that linear regression is adequate, whereas with longer reaches second- or third-order polynomial regression might be necessary.

The technique has been criticised on two grounds by O'Neill and Abrahams (1984). Firstly, the technique was unable to handle smaller undulations in the long profile at a scale greater than or smaller than that of an individual pool-riffle unit. Secondly, small deviations in the bed profile may result in isolated, minor residuals of either sign. The first problem may be overcome by pre-processing the data (Carling and Orr, 2000), whilst the second problem may be avoided by only including residuals of a given deviation from the regression line, also known as the 'bed form differencing technique' (O'Neill and Abrahams, 1984).

Clifford (1990) suggests that the bed differencing technique cannot be entirely objective, because the cumulative elevation difference which determines the threshold value for bedform identification is based on the subjective choice of a fraction of the standard deviation of the elevation series. Secondly, he states that the technique may not be reproducible within the same series if a constant fraction of the standard deviation (T value) is used (O'Neill and Abrahams recommend using a T value of 0.75), particularly with very short or long series where the standard deviation may be unstable as successive observations are added. Furthermore, Clifford (1990) claims that the zero-crossing technique is limited by its reliance on a single, one-dimensional measure of channel form. Slight differences may exist in the channel long profile depending upon planform line taken, for example, between the thalweg or the channel centre line. Although Clifford (1990; 1993a) states that there is no truly objective quantitative identification of riffle-pool sequences, autoregressive-modelling approaches, which have a physical basis, may overcome these problems.

1.3.3 Theories of riffle-pool formation

The most coherent hydraulically based theory of riffle-pool formation is that developed by Yalin (1971; 1977; 1992) which was elaborated by Richards (1976a; 1978; 1982) to provide the Yalin-Richards hypothesis. These theoretical studies demonstrate that the regularity of riffle spacing is related to the path length of periodic macroturbulent eddies extending across the full width of flow (Yalin, 1971, 1977, 1992). Turbulence generated at the boundary of a straight, uniform channel produces large-scale roller eddies associated with alternate acceleration and deceleration of flow. The scale of the eddies depends upon channel size, and the spacing between

successive fast or slow zones averages $2\pi w$. It may also be possible that two counter-rotating periodic macroturbulent eddies exist in straight channels rather than one, each occupying half the channel width (Hey, 1976). Richards (1976a) supports Yalin, claiming that the autocorrelated nature of macro-scale flow structure is the primary cause of riffle-pool bedforms, which subsequently lead to meandering. Richards (1976) further suggests that riffles and pools form as a response to alternating scour and fill associated with the theoretically determined correlation properties of large-scale eddy motions in open channel flow.

Other theories of riffle-pool formation provide however, a less comprehensive explanation of their geometry and initiation. Yang (1971) developed a theory that riffle-pool sequences occur because natural streams minimise their rate of potential energy expenditure; energy is dissipated less rapidly over a reach consisting of cells with different energy gradients, compared to a uniformly sloping reach. Rapid energy loss along a reach with a uniform gradient would result in scour and compensatory deposition which in turn would alter the form of the bed from uniform to undulating. According to Yang's (1971) law of least-time rate of energy expenditure the stream should form a riffle-pool sequence with a higher average velocity and a steeper water surface slope at the riffle compared to the pool. Yang claimed that the higher velocity gradient at the riffle would result in higher repulsive pressure in the riffle than in the pool, which would have the effect of depressing the bed surface of the pool and raising that of the riffle to form a concave-convex bed profile. This change in elevation continues, tending to increase the velocity gradient between the riffle and pool, until the shear stress at the riffle is so high that the bed material begins to shear. This shearing action in mixed sediments results in a coarsening of the riffle, and deposition of fines washed from the upstream riffle results in a finer grained pool.

Langbein and Leopold (1968) suggest a kinematic wave model for gravel riffle and sand-dune forms, based on the mutual interference of particles during transport. In this model, gravel particles move in groups (riffles) that move slower than the individual particles, which may hop from the downstream end of one group to the upstream end of the other, so that the group appears to move upstream. This model shows some similarities to natural riffle-pool sequences. For example Jackson and

Beschta (1982) describe riffle to riffle leap-frogging of gravel, and Sear (1992) provides tracer data that demonstrate faster virtual velocities of pool sediments. However, it differs from a natural riffle-pool sequence in that the riffles appear mobile, not static. Furthermore the model does not explain sediment sorting or riffle-pool wavelength (Richards, 1982).

An alternative theory for the initiation of an undulating bed profile was developed for step-pool sequences by Whittaker and Jaeggi (1982). In their model it is envisaged that antidunes are formed in association with standing waves, where the waveform of the bed is in phase with the water surface. However it is difficult to envisage the flows necessary to produce standing waves of the scale required to produce the variations in bed surface elevation evident in most riffle-pool sequences.

More recently Clifford (1990; 1993a) and Carling and Orr (2000) have attempted to obtain field data with which to validate and revise the Yalin-Richards hypothesis, which stress the importance of coherent turbulent flow structures in creating localised scour. Clifford (1993a) found that eddy sizes at the scale up to πw in dimension expected in the Yalin model do commonly occur, although these could not be clearly identified as dominant in any of the velocity series recorded on the River Quarne. Instead, the clearest indication of dominant eddy size was of 1-3 m, which appeared to scale to small multiples of grain size or small-scale bedforms. Carling and Orr (2000) who measured eddy lengths of 1-2m supported these empirical observations, on the River Severn for in-bank flows. For bankfull flows in the River Severn numerical modelling estimates arrived at an eddy length scale of 14 m. Clifford (1993a) also identified a small number of larger flow structures 1-4 times the channel width, which correlated to the size of pools. However it was the smaller scale flow structures which predominated, leading Clifford to suggest a re-interpretation of the Yalin-Richards hypothesis that incorporated smaller and more variable flow structures and the associated morphological response / control. Clifford's revised model states that riffle-pool units are initiated by the generation of roller eddies upstream and downstream of a major flow obstacle such as a boulder. The obstacle persists for long enough to fix flow patterns and hence induce significant modification of channel form. However the obstacle is ultimately removed as part of the process of bed

modification via extension scour. Three distinct stages in the process are involved: (1) local scour of a single pool that creates (2) deposition downstream, which then (3) generates the next downstream flow irregularity. The riffle-pool sequence is thus created ‘autogenetically’ as the summation of a sequence of irregularities, each unit of which is formed and maintained only by flow dynamics operating at a local scale. Clifford also suggested that spatial variation in the near-bed turbulent velocity field triggered by incipient riffle-pool topography, leads to differences in bedload entrainment due to structural differences (e.g. Sear 1992; 1996), which further enhance and maintain the sequence in a form-process feedback loop. Thompson *et al.* (1996) attach a note of caution to Clifford’s model claiming it may have problems explaining channel formation when numerous coarse bed elements are present. Furthermore this model may not apply to streams where obstacles are unavailable.

1.3.4 Riffle-pool hydraulics and maintenance

Theories surrounding the maintenance of riffle pool morphology may be separated from those responsible for their initial formation on a uniform bed. Hypotheses of riffle-pool maintenance have usually been centred on the interaction between water discharge, sediment transport, and channel morphology, slope and bed roughness elements. Gilbert (1914) was the first to introduce a model of riffle-pool maintenance based around observations that there may be a reversal in velocity between riffle and pool units as discharge increased. Keller (1971) advanced this model and combined observations with quantitative data to propose the ‘velocity reversal hypothesis’, which has since been used to explain the areal sorting of bed sediments and the maintenance of the riffle-pool form. Keller found that at low flow the near bed velocity of the pool was less than the adjacent riffles. As discharge increased the pool velocity increased at a faster rate than the riffle velocity. Although Keller did not record higher pool velocities, extrapolation of his data suggested a reversal in velocity towards bankfull. Changes in water surface slope (energy gradient) also occur between riffles and pools at different discharges. At low flow the water surface slopes are higher over riffles than pools, but increase at a faster rate over pools than riffles as discharge increases, until eventually the water-surface slopes converge (Thompson *et al.*, 1996). The velocity reversal hypothesis has emerged as the principle area of debate concerning riffle-pool maintenance and sediment transport processes through

riffle-pool sequences (see Milan *et al.*, 2001). A review of the literature by Milan *et al.* (2001) found six studies to support the hypothesis with actual measurements (Andrews, 1979; Lisle, 1979, Teisseyre, 1984; Petit, 1987, Ashworth, 1987 and Sear, 1996). Some accept the hypothesis but were unable to prove it, whilst others strongly disagree (see Table 1, Milan *et al.*, 2001). The main bone of contention surrounds the principle of mass continuity (Bhowmik and Demissie, 1982), where the velocity of the pool cannot be higher than that of the riffle unless the flow area at the pool is less than that of the riffle. For the flow area at the pool to be less than that at a riffle, it would require a smaller channel width at the pool than the riffle, since water depth at the riffle is always less than at the pool. A number of investigators have demonstrated that during most flows, pools have larger cross-sectional areas and should therefore have lower cross-sectionally averaged velocities than riffles (Richards, 1978; Carling, 1991; Carling and Wood, 1994; Thompson *et al.*, 1996; 1999).

According to Thompson *et al.* (1998) the continuity problems associated with the velocity-reversal theory are a consequence of the traditional one-dimensional view of flow. By viewing flow in two-dimensions Thompson *et al* (1996) demonstrated that the formation of re-circulating eddies in pools was able to increase local velocities in the pool troughs. Bedrock protrusions, boulders and debris jams can form flow constrictions upstream from pools, creating large recirculating eddies downstream (Thompson *et al.*, 1998). The constriction can cause ponding and a local increase in water surface slope at pool heads (Lisle, 1986; Miller, 1994; Thompson *et al.*, 1998). Re-circulating eddies reduce the downstream area of flow in pools in a hydraulically constricted area known as a *vena contracta* (Thompson *et al.*, 1998), caused by upstream flow driven by the eddy. This condition satisfies the continuity of mass principle, allowing higher velocities and scour of the pool trough. Thompson *et al*'s model provides an important advance in the understanding of riffle-pool maintenance, however is limited to channels with physical constrictions.

A reversal in mean section velocity in riffle-pool sequences without constrictions to flow in the pool is still theoretically possible. In streams with high sediment supply, Clifford and Richards (1992) suggest that if the pool fills substantially with gravel at high discharge the cross-sectional area may decrease sufficiently to allow a reversal in velocity. In a supply-limited situation however, a reversal would require systematic

changes in geometry or flow resistance differences, which may not be present between all riffle and pool sections (Clifford and Richards, 1992).

Alternative mechanisms for riffle-pool maintenance

Sear (1992; 1996), Clifford and Richards (1992) and Clifford (1993b) stress the importance of contrasts in bed structure in riffle-pool maintenance and claim this can explain maintenance without recourse to hydraulic theory. Riffle sediments have a tendency to be more tightly packed (Sear, 1992; 1996; Clifford, 1993b) and exhibit a variety of structures involving grain interlock, imbrication, or clustering (e.g. Brayshaw *et al.*, 1983; Kirchener *et al.*, 1990; Church *et al.*, 1998). Bed structure is enhanced by *insitu* gravel vibration caused by chaotic, turbulent flow, which dominate during low magnitude high frequency flows (Sear, 1996). This vibration may also allow fine grained sediments to infiltrate gravel voids (Schächli, 1992; 1995), causing a cementation effect (Reid and Frostick, 1984). Locked and buried clasts tend to move shorter distances than free surface clasts (Hassan and Church, 1992), and have higher critical thresholds for motion (θ_c) than the loosely packed fines in pools (Sear, 1996). Thus the riffles are maintained as topographic highs, as they are more difficult to scour, and the pools are maintained as topographic lows, as they scour more easily. The importance of relative bed structural effects in streams which show coarse lag deposits in the pools is unknown, with the implication being that the lower compaction experienced in the pool sediments may be counteracted by its coarser grain size.

Teisseyre (1984) provides a qualitative account of the role of three-dimensional flow structure in riffle-pool maintenance, suggesting that transverse secondary flows and longitudinal re-circulating eddies can be significant sediment transporters and sorters. Bathurst (1979) has also provided data that demonstrates the effects of secondary flows on increasing shear stresses, particularly at medium discharges. Thompson *et al.* (1999) suggest that re-circulating eddies triggered by obstructions such as boulders in pools can cause locally high shear stress as well as reducing the wetted cross-section area enough to induce velocity reversal. The role of three-dimensional flow is discussed further in Chapter Nine.

Wilkinson *et al.* (2000) argue that the tractive force reversal theory does not provide an adequate explanation of riffle-pool maintenance as it has only been confirmed in some isolated riffle-pool sequences. Instead, Wilkinson *et al.* (2000) propose an alternative mechanism for riffle-pool maintenance based upon sediment continuity. Sediment continuity can be conceptualised as a mass balance over a small reach of channel. Where a positive sediment transport gradient exists, more sediment is removed from the downstream end of the reach than is supplied to the upstream end. This results in a decrease in bed elevation as the bed supplies sediment to make up the difference. With this model, scour and deposition are found to occur where there is a longitudinal gradient in the sediment transport rate and mean bed shear stress along the channel. Scour occurs in regions of the channel with a positive shear stress gradient and deposition in regions of the channel where there is a negative shear stress gradient. Aggradation at the riffle crest during a flood, requires a negative shear stress gradient, whereas pool scour requires a positive shear stress gradient along the length of the pool. This contrasts with Keller's reversal hypothesis, which requires a tractive force minimum over the riffle crest for it to aggrade and a tractive force maximum in the centre of the pool for it to scour.

1.4 Gravel-bed sediment structure

Before considering sediment transport and sorting through riffles and pools, it is first necessary to consider the sedimentological characteristics of upland temperate gravel beds similar to the Rede study site used in this investigation. The sediments deposited within the bed of a river display both vertical and lateral structural variability (Carling and Reader; 1982; Milan *et al.*, 2000). The bed is composed of two interrelated components: a coarse surface layer and a finer sub-surface. The surface layer plays an important role in determining the form of sediment transport, regulates the availability of streambed sediment and controls the relationship between streamflow and bedload discharge (Milhous, 1973). The difference between the size characteristics of the surface and sub-surface sediments has important implications for mobility, as this effects the equal mobility criterion described later in section 1.5.2. A progressive increase in the difference between surface and subsurface sediments should result in a progressive decrease in entrainment threshold or critical Shields function(θ_c) (Clifford, 1990). If the ratio of surface to subsurface sediment sizes shows a

difference so that θ_c for the pool is less than θ_c for the riffle, then pools are likely to be scoured and riffles maintained for a given tractive force.

1.4.1 Surface layer texture

The coarse surface layer in gravel-bed rivers has been variously termed the 'armour' in the more recent literature, 'pavement' in the older literature (Gomez, 1984), and 'censored' layer (Bray and Church, 1980; Carling, 1981). Armour and pavements are usually only one-grain thick, whereas censored layers comprise more than one grain. Both armours and pavements may be termed 'static' or 'mobile' depending upon their mobility. Static armours are found where there is no supply of gravel from upstream, e.g. below reservoirs (Petts, 1984; Milan, 1994). In this case the bed surface is immobile at all flows below the historical maximum discharge (Sutherland, 1987; Parker and Sutherland, 1990). Mobile armours develop in gravel-bed streams where bed surface disruption is a more common feature.

There has been considerable debate concerning the definition of the surface layer (Carling, 1981; Milhous, 1981; Parker, 1981), which led Bray and Church (1982) to conclude that it was not yet possible to make a definitive description of the mechanism of gravel-bed formation. Richards and Clifford (1991) suggest that much of the problem surrounding a genetic classification of the surface layer is that historically the term 'armour' has been used collectively regardless of the mode of formation. Gomez (1984) suggests that a genetic classification of the surface layer is not possible due to an incomplete understanding of the processes surrounding its formation. However, two general classifications of the surface layer appear to exist based upon its relative mobility. Bray and Church (1980) refer to the armour as a temporary protection frequently removed, whereas a pavement is a semi-permanent feature. This contradicts several other studies which suggest pavements experience regular mobilisation (e.g. several times a year) of most grain sizes (Livesey, 1965; Parker *et al.*, 1982a and 1982b; Raudkivi and Ettema, 1982; Komar and Carling, 1991). However, when the surface is so coarse that it seldom moves, it is called an armour layer. Richards and Clifford (1991) highlight four main explanations for the formation of coarse surface layers, which may occur in any combination. These are (i) lateral winnowing (Tanner, 1964), (ii) vertical winnowing (Parker and Klingeman,

1982), (iii) equal mobility (Parker *et al.*, 1982a), (iv) traction clogging (Everts, 1973; Allen, 1983). As will be explained in more detail in section 1.5.1, a static armour results from selective transport processes of lateral winnowing (Sutherland, 1987; Parker and Sutherland, 1990), whilst section 1.5.3 shall demonstrate that mobile armours result from vertical winnowing (Parker and Klingeman, 1982).

1.4.2 Variations in surface structure and implications for mobility

A variety of structures involving imbrication, interlock or clustering may be found on a gravel-bed surface (Laronne and Carson, 1976; Brayshaw *et al.*, 1983; Kirchner *et al.*, 1990; Buffington *et al.*, 1992; Church *et al.*, 1998) and may alter the mobility of different areas of the bed. More recently it has been recognised that the surface of poorly sorted, bimodal sediments found in gravel bed rivers is often organised into patches of finer and coarser (armoured) sediment. These sediment patches have been observed in flume studies (Wilcock and Southard, 1988; Kuhnle, 1993a; Paola *et al.*, 1992; Paola and Seal, 1995; Toro-Escobar *et al.*, 2000) and in the field (Laronne and Carson, 1976; Mosley and Tindale, 1985; Lisle and Hilton, 1999; Laronne *et al.*, 2000). The coarser patches tend to be better sorted than the reach on average and have the effect of reducing the mobility of the coarser material whilst increasing that of the fines (Paola and Seal, 1995; Laronne *et al.*, 2000).

1.4.3 Subsurface sediments

This component comprises the bulk of the channel bed with grain sizes typically two to three times finer than the surface layer (e.g. Parker and Klingeman, 1982; Sutherland, 1987; Wilcock, 1989). Subsurface sediments usually have a greater range of grain sizes which can be divided into (i) a coarse gravel population >4mm (framework), the void spaces of which are interspersed with (ii) a finer matrix population (<2mm) of sands silts and clays. On a weight frequency basis these two components may be clearly distinguishable as peaks on a bimodal grain-size distribution, with a saddle frequency interval separating the two populations (Carling and Reader, 1982; Wolcott, 1988; Milan, 1994). Fluvial sediments are commonly deficient in the 2-4mm size range (Carling, 1989; Milan *et al.*, 2000), although Wolcott (1988) suggests that the gap may occur anywhere between 1 and 10mm. Three hypotheses have been proposed to explain bi- or poly-modality in fluvial

sediments. The first hypotheses negates the importance of fluvial action, the second includes it as a causal factor, whilst the third claims that a stream may preferentially entrain the 'gap' material, which is carried away due to its increased mobility (Blatt *et al.*, 1980; Russel, 1968, Sundborg, 1956). Subsurface sediments may be classified according to the concentration of matrix material present in the framework void spaces. Where the matrix is less than 32% and the framework particles are in tangential contact with one another, then the substrate is termed 'framework supported' (Carling and Glaister, 1987; Church *et al.*, 1987). However, if the quantity of matrix exceeds this figure, the deposit is 'matrix dominated'. A framework gravel with open void spaces, which is free of fines may be termed 'openwork' (Cary, 1951).

In order to further understand the role of sediment structure and sorting patterns in the maintenance of riffles and pools, it is useful to understand the factors governing the mobility of sediment in river channels and discuss the theories of selective transport and equal mobility. This background literature is pertinent to the research presented in Chapters Six and Seven.

1.5 Incipient motion

Most investigators use a standard or modified form of the Shields (1936) entrainment function to define incipient motion of a grain size of interest, regardless of whether equal mobility or selective transport operates within the channel (Buffington and Montgomery, 1997). Shields ran a series of flume experiments with uniform material (<3 mm in diameter) organised into planar beds, and related the tangential fluid stress at the boundary responsible for grain movement to the weight per unit area of the grains in its surface layer. Thus the Shields entrainment function, or dimensionless critical shear stress (θ_c), may be defined as;

$$\theta_c = \tau_c / (\rho_s - \rho_w) g D_i \quad (1.1)$$

where τ_c is the critical shear stress responsible for grain movement, ρ_s and ρ_w are sediment and fluid densities respectively, g is gravitational acceleration and D_i is the

grain size of interest. In a plot of θ_c versus grain Reynolds¹ number (Re^*_c), Shields demonstrated that θ_c reached a constant value of about 0.06 under hydraulically rough bed conditions evident in natural streams ($Re^*=489$), although considerable scatter was also evident (Buffington and Montgomery, 1997). From this it was deduced that critical shear stresses were directly proportional to grain size, which suggests that grain weight is the principal force restricting movement. Coarser grains are less mobile due to their greater inertia and therefore require greater shear stresses for mobilisation (Powell, 1998). Buffington and Montgomery (1997) indicate that there have been numerous revisions and updates to the Shields curve (e.g. Shields, 1936; Grass, 1970; Gessler, 1971; Paintal, 1971). Latterly it has been recognised that incipient motion of a particular grain size is inherently a statistical problem, which depends on probability functions of both turbulent shear stress at the bed and intergranular geometry (i.e. friction angles) of the grains on the bed controlled by shape, sorting and packing (Miller and Byrne, 1966; Li and Komar, 1986; Kirchner *et al.*, 1990; Buffington *et al.*, 1992).

Analysis of the threshold shear stress (τ_c) for initial movement has been used to demonstrate the mobility of mixed sized sediments by many workers (e.g. Andrews, 1983, Ashworth and Ferguson, 1989). The values for the τ_c and b exponents have varied widely in the literature and can be partly explained by differences in the two methods used to determine θ_c : the largest-grain method and the reference-transport method (Johnston *et al.*, 1998). The largest-grain method (e.g. Komar, 1989) assumes that the largest mobile grain size collected in a bed load sample is indicative of the initial motion conditions as long as larger grains are available for transport. The reference-transport method (e.g. Parker *et al.*, 1982a; Wilcock and Southard, 1988; 1989) involves measuring transport rates for individual size fractions for a number of different flows. The relation between shear stress and transport rate is then used to find a θ_c that produces a small reference transport rate for that size fraction. Wilcock (1988; 1992b) argues that the largest grain method produces a variation in θ_c with $D_i^{0.5}$ ($b \approx -0.5$), whilst the reference transport method indicates little dependence of θ_c upon D_i ($b \approx -1$). In principle, the two initial motion methods should give identical

¹ $Re^*c = u^*c k_s/v$, where u^*c is the critical shear velocity for incipient motion ($u^*c = (\tau_c/\rho)^{1/2}$), k_s is the boundary roughness length scale, and v is the kinematic viscosity; Shields (1936) set $k_s = D_{50}$.

results except when θ_c is independent of D_i . However, scaling and sampling problems make it very difficult to obtain representative and comparable estimates of θ_c for different size fractions (Wilcock, 1988; Dietrich and Whiting, 1989; Komar and Shih, 1992). Selective entrainment may also vary with the degree of sorting and bimodality (Kuhne, 1993a; 1993b; Wilcock, 1992a; 1993) and flow intensity (Parker *et al.*, 1982b; Diplas, 1987; Ashworth and Ferguson, 1989).

1.5.1 Size -selective entrainment and static armouring

Many investigators have demonstrated sediment sorting patterns which are consistent with preferential entrainment of certain grain-sizes. Ashworth and Ferguson (1989), working on the Allt Dubhaig and River Feshie, Scotland, contend that although equal mobility may occur at very high shear stresses, size-selective entrainment has to be responsible for the rapid downstream fining observed in many streams. This is because equal mobility only allows fining to occur as a result of abrasion during transport or weathering. For thirteen different rivers in the USA, New Zealand and the UK, Lisle (1995) has also demonstrated that significant selective transport of finer bedload over a more stable substrate of coarser bed material can occur

Surface layer coarsening or armouring may result from a combination of selective transport and sediment supply starvation (Dietrich *et al.*, 1989; Buffington and Montgomery, 1999). This has been observed in the field below reservoirs, where regulated clear-water flows are competent enough to scavenge fines from the surface layer (Petts, 1984a; 1984b; Milan, 1994; 1996). The type of armour that develops is usually immobile at all flows up to the historical maximum (Powell, 1998), and is commonly termed static or stable (Sutherland, 1987; Parker and Sutherland, 1990). Static armours tend to have a wide range of τ_c for different sized particles. The armour surface is broken when the coarsest material is entrained which then allows the subsurface material to be transported. On the falling limb of the hydrograph the coarse clasts are preferentially deposited rapidly reforming the surface layer. Fines are then removed from the surface layer through lateral winnowing (Klingeman and Emmett, 1982; Gomez, 1989).

1.5.2 Relative mobility of grains in mixed-sized sediments

Shields (1936) based his research on grains with uniform size. Application of the Shields threshold curve to mixed sediments found in natural channels involves assumption of a characteristic size for the whole deposit such as the median grain size (D_{50}). τ_c for individual size fractions in mixed sediments differ markedly from those found for uniform size sediment. A mixture of grain sizes influences the τ_c for a grain size fraction in two ways. Firstly, small grains which sit among coarser grains have larger friction angles (resistance to movement) than larger grains sitting among relatively fine grains. Secondly, relatively fine grains have less relative protrusion as they are sheltered or hidden from the flow in the wakes created by adjacent coarser grains, thus reducing the fluid forces acting on the grain (Fenton and Abbott, 1977; Carling *et al.*, 1992). Both factors lead to greater τ_c for grains which are finer than the median grain size of the surface layer D_j and a smaller τ_c for grains which are coarser than D_j .

With this in mind Parker and Klingeman (1982) proposed an empirical equation of the type;

$$\theta_c = a(D_i/D_j)^b \quad (1.2)$$

where a and b are empirical coefficients. a is equivalent to θ_{c50} the critical dimensionless shear stress when $D_i = D_{50}$, and b is a hiding factor which quantifies the dependence of θ_c on relative grain size ($b < 0$). Values for the b exponent are of particular significance; if $b = 0$ then sediment entrainment is dependent solely upon grain size. However an exponent of -1 would indicate that the absolute weight of a grain is completely compensated for by the relative size effects and that the τ_c for different size fractions are independent of grain size. Estimates of b in (1.2) have ranged from -0.43 to almost -1.0 for flume and field studies (Day, 1980; Parker and Klingeman; 1982; Andrews, 1983; Hammond *et al.*, 1984; Wilcock and Southard, 1988; Ashworth and Ferguson, 1989; Petit, 1989; 1990; Carling *et al.*, 1992; Sear, 1996), suggesting significant differences in grain-to-grain interactions between sediment mixtures (Johnston *et al.*, 1998).

1.5.3 Equal mobility hypothesis and mobile armouring

Parker and Klingeman (1982), Parker *et al.* (1982a; 1982b), Andrews (1983), Andrews and Erman (1986) and Andrews and Parker (1987) suggest that hiding and protrusion effects can be strong enough that the τ_c required to entrain a particle increases only slightly, if at all, with its diameter. Parker *et al.* (1982a) conducted experiments on Oak Creek, Oregon USA, a small stream with a well-developed armour layer. Data derived from flows above the critical discharge for mobilisation of the armour and sub-surface sediments produced an entrainment function (b exponent) of -0.982 . This suggested that once the critical shear stress was reached, exceeding the threshold value required to disturb the armour, mobility (for equilibrium transport conditions) was equal for all sizes encountered (exponent virtually -1). Furthermore the bedload grain size distribution was equivalent to that of the sub-surface bed material, where $p_i/f_i \approx 1.0$ for all i where p_i is the proportion of the i th size in the bed load and f_i is the proportion of that size in the sub-surface bed material (Andrews and Parker, 1987). This effect equalises the long-term mobility of small and large particles so that there is no progressive coarsening or fining of the bed at a point. It is suggested by Parker and co-workers that under equilibrium conditions the lesser mobility of coarser clasts is compensated for by their over-representation on the bed surface through a process of vertical winnowing of finer grains (Parker and Klingeman, 1982). Surface coarsening through vertical winnowing acts to equalise the mobility of different sizes by counterbalancing the intrinsic lesser mobility of relatively coarse particles (Parker *et al.*, 1982b; Andrews and Parker, 1987). Estimates of τ_c can therefore be estimated from the D_{50} and an appropriate value of θ_c (Gordon, *et al.*, 1992; Wilcock, 1992a). Armour layers produced by vertical winnowing are termed mobile armours. A mobile armour requires the framework clasts to move and thus allow fines to infiltrate void spaces, whereas finer grain sizes are selectively transported around coarser immobile / less mobile clasts in the formation of a static armour.

A large body of literature exists concerning sediment mobility, some of which supports equal mobility and others selective transport (e.g. Andrews and Parker, 1987; Richards, 1990; Church *et al.*, 1991; Church and Hassan, 1992, Gomez, 1995; Lisle, 1995; Wathen *et al.*, 1995; Komar, 1996). The channel-averaged data of Parker *et al.*

(1982b), and Andrews and Parker (1987) appear to provide evidence of equal mobility, although considerable scatter is evident in the data. Some of the original data obtained by Parker and his colleagues, used to formulate the equal mobility hypothesis from Oak Creek, US, has since come under scrutiny. Komar (1987) reanalysed some of this data and claimed that there was no common threshold for motion of gravels. Ashworth and Ferguson however present strong evidence for size selective transport on the Allt Dubhaig, and Church *et al.* (1991) concede that for river reaches which do not show any strong downstream fining trends, the notion of equal mobility must hold in a general sense. In one of the most critical interrogations of the equal mobility hypothesis, Church *et al.* (1991) analysed fine bedload $<2000\mu\text{m}$ and found 'near' equal mobility for washload material ($<210\mu\text{m}$ material), whereas bedload material $210\mu\text{m}-2000\mu\text{m}$ showed evidence of being selectively transported. The issue of mobility in the finer fractions, which has been considered much less in comparison to gravel, is considered in detail in Chapter Five.

1.5.4 Mobility of sediments through riffles and pools

A number of workers have demonstrated (using tracers) greater transport distances of sediments located in pools in comparison to riffles (e.g Sear, 1992a; 1996; Ashworth 1987; Keller unpublished (in Sear, 1996); Thorne, unpublished (in Sear, 1996) reflecting greater tractive forces of pools during high flows. Sear (1996) was able to provide a slightly better spatial resolution and demonstrated that (i) pool head sediments could be transported further than pool trough sediments, (ii) pool trough sediments could be transported further than pool tail sediments, and (iii) pool tail sediments could be transported further than riffle sediments. Although transport distance for bedload clasts has been shown to reflect the spatial patterns of shear stress, Sear (1996) has also suggested that differences in bed structure may strongly influence mobility (see section 1.3.4).

1.6 Sediment sorting in the riffle-pool sequence

The majority of workers suggest variations in sorting of the surface layer of sediments between pools and riffles, claiming that riffles are coarser and better sorted than pools implying the operation of selective transport processes (Table 1.1). There are a number of investigators, however, who claim that it is the pools which should be

Table 1.1 Summary of a range of studies documenting textural differences between the bed sediments of riffles and pools.

Investigator	River	Riffle	Pool
Hack (1957)		No difference	No difference
Leopold <i>et al.</i> (1964)		Coarser	Finer
Yang (1971)	Lab flume and Kaskaskia River, Illinois, US	Coarser	Finer
Keller (1971; 1972)	Dry Creek, US	$D_{50} = 32\text{mm}$	$D_{50} = 10\text{mm}$
Church (1972)		Coarser	Finer
Cherkauer (1973)	Treia River, Italy	Cobbles and boulders, little matrix	Sand and fine gravel
Richards (1976a and b; 1978)	River Fowey, Cornwall UK	45-60mm	37-52mm
Lisle (1979), Andrews (1984)	East Fork River, Wyoming, US	Coarser at low flow, Finer at high flow	Finer at low flow, coarser at high flow
Milne (1982)	Kingledoors Burn, Tweed, Scotland, Peeblesshire, UK	$D_{50} = 43\text{mm}$	$D_{50} = 36\text{mm}$
Bhowmik and Demissie (1982)	Kaskaskia River, Illinois, US	Coarser $D_{max} = 46\text{mm}$	Finer $D_{min} = 0.034\text{mm}$
Hirsch and Abrahams (1984)	Cattaraugus Creek, New York, US	Coarser and better sorted, $D_x = 57\text{mm}$	Finer and less well sorted, $D_x = 28\text{mm}$
Ashworth (1987)	Allt Dubaig, Scotland, Reach A Reach B Reach C Reach D Reach E River Feshie, Scotland, UK	$D_{50} = 113\text{mm}$ $D_{50} = 87\text{mm}$ $D_{50} = 70\text{mm}$ $D_{50} = 78\text{mm}$ $D_{50} = 40\text{mm}$ $D_{50} = 62\text{mm}$	$D_{50} = 125\text{mm}$ $D_{50} = 120\text{mm}$ $D_{50} = 59\text{ mm}$ $D_{50} = 64\text{mm}$ $D_{50} = 40\text{mm}$ $D_{50} = 70\text{mm}$
Petit (1987)	La Rulles, Ardenne, France	15.2mm	50-100mm
Carling (1991)	River Severn, Shrewsbury, UK	$D_{50} = 25\text{mm}$	$D_{50} = 43\text{mm}$
Clifford (1993b)	River Quarne, Exmoor, UK	Coarser	Finer
Sear (1996)	River North Tyne, UK	$D_{50} = 60\text{mm}$	$D_{50} = 43\text{mm}$
Robert (1997)	Little Rouge River, Ontario, Canada	Coarser	Finer
Thompson <i>et al.</i> (1996; 1999)	North Saint Vrain Creek, Colorado, US	Finer x difference = 4.8mm max difference = 8.8mm Reach $D_{50} = 95\text{mm}$	Coarser
Wilkinson <i>et al.</i> (2000)	Steavenson River, Marysville, Victoria, Australia	76mm	50mm

coarser than the riffles (e.g. Bhowmik and Demissie, 1982, Thompson *et al.*, 1999). The pattern of surface sediment grain size may be linked to the reversal mechanism (Keller, 1971) by which riffle-pool morphology can be maintained. In streams which show a competence reversal, pool troughs represent zones of maximum tractive force during peak flood events above the reversal threshold. Keller (1971) suggests that at flows below the reversal threshold only relatively fine material is selectively transported. The bottom velocity of the pool is less than that of the riffle; hence the largest material which can be transported by the riffle is trapped in the downstream pool. When the bottom velocity is equal in both the pool and in the riffle then material which can be transported through a riffle is also transported through the next pool. As discharge rises, the pool bottom velocity eventually exceeds that of the riffles. As the threshold for the transport of coarse material on the riffles is exceeded, bed particles will be transported down to the next pool, whereupon they are rapidly transported down to the next riffle by the greater tractive force of the pool. During peak flood flows above the reversal, pools may transport any bedload particle that moves into the pool. At high flow, the only stable areas for coarse material are on bars and riffles, where there is less tractive force. On the falling limb of the hydrograph, the coarse material is stranded on the riffles. Consequently, the largest clasts are found on riffles, and relatively finer material is found in pools. Jackson and Beschta's (1982) two-phase sediment transport model employs Keller's (1971) velocity reversal hypothesis, suggesting that gravel transport (Phase 2) is initiated when tractive force of the pools exceeds that of the adjacent riffles, whereupon the surface armour is disrupted on the riffles and coarse bedload is transported downstream. As pool tractive forces tend to exceed those of the riffles, sediments are not deposited in the pools. Instead the pools are scoured and sediments are deposited on the downstream riffle if the competence is low enough. Phase 2 bedload transport may therefore be conceptualised as a 'leapfrogging' of bed material downstream from riffle to riffle (Jackson and Beschta, 1982). Below the reversal threshold and for most of the flow range, Phase 1 transport (sand) dominates.

On the other hand, Bhowmik and Demissie (1982) and Thompson *et al.* (1999) contend that the coarsest bed material should be found in the pool troughs as pools represent zones of maximum competence. Bowman's (1977) model also predicted that bed sediments became coarser with depth, thus reflecting high flow hydraulics.

Any fines found in pools were thought to result of deposition during the waning limb of the flood hydrograph. These ideas are logical if the high flow sorting pattern is considered alone. However grain size is most commonly observed at low flow, and hence the grain-size patterns recorded by most investigators are most likely to reflect a range of flow and sediment supply scenarios. Some studies have highlighted the difficulty in gaining reliable grain size data particularly for pools (Richards, 1976a; Carling, 1991), and some of the published data may include information on low flow deposits or an unrepresentative mixture of high and low flow materials. Several studies have reported coarse sediments in pools (e.g. Gilbert, 1914; Ashworth, 1987), most of which suggest that these are lag deposits derived from erosion of bank material or scour into till deposits (Keller, 1982). This has also been suggested by Leopold *et al.* (1964) to explain some of Hack's (1957) data.

The role of fine sediment supply in determining the observed low flow grain size has been shown to be significant (e.g. Lisle and Hilton, 1992; 1999). In streams with a high supply of fines, material deposited on riffles during high flow is selectively winnowed into the less competent pools on the falling limb of the hydrograph where it is stored until the next high flow event. In supply-limited streams the quantity of fines stored in pools is considerably reduced, hence the high flow sorting patterns are easier to observe and are not disguised by low flow deposits. Bhowmik and Demissie (1982) claim low flow winnowing to be a primary factor responsible for the reported sorting differences between riffles and pools, rather than high flow velocity reversal as suggested by Keller (1971). Thus the existence of finer pools may be considered to be dependent upon sufficient fine sediment supply. Carling (1991) however states that although winnowing may explain small sedimentological differences shown in some streams (e.g. Wolman, 1954; Hack, 1957), it does not explain the cases where riffle sediments are much coarser (Church, 1972; Hirsch and Abrahams, 1981). Furthermore winnowing of fines cannot explain the maintenance of the riffle-pool form; rather it is the re-distribution of gravel that must occur before morphological change can take place (Carling, 1991).

1.6.1 Routing of gravel (Phase 2 bedload) through the riffle-pool sequence

Data are limited concerning the detailed spatial deposition and routing patterns of the full grain size distribution transported as bedload through river channels. Attention

has generally been focused towards scour location and distance of movement rather than deposition location and dynamics (e.g. Ashworth, 1987; Sear, 1992; 1996). For gravel, it is generally accepted that clasts are exchanged between morphological highs (riffles and bars) at high flow and they do not settle in pools due to the greater forces (Keller, 1971; Parker and Peterson, 1980; Jackson and Beschta, 1982). Smaller-scale re-distribution of gravel may also occur at intermediate flows where redeposition of clasts on pool-heads may occur (Lisle, 1982). Movement of pool trough sediments and those located on the stoss slope of riffles has received very little attention (Carling, 1991). There is a clear research need for a morphologically-based account of tracer movements for different flow stages. Sear (1992b; 1996) provides an improved spatial resolution showing size selective sorting through the riffle-pool sequence with a downstream fining shown for tracer material deposited in pools. Coarse gravel (>20mm) appeared to be stored at the pool head (supporting Lisle, 1982) and riffle (supporting Jackson and Beschta, 1982), material between 2 and 16mm was stored in the pool trough and tail, whilst sand was distributed throughout the riffle-pool sequence as infiltrated fines and wake deposits. Thompson *et al.* (1996) was able to demonstrate a more detailed spatial account of deposition using painted pebbles showing the coarsest clasts $D_x = 110\text{mm}$ to be deposited in pool troughs, with progressively finer material being deposited on pool exit slopes ($D_x = 94\text{mm}$), runs ($D_x = 78\text{mm}$), steps ($D_x = 72\text{mm}$), and riffles ($D_x = 57\text{mm}$) respectively. However from their paper, it is unspecified whether coarser material had moved into the pools or if the observed sorting had resulted from preferential scour of finer tracers from pools, leading to formation of a lag layer (see section 1.6). Data from Thompson *et al.* (1996) supported a number of Sear's (1996) results, demonstrating that pool exit slopes act as important depositional sites limiting the downstream movement of coarser clasts.

1.6.2 Routing and sorting of fines (Phase 1 bedload)

Compared to Phase 2 bedload there is much less literature concerning the lateral movement of fine sediments. Fine sediment trapping work which has been conducted appears to suggest that fractions $<250\mu\text{m}$ may be transported in suspension (Acornley and Sear, 1999), whilst coarser sediments ($250\text{-}4000\mu\text{m}$) may be transported predominantly as bedload (Church *et al.*, 1991; Acornley and Sear, 1999). In upland

streams sand transported as the saltation component of the bedload can be responsible for the majority of matrices found in the subsurface (e.g. Lisle, 1989).

In addition to the literature on winnowing of fines and sorting through the riffle-pool sequence, some work has been conducted upon spatial patterns of fine sediment accumulation and grain-size. Much of the information available however is restricted to riffles (with the exception of Carling and McCahon, 1987, and Lisle and Hilton, 1999), the common focus of the research being siltation of salmonid spawning grounds, or heavy mineral / placer studies. Carling and McCahon's (1987) experiments on the upland Great Eggleshope Beck, UK, demonstrated that the accumulation rate of fines increased linearly from the outside of a river bend toward the inside. Similar variation was identified across a riffle-pool sequence; for a 10% increment in stream width, the accumulation rate increased by $119\text{ g m}^{-2} \text{ week}^{-1}$ in the pool and $104\text{ g m}^{-2} \text{ week}^{-1}$ over the riffle. The velocity pattern appeared to influence bedload fractions more than finer material, which was usually transported in suspension. The 2-4mm fraction was found to show enhanced accumulation rates (and inferred transport rates) in high velocity zones in the pool and a number of other high velocity threads across shallower areas. Welton (1980) also shows spatial variation in his measurements for Tadnoll Brook, UK, a lowland chalk stream, with $5\text{ kg m}^{-2} \text{ day}^{-1}$ deposited along the thalweg and up to $70\text{ kg m}^{-2} \text{ day}^{-1}$ deposited along the channel margins. Fines deposited in this low energy stream were probably dominated by grades transported in suspension rather than bedload, which show enhanced deposition along the channel margins due to the lower velocities found in these areas. Frostick *et al.* (1984) identify maximum infiltration rates in zones of high velocity, whereas Carling and McCahon (1987) identify slack-water areas as areas of maximum deposition. In general it appears that bedload material correlates most successfully with local hydraulics, whereas suspended material tends to be more equally dispersed, possibly due to the effects of secondary flows and turbulence. Lisle and Hilton (1999) used the similarity shown in the grain-size distribution of fine sediment drapes, found in the pools of eleven out of sixteen streams situated in California and southern Oregon, US, and sub-surface riffle matrix to show that fines had been routed from upstream riffles via winnowing.

1.6.3 Size sorting

Thoms (1987) was able to demonstrate down- and cross-riffle variation in both the quantity and grain-size of accumulating sediments. In his work on the lowland Black Brook, UK, maximum accumulation and coarser-grained material were found to infiltrate traps situated at riffle heads. In contrast lower accumulation rates and finer material infiltrated riffle tail traps, where the size differences were attributed to winnowing out of finer grades from the riffle head. Traps located in the channel centre also collected greater quantities and coarser fines in comparison with the channel margins. These patterns of infiltration appeared to be related to the interrelationships between sediment supply and near-bed hydraulics.

More recent flume work by Allan and Frostick (1999), demonstrates that the spatial variation in quantity of fine sediment accumulation and grain size can depend upon whether fine bedload is transported over a stable gravel bed or one which is mobilised fully or partly (jiggled) during a flood. Over a stable bed where shear stresses are not capable of moving the framework gravels, fines may be winnowed across the surface and may infiltrate near-surface void spaces forming sand seals (e.g. Beschta and Jackson, 1979); surface fine bedload was shown to fine downstream in this situation. When shear stresses are great enough to jiggle the gravel, framework dilation occurs just prior to entrainment causing fines which are being winnowed across the surface to be sucked into deeper void spaces (Venturi effect). Higher shear stresses appear to result in greater path lengths for the coarser / heavier grains, possibly due to inertial effects resulting in downstream coarsening. This would suggest that the down-riffle fining in matrices shown by Thoms (1987) was purely a reflection of winnowing processes of a stable gravel bed, and that no gravel disturbance had occurred.

1.7 Vertical sorting mechanisms

As was noted in section 1.5.2, the mixture of a coarse gravel framework and a finer matrix of fines found in gravel bed rivers (Carling and Reader, 1982; Milan *et al.*, 2000) may result in reduced mobility for finer material deposited in the wake of coarser clasts (Einstein, 1968; Fenton and Abbot, 1977). Fines may also infiltrate interstitial voids between gravel framework clasts where they are completely protected from the flow until the gravel is disturbed. Vertical sorting of the stream bed as a result of vertical winnowing of fines over both a stable and mobile gravel bed has

been demonstrated by a wide range of laboratory (Einstein, 1968; Beschta and Jackson, 1979; Carling, 1984; Schachli, 1992; 1995; Allan and Frostick, 1999) and field studies (e.g. Frostick *et al.*, 1984). Two different styles of infiltration appear to exist which are related to the size of the infiltrating fines and the size and shape of the receiving gravel framework void spaces (Frostick *et al.*, 1984) and hydraulic conditions (Beschta and Jackson, 1979; Allan and Frostick, 1999) respectively. Over stable framework beds it appears that finer grades (e.g. silts) infiltrate deeper and often fill the voids of an openwork gravel from the base upwards (Einstein, 1968). Conversely, coarser grades (sands and fine gravel) may form near-surface seals, bridging the framework voids and preventing further ingress.

The role of hydraulics has also been demonstrated as being influential (e.g. Beschta and Jackson, 1979; Schachli, 1992; 1995; Allan and Frostick, 1999). Over stable beds, Beschta and Jackson (1979) found greater depths of fine sediment intrusion at higher τ , although this has been disputed by Carling (1984). At τ great enough to disrupt the gravel framework however, framework dilation can occur which can open up previously blocked void spaces. Dilation causes a change in pressure differentials between the void spaces and induces a sucking effect (Venturi effect) that can encourage deeper penetration of fines (Allan and Frostick, 1999; Schachli, 1992; 1995). At even greater τ , total flushing or desiltation of interstitial framework voids may occur (Schachli 1992; 1995).

1.8 Study objectives, experimental design and controlling variables

This thesis seeks to provide an improved explanation of *maintenance* of the riffle-pool form through the investigation of hydraulic character, sediment sorting mechanisms and channel morphology. Although not measured directly some thought must also be given toward potential models of *formation*, as these may condition / control subsequent models of maintenance. The critical evaluation of the various models of riffle-pool formation and maintenance presented in Chapter One has permitted several objectives to be developed. These are to;

- a) Evaluate the tractive force reversal hypothesis of (Keller, 1971) and examine its success at explaining riffle-pool maintenance,

- b) Examine the significance of bed structure contrasts between riffles and pools in altering sediment mobility and thus maintaining the riffle-pool sequence, particularly exploring the role of fine sediments (Reid and Frostick, 1984; Clifford and Richards, 1992; Sear, 1992; 1996; Clifford, 1993b),
- c) Test whether sediment transport and sorting processes through a riffle-pool sequence support the occurrence of tractive force reversal (e.g. Jackson and Beschta, 1982),
- d) Explore the role of hydrograph character (magnitude, frequency, peakedness) in riffle-pool maintenance (e.g. Sear, 1992a and b),
- e) Determine the role of site character in riffle-pool formation and maintenance,
- f) Evaluate other factors that may explain riffle-pool maintenance; i) significance of three dimensional flow, ii) importance of obstacles (Clifford, 1993a; Thompson *et al.*, 1999), iii) sediment continuity (Wilkinson *et al.*, 2000)

The experimental design used to tackle these objectives and the various controlling variables at the Rede study site is presented in Table 1.2.

Tractive force reversal

Further data are required regarding stage-dependent variation in tractive force throughout riffle-pool sequences, that address the following issues (that have led to the controversial nature of Keller's (1971) reversal hypothesis);

- a) poor spatial and temporal resolution of hydraulic measures. There is a particular need for; (i) data at bankfull discharge, (ii) more data points throughout riffle-pool units, and for (iii) sequences of riffles and pools to be monitored rather than comparisons made between discrete units situated large distances away from one another,
- b) lack of standardisation in the hydraulic measures used in different studies. For example τ (from velocity profiles, from $\rho_w g R_s$, point and section average measures), stream power (Ω), v (section average from Q/A), bed and profile average from current meter readings,

Study objectives	Experimental design	Controlling variables in Rede reach
1) Evaluate the tractive force reversal hypothesis of (Keller, 1971) and examine its success at explaining riffle-pool maintenance	<ul style="list-style-type: none"> • Spatial and temporal hydraulic survey (point and cross-section average) • v depth average and bed estimated from current meter survey and mean from A / Q • τ from velocity profiles and $\rho g ds$ • Ω • Sequence of 3 riffles and 4 pools • Up to 530 points measured in reach 	<ul style="list-style-type: none"> • Q regime / hydrograph character • Channel form; variation in cross-sectional wetted area (degree of expansion and contraction), depth / hydraulic radius, slope (bed, valley) ($\tau = \rho g ds$) • Pool geometry (Thompson <i>et al.</i>, 1998) • 3D flow structure • Channel obstacles; e.g. bank collapse in pools reducing cross-sectional area • Sediment supply • Type of extrinsic sediment supply; fluvio-glacial / alluvium, re-working of non-fluvial sediment; alluvium and fluvio-glacial outwash • Grain roughness; coarser pools increase chance of reversal (Carting and Wood, 1994)
2) Examine the significance of bed structure contrasts between riffles and pools in altering sediment mobility and thus maintaining the riffle-pool sequence (Sear, 1992; 1996; Clifford, 1993b)	<ul style="list-style-type: none"> • Spatial compaction survey using a cone penetrometer • Surface and subsurface grain size characteristics; % sub 2 mm • Gravel tracer survey to determine difference in θ_c between riffles and pools 	<ul style="list-style-type: none"> • Sediment supply • Turbulent flow at riffles during low discharges • Hydrograph character; duration and competence of lower discharges • Large clasts extending into flow, induce turbulent flow structures (e.g. Buffin-Bélanger and Roy, 1998). • Comparatively greater τ at riffles during low flows • Fine sediment infiltration, cementation during low flows (e.g. Reid and Frostick, 1984)
3) Test whether sediment transport / sorting processes through a riffle-pool sequence support the occurrence of tractive force reversal (e.g. Jackson and Beschta, 1982)	<ul style="list-style-type: none"> • Surface grain size character of riffle pool units, and sub-units • Sediment tracing; gravel and sand • Spatial and temporal basket trapping of phase 1 bedload 	<ul style="list-style-type: none"> • Sediment supply • Hydrograph shape • Spatial and temporal variation in tractive force • Existing grain and form roughness (e.g. angle of pool exit slope) • Turbulent flow
4) Explore the role of hydrograph character (magnitude, frequency, peakedness) in riffle-pool maintenance (e.g. Sear, 1992)	<ul style="list-style-type: none"> • Discharge measurement. • Clast tracer surveys • Re-survey of riffle-pool morphology 	<ul style="list-style-type: none"> • Climate; precipitation magnitude and frequency • Flow regulation • Land-use • Geology
5) Determine the role of site character in riffle-pool formation and maintenance	<ul style="list-style-type: none"> • Review of the published literature, and assessment of Rede site 	
6) Evaluate other factors that may explain riffle-pool maintenance	<ul style="list-style-type: none"> • Qualitative observation and literature review 	
a) Significance of turbulent flow structures	<ul style="list-style-type: none"> • Literature review, qualitative observation in the field 	<ul style="list-style-type: none"> • Form and grain roughness • Discharge character • Channel morphology
b) Importance of obstacles (Clifford, 1993a; Thompson <i>et al.</i> , 1999)	<ul style="list-style-type: none"> • Assessment of coarse clasts / occurrence of obstacles in pools and stage of pool development in Clifford's (1993a) model 	<ul style="list-style-type: none"> • Availability of obstacles, e.g. reworking of glacial deposits with occasional large clasts, trees, bedrock outcrops etc. • Relative grain roughness, projection into flow. • Hydrograph; duration of flow stages able to submerge obstacle and allow turbulent flow structures to develop; longer duration more scour induced by turbulent eddies
c) Sediment continuity (Wilkinson <i>et al.</i> , 2000)	<ul style="list-style-type: none"> • Analysis of literature 	<ul style="list-style-type: none"> • Longitudinal tractive force gradient • Bed slope • Sediment supply; Low supply – scour, high supply – less scour / scour and fill

Table 1.2 Study objectives, experimental design and controlling variables on the Rede study reach

- c) differences in controlling site variables e.g. sediment supply and source, hydrograph character, past history of valley and floodplain, lack of distinction between processes in straight and sinuous reaches.

This investigation will address these issues by utilising a range of tractive force measures over the full discharge range, whilst utilising a high density spatial coverage through a sequence of three riffles and four pools. There is a wide range of variables listed in Table 1.2 that may influence or even control whether tractive force reversal occurs. For reversal to occur floods must be of sufficient magnitude (usually around bankfull), and must occur frequently enough to scour and maintain pools, whilst at the same time deposit and transfer sediments onto and between the riffles. Channel morphology may also control whether reversal occurs. Firstly, flow contraction into pools and expansion onto riffles, forced by morphology, promotes greater tractive force in the pools at high flow. Secondly, reversal in cross-section average velocity may only occur if the pool cross-section wetted area remains below that of the pool at high flow, according to the continuity of mass principle. Thompson *et al.* (1998) also indicate that an increase in pool length during a flood will act to increase pool centre velocities. Hydraulic radius and channel slope also influence shear stress and stream power, the former controlled by discharge and sediment supply, and the latter by valley gradient. Three-dimensional flow structure in the form of transverse secondary flows and longitudinal roller eddies, may further influence tractive force (Bathurst, 1979; Teisseyre, 1984; Thompson, 1986). However, due to equipment restrictions, this study is limited to a one-dimensional analysis of flow. Qualitative observations concerning three-dimensional flow are however made. Both cross-section average velocity and three-dimensional flow structure are influenced by the presence of obstructions in the pool cross-section (e.g. Thompson *et al.*, 1999), which requires an assessment of any influence of obstructions upon pools at the study site used in this investigation, and those reported in the literature.

Sediment supply can also influence tractive force reversal; if pool competence exceeds supply, cross-section areas change little or enlarge during a flood decreasing the chance of reversal. Conversely in high supply conditions, the pool cross-section areas may reduce sufficiently to raise velocity, effectively increasing the chance of reversal (Clifford and Richards, 1992). As was described in section 1.6, supply also

influences sorting contrasts between riffles and pools. The mechanism by which sediment is supplied to the channel may also influence hydraulic and sediment transport behaviour of the riffle-pool sequence. In self-formed alluvial channels, every grain comprising the channel boundary may be mobilised. However a stream that is re-working valley fill deposits, composed of relict Pleistocene deposits such as boulder clay for example, may not be able to mobilise the coarser clasts. Mobility is further reduced as the fine sediment component is more cohesive due to the greater clay content, in comparison to a fluvial deposit. In supply-limited streams, this situation could lead to coarser pools in comparison to the riffles, increasing grain roughness and the stability of the pool bed, although increasing the likelihood of tractive force reversal (Carling and Wood, 1994). An assessment of sediment supply and sources will be made at the study site on the River Rede, and the literature is summarised in Chapter Nine to identify its significance to riffle-pool maintenance.

Bed structure contrasts

The literature review presented in Chapter One clearly highlights the possibility of alternative mechanisms being responsible for riffle-pool maintenance. One example is that of bed structure contrasts between riffles and pools, proposed by Sear (1992; 1996), Clifford and Richards (1992) and Clifford (1993b) (see section 1.5.4), which claims that riffle-pool morphology can be explained without recourse to a hydraulic theory of maintenance. These workers mainly discuss the significance of the arrangement of coarse particles in influencing the force required for transport, i.e. the less structured and softer the bed sediment is, the easier it is to mobilise. However the role of interstitial fine sediments has largely been ignored, even though it has been suggested that fines can cement framework clasts together and inhibit transport (Reid and Frostick, 1984). Information on the fine sediments in riffles and pools will be obtained from freeze-cores (Milan *et al.*, 2000). This will provide data on the grain size of the fines (percentage clay, silt and sand) and information on bed structure / clast arrangement. Temporal information on the sizes of fines infiltrating gravel interstices may be assessed using an array of traps situated throughout the riffle-pool sequence (e.g. Thoms, 1987; Sear, 1992). Sediment structure variation may also be assessed using a penetrometer device (Sangerlat, 1979), across a network of points (182 are used throughout the Rede study reach in this investigation). The spatial network of compaction data will allow relationships to be drawn between the degree

of mobility, flow and morphology. Spatial variation in the threshold for motion (θ_c) of pool and riffle gravel may be assessed from hydraulic and tracer transport data, which may be used to support the penetrometer findings.

A variety of factors may influence sediment structure at the study site (Table 1.2). For example, high sediment supply will prevent armouring and lead to a looser bed structure (Dietrich *et al.*, 1989). Winnowing of fines into pools downstream and infiltration of clays and silts into gravel interstitial spaces is likely to develop bed structure and increase the compaction of riffles. Turbulent flow and greater τ at riffles during low discharge is also thought to be important in the development of bed structure (Sear, 1996), which may be further influenced by the presence of coarse protruding clasts or pebble clusters (Buffin-Bélanger and Roy, 1998). Hence the duration of flows below that capable of disturbing gravel, particularly the surface layer, is a further significant factor to take into consideration.

Sediment transport / sorting

As discussed in section 1.6, grain size differences between riffles and pools can provide information about tractive force. However there is considerable discrepancy in the literature (i.e. both finer grained and coarser grained pools, in comparison to the riffles, could both indicate tractive force reversal) which is likely to reflect sediment supply, hydrograph character, and whether or not the channel is truly self-formed and transporting its own sediments or re-working glacial, or alluvial material. In streams with a high supply and a smooth response hydrograph, pools may be finer than riffles at low flow, however streams with a low sediment supply and a flashy hydrograph may show coarser pools at low flow. Once an assessment of sediment supply and sources has been made at the study site used in the present investigation, low flow grain size character may then be used to interpret tractive force patterns.

The routing of gravel and sand may also provide information on tractive force patterns, which may be investigated using tracing techniques (Table 1.2). If tractive force reversal is evident, gravel should be transferred from riffles through the pool downstream to the next riffle (e.g. Jackson and Beschta, 1982). If tractive force reversal does not occur, then some gravel would be expected to be deposited in the

pool (e.g. Haschenburger and Church, 1998). Fine grained sediments should be deposited in areas of low shear stress; such as the pool tail (Lisle and Hilton, 1992; 1999). A number of factors could effect sediment routing such as flood magnitude and duration (Sear, 1992), grain and form roughness. The later could influence sediment deposition loci; high grain roughness increases the number of sites for deposition of finer grained material, e.g. on the lee of coarser clasts, whereas steep exit slopes of pools (high form roughness) could limit the number of grains that leave the pool (Thompson *et al.*, 1999). There is also some evidence to suggest three dimensional flow structure can influence sediment sorting patterns (e.g. Teisseyre, 1984), which will be assessed qualitatively in this investigation.

Hydrograph character

Riffle-pool morphology is adjusted to the hydrograph character as this determines the magnitude and frequency of sediment transport events and tractive force reversals. Sear (1992) has indicated that reduction of hydrograph peaks and an increase in the frequency of medium flows can alter scour and deposition loci of gravel clasts in a riffle-pool sequence, which may have an impact the stability of riffle-pool morphology, as it would encourage aggradation of pool tails and scouring of riffles and pool heads. Bathurst (1979) further indicates that transverse secondary flow structures are most well developed during the middle range of discharges, which also could have an effect on sediment transport and morphology. Further analysis of scour and deposition loci of gravel in relation to riffle-pool topography are required for a range of flood magnitudes and durations. A gravel tracer study in conjunction with morphological re-survey and analysis of discharge data will be used to examine this further.

Site character

The literature review presented in Chapter One, highlighted the difficulty in designating a general model of both formation and maintenance of riffle-pool morphology in different river reaches. The mode of maintenance e.g. tractive force reversal (Keller, 1971) could be site-specific, related to channel morphology (e.g. sinuosity, channel width differences between riffles and pools), form and grain roughness differences, sediment supply and hydrograph character. These characteristics may in turn be influenced by pre-existing landscape. For example, a

river channel may be confined in its valley (possibly glacial origin), and may be re-working non-fluvial sediments. By grouping reach-scale characteristics of riffle-pool sequences from the published literature, it may be possible to link common models of formation and / or maintenance. The significance of straight and sinuous riffle-pool sequences is also summarised after further consideration of the literature presented in Chapter Nine.

Other factors

It is clear that three-dimensional macro-scale turbulent flow structures (e.g. roller eddies) are important in the formation of riffles and pools (Yalin, 1971; Richards, 1976). Although less intensively researched, they are also significant in maintenance of the riffle-pool form (Bathurst, 1979; Teisseyre, 1984; Thompson, 1986; Thompson *et al.*, 1998; 1999). Smaller-scale flow structures during periods of low flow have also been considered important at riffle locations, encouraging infiltration of fines and increased compaction and bed structuring (Sear, 1996), which could explain riffle-pool maintenance in some instances. A qualitative assessment concerning the significance of three-dimensional flow structure is made in the field and through analysis of the literature.

Obstructions to flow within channels have been shown to alter three dimensional flow structure and initiate pool-riffle morphology (Clifford, 1993a). Thompson *et al.* (1999) has also demonstrated their significance in the maintenance of the riffle-pool sequence, by encouraging velocity reversal. The significance of obstacles in riffle-pool formation and maintenance is assessed through the analysis of past literature, and an assessment of the occurrence coarse clasts at the Rede field site.

Although not included in the initial experimental design of this investigation, the applicability of the sediment continuity model (Wilkinson *et al.*, 2000) to riffle-pool formation and maintenance should be taken into account and will be assessed through analysis of the published literature.

Chapter Two

Study site and methodology

2.1 Introduction

This chapter will describe the characteristics of the study reach and catchment and introduce the sampling methodologies used throughout the investigation. To fulfil the thesis objectives (section 1.8), a comprehensive spatial and temporal set of data taken from a riffle-pool sequence was required concerning; (i) riffle-pool hydraulics, (ii) discharge character, (iii) sediment sorting, (iv) routing of gravel and sand bedload (v) grain size, (vi) sediment mobility, (vii) fine sediment infiltration, (viii) bed structure and (ix) morphology. Riffle-pool formation and maintenance is related to the complex interaction of these variables (Figure 2.1), and it is therefore essential to assess them fully to improve understanding of the riffle-pool form. It is important to highlight the influence of sediment supply upon the outcome of a number of the processes shown in Figure 2.1. For example although there is a tendency for most pools to show higher tractive force than riffles at high flow (e.g. Keller, 1971), the potential for the bed to scour and maintain the pool can be counteracted in conditions of very high sediment supply. It is feasible to get a situation during a flood event where, although the pool is competent to transport every grain size fed into the pool, it is not competent to transport the quantity of sediment fed into it. In this situation the pool acts as a bottleneck and may fill with sediment (Lisle pers comm, 1998). Although not discussed in models of formation (section 1.3.3), sediment supply is likely to be an important factor. In high supply scenarios riffle pool morphology is less likely to form, which partly explains (along with hydrograph shape) the low relief bed topography exhibited in semi arid ephemeral alluvial streams (e.g. Powell, 1988). Surface grain size variability between riffles and pools, and hence grain roughness, which is usually observed at low flow, can also be strongly influenced by sediment supply. The grain size patterns may reflect high flow competence when sediment supply is low (e.g. Bowman, 1977), however in high supply scenarios the high flow tractive force pattern may be masked (e.g. Lisle and Hilton, 1982).

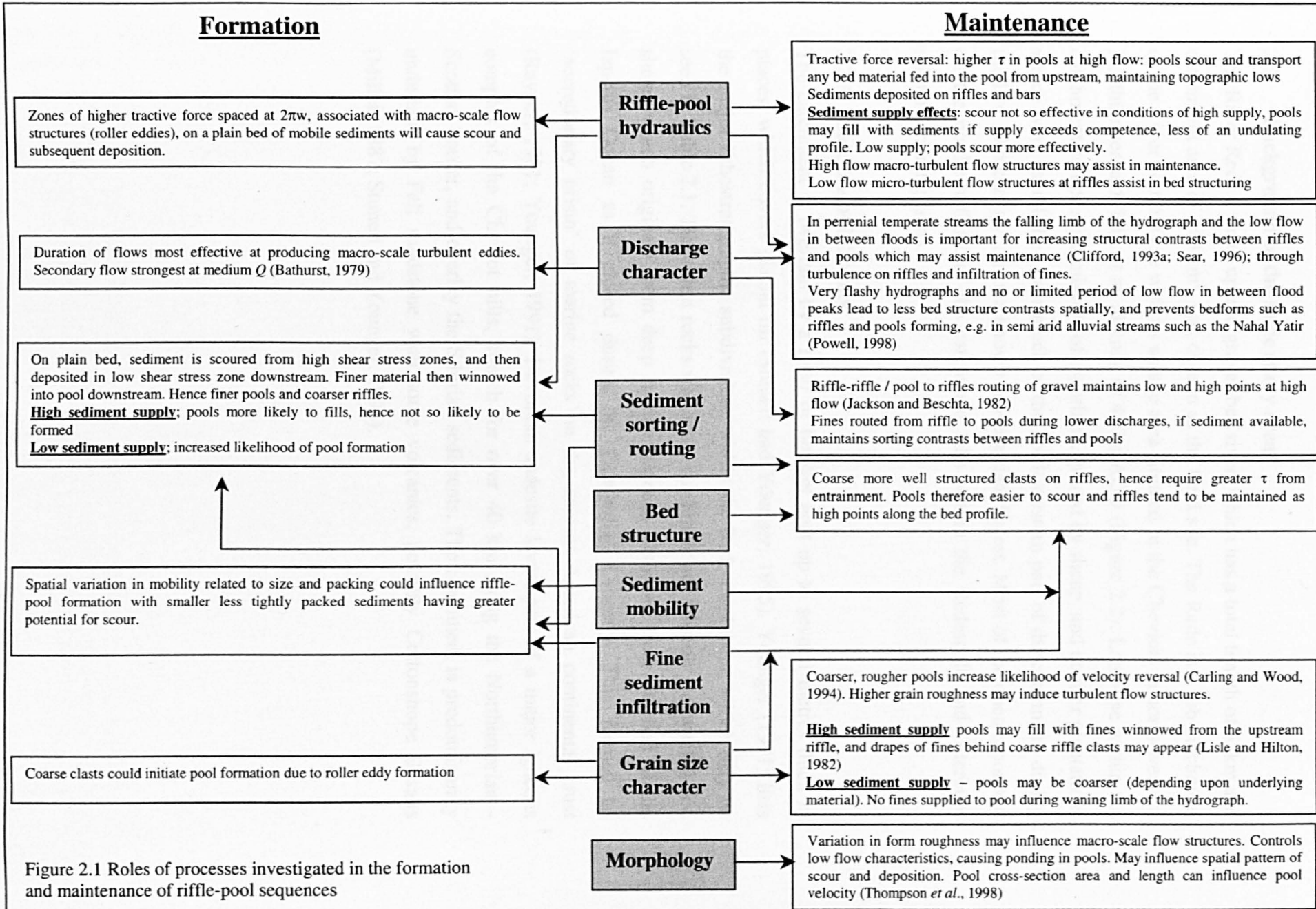


Figure 2.1 Roles of processes investigated in the formation and maintenance of riffle-pool sequences

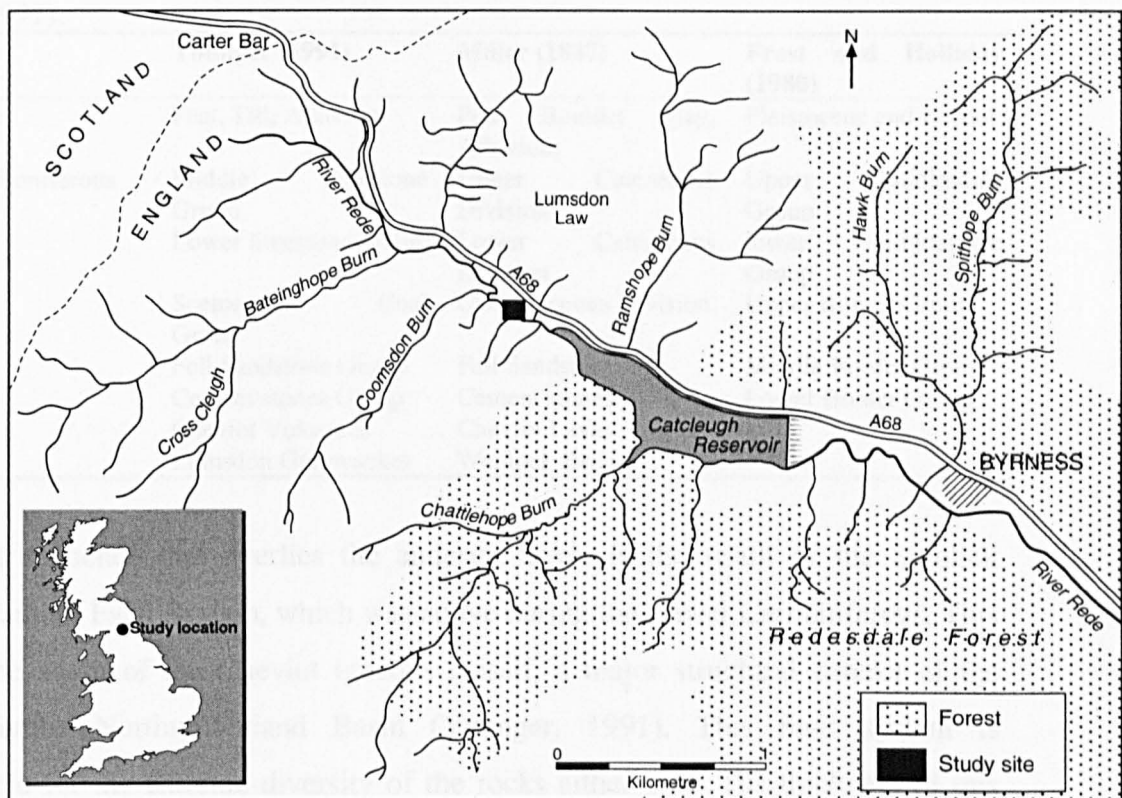
2.2 Background to the Rede study area

The River Rede a small upland gravel-bed river, which has a total length of 58km and catchment area of 340 km², was chosen as the field site. The Rede is a sub-catchment of the River North Tyne with its source area situated in the Cheviots in north-western Northumberland, UK, at an altitude of 490m AOD (Figure 2.2). Land-use within the catchment comprises a mixture of moorland, grazed by sheep, and conifer plantations which were established over much of the north-western part of the catchment during the late 19th century, an area known as Redesdale Forest. Most of the open moorland on the northern flank of the catchment falls within the Redesdale and Otterburn military training areas.

2.2.1 Catchment lithology

The catchment is overlain by a layer of blanket peat up to several metres thick in places, which covers glacial till (Stunell and Younger, 1995). Younger (1991) lists the major lithostratigraphic subdivisions within the Rede catchment, which may be seen in Table 2.1. The oldest rocks within the catchment are Silurian greywackes and shales which originate from deep marine deposits obducted from the bed of the Iapetus Ocean as it closed during the Caledonian Orogeny. This formed an ‘accretionary prism’ of marine rocks on the ancient American continental crust (Rayner, 1981; Younger, 1991). Devonian andesite lavas, part of a major igneous complex of the Cheviot hills, stretch for over 40 km along the Northumbrian - Scottish border, and overlay the Silurian sediments. The catchment is predominantly underlain by Fell sandstone with some volcanics, possibly Cottonshope Basalts (Miller, 1887; Stunell and Younger, 1995).

(a)



(b)

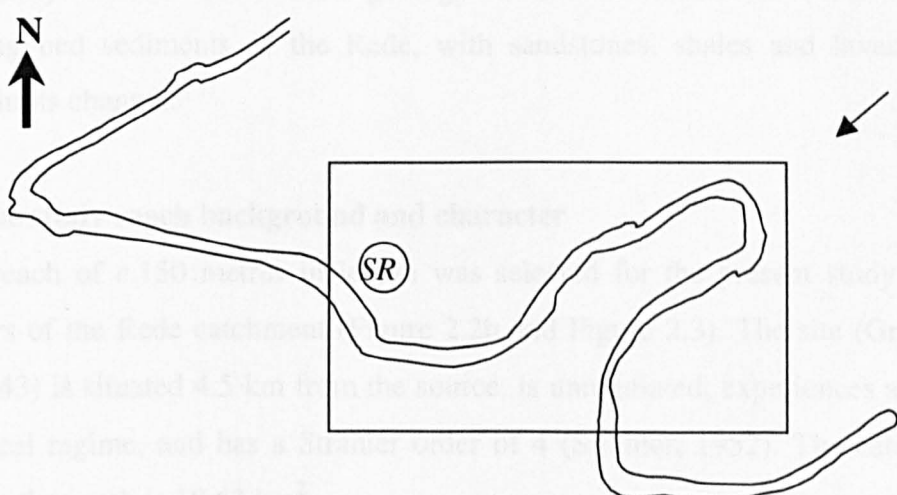


Figure 2.2 The Rede study catchment; (a) catchment map, (b) study reach location showing the position of the stage recorder (SR). The arrow indicates the perspective at which all other maps of the study reach are graphically presented throughout the thesis, looking upstream from the survey position.

Table 2.1 Major stratigraphic sub-divisions in the Rede catchment (after Younger, 1991).

Age	Younger (1991)	Miller (1887)	Frost and Holliday (1980)	
Quaternary	Peat, Till, Alluvium	Peat, Boulder Clay, Alluvium		Pleistocene and Recent
Lower Carboniferous	Middle limestone Group Lower limestone group Scemerston Group Fell Sandstone Group Cement stones Group Cheviot Volcanics	Upper Division Lower Division Coal	Calcareous Calcareous Carbonaceous Division	Upper Group lower Group Upper Border Group
Devonian			Fell Sandstones Cement stones	Middle Border Group
Silurian	Lumsdon Greywackes		Cheviot Lavas Wenlock Beds	Lower Border Group -

The next sequence that overlies the andesite lavas, is the result of the Stublick Ninety-Fathom Fault System, which was active during the Lower Carboniferous. This lies to the south of the Cheviot igneous massif, a major structural control of the Carboniferous Northumberland Basin (Younger, 1991). This fault system is responsible for the extreme diversity of the rocks either side. The thickness of this material in the Rede catchment reaches 4500m (Fordham, 1989), and is predominantly clastic. The mixed geology of the catchment is evident when considering bed sediments of the Rede, with sandstones, shales and lavas being observed in its channel.

2.2.2 The study reach background and character

A study reach of *c.*150 metres in length was selected for the present study in the headwaters of the Rede catchment (Figure 2.2b and Figure 2.3). The site (Grid ref.: NT 721 043) is situated 4.5 km from the source, is unregulated, experiences a flashy hydrological regime, and has a Strahler order of 4 (Strahler, 1952). The catchment area above the reach is 18.63 km².

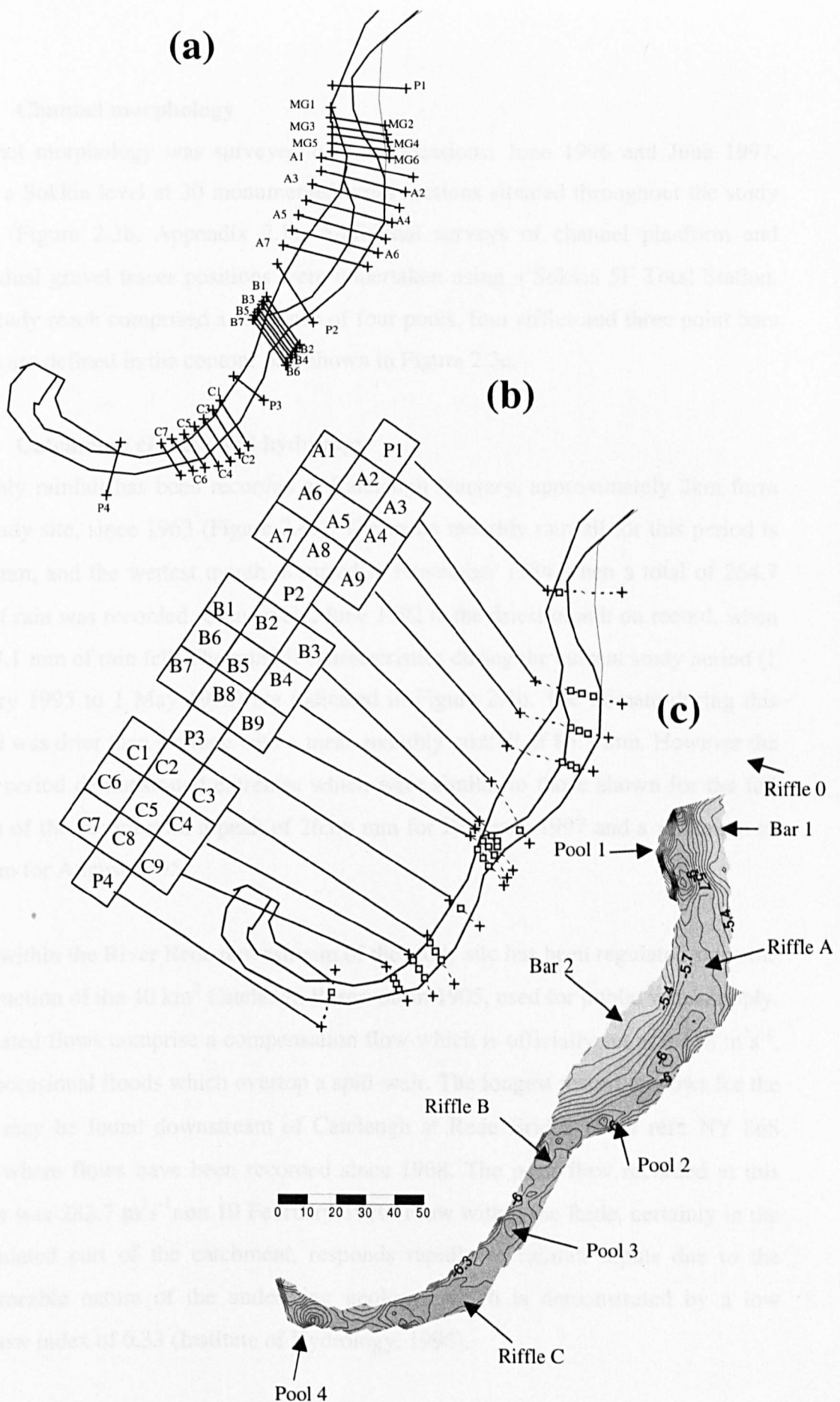


Figure 2.3 Study reach details, (a) position of cross-sections, (b) position of basket traps and cell-based survey shown by squares, (c) contour map of riffle-pool morphology

2.2.3 Channel morphology

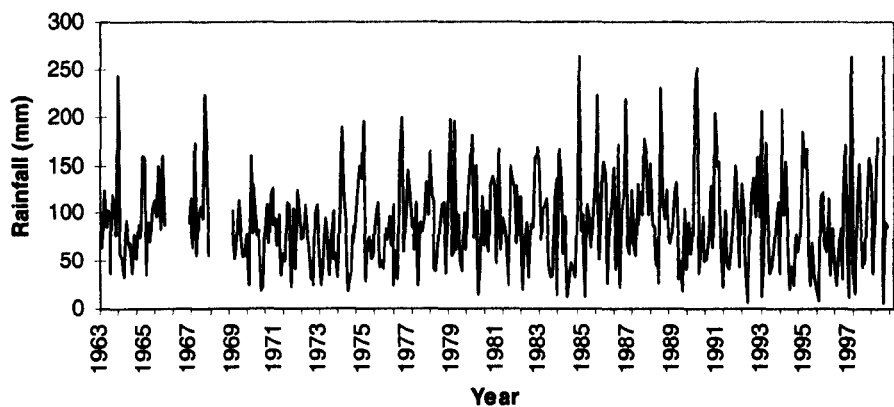
Channel morphology was surveyed on two occasions; June 1996 and June 1997, using a Sokkia level at 30 monumented cross-sections situated throughout the study reach (Figure 2.3b, Appendix 2.1). Additional surveys of channel planform and individual gravel tracer positions were undertaken using a Sokkia 5F Total Station. The study reach comprised a sequence of four pools, four riffles and three point bars which are defined in the contour plot shown in Figure 2.3c.

2.2.4 Catchment climate and hydrology

Monthly rainfall has been recorded at Catcleugh Nursery, approximately 2km from the study site, since 1963 (Figure 2.4a). The mean monthly rainfall for this period is 91.2 mm, and the wettest month occurred in November 1984 when a total of 264.7 mm of rain was recorded. Conversely, June 1992 is the driest month on record, when only 7.1 mm of rain fell. The rainfall characteristics during the current study period (1 January 1995 to 1 May 1998) are indicated in Figure 2.4b. The climate during this period was drier than average with a mean monthly rainfall of 83.3 mm. However the study period demonstrated extremes which were similar to those shown for the full length of the record with a peak of 263.6 mm for February 1997 and a minimum of 8.9 mm for August 1995.

Flow within the River Rede downstream of the study site has been regulated since the construction of the 40 km² Catcleugh Reservoir in 1905, used for public water supply. Regulated flows comprise a compensation flow which is officially set at 0.158 m³s⁻¹, with occasional floods which overtop a spill-weir. The longest record of flows for the Rede may be found downstream of Catcleugh at Rede Bridge (Grid ref.: NY 868 832), where flows have been recorded since 1968. The peak flow recorded at this station was 282.7 m³s⁻¹, on 19 February 1970. Flow within the Rede, certainly in the unregulated part of the catchment, responds rapidly to rainfall inputs due to the impermeable nature of the underlying geology, which is demonstrated by a low baseflow index of 0.33 (Institute of Hydrology, 1998).

(a)



(b)

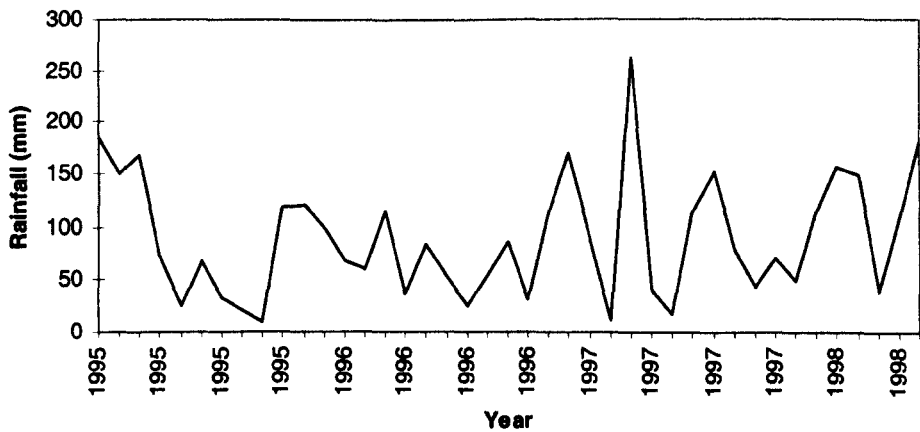


Figure 2.4 Mean monthly rainfall characteristics at Catcleugh Nursery, (a) full record for 1 Feb 1963 to 1 May 1998, (b) rainfall characteristics for the study period 1 January 1995 to 1st May 1998 (source: Northumbrian Water plc).

2.3 Calculation of discharge

A continuous stage recorder was installed at the upstream end of the study site (Figure 2.2b). Stage (E) was calibrated against discharge (Q) at eight different flows between $0.18 \text{ m}^3\text{s}^{-1}$ and $3.47 \text{ m}^3\text{s}^{-1}$. Log-log regression shown in Figure 2.5a and equation 2.1 was found to fit the relationship ($r^2=0.99$, $p<0.001$), however this over-estimated discharge at flows over $3.2 \text{ m}^3\text{s}^{-1}$ (approximately half bankfull and above). A linear regression ($r^2=0.95$, $p<0.001$) was used to estimate flows greater than this (Figure 2.5b, equation 2.2). Conversely, linear regression was found to underestimate base flow conditions ($<0.5 \text{ m}^3\text{s}^{-1}$).

$$Q = 21.204E^{2.73} \quad (2.1)$$

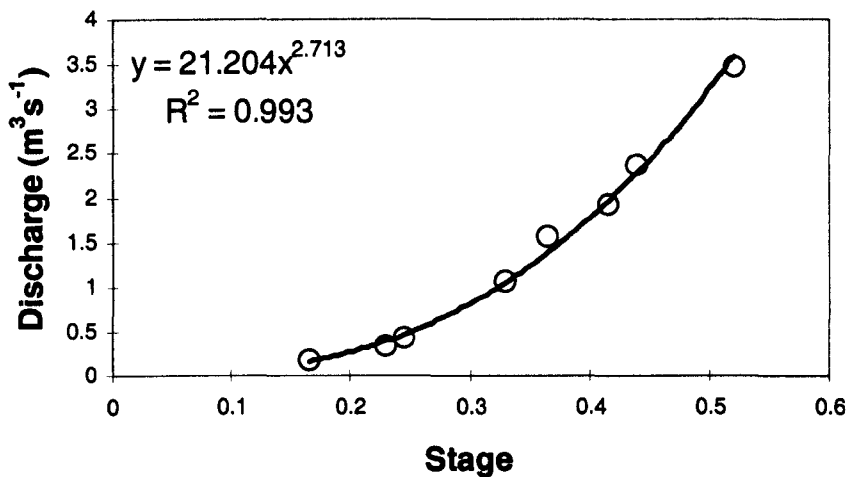
$$Q = 9.3378E-1.7487 \quad (2.2)$$

2.4 Sediment tracing

To provide quantitative information upon the routing and sorting of sand and gravel (Phase 1 and Phase 2 bedload) through the Rede riffle-pool sequence it was decided to employ tracing methodologies, in conjunction with a detailed temporal and spatial sediment sampling programme. Tracers may be used to measure entrainment rates and grain displacement lengths and provide an alternative to direct sampling of bedload, thus providing information on mobility and sediment routing / sorting. Tracer research has been focused towards three main areas since the 1960's;

- 1) initiation of motion (Hey, 1975; Carling, 1983a; Petit, 1990; Ferguson and Wathen, 1998),
- 2) path length in relation to hydraulic variables (Butler, 1977; Ashworth and Ferguson, 1989; Carling, 1987; Hassan and Church, 1992), and
- 3) studies of the structural and morphological controls on transport (Keller, 1970; Larrone and Carson, 1976; Thorne and Lewin, 1979; Brayshaw, 1985; Petit, 1987; Ashworth, 1987; Hassan, and Church, 1992; Sear, 1996, Thompson *et al.*, 1996)

(a)



(b)

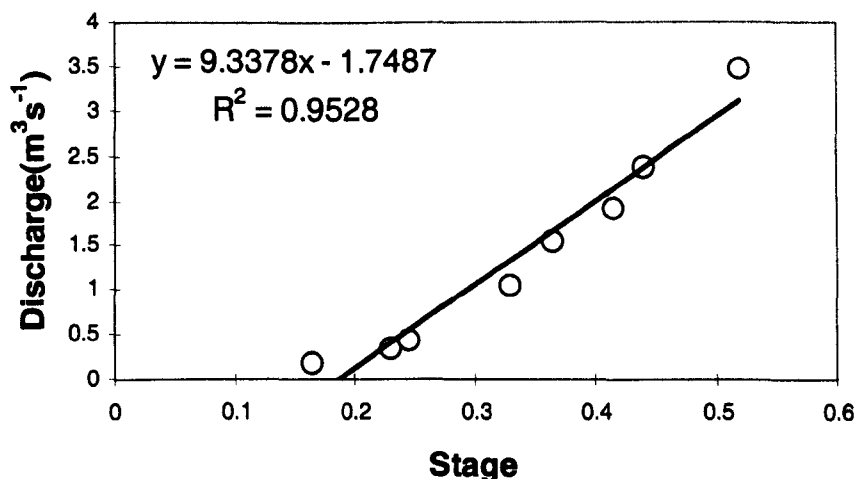


Figure 2.5 Stage discharge relationship for the River Rede study site, a) log-log regression, b) linear regression.

Although the use of tracers is not as common as direct sampling techniques, it offers a number of advantages. Tracers provide more insight into the stochastic and spatially variable nature of bedload transport because the size, shape and density of mobile and immobile material is predetermined, which is an unknown factor in direct sampling (Wilcock, 1989). Tracers also provide logistical and safety advantages since they can be installed and monitored at low flow, thus avoiding direct sampling during a flood episode. Small transport rates are likely to be more accurate than estimates derived from direct sampling of bedload, where errors may exceed measured rates (Wilcock, 1997).

2.4.2 Tracing gravel (Phase 2 bedload)

There has been a wide range of techniques employed to trace sediments in fluvial systems which have experienced variable success. To optimise success, tracers must be;

- 1) stable against premature loss of tagging,
- 2) reasonably inexpensive,
- 3) detectable at low concentrations,
- 4) non-toxic to aquatic or human life,
- 5) allow repeated experiments within a reach either by the decay of the original tracers or through readily identifiable characteristics, and finally
- 6) be able to accurately mimic the size, density and shape of the natural sediments (Arkell, 1985).

Techniques that have been used to monitor gravel (Phase 2) bedload may be divided into six categories;

- 1) painted particles (e.g. Ashworth 1987, Thompson *et al.*, 1996),
- 2) magnetics (Arkell, 1985, Sear, 1996);
- 3) radio transmitters (Emmett *et al.*, 1992),
- 4) exotics, such as limestone (Mosely, 1978);
- 5) fluorescence (Rathburn and Kennedy, 1978); and
- 6) radioactivity (Crickmore, 1967).

Several limitations are evident with some of these methods. Painted particles are cheap, however impractical below 8-11 mm due to poor visibility. Recovery rates are moderate due to burial during bedload transport events (see Table 8.1 in Hassan and Church, 1992). The use of magnetics overcomes this drawback to a degree as buried particles can still be detected using a search coil. Radio transmitters may also improve recovery rates, however these are restricted to coarser grain sizes and are expensive. Fluorescence and radioactivity are useful for finer grain sizes, however the later may cause harm to aquatic life.

Due to financial restrictions, and the short time-span of this investigation (in comparison to Ferguson and co-workers investigation on the Allt Dubaig for example) a painted clast tracer study was undertaken. This was deemed adequate to provide information concerning the sorting and routing of gravel though the Rede riffle-pool sequence and information on the hydraulic conditions for initial entrainment. Prior to the gravel tracer survey, cross-profile re-survey had suggested only minor areas of scour and fill on riffles, which suggested that burial depths would be negligible and therefore recovery rates would be reasonable. Transport paths of individual clasts of coarse-grained material were traced using 288 measured and weighed painted clasts, placed throughout the study reach (Figure 2.6). For each clast the a, b, and c axis were recorded in order to provide information concerning size and shape of the material, and a colour coding system was used to aid interpretation (Table 2.2). The overall size information and individual size distributions of tracers emplaced in each riffle and pool are shown in Figure 2.7 and Table 2.2. The shape classification of Zingg (1935) was used to classify the tracer clasts. This information is demonstrated for the overall sample and for each riffle and pool emplacement unit (Table 2.2). The tracer shape distribution mimicked that of the natural bed sediments which were dominated by discs (Milan *et al.*, 1999). After a period of competent flow to allow tracer clasts to be incorporated into the bed fabric (Hassan and Church, 1992), all tracer pebbles were surveyed using a Sokkia set 5F Total Station (Figure 2.6). Recovery of tracers was restricted to those found on the bed surface. A glass-bottomed bucket was used to identify submerged clasts, and where found, each tracer

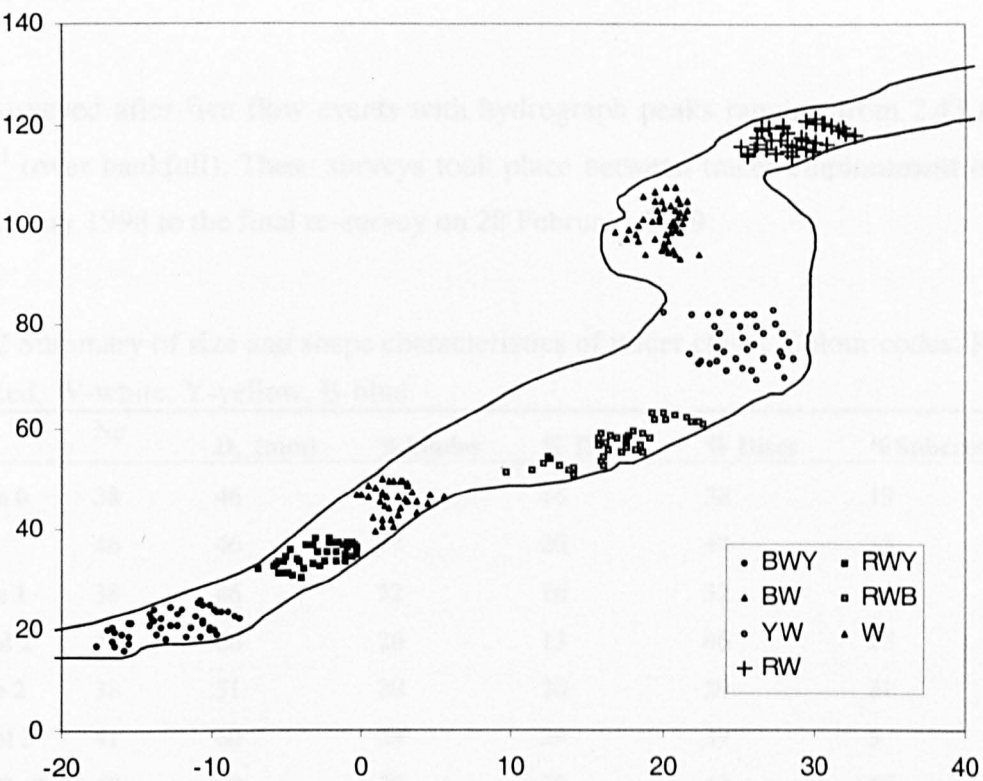


Figure 2.6 Emplacement positions of gravel tracers in the Rede riffle-pool sequence. Labels shown in key correspond to a colour coding information presented in Table 2.2. x and y axis is distance in metres.

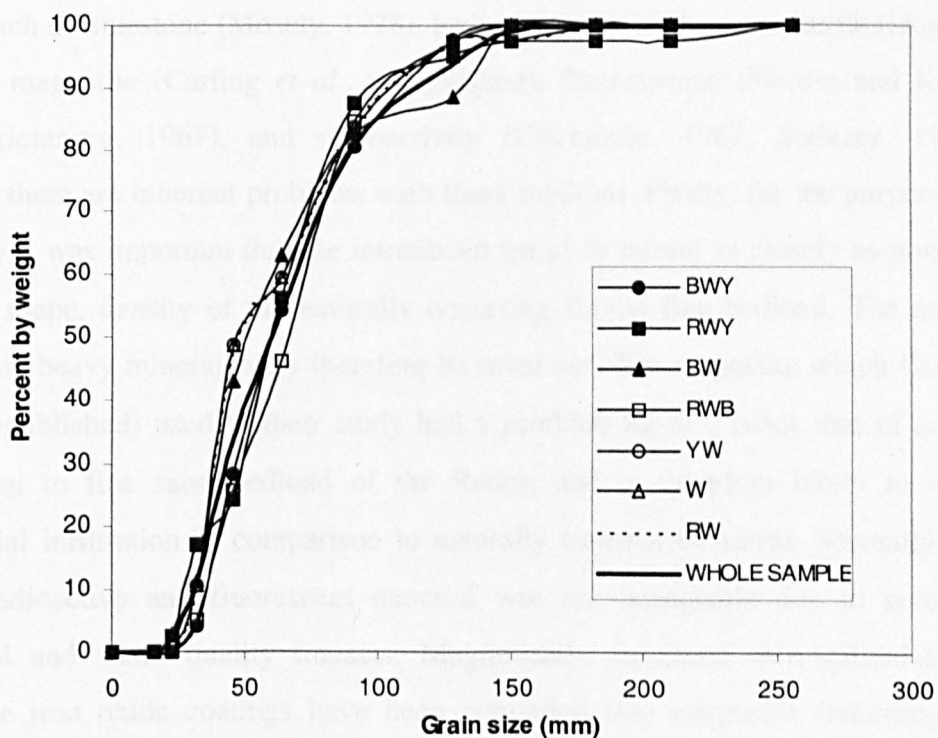


Figure 2.7 Grain size distribution of gravel tracers emplaced throughout the Rede riffle-pool sequence.

was re-surveyed after five flow events with hydrograph peaks ranging from 2.43 to $9.92\text{m}^3\text{s}^{-1}$ (over bankfull). These surveys took place between tracer emplacement on the 21 January 1998 to the final re-survey on 28 February 1999.

Table 2.2 Summary of size and shape characteristics of tracer clasts. Colour codes; R-Red, W-white, Y-yellow, B-blue.

Code	No	D_{50} (mm)	% Blades	% Rods	% Discs	% Spheres
RW-Riffle 0	38	46	27	16	38	19
W-Pool 1	46	46	17	20	48	15
YW-Riffle 1	38	46	32	16	32	19
RWB-Pool 2	40	66	26	13	46	15
BW-Riffle 2	38	51	20	20	29	31
RWY-Pool 3	41	60	29	29	37	5
BWY-Riffle 3	47	60	22	20	43	15
TOTAL	288	60	25	19	40	17

2.4.3 Tracing sand (Phase 1 bedload)

Attempts at monitoring fine sediment movement have usually involved the use of exotics such as limestone (Moseley, 1978), heavy minerals such as cassiterite (Hughes, 1992) or magnetite (Carling *et al.*, unpublished), fluorescence (Nordin and Kelly, 1978; Crickmore, 1967), and radioactivity (Crickmore, 1967; Stelczer, 1981). However there are inherent problems with these methods. Firstly, for the purposes of this study it was important that the introduced tracer to mimic as closely as possible the size, shape, density of the naturally occurring fluvial fine bedload. The use of exotics and heavy minerals may therefore be ruled out. The magnetite which Carling *et al.* (unpublished) used in their study had a $\rho_s=5200\text{ kg m}^{-3}$, twice that of quartz (equivalent to fine sand bedload of the Rede), and is therefore likely to show preferential infiltration in comparison to naturally transported sands. Secondly, the use of radioactive and fluorescent material was not acceptable due to potential ecological and water quality impacts. Magnetically enhanced iron-stained sands where the iron oxide coatings have been converted into magnetite (retaining the original density of the sand) was chosen to monitor the development of fine bedload. The technique appeared to be a suitable option bearing in mind the optimum tracer attributes listed in section 2.4.2.

2.4.4 Magnetic Tracing of fluvial sediments

Previous studies which have applied magnetics to gravel bed rivers have usually focussed upon a wider range of grain sizes (e.g. Arkell, 1985; Sear, 1992a). Magnetic tracing of fluvial material may be divided into two categories. Firstly, there have been investigations which have traced clasts with magnets or some form of metal plug/tag inserted into them (e.g. Butler, 1977; Ergenzinger and Conrady, 1982; Reid *et al.*, 1984). Another common technique is to trace material which either has (i) a naturally high magnetic susceptibility (e.g. Gottesfeld, 1997) or (ii) which has had its magnetism artificially enhanced in some way (environmental magnetism). As magnets cannot be inserted into sand grains, the latter option (ii) appeared more appropriate. In this investigation it was decided to introduce magnetically enhanced sand into the Rede channel.

Much of the pioneering work in environmental magnetism has been conducted by Thompson and Oldfield (1986), whilst Arkell (1985) Arkell *et al.* (1983) and Rummery *et al.* (1979) have demonstrated the application of artificially enhanced iron rich bedload to sediment tracing through fluvial systems. This technique has largely been restricted to coarse bedload in fluvial systems. However, van der Post *et al.* (1994) have recently demonstrated the application of artificially magnetically-enhanced sand for detecting tidal induced movement of beach sands. This is the technique which is employed in the current investigation. The magnetic signature of this material may be detected using a range of measures.

2.4.5 Magnetic measures and detection

There are three commonly used magnetic measurements; Magnetic Susceptibility (K and χ), Isothermal Remnant Magnetisation (IRM), and Anhysteretic Remnant Magnetisation (ARM). One type of magnetic measure (Magnetic Susceptibility) was deemed suitable for use in the present investigation. Susceptibility measurements have proved the most useful in determining the direction of tracer movement and spatial and temporal changes in tracer concentration within fluvial environments (e.g. Arkell, 1985). Magnetic Susceptibility may be used as an indicator of the ease of which a sample can be magnetised, and may be defined as $K=M/H$ where H is the applied field and M is the volume magnetisation induced in a material of

susceptibility K. Susceptibility values give a general indication of the concentration of ferrimagnetic minerals such as magnetite and maghaematite.

Susceptibility may either be measured directly in the field using a portable meter or measured in the laboratory using sensors designed to scan cores of sediment or 10 ml subsamples. For example, Arkell (1985) detected tracer movement in fluvial environments, by using a combination of a Bartington loop field search probe (rather like a metal detector), and a hand-held ferrite probe - which permitted detailed searching for buried particles after sections of bar sediment had been excavated. Finer sediments were recovered after sieving sub-samples and were analysed for volumetric susceptibility (m^3kg^{-1}) which can be calibrated with sediment weight (Arkell, 1985). These latter measurements permit a mass-specific assessment by drying the sample and dividing the K reading by the mass to give units in m^3kg^{-1} , denoted by the symbol χ .

In the present investigation, relative changes in tracer concentration through the riffle-pool sequence over time were mapped by measuring volume magnetic susceptibility (κ), using two approaches. Firstly a submersible Bartington MS1 susceptibility meter and a 20cm diameter search coil was used to take readings at 1m intervals along each of 30 cross-sections throughout the study reach and at randomly surveyed positions further downstream (Figure 2.3a). The instrument shows many similarities to a metal detector, and responds to changes in magnetic flux around the coil sensor as a result of changes in the volume of magnetic material present. As the loop is open (therefore measuring variable volumes) the readings taken are dimensionless and provide a semi-quantitative assessment of the presence and volume of tracer at a point. Whether this technique is suitable for taking surface readings, effective detection declines with distance from the loop following the inverse square law. The maximum depth detection for all but the strongest (and largest) magnetic sources, will be approximately the diameter of the loop (20cm).

Although volumetric susceptibility (κ) is a function of the size and shape of grains, Arkell *et al.* (1983), Currie and Bornhold (1983) and Rao and Kshirasagar (1991) have demonstrated that for a given grain-size distribution of magnetic material, κ increases linearly with tracer concentration, as long as the background host sediment has a low magnetic susceptibility. Arkell (1985) showed that finer clasts have a much more uniform enhancement and enable accurate calibration curves to be drawn of χ versus percentage concentration of tracer material. A calibration curve for the tracer used in this study is shown in Figure 2.8.

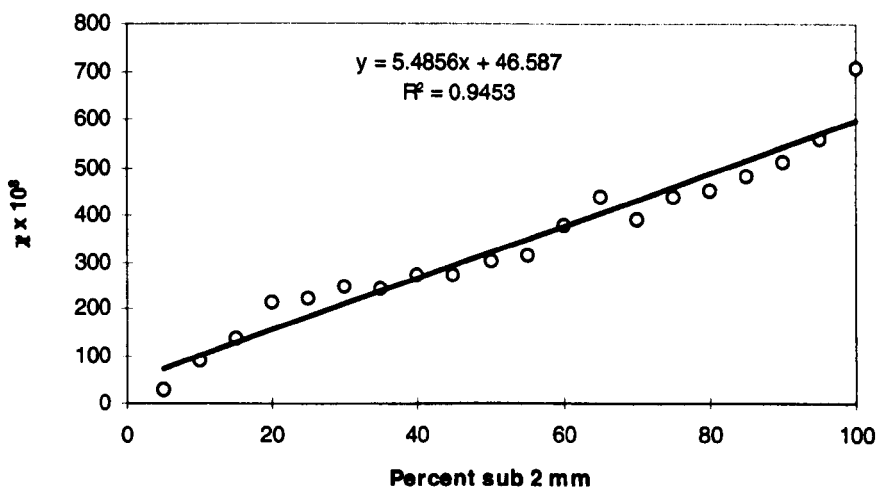


Figure 2.8 Calibration curve for estimating the percentage by weight tracer material within a sample of a given magnetic susceptibility.

The concentration, size and position of the magnetic material in relation to the search loop also affect the readings obtained by the search loop. The instrument does not provide any distinction between particle sizes (Arkell, 1983). This is easily overcome when measuring coarse clasts (>10mm) which can be picked up and measured in the field. It is not possible however to measure the volume or mass of fines (<2mm) in a given area in the same way, although trapping and freeze-coring the material may partly overcome this problem. The samples obtained in this manner may be measured for their magnetic signature in the laboratory much more accurately after sieving, drying and weighing. However the instrument is useful for rapid reconnaissance of tracer movement after floods.

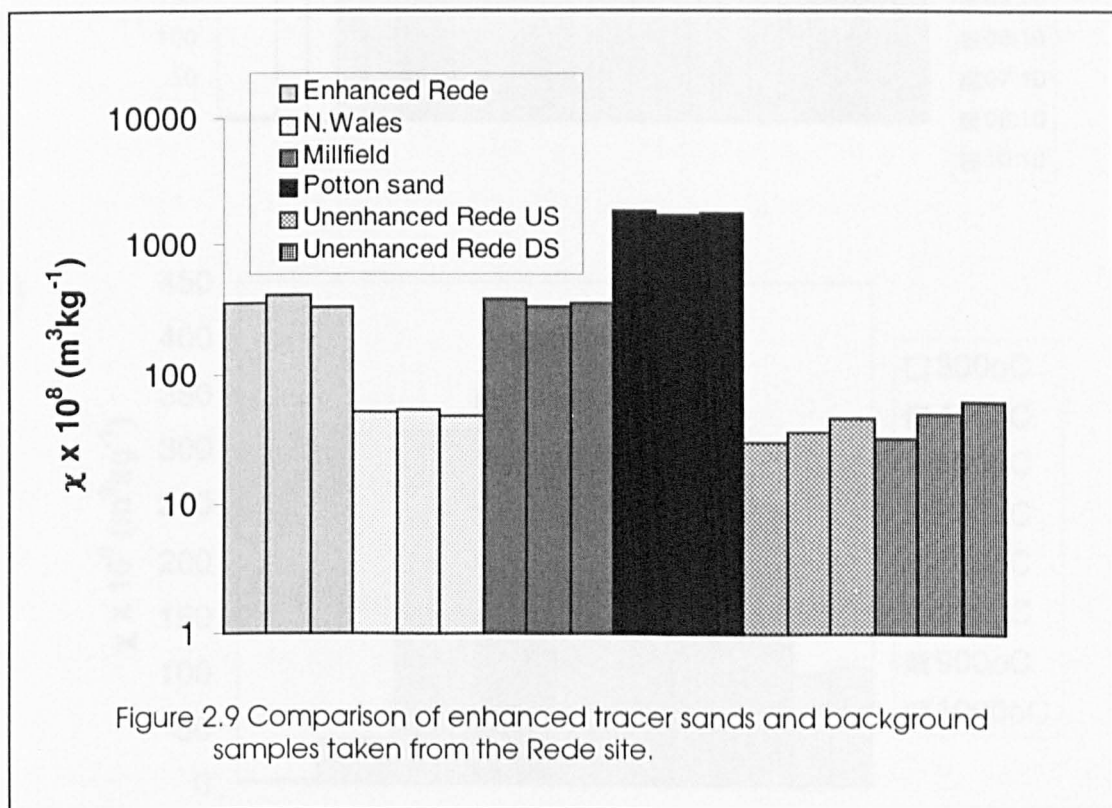
Susceptibility measurements of <2mm material were conducted upon subsamples of sand collected in basket traps (discussed in Chapter Five), and channel storage areas (e.g. bar tops). To examine infiltration of tracer into the subsurface sediment voids, freeze-cores were taken on two occasions after tracer movement (July 1996 and March 1997). Cores were sectioned at 15 cm intervals, dried and sieved, and the sub 2mm fraction retained for magnetic analyses. Magnetic susceptibility measurements on 10 ml sub-samples of this matrix material were then made in the laboratory using a magnetic susceptibility meter developed at the Department of Physics University of Newcastle upon Tyne. These readings could then be made mass specific by dividing the κ reading by the mass to give units in m^3kg^{-1} denoted by the symbol χ .

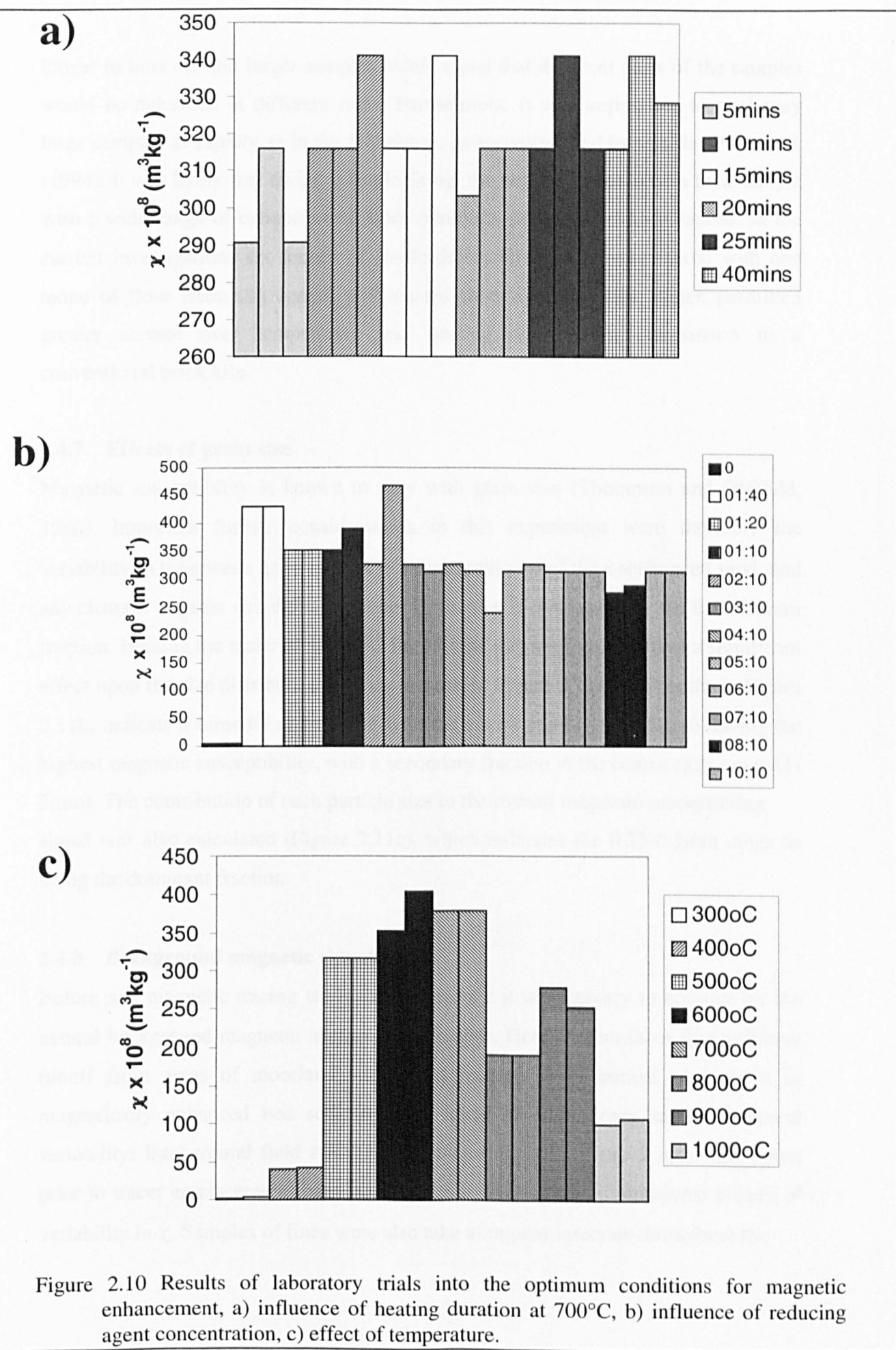
2.4.6 Magnetic tracer manufacture

The manufacture of the tracer used by van der Post *et al.* (1994) is a modification of the technique of Arkell (1985), Oldfield *et al.* (1981), Arkell *et al.* (1982) and Rummery *et al.* (1979). By heating iron rich sediments the 'apparent field reversible in-phase magnetic susceptibility' (χ) is reversed. The enhancement process is dependent upon the degree to which the red coloured iron-oxide coatings on the outside of the material being used (in this study on the silica sand grains) can be converted into magnetite (black) /maghaemite (pink). The enhancement procedure is as follows; firstly an iron-stained (red) sand must be obtained. Suitable locations in the UK include glacial outwash deposits derived from Triassic rocks in North Wales, Cheshire and Shropshire, and from the Cretaceous Greensand quarries in Bedfordshire. The process of magnetic enhancement, as recommended by van der Post *et al.* (1994), involves toasting the sand at high temperatures ($\sim 700^\circ\text{C}$) for two hours in a reducing atmosphere (achieved by mixing flour into the sand), followed by rapid cooling in air.

To investigate these conditions further, a series of laboratory experiments were conducted on a small scale (10g samples) to identify 1) degree of enhancement of four different sands, and 2) the optimum conditions for enhancement for the chosen sand. Figure 2.9 illustrates the degree of enhancement in a range of different sands,

suggesting Greensand to be a suitable material in agreement with van der Post *et al.* (1994). Based upon these findings and van der Post's recommendations it was decided to use Greensand (code; NT53), obtained from Potton, Bedfordshire, as the tracer material in the current investigation. The variables chosen for the second group of tests were; temperature, atmosphere (i.e. organic flour concentration), and period of heating. The results are demonstrated in Figures 2.10 a-c where it can be seen that the optimum temperature is between 600 and 700 °C which further agrees with van der Post *et al.* (1994). The concentration of organic material used to control atmosphere did not appear too critical, and low concentrations (1 part in 40 to 1 part in 5) appeared slightly more favourable. The duration of heating also did not appear to be a critical factor. It is important to note that although these experiments provide some useful information which may be used to design an optimum enhancement model, realistically they provide only a rough guideline, due to the differences in scale. It is not possible to simulate laboratory conditions exactly when dealing with large samples (the six tonnes used in this research project), in large kilns. Large kilns take





longer to heat up, and larger samples would mean that different parts of the samples would be enhanced at different rates. Furthermore, it was impossible to cool very large samples as rapidly as in the laboratory, as recommended by van der Post *et al.* (1994). It was likely that during a single firing, the net result would be a bulk sample with a wide range of enhancement, from optimum through to over-enhanced. In the current investigations six tonnes of Bedfordshire Greensand were mixed with one tonne of flour (reducing agent), and toasted in a ‘specials’ kiln, which permitted greater control over temperature and heating duration in comparison to a conventional brick kiln.

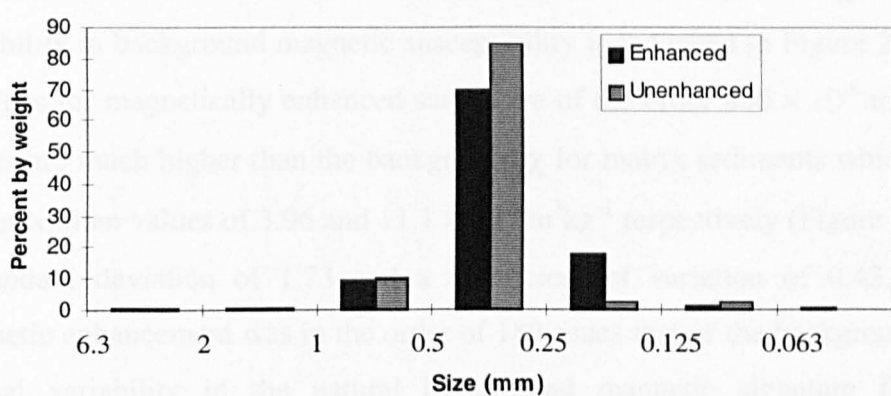
2.4.7 Effects of grain size

Magnetic susceptibility is known to vary with grain size (Thompson and Oldfield, 1986). Important further considerations in this experiment were therefore the variability in χ between grain sizes, the initial grain size of the unenhanced sand, and any changes in grain size during heating. Grain-size is dominated by the 0.25-0.5mm fraction. Heating the material at 700°C for 15mins was not found to have a significant effect upon the size distribution, as may be seen in Figure 2.11a. The results in Figure 2.11b, indicate a bimodal distribution with the coarse sand (0.25-0.5mm) having the highest magnetic susceptibility, with a secondary fraction in the coarse sand range (1-2mm). The contribution of each particle size to the overall magnetic susceptibility signal was also calculated (Figure 2.11c), which indicates the 0.25-0.5mm range as being the dominant fraction.

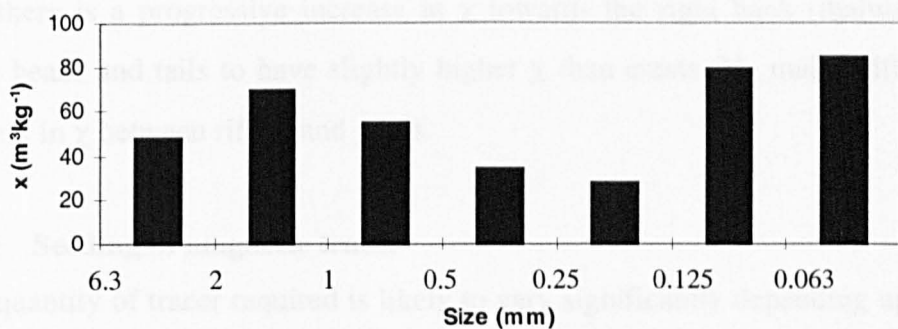
2.4.8 Background magnetic signature

Before any magnetic tracing study can commence it is necessary to account for the natural background magnetic mineral assemblages. Heavy minerals or fine sediment runoff from areas of moorland which had recently been burned may result in magnetically enhanced bed sediment, the latter of which may induce temporal variability. Background field susceptibility measurements of sub 2 mm were taken prior to tracer emplacement from freeze-cores to give a three-dimensional picture of variability in χ . Samples of fines were also take at regular intervals throughout the

(a)



(b)



(c)

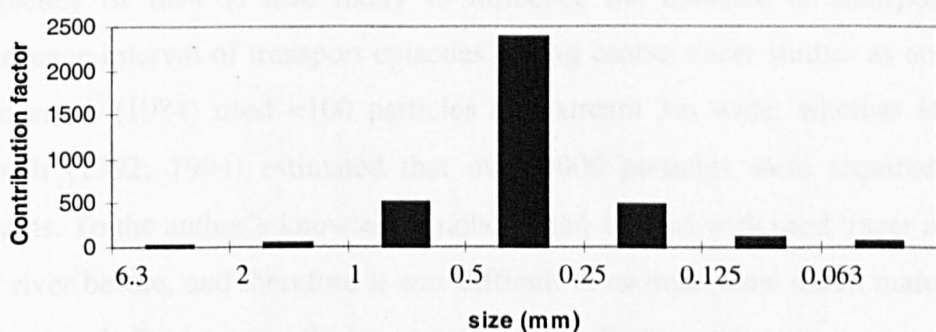


Figure 2.11 Grain size factors, for Phase 1 tracer; a) grain size distribution of unenhanced and enhanced Greensand tracer material, b) variation in χ with grain size, c) contribution factor of χ by each grain size fraction.

study to test for any seasonal variation in χ . However, this was found to be negligible. The sub 2 mm fines sieved from each core section were analysed for χ . The degree of variability in background magnetic susceptibility is indicated in Figure 2.12. Typical χ values for magnetically enhanced sand were of the order $800 \times 10^{-8} \text{ m}^3\text{kg}^{-1}$. These values are much higher than the background χ for matrix sediments which had mean and maximum values of 3.96 and $11.1 \times 10^{-8} \text{ m}^3\text{kg}^{-1}$ respectively (Figure 12.12), with a standard deviation of 1.73 and a coefficient of variation of 0.43 . Hence the magnetic enhancement was in the order of 180 times that of the background material. Spatial variability in the natural background magnetic signature for different morphological units is displayed in the bar charts in Figure 2.13, where it can be seen that there is a progressive increase in χ towards the right bank (thalweg), and for riffle heads and tails to have slightly higher χ than crests. No major differences are evident in χ between riffles and pools.

2.4.9 Seeding of magnetic tracer

The quantity of tracer required is likely to vary significantly depending upon the size of the channel and flow regime. A large channel with a flashy regime would require more tracer than a small slow response channel, for example. The magnitude and frequency of flow is also likely to influence the distance of transport and the recurrence interval of transport episodes. Using coarse tracer studies as an analogue, Reid *et al.* (1984) used <100 particles in a stream 3m wide, whereas Hassan and Church (1992; 1994) estimated that over 1000 particles were required in larger streams. To the author's knowledge, nobody had worked with sand tracer in a gravel-bed river before, and therefore it was difficult to estimate how much material would be required. Due to the flashy regime of the Rede catchment it was decided to introduce 2316 kg (dry weight) to the Rede channel. The rest of the magnetically enhanced sand was used in a separate experiment, not discussed in this thesis. The material was seeded, during low flow conditions ($0.23 \text{ m}^3\text{s}^{-1}$) on 20 April 1996, across the tail end of pool 1 and head of the upstream riffle A in order to simulate the commonly reported zone of fine sediment deposition and storage (Lisle and Hilton, 1982; 1999) (Figure 2.14). This area was divided into 15 cells and the material was deposited by hand and distributed evenly across the streambed using rakes (Plate 2.1).

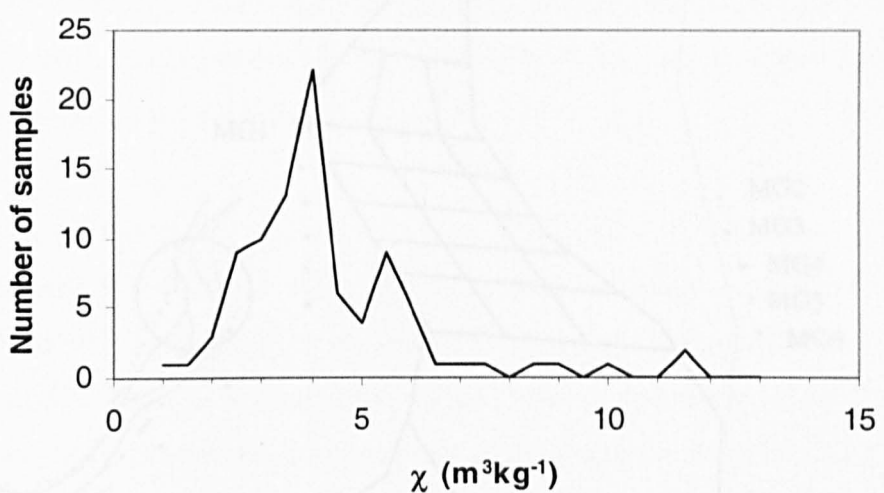


Figure 2.12 The natural background χ distribution, assessed from freeze-core samples taken from the Rede channel bed.

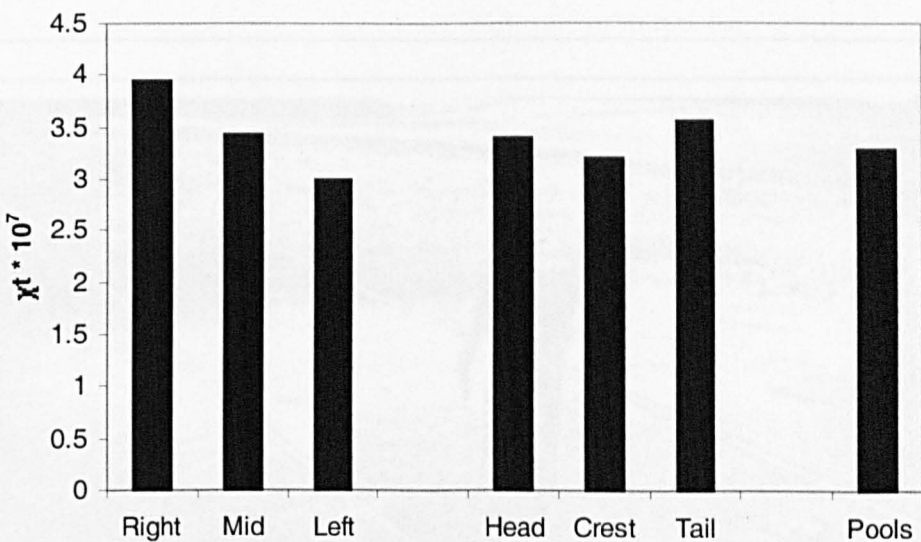


Figure 2.13 Variation in the mean background χ_t for riffle sub-units and pools.

2.1.1.1 Tracer sampling methods

information on both the surface and near-surface sediments is required in order to provide information for comparison with the tracer calculations in Chapter Five and to provide information on the tracer dispersal through the vadose zone through the Redcliffe

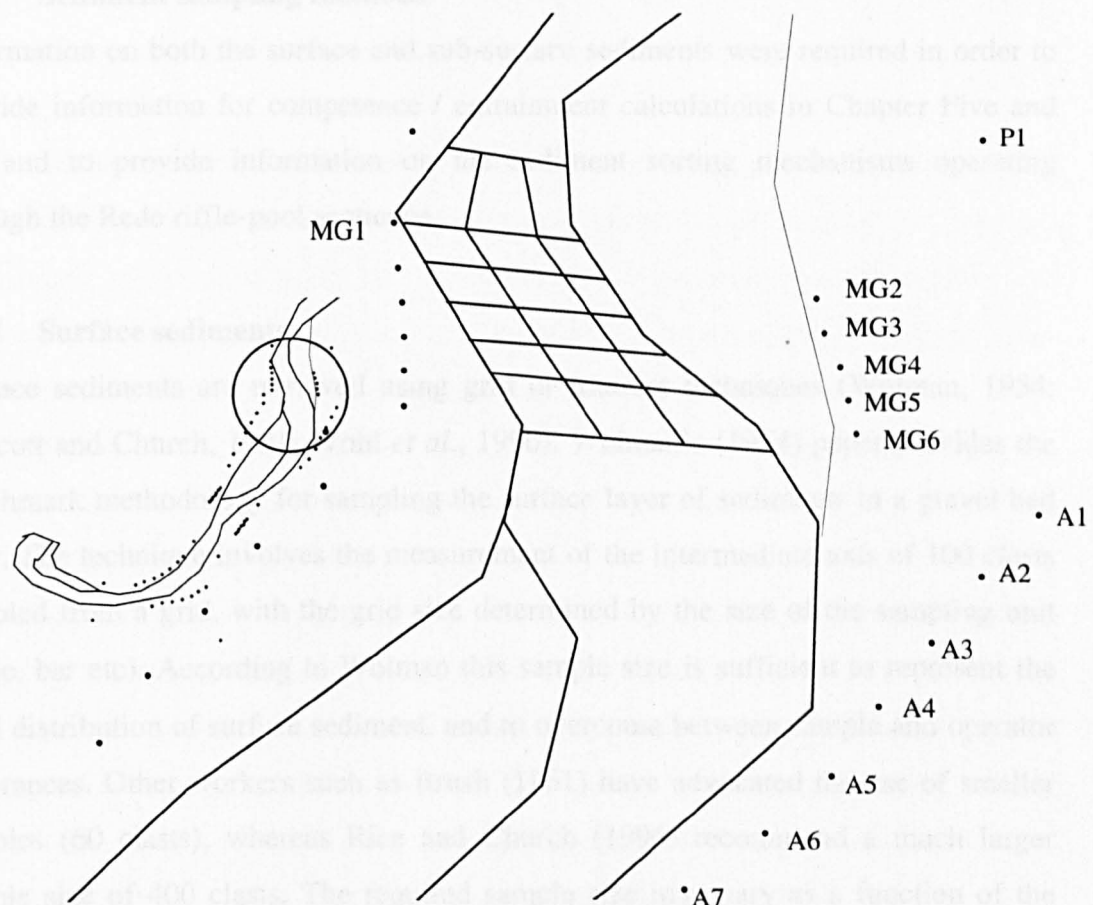


Figure 2.14 Emplacement location for tracer sands.



Plate 2.1 Seeding of magnetic tracer material

2.5 Sediment sampling methods

Information on both the surface and sub-surface sediments were required in order to provide information for competence / entrainment calculations in Chapter Five and Six and to provide information on the sediment sorting mechanisms operating through the Rede riffle-pool sequence.

2.5.1 Surface sediments

Surface sediments are retrieved using grid or transect techniques (Wolman, 1954; Wolcott and Church, 1991; Wohl *et al.*, 1996). Wolman's (1954) paper provides the benchmark methodology for sampling the surface layer of sediments in a gravel bed river. The technique involves the measurement of the intermediate axis of 100 clasts sampled from a grid, with the grid size determined by the size of the sampling unit (riffle, bar etc). According to Wolman this sample size is sufficient to represent the areal distribution of surface sediment, and to overcome between sample and operator differences. Other workers such as Brush (1961) have advocated the use of smaller samples (60 clasts), whereas Rice and Church (1996) recommend a much larger sample size of 400 clasts. The required sample size may vary as a function of the desired precision or site conditions (Hey and Thorne, 1983; Church *et al.*, 1987; Wolcott and Church, 1991), or grain shape and sorting (Milan *et al.*, 1999). Most investigations into the size of the surface layer still utilise Wolman's 100 clast count and therefore it was used for this study.

Surface sediments in this investigation were sampled using a modified grid-by-number technique (Wolman, 1954) whereby sediments were sampled from cells within morphological units (Figure 2.3). Riffles were split into nine cells to permit longitudinal variation to be assessed between riffle heads, crests and tails, and to allow any cross-riffle variation between right-bank, mid-channel and left-banks to be assessed. Due to their small area, pools were not split into cells, whereas bars were split into three cells; head middle, and tail. A total of 2200 particles were taken from the reach whilst walking randomly in each cell with eyes diverted from the streambed; 50 clasts per cell, 450 per riffle, 100 per pool, 150 per bar. All three axes were measured in order to provide information on both grain size and shape. A

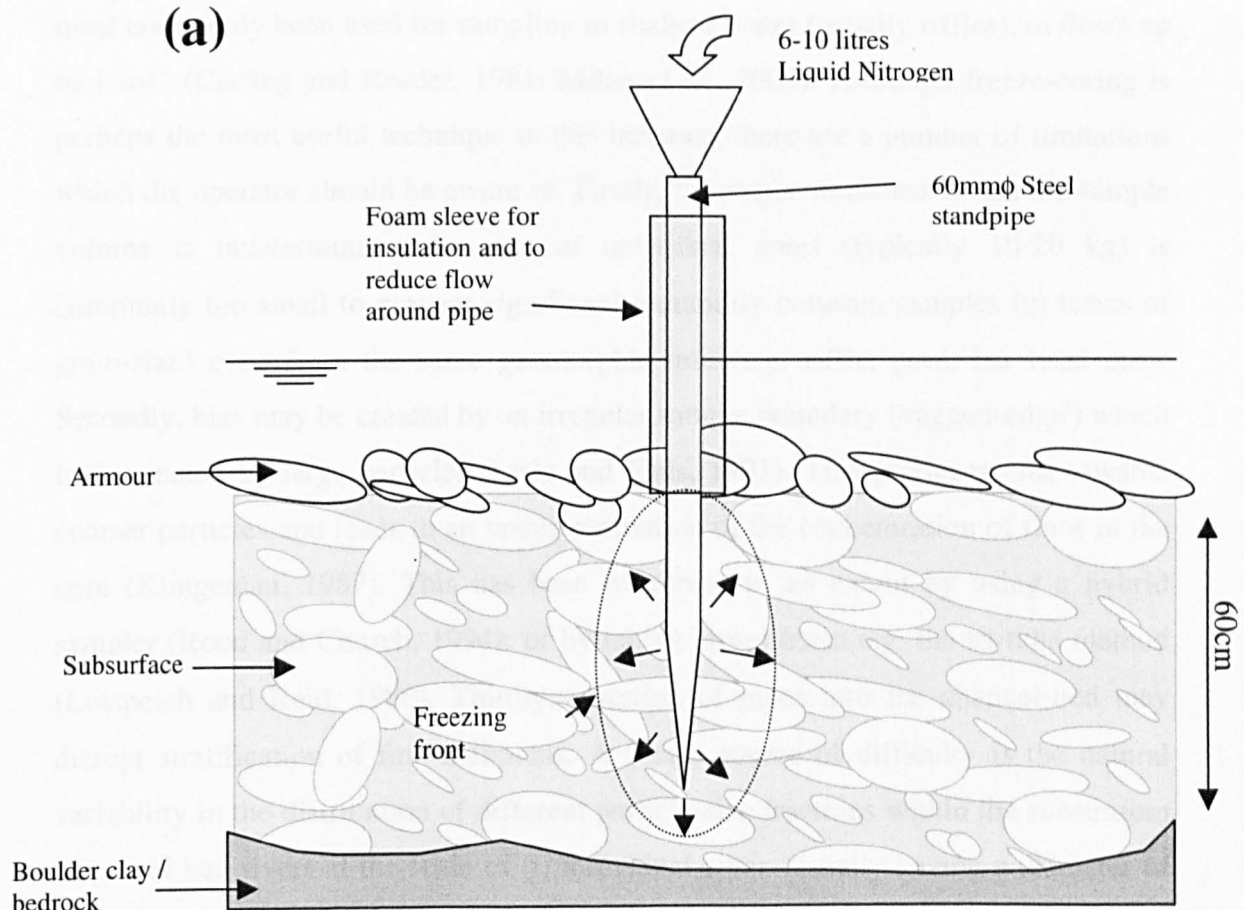
problem with surface sampling is that the finer sizes (2-8 mm) are often under-represented, and as a consequence the size distribution was truncated at 8 mm.

2.5.2 Subsurface sediments and the application of freeze-coring techniques

Information on the sub-surface sediments was required for competence / entrainment estimations, to assess mobility i.e. where $pi/fi \approx 1.0$ grains are equally mobile (see section 1.5.3), and also to measure the concentrations of infiltrated magnetic fine bedload tracer. Information was required on the full particle size distribution of submerged sub-surface sediments, including fine matrix sediments. Although a variety of different sampling methodologies have been used to retrieve volumetric sediment samples from gravel bed rivers (for reviews see Kellerhals and Bray, 1971; Klingeman and Emmett, 1982), few have managed to retain all sizes present without disrupting the structural arrangement of the sediment fabric. Early methods such as grab (spade excavation), pipe scoop, surber and cookie cutter, under-represent the fine sediment population due to wash-out (elutriation) under flowing water (Thoms, 1992; Petts and Thoms, 1986). For example, Thoms (1992) found these methods to under-represent the fine sediment population (sub 2 mm) by up to 400%. Furthermore, these methods can be biased towards the collection of surface sediments. The most widely employed devices have been 'bulk core' samplers (e.g. McNeil and Ahnell, 1960). This sampler, although capable of retrieving a large sample size, does not permit either vertical stratification of grain size, or accurate information on fine-grained sediments.

A common technique, shown in Figure 2.15a, which fulfils these criteria is freeze-coring (e.g. Carling and Reader, 1981; Rood and Church, 1994). By taking frozen cores *in situ* it is possible to assess the full grain-size distribution and the concentrations of fine-grained particles commonly washed out when using other methods. Information on the vertical variation in grain-size parameters may also be obtained by splitting cores into sections. Furthermore information may be obtained concerning the depth of substrate (Milan *et al.*, 2000). Freeze-coring techniques have

(a)



(b)

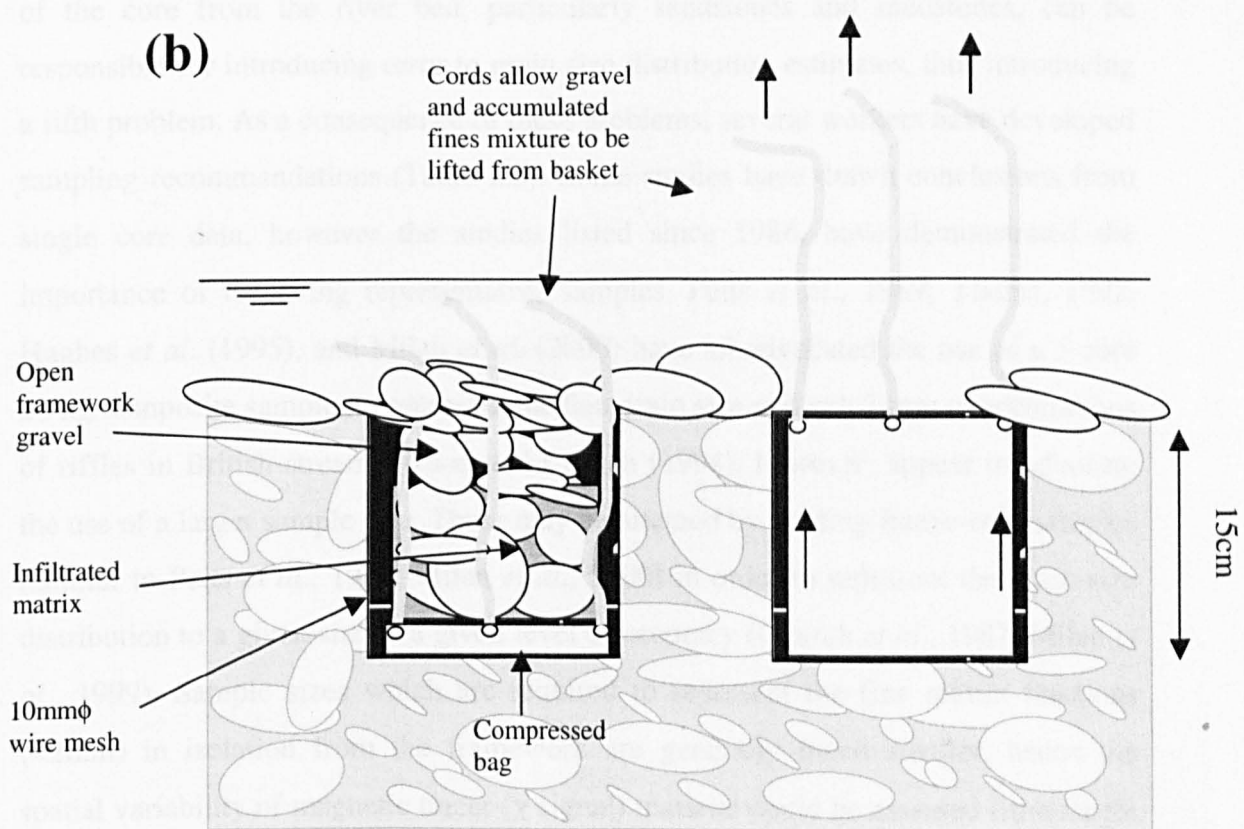


Figure 2.15 Sediment sampling techniques, (a) freeze-coring, (b) basket trap sampling.

most commonly been used for sampling in shallow water (usually riffles), in flows up to 1 ms^{-1} (Carling and Reader, 1981; Milan *et al.*, 2000). Although freeze-coring is perhaps the most useful technique in this instance, there are a number of limitations which the operator should be aware of. Firstly, the major weakness is that the sample volume is indeterminate, the size of individual cores (typically 10-20 kg) is commonly too small to prevent significant variability between samples (in terms of grain-size) even from the same geomorphic unit (e.g. riffle, pool, bar head etc.). Secondly, bias may be created by an irregular sample boundary ('ragged-edge') which is dominated by large particles (Lisle and Eads, 1991). This produces bias towards coarser particles and leads to an under-estimation of the concentration of fines in the core (Klingeman, 1987). This has been overcome to an extent by using a hybrid sampler (Rood and Church, 1994); or by taking larger cores e.g. the tri-tube method (Lotspeich and Reid, 1980). Thirdly, insertion of pipes into the channel-bed may disrupt stratification of fine-sediments. A fourth source of difficulty is the natural variability in the distribution of different particle-size fractions within the substratum of gravel bed rivers at the scale of (i) individual cores (usually having a diameter of 30 - 40 cm), (ii) bedform, and (iii) reach. Fracturing of fragile particles upon retrieval of the core from the river bed, particularly sandstones and mudstones, can be responsible for introducing error to grain size distribution estimates, thus introducing a fifth problem. As a consequence of these problems, several workers have developed sampling recommendations (Table 2.3). Some studies have drawn conclusions from single core data, however the studies listed since 1986, have demonstrated the importance of retrieving representative samples. Petts *et al.*, 1989; Thoms, 1992, Hughes *et al.* (1995), and Milan *et al.* (2000) have all advocated the use of a 5 core 20 kg composite sample, to represent median grain size and sub 2 mm concentrations of riffles in British streams. Rood and Church (1994), however, appear to advocate the use of a larger sample size. These may be attained by pooling freeze-core samples (similar to Petts *et al.*, 1989; Milan *et al.*, 2000) in order to represent the grain-size distribution to a given size at a given level of accuracy (Church *et al.*, 1987, Milan *et al.*, 1999). Sample sizes which are required to represent the fine matrix fractions (<2mm) in isolation from the framework are generally much smaller, hence the spatial variability of magnetic tracer (χ signal) material could be assessed from single cores (Church *et al.*, 1987; Milan *et al.* 1999).

Table 2.3 Sampling guidelines previously recommended when using freeze-coring techniques.

Study and site	Equipment specifications	Sampling recommendations
Rood and Church (1994). Nechako River, B.C., Klondike, McQueston and Mayo Rivers, Yukon Territory, Canada.	Hybrid McNeil-type and freeze-core sampler. Alloy steel pipe 5cm Ø, liquid nitrogen.	Thirty to fifty 13.5kg cores pooled to represent sub 2mm concentrations to within a precision of 10%
Thoms (1992)	Copper standpipe 2.5 cm Ø, liquid carbon dioxide	Five 4kg cores required to characterise median grain size allowing for a 5% error at the 0.05 confidence level.
Hughes (1992) Hughes <i>et al.</i> (1995)	Copper standpipe 2.5 cm Ø, liquid carbon dioxide	Five cores and a pooled weight of 20kg to provide reproducible results allowing for $\pm 3\%$ on estimates of sub 1mm concentrations.
Petts <i>et al.</i> , (1989) Petts and Thoms (1986), Petts (1987)	Copper standpipe 2.5 cm Ø, liquid carbon dioxide	Five 4kg cores pooled 20kg to provide reproducible results allowing for $\pm 3\%$ on estimates of sub 1mm concentrations.
Milan <i>et al.</i> , in 2000		
Carling and Reader (1981)	Copper standpipe 2.5 cm Ø, liquid carbon dioxide	Single cores analysed
Lotspeich and Reid (1980)	Tri-tube freeze-corer, liquid carbon dioxide	Single large cores

The sampling strategy used in this study was different to those listed in Table 2.3, as a high spatial resolution was required to pick up tracer routing patterns. A cell-based sampling strategy was designed (Figure 2.3b), whereby a single 60 cm freeze-core was taken from each of the riffle cells, and a bulk 5-core sample from each pool. For the initial background survey in July 1995 two cores were taken from each cell, whereas subsequent surveys in July 1996 and March 1997, a single core was taken from each cell. Cores were bulked to provide information for morphological units as a whole, thus meeting the sample-size criteria discussed by Church *et al.* (1987) and Milan *et al.* (1999).

2.5.3 Fine bedload transport and trapping

Fine bedload traps or baskets have been used widely to assess both siltation of gravel bed rivers (e.g. Thoms, 1992; Carling and McCahon, 1987, Davey *et al.*, 1987, Sear,

1993 and Lisle and Eads, 1992) and fine bedload mobility (Church *et al.*, 1991). In the present investigation the traps employed had two purposes; firstly to assess the accumulation rates and mobility of fine bedload (Chapter Five), and secondly to monitor the routing of a magnetic tracer through the study reach (Chapter Seven). The baskets employed in this study were similar to the design of Sear (1993), in as much as each basket was 0.15 m deep with a surface area of 314 cm² (Figure 2.15b). Each basket was constructed from 10 mm wire mesh and permitted intragravel movement of fines, which can contribute significant quantities of fines (Carling, 1984; Sear, 1993).

Thirty-one traps were positioned along transects in the study reach at the centre of each sampling cell (Figure 2.3b). To assist efficient retrieval of trapped fines, a compressed plastic bag was folded and placed at the base of the basket *sensu* Lisle and Eads (1992). Cables attached to the wire rim of the bag lead to the water surface. The baskets were then filled with a representative substrate framework which was truncated at 2 mm, obtained from freeze-cores (acquired from within a 2 m radius of the final position of the basket within the channel bed). A representative armour layer comprising grains obtained in the vicinity of each trap was constructed over each basket once it had been set within the streambed. Each armour layer particle was painted in order to assist identification of trap position and to provide a visual estimate of any gravel transport which had occurred post flood event. On sampling, the surface layer was removed and the compressed bag was then pulled upwards *via* the cables in order to minimise loss of fines under flowing water. On removal from the bed, the framework and accumulated fines mixture retained within the bag were wet sieved through a 2 mm sieve in the field and the organics floated off in a bucket. The bag was then returned to the basket and compressed, and the framework material retained within the sieve was returned to the basket on top of the compressed bag. Further analysis then concentrated on the inorganic fraction. The fines mixture was then passed through a 125 µm sieve, sealed in plastic bags, and taken back for size and dry weight analysis in the laboratory. Although a sub-sample of the <125 µm was retained, it was not included in the analysis as it was considered to be washload (Church *et al.*, 1991) rather than bedload. In upland gravel-bed rivers the majority of fines transported tends to be sands transported as bedload. For example, Lisle (1989)

noted that as little as 20% of the fines which entered his traps were derived from suspended load. Analysis of suspended sediment data on the Rede (Appendix 2.2) indicated maximum concentrations of only 50 mg l^{-1} , which are low in comparison to other British rivers (Walling and Webb, 1987). Concentrations of suspended sediments were generally too low to conduct grain-size analysis, however visual inspection of filter papers revealed that the suspended load was generally dominated by silt- (4-63 mm), however some fine sand grains were visible for flows $>2 \text{ m}^3 \text{s}^{-1}$. It would appear reasonable to assume therefore that the majority of fine sediments infiltrating traps would be derived from saltated bedload sources rather than suspended load.

2.5.4 Strategy to detect fine-tracer development

A combination of freeze-coring and trapping of sediments was used to assess the spatial and temporal development of fine tracer material through the Rede riffle-pool sequence. Freeze-coring was undertaken twice after tracer emplacement, firstly following the first major flood after emplacement (July 1996), and secondly the following spring (March 1997). It was not possible to conduct a flood-by-flood survey due to the labour effort required. A finer temporal resolution of tracer development was obtained by sampling basket traps on a flood-by-flood basis.

2.5.5 Laboratory procedures and grain-size analysis

Sedimentological analysis followed the steps outlined in Milan (1994). Freeze-core sediment samples are air dried at 50°C and then passed through a series of nested sieves. The adopted sieve sizes follow an existing methodological protocol, in order that direct comparison could be made with freeze-core sediment sampling over a range of UK streams (Milan *et al.*, 2000). Sediments were sieved through 63, 37.5, 20, 6.3 and 2 mm mesh sizes. Matrix sediments from freeze-cores, and fine bedload sediments from traps, that passed through the 2 mm sieve were wet sieved through 1, 0.5, 0.25 and 0.125 mm sieves. The grain-size distribution of the sub 0.125 mm material was determined by laser diffraction (Agrawal *et al.*, 1993). Fine bedload (sand fraction) obtained from the basket traps were also dried at 50°C in a fan oven and weighed, and then a 200g sub-sample was wet sieved through 2 mm, 1 mm, 500 μm , 250 μm , 125 μm aperture sieves.

2.6 Approaches to estimating hydraulics through a riffle-pool sequence

It is extremely problematic to obtain a detailed spatial and temporal data set concerning flow hydraulics over the full discharge range within a natural river channel. It is useful therefore to assess past methodological approaches, rank their relative success and highlight any limitations before selecting appropriate procedures for the River Rede.

2.6.1 Past approaches and associated problems

Discharge range

The majority of observations of tractive force variability through riffle-pool sequences have been taken at low discharge, with very few studies presenting data at bankfull and over. Even in Keller's (1971) original study, where he proposed the velocity reversal hypothesis, he was only able to postulate an equalisation in velocity (as he was unable to take measurements at the bankfull discharge). Furthermore the frequency of observations of tractive force over the discharge range is extremely limited. For example, Robert (1997) only took three measurements between baseflow and two-thirds bankfull, again missing out vital data which needs to be obtained at and over bankfull discharge. Data that was obtained at around bankfull by Carling (1991) indicate significant non-linearity in logarithmic plots between flow geometry variables and discharge. However, Clifford and Richards (1992) point out that log-log plots must be interpreted with care, as convergent plots may mask absolute increases in the difference between two quantities plotted in this way.

Range of parameters

A wide range of parameters has been used to quantify hydraulic variations through riffles and pools (Table 2.4). Of these studies, only Clifford and Richards (1992),

Table 2.4 Range of parameters used to quantify riffle-pool hydraulics

Author	Parameter
Clifford and Richards (1992)	Profile averaged and bed velocity, section averaged velocity, mean section averaged shear stress (Du Boys), Local shear stress from velocity profiles
Keller (1971)	Mean bottom velocity
Andrews (1979), Teisseyre (1984)	Mean section velocity
Lisle (1979)	Mean boundary shear stress
Carling (1991)	Section average shear velocity
O'Conner <i>et al.</i> (1986)	Stream power
Jackson and Beschta (1981), Ashworth (1987), Petit (1987)	Point measures of shear stress and velocity
Bhowmik and Demissie (1982)	Froude number
Thompson <i>et al.</i> (1999)	Water surface slopes

Teisseyre (1984) and Carling (1991) use more than one parameter in their study, although Teisseyre's study is restricted to three observations, while Carling's study is limited to section-averaged data. Clifford and Richards (1992) point out that patterns in the behaviour of section-averaged and point measurements at riffles and pools are not necessarily equivalent as measures of flow competence may be suspect, and only valid where flow is strictly uniform. Clifford and Richards (1992) provide the greatest range of parameters for a single reach, although their study was also problematic. Firstly they fail to measure the full discharge range and secondly there were severe problems with estimating shear stress from what is currently the most utilised and accepted method of calculating point boundary shear stress in natural channels; namely velocity profiling or 'the law of the wall'. Using this technique, shear stress for a fully rough turbulent boundary layer is given by;

$$\frac{\tau_o}{\rho_w} = \left[\frac{(u_2 - u_1)}{(2.3/\kappa) \log(y_2/y_1)} \right]^2 \quad (2.3)$$

where u_1 and u_2 are point mean velocities, y_1 and y_2 are depths from the bed at which u_1 and u_2 were measured, κ is the von Karman constant, usually taken as being equal to 0.41, and ρ_w is the fluid density, which for water is taken as being equal to 1000 kgm^3 . Clifford and Richards (1992) demonstrated that sinuous shallow streams with large grain roughness elements; introduced a high degree of scatter to the velocity profile, so much so that interpretations regarding riffle-pool hydraulics were meaningless.

Inferring sediment transport from hydraulics

Prediction of sediment transport pathways are only reliable in transport-limited conditions (Clifford and Richards, 1992; Lisle pers comm., 1998). For a reversal in mean velocity to occur at high discharge, the pool would have to fill with gravel to reduce the cross-sectional area sufficiently to satisfy the continuity-of-mass principle. In a supply-limited situation however, a reversal would require systematic changes in geometry or flow resistance differences, which may not be present between all riffle and pool sections (Clifford and Richards, 1992). The implication of this is that scour at the pool and fill at the riffle may not always occur. The use of mean boundary shear stress as an index of sediment transport may have low success as undulating bed topography may result in the near-bed (grain) component of total stress being out of balance with the downstream propulsive force (Clifford and Richards, 1992). Furthermore, bed structure may vary spatially between and within riffle-pool units (Sear, 1996), leading to a reduction in the critical shear stress for entrainment for clasts situated in loosely packed arrangements.

Spatial integrity of measurement

There has been little standardisation in terms of spatial integrity of hydraulic measurements in the field. For example, Carling (1991), working on the River Severn, had to rigorously analyse his velocity profiles from adjacent verticals to ensure uniformity between verticals in order to obtain a meaningful cross-section average. Some conclusions regarding velocity reversal between a riffle and a pool

have been made using riffles and pools which have been up to 1km apart (e.g. Lisle, 1979; Andrews, 1979; Jackson and Beschta, 1981). There is a lack of studies which have concentrated on sinuous reaches and relatively few studies support the occurrence of velocity reversal in meandering reaches (Clifford and Richards, 1992, Keller and Floresheim, 1993). The issue of site specificity shall be revisited in Chapter Nine.

In my thesis, I decided to use a range of measures to assess tractive force through the Rede riffle-pool sequence; (i) cross-section average velocity, (ii) near bed velocity, (iii) profile-averaged velocity, (iv) point τ from velocity profiles, (v) mean τ , estimated using the Du Boys formula, and (vi) point τ , estimated using the Du Boys Formula.

2.6.2 Determination of velocity

This parameter was used in an effort to ascertain whether velocity reversal hypothesis could be applied in the case of the River Rede. A number of velocity parameters were measured;

- 1)** Cross-sectionally averaged velocity was estimated from stage data obtained at seven cross-sections situated at the crest of the riffles and in the troughs of the pools. Continuous discharge was measured at a permanent gauging station situated 50 metres upstream of the riffle-pool sequence under study. Velocities were obtained by dividing the discharge peaks for twenty-one flood hydrographs by the wetted area derived from each of the cross-sections.
- 2)** Bed velocity was measured using an electromagnetic current meter 0.01m from the bed, at nine points on three riffles and three points in the pools for three different flows from baseflow to about half bank full; $0.3, 1.0$ and $3.6 \text{ m}^3 \text{ s}^{-1}$.
- 3)** Profile averaged velocity was measured at 0.6 depth in conjunction with bed velocity, using the same spatial and temporal resolution as bed velocity. A third

velocity measurement was taken at 0.8 depth to enable point boundary shear stress to be calculated using equation 2.3 above.

2.6.3 Determination of boundary shear stresses

Three measures of boundary shear stress were used;

- 1) Point boundary shear stress estimated from velocity profiles
- 2) Mean boundary shear stress estimated from the Du Boys equation
- 3) Point boundary shear stress estimated from a modified Du Boys equation (using depth instead of hydraulic radius)

It was initially planned that through use of velocity profiling and equation 2.3, a high resolution point boundary shear stress survey through the Rede riffle-pool sequence would be undertaken. This was done for up to thirty-six points throughout the Rede riffle pool sequence for three different discharges; 0.3, 1.0 and $3.6 \text{ m}^3 \text{ s}^{-1}$. The Rede data for the velocity profile survey is more spatially detailed than Robert (1997) and covers a similar flow range. Obtaining the same detail of measurements throughout the Rede riffle-pool sequence at higher discharges proved extremely problematic. Firstly, there was the problem of being on-site during a bankfull flows or those close to bankfull. Secondly, the duration of bankfull flow tended to be relatively short (around 1 hour) compared to the duration required to take up to 36 point velocity profiles (up to 3 hours). Hence the shear stresses measured at the start of a survey would be taken at different discharges and at a different stages on the flood hydrograph compared to those taken at the start of the survey. Thirdly, there is the problem of taking velocity measurements in deep fast flowing water. This requires bridges or platforms across the channel, which were not available for my study. Finally, there is the problem caused by taking velocity profiles where there are large grain roughness elements. Such elements can result in negative velocity profiles (Clifford and Richards, 1992), a feature seen in the Rede at low flows. As a result it was decided to employ estimates of boundary shear stress derived from the slope depth product or the Du Boys formulae for flows greater than $4 \text{ m}^3 \text{ s}^{-1}$.

2.6.4 Mean and point boundary shear stress

Water surface profiles were surveyed on five occasions (Figure 2.16), using a combination of water surface and strand-line measurements, for stages ranging from summer base flow to approximately bankfull discharge. Additional slope information was obtained for 21 separate flows by obtaining stage-board readings above and below each riffle. These slopes typically ranged between 0.03 and 2%. Cross-stream depth distributions were recorded at each of the cross-sections by subtracting water surface from bed surface elevation. As it was impossible to observe the bed at the higher stages, the coarseness of the bed material introduces some imprecision in the measurement of bed elevations. The thickness of the line indicating the bed in Figure 2.15 was scaled to represent the likely error margin ($\pm D_{50}$).

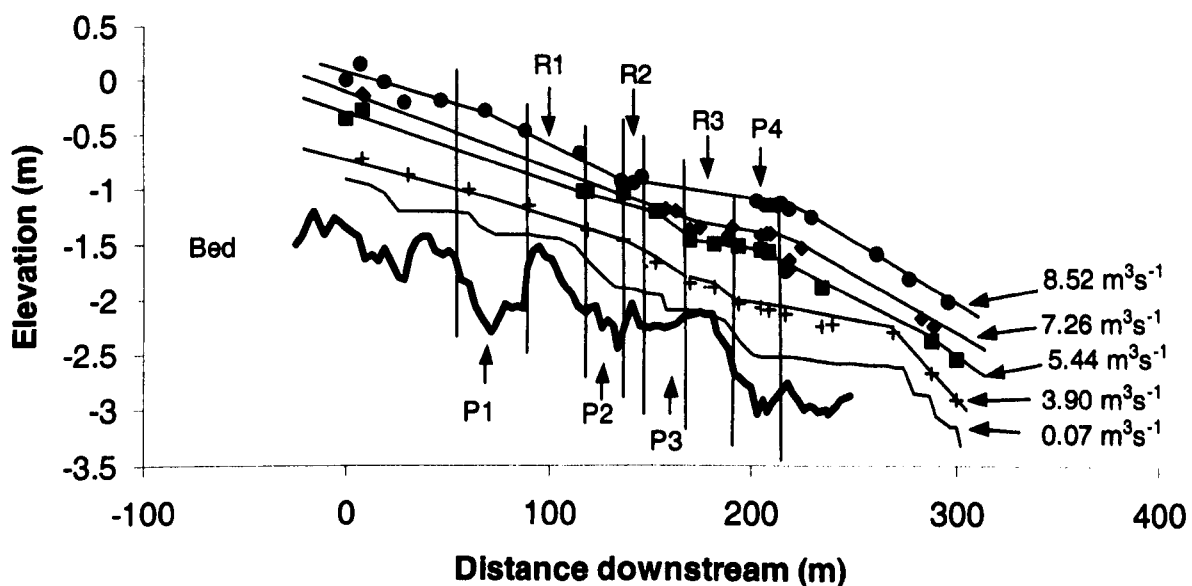


Figure 2.16 Bed long profile of the Rede riffle pool sequence and water surface profiles surveyed over five flows of varying magnitude. Line thickness for bed profile approximates to the reach D_{50} .

The survey data were then entered into the Du Boys equation to calculate local bed shear stresses (τ_o), assuming that the flow was approximately uniform and that the energy slope could be approximated by the local water surface slope.

$$\tau_o = \rho_w g R S \quad (2.4)$$

Where, R is the hydraulic radius, g is acceleration due to gravity, ρ_w is the density of water, and S is the energy slope which is approximated as being equal to the water surface slope. Point boundary shear stress was estimated by substituting R with point depth (d), this is a commonly accepted procedure (e.g. Ferguson and Wathen, 1998). Strictly, equation 2.2 should only be applied to uniform flow (Bathurst, 1982) and where super-elevation effects encountered at bends are minimal. This is because riffle-pool morphology introduces flow convergence and divergence, acceleration and deceleration, the magnitude of which is related to the degree of change in cross-sectional wetted area with distance downstream between sections. Milan *et al.* (2001) demonstrate however that these non-uniform and super-elevation effects were minimal for the flows under scrutiny in the Rede study reach.

2.7 Spatial analysis

Both the sediment and hydraulic sampling strategies used throughout this investigation provided a high spatial resolution which enabled the use of a contouring package 'Surfer' (Surfer Mapping System, Golden Software Incorporated), to aid interpretation of the data. The Surfer program produces surfaces from spatially referenced data. Interpolation of x , y , z is necessary particularly in areas where data are sparse. To prevent inaccurate inferences from areas where data are limited, it is advantageous to use an interpolation method such as Kriging, which provides error estimates on the interpolated values. Kriging is a form of weighted local averaging based on the theory of regionalise variables (Matheron, 1971; Olea, 1975). Mather (1993) suggests that Kriging is an optimal interpolator in the sense that each interpolated value is unbiased and its estimated variance is a minimum.

2.8 Summary and conclusions

This chapter has introduced the characteristics of the study sites and considered the sampling methodologies used in the present investigation, highlighting some of the limitations which must be realised before interpreting any of the data. The following chapter details the sedimentology of the Rede riffle-pool sequence, presenting data obtained from the Wolman grid and freeze-core sampling exercise.

Chapter Three

Sedimentology of the Rede riffle-pool sequence

3.1 Introduction

As reported in Chapter One (section 1.6), riffle-pool sequences are usually reported as displaying distinct spatial variation in the grain-size of the surface sediments, where riffle sediments are coarser (Leopold *et al.*, 1964; Keller, 1971; Yang, 1971; Cherkauer, 1971; Bhowmik and Demissie, 1982; Teisseyre, 1984, Lisle and Hilton, 1982; 1999), and in some instances better sorted (Hirsch and Abrahams, 1984; Carling, 1991) than pool sediments. This spatial pattern of surface sediment sorting undermines riffle-pool maintenance theory, in particular Keller's (1971) velocity reversal hypothesis and Jackson and Beschta's (1982) two-phase bedload transport model. Fine gravel and sand (Phase 1 bedload) is winnowed from riffles into pools over most of the flow range during which period the riffles are more competent than pools. At flows approaching bankfull, the tractive force of the pool exceeds that of the adjacent riffles, and any gravel (Phase 2 bedload) scoured from riffles passes through the pools and gets deposited on riffles further downstream (Keller, 1971; Jackson and Beschta, 1982). On the falling limb of the hydrograph sand and fine gravel is winnowed from the riffles and deposited in the pools, thus leading to pools becoming finer than the riffles.

Recent studies suggest that fundamental sedimentological differences between pools and riffles may explain some of the observations of sediment transport behaviour (Clifford and Richards, 1992; Sear, 1992a; 1996; Clifford, 1993b). In section 1.5 it was demonstrated from the Shields curve that τ_c was directly proportional to D_s , suggesting that grain weight was the principle force restricting movement. D_s variability in a riffle-pool sequence should therefore show differences in τ_c required to scour different areas of the bed. However, as was shown in section 1.5.3 and 1.5.4, differences in grain size (e.g. Shields, 1936), shape (e.g. Schmidt and Ergenzinger, 1992), and packing (e.g. Sear, 1996) between riffles and pools result in differential critical entrainment thresholds for bed sediment clasts. The objective of this chapter is to identify the extent and pattern of sedimentological variability, including vertical

and lateral variability in grain size, shape, structure and strength for the Rede study site. Although it is clear from section 1.6 that attention needs to be given to accurate measurement of high flow grain size in streams which have a high supply of fine bedload, the study of supply-limited streams (such as the Rede) may provide further insight into high flow sorting processes. These data will be used in conjunction with hydraulic data (Chapter Four) and sediment tracer data (Chapters Five-Eight) to provide a detailed insight into sediment transport dynamics in an upland gravel-bed river.

3.2 Sampling strategy

The study reach was divided into cells (Figure 3.1). This cell-based sampling strategy allowed an examination of variation in sediment character throughout morphological sub-units. Three riffles, four pools and three point bars were sampled on an intensive basis and three further riffles and one pool was sampled less intensively. The three main riffles (A, B and C) were each divided into 9 cells. This system allowed comparisons to be made between morphological sub-units. For example by combining the data from riffle heads (cells 1, 2 and 3), a comparison could be made with riffle crests (cells 4, 5 and 6) or tails (cells, 7, 8 and 9). Likewise the right-bank sediments (cells 1, 6 and 7) could be compared with mid-channel (cells 4, 5 and 6) or left-bank sediments (cells 3, 4 and 9). Pools were not subdivided due to their smaller size, however bars were split into a bar head, bar mid-point and bar tail zones.

3.2.1 Sediment sampling

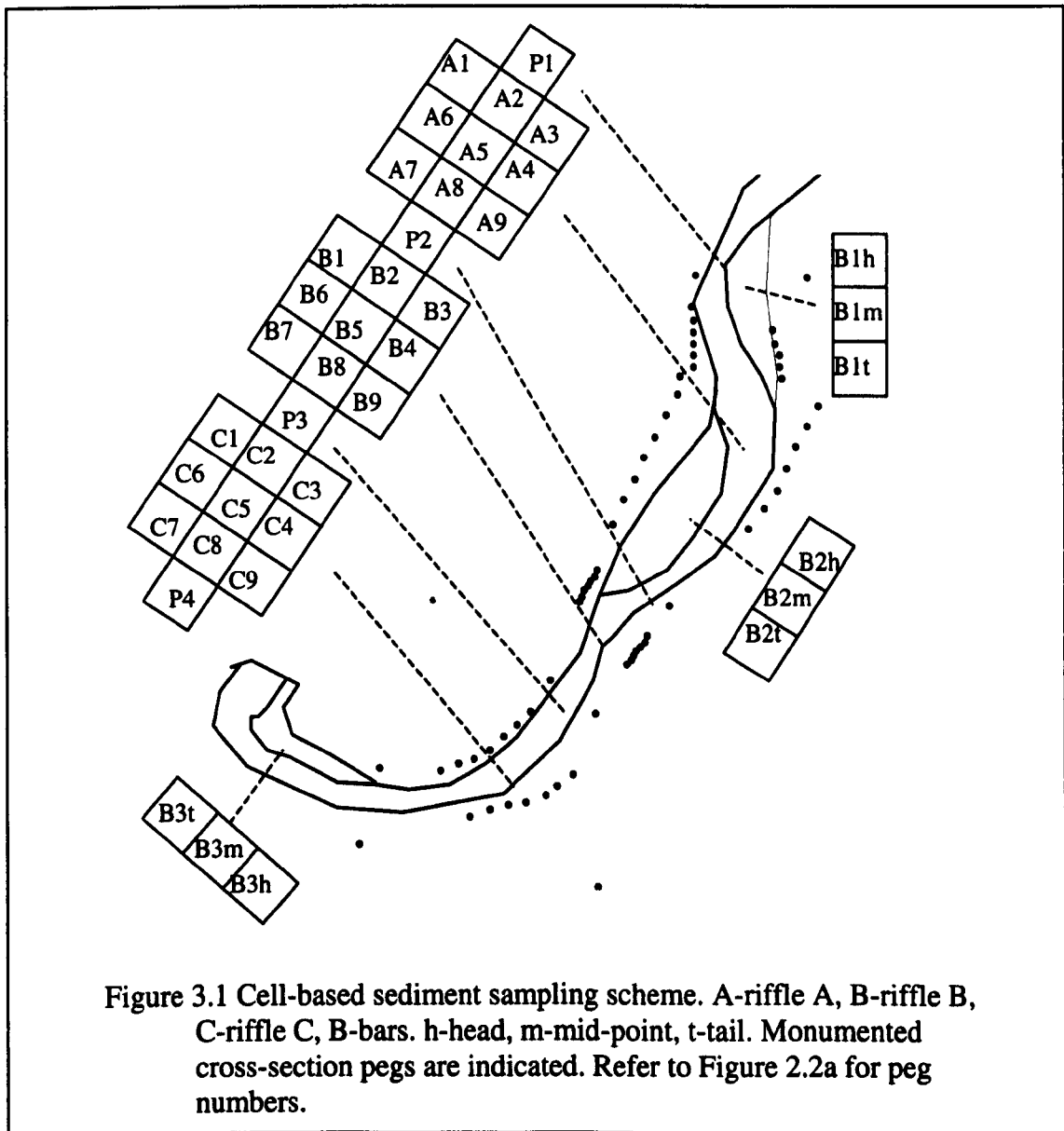
Surface – Wolman grid sampling

In each of the riffle and bar cells, a, b and c-axes of 50 particles were recorded; a total of 450 particles per riffle, and 150 particles per bar. For the pools, 100 particles were taken (see section 2.5.1).

Sub-surface: Freeze-core sampling

Two freeze-cores were taken from each cell at riffles A, B and C, whereas composite samples of 5 cores were retrieved from each of the pools and the other riffles following a standardised protocol (Petts *et al.*, 1989; Milan *et al.*, 2000). Sediments were sampled to a maximum depth of 60 cm, although this was sometimes limited by

the depth of available gravel. Upon retrieval each frozen core was sectioned into 15 cm intervals using a hammer and chisel, after which they were returned to the laboratory to be analysed for their grain size characteristics (see section 2.5.2 and 2.5.5).



Bed compaction

The spatial variability in bed strength was examined by conducting a cone penetrometer survey (Sear, 1992a, 1992c). This technique involves the application of a known force on a standard penetration point. The number of blows taken to advance the point a given distance is recorded (Sangerlat, 1979). The distance used on the Rede was 0.1 m which approximated to the D_{50} of the surface gravels. The values recorded in this way reflect the composite effect of the weight of the surrounding grains, packing density and degree of grain interlock (Sear, 1992a). Bed strength was tested along each of the thirty cross sections and random points, giving a total of 182 points throughout the Rede riffle-pool sequence.

3.3 Results

3.3.1 Surface layer: general characteristics

The surface layer of the Rede channel comprised occasional large immobile cobbles and boulders surrounded by patches of coarse and medium gravel (Plate 3.1). The



Plate 3.1 Bed surface of the Rede channel demonstrating the patchy surface structure.

coarse particles tended to be moss-covered, indicative of low frequency transport. However, surface layer mobilisation, probably of the gravel patches, did appear to take place, a fact which was further substantiated by the gravel tracer movement discussed in Chapters Six and Eight. Consequently it was difficult to categorise the surface layer based upon previous typologies suggested in the literature (e.g. Gomez, 1984). The gravel patches appear to display armoured characteristics, however it is unlikely that 'whole bed' mobilisation ever takes place due to the presence of the large clasts in the bed. These appeared to be larger patch features in comparison to those discussed by Larronne *et al.* (2000).

3.3.2 Surface layer: grain-size characteristics

Table 3.1 demonstrates the grain-size characteristics of the surface layer in riffles, pools and bars. A multiple comparisons analysis of variance (F ratio test) indicates

Table 3.1 Summary surface layer characteristics of individual geomorphic units

Site	D_{16}	D_{50}	D_{84}	Sorting
Riffles				
Control	33	70	125	0.96
A	41	75	133	0.85
B	44	84	150	0.89
C	56	96	150	0.71
D	55	90	170	0.81
E	60	100	155	0.69
F	51	90	133	0.69
G	34	70	133	0.98
Mean	45	85	145	0.84
Bars				
1	18	39	73	1.00
2	33	64	116	0.91
Mean	23	50	100	1.01
Pools				
1	82	120	190	0.61
2	72	120	195	0.49
3	86	115	170	0.74
4	43	82	120	0.74
5	83	123	194	0.61
Mean	65	110	171	0.70

The sorting index used is the Graphic Standard Deviation (σ_0) (Folk, 1974), which measures the deviation of the 16th and 84th percentiles ($\phi_{84} - \phi_{16}$)/2, where ϕ is the particle size in ϕ units at which $n\%$ by mass is finer.

pools to be significantly coarser than riffles and both riffles and pools to be significantly coarser than bar sediments ($p<0.001$). This is interesting as pools are

usually reported as being finer than riffles (e.g. Sear, 1992a). Pools are slightly better sorted on average than riffles, with the poorest sorting shown on bar surfaces. A summary of grain size variability for permanently submerged morphological sub-units is demonstrated in the box and whisker plots shown in Figure 3.2, while more detailed cell-based information is shown in Figure 3.3 and contour plots (Figure 3.4). The coarse nature of pools and the finer nature of the riffles and point bars, which appear to act as storage zones (with poorer sorting) are noticeable. The coarsest cell appears at the tail of Riffle C along the left-bank, whereas the finest cell appears at the crest of Riffle A on the right-bank (excluding bar data). Whilst a general downstream pattern across riffles did not appear to exist, some riffles tended to be coarser at the head. An example was Riffle A, (right hand bank, channel centre), whereas others were either coarsest at their crest, or tail (e.g. Riffle C).

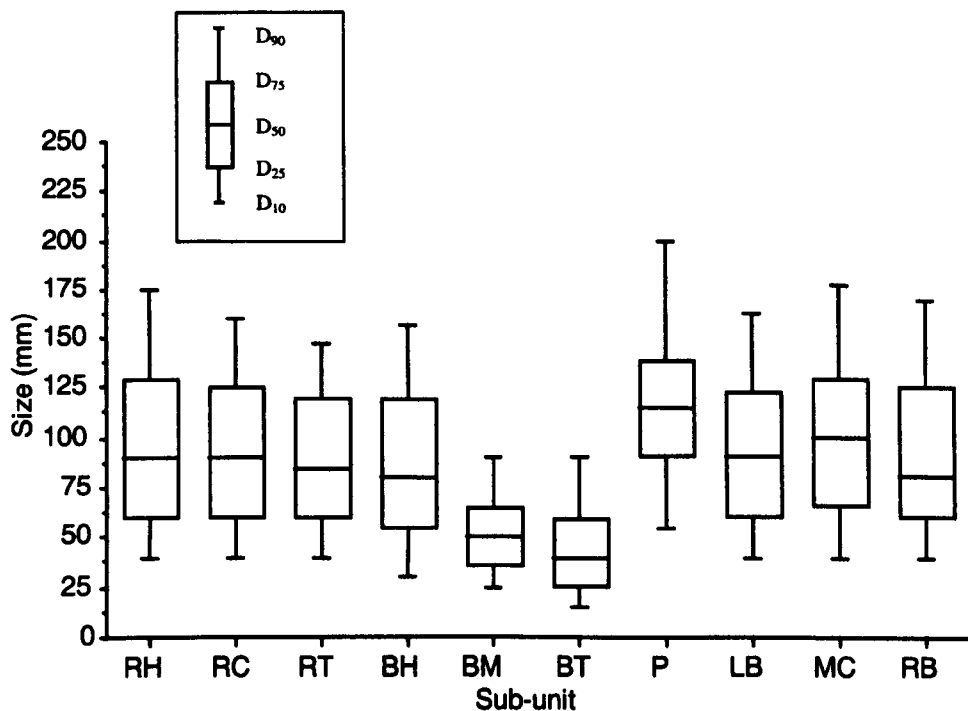
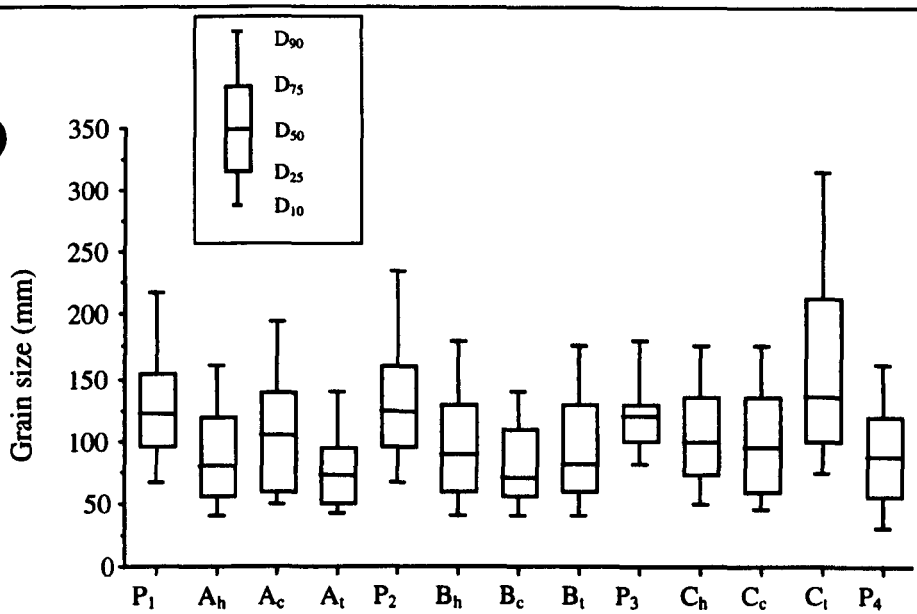
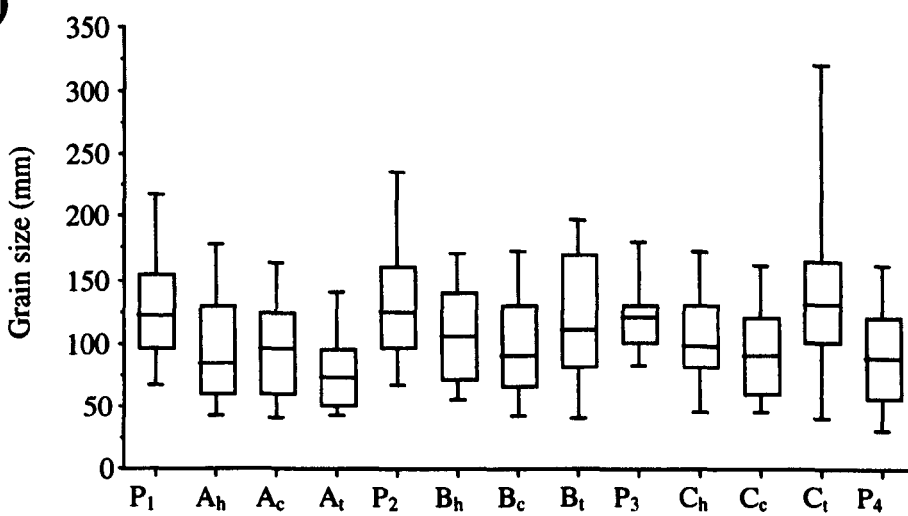


Figure 3.2 Variation in median grain-size for surface (armour) layer sediments for morphological sub-units. RH – riffle head, RC – riffle crest, RT – riffle tail, P – pool, LB – left bank, MC – mid-channel, RB – right bank.

(a)



(b)



(c)

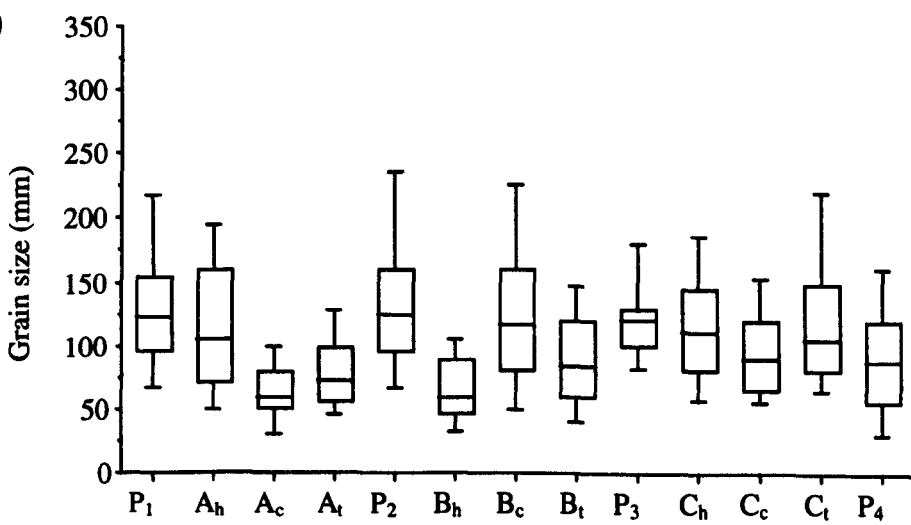


Figure 3.3 Downstream pattern in surface grain size from cell-based data; (a) right-bank, (b) mid-channel, (c) left-bank. A-riffle A, B-riffle B, C-riffle C, h-head, c-crest, t-tail, P-pool. Each box for the riffle sub-units represents the statistics for a 50 stone sample, and the pools for a 100 stone sample.

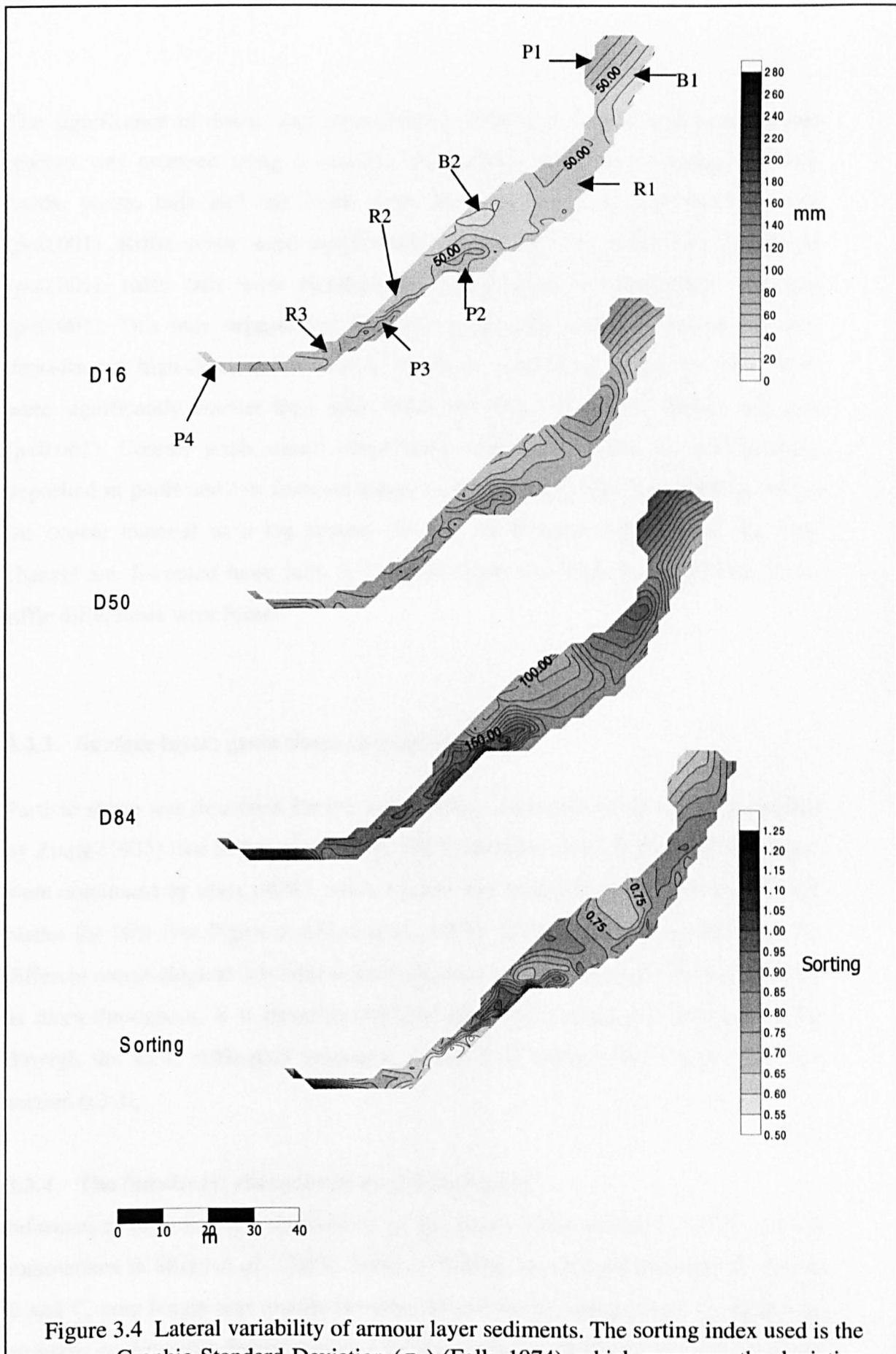


Figure 3.4 Lateral variability of armour layer sediments. The sorting index used is the Graphic Standard Deviation (σ_G) (Folk, 1974), which measures the deviation of the 16th and 84th percentiles $(\phi_{84} - \phi_{16})/2$, where ϕ_n is the particle size in ϕ units at which $n\%$ by mass is finer.

The significance of down- and cross-stream variation for riffles and pools at both reaches was assessed using a multiple comparisons Analysis of Variance. Riffle heads, crests, tails and bar heads were all significantly coarser than bar tails ($p<0.001$). Riffle crests were significantly coarser than bar heads and mid-points ($p<0.001$), riffle tails were significantly coarser than bar mid-points and tails ($p<0.001$). This may suggest that these are preferential areas for coarse sediment deposition at high flow, and/or areas of enhanced winnowing during low flow. Pools were significantly coarser than riffle heads and tails, bar heads, centres and tails ($p<0.001$). Coarser pools would either imply that coarse clasts are preferentially deposited in pools and / or fines are preferentially flushed from pools leaving behind the coarse material as a lag deposit. Sorting mechanisms operating in the Rede channel are discussed more fully in Chapters Eight and Nine. No significant cross-riffle differences were found.

3.3.3 Surface layer: grain shape characteristics

Particle shape was described for the Rede surface sediments using a scheme devised by Zingg (1935) (see Milan *et al.*, 1999, p90 for details). Overall, the Rede sediments were dominated by discs (40%), while equants and rods both accounted for 22% and blades for 16% (see Figure 5, Milan *et al.*, 1999). Differences in the grain shape for different morphological sub-units were negligible, with the dominant shape remaining as discs throughout. It is therefore unlikely that shape influences sediment sorting through the Rede riffle-pool sequence. Tracer data support this supposition (see section 6.3.3).

3.3.4 The Substrate: characteristics of freeze cores

Information regarding the dimensions of the freeze-cores obtained in this study is summarised in Milan *et al.* (1999, Table 2). Taking into account the study Riffles A, B and C, core length was usually between 50 and 60 cm, although gravel depth was probably considerably deeper than this at these locations. Shorter cores were retrieved from riffle C due to shallow gravel (5-10cm in places), which was found to overlie

boulder clay. The gravel clay boundary was clearly identifiable in freeze cores. Shorter cores were retrieved from the other study riffles and some of the pools. Cores tended to be heavier when compared with previous studies (Milan, 1994; Milan *et al.*, 2000), partly due to coarse cobbles embedded within the substrate sticking to the outside of the core. The average core weight was 16 kg and the average volume of a core was 6354 ml. In some instances a single clast would exceed the weight of the rest of the core sample (Plate 3.2), a factor which could skew the grain-size distribution and drastically alter grain-size indices and the percentage by weight concentration of fines. Although full baseline grain-size data are presented here as combined (bulked) freeze-core samples, it is recognised that truncation of the grain-size distribution is necessary to ensure that each grain-size class included is represented in their true proportions. The background literature to this issue and application of truncation recommendations to the Rede data is discussed in Milan *et al.* (1999).



Plate 3.2 Freeze-core demonstrating large clast in the upper 0-15cm of substrate

3.3.5 Sub-surface grain-size characteristics

The full grain-size distribution for the bulked freeze-core data-set (80 cores) and range for all freeze cores taken from riffles are presented in Figure 3.5. The presence

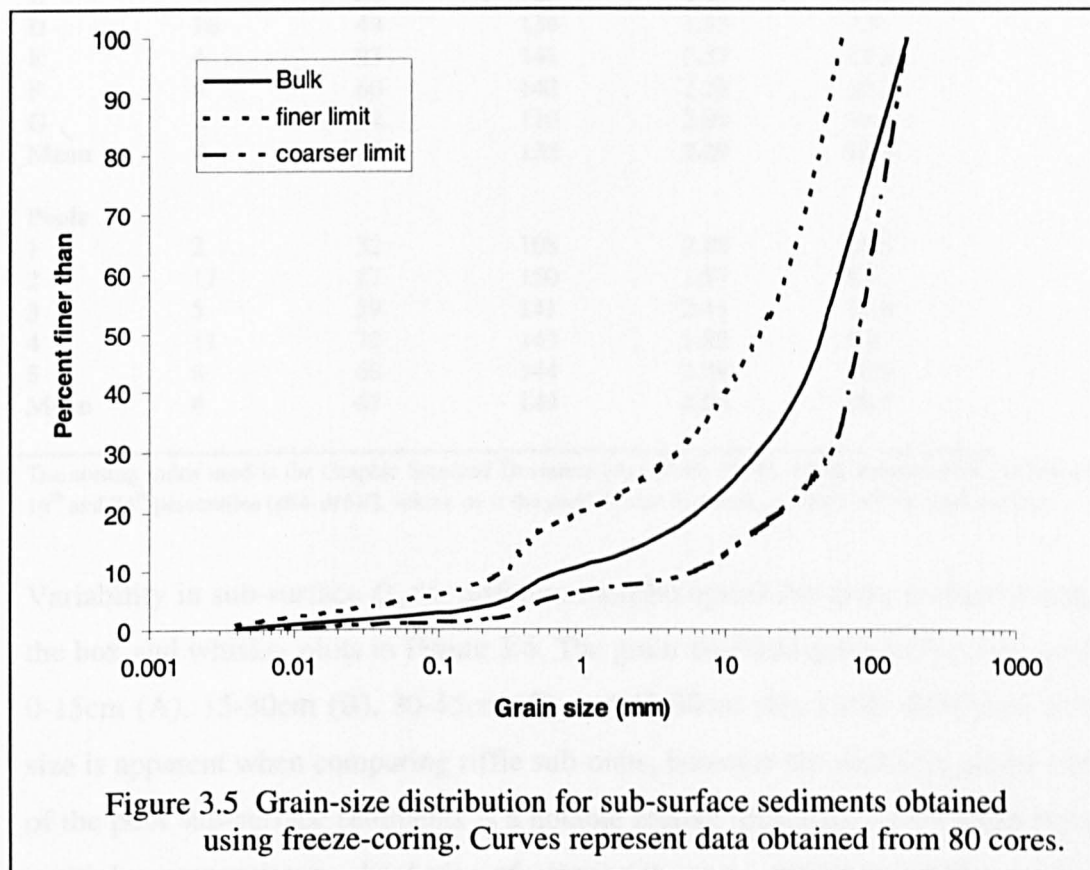


Figure 3.5 Grain-size distribution for sub-surface sediments obtained using freeze-coring. Curves represent data obtained from 80 cores.

of a dominant framework and sub-dominant matrix population resulted in a weakly bimodal grain-size distribution, and a framework-supported structure. Grain size statistics taken from these curves are summarised in Table 3.2. The sub-surface appeared considerably finer than the surface layer in riffles and pools, due to the presence of a matrix mode with between 7 and 19% (by weight). For example, the overall sub-surface D_{50} for riffles was 48mm in comparison to an armour D_{50} of 85mm. Sub-surface sediments tended to be more poorly sorted in comparison with the surface layer material, reflecting the presence of matrix material held in the framework voids (Milan *et al.*, 1999, Figure 7).

Table 3.2 Summary substrate grain-size characteristics

Site	D_{16}	D_{50}	D_{84}	Sorting	Matrix (%)
Riffles					
Control	3	34	116	2.64	15.2
A	3	37	137	2.76	15.6
B	4	49	134	2.53	11.9
C	4	50	153	2.63	12.3
D	16	49	134	1.53	7.7
E	4	93	141	2.57	12.3
F	6	60	142	2.28	10.2
G	2	34	110	2.89	19.3
Mean	4	48	133	2.29	12.8
Pools					
1	2	32	108	2.88	16.5
2	17	87	150	1.57	8.7
3	5	59	141	2.41	11.8
4	11	72	145	1.86	9.0
5	6	68	144	2.29	10.9
Mean	6	67	144	2.53	10.7

The sorting index used is the Graphic Standard Deviation (σ_G) (Folk, 1974), which measures the deviation of the 16th and 84th percentiles ($\phi_{84} - \phi_{16}$)/2, where ϕn is the particle size in ϕ units at which $n\%$ by mass is finer.

Variability in sub-surface D_{84} for different morphological sub-units is demonstrated in the box and whisker plots in Figure 3.6. The grain size data given is for core sections; 0-15cm (A), 15-30cm (B), 30-45cm (C) and 45-60cm (D). Little difference in grain size is apparent when comparing riffle sub-units, however the distinctly coarser nature of the pool sub-surface sediments is a notable feature throughout the sample depth. A multiple comparisons Analysis of Variance test revealed highly significant differences ($p<0.001$) between pools and all riffle sub-units at every depth sampled, whereas no significant differences were found between the median grain size of riffle sub-units.

3.3.6 The matrix

The matrix (sub 2 mm) generally accounted for between 7 and 19% (by weight) of the bulked core samples. Little overall difference was evident between the concentrations of fines in riffles or pools, however some differences were apparent when consideration was given to matrix concentrations within morphological sub-units at different depths within the bed (Figure 3.7). Pools consistently recorded lower concentrations of matrix in comparison to the riffle sub-units. Multiple comparisons analysis of variance revealed significant downstream differences between pools and riffle heads, crests and tails at 15-30cm ($p<0.001$), and riffle heads and tails at 45-

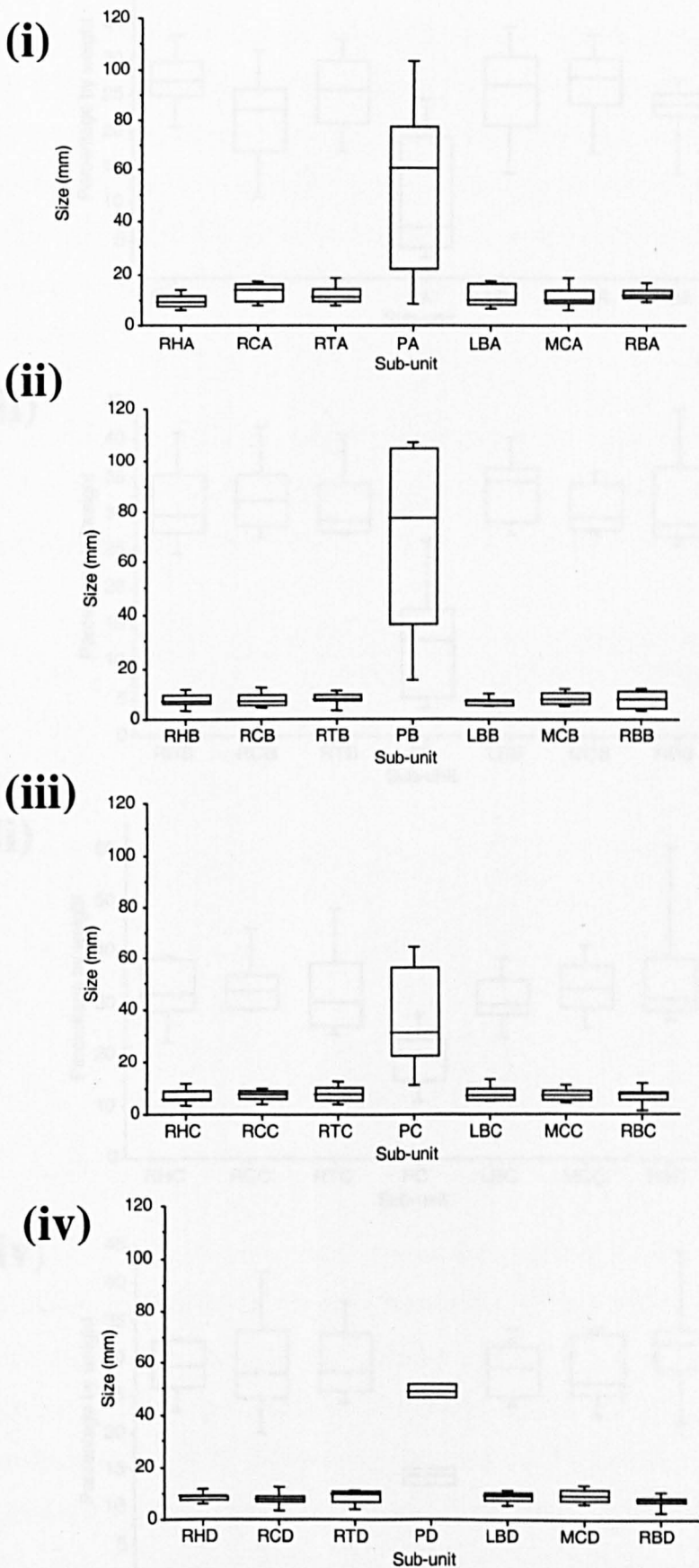


Figure 3.6 Variation in median grain size of sub-surface sediments for morphological sub-units for (i) 0-15cm (A), (ii) 15-30cm (B), (iii) 30-45cm (C), (iv) 45-60cm (D). RH-riffle heads, RC-riffle crests, RT-riffle-tails, P-pools, LB-left-bank, MC-mid-channel, RB-right-bank.

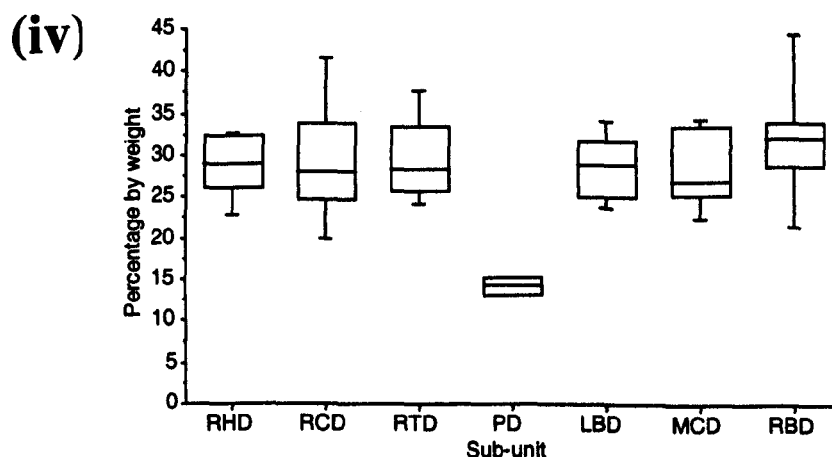
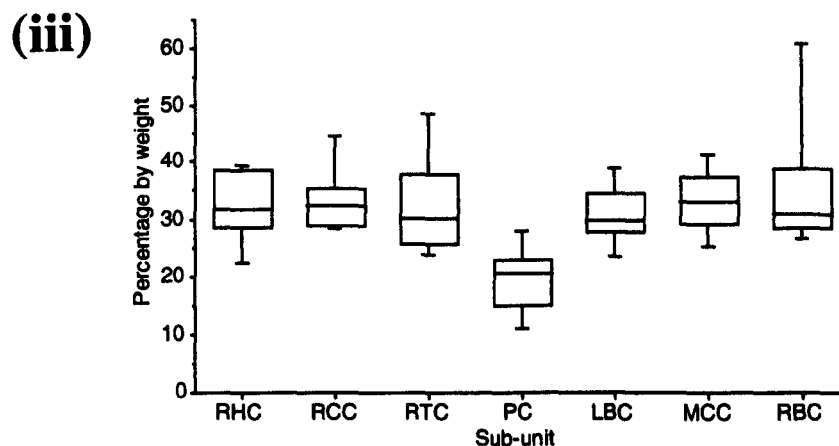
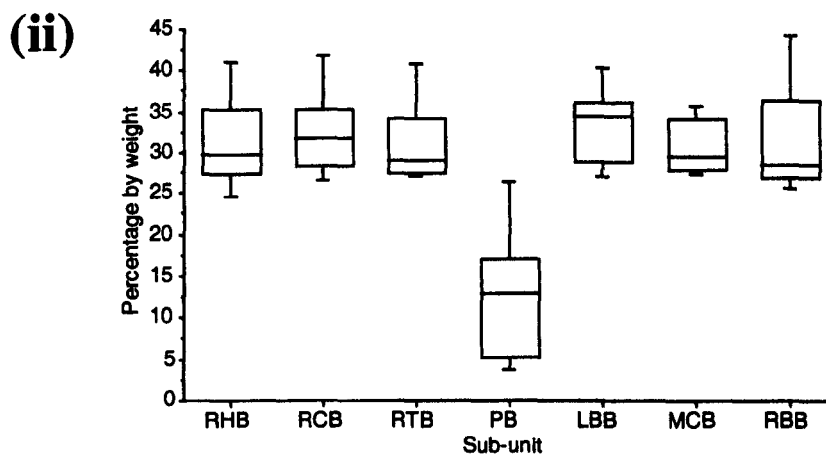
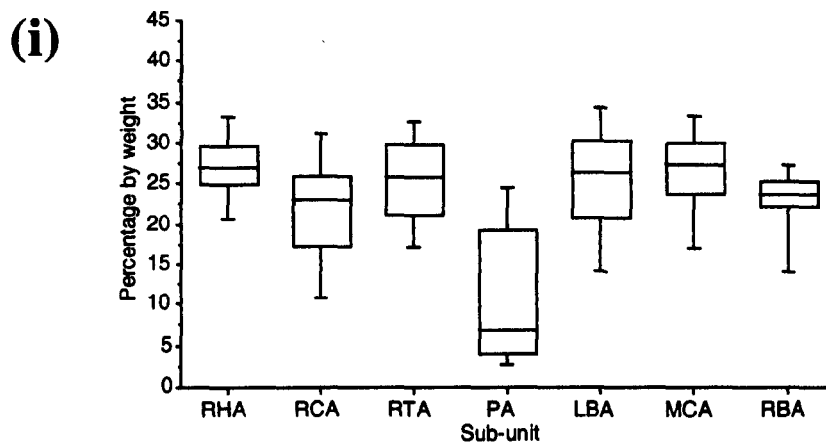


Figure 3.7 Variation in the percentage by weight of matrix (<2mm) sediments morphological sub-units for (i) 0-15cm (A), (ii) 15-30cm (B), (iii) 30-45cm (C), (iv) 45-60cm. RH – riffle head, RC – riffle crest, RT – riffle tail, P – pool, LB – left bank, MC – mid-channel, RB – right bank.

60cm ($p<0.001$). Cross-channel differences were also significant between pools and each cross channel sub-unit for the surface 0-15cm and 45-60cm ($p<0.001$), and for the left-and right-bank for 15-30cm. No significant differences were evident between the concentration of matrix sediments when comparing cross-channel riffle sub-units alone. Riffle crests and the right-bank tended, however, to contain slightly lower concentrations of fines, possibly reflecting hydraulic character in this region (see Chapter Four).

Table 3.3 presents the percent weight of sediment in each size fraction. Matrix sediments were dominated by sand-sized material with 79.9% on average (matrix in isolation). Silt and clay account for 17.1% and 3.0% respectively, with the dominant

Table 3.3 Summary of matrix size distribution of individual geomorphic units

Site	2-1	0.5-1	0.25-0.5	0.063-0.25	0.004-0.063	<0.004
Riffles						
Control	1.44	2.51	5.48	2.82	2.57	0.38
A	2.31	2.82	5.12	2.26	2.60	0.47
B	2.07	2.17	3.50	1.73	2.03	0.37
C	2.36	2.36	3.63	1.71	1.90	0.33
D	1.48	1.59	2.34	1.05	1.07	0.17
E	2.35	2.52	3.70	1.68	1.75	0.29
F	1.94	2.06	3.00	1.42	1.56	0.27
G	3.71	3.99	5.85	2.63	2.71	0.44
Mean	2.71	2.39	3.96	1.85	2.09	0.37
Pools						
1	1.88	1.93	4.21	4.48	3.51	0.49
2	1.17	1.00	2.41	1.71	2.05	0.40
3	1.53	1.54	3.16	2.18	2.77	0.57
4	1.13	1.36	3.20	1.70	1.43	0.22
5	1.31	1.55	3.59	2.12	1.97	0.32
Mean	1.36	1.35	2.99	2.12	2.34	0.44

size fraction in the 0.25-0.5 mm class. Overall the matrix sediments of riffles contain slightly greater proportions of material between 0.25 and 2.0 mm than the pools. Grain-size statistics for the matrix in isolation are presented in Table 3.4, where it appears that the median grain size of the matrix sediments (D_{50m}) of the pools are slightly coarser (D_{50m} of 0.22 mm on average) than the riffles (D_{50m} of 0.17 mm). The matrix sediments appear to be extremely poorly sorted for riffles, whereas pools are very poorly sorted. Variation in D_{50m} for morphological sub-units is demonstrated in Figure 3.8, where the coarser nature of the pools in comparison to the riffle sub-units is a feature found at every depth sampled within the bed. A further general feature is a

Table 3.4 Structure of matrix sediments in isolation

Site	D_{16}	D_{50}	D_{84}	Sort. _n
Riffles				
Control	0.03	0.18	0.60	2.2
A	0.01	0.16	0.60	3.0
B	0.00	0.15	0.61	4.6
C	0.00	0.13	0.56	4.6
D	0.00	0.12	0.55	4.6
E	0.00	0.13	0.50	4.5
F	0.00	0.14	0.56	4.6
G	0.03	0.13	0.50	4.1
Mean	0.00	0.17	0.60	4.6
Pools				
1				
2	0.02	0.24	0.76	2.6
3	0.02	0.22	0.73	2.6
4	0.02	0.19	0.62	2.5
5	0.02	0.20	0.64	2.5
Mean	0.02	0.22	0.77	2.6

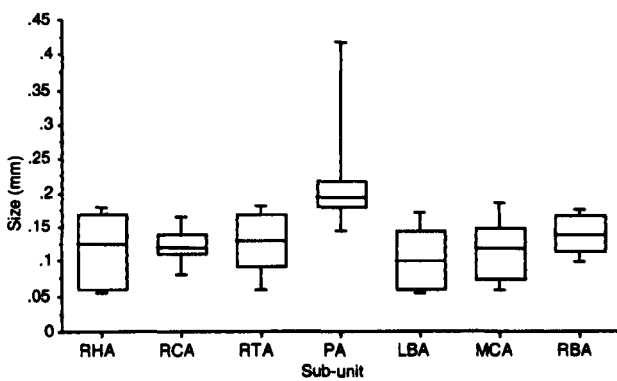
The sorting index used is the Graphic Standard Deviation (σ_0) (Folk, 1974), which measures the deviation of the 16th and 84th percentiles ($\phi_{84} - \phi_{16}$)/2, where ϕ_n is the particle size in ϕ units at which $n\%$ by mass is finer.

down riffle coarsening in matrix size and for the right-bank to have a coarser matrix for the surface 15cm. Multiple comparisons Analysis of Variance reveal however that differences between riffle sub-units and pools were not significant at the 0.001 level. However the matrix sediments found in riffle tails was found to be significantly coarser than riffle heads and crests ($p<0.001$).

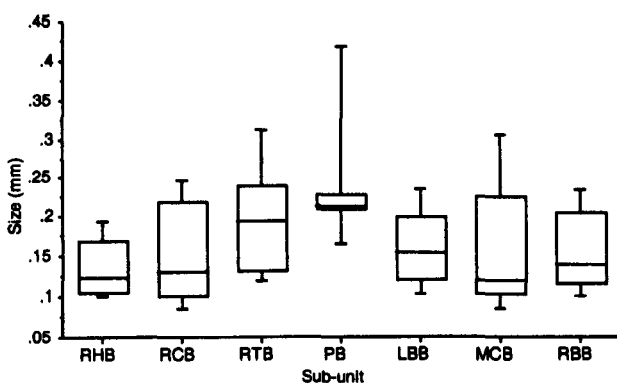
3.3.7 Riffle-pool scale vertical variability

Vertical variability in grain-size distribution for riffles and pools is demonstrated in Figure 3.9. The greatest difference in grain size characteristics appears to be between the surface sediments and the top 0-15 cm of substrate, which is evident for both riffles and pools. Surface coarsening (armouring) appears to be a feature in pools as well as riffles. Vertical grain-size characteristics (D_s and percentage matrix) for riffle sub-units and pools are demonstrated in more detail in the box and whisker plots (Figure 3.10 & 11), where the general pattern shown throughout the reach is for the surface 0-15 cm of substrate to be relatively coarse and have the lowest concentration of fine sediments, regardless of geomorphic sub-unit. The differences in median grain size between sub-surface sediment layers was not significant at the 99% level of confidence, however the coarse nature of the pool sub-surface sediments in comparison to the riffles is again evident (see Figure 3.10d). Differences in grain-size

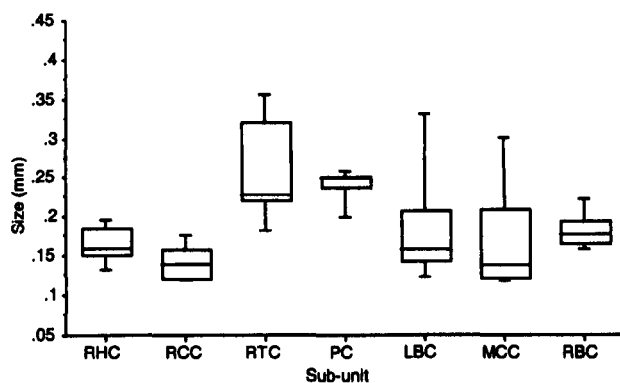
(i)



(ii)



(iii)



(iv)

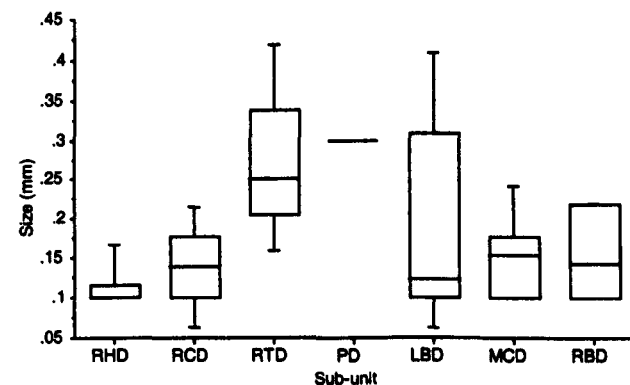
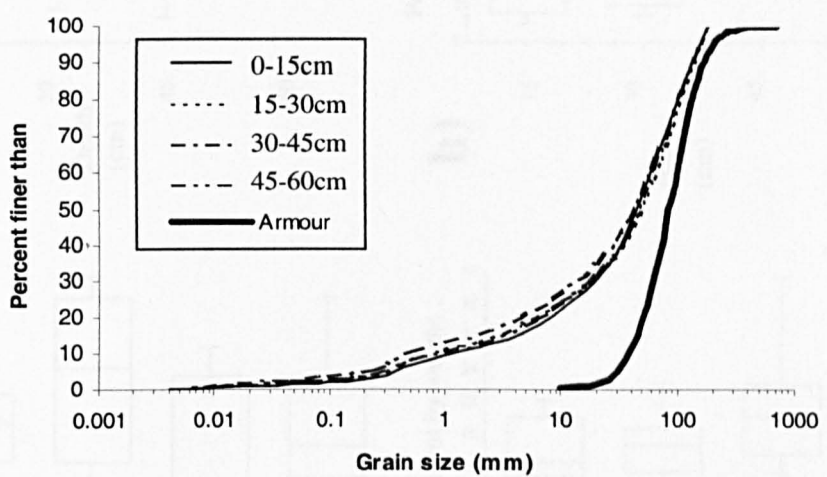


Figure 3.8 Variation in median grain size of matrix sediments for morphological sub-units for (i) 0-15cm (A), (ii) 15-30cm (B), (iii) 30-45cm (C), (iv) 45-60cm. RH – riffle head, RC – riffle crest, RT – riffle tail, P – pool, LB – left bank, MC – mid-channel, RB – right bank.

(a)



(b)

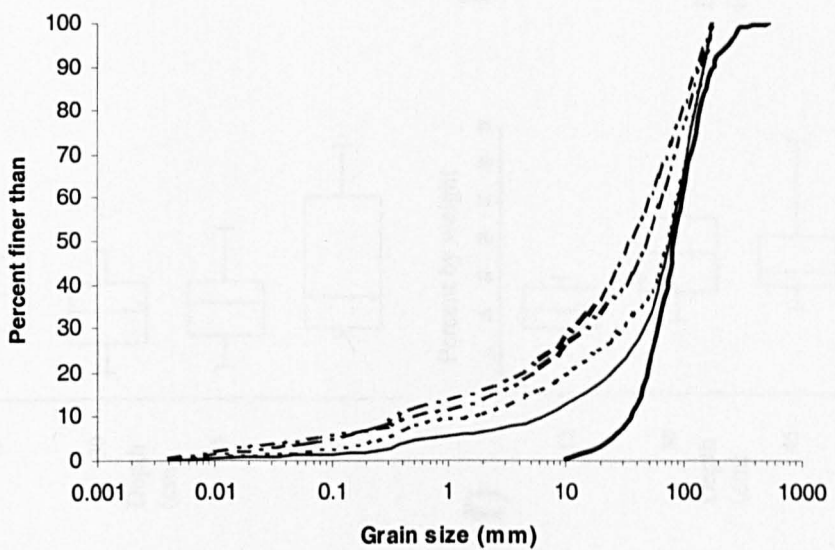


Figure 3.9 Grain-size distributions for the River Rede study reach for (a) Riffle and (b) pools. Armour layer data represent that of a 1050 stone sample, for riffles and a 500 stone sample for pools. Freeze-core data were obtained from an 80 core sample.

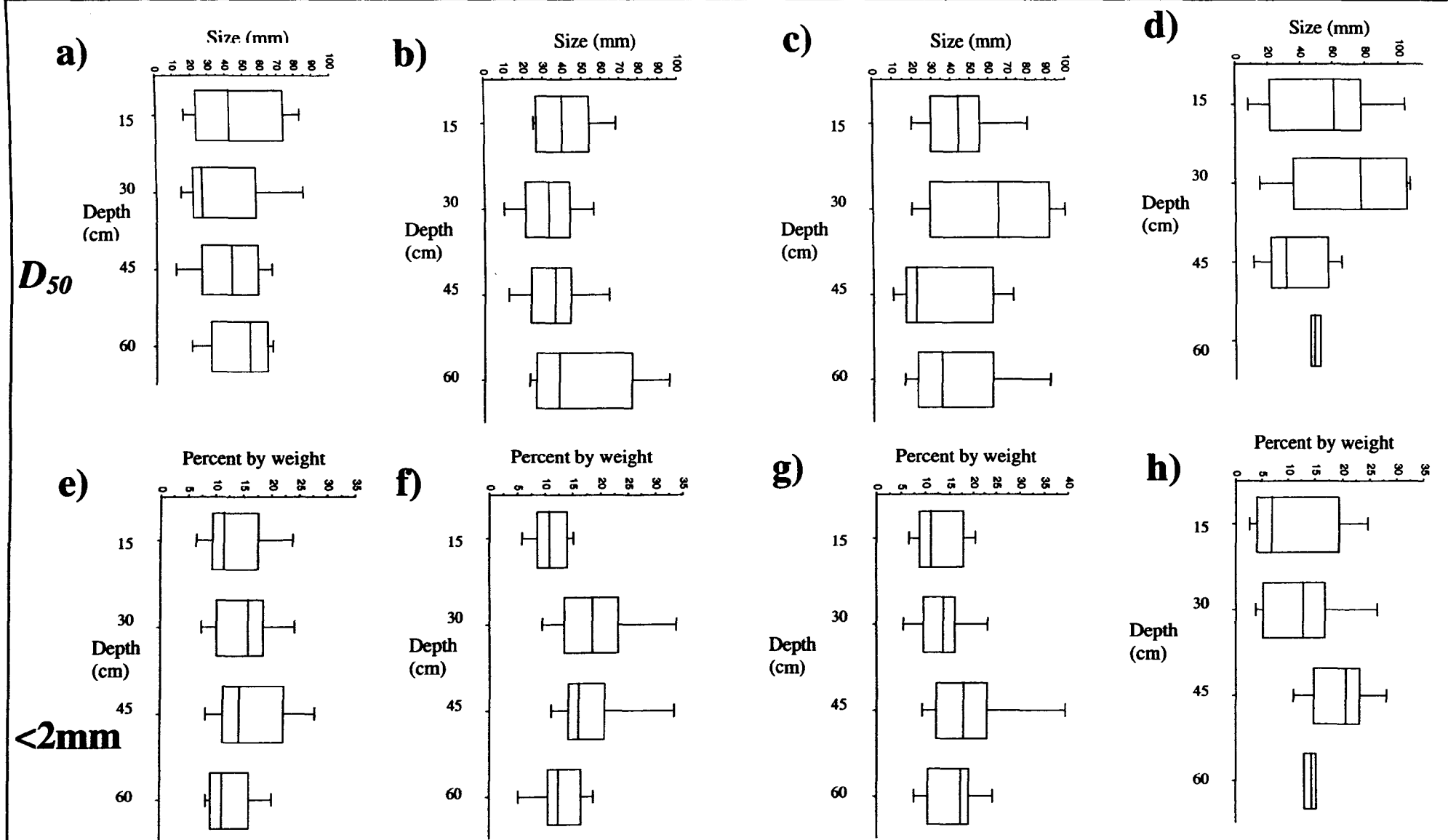


Figure 3.10 Vertical variation in median grain size for a) riffle heads, b) riffle crests, c) riffle tails, d) pools, and sub 2mm concentrations for e) riffle heads, f) riffle crests, g) riffle tails, h) pools

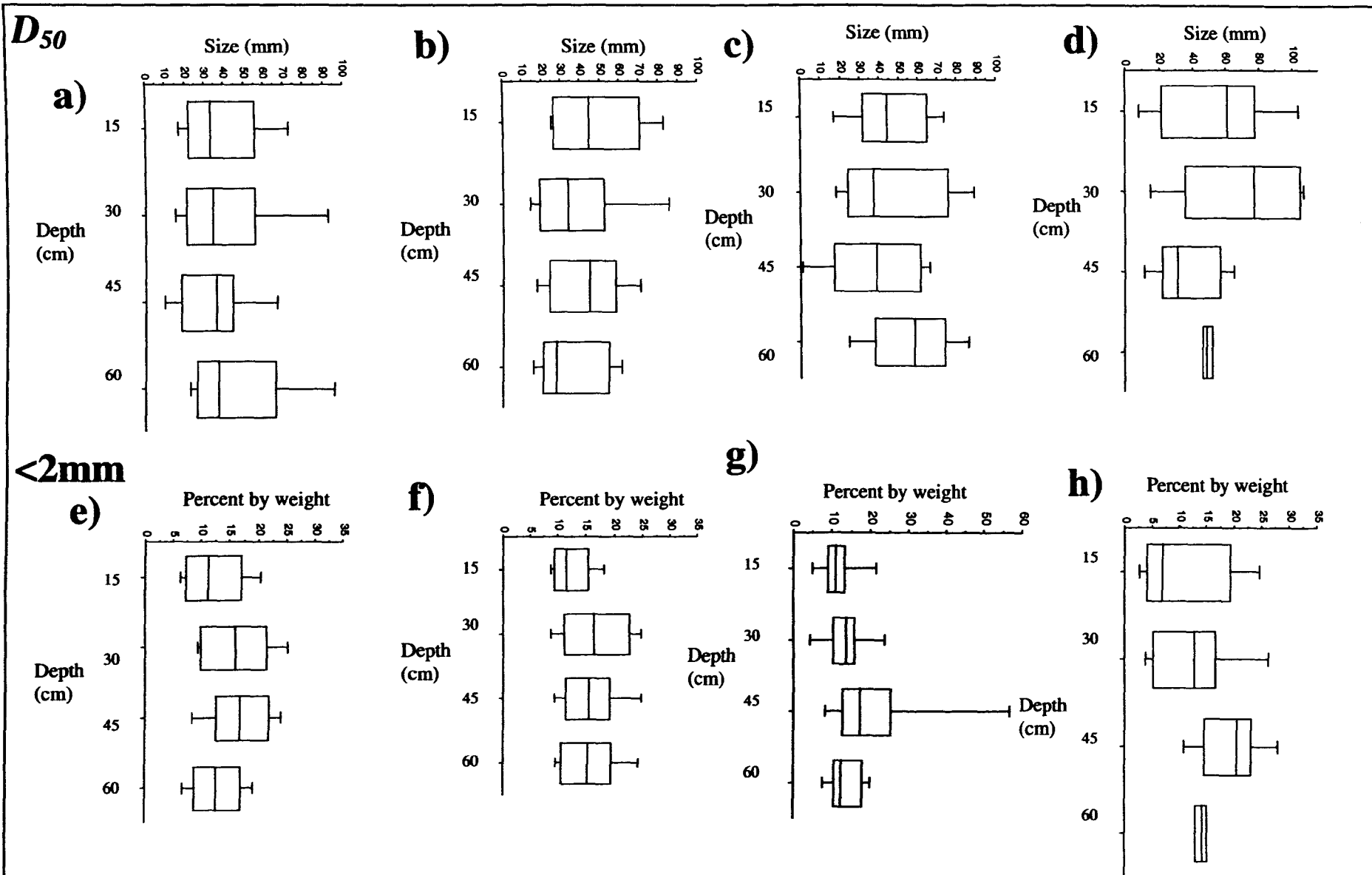


Figure 3.11 Vertical variation in median grain size for a) lef-bank, b) mid-channel, c) right-bank, d) pools, and sub 2mm concentrations for e) left-bank, f) mid-channel, g) right-bank, h) pools

characteristics between the riffle sub-units alone were not significant, with the exception of riffle tails (Figure 3.10c), where the near-surface 0-15cm of substrate of all other sub-units appeared to be coarser and had lower concentrations of matrix material in comparison to the 15-30cm layer. Beyond the 15-30cm layer, there appeared to be general coarsening, with the 45-60cm core sections recording similar D_s and matrix values to the near-surface sediments.

3.3.8 Bed compaction / strength

Variation in bed strength for morphological sub-units is summarised for the whole reach in the box and whisker plots (Figure 3.12). It may be seen that riffle crests and tails have the greatest overall compaction, whilst bar tails appear to accumulate the softest sediment fabric. Low compaction reflects the fine grain size and poor sorting of sediments found at bar tails. Also noticeable is that pools tend to have lower compaction than riffles, although application of a multiple comparisons Analysis of Variance did not reveal this difference to be significant at the

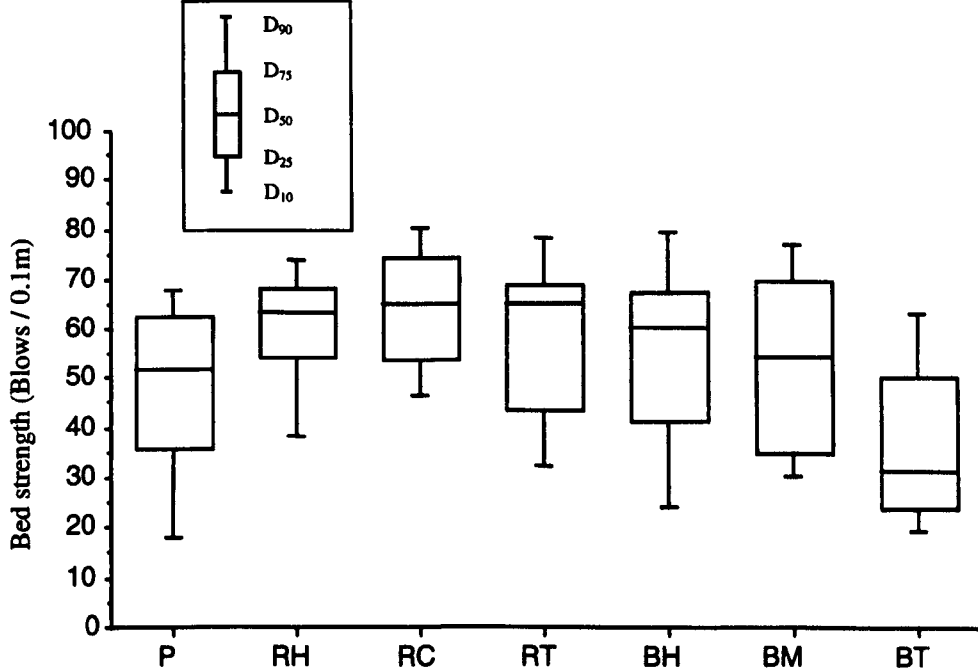


Figure 3.12 Variation in bed strength / compaction for different morphological sub-units; P-pools, RH-riffle heads, RC-riffle crests, RT-riffle tails; BH-bar heads, BM-bar midpoints, BT-bar tails..

99% level. In contrast, riffle heads, crests and bar midpoints were found to be significantly more compact than bar tails ($p<0.001$).

Variation in bed structure may be observed in more detail with reference to the contour plots in Figures 3.13, 3.14 and 3.15 which demonstrate the spatial variability in bed structure (obtained from the cone penetrometer readings) throughout the Rede study riffle-pool sequence. Overall it is the upstream part of the reach that displays the lowest compaction compared to readings obtained from the lower part of the study reach. Figure 3.13 demonstrates bed compaction for the upstream end of study reach, incorporating Pool 1, Riffle B and Pool 2, Point Bar 1 and Point Bar 2. Apart from a small area of bank collapse on the outer bank of the meander bend at Pool 1, the two least compact bed surfaces are found on exposed bar surfaces, where fine gravels and sands dominated sediments. Considering the permanently submerged zones, the most compact area appears towards the head of the riffle (A) and Pool 2, whilst the softest area is located at the tail of the riffle, with the crest being of intermediate compaction. Moving further downstream, the most compact area of Riffle 2 may be found around the crest area (Figure 3.14), whereas the head, tail, and Pool 3 seem to be slightly less compact. The most compact section of the whole reach is found on Riffle C (Figure 3.15), which is probably a reflection of the higher energy gradient in this area promoting armouring (see Figure 2.16). As freeze-core evidence suggests, gravel was very thin in places (<15cm) across Riffle C, overlying boulder clay. The bed strength properties in this zone therefore could reflect the influence of the underlying boulder clay rather than fluvial sediment. The head and tail of Riffle C exhibit slightly lower compaction in comparison to the crest, similar to that shown for Riffle B. Cross channel variability in compaction at Riffle C was also evident with the channel centre showing greater compaction in comparison to the channel margins. Pool 4 displays lower compaction.

3.4 Discussion and conclusions

The objective of this part of the research project was to identify the extent and pattern of sedimentological variability within the study reaches in order to provide baseline information on sediment sorting patterns through a riffle-pool sequence. Sediment

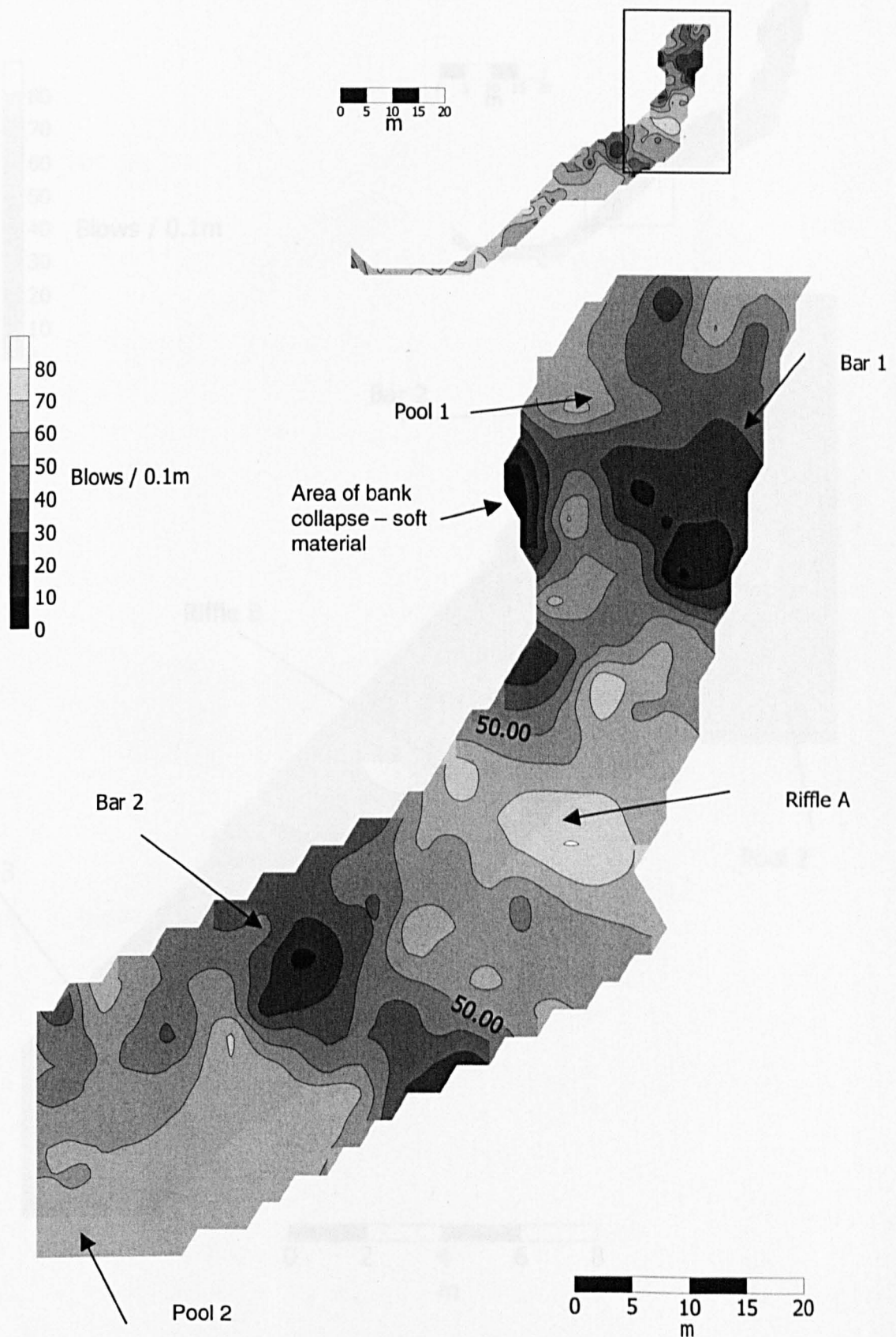


Figure 3.13 Contour plot of bed compaction for the upstream section of site; pool 1, riffle 1, pool 2.

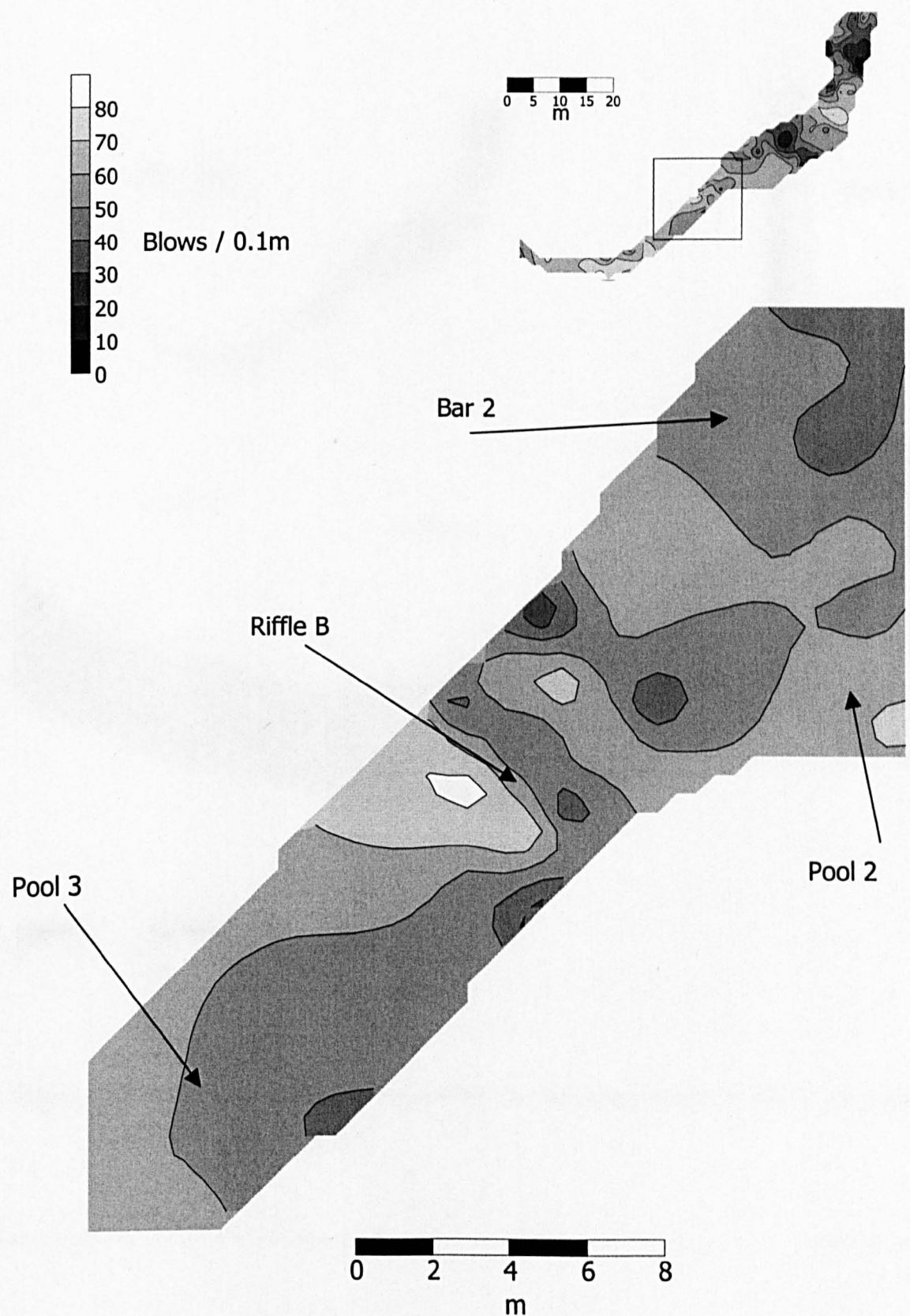


Figure 3.14 Contour plot of bed compaction for the middle section of the study site: pool 2, riffle B, pool 3.

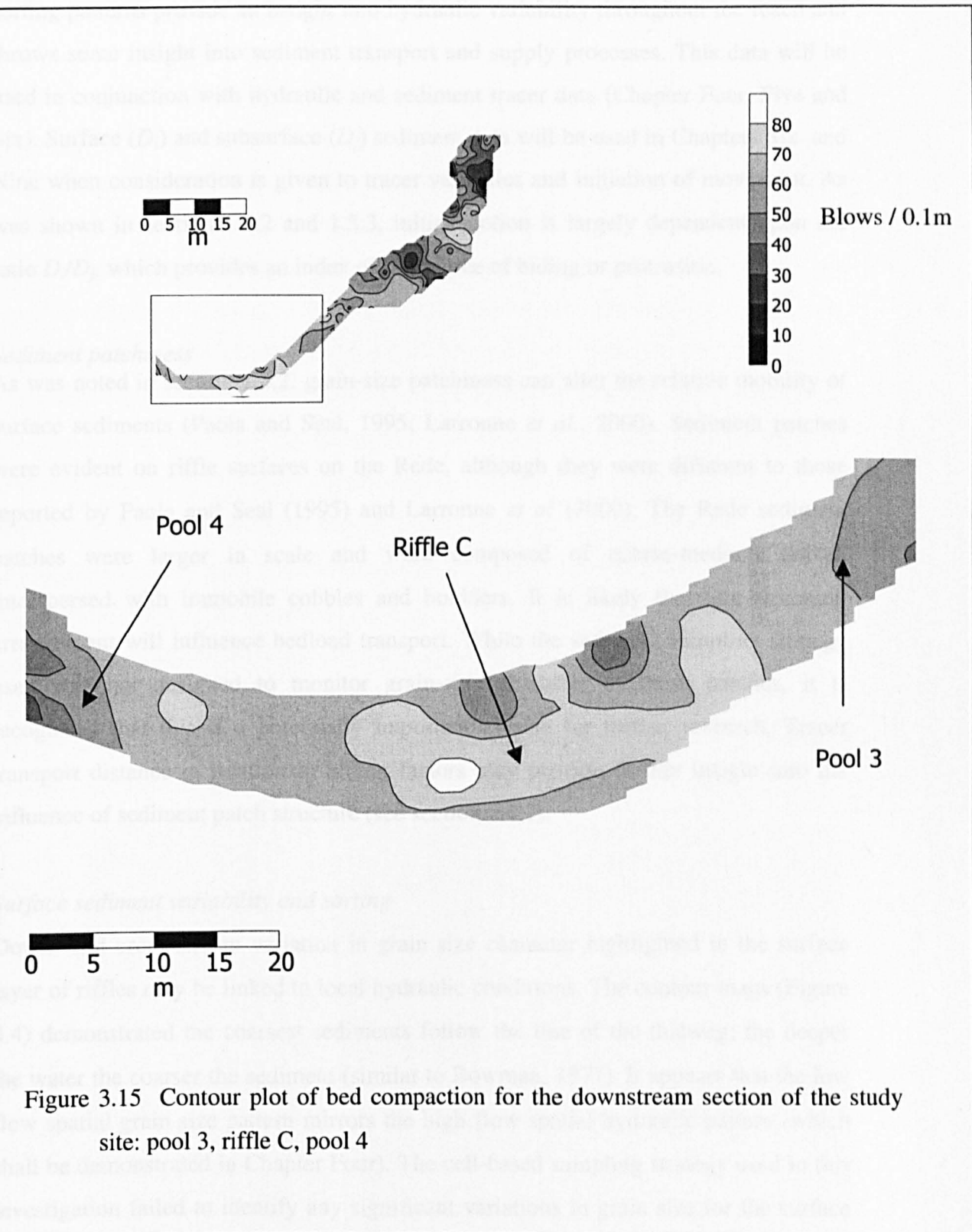


Figure 3.15 Contour plot of bed compaction for the downstream section of the study site: pool 3, riffle C, pool 4

sorting patterns provide an insight into hydraulic variability throughout the reach and throws some insight into sediment transport and supply processes. This data will be used in conjunction with hydraulic and sediment tracer data (Chapter Four, Five and Six). Surface (D_i) and subsurface (D_j) sediment data will be used in Chapters Six and Nine when consideration is given to tracer velocities and initiation of movement. As was shown in section 1.5.2 and 1.5.3, initial motion is largely dependent upon the ratio D_i/D_j , which provides an index of the degree of hiding or protrusion.

Sediment patchiness

As was noted in section 1.4.2, grain-size patchiness can alter the relative mobility of surface sediments (Paola and Seal, 1995; Larronne *et al.*, 2000). Sediment patches were evident on riffle surfaces on the Rede, although they were different to those reported by Paola and Seal (1995) and Larronne *et al* (2000). The Rede sediment patches were larger in scale and were composed of coarse-medium gravel, interspersed with immobile cobbles and boulders. It is likely that this structural arrangement will influence bedload transport. While the sediment sampling strategy used was not designed to monitor grain-size character of these patches, it is recognised that this is a potentially important avenue for further research. Tracer transport distance in relation to hiding factors may provide further insight into the influence of sediment patch structure (see section 6.4.1).

Surface sediment variability and sorting

Down- and cross-stream variation in grain size character highlighted in the surface layer of riffles may be linked to local hydraulic conditions. The contour maps (Figure 3.4) demonstrated the coarsest sediments follow the line of the thalweg; the deeper the water the coarser the sediment (similar to Bowman, 1977). It appears that the low flow spatial grain size pattern mirrors the high flow spatial hydraulic pattern (which shall be demonstrated in Chapter Four). The cell-based sampling strategy used in this investigation failed to identify any significant variations in grain size for the surface sediment within-riffles, however strong differences were found between pools and riffles. Pools appeared coarser than riffles in the surface and sub-surface layer, a feature less commonly reported in the literature. Coarse immobile lag deposits have been reported in several early studies (e.g. Gilbert, 1914, Hack, 1957) which have

been later explained by Leopold *et al.* (1964) to result from the erosion of bank materials. Keller (1982) suggests that in streams with a very low supply of fine bed material, pool troughs may scour into basal till or expose bed rock. A similar explanation was also used in a later study by Ashworth (1987). An alternative explanation would be that coarse clasts are transported into the pool, as implied by Thompson *et al.* (1996) in a tracer study. Tracer data presented in Chapter Eight should elucidate the sorting mechanisms operating in the Rede channel and whether clasts are deposited in pools. Without tracer information, observations on the Rede suggest that relict deposits become exposed as a result of erosion on the outer bank of a meander bend (Plate 3.3). Some of this material may be too coarse for contemporary flows to transport, or may be transported only very occasionally, whereas the finer gravel is flushed onto the downstream riffle at high flow. Coarse pool sediments also provide an indication of the sediment supply dynamics within the Rede. Lisle and Hilton (1992; 1999) have demonstrated that sand drapes develop on pool exit slopes where the supply of this material is high, whereas drape development is poor in supply limited situations. This would suggest therefore that that fine bedload is strictly supply-limited in the Rede channel. Instead of pools acting as low flow storage zones, fine gravel and sand appears to accumulate on bar surfaces as found by Laronne and Duncan (1992) and Mosely and Tindale (1995) in their studies.



Plate 3.3 Lag deposits in Pool 1, river Rede. Coarse clasts drop into pool

Hydraulic character

The observed low-flow grain-size character can also provide some insight into the hydraulic character of the Rede riffle-pool sequence. Some workers contend that if the pools are zones of maximum competence at peak discharge - following Keller's (1971) model, then they should display the coarsest surface sediments (e.g. Bhowmik and Demmissie, 1982a; Thompson *et al.*, 1999). It may be postulated therefore that the finer grain sizes usually reported for pools (see Table 1.1) are a result of finer deposits winnowed from the upstream riffle during lower discharges in streams with a high sand supply. This calls in to question the issue of sediment sampling time in relation to the flood hydrograph. In order to measure the grain size that reflects maximum competence in a stream with a high sediment supply, sampling would have to be conducted during high flow.

Vertical variability

Vertical variability in bed structure is a common feature in gravel-bed rivers (see sections 1.4 and 1.7), with the surface layer usually displaying coarser characteristics in comparison to the sub-surface (Gomez, 1984). Considerable vertical variability was found in grain size and matrix concentrations, especially between the surface and sub-surface sediments, and a coarsening upward sequence was usually evident in the 45-0cm zone in the sub-surface sediments. Greatest concentrations of fine sediments are usually found at a depth >15 cm below the bed surface. The 0-15 cm layer of sub-surface sediment is relatively free of fine matrix in both riffles and pools, although pools contain the lowest concentrations. Significant within-riffle variation was evident for the 0-15cm layer's matrix sediments, where riffle tails were found to be significantly coarser than riffle heads. Low flow modification in the form of lateral and vertical winnowing may play a significant role in determining the observed spatial pattern in grain size, where the matrix (particularly the finest grades: clay and silt) are preferentially flushed from gravel voids (Dietrich *et al.*, 1989; Parker and Klingeman, 1982). Armouring is enhanced when sediment supply is low; however armouring is reduced when sediment supply is increased (Dietrich *et al.*, 1989). Armouring has implications for sediment mobility; under equilibrium transport conditions, surface coarsening through vertical winnowing may equalise the mobility of different sizes by counterbalancing the intrinsic lesser mobility of relatively coarse

particles (Parker *et al.*, 1982b; Andrews and Parker, 1987). Fine sediment development is described in Chapter Seven and will provide further insight into fine sediment sorting mechanisms and the winnowing process.

Grain shape

Clifford (1993) has suggested that sorting via grain shape may be more important than size sorting. Teisseyre (1984) has also highlighted shape sorting in response to three-dimensional flow. Ashworth and Ferguson (1989) and Li and Komar (1986) have found that sphericity has a significant positive influence on travel distance, whereas Schmidt and Ergenzinger (1992) have suggested particle elongation to be important with greater travel distances for rod-shaped clasts. The Rede data and some other studies have failed to demonstrate significant shape differences between riffles and pools (e.g. Sear, 1992). It is unlikely therefore that grain shape sorting is a very important process on the Rede. This supposition is tested with tracer data in section 6.3.3.

Bed structure

Sear (1996) suggests that differences in bed structure may be a significant factor in determining differential mobility between riffle and pool sediments. Differences in bed structure between morphological sub-units on the Rede were identified, with riffles being the zones of maximum bed strength, and bar tails zones of least bed strength. Pools were found to have lower bed strength in comparison with riffles. This finding is similar to that of Sear (1996) who demonstrated that riffle sediments were more tightly packed and exhibited a higher frequency of stable sediment structures, whereas pool sediments were loosely packed and relatively low in structure. This spatial pattern in sediment structure may be explained through sorting processes. During high frequency low and intermediate discharges, the riffle areas experience chaotic, turbulent flows that develop structure through *in situ* particle vibration and sporadic particle motion (Sear, 1996). During low flow, vertical and lateral winnowing of fines from the surface gravel may occur. Fines which infiltrate intragravel voids can act to cement gravel framework clasts together (Reid and Frostick., 1984; Frostick *et al* ., 1984). This along with the increased coarseness of the surface layer results in greater compaction. Bar tails appear to act as accumulation

zones for winnowed fines on the waning limb of the hydrograph (Laronne and Duncan, 1992). The sediments in this sub-unit are poorly structured and loosely arranged. Pool surface particles were not cemented together with matrix or lodged in a tight / imbricated structure like the riffle sediments. Low pool shear stresses at low flow and fine sediment starvation from the upstream riffle may reduce the likelihood of infiltration of fines and cementation of coarse particles in pools, and may further explain the low compaction readings obtained in the cone penetrometer survey. Sear (1996) further suggests that the poorly developed bed structure in pools may reflect (i) lack of turbulent flow at low discharges, and (ii) the relatively narrow shear stress fields required to entrain pool material. Consequently clasts located on riffles are likely to exhibit higher entrainment thresholds (θ_c) which act to maintain these units as topographic highs, whilst sediments in pools tend to be mobilised at discharges below those necessary to mobilise riffle sediments. Although Sear's (1996) model is significant in the maintenance of some riffle-pool sequences, it is unlikely that differences in bed structure between riffles and pools is the only mechanism responsible. In situations where the pool sediments are coarser than the riffles, as found on the River Rede, the grain size could potentially counteract the reduced compaction effect. Furthermore, variability in pool morphology, particularly the angle of the pool exit slope, is known to influence the size of material leaving the pool (Thompson *et al.*, 1998). Even though the pool bed may be less compact compared to the riffle, a higher shear stress may still be required to transport the coarse pool grains over the positive gradient of the exit slope, compared to the shear stress required to move a similar sized grain the same distance on a riffle. Attention must also be given therefore to hydraulic and sediment routing models, however further attention to Sear's (1996) hypothesis is given in Chapter Six.

Boulders and pool initiation

Some boulders are evident in the bed sediments of the Rede which are probably derived from glacial processes. These could have the potential of initiating pools in the manner described by Clifford (1993a). However this is unlikely as coarse boulders tended not to be observed in the region of pools found at the Rede site.

3.5 Summary

- 1) Riffles on the River Rede are composed of patches of medium-coarse gravel which are separated by occasional coarse immobile boulders. Pools are covered by coarse lag gravel, and bars appear to store the full mobile grain-size range, including sand;
- 2) Pools are significantly coarser ($D_s = 110\text{mm}$) ($p<0.001$) than riffles ($D_s = 85\text{mm}$) in the Rede channel, and bars display the finest characteristics ($D_s = 50$);
- 3) In comparison with riffles and bars the surface sediments of pools were slightly better sorted on average;
- 4) Pool matrix sediments are also coarser and better sorted ($D_s = 0.22\text{mm}$) than riffle matrix sediments ($D_s = 0.17\text{mm}$), although this is not statistically significant;
- 5) Riffle tails were significantly coarser than riffle heads ($p<0.001$), and there was a tendency for the right-bank sub-surface sediments to contain coarser matrix material in comparison to the left bank and mid-channel, however this was not found to be statistically significant;
- 6) The sub-surface sediments were much finer (18mm compared with 85mm) than the surface as they contained both a significant proportion (17-26%) of matrix material;
- 7) Riffle heads, crests and bar midpoints were found to be significantly more compact in comparison to bar tails ($p<0.001$).

Chapter Four discusses the stage-dependent hydraulic character of the Rede riffle-pool sequence and discusses the implications of this upon the observed sediment sorting pattern shown in Chapter Three. In particular, Keller's reversal hypothesis is tested as a mechanism for maintaining riffle-pool morphology.

Chapter Four

Hydraulic characteristics of the Rede riffle-pool sequence

4.1 Introduction

The hydraulic character of the riffle-pool sequence has been used to explain sediment sorting and maintenance of the unit (Carling, 1991; Bhowmik and Demissie, 1982; Clifford and Richards, 1992). As was described in section 1.3.4, Keller (1971) proposed a velocity reversal hypothesis which has remained the key theory as to the maintenance of the riffle-pool form. However, as highlighted by Milan *et al.* (2001), and in section 1.3.4, the theory has been the subject of considerable debate. This Chapter will contribute to this debate by providing high-resolution data concerning the spatial variation in velocity and boundary shear stress (tractive force) with stage. Here, cross-section average velocity data is presented for 21 discharges, ranging from baseflow to over bankfull and is used to test Keller's hypothesis for the Rede. Greater spatial resolution is then provided concerning tractive force variability over the discharge range by using boundary shear stress for five flows (including one at bankfull). Hydraulic data of this nature will help to explain the observed sediment sorting patterns discussed in Chapter Three, and tracer movements which are presented in Chapters Seven and Eight. The data are then used to predict trap-specific and clast specific hydraulics to provide information on grain mobility in Chapters Five and Six.

4.2 Methods and extent of the Rede hydraulic data set

A variety of measures was used to quantify the spatial variability in hydraulics with stage, namely (i) cross-section averaged velocity, (ii) near bed velocity, (iii) profile-averaged velocity, (iv) point τ (from velocity profiles), (v) mean τ (from the Du Boys equation, substituting d for R), and (vi) point τ (estimated from the Du Boys equation). The methods used to obtain data for these various measures of flow hydraulics have been described in section 2.6. The measurements taken for the Rede provide a comprehensive data set concerning stage dependent hydraulics through

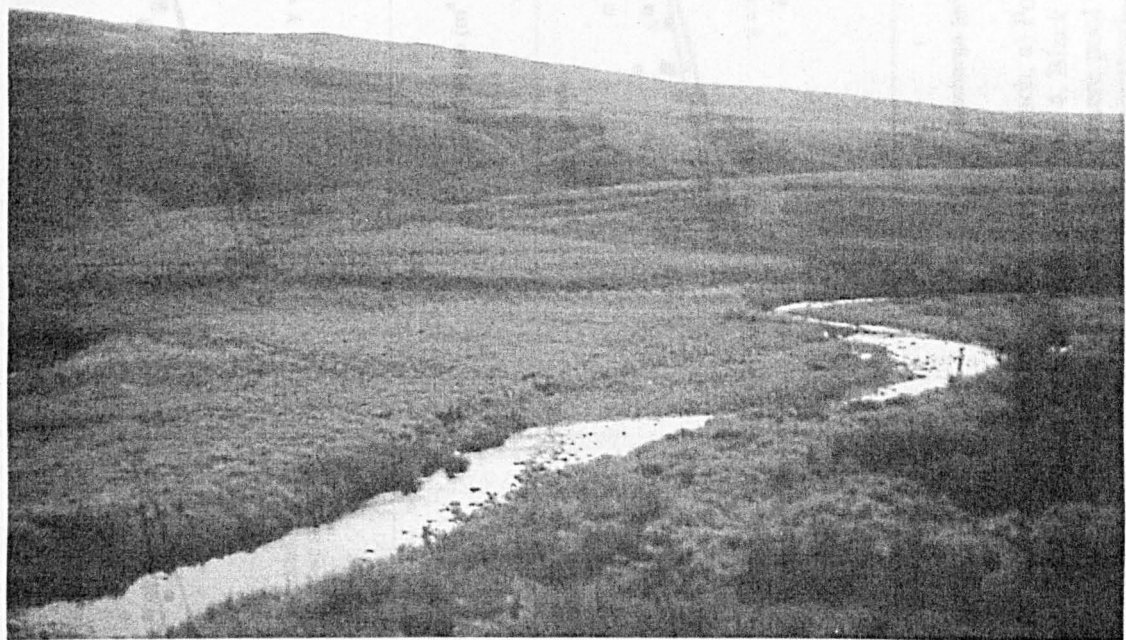
riffle-pool sequences, with data obtained across the full flow range from baseflow ($0.1 \text{ m}^3 \text{ s}^{-1}$) shown in Plate 4.1a, to over bankfull, ($10 \text{ m}^3 \text{ s}^{-1}$) shown in Plate 4.1b.

4.3 Results

4.3.1 Cross-section averaged velocity

Figure 4.1 demonstrates the relationship between cross-sectionally averaged velocity data and discharge for six riffle-pool units throughout the study reach. Velocity-discharge relationships for the other twenty-four cross-sections situated throughout the Rede riffle-pool sequences are presented in Appendix 4.1. Marginal shear stress reversals are evident for four out of the six riffle-pool units (Figures 4.1c-f). In the middle of the reach reversal in velocity occurs when flows exceed around one-third bankfull at $2-3 \text{ m}^3 \text{ s}^{-1}$ (Figure 4.1 c and d), whereas further down the reach a reversal occurs at bankfull discharge at $7-9 \text{ m}^3 \text{ s}^{-1}$ (Figure 4.1e and f). A reversal is not evident at the upstream-most part of the reach between Pool 1-Riffle A and Riffle A-Pool 2, however there is a velocity equalisation at around bankfull. Log-log regressions of the form $v = aQ^b$, presented on Figure 4.1 consistently indicate steeper slope exponents (b) for the pool data, suggesting that pool velocities increase at a faster rate as discharge rises in comparison to the riffles. It is evident that deviation from the log-log relationship is evident particularly at the highest three flows measured. Although the velocity data provides useful information, limitations are encountered due to its cross-section averaged nature. For example, close to bankfull there appears to be a slight reduction in the rate at which velocity increases as discharge progressively rises, which may possibly reflect over-spill on to bar surfaces or on to the floodplain. Furthermore, the increase in wetted cross-sectional area as bar surfaces are drowned may prevent cross-section average velocity reversal occurring at some pool-riffle units (e.g. Pool 1-Riffle A), even though the central core of velocity within the pool trough may exceed that of the adjacent riffles. The boundary shear stress data overcomes these drawbacks to an extent by providing a finer resolution, taking into

a)



b)



Plate 4.1 The Rede riffle-pool sequence at a) low flow ($\approx 0.1 \text{m}^3 \text{s}^{-1}$) August 1995, (b) high flow ($\approx 5 \text{m}^3 \text{s}^{-1}$) May 1996

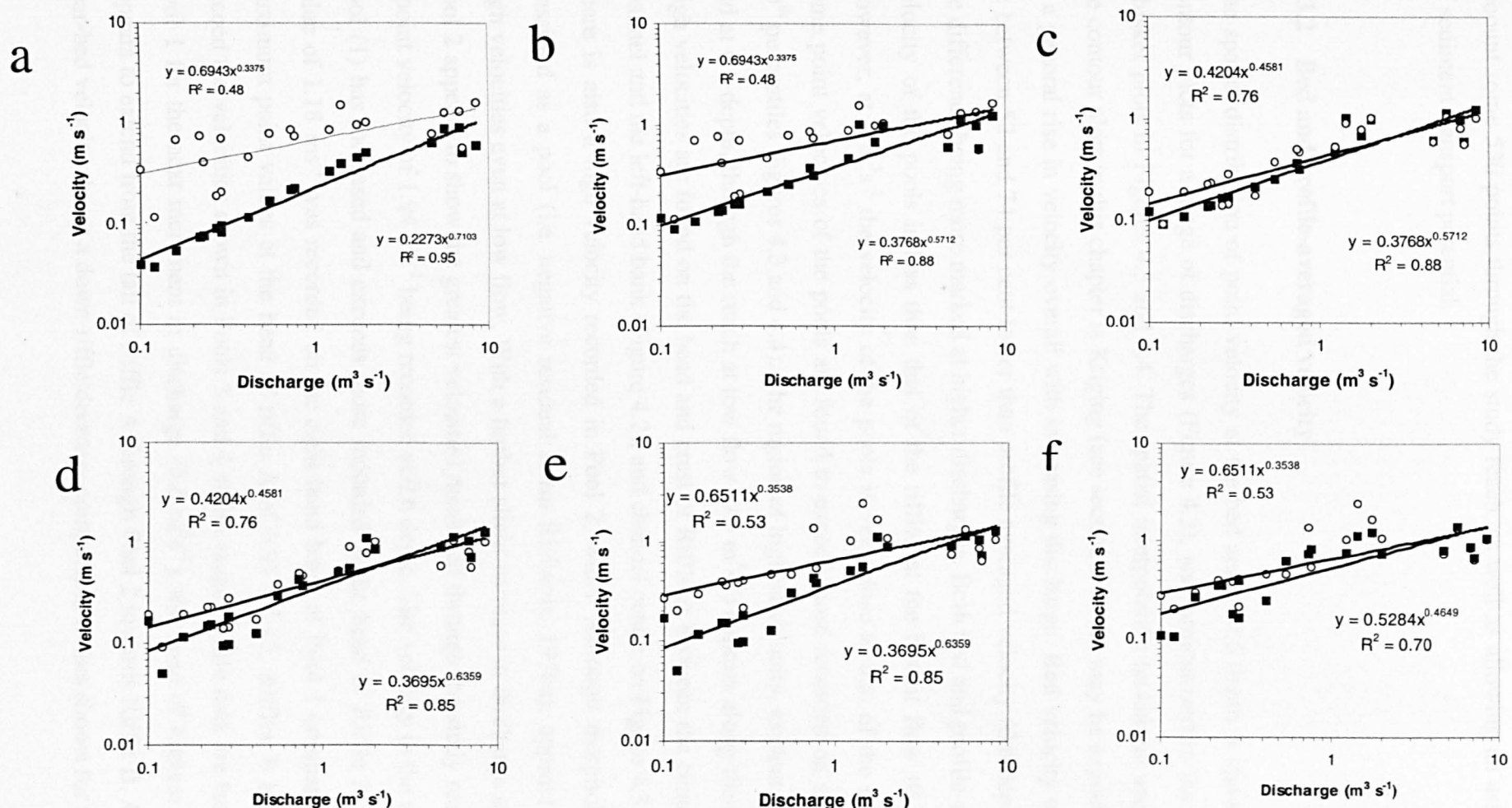


Figure 4.1 Cross-section averaged velocity pattern with increasing discharge for six riffle-pool units throughout the study reach, a) Pool 1 and Riffle 1, b) Riffle 1 and Pool 2, c) Pool 2 and Riffle 2, d) Riffle 2 and Pool 3, e) Pool 3 and Riffle 3, f) Riffle 3 and Pool 4. Black squares represent pool data, open circles represent riffle data. Velocity reversal is evident for four out of six riffle-pool units, where pool velocities exceed riffle velocities at high discharges. Log-log regressions ($p < 0.001$) indicate greater slope exponents for pools, demonstrating a greater rate of increase in velocity in comparison to the riffles for a given rise in discharge.

account some 530 points through the study reach, as well as allowing an assessment of sediment transport potential.

4.3.2 Bed and profile-averaged velocity

The spatial distribution of point velocity at the bed and at 0.6 depth is shown in the contour plots for a range of discharges (Figure 4.2), and summarised in the box and whisker plots in Figures 4.3 and 4.4. The spatial interpolation technique used for all the contour plots in this chapter is Kriging (see section 2.7). As may be expected there is a general rise in velocity overall with increasing discharge. Bed velocity tended to be between 52 and 74 per cent lower than profile averaged velocity (0.6 depth), with the difference being more marked at higher discharges. Both bed and profile-averaged velocity of the pools is less than that of the riffles at the lowest flow ($0.3 \text{ m}^3 \text{s}^{-1}$). However, at $1 \text{ m}^3 \text{s}^{-1}$ the velocity of the pools is very close to that of the riffles and some point velocities of the pools are found to exceed those recorded on riffles (see 90th percentiles Figures 4.3 and 4.4). The region of highest velocity, evident at the bed and at 0.6 depth, through the reach at low flow ($0.3 \text{ m}^3 \text{s}^{-1}$) appears along the thalweg. High velocities are found on the head and crest of Riffle A between the centre of the channel and the left-hand bank (Figure 4.2), and channel centre on Figure 4.3 and 4.4. There is also a high velocity recorded in Pool 2, which although morphologically classified as a pool (i.e. negative residual *sensu* Richards, 1976a), appears to have high velocities even at low flow. With a further slight increase in discharge to $1 \text{ m}^3 \text{s}^{-1}$, Pool 2 appears to show the greatest velocities measured through the study reach, with a point velocity of 1.94 ms^{-1} being recorded at 0.6 depth. The velocity in the upstream pool (1) has increased and exceeds those recorded at the head of Riffle A. A point value of 1.18 ms^{-1} was recorded on the right hand bank of Pool 1 compared with a maximum point values at the head of riffle A of $0.95 \text{ m}^3 \text{s}^{-1}$. Riffles B and C still exceed the velocities shown in Pools 3 and 4 at this stage. While data are lacking for Pool 1 for the next increment in discharge ($3.6 \text{ m}^3 \text{s}^{-1}$), the zone of highest velocity appears to extend from the tail of Riffle A through Pool 2 towards Riffle B. Although near-bed velocity shows a down-riffle decrease comparable to that shown for the

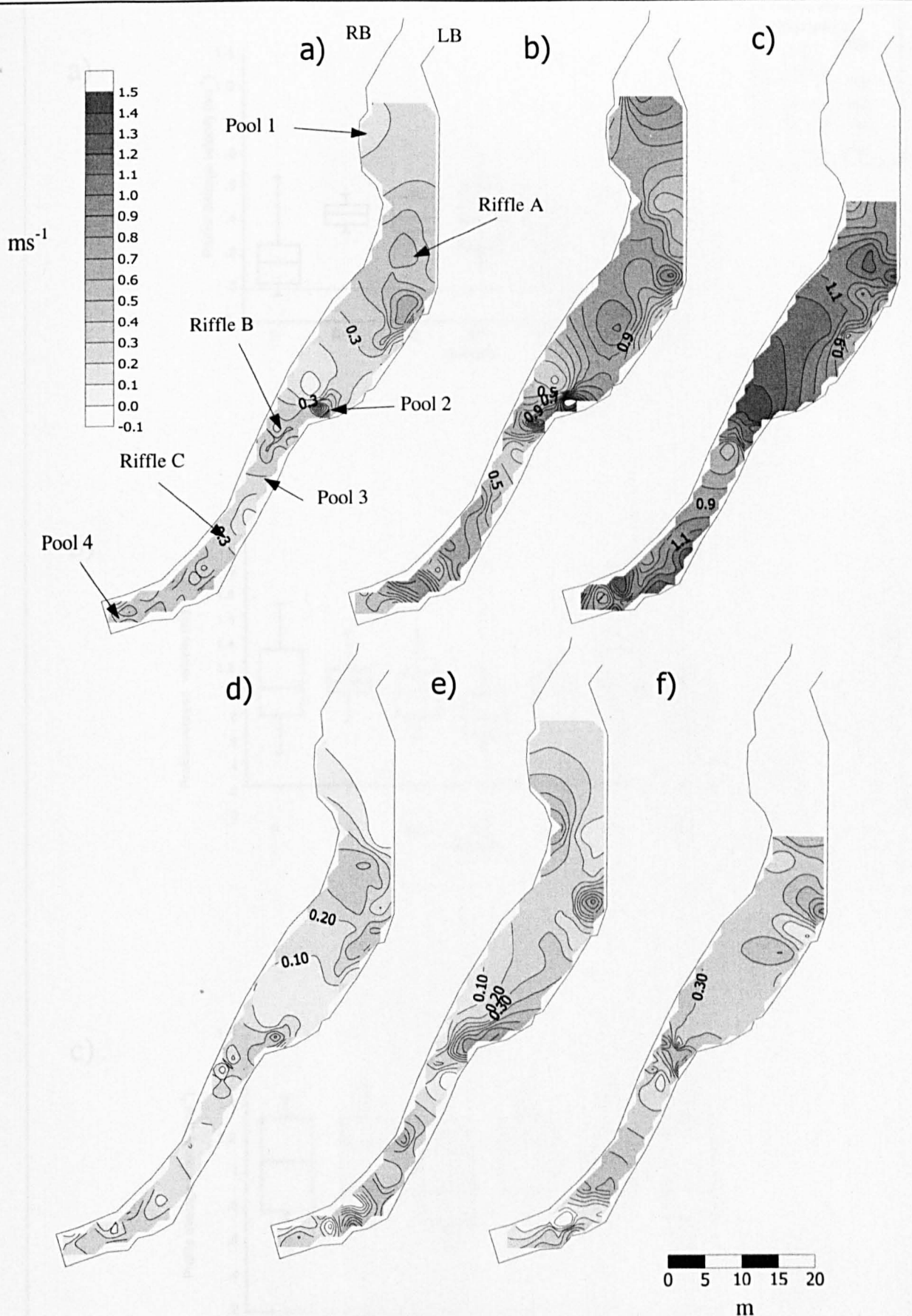
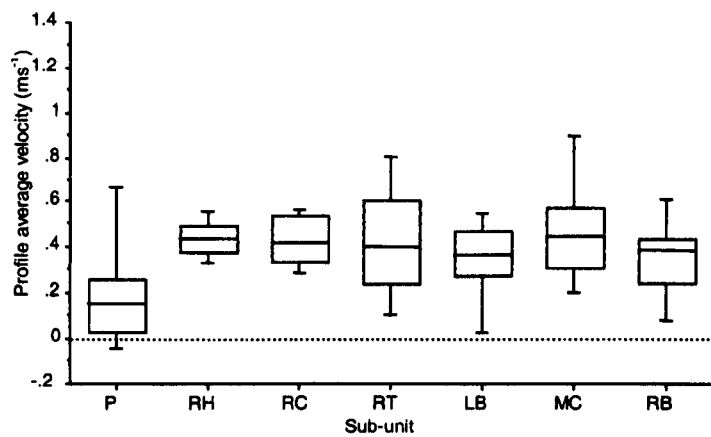
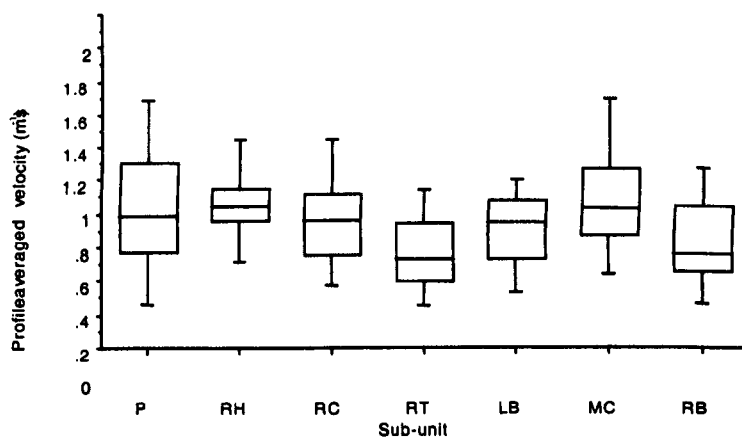


Figure 4.2 Spatial pattern in profile averaged and bed velocity for study reach A for flows $0.3\text{-}3.6 \text{ m}^3 \text{s}^{-1}$, a) Profile average $0.3 \text{ m}^3 \text{s}^{-1}$, b) Profile average $1 \text{ m}^3 \text{s}^{-1}$, c) Profile average $3.6 \text{ m}^3 \text{s}^{-1}$, d) Bed $0.3 \text{ m}^3 \text{s}^{-1}$, e) Bed $1 \text{ m}^3 \text{s}^{-1}$, f) Bed $3.6 \text{ m}^3 \text{s}^{-1}$. RB – right bank, LB – left bank.

a)



b)



c)

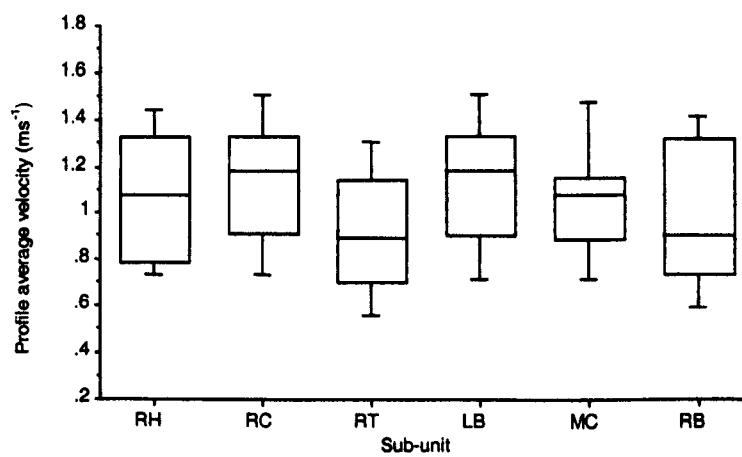
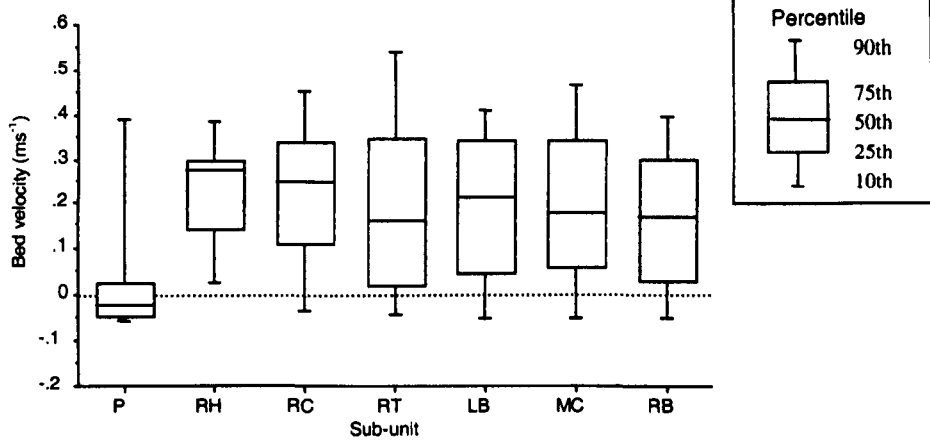
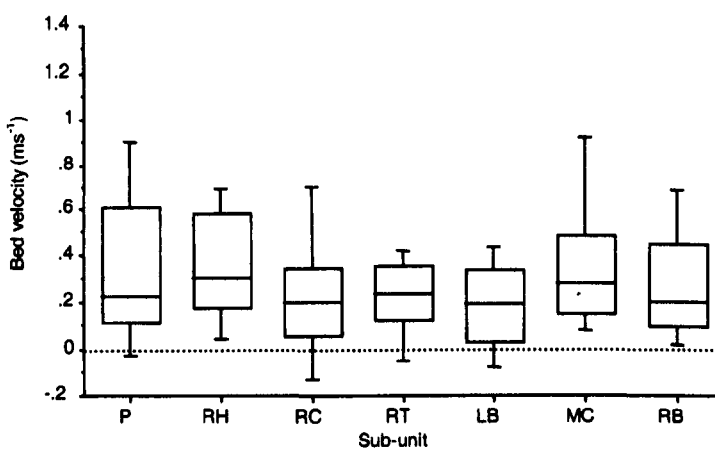


Figure 4.3 Morphological variation in profile averaged velocity (0.6 depth) for a) $0.3 \text{ m}^3 \text{s}^{-1}$, b) $1 \text{ m}^3 \text{s}^{-1}$ and c) $3.6 \text{ m}^3 \text{s}^{-1}$. No pool data available for $3.6 \text{ m}^3 \text{s}^{-1}$. RH-riffle head, RC-riffle crest, RT-riffle tail, P-pool, LB-left bank. MC mid-channel. RB-right bank.

a)



b)



c)

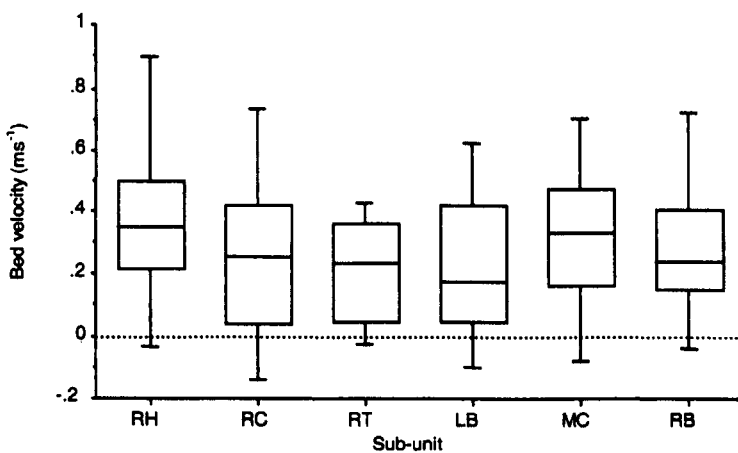


Figure 4.4 Morphological variation in near-bed velocity for a) $0.3 \text{ m}^3 \text{s}^{-1}$, b) $1 \text{ m}^3 \text{s}^{-1}$ and c) $3.6 \text{ m}^3 \text{s}^{-1}$. No pool data available for $3.6 \text{ m}^3 \text{s}^{-1}$. RH-riffle head, RC-riffle crest, RT-riffle tail, P-pool, LB-left bank, MC mid-channel, RB-right bank.

previous two lower flows, profile averaged velocity is found to be highest at riffle crest and lowest at the tail. Near-bed velocity is also highest in the channel centre at $3.6 \text{ m}^3 \text{s}^{-1}$, similar to the lower two flows. However profile-averaged velocity shows a steady increase from the shallower right bank towards the deeper left-bank (thalweg).

4.3.3 Boundary shear stress distribution

Point boundary shear stresses measured from velocity profiles

Spatial variability in boundary shear stress distribution calculated from velocity profiles is demonstrated for a range of discharges (Figure 4.5), and summarised in Figure 4.6). As may be expected there is a general increase in shear stress with increasing discharge. This is a reflection of the vertical velocity differences, as was mentioned in section 4.3.2, where at the highest flow recorded there was a 74% difference between bed and 0.6 depth at $3.6 \text{ m}^3 \text{s}^{-1}$. At low flow, shear stresses for the pools are generally less than 10 N m^{-2} , whereas shear stresses for the riffles are generally greater with a maximum of 67 N m^{-2} being recorded on the crest of riffle A (Figure 4.5). At this flow ($0.3 \text{ m}^3 \text{s}^{-1}$), all riffle sub-units have lower τ than the pools. There is little difference between the average τ down-riffle, however channel centres (MC) show greater τ than the margins. With further increase in discharge, there is a noticeable difference in the pattern of point boundary shear stress in comparison to both bed and profile-averaged velocity. The reversal in velocity shown for Pool 2 and Pool 1 at around $1 \text{ m}^3 \text{s}^{-1}$ is not evident in the shear stress data (Figure 4.5a). The highest shear stress at this flow was found at the head of Riffle B towards the right bank where a shear stress of 230 N m^{-2} was recorded. The highest shear stress for a pool is shown in Pool 4 with 34 N m^{-2} . Pool τ are still below those recorded in all riffle sub-units. There is some change in the distribution of τ over riffles however, with greatest τ being shown at riffle heads and least at tails. Furthermore there is a gradual increase in τ from the right to left bank towards the thalweg location, a similar pattern to that shown in the velocity data at $3.6 \text{ m}^3 \text{s}^{-1}$. Again at the highest flow, data are lacking for the pools. τ at riffle heads are reduced (possibly suggesting that these areas may transport sediments less rapidly and may result in deposition), however τ at

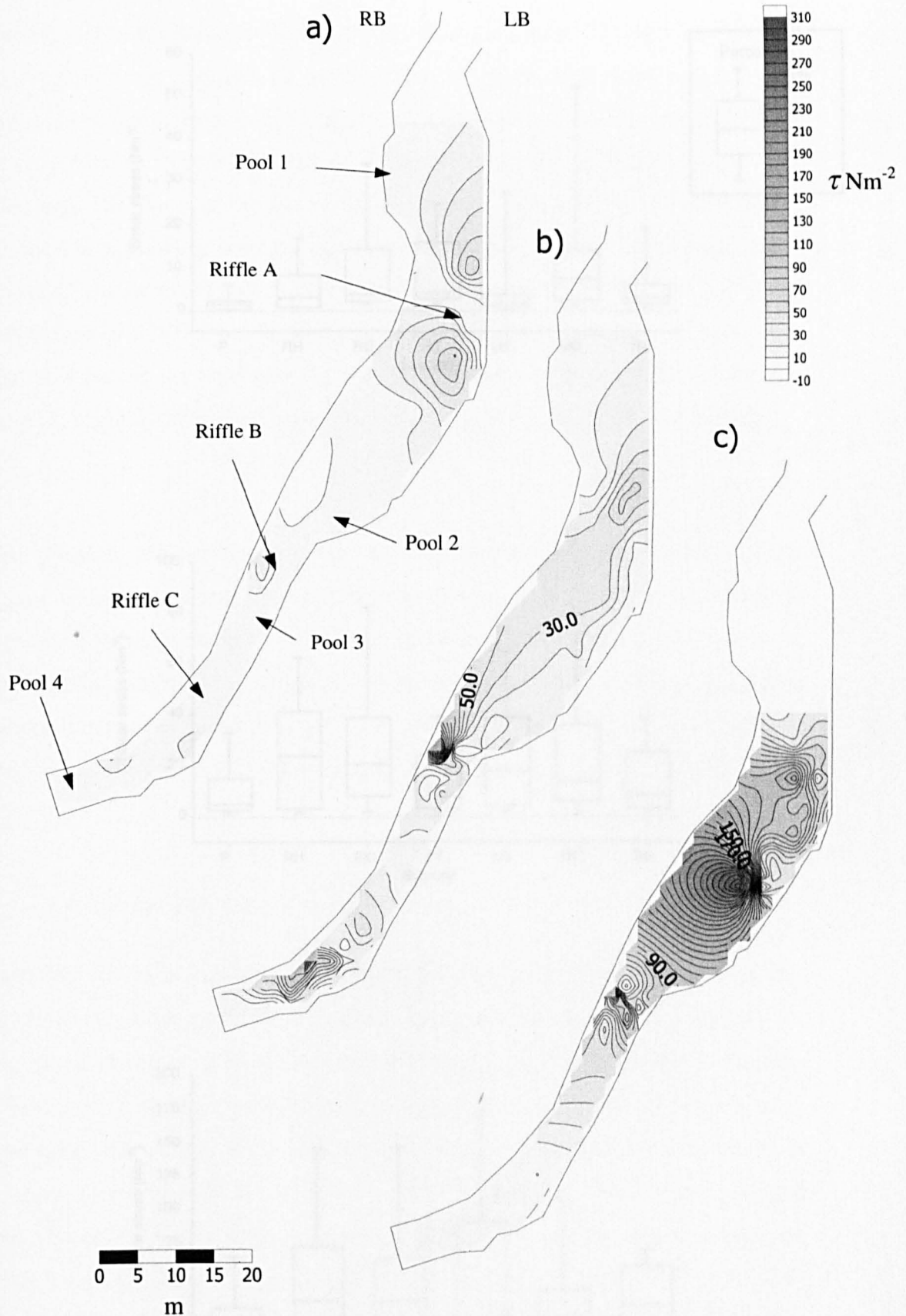
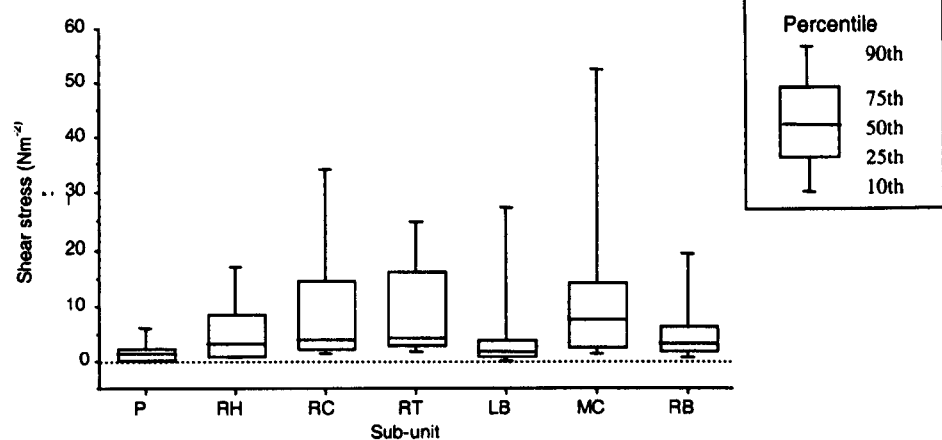
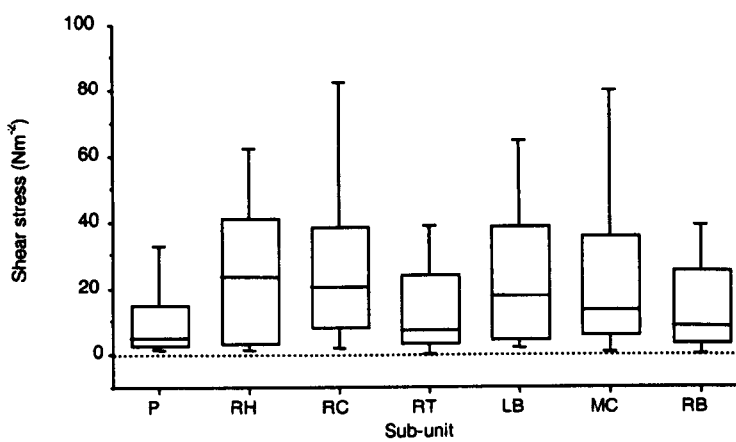


Figure 4.5 Spatial pattern of point shear stress estimated from velocity profiles for study at flows of a) $0.3 \text{ m}^3 \text{s}^{-1}$, b) $1 \text{ m}^3 \text{s}^{-1}$, c) $3.6 \text{ m}^3 \text{s}^{-1}$. LB-left bank, RB-right bank.

a)



b)



c)

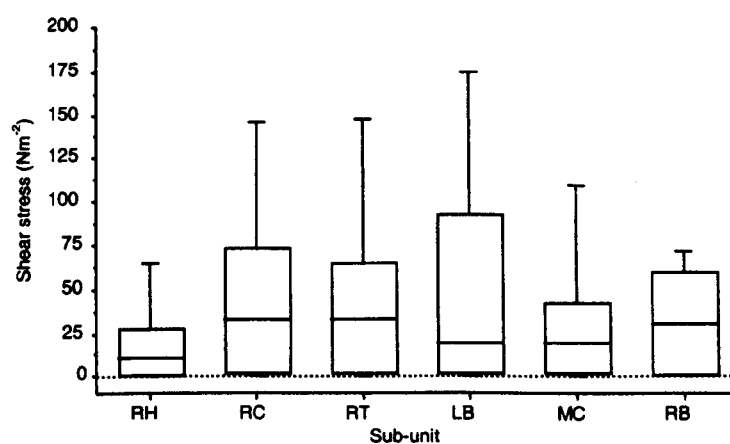


Figure 4.6 Morphological variation in shear stress calculated from velocity profiling and equation 2.3
 a) $0.3 \text{ m}^3 \text{s}^{-1}$, b) $1 \text{ m}^3 \text{s}^{-1}$ and c) $3.6 \text{ m}^3 \text{s}^{-1}$. No pool data available for $3.6 \text{ m}^3 \text{s}^{-1}$. RH-riffle head, RC-riffle crest, RT-riffle tail, P-pool, LB-left bank, MC mid-channel, RB-right bank.

riffle crests and tails remain similar to the previous discharge. The right bank shows slightly higher τ on average compared to the left bank and mid-channel zones, contrasting with the velocity data for this flow. However it is evident that peak shear stresses are located towards the tail of Riffle A where the maximum point value recorded was 334 Nm^{-2} in the centre of the channel. Shear stresses over Riffle C appear show a substantial decrease compared to the previous two discharges where values are in the order of only 1 Nm^{-2} , and a maximum value of 4 Nm^{-2} is found towards the tail of this riffle. Although point boundary shear stress data obtained from velocity profiles are not available for the pools above and below Riffle C for this discharge, it is highly likely that shear stresses are greater in the pools (i.e. $>1 \text{ Nm}^{-2}$).

Velocity profiling has provided a useful data set regarding boundary shear stress at discharges up to around half bankfull, but no evidence was found for a reversal in shear stress at these discharges even though this was evident when considering point velocity. Spatial patterns in shear stress data are now presented for flows greater than half bankfull estimated using the depth slope product. Data for lower flows are also included to aid interpretation and for comparative purposes.

Cross-section average shear stress using Du Boys

Contour plots shown in Figures 4.7 demonstrate the spatial variations in cross-section average boundary shear stress. Water surface slopes used to calculate τ using equation 2.3, are given in Figure 2.16. Cross-section averaged shear stresses are lower than some of the point values, particularly those recorded in the trough of pools at high flow recorded due to their cross-sectionally averaged nature. A general increase in shear stress is evident with an increase in discharge, however more complex spatial patterns also exist. At the lowest discharge ($0.1 \text{ m}^3 \text{s}^{-1}$) there are similarities in the spatial distribution of shear stress to that shown at $0.3 \text{ m}^3 \text{s}^{-1}$ measured using velocity profiling (compare Fig 4.7a with 4.5a), with peaks of 24 Nm^{-2} shown at the tail of riffle A, towards the left hand bank. With a further increase in discharge to $2 \text{ m}^3 \text{s}^{-1}$, similarities are again demonstrated between the velocity profile data obtained at $3.6 \text{ m}^3 \text{s}^{-1}$, with high shear stresses being located at the tail of Riffle A

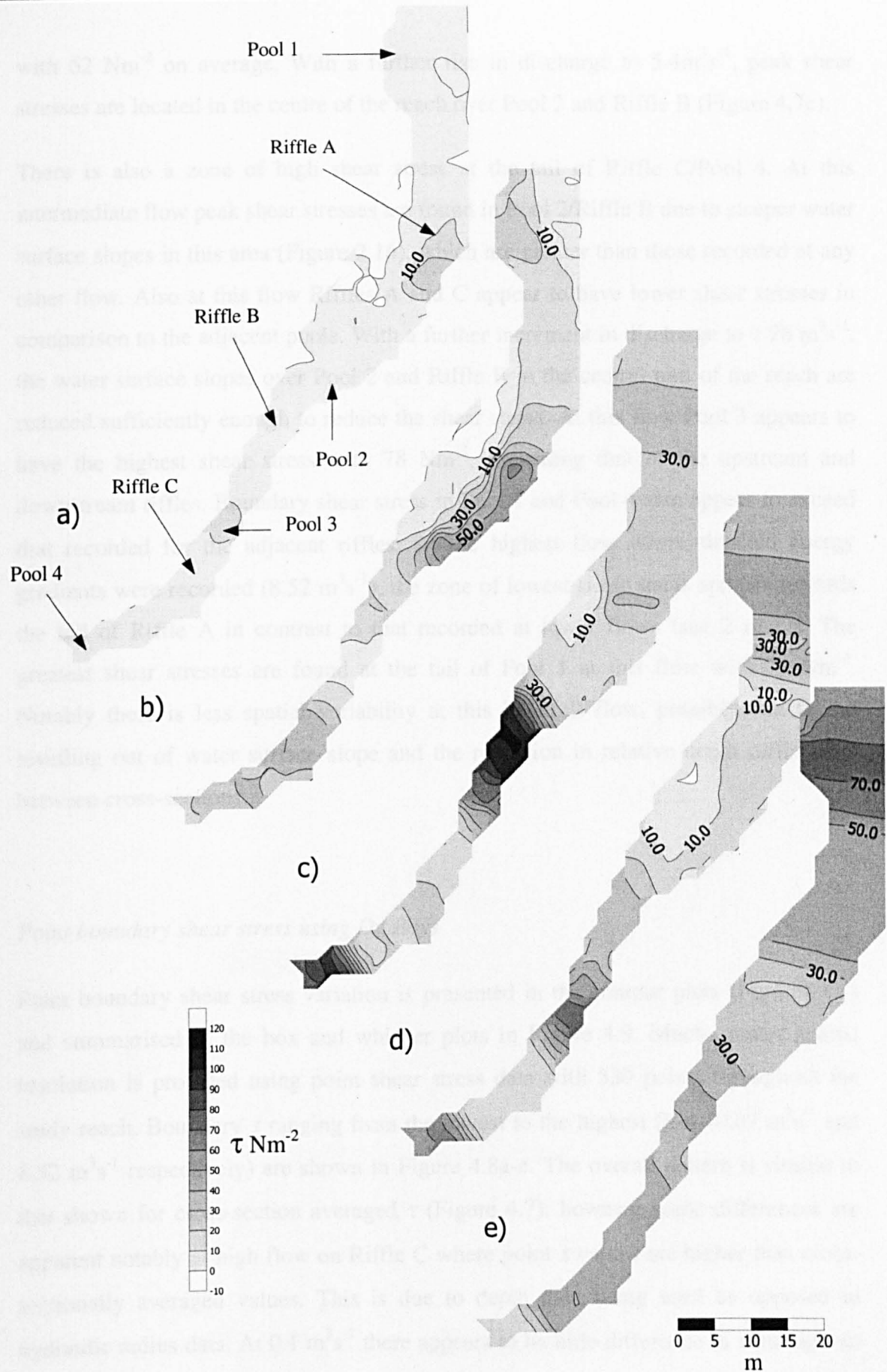


Figure 4.7 Spatial variability of cross-section average shear stress estimated using the Du Boys equation for flows of a) $0.1 \text{ m}^3 \text{s}^{-1}$, b) $2 \text{ m}^3 \text{s}^{-1}$, c) $5.44 \text{ m}^3 \text{s}^{-1}$, d) $7.26 \text{ m}^3 \text{s}^{-1}$, e) $8.52 \text{ m}^3 \text{s}^{-1}$

with 62 Nm^{-2} on average. With a further rise in discharge to $5.4 \text{ m}^3 \text{s}^{-1}$, peak shear stresses are located in the centre of the reach over Pool 2 and Riffle B (Figure 4.7c).

There is also a zone of high shear stress at the tail of Riffle C/Pool 4. At this intermediate flow peak shear stresses are found in Pool 2/Riffle B due to steeper water surface slopes in this area (Figure 2.16), which are greater than those recorded at any other flow. Also at this flow Riffles A and C appear to have lower shear stresses in comparison to the adjacent pools. With a further increment in discharge to $7.26 \text{ m}^3 \text{s}^{-1}$, the water surface slopes over Pool 2 and Riffle B in the central part of the reach are reduced sufficiently enough to reduce the shear stress. At this flow Pool 3 appears to have the highest shear stress with 78 Nm^{-2} , exceeding that of the upstream and downstream riffles. Boundary shear stress in Pool 1 and Pool 4 also appear to exceed that recorded for the adjacent riffles. At the highest flow where detailed energy gradients were recorded ($8.52 \text{ m}^3 \text{s}^{-1}$), the zone of lowest shear stress appears towards the tail of Riffle A in contrast to that recorded at lower flows (see $2 \text{ m}^3 \text{s}^{-1}$). The greatest shear stresses are found at the tail of Pool 1 at this flow with 79 Nm^{-2} . Notably there is less spatial variability at this bankfull flow, possibly due to the levelling out of water surface slope and the reduction in relative depth differences between cross-sections.

Point boundary shear stress using Du Boys

Point boundary shear stress variation is presented in the contour plots (Figures 4.8) and summarised in the box and whisker plots in Figure 4.9. Much greater spatial resolution is provided using point shear stress data with 530 points throughout the study reach. Boundary τ ranging from the lowest to the highest flow ($0.07 \text{ m}^3 \text{s}^{-1}$ and $8.52 \text{ m}^3 \text{s}^{-1}$ respectively) are shown in Figure 4.8a-e. The overall pattern is similar to that shown for cross-section averaged τ (Figure 4.7); however some differences are apparent notably at high flow on Riffle C where point τ values are higher than cross-sectionally averaged values. This is due to depth data being used as opposed to hydraulic radius data. At $0.1 \text{ m}^3 \text{s}^{-1}$ there appears to be little difference in τ throughout the reach (Figure 4.8a). The box and whisker plots summarise τ variation for different morphological units. At the lowest flow of $0.07 \text{ m}^3 \text{s}^{-1}$, there appears to be very little

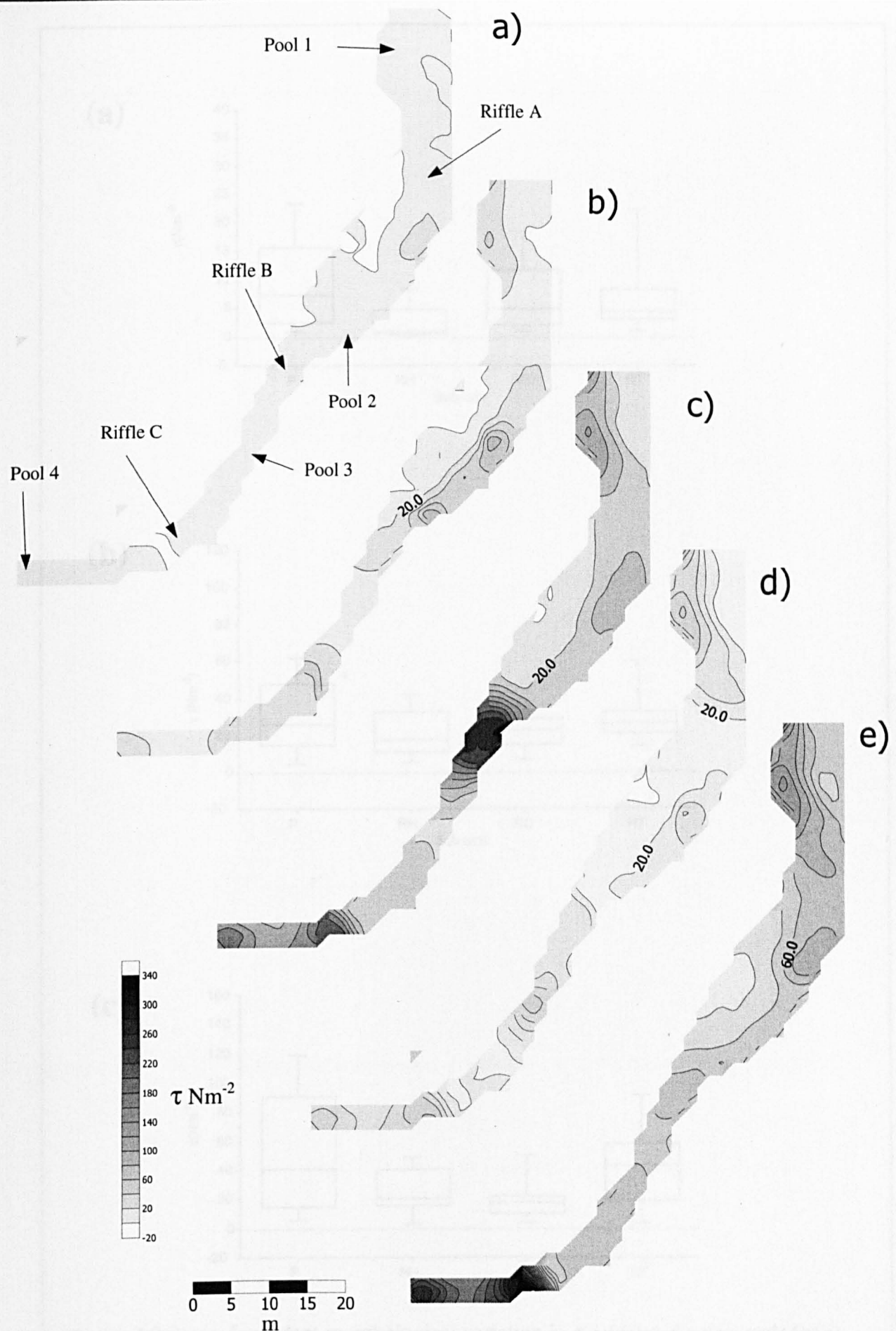


Figure 4.8 Spatial variability of point shear stress estimated using the Du Boys equation for a) $0.1 \text{ m}^3\text{s}^{-1}$, b) $2 \text{ m}^3\text{s}^{-1}$, c) $5.44 \text{ m}^3\text{s}^{-1}$, d) $7.26 \text{ m}^3\text{s}^{-1}$, e) $8.52 \text{ m}^3\text{s}^{-1}$

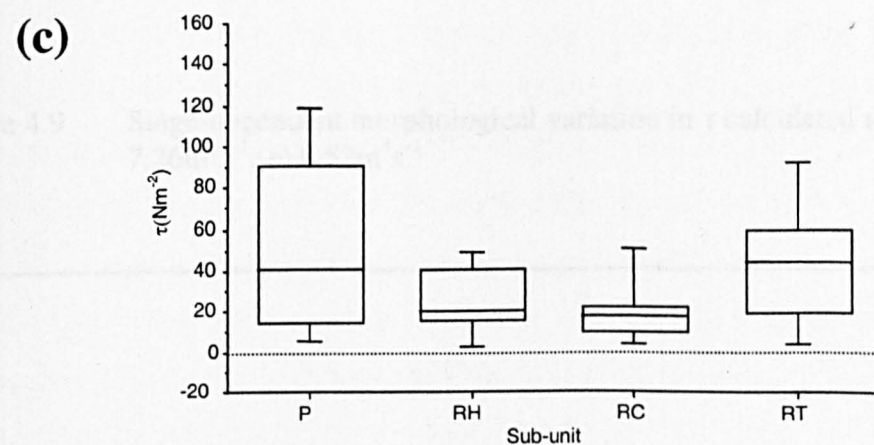
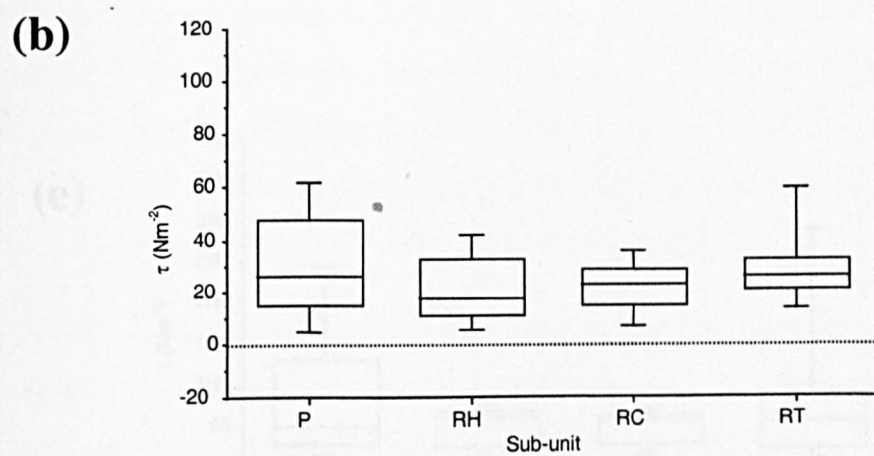
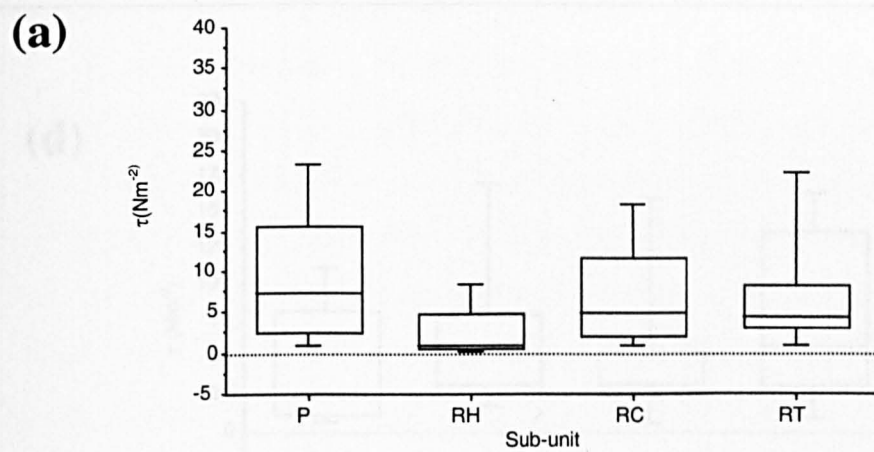
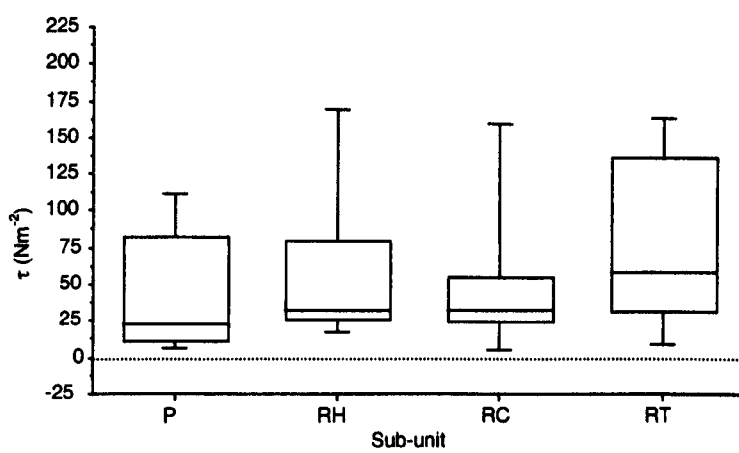


Figure 4.9 Stage-dependent morphological variation in τ calculated using ρ gds for a) $0.1 \text{ m}^3 \text{s}^{-1}$, b) $2 \text{ m}^3 \text{s}^{-1}$, c) $5.44 \text{ m}^3 \text{s}^{-1}$ d) $7.26 \text{ m}^3 \text{s}^{-1}$, e) $8.52 \text{ m}^3 \text{s}^{-1}$

(d)



(e)

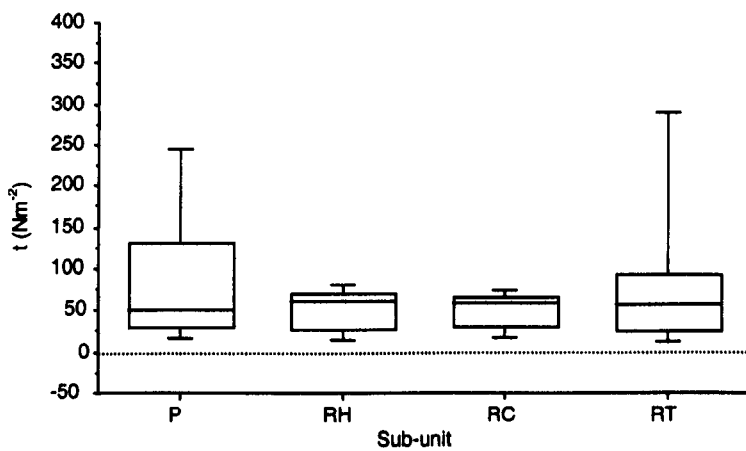


Figure 4.9 Stage-dependent morphological variation in τ calculated using ρ_{gds} for d) $7.26 \text{ m}^3 \text{ s}^{-1}$, e) $8.52 \text{ m}^3 \text{ s}^{-1}$

differentiation between sub-units, although surprisingly pools record marginally higher τ . This is possibly due to the influence of Pool 2 which occasionally appeared to exhibit high low-flow water surface slopes at the head of the pool due to the effects of slumped bank material which acted as a constriction to flow. Conversely, riffle heads record the lowest τ (Figure 4.9a). With a slight increase in discharge to $2 \text{ m}^3\text{s}^{-1}$, τ are generally higher, however there is little difference in τ between morphological units, when consideration is given to averaged data (Figure 4.9b). Pools are still showing slightly higher τ in comparison to riffles, and there appears to be a down-riffle increase in τ , with riffle tails showing the highest τ . Considering point τ distribution, the highest τ zones are situated on the head of Riffle A on the left-hand bank, on the head of Pool 2 and the tail of Riffle C/head of Pool 4 (Table 4.1). Pool 1 and Pool 3 have very gentle water surface slopes (0.03-0.4%) and experience very low τ (Figure 2.13). Conversely, the steepest slope recorded at low flow is found on Riffle 1 with 1.8%. Notably, some point boundary τ in Pool 2, Pool 3 and Pool 4 were greater than on the adjacent riffles. This was a feature also evident when considering point velocities as a unit of tractive force (see section 4.4.2).

At higher discharges, water surface topography is smoother and, particularly at the two highest flows, flow is gradually varied and may be considered (as a first approximation) to be uniform (Milan *et al.*, 2001) (see Figure 2.16). Pools and riffle tails are high τ zones, with pools showing the highest τ values. Riffle heads and crests tend to be zones of relatively low τ at this flow (Figure 4.9c). High shear stresses are particularly evident in the middle and downstream portions of the reach, where mean values of 120 Nm^{-2} and 101 Nm^{-2} were found in Pool 2 and Pool 4 respectively (Figure 4.8b). At $5.44 \text{ m}^3\text{s}^{-1}$ the boundary shear stress in Pool 1 exceeds that of the downstream riffle (Riffle A), conflicting with the velocity data which suggested an equalisation rather than a reversal (Figure 4.1a). However, it should be noted that the high pool τ values are only located in the deeper part of the pool, areas of the bar which begin to be submerged at this stage actually have lower shear stress in comparison to the riffle downstream. The cross-section average velocity data takes into account the submerged area over the bar surface, which results in lower average velocities than those likely to be encountered in the deep part of the pool. At this same discharge Riffle A and Riffle A all show slight τ increases, while Riffle B and

	P1	P1-R1	R1	R1-P2	P2	P2-R2	R2	R2-P3	P3	P3-R3	R3	R3-P4	P4	
Slope range	0.0003-0.0094	Reversal at 7.26 m ³ s ⁻¹	0.0028-0.0184	Reversal at 3.9 m ³ s ⁻¹ and 8.52 m ³ s ⁻¹	0.0028-0.0184	Pool shows greater slope at low flow	0.0022-0.0203	Reversal at 7.26 m ³ s ⁻¹	0.0021-0.0123	Pool has greater slope at low flow	0.0023-0.0128	Two reversals at 5.44 and 8.52 m ³ s ⁻¹	0.0045-0.0124	
Channel wetted width range (m)	3.5 – 18.4		6.7 – 19.0		3.0 – 15.0		5.0 – 14.7		3.5 – 9.3		6.0 – 11.9		3.0 – 10.0	
124	Shear stress range (Nm ⁻²)	0.03-176.9	Reversal at 5.44 m ³ s ⁻¹	1.9-94.18	Reversal at 5.44 m ³ s ⁻¹ and 8.52 m ³ s ⁻¹	4.96-116.32	Reversal at 7.26 m ³ s ⁻¹	0.06-207.39	Reversal at 3.9 m ³ s ⁻¹ and 8.52 m ³ s ⁻¹	7.98-123.14	Reversal at 3.9 m ³ s ⁻¹ and 8.52 m ³ s ⁻¹	0.7-72.49	Reversal at 5.44 m ³ s ⁻¹	0.05-350.35
Grain roughness (mm)	$D_{84}=193$ $D_{50}=120$ $D_{16}=83$		$D_{84}=132$ $D_{50}=79$ $D_{16}=43$		$D_{84}=190$ $D_{50}=120$ $D_{16}=73$		$D_{84}=152$ $D_{50}=85$ $D_{16}=45$		$D_{84}=164$ $D_{50}=112$ $D_{16}=86$		$D_{84}=173$ $D_{50}=101$ $D_{16}=66$		$D_{84}=120$ $D_{50}=82$ $D_{16}=42$	
Entrainment potential	$Q>5.44$ m ³ s ⁻¹	$Q>7.27$ m ³ s ⁻¹	$Q>7.27$ m ³ s ⁻¹	$Q>7.27$ m ³ s ⁻¹	$Q>3.90$ m ³ s ⁻¹	$Q>3.90$ m ³ s ⁻¹	$Q>5.44$ m ³ s ⁻¹	$Q>5.44$ m ³ s ⁻¹	$Q>7.26$ m ³ s ⁻¹	$Q>7.26$ m ³ s ⁻¹	$Q>8.52$ m ³ s ⁻¹	$Q>5.44$ m ³ s ⁻¹	$Q>5.44$ m ³ s ⁻¹	

Table 4.1 Summary of changes in boundary shear stress with increasing discharge. Also included are the factors which influence riffle-pool hydraulics.

Riffle C still displays higher τ values than Pool 3. The reversal noted in the cross-sectionally averaged velocity data between Pool 2-Riffle B is also evident in the boundary τ data at this flow. Boundary τ peaks are now located at the head and centre of Pool 2, and throughout Riffle C and Pool 4.

At $7.26 \text{ m}^3\text{s}^{-1}$, just below bankfull flow, pool troughs appear to be showing lower τ in comparison to riffles (Figure 4.9d). Riffle tails (the lower part of which could also be considered as pool heads) are zones of highest τ . Little difference is evident between the τ shown at riffle heads and crests. When consideration is given to individual morphological units, however, there is evidence for pool τ to exceed that of riffles at this flow. Boundary τ in Pool 1 reaches its maximum with the tail of Pool 1 showing a slight increase in shear stress. However, the head of Riffle A shows a reduction in shear stress and downstream of Pool 1 there is a general decline in stresses compared to those under the previous discharge of $5.44 \text{ m}^3\text{s}^{-1}$ (Figure 4.8c). Shear stress reversals are in evidence between Pool 1-Riffle A, Riffle B-Pool 3 and Pool 3-Riffle C where pool shear stress exceeds riffle. Mean boundary shear stresses in Pool 1 and Pool 4 remain higher than those on Riffle A and Riffle C respectively. Other notable changes are that the high shear stress zone on the crest of Riffle A near the left-hand bank re-emerges. The region of high shear found in Pool 2 at the previous flow shows a slight reduction, and the peak stress is found further downstream towards the tail of Pool 2 and the head of Riffle B. The tail of Riffle B and Pool 3 show low shear stresses whereas Riffle C and Pool 4 both show a further increase.

At bankfull discharge ($8.52 \text{ m}^3\text{s}^{-1}$) there is a general reduction and little difference in water surface slope between morphological units (Figure 2.16). Considering morphological sub-units there appear to be little overall difference on average with τ generally around 50 Nm^{-2} . Peaks are found again in pools and riffle tails, the latter showing the greatest range in τ (Figure 4.9e), compared to the narrower range of values found at riffle heads and crests. A maximum boundary τ of 225 Nm^{-2} is found in Pool 4 at this flow. This area shows differences in the cross-sectionally averaged data, which suggests this zone has a much lower τ . The upstream bar surface adjacent to Pool 1 is fully drowned, and an increase in boundary τ may be observed on the shallow water over the bar surface (Figure 4.8d). Most of the pool-riffle units, with

the exception of Riffle C-Pool 4, show a trend towards equalisation; however the pool shear stresses still generally exceed those on the riffles. Overall the boundary shear stress data support the cross-sectionally velocity data, with the exception of Pool 1-Riffle A and Riffle A-Pool 2.

4.3.4 Prediction of boundary shear stress

To draw relationships between tractive force and sediment transport within the Rede study reach it was important to obtain an estimate of τ for each flood analysed during basket sampling and sediment tracing. However, it was impossible to physically measure τ in the field for each flood event for specific points on the bed (e.g. clast location). By using the hydraulic data (d , s and Q), tacheometric survey data and spatial interpolation techniques it was possible to obtain an estimate of maximum τ for specific points on the bed. Water slope was measured by surveying the water's edge for the lowest flow ($0.1 \text{ m}^3 \text{s}^{-1}$) and trash lines for four other flood flows up to bankfull. (Figure 2.16). Lower resolution water slope data was also obtained from stage-board readings which were positioned at the head and tail of riffles, allowing a mean slope for each riffle and pool to be calculated. As each stage board had its level surveyed relative to the cross-section datum, by plotting water surface slope against distance downstream, it was possible to read off water elevations at each cross-section position. It was then possible to construct stage-discharge relationships for each of 30 cross-sections throughout the study reach. Using linear regression it was then possible to predict water elevation for each point across each cross-section for a given Q (Appendix 4.2). This provided 530 point values of d which could then be contoured in Surfer, using Kriging as the interpolation method. An estimate of the τ responsible for initiating the movement of a clast for a particular point on the bed surface for a given Q , could then be derived by subtracting the bed elevation (z) at the pre-flood clast's position (x, y) from the same point on the interpolated water elevation surface. τ could then be calculated by entering the d value into ρgds , using s predicted for individual riffles and pools (Appendix 4.3).

There are of course a number of assumptions and limitations to this technique. For example the method assumes;

- 1) a relatively stable bed surface with little scour and fill occurring at each cross-section,
- 2) that super-elevation effects are minimal,
- 3) the maximum point τ for a given flood was responsible for initiating motion, when movement may have occurred before the flood peak

Scour and fill occurs throughout the study reach and is most pronounced on the pool cross-sections, however riffles appear relatively stable (Appendix 2.1). More confidence may therefore be expressed in τ predicted from riffle data. Super-elevation effects are thought to be minimal throughout the Rede study reach (see Milan *et al.*, 2001). Even though problems exist, this technique provides a useful tool for estimating point specific hydraulics in situations where it is impossible to take physical measurements.

Average estimates of τ were required for the reach as a whole and for riffle and pools separately. Average τ was estimated using the 75th percentile depth for riffles, pools and reach, and a mean water surface slope of 0.00728. The choice of 75th percentile depth follows a similar procedure conducted by Ferguson and Wathen (1998, p2033), who chose a depth "midway between the mean and the maximum from the section". The rationale behind this procedure is that gravel transport tends to be concentrated near the thalweg, hence τ would be underestimated by using mean depth in what were generally non-trapezoidal cross-sections (Appendix 2.1). τ calculated in this manner reflects changes in depth rather than slope, and shows a strong dependence upon discharge as demonstrated by the following regression equations;

Reach

$$\tau = 10.141Q + 16.178 \quad n=5, \quad r^2=0.959 \quad p=<0.01 \quad SE=7.99 \quad (4.1)$$

Riffle

$$\tau = 9.9536Q + 4.5223 \quad n=5, \quad r^2=0.968 \quad p=<0.01 \quad SE=6.92 \quad (4.2)$$

Pool

$$\tau = 9.9316Q + 19.352 \quad n=5, \quad r^2=0.946 \quad p=<0.01 \quad SE=8.99 \quad (4.3)$$

4.4 Discussion and conclusions

4.4.1 Tractive force variation through pools and riffles

The results for the River Rede show some support for Keller's (1971) velocity reversal hypothesis, however considerable spatial complexity is involved. A reversal was found for cross-sectionally average velocity data for four out of the six riffle-pool units along the study reach. The remaining two riffle-pool units showed an equalisation in velocity at around bankfull. When consideration is given to profile averaged velocity at-a-point it is possible to find higher velocities in the pools at flows much lower than bankfull ($1\text{m}^3\text{s}^{-1}$). Shear stress data estimated from velocity profiling did not reveal a reversal, possibly due to the limited range of flows considered. However when consideration was given to section-averaged and point shear stress calculated from the Du Boys equation, reversals were evident for individual riffle-pool units. As reversals tended not to be synchronous between riffle-pool units at particular discharges, they were masked when data from each pool and riffle-sub-unit were combined (Figure 4.9).

A summary of the variability in key variables at each riffle-pool is shown in Table 4.1 (from Milan *et al.*, 2001), which also demonstrates the change in energy slope and grain and form roughness between units. It may be seen that shear stress reversal tends to be accompanied by an equalisation or a reversal in energy slope, and sometimes reversals can occur at different stages on the hydrograph. The study reach on the Rede should favour the phenomenon of tractive force reversal for two reasons. Firstly, its pool sediments are coarser than those on the riffles, increasing the grain roughness of the pools. Secondly, pool channel widths are much narrower than those of riffles. Carling and Wood (1994) have demonstrated, using computer simulation, the increased potential for velocity reversal where the pools have a higher grain roughness and where riffles are in excess of 50 per cent wider than the pools. This relates to one of the key issues surrounding the velocity reversal debate, namely the continuity of mass principle. Many workers contend that pool cross-sectionally averaged velocity can only exceed that of the riffle if the pool cross-sectional area is less than the adjacent riffle (Bhowmik and Demissie, 1982, and section 1.3.4). Some investigators have demonstrated larger cross-sectional areas for pools at high flow (e.g. Richards, 1978; Carling, 1991; Carling and Wood, 1994; Thompson *et al.*, 1996;

1999). For the Rede (Figure 4.10), it can be seen that pools have larger cross-sectional areas than riffles at low flow (up to $5.44 \text{ m}^3\text{s}^{-1}$). After approximately two-thirds bankfull, Pool 3 and Pool 4 have lower cross-section areas than the adjacent riffles, and at $7.26 \text{ m}^3\text{s}^{-1}$ and $8.52 \text{ m}^3\text{s}^{-1}$ Pool 2, Pool 3 and Pool 4 have lower cross-section areas in comparison to adjacent riffles. The area of Pool 1 however is always larger than the adjacent riffles (this is a particularly deep pool). Although the cross-section areas of some pools is only marginally lower than the adjacent riffles, this is sufficient to satisfy the continuity of mass principle and thus allow marginal velocity reversal to occur on the Rede.

4.4.2 Problems with cross-sectional measures

Deviation from the log-log relationship between mean section velocity and discharge was demonstrated for the Rede data at flows approaching bankfull. However log-log regression fitted reasonably well. This was also highlighted by Carling's (1991) data for the River Severn where he utilised a polynomial function for his data, and is also an issue raised by Clifford and Richards (1992). The deviation from the log-log relationship may be a result of overspilling onto some areas of the floodplain where areas of the bank are lower or damaged. Overspilling in the middle of the reach was observed on several occasions at around bankfull. This may explain the lack of reversal for Pools 1 and 2.

4.4.3 Problems with velocity profiling

Although recent studies such as Robert (1997) and Carling (1991) have used velocity profiling to assess flow hydraulics in natural channels, problems may be encountered if large roughness elements are present. Bray (1980) has shown that the technique is particularly problematic where the depth to grain size ratio is less than *ca.*3. Furthermore, Clifford and Richards (1992) have confirmed these problems with velocity profile data obtained from the River Quarne, where negative velocity gradients were occasionally obtained. It is possible that this feature may be induced by turbulent flow structures such as the strong sweeping events found in the vicinity

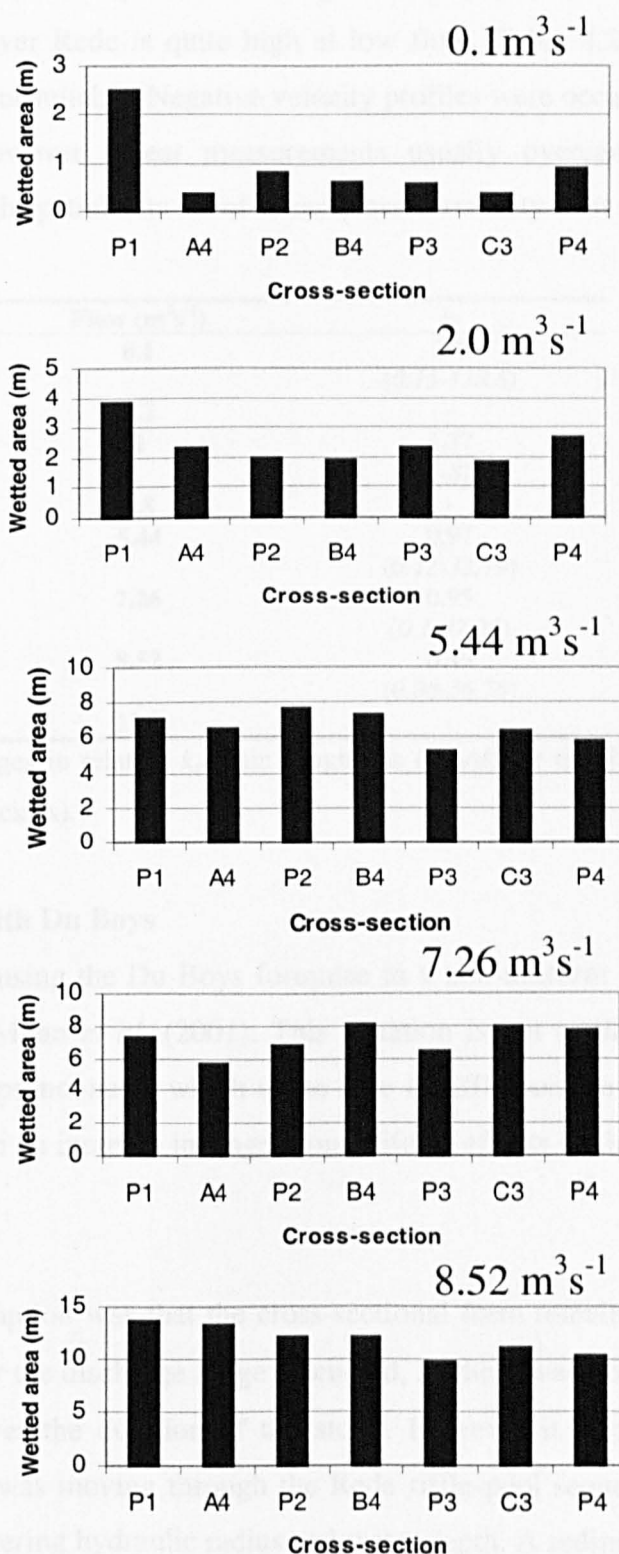


Figure 4.10 Change in cross-section wetted area for cross-sections taken in the trough of the pools and crests of the riffles throughout the Rede study reach.

of pebble clusters, reported by Buffin-Bélanger and Roy (1998). The depth to grain-size ratio on the River Rede is quite high at low flow (Table 4.2), suggesting that velocity profiling is unsuitable. Negative velocity profiles were occasionally found for the Rede data. However repeat measurements usually overcame this problem, permitting a thorough spatial data set of shear stress variability over three flows.

Flow (m^3s^{-1})	k_r
0.1	3.7 (0.15-138.8)
0.2	-
2	1.37 (0.1-87.5)
4.8	-
5.44	0.97 (0.12-32.79)
7.26	0.95 (0.1-47.21)
8.52	0.49 (0.08-36.76)
12.5	-

Table 4.2 Mean changes in relative k_r grain roughness (D_{84}/d) for the Rede with discharge (range is shown in brackets).

4.4.4 Problems with Du Boys

The problems with using the Du Boys formulae in a non-uniform flow environment were addressed in Milan *et al.* (2001). This equation is not applicable where non-uniform effects are pronounced, which is the case in riffle-pool environments at low flow. However, with an increase in stage, non-uniform effects of the morphology are drowned out.

An additional assumption was that the cross-sectional form remained approximately constant ($\pm D_{50}$) over the discharge range discussed, as there was no significant cross-sectional change over the duration of the study. However it is quite feasible that sufficient sediment was moving through the Rede riffle-pool sequence which would have the effect of altering hydraulic radius and water depth. A sediment 'slug' moving through the system may also be responsible for altering cross-section area and bed slope. Cross-sectional change and sediment budgeting through the Rede riffle-pool sequence is the subject of further investigation by the author and co-workers.

4.5 Summary

- 1) Marginal velocity reversal was found to occur for four out of six riffle-pool units, when considering cross-section average measures;
- 2) The wetted cross-section area of pools is less than that of riffles at high flow, satisfying the continuity of mass principle;
- 3) Point velocity measured using a current meter was able to demonstrate higher velocities in pools at flows as low as $1 \text{ m}^3 \text{s}^{-1}$;
- 4) τ calculated from velocity profiles did not show a reversal, although this could only be measured up to around one-third bankfull;
- 5) τ calculated from ρgds demonstrated reversals when considering point data, however these effects appeared to be masked when point data are averaged for individual riffle or pool units (as in the box and whisker plots);
- 6) Riffle tails / pool heads appear to be zones of high τ at bankfull, exceeding that of riffle crests and heads (low τ zones);
- 7) Zones of high τ and velocity were found in some pools at low flow, which was found to exceed some of the measurements in the riffles. This demonstrates the spatial complexity of tractive force through pools, and that negative residuals of the longitudinal bed profile are not necessarily the lowest velocity areas at low discharge.

Using the techniques described in section 4.3.4, hydraulic conditions may be predicted for a variety of discharge scenarios. This is put to use in the next four Chapters, which will focus on sediment transport. The next chapter specifically focuses upon finer grades (sand), where local hydraulics in the vicinity of traps are predicted using the data from this chapter to provide information on the mobility of this fraction.

Chapter Five

Mobility of bed sediments through a riffle-pool sequence 1: Fine bedload

5.1 Introduction

The rationale behind this Chapter and Chapter Six builds on the arguments presented in section 1.3.4, 1.5, where it was suggested that differences in θ_c for the same flow, such that θ_c (pool) < θ_c (riffle) may result in pool scour and riffle maintenance. Sear (1992; 1996) and Clifford (1993b) have documented the importance of bed structure in the maintenance of riffle-pool morphology and have assessed structure by describing the arrangement of the surface fabric (limited to gravel) or by using a penetrometer device (Sangerlat, 1979). Attention has yet to be given towards the role of fine sediments in bed structure contrasts and riffle-pool maintenance. Infiltration of fine, particularly cohesive, sediments into the void spaces between framework gravels is known to create a powerful cementation effect (Reid and Frostick, 1984; Reid *et al.*, 1984), which may increase θ_c for entrainment. The quantity and grain size of fine sediments accumulating in framework gravel void spaces is likely to change the mobility of bed sediments on both a temporal and spatial basis. This Chapter therefore focuses upon the interaction of sand (Phase 1 bedload) with a gravel bed, and will document its both lateral and vertical development in relation to discharge and τ . The grain sizes considered are those between $125\mu\text{m}$ and $2000\mu\text{m}$ which are predominantly transported as the saltation load component of the bedload, i.e. the material tends to bounce along the bed, or move indirectly by the impact of bouncing particles (Garde and Ranga Raju, 1977). This is in contrast to gravel material which may spend more time in contact with the bed, and move via rolling or sliding. Material finer than $125\mu\text{m}$ is assumed to be transported predominantly in suspension, and is not considered in any great detail here (Acornley and Sear, 1999). An examination of the mobility of sand-size sediments through the Rede riffle-pool sequence is also presented, however due to difficulties in obtaining enough basket trap data from pools, the analysis is restricted to data obtained from riffles. This information should improve understanding of Phase 1 transport processes, particularly winnowing, which will help explain sediment sorting patterns through Rede riffle-pool sequence.

5.2 Experimental design - trapping

Sampling both the quantity and grain size of fines deposited within a natural channel presents a number of problems, most notably the potential loss of finer grades under flowing water. Sampling may be carried out by using a fixed trap structure set within the bed, or alternatively by using some form of portable sampler (e.g. Helley-Smith). However, these methods present many problems. Installing traps within the bed creates disturbance to the bed structure, whilst sampling with a portable sampler makes it difficult to obtain good spatial coverage at high flow over the same sample duration. Two main approaches have been used in the past to collect fine bedload. Firstly, Church *et al.* (1991) used a bed-load trap made out of a concrete pipe (impermeable to intragravel flow) with a bucket inside. The entrance to the trap is covered with a wire mesh to prevent entry of coarser gravels. It was decided not to employ this type of trap as it did not allow intragravel migration of fines, nor did it simulate accumulation in a natural gravel bed. The approach used herein was to sample an array of fixed traps filled with a matrix-free gravel, similar to those used by Sear (1993) and Thoms (1987), removed on a post-flood basis. The mean capacity of the traps (volume of void space) was 2814 ml and ranged from 1700 to 4500 ml. To monitor the mobility of fine bedload (sand), two approaches were used; magnetic tracing and trapping of fine bedload which are described in Chapter Two. Although 31 traps were initially installed throughout the study reach, only 27 (riffle traps only) are included in the analysis in this chapter. Data for pool traps was limited due to damage and burial. The limited data available for pool traps concerning accumulation rates is discussed in Chapter Seven.

The approach used in this Chapter to analyse the mobility of finer grains is that of Church *et al.* (1991). By plotting rating relations between Q and accumulation rate (A) for different grain size fractions, Church *et al.* (1991) were able to estimate thresholds for motion. Using the τ prediction technique in section 4.3.4 it is possible to present rating relations of A against τ , and to estimate the critical thresholds for motion (τ_c). In the present investigation, the use of maximum local τ for the abscissa variate in the rating relations generally provided better correlations than using mean or maximum Q , or mean local τ . This technique requires (1) τ data which are presented for flood peaks using the prediction method described in section 4.3.4., (2) accumulation of fine

bedload data for traps, (3) grain-size data for bedload entering each trap, and (4) Q , d , and s data for predicting τ , see section 4.3.4.

Examination of rating relations

In order to analyse the relationship between shear stress and accumulation rates, rating relations of the form $A = a\tau^b$, where A is accumulation rate ($\text{kg m}^2 \text{ day}^{-1}$), a and b are regression coefficients, τ is boundary shear stress (Nm^{-2}), are developed. Sediment transport rate versus flow data often show a non-linear relationship (e.g. Church *et al.*, 1991), however when both variables are \log_{10} transformed the non-linear relationship is transformed into a linear relationship. The least squares regression line fitted to the \log_{10} transformed data yields a regression in the form:

$$\log_{10} y = a + b \log_{10} x \quad (5.1)$$

Where y is the dependent variable, x is the independent variable, and a and b are regression coefficients. By taking the antilogarithms of both sides of the equation it is possible to obtain an equation for predicting y from x :

$$y = \text{antilog}_{10} x^b \quad (5.2)$$

Expressing this equation in terms of the dependent variable sediment accumulation rate in $\text{kg m}^2 \text{ day}^{-1}$ (A) and the independent variable shear stress in Nm^{-2} (τ) gives the power function:

$$A = a\tau^b \quad (5.3)$$

Log-log regression provides an appropriate means of measuring the dependence of accumulation upon shear stress. Further information on fine sediment mobility may also be obtained by analysing the movement of a tracer which mimics natural bedload.

Transport distance of tracer

In order to examine the relationship between flow and transport distance for sand, a tracer experiment was conducted; the details of which were discussed in Chapter Two. It is impossible to track individual sand particles due to their fine size, therefore the concentration of the tracer cloud in terms of its mass magnetic susceptibility (χ) is used (Sear, 1996). χ measurements were made on trapped basket samples and grab samples in order to determine the longitudinal position of the tracer after sequential floods. A mathematical expression of tracer movement based upon a spatial integration technique (Crickmore, 1967; Arkell, 1985; Sear, 1996) may be made, assuming that the tracer has been well mixed with the bed sediment upon movement. This technique allows the point at which the concentration of magnetic tracer is equal upstream and downstream, or centroid, to be calculated for successive flows. These workers argue that the position of the centroid reflects the subtleties of tracer release and dispersion. The centroid position (P_t), at time t , may be calculated by the formula:

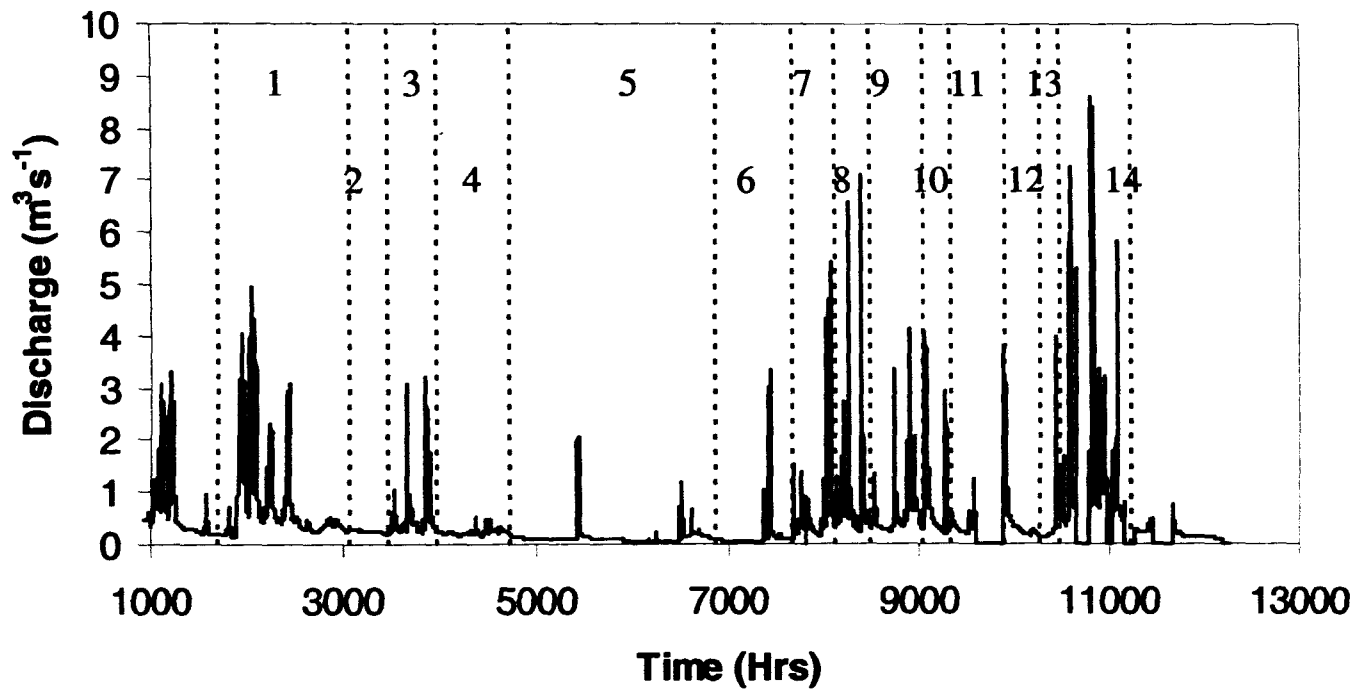
$$\frac{\sum x_i S_i}{\sum S_i} \quad (5.4)$$

Where x_i is the distance downstream of the emplacement site at which a given tracer concentration S_i is found.

5.3 Results

5.3.1 Hydrograph character and sampling periods

The hydrograph for the period where basket traps were sampled is shown in Figure 5.1. The traps were sampled on fourteen occasions between 15th March 1996 and 11th March 1997, covering the end of the 1995-96 winter season, the 1996 summer low flow period, and the whole of the 1996-1997 winter. Tracer movement was monitored



End of Period	Dates
1	15.3.96
2	15.4.96
3	6.5.96
4	6.6.96
5	10.9.96
6	14.10.96
7	2.11.96
8	17.11.96
9	10.12.96
10	22.12.96
11	15.1.97
12	31.1.97
13	8.2.97
14	11.3.97

Figure 5.1 Flow hydrograph for the study period 15th March 1996-11th March 1997. The dotted lines represent the accumulation time between sampling.

on twelve occasions subsequent to emplacement on 20 April 1996. The sampling intervals, indicated on Figure 5.1, were variable usually being sampled after each flood event. Hydrographs tended to be flashy in nature, although some floods reflected snowmelt and were of a longer-term character. An example of a snowmelt hydrograph was the one prior to the first basket sample (15th March 1996). The peak recorded flow during the period of basket sampling was 8.62 m³s⁻¹.

5.3.2 Transport distance

Figure 5.2 demonstrates the relationship between centroid position and a mobilisation index (Qt) for twelve events between 20th April 1996 – 11th March 1997 inclusive, with hydrograph peaks ranging from 0.54-8.62 m³s⁻¹. The flow parameter (dependent variable) was calculated from the peak Q , multiplied by the duration of competent flow in hours (t). Qt was used in favour to stream power due to its stronger relationship with centroid transport distance. The lowest Q where any accumulation was found in the traps was found to be 0.35 m³s⁻¹ (reach average τ using Eq 4.1 >20 Nm⁻²) hence the mobilisation duration was taken to be the period over which this discharge was exceeded. For the first five flow events (solid symbols), which were all below 5.44 m³s⁻¹, prior to November 17th 1996, there appears to be a linear pattern between Qt and transport distance. The maximum tracer distance (L) was in the order of 80m following the first flood of 3.2m³s⁻¹, shortly after seeding of the material onto the river bed (Table 5.1). Some caution must be expressed here, as it is possible that the tracer material may have been ‘overloose’, and not in a structurally stable or natural position. Hence the material may have been transported further than would have naturally have been the case. Alternatively it could be argued that overloose surficial drapes of sand are a natural feature on pool exit slopes, in streams with a high sediment supply (Lisle and Hilton, 1992; 1999). Movement for the next four floods show a linear pattern for Q_{max} . However after the first large winter flood, which peaked at 7.12m³s⁻¹, the centroid appeared to move upstream by 6m (Table 5.1). There are two possible explanations for this. Firstly, tracer which had infiltrated the armour layer and sub-surface framework voids, close to the seeded zone, would have been sheltered from the flow until a large flood capable of disrupting the armour. On disruption of the armour, formerly infiltrated tracer would be re-exposed, which

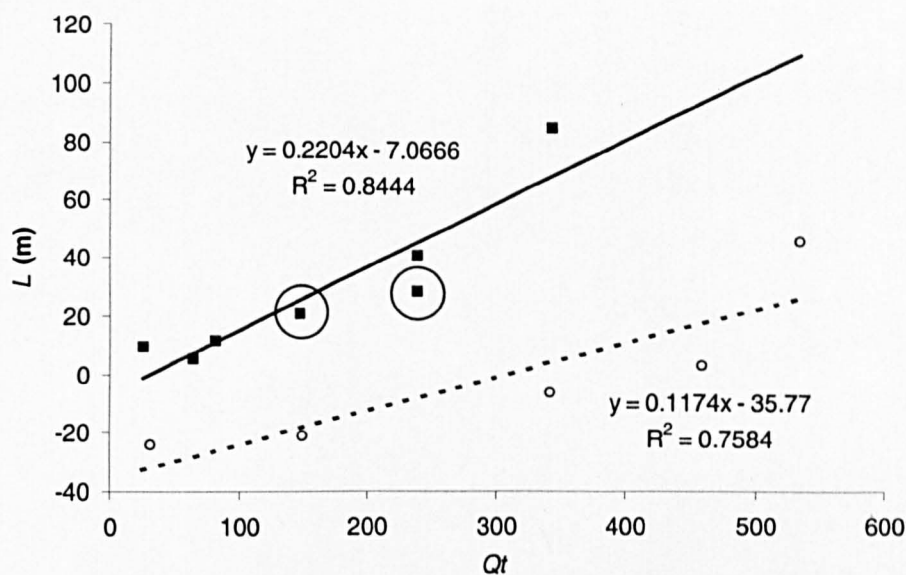


Figure 5.2 Relationship between mobilisation index (Qt) and travel distance of tracer centroid calculated using equation 5.1. Solid symbols represent transport of tracer over a stable armour surface before the first large flood ($7.12 \text{ m}^3 \text{s}^{-1}$), whereas open symbols represent movement of tracer after this flood had mobilised surface possibly re-exposing buried tracer near the seeded zone. Circled points represent two high \bar{L} values obtained after the $7.12 \text{ m}^3 \text{s}^{-1}$ flood.

Date	Centroid position downstream of emplacement site (m)	Movement L (m)	Previous peak Q ($\text{m}^3 \text{s}^{-1}$)
22.5.96	84.8	84.8	3.2
6.6.96	96.3	11.5	0.54
10.9.96	101.8	5.5	2.08
14.10.96	111.1	9.3	3.39
2.11.96	152.2	41.1	5.44
17.11.96	146.2	-6.0	7.12
10.12.96	149.8	3.6	4.13
22.12.96	178.5	28.7	4.09
15.1.97	199.2	20.7	1.23
31.1.97	178.9	-20.3	3.81
8.2.97	155.1	-23.9	3.99
11.3.97	201.4	46.3	8.62

Table 5.1 A flood-by-flood account of tracer position though the Rede riffle-pool sequence

would result in an apparent negative movement of the centroid. A second possibility could be that non-uniform hydraulic nature of the reach, most evident at low discharges, could lead to non-uniform transport of tracer material. For example, excess transport and dilution of the leading edge of the tracer cloud in areas of high τ , and limited movement of the previous tracer centroid in areas of lower τ , could lead to

a perceived upstream movement. The first of these explanations has also been suggested by Sear (1996), and is pursued further here. The suitability of the tracer centroid for monitoring downstream dispersion in a natural channel displaying non-uniform flow and morphology is questionable, due to the 'lumpy' variation in concentration which occurs with distance downstream after flow events. It is recommended that future investigations identify more appropriate methods of monitoring tracer dispersion that take into account the natural variation in hydraulics and morphology found with river channels.

Floods that follow the first large flood peak of the winter tend not to move the tracer as far (with the exception of two flows which are circled on Figure 5.2), and two further surveys reveal tracer recession of around 20m. There appears to be a second linear relationship between flow and transport distance which plots below the first one (open symbols), when taking into account all the floods following the first large flood of the winter (Figure 5.2). The dependence of transport of tracer material upon both competent flow duration and maximum discharge may be described by the following multiple regression relations;

All data

$$L = 7.999 - 5.148Q + 0.132t \quad n=12, \quad p=0.2, \quad r^2=0.544, \quad SE=28.28 \quad (5.5)$$

Before armour disruption

$$L = -5.309 - 1.024Q + 0.228t \quad n=7, \quad p=<0.05, \quad r^2=0.920, \quad SE= 13.22 \quad (5.6)$$

Post armour disruption

$$L = -53.634 + 5.252Q + 0.081t \quad n=5, \quad p=0.15, \quad r^2=0.922, \quad SE=15.48 \quad (5.7)$$

Where L is distance travelled, Q is peak discharge, and t is duration of competent flow. It should be noted that these equations are different for those presented on Figure 5.2, which are for Qt versus L which describe the log-log regression curves in the plots. These equations represent a means of predicting the rate of dispersion of

sand-sized material through a small coarse-grained upland channel, over a stable armour, and after armour disruption. The movement of the tracer centroid shown in Table 5.1 is discussed in more detail in relation to sorting processes through riffle-pool morphology in Chapter Seven. Further information on sediment mobility may be obtained by analysing the grain-size characteristics of material entering traps.

5.3.3 Grain size characteristics of sand entering traps

A summary of the grain size characteristics for fine bedload ($125\mu\text{m}$ - $2000\mu\text{m}$) entering each trap throughout the study reach is presented in Table 5.2 and Figure 5.3. Size data for each trap are presented in Appendix 5.1. The dominant size fraction is fine-medium sand (250 - $500\mu\text{m}$), with a mean of 41 percent by weight, whilst the fine sands (125 - $250\mu\text{m}$) only have a mean of 14 percent by weight. Some variation between the size of infiltrating fines between and within riffles is evident. For example, Riffles A and C tend to have low concentrations of coarse sand (1000 - $2000\mu\text{m}$) in the order of 18 percent by weight, in comparison to Riffle B which has a mean of 25 percent by weight. This may relate to sorting processes and local hydraulics which are discussed further in Chapter Seven. Riffle B is a higher energy riffle in comparison with Riffle A (see Chapter Four), and the fines accumulating in traps here tended to be coarser.

The time series of the variation in the size of fine bedload using average data from all 27 traps over the study period shown in Figure 5.3 indicates some subtle seasonal variation in mean concentration of different size classes being transported with flow. The 125 - $250\mu\text{m}$ size class appears to be the most sensitive to variations in flow. Concentrations of this size class found in bedload traps appear to be enhanced during periods of low flow, whereas during periods of higher winter flow, concentrations of this size-class appear to be diluted. Conversely, the coarser size fractions (500 - $1000\mu\text{m}$, 1000 - $2000\mu\text{m}$) appear to show higher concentrations during periods of high flow and lower concentrations during periods of low flow. The finest fraction (125 - $250\mu\text{m}$) does not appear to be as sensitive to flow as the 250 - $500\mu\text{m}$ size class, but does show some dilution effects at higher discharges.

The next section considers the behaviour of each size fraction and uses rating relations to estimate thresholds for motion for each grain size fraction.

Table 5.2 Percentage by weight composition of sediments entering basket traps.

	1000-2000 μm	500-1000 μm	250-500 μm	125-250 μm
<i>A MEAN</i>	18.41 (2.67-58.67)	25.88 (6.25-47.31)	41.88 (17.33-71.19)	13.84 (1.69-41.38)
<i>B MEAN</i>	25.26 (1.14-67.44)	22.15 (5.59-43.96)	38.93 (9.09-68.72)	13.77 (2.26-39.55)
<i>C MEAN</i>	17.79 (1.09-62.50)	24.76 (4.00-46.20)	43.48 (6.25-74.47)	14.14 (2.53-44.00)
MEAN	20.38 (1.09-67.44)	24.43 (4.00-47.31)	24.43 (4.00-47.31)	13.92 (1.69-44.00)
ALL TRAPS				

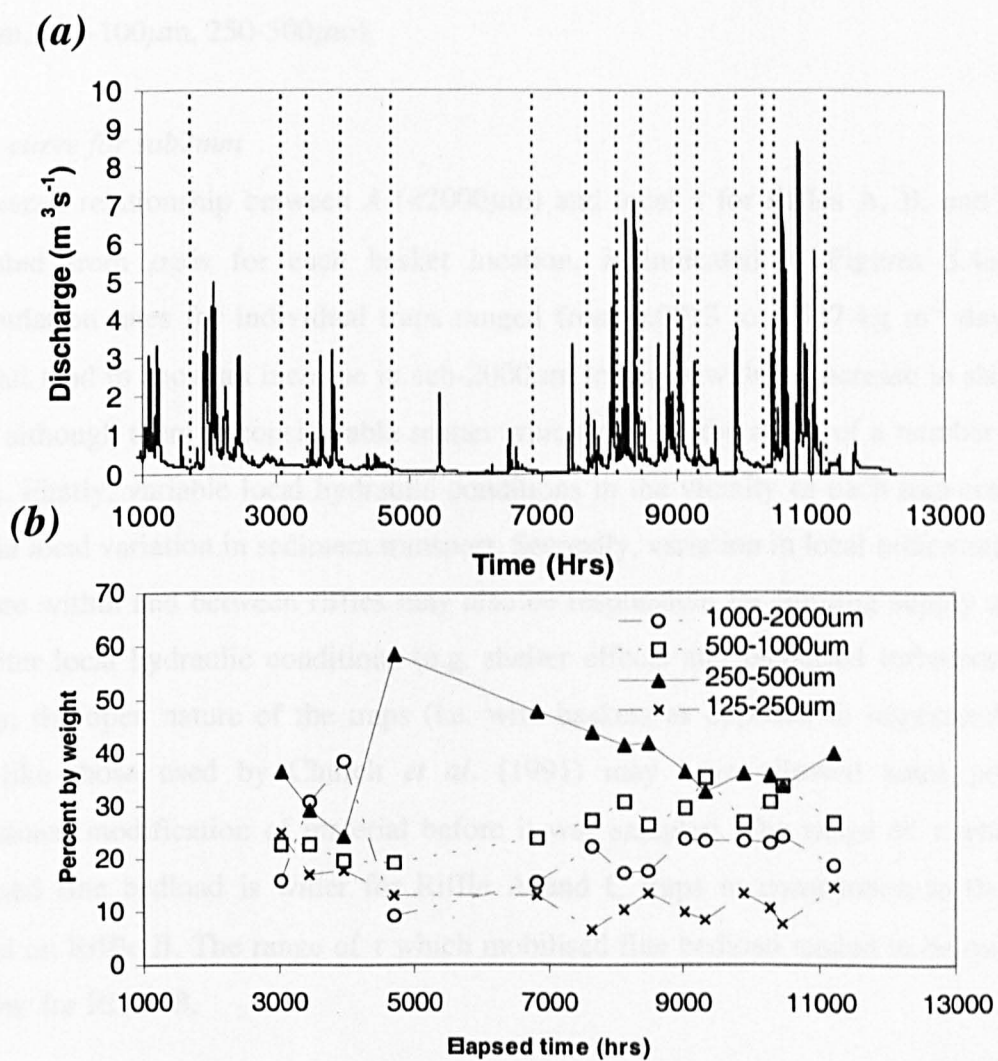


Figure 5.3 Temporal patterns of grain size accumulation in traps. (a) flow, (b) time series of mean percentage by weight of accumulation for different grain size fractions.

5.3.4 Mobility

Trap variability

Accumulation rate at each trap showed a similar pattern, which is indicated by the high correlations among sequences of weights recovered from the traps, given in Appendices 5.2, 5.3, 5.4 and 5.5. Notable exceptions are the correlation coefficients for traps from Riffles B and C, particularly for the 1000-2000 μm size fraction. The general consistency of between-trap accumulation rate indicates that the traps with high correlation coefficients do not have any significant individual biases for different sand size fractions. However there were some traps where significant bias is apparent, these were trap A8 (for 500-1000 μm), B2 (for <2000 μm , 1000-2000 μm , 500-1000 μm , 250-500 μm , 125-250 μm), B3 (for 1000-2000 μm), B4 (for <2000 μm , 1000-2000 μm , 500-100 μm , 250-500 μm).

Rating curve for sub2mm

The overall relationship between A (<2000 μm) and local τ for riffles A, B, and C, calculated from ρ_{gds} for each basket location, is indicated in Figures 5.4a-c. Accumulation rates for individual traps ranged from 0.0013 to 1.527 $\text{kg m}^{-2} \text{ day}^{-1}$. Traps all tend to show an increase in sub-2000 μm loadings with an increase in shear stress, although there is considerable scatter which may be the result of a number of factors. Firstly, variable local hydraulic conditions in the vicinity of each trap could result in local variation in sediment transport. Secondly, variation in local sedimentary structure within and between riffles may also be responsible for limiting supply and may alter local hydraulic conditions (e.g. shelter effects and increased turbulence). Thirdly, the open nature of the traps (i.e. wire baskets as opposed to impermeable walls like those used by Church *et al.* (1991) may have allowed some post-depositional modification of material before it was sampled. The range of τ which mobilised fine bedload is wider for Riffle A and C traps in comparison to those situated on Riffle B. The range of τ which mobilised fine bedload tended to be much narrower for Riffle B,

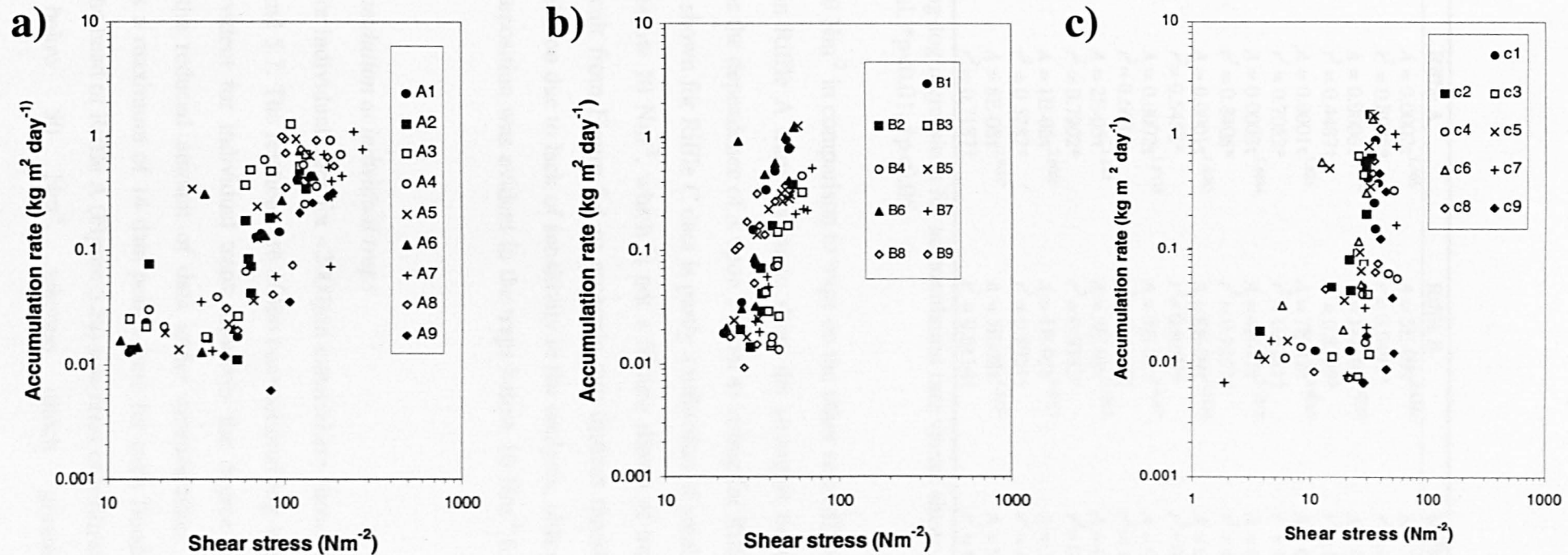


Figure 5.4 Trap rating relations for material $<2\text{mm}$ based on period-averaged samples. The fitted equations (see Table 5.3) are log-log regressions through all of the data for a) riffle A, b) riffle B, and c) riffle C.

Trap number	Riffle A	Riffle B	Riffle C
1	$A = 0.0002\tau^{1.468}$ $r^2 = 0.8025^*$	$A = 5E-09\tau^{4.8361}$ $r^2 = 0.9491^*$	$A = 3E-06\tau^{3.2023}$ $r^2 = 0.6578†$
2	$A = 0.0006\tau^{1.2109}$ $r^2 = 0.4487†$	$A = 1E-09\tau^{4.8727}$ $r^2 = 0.8369^*$	$A = 0.001\tau^{1.6989}$ $r^2 = 0.6036†$
3	$A = 0.0001\tau^{1.825}$ $r^2 = 0.7052^*$	$A = 7E-12\tau^{5.9869}$ $r^2 = 0.6281†$	$A = 6E-05\tau^{2.0928}$ $r^2 = 0.08NS$
4	$A = 0.0003\tau^{1.4884}$ $r^2 = 0.8408^*$	$A = 4E-15\tau^{7.8585}$ $r^2 = 0.7217†$	$A = 0.001\tau^{1.0651}$ $r^2 = 0.4736NS$
5	$A = 0.0001\tau^{1.6985}$ $r^2 = 0.5458^*$	$A = 8E-09\tau^{4.5129}$ $r^2 = 0.8102^*$	$A = 0.0008\tau^{1.7545}$ $r^2 = 0.5802†$
6	$A = 0.0002\tau^{1.5133}$ $r^2 = 0.668^*$	$A = 5E-07\tau^{3.6187}$ $r^2 = 0.4689†$	$A = 0.0031\tau^{1.258}$ $r^2 = 0.374NS$
7	$A = 2E-05\tau^{1.847}$ $r^2 = 0.7902^*$	$A = 3E-08\tau^{3.8931}$ $r^2 = 0.9533^*$	$A = 0.0017\tau^{1.163}$ $r^2 = 0.5224†$
8	$A = 1E-06\tau^{2.6065}$ $r^2 = 0.5282^*$	$A = 1E-05\tau^{2.8077}$ $r^2 = 0.8921†$	$A = 3E-05\tau^{2.5287}$ $r^2 = 0.397NS$
9	$A = 8E-08\tau^{2.9087}$ $r^2 = 0.7187†$	$A = 3E-08\tau^{4.1351}$ $r^2 = 0.6114†$	$A = 9E-05\tau^{1.656}$ $r^2 = 0.0441NS$

Table 5.3 Log-log regressions for accumulation rate versus shear stress for <2000 μm material. * $p<0.01$, † $p<0.05$.

in the range 20-70 Nm^{-2} in comparison to traps on the other two riffles. Accumulation of fine bedload in Riffle A traps appear to show the strongest dependence upon τ ($r^2=0.57$), whereas the dependence of A upon τ is not as strong for Riffle B and C. The poor relationship shown for Riffle C data is partly a reflection of small accumulations of fine bedload below 10 Nm^{-2} , which is not a feature shown at traps on the other riffles. It is difficult from Figure 5.4 to ascertain any distinct threshold for motion from the rating relation due to lack of sensitivity in the analysis, although generally it appears that no deposition was evident in the traps below 10 Nm^{-2} for Riffles A and B.

Variation in accumulation at individual traps

Rating relations for individual traps for <2000 μm material are shown in Table 5.3 and Figures 5.5, 5.6 and 5.7. The relations are of the conventional log-log format $A = \tau^b$. Less scatter is evident for individual traps, however the degree of confidence is reduced due to the reduced amount of data under consideration: for each curve presented there is a maximum of 14 data points (one for each flood event). For the traps situated at the head of Riffle A (Figure 5.5a) low rates of infiltration are found at boundary τ below 50 Nm^{-2} , whereas much greater rates are

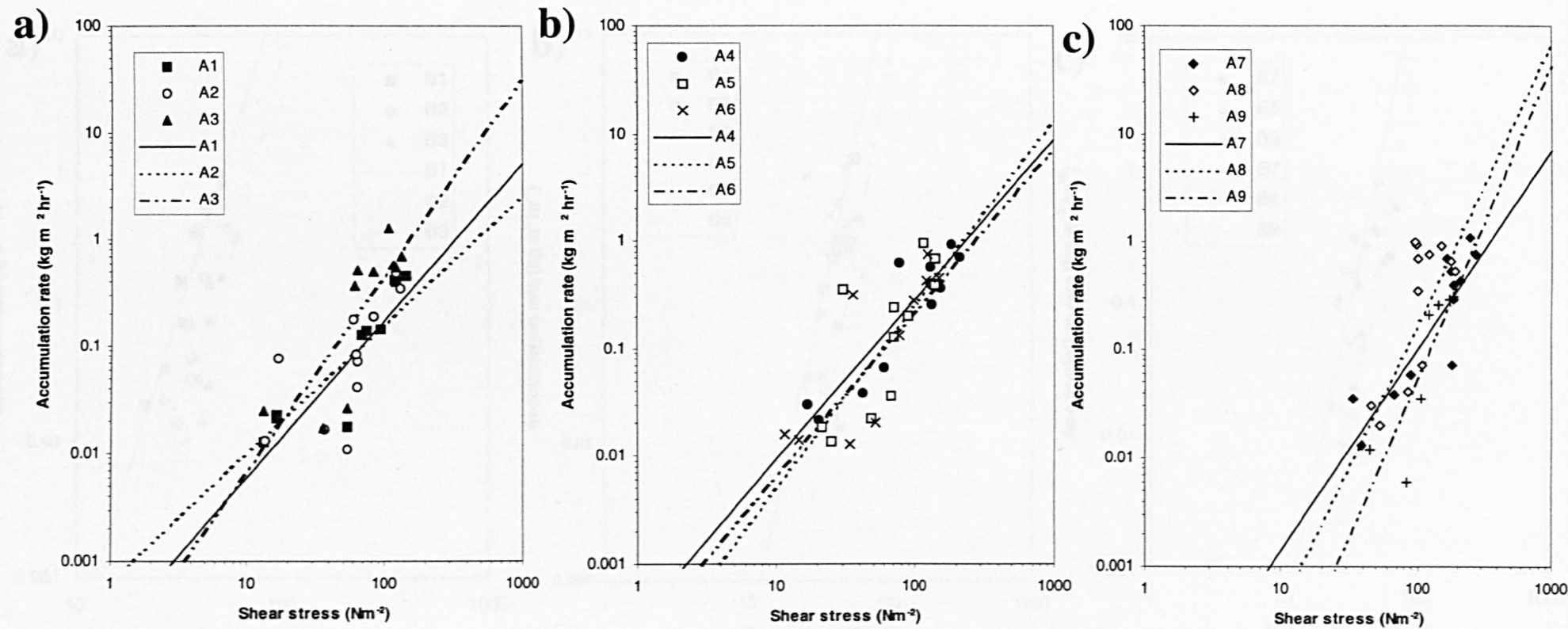


Figure 5.5 Trap rating relations for material $<2\text{mm}$ for riffle A. The fitted relations are the log-log regressions presented in Table 5.8.

a) Traps located at the riffle head, b) traps located at the riffle crest, c) traps located at the riffle tail

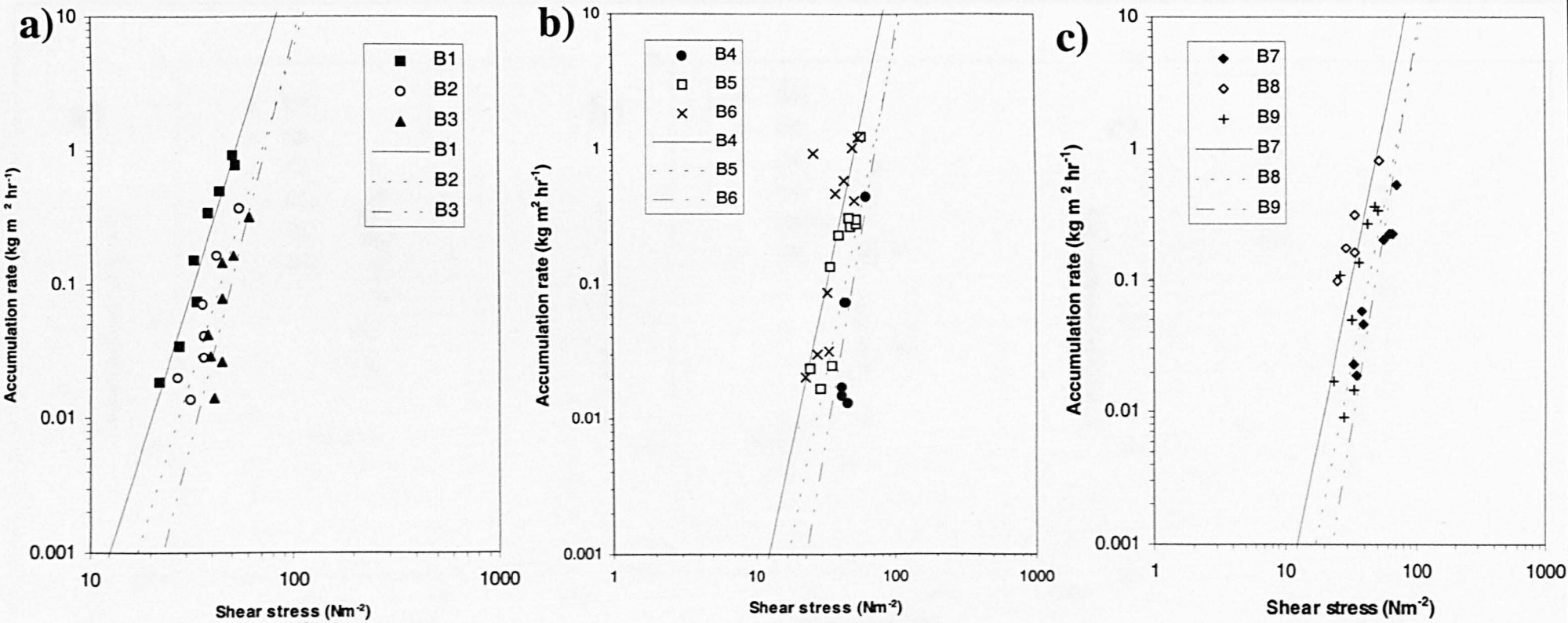


Figure 5.6 Trap rating relations for material $<2\text{mm}$ for riffle B. The fitted relations are the log-log regressions presented in Table 5.8. a) Traps located at the riffle head, b) traps located at the riffle crest, c) traps located at the riffle tail

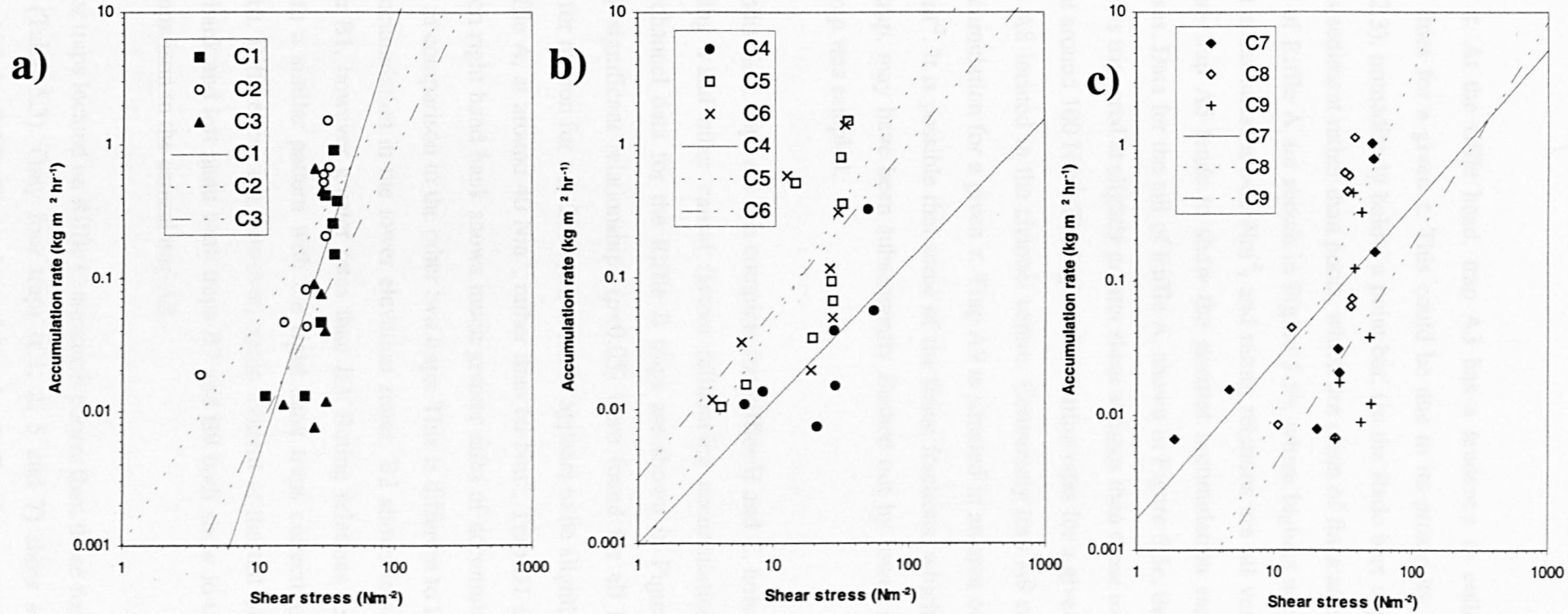


Figure 5.7 Trap rating relations for material <2mm for riffle C. The fitted relations are the log-log regressions presented in Table 5.8. a) Traps located at the riffle head, b) traps located at the riffle crest, c) traps located at the riffle tail

found for higher τ . At the riffle head, trap A3 has a tendency to collect higher concentrations of fines for a given τ . This could be due to its proximity to the left bank (see Figure 2.3), immediately below a point bar, (in the Rede bars appear to act as sources of fines sediment rather than pools, which are clean of fines at base-flow). Data for the crest of Riffle A are shown in Figure 5.5b, where highest accumulation rates are found at shear stresses $>60 \text{ Nm}^{-2}$, and rating relations are all very similar. The channel centre trap A5 tends to show the greatest accumulation especially at higher shear stresses. Data for the tail of Riffle A, shown in Figure 5.5c, demonstrate that most transport is triggered at slightly greater shear stresses than those experienced further up-riffle, at around 100 Nm^{-2} . The highest infiltration rates for a given τ tend to be located at trap A8 located in the channel centre. Conversely trap A9 records the lowest rates of accumulation for a given τ . Trap A9 is situated in an area of high τ in the order of 90 Nm^{-2} . It is possible that some of the finest fractions, which had been deposited in the trap, may have been subsequently flushed out by lower magnitude flows before the trap was sampled.

The data-set for individual traps are less complete for Riffles B and C, however some inferences regarding τ and other causal factors influencing accumulation may be made. The cross-channel data for the Riffle B traps are shown in Figures 5.6a-c, where statistically significant relationships ($p<0.05$) were found for all traps. The general threshold for motion for sub- $2000 \mu\text{m}$ material appears to be slightly lower in comparison to Riffle A, at around 40 Nm^{-2} , rather than 60 Nm^{-2} . Trap B1 situated on the higher elevation right hand bank shows much greater rates of accumulation for a given shear stress in comparison to the other two traps. This is different to the general trend of greater accumulation in the lower elevation zones. B2 shows lower rates of accumulation than B1, however greater rates than B3. Rating relations for the next three traps indicate a similar pattern with the right bank traps collecting the most fines. (Figure 5.6b). Differences are, however, again evident at the tail of Riffle B, where right hand bank and left hand bank traps B7 and B9 both show lower rates of infiltration, in comparison to the central trap A8.

Rating relations for traps located on Riffle C are much poorer than those found for the other two riffles (Table 5.3). Only four traps (C1, 2, 5 and 7) show statistically significant relationships ($p<0.05$). Cross-channel data for Riffle C traps (Figures 5.7a-

c) indicate the general threshold for motion for sub-2mm material to be about half that found for Riffle A, at around 30 Nm^{-2} . Some of the poor relationships displayed between accumulation rate and τ may partly be a result of supply limitation, increased flushing efficiency or suspension of fines rather than transportation via bedload. The right hand bank trap at the riffle head (C1) shows the strongest relationship with shear stress ($r^2=0.7, p<0.05$). Accumulation rates at trap C3 on the left-hand bank did not show a significant relationship with τ ; low accumulation rates are again located in a zone of higher elevation. The traps situated in the crest of the riffle (Figure 5.7b) show a similar pattern. Only the central trap (C5) shows a significant relationship between accumulation rate and shear stress, with accumulation rates also tending to be greater in this zone of lower elevation. Lowest infiltration rates are found at the left-hand bank trap C4 in a zone of higher elevation on the channel margin. Only trap C7 located at the tail of the riffle showed significant relationships between accumulation rate and τ .

My data demonstrates that, for most traps, there is a strong relationship between τ and accumulation of fines. However some traps, particularly those located on Riffle C, do not display a strong relationship between these two variables. Accumulation in the traps must therefore show more dependence upon other variables, such as re-suspension of material through small-scale turbulent pulses, similar to that observed by Carling (1984). In many of the traps, particularly those situated on Riffle C, siltation appeared to be prevented near to the surface of the trap, suggesting that permanent deposition only occurs below a zero velocity plane. Porous walls and top of the traps allow post-depositional exchange of fine sediment between the interstitial spaces and the channel above, further influencing A . Fine bedload sheets (waves) passing through the reach may also account for variable accumulation rates (Carling pers com, 2001), which may be supply dependent and seasonal. Macro-scale turbulent flow structures in the form of high-speed fluid wedges interconnected by low-speed regions (Buffin-Bélanger *et al.* 2000), may also influence accumulation of fines in traps, particularly if associated with the passage of a fine bedload sheet. High speed wedges may result in locally high sand transport rates, whereas the fine bedload waves may move more slowly. Flow structures may be induced by the coarse protruding clasts, particularly evident on Riffle C, which could explain accumulations

recorded below 10 Nm⁻². This explanation is rather speculative and would require testing in the field.

Accumulation tended to be greatest in low elevation zones – where competence is greatest at peak flow (see Chapter Four). This would suggest that post-flood washout of fines in these high shear stress zones was negligible. If washout of material was significant then these traps would contain fewer sediments. High concentrations of fine bedload are likely to reflect the greater rate of delivery.

Multiple regression analysis of A versus τ

To further interrogate trap effects the relationship between τ and accumulation rate, multiple regression was conducted to test the following model;

$$A_{tsi} = a\tau_{si}^{bt} \quad r^2 = 0.92, \quad SE = 0.53 \quad (5.8)$$

where sediment accumulation (A) is dependent on shear stress (τ) regardless of grain size, a and b are regression exponents, t is trap, s is size, i is an individual observation. The statistics for these data are shown in Table 5.4. There appears to be a good fit between the two variables demonstrating a strong dependence of sediment accumulation upon shear stress, and that the trap effect (local position) is important. It is important to note that this equation does not take into account the influence of grain size, which will be demonstrated in the following section.

5.3.5 Size effects

All traps

Subtle differences are apparent for the plots of τ versus A , when grain size is taken into account (Figure 5.8 a-d). These plots demonstrate data from all traps sampled for each grain size after each flood event. The near vertical convergences shown in the data in Figure 5.8, suggest a dominant shear stress range on riffles of between 20 and

Trap	a_i	Standard error a_i	b_i	Standard error b_i	r^2
A1	4.40453E-05	2.8695	1.4978	0.2519	0.65
A2	7.83791E-05	2.9861	1.2977	0.2716	0.34
A3	1.77664E-05	2.8379	1.8894	0.2562	0.63
A4	5.69246E-05	2.7208	1.4994	0.2247	0.67
A5	1.98838E-05	3.4017	1.7471	0.2938	0.46
A6	4.4792E-05	2.5345	1.5496	0.2293	0.58
A7	3.32966E-06	3.5892	1.9264	0.2604	0.67
A8	1.35425E-07	7.7678	2.7749	0.4409	0.43
A9	1.89017E-08	11.3553	2.8768	0.5117	0.59
B1	1.0792E-09	16.7649	4.8382	0.7845	0.75
B2	1.22885E-10	59.5525	5.0846	1.1316	0.63
B3	1.32434E-12	261.6978	5.9975	1.4633	0.42
B4	7.46793E-16	1183.0420	7.8657	1.8506	0.50
B5	1.20587E-09	15.0730	4.5721	0.7302	0.62
B6	1.15878E-07	11.1815	3.5527	0.6688	0.37
B7	1.18304E-08	19.1029	3.6222	0.7575	0.46
B8	1.82348E-06	57.1479	2.8639	1.1413	0.38†
B9	4.83504E-09	17.5106	4.2039	0.8018	0.51
C1	2.16073E-07	6.5781	3.4956	0.5639	0.56
C2	0.000138166	2.6467	1.8291	0.3124	0.52
C3	7.36038E-06	27.7460	2.2481	1.0187	0.07NS
C4	0.000395913	2.7479	0.6907	0.3317	0.31†
C5	0.000185823	2.2090	1.679	0.2569	0.51
C6	0.000635331	2.2289	1.2785	0.2798	0.33
C7	0.000316811	1.8151	1.1544	0.1858	0.40
C8	4.31023E-06	4.5867	2.5766	0.4558	0.35
C9	0.000103753	33.4349	1.2026	0.9571	0.03NS

Table 5.4 Trap rating relations of the form $A = a_i \tau^{b_i}$ for material $<2000\mu\text{m}$. Here, A is the mean rate of sediment accumulation ($\text{kg m}^2 \text{ day}^{-1}$) and τ is the maximum trap shear stress recorded prior to sampling. All r^2 values are significant at $p<0.001$, $\dagger p<0.01$, unless otherwise indicated

60 Nm^{-2} , reflecting a small but dominant range of water surface slope and depths found at riffles. The large degree of scatter evident in this shear stress band, when data from all traps are grouped together, suggests low dependence of accumulation upon shear stress that is probably due to the localised trap effects discussed earlier. As will be shown in Chapter Six, accumulation rate is influenced by relative form and grain roughness. Traps situated in low elevation areas of the bed (high τ zones during a flood) tend to accumulate greater concentrations of fines due to the greater rate of delivery. Progressively lower rates of accumulation are also found in traps with a progressively coarser (rougher) surface layer, which could reflect greater turbulent re-suspension of fines. This would appear to be supported by (Buffin-Bélanger and Roy, 1998) who have demonstrated that coarse clasts and pebble clusters projecting into the flow can induce turbulence. The spatial variability in turbulent flow across riffle

surfaces may explain the highly variable accumulation rates. Furthermore, Cariño
et al. (1998) showed that turbulent pulses are not only responsible for increasing
the accumulation rates, but also for decreasing the shear stress.

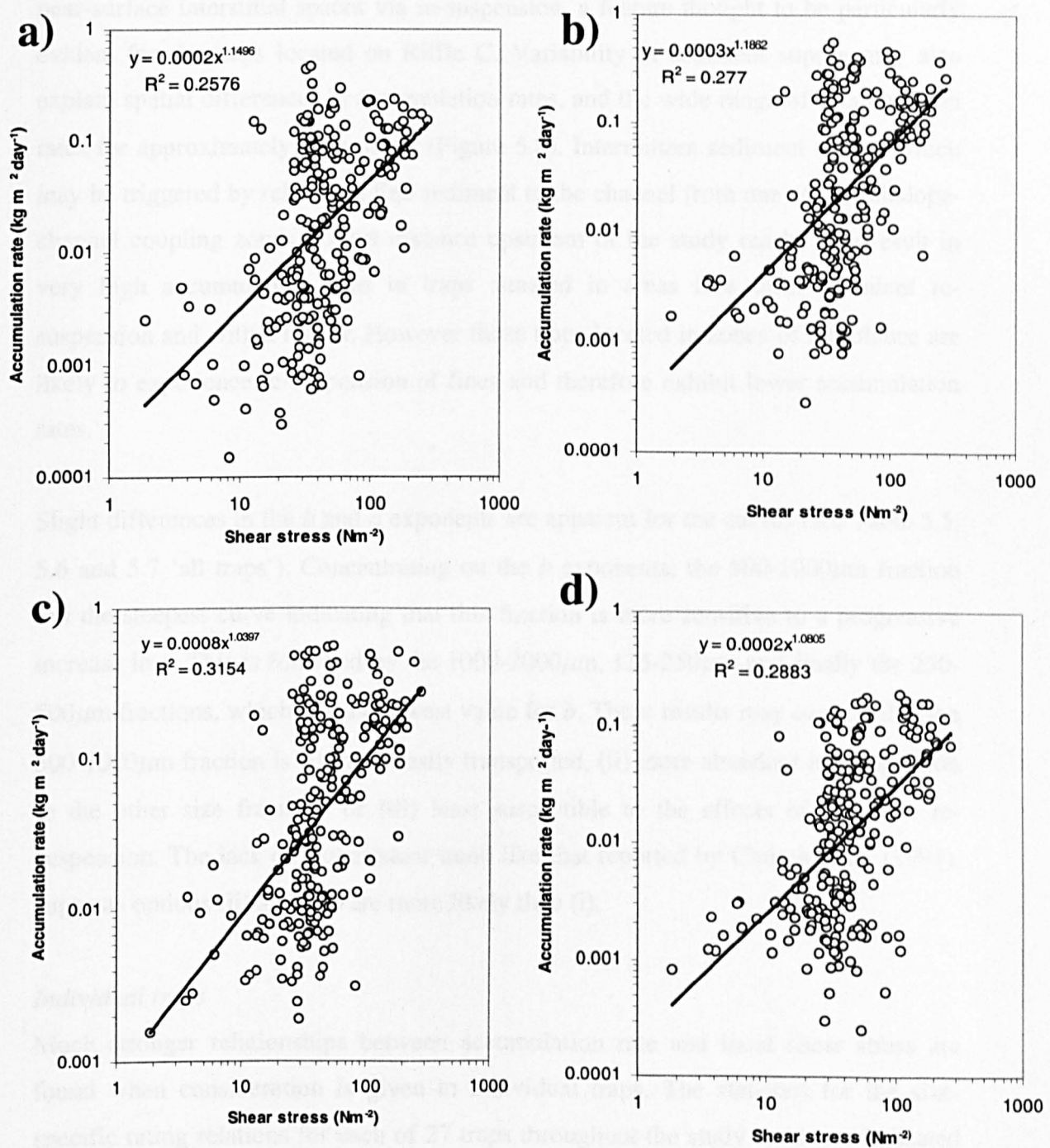


Figure 5.8 Size-specific rating relations for different grain size fractions for all traps, a) 1000-2000 μ m, b) 500-1000 μ m, c) 250-500 μ m and d) 125-250 μ m.

surfaces may explain the highly variable accumulation rates. Furthermore, Carling (1984) has shown that turbulent pulses can not only be responsible for introducing sand into void spaces from suspension, but be responsible for removal of fines from near-surface interstitial spaces via re-suspension, a feature thought to be particularly evident for the traps located on Riffle C. Variability in sediment supply may also explain spatial differences in accumulation rates, and the wide range of accumulation rates for approximately the same τ (Figure 5.8). Intermittent sediment sheets, which may be triggered by release of fine sediment to the channel from one of the hillslope-channel coupling zones a short distance upstream of the study reach, may result in very high accumulation rates in traps situated in areas free from turbulent re-suspension and with a high τ . However those traps located in zones of turbulence are likely to experience re-suspension of fines and therefore exhibit lower accumulation rates.

Slight differences in the b and a exponents are apparent for the curves (see Table 5.5, 5.6 and 5.7 'all traps'). Concentrating on the b exponents; the 500-1000 μm fraction has the steepest curve indicating that this fraction is more sensitive to a progressive increase in τ . This is followed by the 1000-2000 μm , 125-250 μm and finally the 250-500 μm fractions, which has the lowest value for b . These results may suggest that the 500-1000 μm fraction is (i) more easily transported, (ii) more abundant in comparison to the other size fractions or (iii) least susceptible to the effects of turbulent re-suspension. The lack of a consistent trend like that reported by Church *et al.* (1991), suggests options (ii) and (iii) are more likely than (i).

Individual traps

Much stronger relationships between accumulation rate and local shear stress are found when consideration is given to individual traps. The statistics for the size-specific rating relations for each of 27 traps throughout the study reach are indicated in Tables 5.5, 5.6 and 5.7, where r^2 values generally indicate good relationships between shear stress and accumulation for individual size classes ($p=0.05$, unless otherwise specified). Notable exceptions are the traps located on riffle C (C4, C6, C7 and C8).

Size	a_i	Standard error a_i	b_i	Standard error b_i	R^2
Trap A1; N=9; $t_{0.05,7} = 2.37$					
1-2mm	1.42×10^{-5}	2.76E+01	1.11*	0.4793	0.50
500-1000 μ m	1.87×10^{-5}	2.76E+01	1.67	0.4793	0.83
250-500 μ m	9.14×10^{-5}	2.76E+01	1.51	0.4793	0.85
125-250 μ m	1.55×10^{-5}	2.76E+01	1.70	0.4793	0.71
Trap A2; N=11; $t_{0.05,9} = 2.26$					
1-2mm	2.11×10^{-5}	3.21E+01	1.44	0.5168	0.84
500-1000 μ m	8.94×10^{-5}	3.21E+01	1.31	0.5168	0.46
250-500 μ m	4.26×10^{-5}	3.21E+01	1.12	0.5168	0.40
125-250 μ m	4.69×10^{-5}	3.21E+01	1.33	0.5168	0.31†
Trap A3; N=10; $t_{0.05,8} = 2.23$					
1-2mm	1.76×10^{-5}	2.64E+01	1.80	0.4874	0.81
500-1000 μ m	9.87×10^{-6}	2.64E+01	2.10*	0.4874	0.73
250-500 μ m	4.89×10^{-5}	2.64E+01	1.79	0.4874	0.76
125-250 μ m	1.17×10^{-5}	2.64E+01	1.86	0.4874	0.63
Trap A4; N=11; $t_{0.05,9} = 2.20$					
1-2mm	9.33×10^{-5}	2.25E+01	1.37	0.4274	0.81
500-1000 μ m	4.35×10^{-5}	2.25E+01	1.62	0.4274	0.87
250-500 μ m	1.03×10^{-4}	2.25E+01	1.49	0.4274	0.80
125-250 μ m	2.51×10^{-5}	2.25E+01	1.51	0.4274	0.60
Trap A5; N=11; $t_{0.05,9} = 2.26$					
1-2mm	1.66×10^{-5}	5.27E+01	1.78	0.559	0.48
500-1000 μ m	2.62×10^{-5}	5.27E+01	1.73	0.559	0.55
250-500 μ m	5.79×10^{-5}	5.27E+01	1.62	0.559	0.52
125-250 μ m	6.21×10^{-6}	5.27E+01	1.86	0.559	0.47
Trap A6; N=10; $t_{0.05,8} = 2.31$					
1-2mm	6.29×10^{-5}	1.72E+01	1.35	0.4363	0.49
500-1000 μ m	3.58×10^{-5}	1.72E+01	1.60	0.4363	0.70
250-500 μ m	8.25×10^{-5}	1.72E+01	1.58	0.4363	0.72
125-250 μ m	2.17×10^{-5}	1.72E+01	1.67	0.4363	0.61
Trap A7; N=12; $t_{0.05,10} = 2.23$					
1-2mm	2.59×10^{-7}	6.47E+01	2.38*	0.4954	0.78
500-1000 μ m	4.92×10^{-6}	6.47E+01	1.89	0.4954	0.64
250-500 μ m	1.78×10^{-5} *	6.47E+01	1.70	0.4954	0.82
125-250 μ m	5.37×10^{-6}	6.47E+01	1.73	0.4954	0.72
Trap A8; N=12; $t_{0.05,10} = 2.23$					
1-2mm	8.55×10^{-7}	1.22E+03	2.45	0.8387	0.48
500-1000 μ m	2.34×10^{-7}	1.22E+03	2.76	0.8387	0.48
250-500 μ m	2.17×10^{-7}	1.22E+03	2.76	0.8387	0.60
125-250 μ m	7.72×10^{-9}	1.22E+03	3.13	0.8387	0.55
Trap A9; N=7; $t_{0.05,8} = 2.57$					
1-2mm	7.95×10^{-8}	5.17E+03	2.91	0.9734	0.72
500-1000 μ m	4.57×10^{-7} *	5.17E+03	2.12	0.9734	0.52†
250-500 μ m	1.17×10^{-9}	5.17E+03	3.51	0.9734	0.79
125-250 μ m	2.59×10^{-8}	5.17E+03	2.97	0.9734	0.77
ALL TRAPS RIFFLE A; N=93; $t_{0.05,91} = 1.99$					
1-2mm	2.96×10^{-5}		1.53		0.50
500-1000 μ m	2.88×10^{-5}		1.64		0.57
250-500 μ m	1.21×10^{-4}		1.41		0.57
125-250 μ m	0.438		1.14		0.94

Table 5.5 Size-specific rating relations of the form $A_i = a_i \tau^{b_i}$ for individual traps and material $< 2000 \mu\text{m}$, for riffle A.

In the table, A is the mean rate of sediment accumulation in the trap ($\text{kg m}^{-2} \text{ day}^{-1}$), and τ is the peak shear stress (Nm^{-2}) estimated using techniques in Chapter 4. The power functions are adjusted to eliminate bias introduced in the linearised (logarithmic) calculations (cf. Ferguson, 1986). All R^2 values are significant at $\sigma = 0.05$; t is Student's t at $\alpha = 0.05$ with indicated degrees of freedom, used to form the confidence ranges of the parameters. † Value only significant at $\alpha = 0.1$. NS = not significant.

Size	a_i	Standard error a_i	b_i	Standard error b_i	R^2
Trap B1; N=8; $t_{0.05,7} = 2.37$					
1-2mm	1.22×10^{-9}	2.28E+04	4.81	1.4924	0.90
500-1000 μm	4.837×10^{-10}	2.28E+04	5.19*	1.4924	0.96
250-500 μm	4.728×10^{-9}	2.28E+04	4.58	1.4924	0.94
125-250 μm	4.83×10^{-10}	2.28E+04	4.77	1.4924	0.83
Trap B2; N=7; $t_{0.05,5} = 2.57$					
1-2mm	9.334×10^{-10}	2.83E+06	4.64	2.1527	0.77
500-1000 μm	6.77×10^{-11}	2.83E+06	5.19	2.1527	0.82
250-500 μm	1.245×10^{-9}	2.83E+06	4.57	2.1527	0.75
125-250 μm	2.895×10^{-12}	2.83E+06	5.93*	2.1527	0.65
Trap B3; N=8; $t_{0.05,7} = 2.37$					
1-2mm	7.66×10^{-11} *	7.91E+08	4.84	2.7837	0.51†
500-1000 μm	3.55×10^{-13}	7.91E+08	6.18	2.7837	0.60
250-500 μm	1.727×10^{-11}	7.91E+08	5.56	2.7837	0.75
125-250 μm	6.548×10^{-15}	7.91E+08	7.42	2.7837	0.63
Trap B4; N=8; $t_{0.05,4} = 2.78$					
1-2mm	2.08×10^{-13}	2.46E+11	6.37	3.5206	0.37†
500-1000 μm	1.4×10^{-16}	2.46E+11	8.12	3.5206	0.60†
250-500 μm	1.12*	2.46E+11	0.75*	3.5206	0.82
125-250 μm	2.46×10^{-18}	2.46E+11	9.37	3.5206	0.65
Trap B5; N=10; $t_{0.05,6} = 2.31$					
1-2mm	3.57×10^{-9}	1.52E+04	4.44	1.3891	0.72
500-1000 μm	1.65×10^{-10}	1.52E+04	5.19*	1.3891	0.84
250-500 μm	4.09×10^{-9}	1.52E+04	4.31	1.3891	0.81
125-250 μm	8.73×10^{-10}	1.52E+04	4.36	1.3891	0.71
Trap B6; N=10; $t_{0.05,6} = 2.31$					
1-2mm	1.32×10^{-6} *	4.88E+03	2.66*	1.2723	0.42
500-1000 μm	7.25×10^{-8}	4.88E+03	3.82	1.2723	0.47
250-500 μm	2.45×10^{-7}	4.88E+03	3.59	1.2723	0.45
125-250 μm	7.64×10^{-9}	4.88E+03	4.15	1.2723	0.47
Trap B7; N=8; $t_{0.05,6} = 2.45$					
1-2mm	8.02×10^{-7} *	3.74E+04	2.16*	1.4412	0.35†
500-1000 μm	1.51×10^{-9}	3.74E+04	4.15	1.4412	0.88
250-500 μm	1.20×10^{-8}	3.74E+04	3.94	1.4412	0.97
125-250 μm	1.33×10^{-9}	3.74E+04	4.24	1.4412	0.88
Trap B8; N=5; $t_{0.05,5} = 3.18$					
1-2mm	1.26×10^{-5}	2.42E+06	2.49	2.1711	0.78
500-1000 μm	5.68×10^{-7}	2.42E+06	3.35	2.1711	0.87
250-500 μm	2.29×10^{-5}	2.42E+06	2.19	2.1711	0.75†
125-250 μm	6.72×10^{-8}	2.42E+06	3.44	2.1711	0.59†
Trap B9; N=9; $t_{0.05,7} = 2.37$					
1-2mm	3.92×10^{-9}	2.69E+04	4.40	1.5254	0.57
500-1000 μm	5.68×10^{-11}	2.69E+04	5.37	1.5254	0.69
250-500 μm	7.92×10^{-8}	2.69E+04	3.52	1.5254	0.56
125-250 μm	3.09×10^{-8}	2.69E+04	3.53	1.5254	0.42†
ALL TRAPS RIFFLE B; N=72; $t_{0.05,70} = 1.99$					
1-2mm	1.89×10^{-5} *	1.87*		0.11	
500-1000 μm	3.69×10^{-7}	2.96		0.21	
250-500 μm	4.16×10^{-7}	3.10		0.40	
125-250 μm	1.14×10^{-8}	3.76		0.47	

Table 5.6 Size-specific rating relations of the form $A_i = a_i \tau^{b_i}$ for individual traps and material $< 2000 \mu\text{m}$, for riffle B.

In the table, A is the mean rate of sediment accumulation in the trap ($\text{kg m}^{-2} \text{ day}^{-1}$), and τ is the peak shear stress (Nm^{-2}) estimated using techniques in Chapter 4. The power functions are adjusted to eliminate bias introduced in the linearised (logarithmic) calculations (cf. Ferguson, 1986). All R^2 values are significant at $\sigma = 0.05$; t is Student's t at $\alpha = 0.05$ with indicated degrees of freedom, used to form the confidence ranges of the parameters. † Value only significant at $\alpha = 0.1$, NS = not significant.

Trap	a_i	Standard error a_i	b_i	Standard error b_i	R^2
A1	4.40453E-05	2.869459	1.4978	0.2519	0.65
A2	7.83791E-05	2.98607	1.2977	0.2716	0.34
A3	1.77664E-05	2.837919	1.8894	0.2562	0.63
A4	5.69246E-05	2.720821	1.4994	0.2247	0.67
A5	1.98838E-05	3.401731	1.7471	0.2938	0.46
A6	4.4792E-05	2.534545	1.5496	0.2293	0.58
A7	3.32966E-06	3.589219	1.9264	0.2604	0.67
A8	1.35425E-07	7.767835	2.7749	0.4409	0.43
A9	1.89017E-08	11.35534	2.8768	0.5117	0.59
B1	1.0792E-09	16.76486	4.8382	0.7845	0.75
B2	1.22885E-10	59.5525	5.0846	1.1316	0.63
B3	1.32434E-12	261.6978	5.9975	1.4633	0.42
B4	7.46793E-16	1183.042	7.8657	1.8506	0.50
B5	1.20587E-09	15.07301	4.5721	0.7302	0.62
B6	1.15878E-07	11.1815	3.5527	0.6688	0.37
B7	1.18304E-08	19.10293	3.6222	0.7575	0.46
B8	1.82348E-06	57.14786	2.8639	1.1413	0.38†
B9	4.83504E-09	17.51056	4.2039	0.8018	0.51
C1	2.16073E-07	6.578093	3.4956	0.5639	0.56
C2	0.000138166	2.646671	1.8291	0.3124	0.52
C3	7.36038E-06	27.74598	2.2481	1.0187	0.07NS
C4	0.000395913	2.747894	0.6907	0.3317	0.31†
C5	0.000185823	2.209022	1.679	0.2569	0.51
C6	0.000635331	2.228948	1.2785	0.2798	0.33
C7	0.000316811	1.815098	1.1544	0.1858	0.40
C8	4.31023E-06	4.586696	2.5766	0.4558	0.35
C9	0.000103753	33.4349	1.2026	0.9571	0.03NS

Table 5.7 Size-specific rating relations of the form $A_i = a_i \tau^{b_i}$ for individual traps and material $< 2000 \mu\text{m}$, for riffle C.

In the table, A is the mean rate of sediment accumulation in the trap ($\text{kg m}^{-2} \text{ day}^{-1}$), and τ is the peak shear stress (Nm^{-2}) estimated using techniques in Chapter 4. The power functions are adjusted to eliminate bias introduced in the linearised (logarithmic) calculations (cf. Ferguson, 1986). All R^2 values are significant at $\sigma = 0.05$; t is Student's t at $\alpha = 0.05$ with indicated degrees of freedom, used to form the confidence ranges of the parameters. † Value only significant at $\alpha = 0.1$, NS = not significant.

Differences between a and b exponents are apparent for different grain sizes, and the same pattern appears to hold for most of the traps sampled. The values for the intercept (a) tend to be higher for the 250-500 μm fraction than for other size fractions with a maximum of 1.12 found at trap B4. The 250-500 μm fraction also tends to have the lowest slope (b) with a value of 0.75. This suggests that this fraction is the least sensitive to progressive increases in τ in comparison to the other size fractions. Slope values (b -exponent) tend not to differ dramatically between size fractions for each trap on Riffles A and C, however there are large variations found for traps situated on Riffle B, particularly at traps B3 and B4. Steepest curves tend to be found for 125-

250 μm or 500-1000 μm on Riffle A and B. For Riffle C however, it is the 1000-2000 μm size fraction which is the most sensitive to progressive increases in τ , which is reflected in the high b -exponents.

These data appear to suggest some spatial variability in values for the a and b exponents. Generally Riffles A and B conflict with Church *et al.* (1991) who found that the coarser sand fractions tended to be the most sensitive to an increase in flow strength. Riffles A and B suggest that 125-250 μm material is not available at very low τ , but is more abundant at higher τ (hence the curves have high b -exponents). However, data for traps located on Riffle C are more supportive of Church *et al.*'s findings, in that the 1000-2000 μm fraction appears to be the most sensitive grain fraction as shear stress progressively increases. Riffle C is a higher energy riffle (see Chapter Four), and it is possible that some finer fractions may be more likely to be intermittently suspended or saltated over the riffle due to turbulence and therefore are less likely to accumulate in traps, resulting in lower b and higher a exponents. Alternatively, some traps on this riffle may be susceptible to post flood flushing of the finest sand fractions through the gravel interstices.

Detecting a threshold for motion in the sand size classes

To investigate the threshold for motion of different sand size grades the lower portion of the rating curves for each size fraction for Riffle A was plotted (Figure 5.9). Riffle A data was used here as the results of the correlation in Appendices 5.2-5.5 confirmed the greatest between-trap similarity in the sequences of weights recovered for each size class. Regression through data from 'all traps' on Riffle A yielded better r^2 values (see Table 5.5), and as a consequence more confidence can be expressed in the data obtained from Riffle A, rather than the reach as a whole, which exhibits a high degree of scatter and lower r^2 values.

At a practical detection limit of 0.003 kg m² day⁻¹ threshold estimates are found to be almost identical for the 125-500 μm , 500-1000 μm and 1000-2000 μm size fractions, with a range of between 11 and 22 Nm⁻². The 250-500 μm fraction has a slightly lower threshold for motion in comparison to the other sizes with a value of 11 Nm⁻². It is

clear from Figure 5.9 that very low shear stresses are required for initial movement of sand-sized material. This graph appears to demonstrate equal mobility for three out of the four fractions considered. However this analysis is not very critical as problems are encountered when extrapolating the data beyond the measured range and the possibility of variable slope estimates propagating error in the intercept estimate (Church *et al.*, 1991).

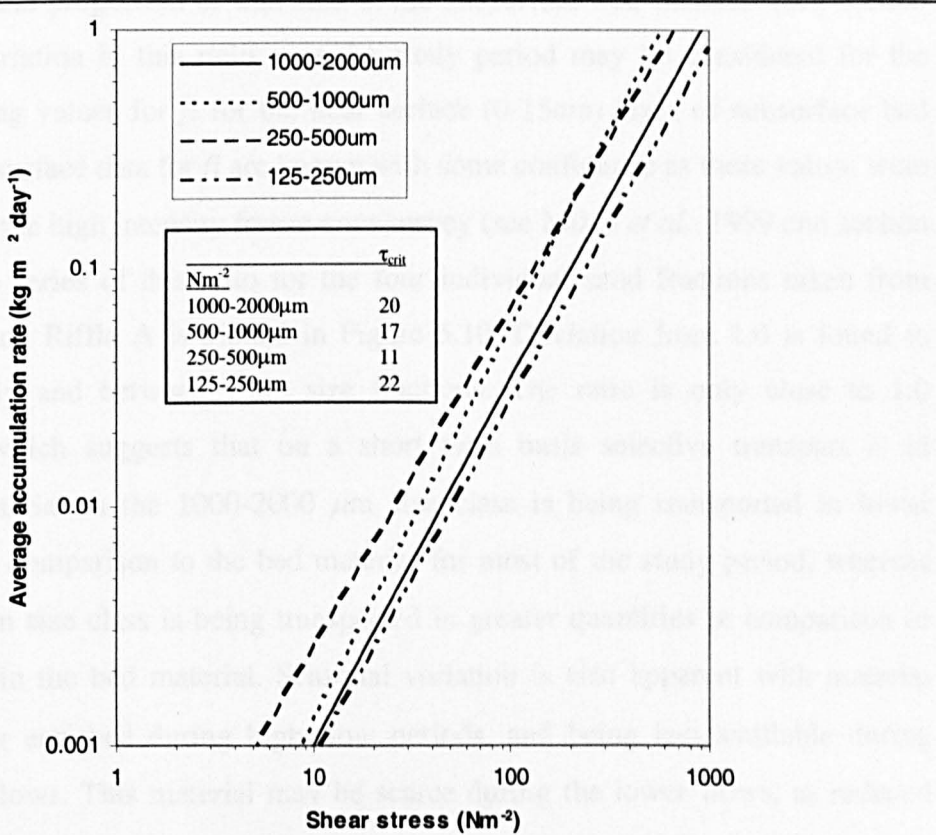


Figure 5.9 Log-log graph representation of size-specific rating relations based on all 9 traps located on riffle A. The fitted relations are the regression equations in Table 5.6 for 'All data' riffle A.

By taking into consideration size effects at each trap and repeating the multiple regression analysis between A and τ the relation is improved;

$$A_{tsi} = a_{ts} \tau_{tsi}^{bts} \quad r^2 = 0.94, \quad SE=0.507 \quad (5.9)$$

This equation takes into account the range of a and b values for different sizes of sediments at each trap, shown in Table 5.5, 5.6 and 5.7. r^2 values indicate a slight

improvement on Equation 5.8, suggesting that the dependence of A upon τ is influenced by the grain size as well as the trap.

Equal mobility in the sand-sized material

According to Andrews and Parker (1983) for grains in transport to be equally mobile, the ratio of $p_i / f_i \equiv 1.0$ for all i , where p_i is the proportion of the i th size in the bed load and f_i is the proportion of that size in the subsurface bed material (see section 1.5.3). The variation in this ratio over the study period may be considered for the Rede data using values for f_i for the near surface (0-15cm) layer of subsurface bed material. Sub-surface data for f_i are known with some confidence as these values were obtained from the high intensity freeze-core survey (see Milan *et al.*, 1999 and section 2.5.2). A time series of this ratio for the four individual sand fractions taken from traps situated on Riffle A is plotted in Figure 5.10. Deviation from 1.0 is found to vary seasonally and between grain size fractions. The ratio is only close to 1.0 temporarily, which suggests that on a short term basis selective transport is in operation. Material in the 1000-2000 μm size class is being transported in lower proportions in comparison to the bed material for most of the study period, whereas the 125-250 μm size class is being transported in greater quantities in comparison to that held within the bed material. Seasonal variation is also apparent with material $>500\mu\text{m}$ being enriched during high flow periods, and being less available during summer low flows. This material may be scarce during the lower flows, as reduced competence is only being capable of transporting the finer grades. In contrast the finer sands $<500\mu\text{m}$ behave in antiphase, tending to be enriched during the lower flow periods and scarce during the winter high flows. High flows appear to dilute the finer grades and may result in suspension of this material. This plot appears to suggest size selectivity over the shorter timescale (season to season), however, when deviation from 1.0 is averaged out over the whole study period, the condition is closer to equal mobility. A seasonal change in sediment source within the catchment may also explain the change in grain size of sediments accumulating in traps. The main sources of fines on the Rede are from erosion scars / bluffs in slope-channel coupling zones, in-channel supply, and run-off from surrounding moorland. Low and intermediate events are likely to be responsible for re-work in-channel sources (such as those deposited on bar surfaces, or on the lee of large clasts) and introducing finer

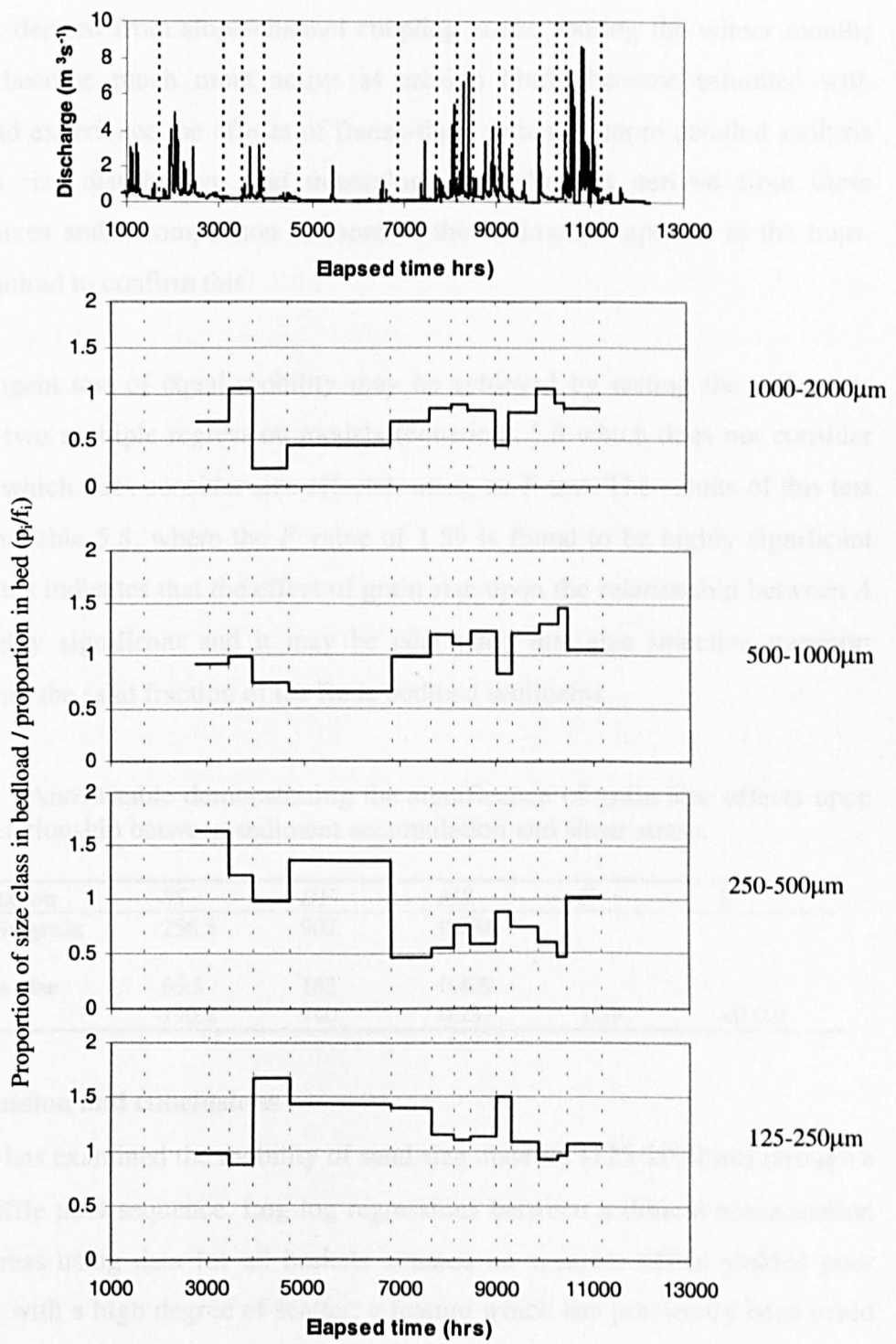


Figure 5.10 Behaviour of p_i/f_i over the thirteen month study period for the weighted average load for all traps located on riffle A. Departure from 1.0 indicates size-selective transport.

grades from run-off into the channel. Larger events are more likely to introduce coarser fines derived from slope-channel coupling zones. During the winter months these areas become much more active as erosion bluffs become saturated with rainwater, and experience the effects of freeze-thaw action. A more detailed analysis of the grain size distributions and mineralogy of sediments derived from these different sources and a comparison to those of the sediments captured in the traps, would be required to confirm this.

A more stringent test of equal mobility may be achieved by testing the difference between the two multiple regression models (equations 5.8 which does not consider size and 5.9 which does consider size effects), using an *F*-test. The results of this test are shown in Table 5.8, where the *F* value of 1.59 is found to be highly significant ($p<0.001$). This indicates that the effect of grain size upon the relationship between *A* and τ is highly significant and it may be concluded that size selective transport operates within the sand fraction of the Rede bedload sediments.

Table 5.8 Anova table demonstrating the significance of grain size effects upon the relationship between sediment accumulation and shear stress.

Source of Variation	SS	DF	MS	F	P
Basic model (No grain size)	256.5	902	0.284		
Effect of Grain Size	66.3	162	0.409		
Residual	190.2	740	0.257	1.59	<0.001

5.4 Discussion and conclusions

This chapter has examined the mobility of sand size material (125-2000 μm) through a gravel-bed riffle pool sequence. Log-log regressions between sediment accumulation and shear stress using data for all baskets situated on separate riffles yielded poor relationships with a high degree of scatter; a feature which has previously been noted by Frostick *et al.* (1985), Carling and McCahon (1987) and Sear (1993). Streamflow and sediment availability can vary over timescales of minutes to hours in flashy streams such as the Rede. Due to the temporal sampling framework which utilised intervals of days to weeks, it was difficult to relate temporally-integrated results from sampling over a whole hydrograph, or series of hydrographs, to detailed instantaneous hydraulic data which assumed uniform flow, when flow may be non-uniform and unsteady (Carling and McCahon, 1987). Although Carling's (1984) work

demonstrated local hydraulics play only a minor role in fine sediment infiltration, data for individual traps demonstrated strong relationships between A and local τ . In general there was a positive relationship between τ and A , although the relation was not always significant. High τ may result in enhanced delivery of fine material to the trap, however they may also result in flush-out of material, as the traps used in this study had porous sidewalls. Turbulent flow is likely to play an important role in both accumulation and re-suspension of fine sediments in framework gravels (Carling, 1984), and may partly explain some of the scatter in the relationships shown by some traps particularly those on Riffle C. Sediment supply will also have a strong influence upon some of the spatial and temporal accumulation patterns shown. Sediment waves or pulses, related to release from storage areas (e.g. slope-channel coupling zones, point bars), may also be responsible for elevating accumulation rates. In Church *et al.*'s (1991) study of fine bedload accumulation over a nival flood, very strong relationships were found between accumulation and discharge. This may reflect the solid-walled traps which he was using, which did not allow for post depositional development. Furthermore, the wire screen / mesh placed over the top of his traps is likely to have prevented turbulent resuspension of fines which had already settled within them. The traps used in this study, however, provide a closer analogue to the development of fines within natural gravels.

Observations of the sub-2000 μm fraction as a whole suggested this material was equally mobile, with little or no accumulation in traps found below a threshold τ of 10 Nm^{-2} (see Figure 5.4). Extrapolation of the lower portion of the rating relations for different size fractions taken from Riffle A supported this observation and demonstrated 'near equal mobility' for three out of the four size fractions considered, the exception being the 250-500 μm fraction which required a lower threshold τ (5 Nm^{-2}) for entrainment. Further examination of rating relations revealed that grain size fraction responded differently to progressive increases in τ . Slope exponents for Riffles A and B tended to be steepest for the 125-1250 μm or the 500-1000 μm fraction, whereas for Riffle C steepest b exponents were found for the 1000-2000 μm fraction. This finding would favour the occurrence of selective transport. Information on the mobility of sand was also obtained from the magnetic tracer survey.

Magnetic tracer survey

Movement of tracer sands was found to occur at flows as little as $0.5\text{m}^3\text{s}^{-1}$ where the centroid was transported a further 11.5m downstream. The lowest flow recorded where fine bedload had accumulated in traps was $0.35\text{m}^3\text{s}^{-1}$, before the tracer experiment was conducted, which equated to a reach $\tau = 20 \text{ Nm}^2$ (supporting the basket trap data). Transport of sand was found to show a strong dependence upon both maximum Q and the duration of competent flow (t), as demonstrated by Figure 5.2 and equations 5.5, 5.6, and 5.7. Observations of tracer sand at flows as low as $0.5 \text{ m}^3\text{s}^{-1}$ suggested that sand is selectively transported over the surface of a stable gravel bed until τ is capable of mobilising surface gravel particles. The plot of Qt versus L shown in Figure 5.2 demonstrated two linear relationships, which may be explained by selective transport processes. The pattern shown is indicative of two phase transport processes (*sensu* Jackson and Beschta, 1982): solid symbols represent transport of tracer over a stable armour bed (stabilised after a long period of summer low flows), whereas open symbols represent movement of tracer after break of the armour layer and bed structure. Tracer may have been stored in the subsurface gravel interstices after penetration of the surface voids (*sensu* Beschta and Jackson, 1979). Following the first major flood of the winter ($7.12\text{m}^3\text{s}^{-1}$), it is feasible that the surface layer was disrupted and mobilised in the vicinity of the seeded zone. This would have resulted in exposure of formerly infiltrated material and higher magnetic susceptibility values close to the original seeded zone. Coarse tracer data show mobilisation of coarse surface (D_{50}) tracers in the seeded zone at or near this discharge (see Chapter Six and Eight).

Flow regime and equal mobility

Substantial variations occurred in the proportions of material which accumulated in traps at during different flow regimes (Figure 5.10). Deviation from equal mobility appears to occur for all grain size classes when consideration is given to seasonal variations. However when the full study period is taken into consideration $p_i / f_i \approx 1.0$ for some grain size fractions. This finding is similar to that of Church *et al.*, (1991), who also found substantial variations in the proportions of material trapped at varying flows, and were able to statistically demonstrate 'near equal mobility' for the $<210\text{mm}$ fraction.

Multiple regression analysis demonstrated a strong dependence of A upon τ , equation 5.8 takes into account any trap effect which may occur as a result of local variations in local hydraulics or sedimentary environment, and Equation 5.9 allows for any size effects, which improved the r^2 value. The difference between these two models was found to be highly significant ($p<0.001$), which means that effect of grain size upon the relationship between τ and A is significant, and that size selective transport is in operation for the sand fraction on the Rede.

Role of fine sediments in riffle-pool maintenance

Data presented in this Chapter indicate that Phase 1 bedload transport appears to be initiated at flows of about 4% bankfull ($0.35 \text{ m}^3 \text{s}^{-1}$). Tracer centroid movement appeared to indicate winnowing of fines across a relatively stable gravel bed until the first large winter of 84% bankfull ($7.12 \text{ m}^3 \text{s}^{-1}$). This would suggest that riffle gravel was relatively stable until this large flood, even though pebble tracer data presented in Chapter Seven will show gravel movement is possible at lower flows (30% bankfull). One possible reason for this is the effect of bed structure upon gravel transport. After long durations of relatively low flows, capable of Phase 1 transport only, riffle sediments can become more compact due to the lateral and vertical redistribution of sands, silts and clays (Reid and Frostick, 1984; Reid *et al.*, 1984). Temporal variability in both the quantity and grain size of sediments accumulating in gravel framework voids is clearly demonstrated in Figure 5.10, and could have a strong influence on gravel mobility. During periods of high flow and regular flooding in the winter months, the grain size of material deposited in gravel interstices tends to be in the coarse sand range ($500\text{-}2000 \mu\text{m}$). However, during the intervening summer months where long periods of low flow predominate, material $<250 \mu\text{m}$ more likely to accumulate in gravel interstices. Transport of coarser sands may reflect disruption of the gravel surface and release of interstitial fines, and extrinsic inputs to the channel. Re-deposition of this material may result in a relatively loose bed structure. Accumulation of finer material ($<250 \mu\text{m}$) during the summer, reflects redistribution of previously deposited fines on the riffles. This finer material is more likely to promote compaction, and reduce the mobility of the bed.

The interaction of fine sediments with the gravel may be of key importance to the maintenance of riffle-pool morphology due to the influence upon mobility of the bed (Clifford, 1993b; Sear, 1996). If mobility of bed sediments are influenced by the quantity and grain size of accumulating fine sediments then it would appear that bed sediment mobility may change over time depending upon flood frequency and magnitude and sediment supply. The binding action of fine sediments needs to be researched further, along with temporal variation in compaction and accumulation.

5.5 Summary

- 1) The lowest discharge where sand accumulated in basket traps was $0.35 \text{ m}^3 \text{s}^{-1}$, which equated to a reach average τ of 20 Nm^{-2} ;
- 2) More detailed analysis for initial motion for individual sand-size fractions was found to fall in the range $11-22 \text{ Nm}^{-2}$;
- 3) A high degree of scatter is evident when A was plotted against τ from all traps throughout the study reach. This may be due to spatial patterns of turbulent flow and sediment supply. This needs to be researched further;
- 4) Tracing experiments indicate that sand movement is not only influenced by flow but also by the interaction with the gravel population. Transport distance (L) showed initially a linear relationship with Qt . However after the first large flood capable of transporting gravel, L deviated and showed negative movement in some instances. This could either be attributed to (i) re-exposure of infiltrated;
- 5) Tracer near to the seeded zone, as a result of removal of surface gravel, or (ii) or net erosion of the downstream mass of tracer after initial movement;
- 6) Statistical analyses of size data indicate that selective transport is in operation for sand-sized sediments on the Rede;
- 7) Deviation from equal mobility shows a seasonal pattern which also varies with size. However there is a suggestion that seasonal variations cancel themselves out over the period of a year, indicating that equal mobility may apply in the longer term. This would be logical, as no strong downstream fining is evident in the Rede reach.

Chapter Six examines the mobility of gravel (Phase 2 bedload) through the Rede riffle-pool sequence, whilst Chapter Seven will describe the routing of fine-bedload

through the Rede riffle-pool sequence and discuss implications of sediment supply upon accumulation rates.

Chapter Six

Mobility of bed sediments through a riffle-pool sequence 2: Coarse bedload

6.1 Introduction

Information concerning initial motion criteria for bed-sediments in gravel bed rivers is crucial to a range of geomorphological and ecological problems. Studies of channel morphological change, bedload transport, palaeohydraulic reconstruction, and flushing flow estimations for fish spawning grounds all require information on the relationship between initial movement of different grain sizes and flow strength. As was highlighted in Chapter One (section 1.5.3), the principle area of debate relating to this issue in mixed size gravels is the concept of sediment 'equal mobility' (Klingeman, 1982; Parker *et al.*, 1982a and b; and Andrews and Parker, 1987). It is also recognised that the mobility of sediment can vary through the riffle-pool sequence and play an important in its maintenance (Clifford, 1990; Clifford, 1993a; Sear, 1996). If the equal mobility hypothesis (Eq 1.2) applies for both riffles and pools, and if the ratio of surface to subsurface grain sizes is different resulting in θ_c (pool) $<$ θ_c (riffle), then pool scour and riffle maintenance will result.

Lower θ_c for pool sediments in comparison to riffles should result in increased transport distances and grain velocities for pool sediments (e.g. Ashworth, 1987; Sear, 1992a; 1996, although greater pool tractive force may also have the same effect. Grain size and τ are known to affect grain velocity (Drake *et al.*, 1988; Wilcock, 1997) as (i) the displacement length of a tracer clast is known to increase absolutely and relatively for a given particle size for a given flow (Ferguson and Wathen, 1998), and (ii) displacement length and frequency increase with τ and Ω . This Chapter examines the mobility of gravel through the Rede study reach and assesses the implications for riffle-pool maintenance. Data are presented on travel distance and tracer velocity for a range of tracer size fractions seeded in pools and riffles monitored on five occasions over a thirteen-month period. These data are used to demonstrate the mobility of different grain sizes and the relationships between transport distance and flow, and tracer velocity and flow.

6.2 Experimental design

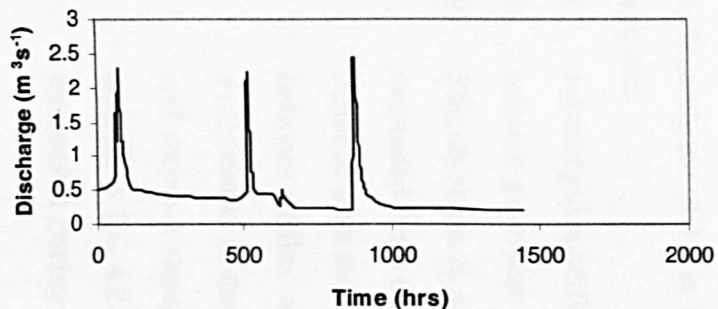
Studies which have addressed the problem of sediment mobility have traditionally used bedload samplers (Andrews, 1983) and flumes (Wilcock, 1997). However, more recently, field-based tracer studies have provided some informative data sets (Church and Hassan, 1992; Ferguson and Wathen, 1998). This latter approach was employed on the Rede where transport distances of individual clasts of coarse-grained material were measured directly by tracking 288 measured and weighed and painted clasts, placed throughout the study reach as described in Chapter Two. The flood hydrographs for the periods between tracer surveys are indicated in Figure 6.1, where it can be seen that hydrograph peaks ranged from 2.17 to $9.92\text{m}^3\text{s}^{-1}$ (over bankfull), between tracer emplacement on the 21 January 1998 to the final re-survey on 28 February 1999.

Stream power $\rho g Q_s$, was used initially to relate gross sediment movement to flow, using the peak discharge of each flood recorded. In order to provide a greater resolution to the analyses, clast-specific hydraulics were estimated using $\rho_w g d_s$. Depth (d) for each cross-section and reach average slope (s) data were estimated using Eq 4.1, which allowed a shear stress surface to be generated in Surfer using Kriging (see Chapter Two and section 4.3.4). The 75th percentile depth for the reach was used as gravel transport tends to be located near the thalweg, and the stress here would be underestimated by using mean depth (Ferguson and Wathen, 1998, section 4.3.4) in what were generally non-trapezoidal sections. By entering the co-ordinates for each clast before each transport event into Surfer it is possible to estimate a point specific shear stress for that clast.

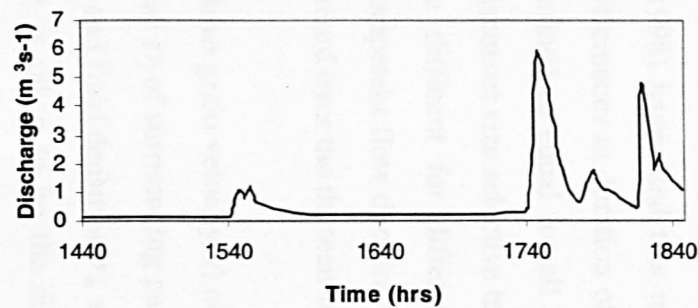
6.2.1 Virtual velocity

To obtain further information on gravel mobility it is useful to gain an insight into the rate of movement of different tracer size fractions. The concept of 'virtual velocity' (Hassan *et al.*, 1992) rather than travel distance provides an appropriate tool here.

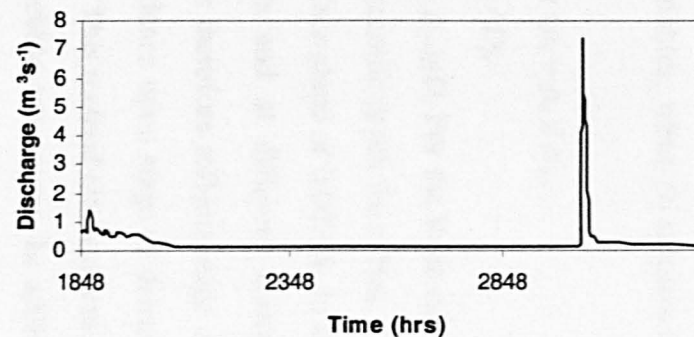
(a)



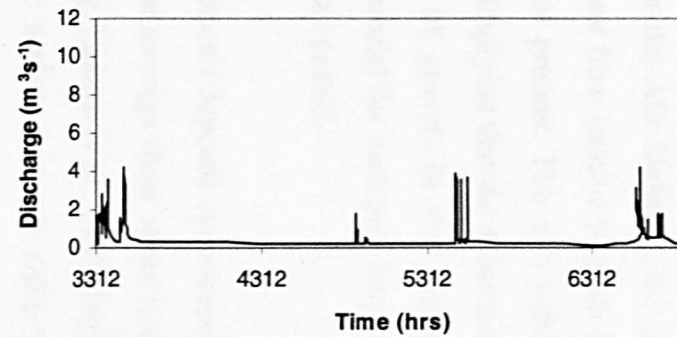
(b)



(c)



(d)



(e)

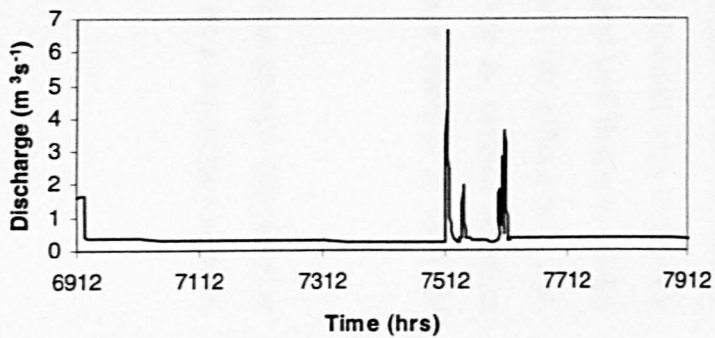


Figure 6.1 Discharge hydrographs for periods in between tracer re-surveys, a) 21/01/98-22/03/98, b) 22/03/98-08/04/98, c) 08/04/98-08/06/98, d) 08/06/98-05/11/98, e) 05/11/98-28/02/99.

Virtual velocity is calculated as distance travelled divided by the duration of competent flow, rather than calendar time which comprises mainly of inactive periods whose percentage flow duration may differ between rivers. Ferguson and Wathen (1998) have used this method on the Allt Dubhaig, but did not take into account differences in duration of competent flow relative to grain size, hence the duration is defined as equal for all grain sizes present. This is a little surprising, as this paper discusses size selective transport, implying that the duration of competent flow should be different for different sizes of gravel. In the present study, a size-specific competent flow duration was calculated for each size fraction for the full hydrograph record over the thirteen-month study period.

Mean grain velocity V_i of size fraction i depends upon tracer diameter D_i , the average size D_j of surrounding particles, the average shear stress τ , acceleration due to gravity g and fluid densities ρ_w and ρ_s (e.g. Hassan *et al.*, 1992; Ferguson and Wathen, 1998). D_j is taken to be the size of the surface material rather than the subsurface (e.g. Church and Hassan, 1992). This is an important consideration as surface material introduces hiding and protrusion effects; the D_{50} of the surface material is used for pools and riffles in this analysis.

According to Ferguson and Wathen (1998), four dimensionless groups characterise the dependence of V_i on these variables, when D_j is taken to be a repeating variable, these are;

- (i) submerged specific gravity $(\rho_s - \rho_w)/\rho_w$,
- (ii) relative grain size $D^* = D_i/D_j$,
- (iii) Shields stress $\theta_c = \tau / (\rho_s - \rho_w)gD$. For the Rede data θ_c was calculated using τ estimated from the 75th percentile depth for riffles, pools and reach, and in this instance a mean water surface slope of 0.00728. In this analysis variations in s between riffles and pools and at different flows are not accounted for. τ calculated in this manner therefore reflects stage changes in d rather than s , and shows a strong dependence upon stage as demonstrated by the regression equations 4.1, 4.2 and 4.3. This method allowed τ to be estimated for the flows monitored during tracer pebble movement. In addition to this, surface grain

size for pools, riffles, and the reach, and tracer grain size D_i were required to calculate a Shields stress defined at (iii).

(iv) dimensionless velocity $V^* = V_i / \sqrt{g}D_i$ was calculated using tracer diameters D_i because velocities of individual size classes were required.

6.3 Results

6.3.1 Recovery rate

An obvious weakness with the painted tracer approach is the loss of clasts due to burial (e.g. Hassan *et al.* (1984). To overcome this problem, the magnetic tracing work for fine bedload on the Rede channel coupled with annual re-survey of fixed cross-sections indicated only minor bed turnover which suggested burial may not be a major problem on the Rede. This fact led to painted clasts being used. Figure 6.2 demonstrates the percentage recovery rates for pools and riffles and shows a slightly greater recovery rate on the riffles and enhanced loss of finer fractions. Recovery rates were reasonable after three events (70-80%), however fell to 30-40% by the fourth re-survey.

6.3.2 Transport distance

The total distance transported for different grain-size classes over the 13 month period is shown in Figure 6.3. It is difficult to distinguish any pattern in the relationship between grain size and transport distance from these data. It is evident that some pebbles moved long distances whereas others, of a similar size, moved only short distances. If the mean distances travelled over the whole study period are taken into account (riffles = 8.35m, pools=8.97m), there is little difference between travel distance for riffles and pools. However if the maximum distance is considered, pools are found to transport clasts further (72.61m) in comparison to riffles (59.7m), reflecting the greater high flow competence of some pools (see Chapter Four). A closer examination of the data is needed to provide an insight into downstream sorting processes operating in the Rede.

By calculating the sum of the mean distances over each of the five flow events studied for individual size classes of tracer particles, a pattern is revealed (Figure 6.4). The

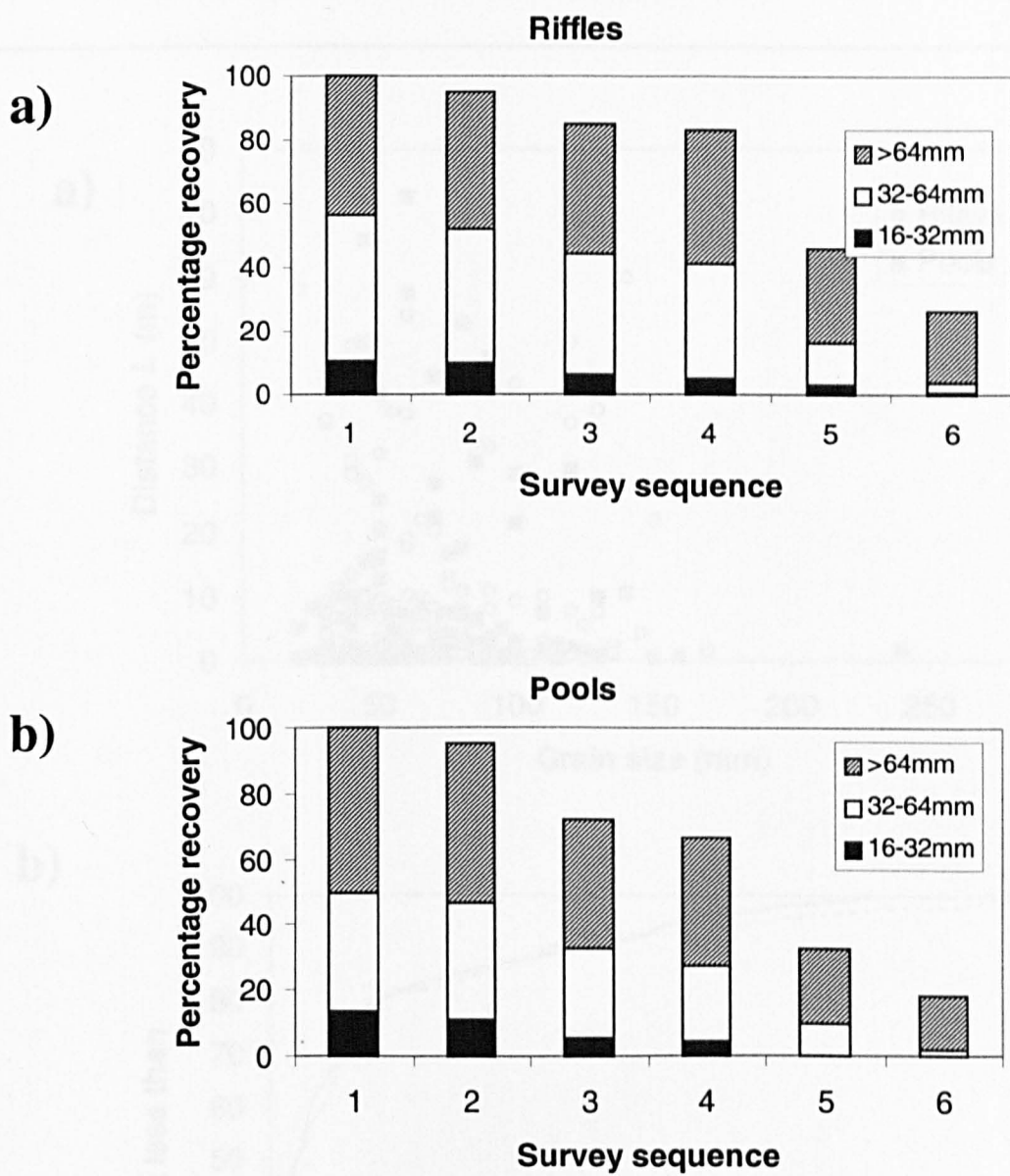


Figure 6.2 Percentage recovery of different size fractions of tracer clasts for each successive surveys for a) riffles, and b) pools.

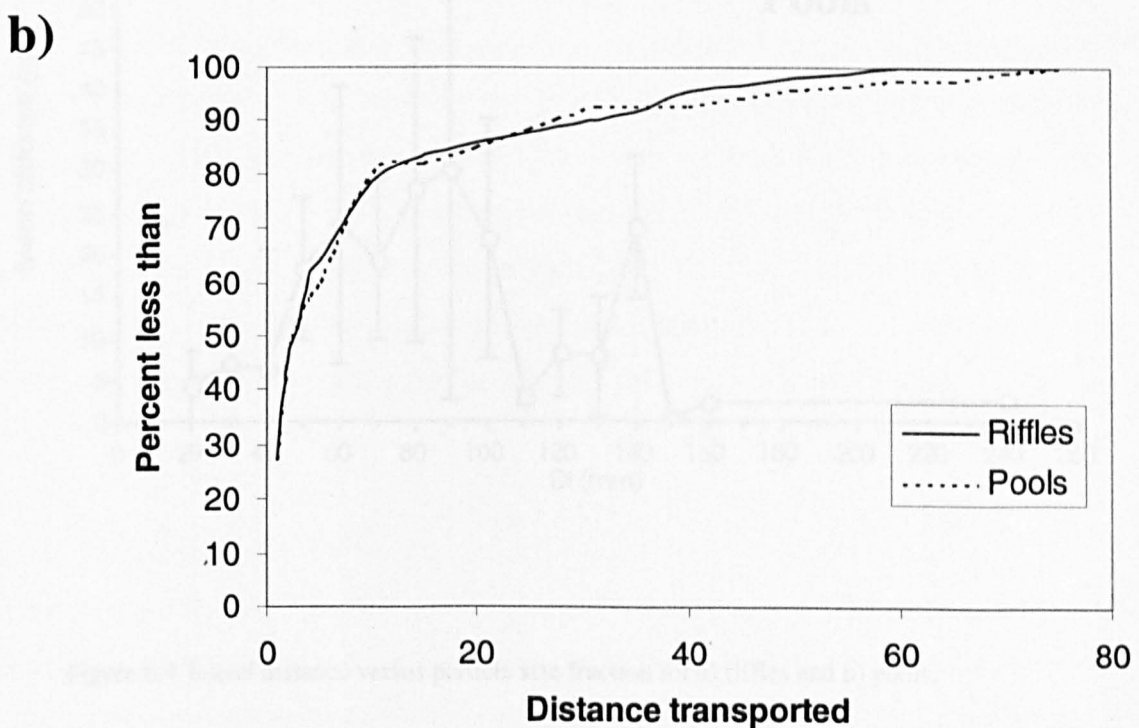
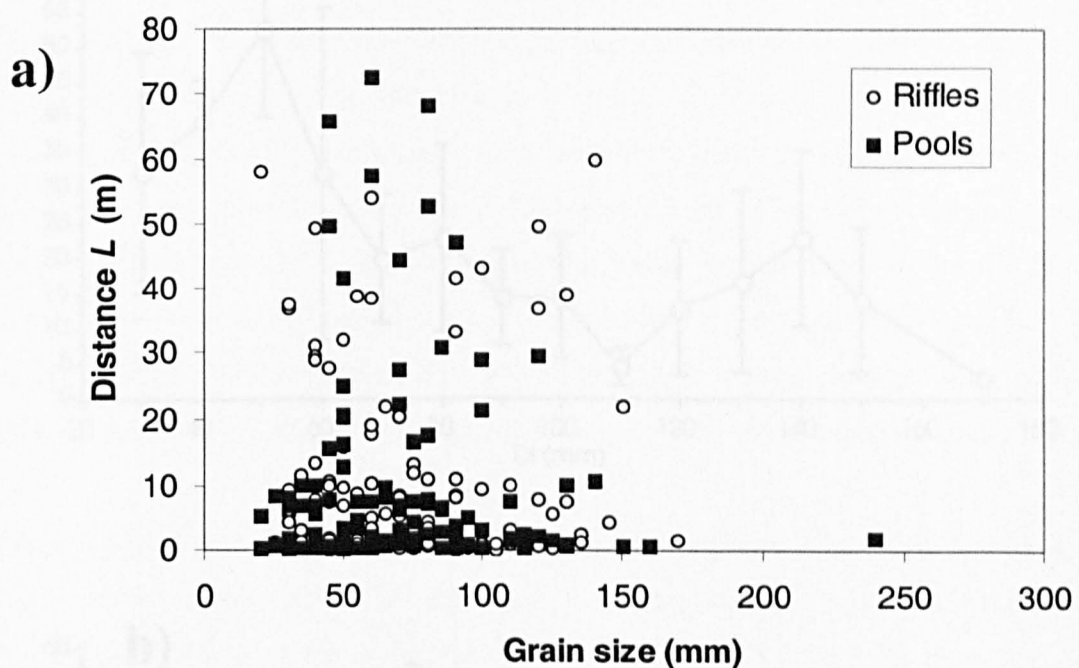


Figure 6.3 Distance of travel a) versus particle size for pools and riffles, b) cumulative distribution of travel distance for pools and riffles demonstrating that around 10% of the pool tracers were transported further than riffle tracers.

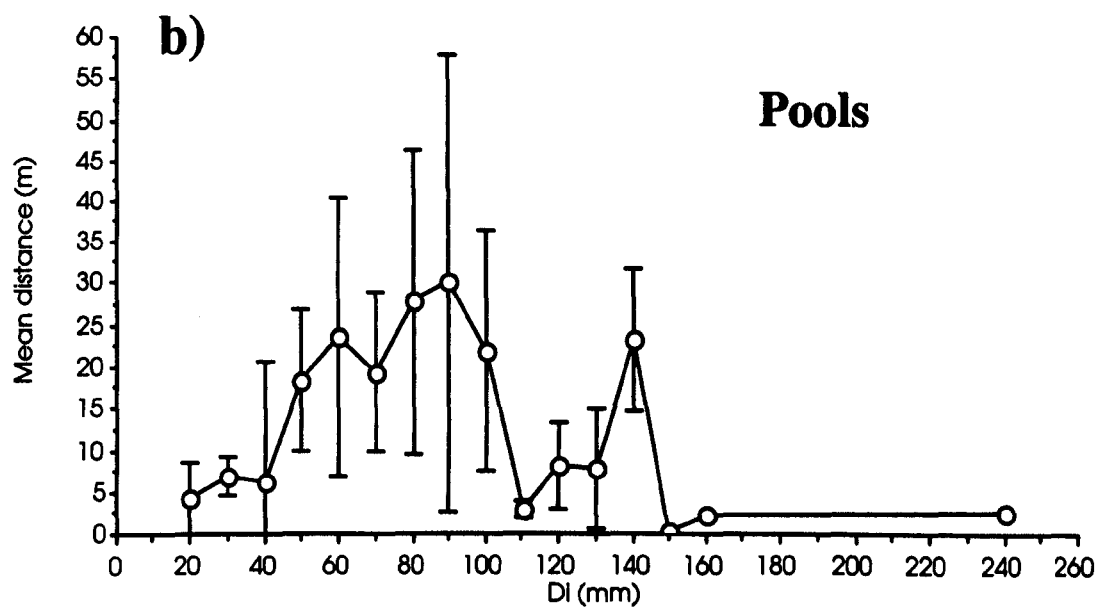
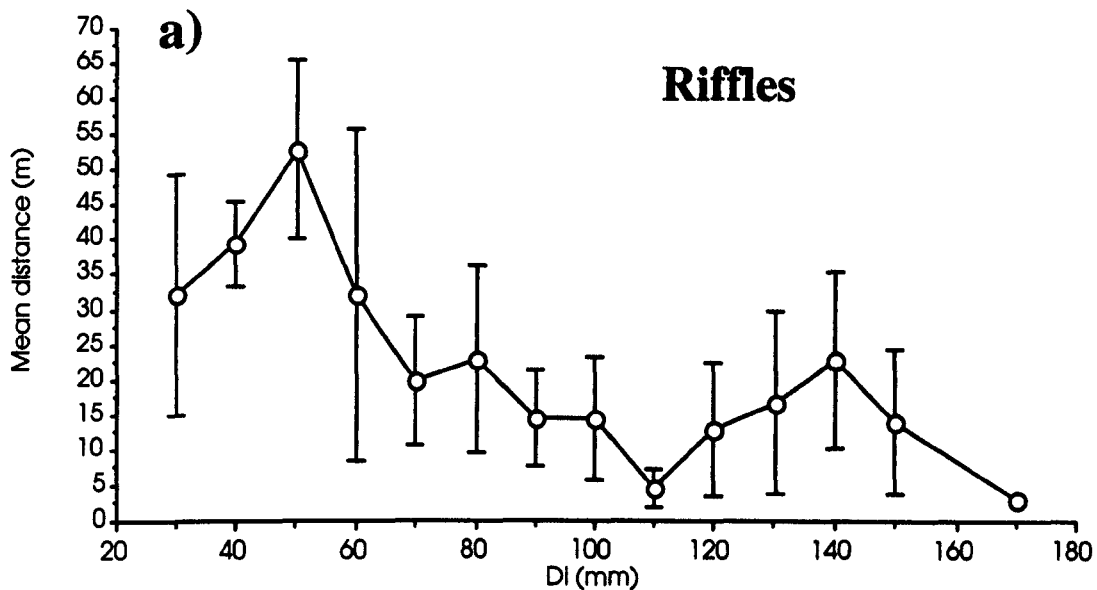


Figure 6.4 Travel distance versus particle size fraction for a) riffles and b) pools.

curves in Figure 6.4 show a bimodal pattern for both pools and riffles, with two grain size peaks in transport distance. For the riffles it appears to be the 50-60mm fraction that travels the furthest, with a secondary transport peak shown for the 140-150mm fraction. For the pool data, the 90-100mm fraction travels the furthest, with a secondary peak found for the 140-150mm fraction. There is a steady increase in transport distance up until the primary peaks for both riffles and pools. However there appears to be a steady decline in transport distance for both riffles and pools after this primary peak until the 110-120mm size fraction (which approximates to the D_{50} for the surface material), which only travels approximately 5m for both riffles and pools. Transport lengths begin to increase once more after this grain size until the secondary peaks are reached after which there is a further decline in travel distance once more.

Evidence for both selective transport and for hiding effects / equal mobility to varying degrees can be demonstrated. A decrease in mean distance with progressively increasing size (falling limb) indicates selective transport, whereas an increase in travel distance with progressively increasing grain size (rising limb) indicates hiding effects. Overall it appears that finer grains are transported further in comparison to coarser material for riffles, however this relationship is not expressed as clearly for the pool data. Hiding effects appear to be a feature for both small and medium size fractions; between 30-50 mm for the riffles and for 20-90 mm for the pools, and for size classes just above the D_{50} for the surface layer; 110-140 mm for both riffles and pools. Hiding effects may be more prevalent in the pools due to the coarser size of the surface sediments in comparison to the adjacent riffles (see Chapter Three).

6.3.3 Shape factors

It has previously been noted by Schmidt and Ergenzinger (1992) that rod-shaped clasts may travel further than other shapes due to their increased exposure to flow. It is therefore necessary to examine the significance of any shape effects upon transport distance. Table 6.1 presents travel distance data for the River Rede channel for pools and riffles, for the thirteen-month monitoring period. Although there is a tendency for rod shaped material to move further, results from an F – test indicate no statistically significant differences for travel distances between different shaped clasts. This analysis suggests that shape factors may be discounted, and that further analysis of the

relationship between flow and sediment movement may concentrate on size effects. The following sections concentrate upon the flow upon sediment movement, and tackle the issues of critical flows for initiation of movement and the equal mobility hypothesis.

Table 6.1 Anova table for distance of travel of different clast shapes, a) Pools, b) Riffles

Anova: Single Factor

(a) Pools

SUMMARY

Groups	Count	Sum	Average	Variance
Blades	103	418.7663	4.065693	55.84978
Rods	104	505.9244	4.864657	137.7017
Discs	222	823.051	3.707437	87.5683
Spheres	58	193.469	3.335672	38.70477

ANOVA

Source of Variation	SS	df	MS	F	P-value	F crit (p=0.001)
Between Groups	122.7025	3	40.90084	0.476731	0.698622	5.508809
Within Groups	41438.71	483	85.79444			
Total	41561.42	486				

Anova: Single Factor

(b) Riffles

SUMMARY

Groups	Count	Sum	Average	Variance
Blades	169	709.9532	4.200907	103.0327
Rods	118	657.007	5.567856	160.8
Discs	247	1006.602	4.075311	67.87112
Spheres	150	557.0084	3.713389	58.93169

ANOVA

Source of Variation	SS	df	MS	F	P-value	F crit (p=0.001)
Between Groups	255.261	3	85.08702	0.939269	0.421192	5.483344
Within Groups	61600.21	680	90.58855			
Total	61855.47	683				

6.3.4 Tracer movement and stream power

Before concentrating upon the effects of local hydraulics upon sediment movement it is informative to analyse the relationship between a gross flow parameter such as peak discharge and travel distance. However, in order to allow relations to be applied to other streams, it is more useful to evaluate maximum stream power (Ω) for the Rede study site from $\rho g Q_s$, for each flood studied (using mean bed slope of 0.0062). The plot of mean transport distance for different grain size classes of tracer against maximum stream power is shown in Figure 6.5, and the log-log relation details in Table 6.2. In this plot the tracer data have been divided up into four grain size categories, rather than using individual clast size. Although information is limited to five events, there appears to be a fairly narrow range of flows for initial motion. Taking the detectable motion to be movement of 0.5m or more, the threshold total Ω for mobilisation appears to lie between 127 and 187 Wm^{-2} , which equated to a unit stream power (ω) of 15.3 and 22.6 Wm^{-2} respectively, recorded at discharges of between 2 and 3 m^3s^{-1} (23- 35% bankfull) in the Rede channel. This compares well with other studies. For example Webber (1971) suggests a stream power of 16 Wm^{-2} is required to mobilise fine gravel, whereas Brookes (1990) suggests a threshold value of 35 Wm^{-2} . There appears to be an almost identical Ω required to mobilise grain sizes between 20 and 120 mm for the riffle tracer data, with the exception of material >120mm which requires greater Ω . Data for pools

Size	a_i	b_i	R^2	Ω_{crit} (Wm^{-2})
<u>Riffles</u>				
>120mm	1E-05	2.0694	0.78*	187
80-120mm	0.0004	1.4731	0.56*	127
40-80mm	4E-05	1.9181	0.77†	137
20-40mm	8E-06	2.2538	0.87*	135
Mean	4E-05	1.9286	0.70	134
<u>Pools</u>				
>120mm	6E-05	1.8012	0.59*	151
80-120mm	3E-05	1.9388	0.59*	151
40-80mm	6E-05	1.8513	0.85†	132
20-40mm	5E-07	2.7111	0.92†	164
Mean	2E-05	2.0609	0.71	137

Table 6.2 Size-specific rating relations of the form $L = a\Omega^b$, where L is the mean distance of transport for tracer data taken from riffles and pools, Ω is stream power and a and b are regression coefficients. * r^2 significant at $\sigma = 0.05$, † $\sigma = 0.1$.

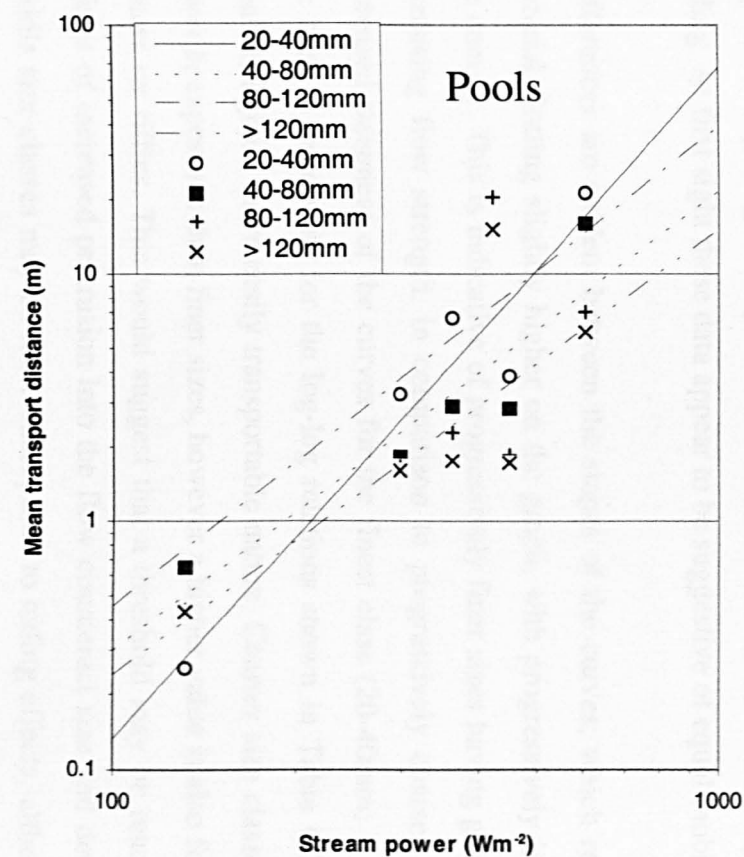
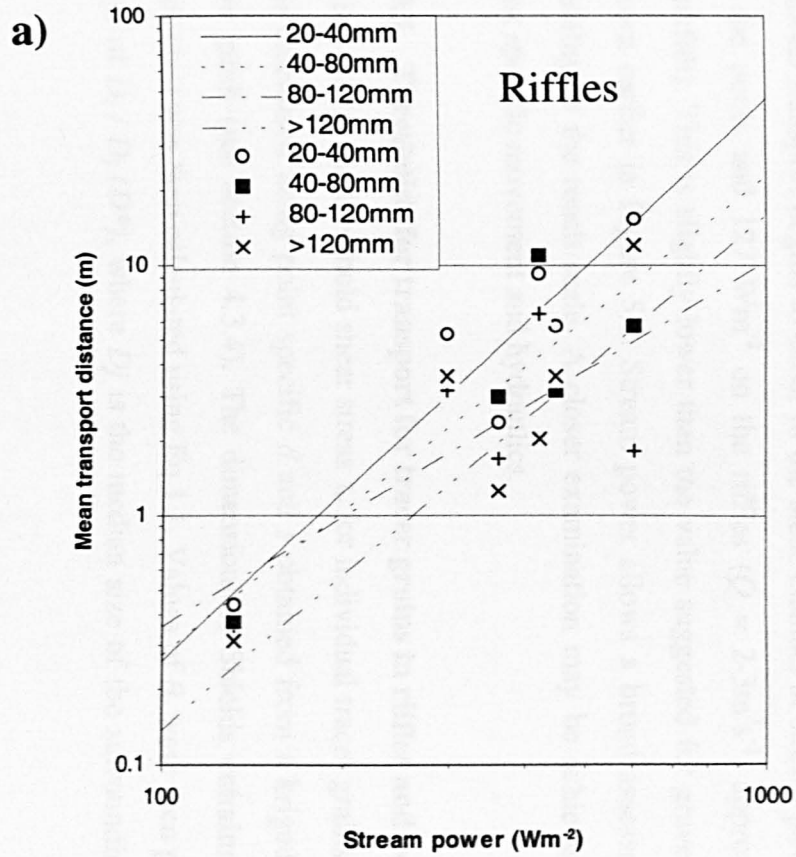


Figure 6.5 Log-log rating curves for size-specific mean transport distance versus stream power ($\rho g Q_s$) for a) Riffles and b) Pools. The size specific rating relations are presented in Table 6.2.

indicate that the Ω required to mobilise the finest fraction (20-40mm) in the pools appear to require greater powers than coarser material, which may be indicative of hiding. At first sight these data appear to be suggestive of equal mobility.

Differences are evident between the slopes of the curves; which results in the finer material plotting slightly higher on the graph, with progressively increasing Ω , than the coarser. This is indicative of progressively finer sizes having greater sensitivity to increasing flow strength, in comparison to progressively coarser size grades. The increased steepness of the curves for the finest class (20-40mm) is demonstrated by the high b_i exponents for the log-log relations shown in Table 6.2, reflecting their smaller, lighter, more easily transportable nature. Coarser size classes generally have lower b_i exponents than finer sizes, however a higher value is also found for >120mm tracers on riffles. This would suggest that a threshold may be reached whereby the effects of increased protrusion into the flow counteract size and density effects. The middle size classes may be more susceptible to hiding effects, although it is difficult to be sure from this limited data set. These data provide evidence of both size selectivity and protrusion effects.

From these data it may be reasonable to assume that some bed surface disruption and bedload transport begins to occur in the Rede channel at stream powers of 132 Wm^{-2} in the pools and 127 Wm^{-2} on the riffles ($Q = 2-3 \text{ m}^3 \text{s}^{-1}$, approximately 23-35% bankfull). This is slightly lower than the value suggested for gravel bed disturbance shown earlier in Figure 5.2. Stream power allows a broad assessment of sediment mobility at the reach scale. A closer examination may be achieved by focusing on clast specific movement and hydraulics.

6.3.5 Thresholds for transport for tracer grains in riffles and pools

In this study, the threshold shear stress τ_c for individual tracer grains mobilised $>0.5\text{m}$ was calculated using point specific d and s obtained from a kriged surface for each flow peak (see section 4.3.4). The dimensionless Shields entrainment function for each clast was then calculated using Eq 1.1. Values of θ_c were then plotted against the ratio of $D_i / D_j (D^*)$, where D_j is the median size of the surrounding particles. D_j is

relevant through hiding and protrusion effects and should therefore refer to the surface layer not the subsurface (Ashworth and Ferguson, 1989).

The resultant curves, given in Figure 6.6, produced for riffle and pool data both demonstrate the higher entrainment thresholds required for particles which are finer

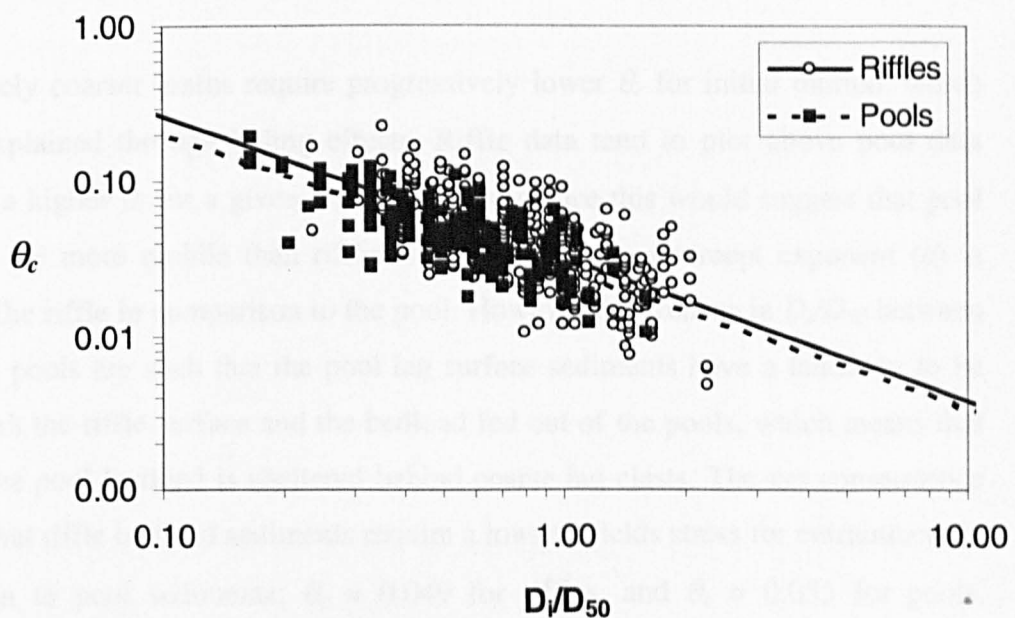


Figure 6.6 Decrease in critical dimensionless shear stress for entrainment with increasing grain size relative to the bed, as inferred from individual tracer clast movement ($>0.5\text{m}$), transported at different shear stresses in riffles and pools. Slope (b -exponent) would be 0 for simple Shields-type size-selective entrainment and -1.0 for equal mobility of all grain sizes.

than the surface layer. The curves demonstrate a negative dependence of θ_c upon relative grain size (D_r/D_{50}). The equations for the log-log curves shown in Figure 6.6 are:

Reach

$$\theta_c = 0.031 \text{ } Di/Dj^{-0.829} \quad n=618, r^2 = 0.485, SE = 0.187 \quad (6.1)$$

Riffles

$$\theta_c = 0.032 \text{ } Di/Dj^{-0.924} \quad n=371, r^2 = 0.461, SE = 0.203 \quad (6.2)$$

Pools

$$\theta_c = 0.027 \text{ } Di/Dj^{-0.889} \quad n=247, r^2 = 0.585, SE = 0.147 \quad (6.3)$$

Progressively coarser grains require progressively lower θ_c for initial motion, which may be explained through hiding effects. Riffle data tend to plot above pool data indicating a higher θ_c for a given D/D_{50} . At first glance this would suggest that pool sediments are more mobile than riffles sediments, as the intercept exponent (a) is larger for the riffle in comparison to the pool. However differences in D/D_{50} between riffles and pools are such that the pool lag surface sediments have a tendency to be coarser than the riffle surface and the bedload fed out of the pools, which means that much of the pool bedload is sheltered behind coarse lag clasts. The net consequence of this is that riffle bedload sediments require a lower Shields stress for entrainment in comparison to pool sediments; $\theta_c = 0.049$ for riffles, and $\theta_c = 0.055$ for pools, compared with a mean $\theta_c = 0.051$ for the whole Rede channel. The data show some overlap; however results from an *F*-test presented in Table 6.3 suggest the values for θ_c for riffles and pools are significantly different ($p = 0.05$). Values for τ_c obtained using θ_c predicted using the regression equations 6.2 and 6.3 for surface sediments in the grain size range 10-120mm are; 37.5-45.3 Nm^{-2} on riffles, compared with 39.5-52.1 Nm^{-2} in pools. Again, higher τ_c are required in pools due to the coarse nature of the lag deposit which surrounds the bedload. If pools were assumed to have the same surface grain size as the riffles, then τ_c would be lower than the riffles ranging between 28.8-37.9 Nm^{-2} .

The slope terms in the equations (b – exponents) are close to the -1.0 required for equal mobility to dominate the transport process (Parker and Klingeman, 1982),

which would suggest the degree of size selectivity is significantly reduced, in favour of equal mobility.

Table 6.3 Anova table, comparing Shields dimensionless entrainment function data for riffles and pools.

Anova: Single Factor

SUMMARY

Groups	Count	Sum	Average	Variance
Riffles	371.000	18.189	0.049	0.001
Pools	247.000	13.610	0.055	0.001

ANOVA

Source of Variation	SS	df	MS	F	P-value	F crit
Between Groups	0.005	1.000	0.005	5.880	0.016	(p=0.05) 3.857
Within Groups	0.574	616.000	0.001			
Total	0.579	617.000				

6.3.6 Mobility and size selectivity for riffles and pools and a comparison with other published data

Further analyses of mobility and size selectivity require non-dimensional scaling of travel distance and grain size in order to compare travel distance between floods and other streams. Church and Hassan (1992) applied this scaling technique for single events on a range of rivers to demonstrate the relationship between geometric mean grain size fractions (D_i), with mean travel distance (L_i). The best-fit curve for through all of this data was;

$$\text{Log } L_i^* = 0.232 + 1.35 \log (1 - \log D_i^*) \quad (6.4)$$

Where L_i^* is L_i scaled by the mean distance L_{50s} for the fraction containing the median surface grain size and D_i^* is D_i scaled by the median subsurface grain size D_{50s} . Tracer size data from the Rede was split into 10mm fractions and analysed in the

same manner as by Church and Hassan. The results for the Rede reach as a whole over five events follow a similar convex-up shape, and only deviate slightly from Church and Hassan's curve, plotting slightly above (Figure 6.7). The curve suggests that for tracer grain sizes progressively coarser than the D_{50} of the surrounding particles, that travel distance drops off rapidly, whereas tracer grains which were progressively finer than the surrounding surface material, travel distance increases but at a less rapid rate.

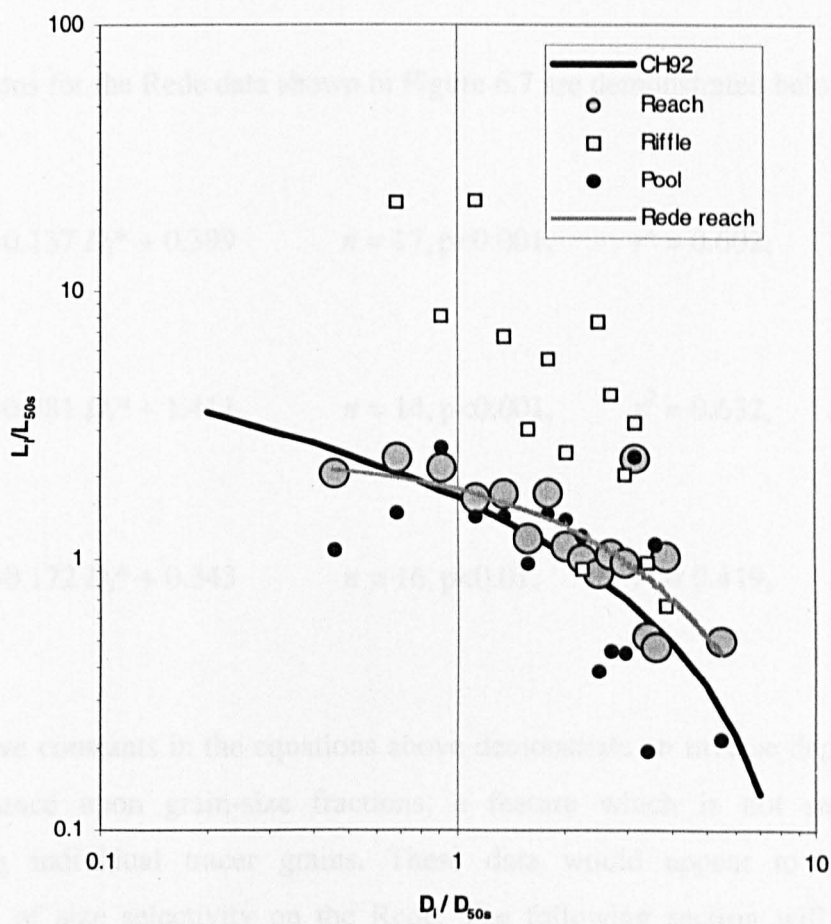


Figure 6.7 Relative travel distance of each size fraction for the Rede reach as a whole, and riffles and pools separately. The curve labelled CH92 is the function fitted by Church and Hassan (1992) to single-event data from previous studies (equation 6.4 in the text).

When riffle and pool data are considered independently there is considerable deviation shown for the riffle data, particularly evident when grain sizes smaller than the size of the surrounding bed material are considered. Travel distance appears to increase more rapidly for grain sizes progressively finer than the surrounding material for riffles in comparison to the pools, grouped Rede data, and Church and Hassan's data. This possibly reflects the lower θ_c values obtained for riffle data (Figure 6.6). This demonstrates that gravel which is finer than the D_{50} of the surrounding grains is more mobile on the riffles in comparison to the pools. Some of the coarser riffle size fractions are found to plot slightly below the pool data, suggesting that these are more mobile than in the pools.

The equations for the Rede data shown in Figure 6.7 are demonstrated below;

Reach

$$\text{Log } L_i^* = -0.137 D_i^* + 0.399 \quad n = 17, p < 0.001, \quad r^2 = 0.602, \quad SE = 0.152 \quad (6.5)$$

Riffles

$$\text{Log } L_i^* = -0.381 D_i^* + 1.411 \quad n = 14, p < 0.001, \quad r^2 = 0.632, \quad SE = 0.297 \quad (6.6)$$

Pools

$$\text{Log } L_i^* = -0.172 D_i^* + 0.343 \quad n = 16, p < 0.01, \quad r^2 = 0.419, \quad SE = 0.273 \quad (6.7)$$

The negative constants in the equations above demonstrate an inverse dependence of travel distance upon grain-size fractions, a feature which is not shown when considering individual tracer grains. These data would appear to support the occurrence of size selectivity on the Rede. The following section will look more closely at the controls on grain movement, and will demonstrate the dependence of sediment movement (Virtual velocity) upon relative grain size and shear stress.

6.3.7 Virtual velocity of tracers – dependence upon scaled tracer size and dimensionless shields entrainment function.

Dependence of V^* upon D^*

Virtual velocities of individual tracer size classes varied from 0.86 m day^{-1} (20 mm) to 186 m day^{-1} (130 mm) for pools and 3.98 m day^{-1} (30 mm) to 404 m day^{-1} (130 mm) for riffles. The mean virtual velocity for the reach as a whole and for riffles was 76.0 m day^{-1} whereas for pools it was 41.3 m day^{-1} . This is not what was expected as pools tend to show higher τ at high flow (see Chapter 4). The relationship between V^* (virtual velocity) and D^* (relative grain size) is demonstrated in Figure 6.8, where

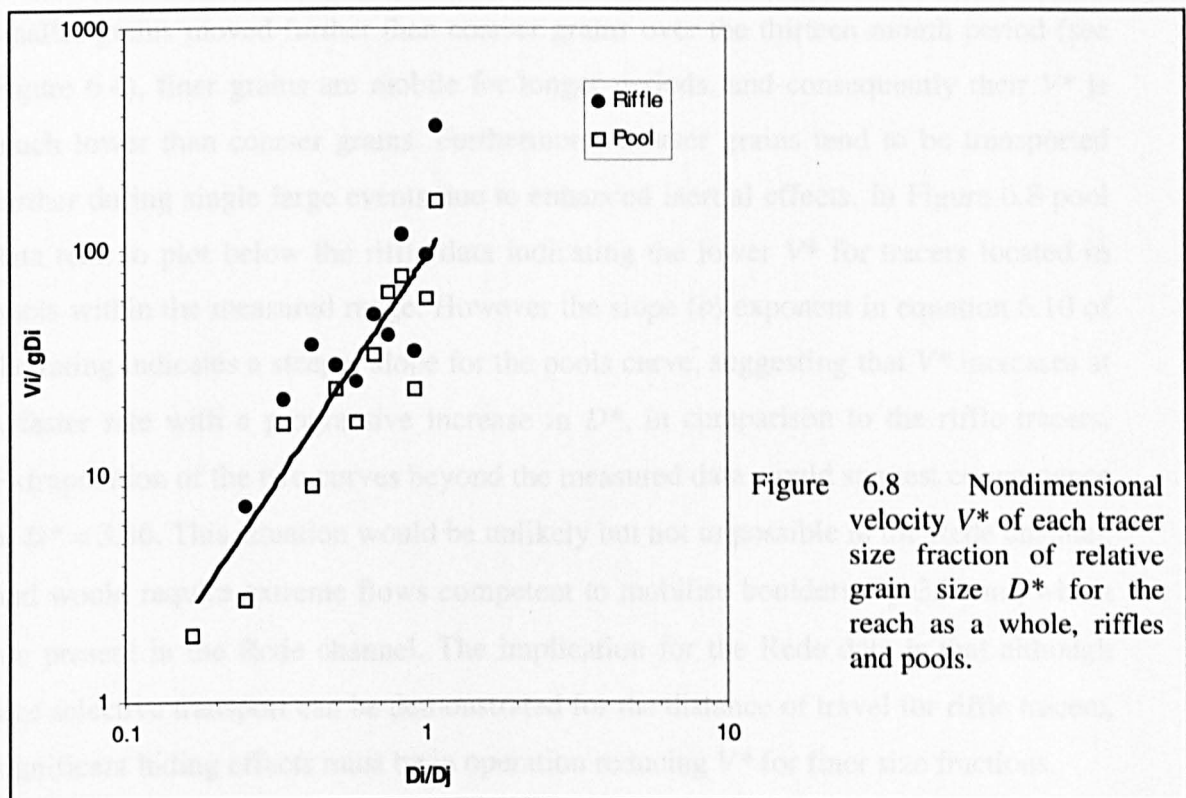


Figure 6.8 Nondimensional velocity V^* of each tracer size fraction of relative grain size D^* for the reach as a whole, riffles and pools.

there appears to be a strong positive log-log relationship. The regression equations for the reach, riffles and pools, are as follows;

Reach

$$V^* = 94.818 D^{*2.021} \quad n=23, \quad r^2=0.77, \quad p<0.001, \quad SE = 0.258 \quad (6.8)$$

Riffle

$$V^* = 109.27 D^{*1.793} \quad n=11, \quad r^2=0.70, \quad p<0.01, \quad SE = 0.253 \quad (6.9)$$

Pool

$$V^* = 77.569 D^{*2.075} \quad n=12, \quad r^2=0.85, \quad p<0.001, \quad SE = 0.231 \quad (6.10)$$

This relationship demonstrates that progressively coarser grains relative to the surrounding surface material have progressively higher virtual velocities. Although smaller grains moved further than coarser grains over the thirteen month period (see Figure 6.4), finer grains are mobile for longer periods, and consequently their V^* is much lower than coarser grains. Furthermore, coarser grains tend to be transported further during single large events due to enhanced inertial effects. In Figure 6.8 pool data tend to plot below the riffle data indicating the lower V^* for tracers located in pools within the measured range. However the slope (b) exponent in equation 6.10 of the rating indicates a steeper slope for the pools curve, suggesting that V^* increases at a faster rate with a progressive increase in D^* , in comparison to the riffle tracers. Extrapolation of the two curves beyond the measured data would suggest convergence at $D^* = 3.36$. This situation would be unlikely but not impossible in the Rede channel, and would require extreme flows competent to mobilise boulders $D_g \approx 350\text{mm}$, which are present in the Rede channel. The implication for the Rede data is that although size selective transport can be demonstrated for the distance of travel for riffle tracers, significant hiding effects must be in operation reducing V^* for finer size fractions.

Dependence of V^ upon θ_c*

An alternative approach of predicting V^* is from the grain Shields entrainment function θ_c since this involves the three likely controlling variables D_i , D_j , and τ_j . These data are plotted in Figure 6.9, where V^* appears to show a strong negative dependence upon θ_c . This may at first seem paradoxical, as the greater the ratio of propulsive to resistive forces would imply greater transport potential hence greater

V^* . However, as was noted in Figure 6.6, hiding effects result in a negative relationship between θ_c and D^* , so that grain sizes finer than the surrounding surface D_{50} require a greater θ_c for mobilisation compared to grains coarser than the surrounding bed surface material which protrude into the flow. Furthermore, as was established in Figure 6.8, progressively finer tracer grains have lower V^* due to the much longer duration of competent flow relative to path length compared to coarser clasts. Hence in Figure 6.9, progressively higher θ_c values predict progressively lower V^* as it is the finer grains which are being selected.

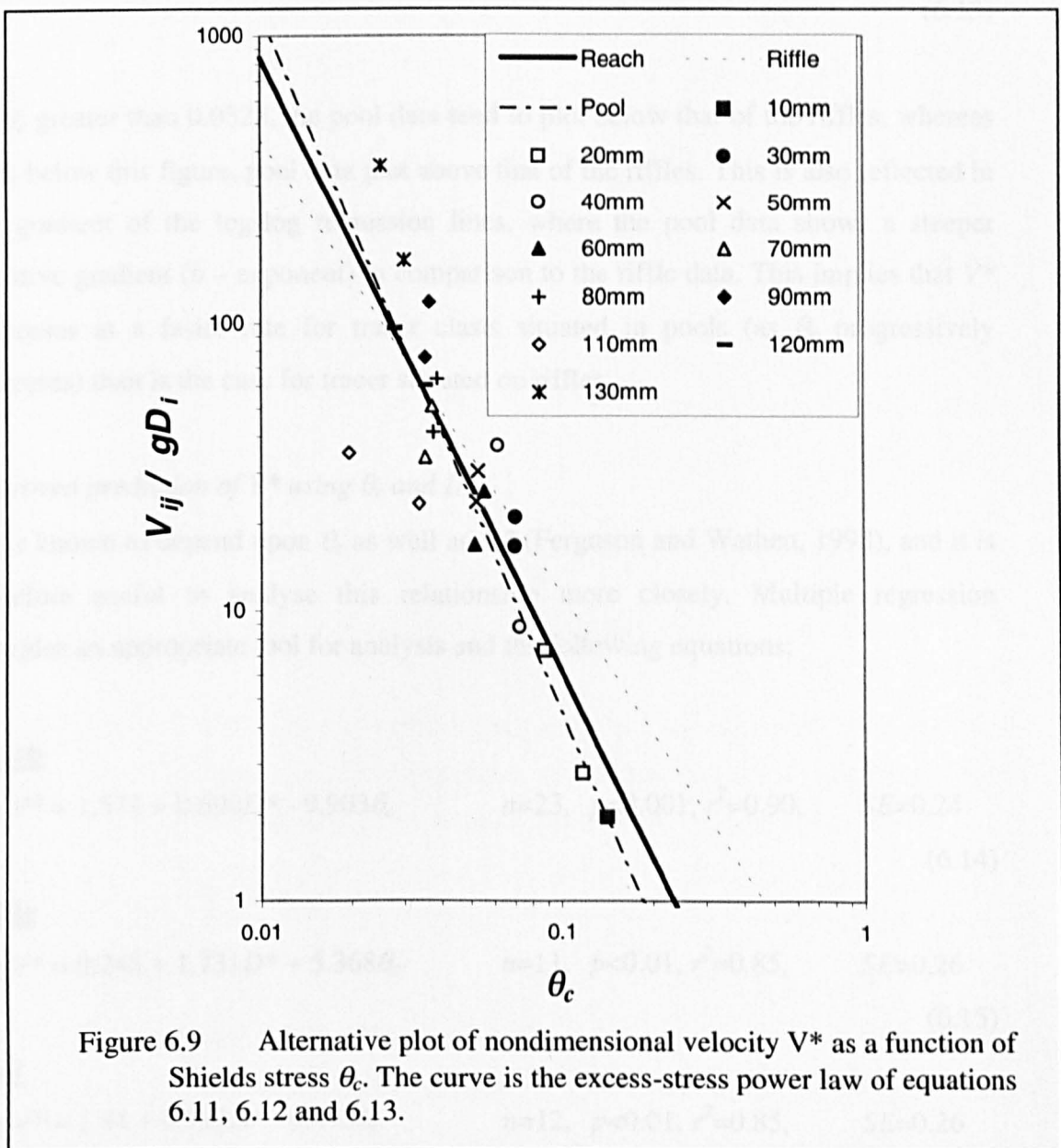


Figure 6.9 Alternative plot of nondimensional velocity V^* as a function of Shields stress θ_c . The curve is the excess-stress power law of equations 6.11, 6.12 and 6.13.

The log-log regression equations for the curves in Figure 6.9 are show below;

Reach

$$V^* = 0.0456\theta_c^{-2.1326} \quad n=23, \quad r^2=0.73, \quad p<0.001, \quad SE=0.277 \quad (6.11)$$

Riffle

$$V^* = 0.2982\theta_c^{-1.5836} \quad n=11, \quad r^2=0.52, \quad p<0.05, \quad SE=0.323 \quad (6.12)$$

Pools

$$V^* = 0.0168\theta_c^{-2.4253} \quad n=12, \quad r^2=0.88, \quad p<0.001, \quad SE=0.207 \quad (6.13)$$

At θ_c greater than 0.0328, the pool data tend to plot below that of the riffles, whereas at θ_c below this figure, pool data plot above that of the riffles. This is also reflected in the gradient of the log-log regression lines, where the pool data shows a steeper negative gradient (b – exponent) in comparison to the riffle data. This implies that V^* decreases at a faster rate for tracer clasts situated in pools (as θ_c progressively increases) than is the case for tracer situated on riffles.

Improved prediction of V^ using θ_c and D^**

V^* is known to depend upon θ_c as well as D^* (Ferguson and Wathen, 1998), and it is therefore useful to analyse this relationship more closely. Multiple regression provides an appropriate tool for analysis and the following equations;

Reach

$$\log V^* = 1.571 + 0.690D^* - 9.903\theta_c \quad n=23, \quad p<0.001, \quad r^2=0.90, \quad SE=0.24 \quad (6.14)$$

Riffle

$$\log V^* = 0.248 + 1.731D^* + 5.368\theta_c \quad n=11, \quad p<0.01, \quad r^2=0.85, \quad SE=0.26 \quad (6.15)$$

Pool

$$\log V^* = 1.44 + 0.732D^* - 9.473\theta_c \quad n=12, \quad p<0.01, \quad r^2=0.85, \quad SE=0.26 \quad (6.16)$$

These equations tend to improve the prediction of V^* ($r^2 > 0.85, p < 0.01$). This is best illustrated by plotting the observed and predicted values of V^* , shown in Figure 6.10 where points fall very close to the 1:1 line.

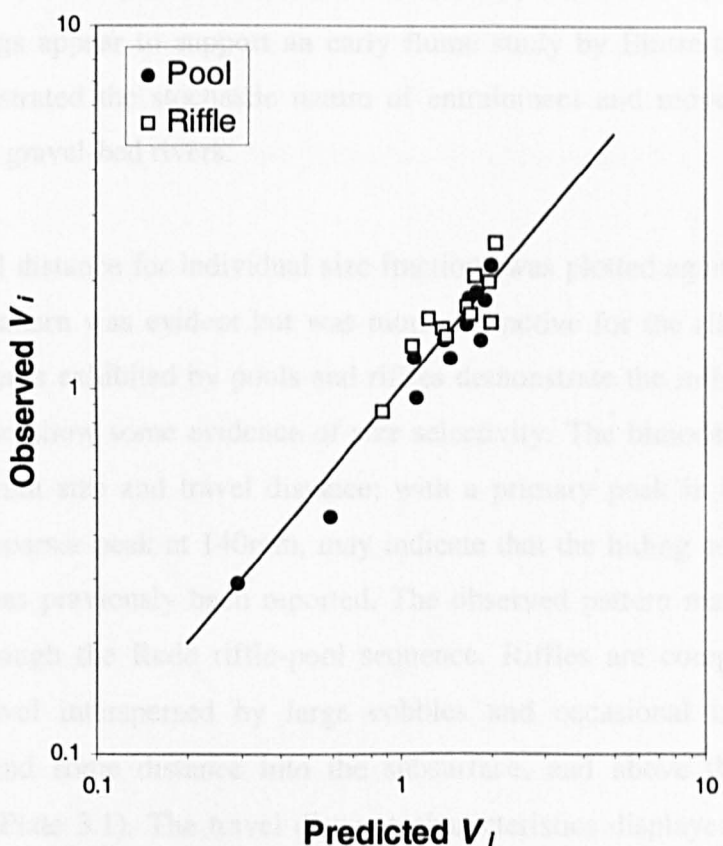


Figure 6.10 Comparison of observed nondimensional velocities V^* for different size fractions for riffles and pools with values predicted from relative grain size D^* and Shields stress θ_c using equations 6.14, 6.15 and 6.16.

6.4 Discussion and conclusions

This chapter has investigated gravel mobility (θ_c , clast travel distance, and velocity in relation to size and shear stress / stream power) through a gravel bed river displaying riffle-pool morphology.

6.4.1 Size selectivity and travel distance

When consideration was given to the total travel distance of individual tracer grains over the study period there was no clear pattern exhibited between grain size and travel distance. This lack of a relationship has been found in a number of other streams such as Harris Creek (Hassan and Church, 1992), Allt Dubhaig (Ashworth, 1987) and the semi-arid Nahal Hebron (Hassan, 1988), which all produce a similar plot (Figure 6.3a) to the Rede (see Hassan and Church, 1992). The Rede data and all these previous findings appear to support an early flume study by Einstein (1937), which clearly demonstrated the stochastic nature of entrainment and movement of individual particles in gravel-bed rivers.

When the mean travel distance for individual size fractions was plotted against grain size, a downstream pattern was evident but was more distinctive for the riffle data. The downstream patterns exhibited by pools and riffles demonstrate the influence of hiding factors and also show some evidence of size selectivity. The bimodal pattern expressed between grain size and travel distance; with a primary peak in the fine-medium sizes and a coarser peak at 140mm, may indicate that the hiding concept is more complex than has previously been reported. The observed pattern may reflect the bed structure through the Rede riffle-pool sequence. Riffles are composed of patches of finer gravel interspersed by large cobbles and occasional immobile boulders, which extend some distance into the subsurface, and above the water surface at low flow (Plate 3.1). The travel distance characteristics displayed for the riffle tracers between 10mm and 110mm may display transport operating through the gravel patches, where a finer D_{50} surface layer has some control on mobility up until 50mm (tracers finer are subject to hiding factors). Tracers coarser than this controlling grain size operate on a size selective basis. The smaller lighter material is transported furthest whereas the larger heavier material is transported the least until protrusion effects begin to play a role. Tracer clasts coarser than the surface D_{50} (120mm) begin to be transported further due to the increased protrusion into the flow. These effects reach a maximum at 140mm (roughly the D_{50} of the coarser control clasts). Eventually protrusion effects appear to be counteracted by size and weight of the material, resulting in reduced transport distance for grains coarser than 140mm. In the pools, size selectivity only appears to operate for the 100-110mm and >140mm tracer

clasts. Transport distance for tracer clasts shows a progressive increase between 20 and 90mm, and 110-140mm, reflecting the increased exposure to flow.

There was little difference in the mean transport distance for tracer clasts situated in riffles and pools, although riffle clasts below 80mm riffles tended to be transported further than those same sizes in the pools. This may reflect the lower θ_c values obtained for riffle sediments (see section 6.4.2). There was some evidence however that sizes between 80 and 120mm were transported further in the pools, reflecting the higher maximum (Chapter Four). The frequency and duration of critical flows also is likely to play role in determining which size fractions are transported the furthest.

When travel distance L_i^* is scaled by mean distance L_{50s} containing the median surface grain size and D_i^* is D_i scaled by the median subsurface grain size D_{50s} , the pattern for the reach as a whole resemble the findings of Church and Hassan (1992) and Ferguson and Wathen (1998) very closely. According to Ferguson and Wathen, this provides evidence of size-selectivity. For tracer grains progressively finer than the subsurface material, travel distance increases slowly, whereas the decrease in travel distance is much more rapid with grains progressively coarser than the surface layer. This pattern may be explained by the different dominant controls of entrainment on different size fractions. Smaller fractions are influenced by hiding factors; hence the slow decline in travel distance. In this instance the general bed texture is important. Transport distance for clasts coarser than the subsurface D_{50} are influenced by inertial effects, so that individual grain size is critical. Similar patterns of enhanced size selectivity for coarser clasts has also been observed by Wilcock and McArdell (1993) who studied fractional bedload fluxes in their flume experiments.

When the data for riffles and pools are considered separately, considerable deviation from Church and Hassan's data is evident for the riffles. Riffle data tend to plot above Church and Hassan's data and show a much steeper decline in travel distance with a progressive increase in relative grain size. Conversely pool data plot very close to Church and Hassan's data, producing a similar shaped curve. This would suggest that travel distance of tracers situated on riffles is much more sensitive to relative grain size in comparison to those situated in the pools. Furthermore, there is no distinctive

change in slope in the relationship for tracer grain sizes below the subsurface D_{50} , which suggests hiding factors are not as important in comparison to pools.

6.4.2 Grain mobility

Grain mobility was investigated initially on a gross basis by plotting the mean travel distance of grain size fractions against reach stream power. The data suggested that the threshold for the 20-120mm tracers was almost identical for the riffles, whereas for the pools, it was the 80-120mm size class which had a lower threshold for motion, and the 20-40mm size fraction required higher stream powers for mobilisation. Although these data are limited to observations over five events, it does appear to suggest that hiding factors significantly influence threshold conditions for mobilisation of bed material, however also indicate that some size selectivity operates in conjunction.

Differences between riffles and pools

A more critical analysis of mobility was conducted by plotting the dimensionless θ_c against D^* . The values obtained from the Rede tracer data fall close to those traditionally assumed for poorly sorted gravels, with a mean $\theta_c = 0.051$ for the whole Rede channel, $\theta_c = 0.049$ for riffles, and $\theta_c = 0.055$ for pools. Values customarily assumed for θ_c are 0.06 for well-sorted sediments and 0.047 for poorly sorted sediments (Miller *et al.*, 1977), although Buffington and Montgomery (1997) have highlighted that values may range from 0.052 to 0.086 for reference-based studies and 0.030 to 0.073 for visually-based studies.

θ_c values for pools were found to be significantly higher than those for riffles, suggesting that riffle sediments are more easily entrained in comparison to pools. This difference was evident even though riffle data tended to plot above pool data (Figure 6.6). High θ_c values for pools may be explained by the coarser nature of the surrounding lag sediments which shelter bedload material. If the pool surface grain size was equal to or finer than the surface layer of the riffles, then θ_c values for pools would be lower than those found on the riffles. This is opposite to that found by Sear (1996) for the North Tyne, who attributed his findings to bed structure condition. Riffles tend to be more highly structured, armoured and compact, whereas the

sediment in pools tended to be loosely packed and more mobile. The information regarding bed structure for the Rede obtained from a penetrometer survey (data presented in section 3.3.6), did provide some evidence for pools and bars containing less compact material in comparison to riffles. However it appears that hiding effects caused by coarse lag deposits in the pools may be more influential. The ratio of surface to subsurface material is greater for pools in comparison to riffles, hence θ_c derived from Eq 1.2 are higher. Travel distance data for pool tracers suggest that transport of sizes below the D_{50} of the pool are strongly influenced by hiding effects. However protrusion effects become more important at sizes at or above the pool D_{50} , as demonstrated by greater transport distances for 80-120mm grains.

Equal mobility hypothesis

Log-log regression plotted through the data indicated an appreciable dependence of θ_c upon D^* . The slope exponent of the rating relation provides information on the mode of transport. It has been suggested by Parker and co-workers that a b exponent equal to -1.0 signifies equal mobility for all grain size present on the bed, whereas a b exponent equal to 0 indicates selective transport for all grain sizes. Parker *et al.* (1982) working on Oak Creek in Oregon found:

$$\theta_c = 0.0876 \ Di/Dj^{-0.982} \quad (6.17)$$

and regarded the b -exponent as effectively -1, indicating equal mobility of all size classes of material. Both riffle and pool b -exponents for the Rede are very close to equal mobility, suggesting that hiding factors may significantly influence the sediment transport regime even though other evidence shows some size selectivity. The b -exponent found for the majority of other rivers tends to be lower, indicating slight size selectivity. For example Ashworth and Ferguson (1989) for the Allt Dubhaig and the Feshie concluded;

$$\theta_c = 0.072 \ Di/Dj^{-0.65} \quad (\text{Allt Dubhaig}) \quad (6.18)$$

$$\theta_c = 0.054 \ Di/Dj^{-0.67} \quad (\text{Feshie}) \quad (6.19)$$

while Sear (1996) found lower b -exponents (indicating stronger size selectivity) for the North Tyne;

$$\theta_c = 0.034 \text{ } Di/Dj^{-0.535} \quad (\text{pools}) \quad (6.20)$$

$$\theta = 0.072 \text{ } Di/Dj^{-0.595} \quad (\text{riffles}) \quad (6.21)$$

The findings of Ashworth and Ferguson (1989) for the Lyngsdalva in Norway, however are closer to the equal mobility condition presented by Andrews (1983) for the East Fork, Snake and the Clearwater Rivers in Idaho;

$$\theta_c = 0.087 \text{ } Di/Dj^{-0.92} \quad (\text{Lyngsdalva}) \quad (6.22)$$

6.4.3 Virtual velocity, shear stress and grain size

The data obtained from painted pebble transport measurements on the Rede permitted predictive relations to be drawn between the velocity of tracer clasts and (i) grain size, and (ii) shear stress. Dimensionless variables were employed for generality and transferability. Three main variables are known to influence virtual velocity V_i ; (i) D_i of the individual tracer pebble, which determines its inertia, (ii) D_j of the surrounding surface particles, which control hiding and protrusion effects, and (iii) τ_j the typical bankfull shear stress which drives mobilisation (Ferguson and Wathen, 1998). The best predictor was given by multiple regression of θ_c and D^* on to V^* . The resulting equations 6.14, 6.15 and 6.16, predict V^* very successfully. Coarser material appears to travel faster than finer material even though finer material travelled further over the thirteen-month study period. Furthermore there is a negative relationship between θ_c and V^* , suggesting that particles which require a higher θ_c for mobilisation, travel slower than grains which require a lower θ_c . This is likely to be a reflection of relative grain size hiding effects. Tracer grains with a lower V^* reflect shielded finer material which requires a higher θ_c for mobilisation. Conversely, the faster tracer grains reflect coarser material which protrudes into the flow and requires a lower θ_c for

mobilisation. It is important to note that this is opposite to the findings of Ferguson and Wathen (1998) for the Allt Dubhaig, who concluded that faster grain velocities for finer size fraction reflected size-selective transport. The reason for this difference is that Ferguson and Wathen assumed an identical competence time regardless of grain size, whereas the analyses used here for the Rede uses competence times for different grain sizes. It should be noted if calendar time were used instead of mobilisation time, progressively finer material would have higher velocities (travelling further) in comparison to progressively coarser material (travelling shorter distances).

6.5 Summary

- 1) Tracer movement was successfully monitored over five flows; an 80% recovery rate was found for the first three flows, however by the final re-survey thirteen months after seeding, the recovery rate had fallen to only 20%. This highlights the limitations of using painted clasts in tracer experiments;
- 2) Although rods were transported further than other shapes this difference was not statistically significant, suggesting that travel distance was independent of shape.
- 3) A bimodal distribution in size versus distance was evident suggesting the existence of both hiding and selective transport which appears to be controlled by two grain sizes;
- 4) The grain size which travels the least approximates to the D_{50} for the reach, this may be considered the 'equilibrium' grain size;
- 5) Evidence of both size selectivity and hiding effects (which drive equal mobility) may be found from plots of size fraction versus travel distance. No relationship was evident between event-based single clast travel distance and b-axis size;
- 6) Transport distance increases with increasing Ω at faster rates for finer sizes of sediments which suggests some selective transport is operating. However initial Ω suggested very similar Ω or slightly lower Ω for progressively coarser fractions, suggesting near-equal mobility;
- 7) θ_c decreases with increasing D^* . θ_c is significantly higher for pools in comparison to riffles ($p<0.05$) which suggests that pool sediments less more mobile. This may

be explained by the ratio of surface to sub-surface sediments which is greater in pools due to the existence of a coarse lag deposit (see Chapter Three);

- 8) b -exponents are very close to Parker and Klingeman's (1982) equal-mobility value of -1.0 , suggesting the occurrence of only minor size selectivity in the Rede channel;
- 9) Scaled travel distance L/Ld_{50s} for the reach as a whole showed a very similar relationship with scaled grain size D^* to that of Church and Hassan (1992) and Ferguson and Wathen (1998). Riffle data however showed considerable deviation, particularly for grains $< D_{50s}$;
- 10) V^* shows a strong positive dependence upon D^* , reflecting increased mobility with increasing protrusion into the flow;
- 11) V^* shows a strong negative dependence upon θ_c reflecting the higher velocities and lower θ_c required to mobilise progressively coarser grains;
- 12) Multiple regression demonstrates a strong dependence of V^* upon two controlling variables; θ_c and D^* ($R^2 > 0.85, p > 0.01$).

Chapters Five and Six have considered the mobility and transport of gravel and sand and through riffle-pool topography. The existence of coarser pools in comparison to the riffles on the Rede (see Chapter Three) suggests that a variation to the traditional sediment sorting models discussed in Chapter One may exist. The following two chapters consider the routing and sorting of gravel and sand through the Rede riffle-pool sequence.

Chapter Seven

Phase 1 sediment routing through a riffle-pool sequence

7.1 Introduction

During the majority of the flow range, riffles have greater tractive force in comparison to the pools. During these periods flows tend only to be competent enough to mobilise sand and fine gravel. It is generally accepted that during these flows any excess fine bedload, which was deposited on the riffle at high flow, is routed over the static riffle armour and transferred into zones of lower tractive force such as pool tails (Jackson and Beschta, 1982; Lisle and Hilton, 1992, 1999). Fines are stored in pools until the next high flow event where they are scoured and eventually transferred into pools situated further downstream (Wohl *et al.*, 1993; Clifford, 1993b). A number of workers (Sawada *et al.*, 1985; Lisle and Hilton, 1992; 1999; Lisle and Madej, 1992; Wiele *et al.*, 1996) describe the importance of supply dependency and winnowing processes upon storage of fines. Fine bedload is highly mobile and 'supply-dependent' insofar as the net transport over a given period is more dependent upon the fines stored on the bed or supplied to the channel from extrinsic sources (e.g. eroding bluffs on hillslopes adjacent to the channel), than on the duration and magnitude of the stream flow. As the supply of fine bed material increases, the void spaces between framework particles in the riffle substrate become filled, resulting in greater volumes of exposed fines on the bed surface which may be subject to winnowing. This chapter examines spatial patterns of fine bedload routing (accumulation), storage, and grain size, through the Rede riffle-pool sequence to test this traditional model of sorting. The ecological significance of fine sediment accumulation in river gravels should also be raised. Data presented in this Chapter may also be of use to fisheries ecologists interested in siltation rates. Of particular use is the close attention to spatial variation in accumulation rates, which Acornley and Sear (1999) claim can be highly variable and linked to local hydraulic conditions.

7.2 Approach

To analyse the routing and sorting of sand (the major constituent of Phase 1 bedload), a combination of basket trap sampling and sediment tracing was employed (see Chapter Two for methodological details). The mass of fine sediment entering the traps

was recorded and converted into an accumulation rate ($\text{kg m}^{-2} \text{ day}^{-1}$) using the calendar time between sampling and the area of the trap 0.05m^2 . The accumulation rates for each trap position gives an indicating of preferential Phase 1 sediment routing zones at high flow, and are not low flow storage areas. High accumulation rates in traps indicate high rates of sediment delivery. Grain size analysis was also conducted on basket samples to provide further information on size sorting across riffle surfaces (see Chapter Five, Appendix 5.1).

A tracing technique previously developed for monitoring movement of beach sands (van der Post *et al.*, 1994) was chosen to provide further information about sorting of sand (particularly storage areas) through the Rede riffle-pool sequence. The details of the tracer manufacture process and tracer deployment are described in Chapter Two (see sections 2.4.6 and 2.4.9), whilst tracer detection in the field and laboratory is described in section 2.4.5.

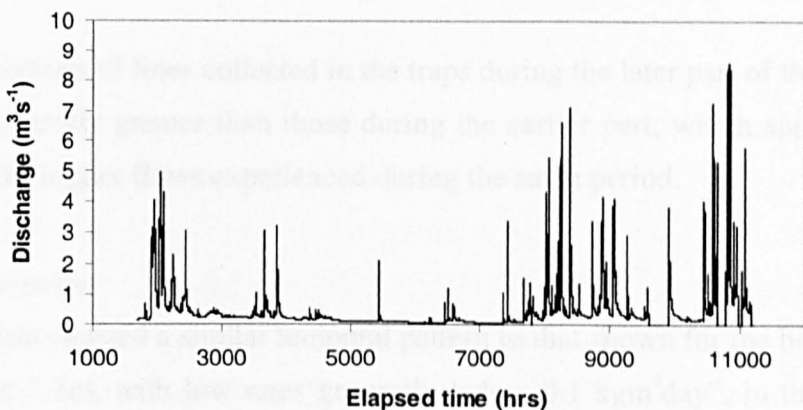
7.3 Results I: Basket traps – temporal and spatial variability in accumulation and grain size

7.3.1 Temporal variation in accumulation rate

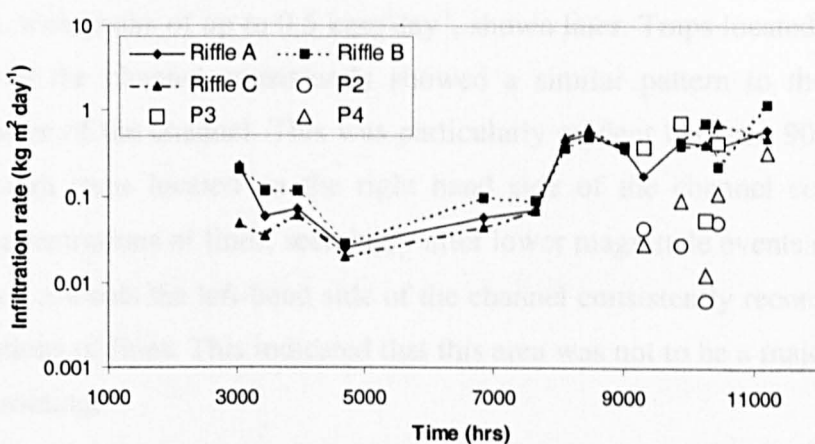
i) Overall pattern

The time series for overall accumulation rates are demonstrated in Figure 7.1, alongside the discharge information for the same period (15th March 1996 to 11th March 1997). Overall individual basket accumulation rates (for riffles) ranged between 0.0013 and $1.527 \text{ kg m}^{-2} \text{ day}^{-1}$. The limited data for pools suggested a much lower accumulation rate on average in comparison to riffles, with the exception of Pool 3. The highest rate of accumulation was found in traps at Riffle B after a flow of $7.12 \text{ m}^3 \text{s}^{-1}$. The mean temporal rate of accumulation showed a similar pattern between riffles however slight variations were encountered. During the first half of the investigation (<8000 hrs) traps at Riffle B appeared to collect greater concentrations of fines coinciding with floods of a lower magnitude ($<5\text{m}^3 \text{s}^{-1}$) than those recorded later on in the study. During the later period it is the traps located at Riffle C which appear to collect slightly more fines than the other two riffles, a factor particularly evident after discharges greater than $5\text{m}^3 \text{s}^{-1}$. In the early part of the study when flows recorded were $<5\text{m}^3 \text{s}^{-1}$ (<8000hrs) these traps had collected the lowest concentrations

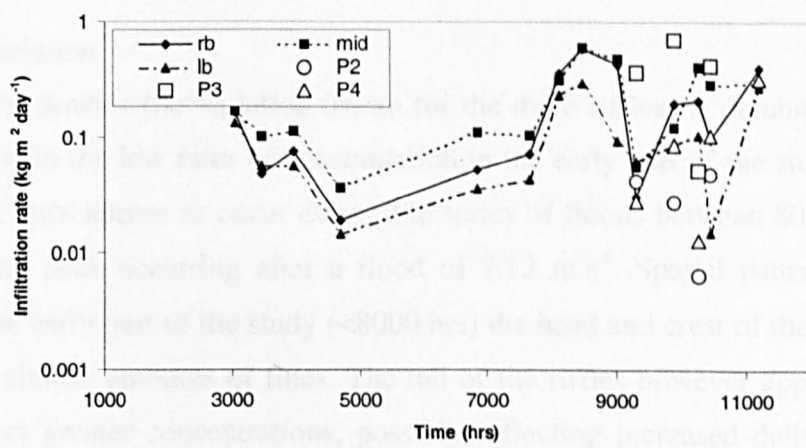
a)



b)



c)



d)

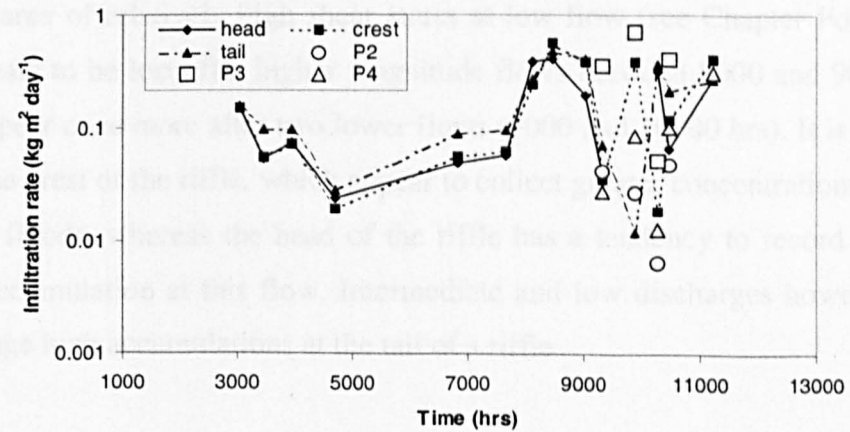


Figure 7.1 Temporal and spatial variability in infiltration rates, a) Discharge, b) between riffle, c) cross-channel variability, d) longitudinal variability. Rb- right bank, lb- left bank, mid- mid channel, P- pool.

of fines. Concentrations of fines collected in the traps during the later part of the study (>8000hrs) are generally greater than those during the earlier part, which appears to be a response to the higher flows experienced during the same period.

ii) Cross riffle variation

The cross-riffle data showed a similar temporal pattern to that shown for the between-riffle data (Figure 7.1c), with low rates generally below $0.1 \text{ kgm}^2\text{day}^{-1}$, in the early part of the study, with peaks of up to $0.5 \text{ kgm}^2\text{day}^{-1}$, shown later. Traps located on the right hand side of the channel consistently showed a similar pattern to the traps located in the centre of the channel. This was particularly evident between 9000 and 10000 hrs, although traps located on the right hand side of the channel collected slightly lower concentrations of fines, seemingly after lower magnitude events (<8000 hrs). Traps located towards the left-hand side of the channel consistently recorded the lowest concentrations of fines. This indicated that this area was not to be a major zone for fine bedload routing.

iii) Down riffle variation

The time-series for down-riffle variation (mean for the three riffles) is demonstrated in Figure 7.1d. Again the low rates of accumulation in the early part of the study are highlighted. Peak rates appear to occur during the series of floods between 8000 and 9000 hrs, with the peak occurring after a flood of $7.12 \text{ m}^3\text{s}^{-1}$. Spatial patterns are evident; during the early part of the study (<8000 hrs) the head and crest of the riffles appear to collect similar amounts of fines. The tail of the riffles however appears to consistently collect greater concentrations, possibly reflecting increased delivery at low flow in this area of relatively high shear stress at low flow (see Chapter Four). This pattern appears to be lost after higher magnitude flows between 8000 and 9000 hrs, only to re-appear once more after two lower flows (9000 and 10000 hrs). It is the traps located at the crest of the riffle, which appear to collect greater concentrations of fines after larger floods, whereas the head of the riffle has a tendency to record the lowest rates of accumulation at this flow. Intermediate and low discharges however appear to encourage high accumulations at the tail of a riffle.

iv) Pool-riffle variation

Pools 2 and 4 (see Figure 2.3 c) consistently showed lower accumulations of fines in comparison to the riffles above and below. Pool 2 tended to collect the lowest concentrations, whilst Pool 3 collected the greatest. On two occasions this pool collected more fines than the adjacent riffles. Notably, Pool 3 is not as deep as the other two pools which were sampled, is on a straight section of channel and is not as susceptible to scour as the other two. Pool 3 has characteristics closer to a glide (Padmore, 1998). Fines have to be fed through this pool as it lies on a straight section of channel, whereas on meandering sections, fines can be fed over bar surfaces instead of through the pool trough.

7.3.2 Temporal variation in the grain-size of accumulating sediments

i) Down riffle size variation

For each riffle, Figure 7.2 shows the down-riffle variation in grain size of sand (63-2000 μ m) infiltrating traps. Coarser sediments were found to infiltrate traps in response to the higher magnitude flood events experienced in the later half of the study. There is a tendency for either the tail (and less frequently the crest) of riffles to collect coarser sediments, with the head of the riffle collecting the finest sediments. Riffle C demonstrates an increase in grain size and less fluctuation in comparison to Riffles A and B in the later part of the study, which is possibly related to the occurrence of higher magnitude floods.

ii) Cross riffle size variation

The variation in median grain size characteristics for accumulating sand (63-2000 μ m) across each riffle is shown in Figure 7.3. For each riffle it appears that there is a trend for coarser material to have been retrieved during the later part of the study (>8000hrs), which appears to reflect the higher magnitude flows experienced during this period. Also evident is the coarser nature of the fines accumulating in traps located in the centre of the channel. The pattern (shown most strongly for Riffles A and B) was for traps located on the left hand side of the channel to collect slightly finer sediments than the middle of the channel, and for the right hand bank to collect the finest sediments. From these results, clear spatial patterns of fine sediment

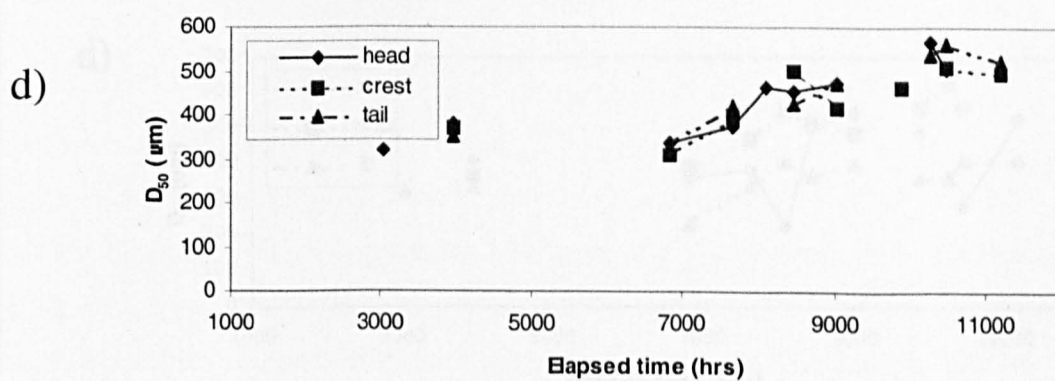
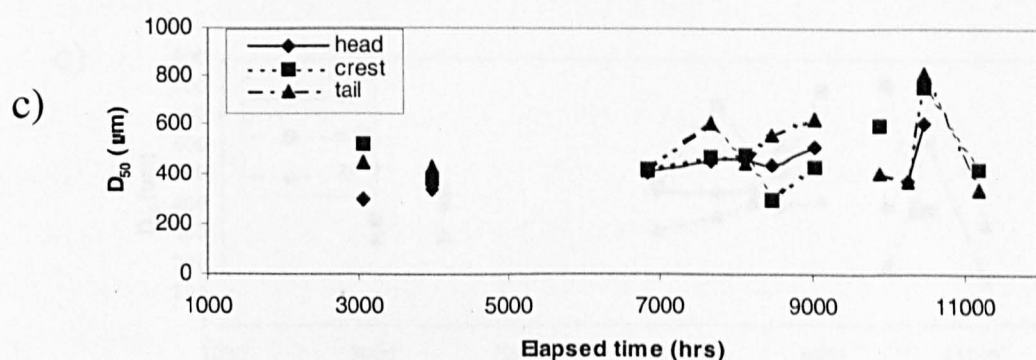
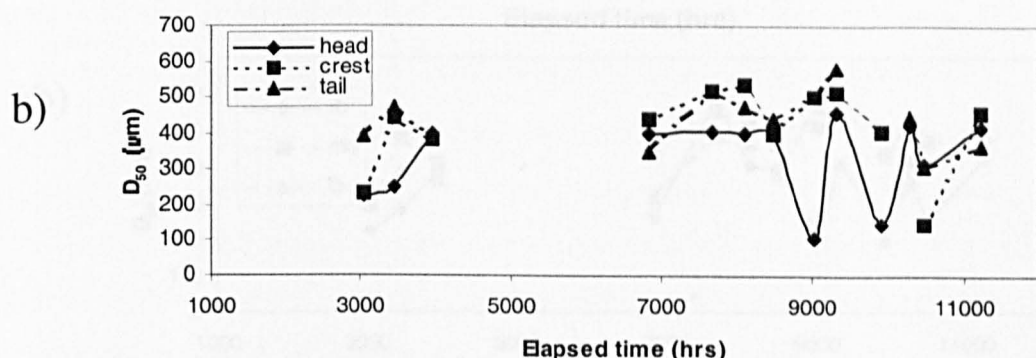
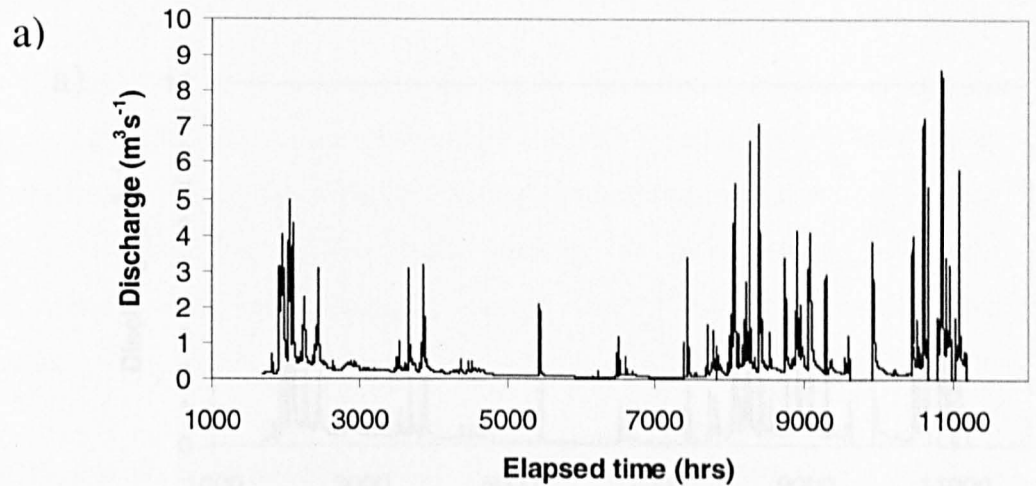


Figure 7.2 Longitudinal temporal variability in grain size of accumulating fines for the head, crest and tail of each study riffle. b) riffle A, c) riffle B, d) riffle C.

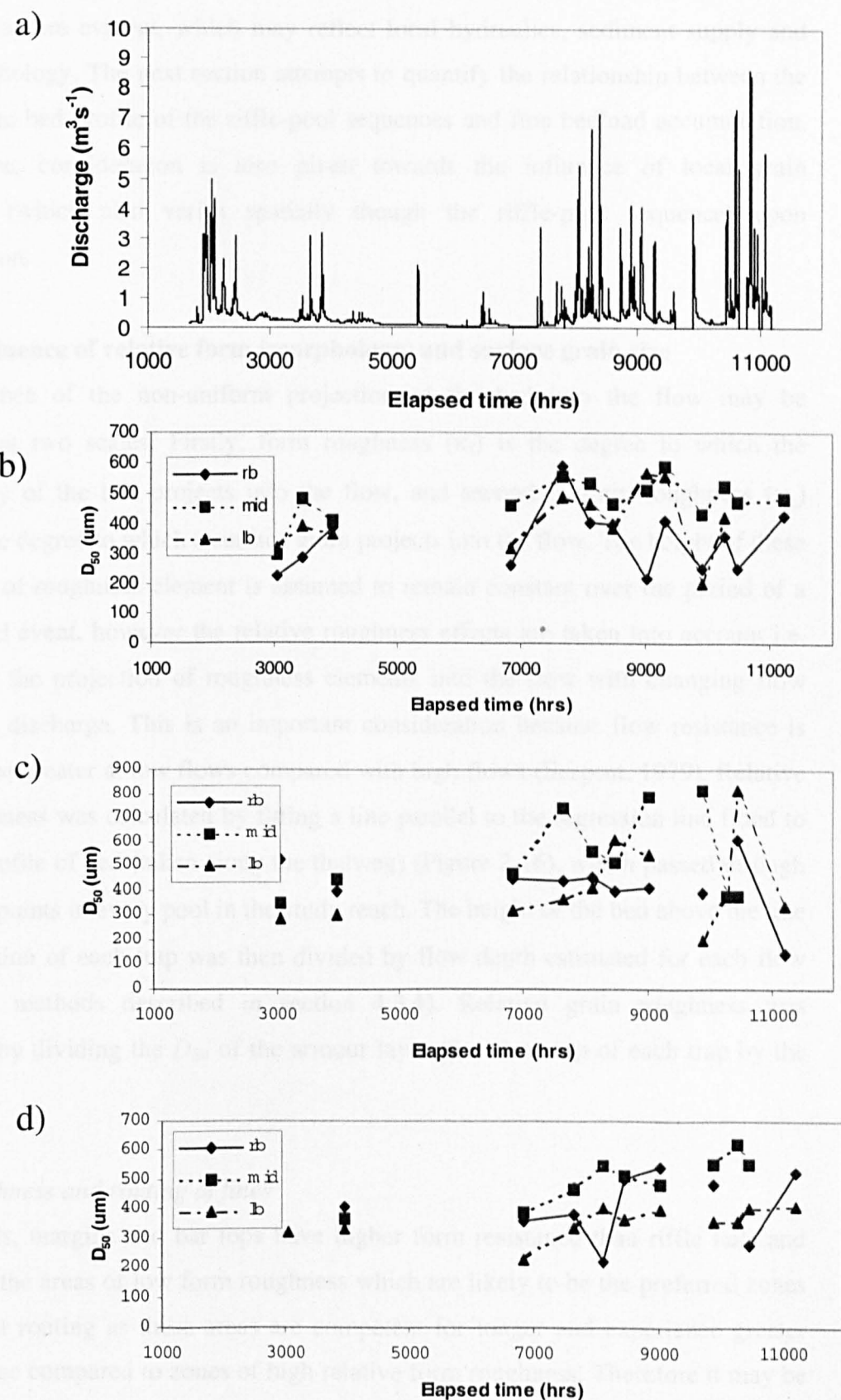


Figure 7.3 Cross-channel temporal variability of grain size for each study riffle. b) riffle A, c) riffle B, d) riffle C. Rb-right bank looking downstream, lb-left bank, mid-mid-channel.

accumulation are evident, which may reflect local hydraulics, sediment supply and local morphology. The next section attempts to quantify the relationship between the non-uniform bed profile of the riffle-pool sequences and fine bedload accumulation. Furthermore, consideration is also given towards the influence of local grain roughness (which also varies spatially though the riffle-pool sequence) upon accumulation.

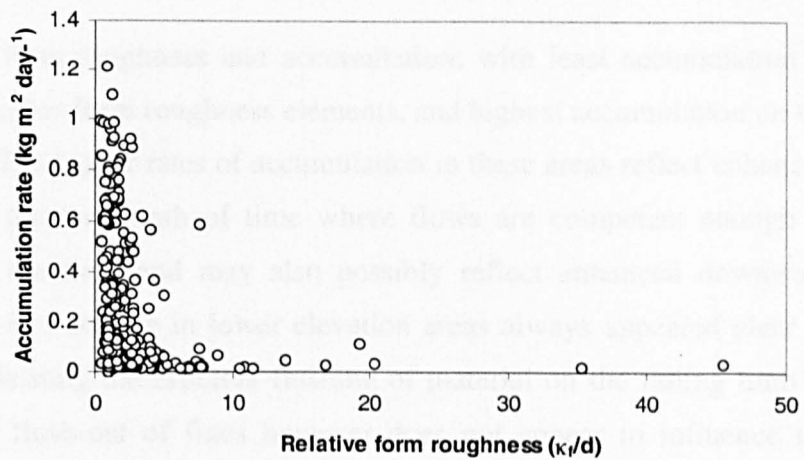
7.3.3 Influence of relative form (morphology) and surface grain size

The influence of the non-uniform projection of the bed into the flow may be expressed at two scales. Firstly, form roughness (κ_f) is the degree to which the morphology of the bed projects into the flow, and second is grain roughness (κ_g) which is the degree to which a surface grain projects into the flow. The height of these two scales of roughness element is assumed to remain constant over the period of a single flood event, however the relative roughness effects are taken into account i.e. changes in the projection of roughness elements into the flow with changing flow depth with discharge. This is an important consideration because flow resistance is known to be greater at low flows compared with high flows (Sargent, 1979). Relative form roughness was calculated by fitting a line parallel to the regression line fitted to the long profile of bed (taken along the thalweg) (Figure 2.16), which passed through the lowest points in every pool in the study reach. The height of the bed above the line at the position of each trap was then divided by flow depth estimated for each flow (using the methods described in section 4.3.4). Relative grain roughness was calculated by dividing the D_{84} of the armour layer placed on top of each trap by the flow depth.

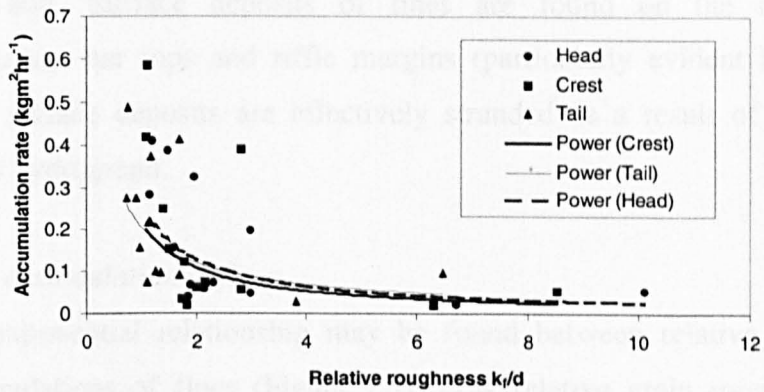
Form roughness and routing of fines

Riffle heads, margins and bar tops have higher form resistance than riffle tails and pools. It is the areas of low form roughness which are likely to be the preferred zones of sediment routing as these areas are competent for longer and experience greater tractive force compared to zones of high relative form roughness. Therefore it may be expected that bars, riffle heads and margins would tend to have lower accumulation rates in comparison riffle centres and tails. The plot of relative form roughness versus accumulation in Figure 7.4 provides the expected pattern, with a negative exponential

a)



b)



c)

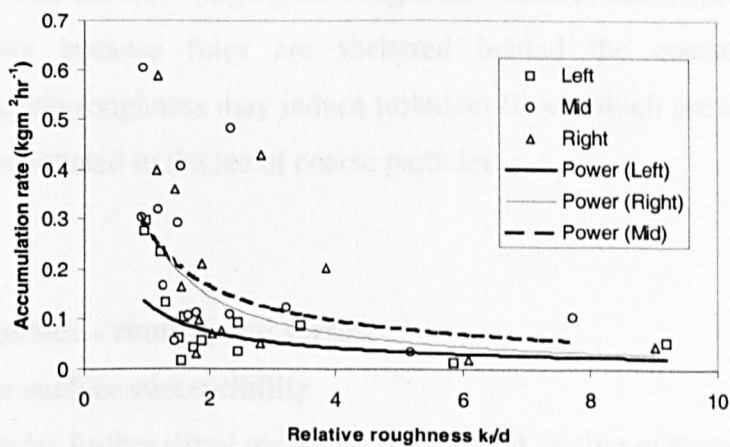


Figure 7.4 Plots indicating the relationship between accumulation rate and variation in relative roughness a) all data b) down riffle and c) cross-riffle. The overall trend is for greater relative form roughness to discourage accumulation of fines. Power functions fitted to the data indicate the head / crest and right/left part of the riffles exhibit greater relative form roughness and as a result lower accumulation rates. Conversely riffle tails and centres have the lowest form roughness and greatest accumulation rates. At low relative roughness during high flow the right hand bank may collect similar amounts of fines to the channel centre as roughness effects are drowned out. The left hand bank always collects less fines than the middle or right hand side of the channel. The riffle tail collects more fines during lower magnitude flow events when form roughness effects are comparatively small for the riffle tail in comparison to the head and the crest. However, during higher flow, when the form roughness effects are lessened, greatest concentrations of fines are located at the head and crest of riffles. Again it is important to note that it is the zones of high form roughness which act as storage zones.

relationship between form roughness and accumulation; with least accumulation in traps situated on the higher form roughness elements, and highest accumulation on the low roughness areas. The higher rates of accumulation in these areas reflect enhanced delivery of material; greater length of time where flows are competent enough to transport material to the trap, and may also possibly reflect enhanced downward hydraulic forces. The bed surface in lower elevation areas always appeared clear of fines at low flow, indicating the efficient flushing of material on the falling limb of the hydrograph. This flush-out of fines however does not appear to influence the quantity of material stored in the traps, although there is a suggestion that it may influence its grain size. Surface deposits of fines are found on the higher elevation/roughness areas; bar tops and riffle margins (particularly evident in the tracer study). These surface deposits are effectively stranded as a result of rapid recession on the flood hydrograph.

Grain roughness and accumulation of fines

A similar negative exponential relationship may be found between relative grain roughness and accumulations of fines (Figure 7.5). Low relative grain roughness appears to improve the delivery of fines over the bed surface to traps. This suggests that gravel protrusion into the flow (high grain roughness) reduces sediment delivery to the traps, possibly because fines are sheltered behind the coarse clasts. Alternatively, higher grain roughness may induce turbulent flows which prevent fines from settling into traps situated in the lee of coarse particles.

7.4 Results II: Magnetics – routing and sorting

7.4.1 Dimensionless surface susceptibility

Magnetic tracing provides further detail regarding routing and sorting of fines through the Rede riffle-pool sequence. Surface susceptibility data obtained using the Bartington loop sensor was obtained on three occasions; (i) before tracer emplacement, (ii) 1 week after tracer emplacement during low flow, and (iii) after the first flood event post tracer emplacement (Figure 7.6a-c). The pre-emplacement survey demonstrates the natural background susceptibility. Background surface susceptibility (Figure 7.6a) was in the ranges $10-192 \times 10^{-8} \text{ m}^3\text{kg}^{-1}$. The two

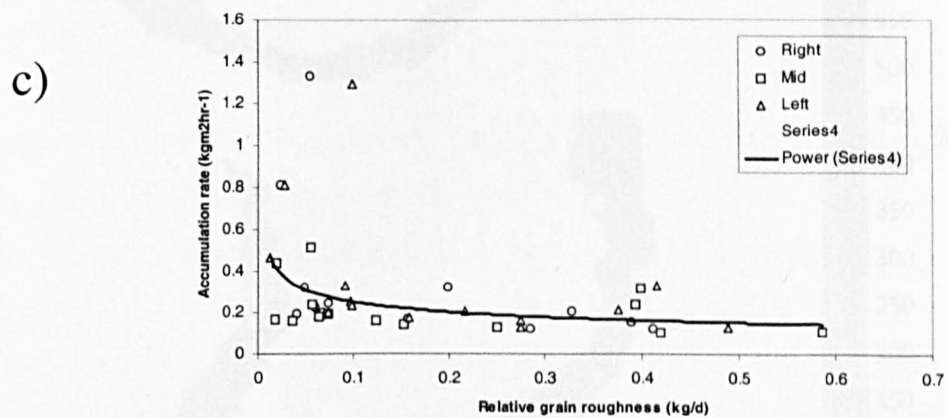
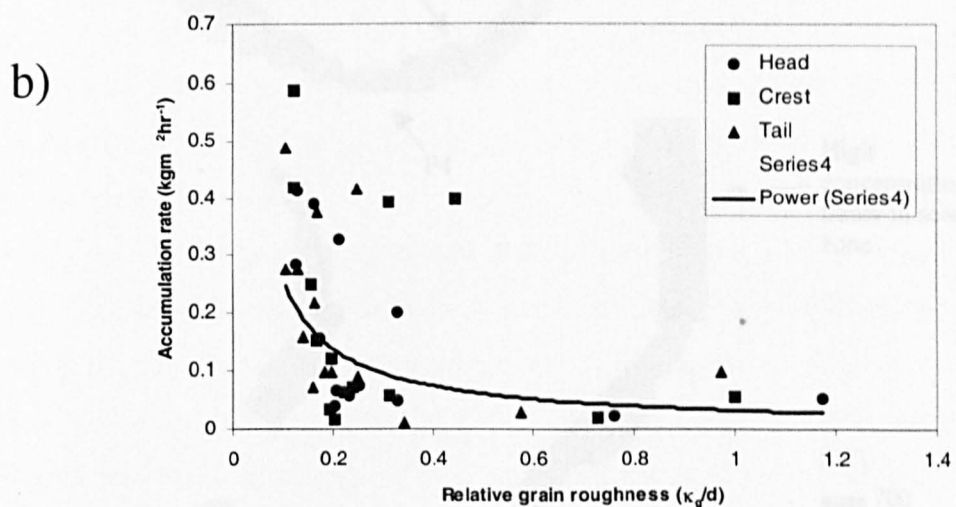
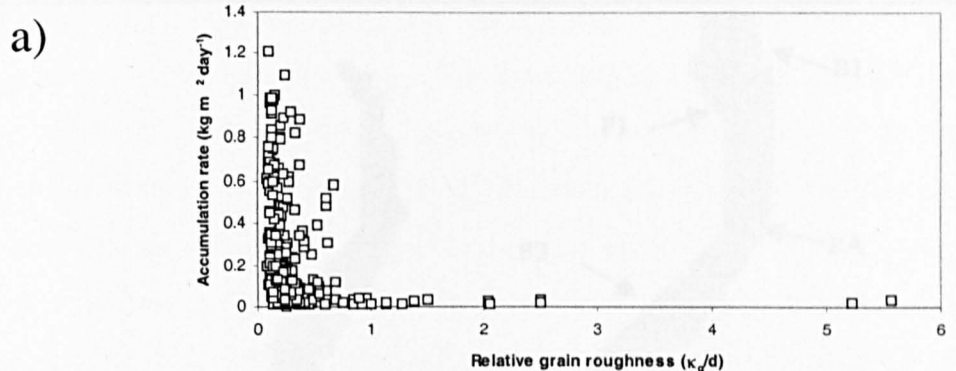


Figure 7.5 Plot indicating the relationship between relative grain roughness and rate of accumulation of fines in traps a) all data b) down riffle and c) cross riffle. Lines fitted are power functions fitted to all the data. Although greater accumulations of fines are found for traps located in zones of low grain roughness, it is important to note that these areas are not storage zones unless substrate void space is available.

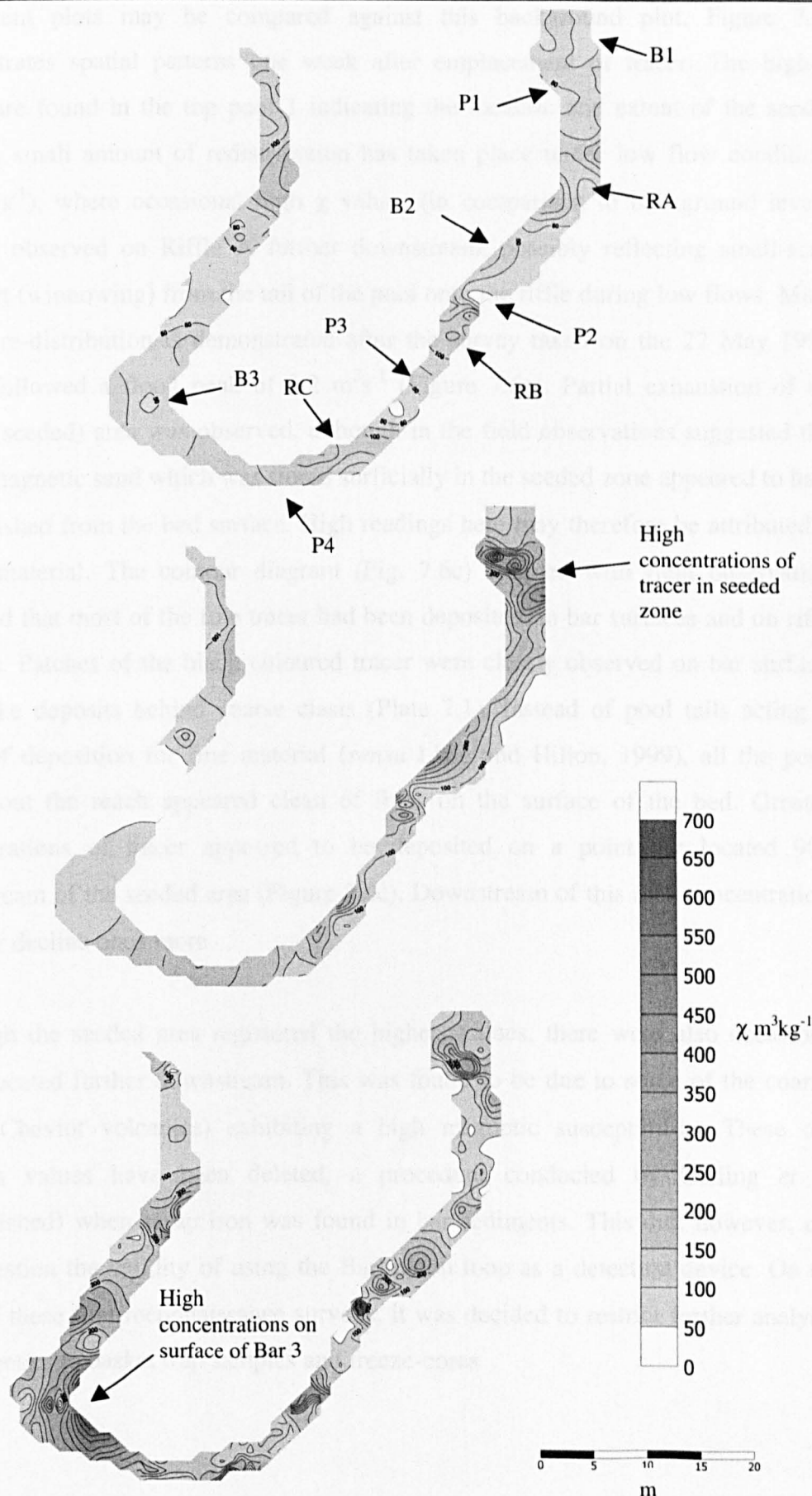


Figure 7.6 Spatial distribution in surface magnetic susceptibility χ , a) background before any emplacement of tracer, b) 1 week after emplacement 30/4/96, c) post flood 22/5/96.

subsequent plots may be compared against this background plot. Figure 7.6b demonstrates spatial patterns one week after emplacement of tracer. The highest values are found in the top pool 1 indicating the location and extent of the seeded zone. A small amount of redistribution has taken place under low flow conditions ($<0.5\text{m}^3\text{s}^{-1}$), where occasional high χ values (in comparison to background levels) may be observed on Riffle A further downstream, possibly reflecting small-scale transport (winnowing) from the tail of the pool onto the riffle during low flows. Much greater re-distribution is demonstrated after the survey taken on the 22 May 1996, which followed a flood peak of $3.2\text{ m}^3\text{s}^{-1}$ (Figure 7.6c). Partial exhaustion of the source (seeded) area was observed, although in the field observations suggested that all the magnetic sand which was stored surficially in the seeded zone appeared to have been flushed from the bed surface. High readings here may therefore be attributed to buried material. The contour diagram (Fig. 7.6c) coupled with field observation, indicated that most of the fine tracer had been deposited on bar surfaces and on riffle margins. Patches of the black coloured tracer were clearly observed on bar surfaces and wake deposits behind coarse clasts (Plate 7.1). Instead of pool tails acting as zones of deposition for fine material (*sensu* Lisle and Hilton, 1999), all the pools throughout the reach appeared clean of fines on the surface of the bed. Greatest concentrations of tracer appeared to be deposited on a point bar located 90m downstream of the seeded area (Figure 7.6c). Downstream of this area concentrations of tracer decline once more.

Although the seeded area registered the highest values, there were also occasional peaks located further downstream. This was found to be due to some of the coarser clasts (Cheviot volcanics) exhibiting a high magnetic susceptibility. These odd spurious values have been deleted, a procedure conducted by Carling *et al.* (unpublished) when scrap iron was found in bar sediments. This did, however, call into question the validity of using the Bartington loop as a detection device. On the basis of these first reconnaissance surveys, it was decided to restrict further analyses of magnetics to basket trap samples and freeze-cores

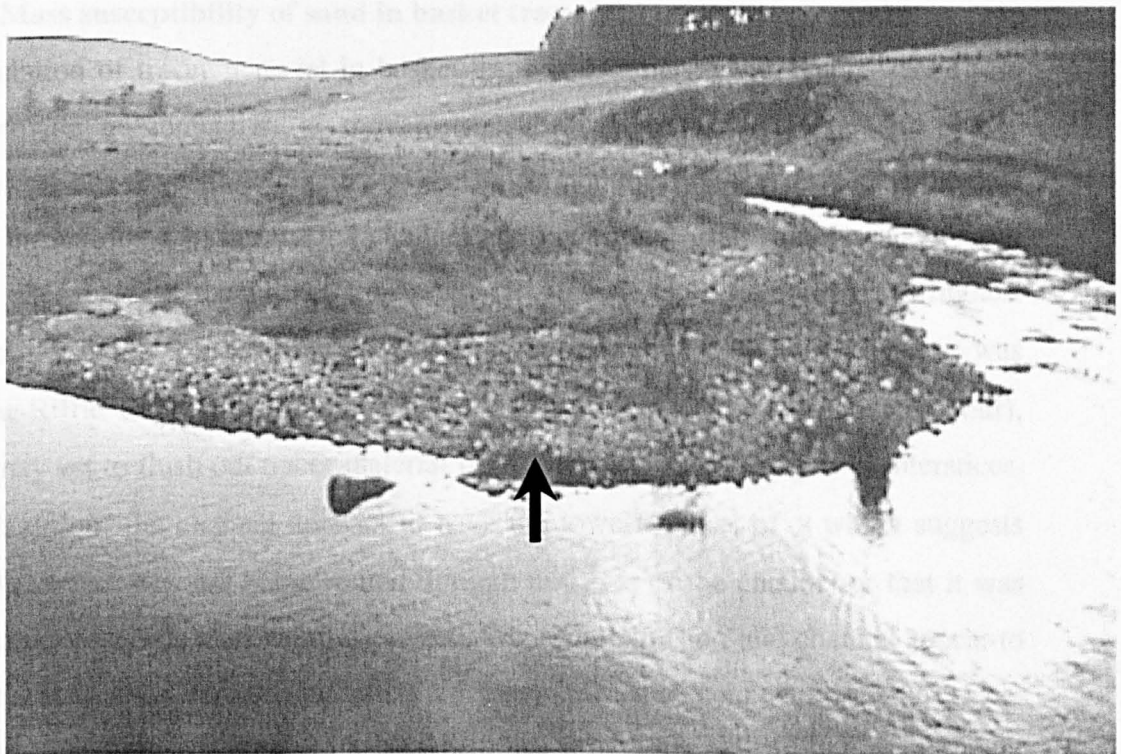


Plate 7.1 Deposition of magnetic sand on bar surfaces, indicated by the arrows

7.4.2 Mass susceptibility of sand in basket traps (χ)

Accumulation of tracer material in basket traps is summarised in Figure 7.7. These plots provide an indication of movement and dilution through time and space, however are not as spatially detailed as the Bartington loop survey results, as the data tend to be restricted to the wetted channel and occasional grab samples taken from storage sites beyond the basket trap range. Riffles A and C recorded the highest values for χ before the first large winter floods (<8000hrs), whereas Lower χ was found at Riffle B possibly reflects greater τ in this area (shown in Chapter Four), which may act to flush out tracer material from the bed surface and gravel interstices. The left side of the channel appears to have the lowest values of χ which suggests either that tracer was not being routed through this area of the channel or that it was flushed out of baskets after being deposited. The right bank and mid channel appear to be favourable sites for accumulation of tracer. Greater concentrations of tracer appeared to be found on the right bank which lies at a higher elevation. Fine sediment which accumulated in riffle head traps also appeared to contain greater concentrations of tracer material, even though these same areas collected the least loadings of fines overall (section 7.3.1), which may suggest post depositional wash-out is not as effective here compared to the crest and tail traps.

Tracer movement may be assessed further by tracking the centroid (section 5.2 and 5.3.2), by describing its movement in relation to channel morphology. The centroid may be calculated using equation 5.1 (Crickmore, 1967). Table 5.1 demonstrates the sequential positions of the centroid after a range of flows. Description of the longitudinal movement of tracer is further assisted with reference to the spatial and temporal patterns of magnetic susceptibility recorded from basket trap samples, which has been contoured in Appendix 7.1 a-m.

(i) Centroid movement

Data for the first flood (22.5.96) of $3.2 \text{ m}^3\text{s}^{-1}$ demonstrate little spatial variability in susceptibility values for tracer material caught in traps. Basket trap values coupled with grab samples taken further downstream and surface susceptibility data obtained using the Bartington Loop indicate that tracer material had been transported beyond

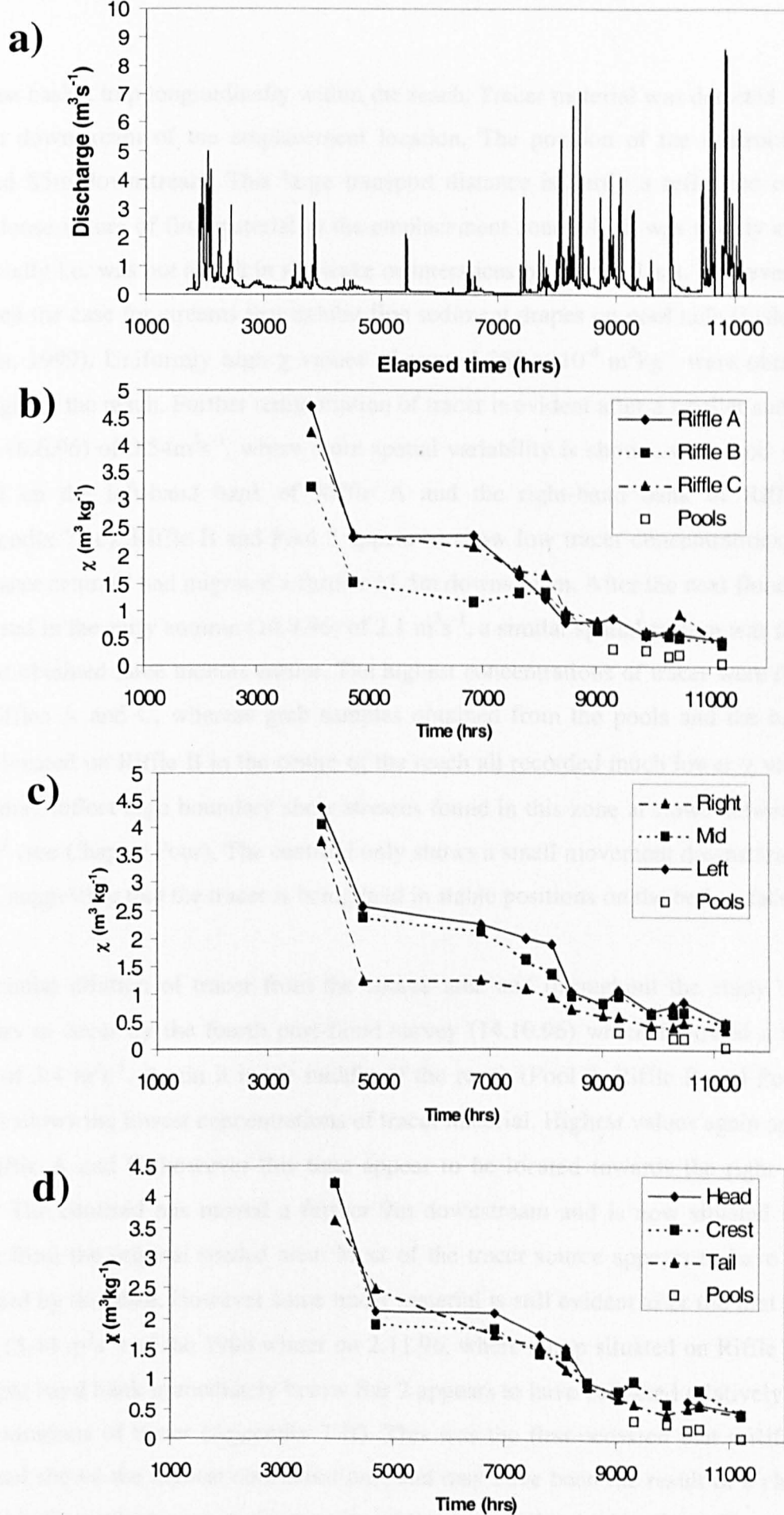


Figure 7.7 Temporal and spatial variation in χ ($\times 10^6$), a) Discharge, b) between riffle, c) cross-channel variability, d) longitudinal (down riffle) variability.

the last basket trap longitudinally within the reach. Tracer material was detected up to 148m downstream of the emplacement location. The position of the centroid had moved 85m downstream. This large transport distance is partly a reflection of the over-loose nature of fine material in the emplacement zone which was mainly stored superficially i.e. was not stored in the wake or interstices of coarse clasts. However this is often the case for streams that exhibit fine sediment drapes on pool tails (Lisle and Hilton, 1999). Uniformly high χ values of around $350 \times 10^{-8} \text{ m}^3\text{kg}^{-1}$ were obtained throughout the reach. Further redistribution of tracer is evident after a smaller summer flood (6.6.96) of $0.54 \text{ m}^3\text{s}^{-1}$, where more spatial variability is shown, with 'hot' spots found on the left-hand bank of Riffle A and the right-hand bank of Riffle C (Appendix 7.1c). Riffle B and Pool 3 appear to show low tracer concentrations, and the tracer centroid had migrated a further 11.5m downstream. After the next flood that occurred in the early autumn (10.9.96) of $2.1 \text{ m}^3\text{s}^{-1}$, a similar spatial pattern was found to that obtained three months earlier. The highest concentrations of tracer were found on Riffles A and C, whereas grab samples obtained from the pools and the basket traps located on Riffle B in the centre of the reach all recorded much lower χ values. This may reflect high boundary shear stresses found in this zone at flows between 2- $6 \text{ m}^3\text{s}^{-1}$ (see Chapter Four). The centroid only shows a small movement downstream of 5.5m, suggesting that the tracer is being held in stable positions on the bed surface.

Substantial dilution of tracer from the source area and throughout the study reach appears to occur by the fourth post-flood survey (14.10.96) which followed a flood peak of $3.4 \text{ m}^3\text{s}^{-1}$. Again it is the middle of the reach (Pool 2, Riffle B and Pool 3) which shows the lowest concentrations of tracer material. Highest values again appear on Riffle A and C, however this time appear to be located towards the right hand bank. The centroid has moved a further 9m downstream and is now situated some 111m from the original seeded area. Most of the tracer source appears to have been depleted by this date. However some tracer material is still evident after the first large flood ($5.44 \text{ m}^3\text{s}^{-1}$) of the 1996 winter on 2.11.96, where a trap situated on Riffle B on the right hand bank immediately below Bar 2 appears to have collected relatively high concentrations of tracer (Appendix 7.1f). This was the first occasion that a Riffle B trap had shown the highest concentrations, and may have been the result of a change in hydraulic environment in the vicinity of the trap at this higher flow. The trap is

located on the lee side of Bar 2 and away from the highest shear stresses which are found on the right hand bank in this area. A still-water zone was observed in this area at high flows which may have allowed settling out of fines winnowed from the bar surface upstream. There is a much greater movement in the position of the centroid in comparison to the previous three flood events, which possibly reflects disruption of coarse particles in the surface layer resulting in release of interstitial stored fines, wake deposits, or mobilisation of previous tracer deposits on morphological highs. After a further flow of 84% bankfull ($7.12 \text{ m}^3 \text{s}^{-1}$) on 17.11.96 tracer concentrations are generally approaching background levels. However tracer is still detectable, with highest concentrations being found unexpectedly at the head of Riffle A. Again this is likely to be due to disruption of the armour layer, which from coarser tracer evidence appears to occur between 35% and 47% bankfull (see section 6.3.4). This surface disrupted has resulted in the release of buried/infiltrated material, which results in the position of the centroid appearing to move backwards by 6m (Table 6.1).

Following the next two flows in December 1996, which were both of the same order of magnitude ($4\text{m}^3 \text{s}^{-1}$), a slightly elevated magnetic signal is still a feature at the head/crest of Riffle A, whilst the rest of the reach is barely above background levels (Appendix 7.1). Over this period the tracer centroid has progressed another 32m downstream. After the next flood event ($1.23\text{m}^3 \text{s}^{-1}$), tracer material is barely detectable within the reach once more, however when data from both basket traps and grab samples were combined it was apparent that the tracer centroid had migrated a further 21m downstream. The next two floods in late January and early February were around half-bankfull discharge and appear to indicate a subtle release of fines stored beneath the surface layer in the zone of tracer emplacement. Although susceptibility readings were not as high as earlier in the investigation, increases in comparison to the previous flow were evident. Again these higher levels appear towards the head of riffle A suggesting capture from a local source i.e. the emplacement zone. Although these two flows of just below $4\text{m}^3 \text{s}^{-1}$ may not have been capable of mobilising the surface D_{50} , patchy localised scour is still possible. The re-emergence of tracer material close to the seeded zone again has the effect of moving the centroid back upstream on both occasions by around 20m (Table 5.1), a feature noted also on the North Tyne by Sear (1996). The last samples were taken in March 1997 after the largest flood (over the period of tracer monitoring) of $8.6\text{m}^3 \text{s}^{-1}$. By this stage of the

investigation it is virtually impossible to separate tracer material within the study reach from background levels. However, computation of equation 5.1 suggests a further centroid migration of 46m.

7.4.3 Vertical sorting of tracer (Phase 1 material)

To examine any interstitial storage and vertical sorting of tracer, freeze-core samples were examined on two occasions after emplacement (July 1996 and March 1997). Variations in background χ in the matrix sediments with depth obtained from freeze-cores are indicated in Appendix 7.2, where there appears to be a general increase with depth. The range of values for the lower core sections (45-60cm) also tend to be widest whereas the near-surface 0-15cm has the narrowest range, as indicated by the 95% bars. Only limited infiltration of tracer appears to have occurred and was not a general feature. This is due to the void spaces between gravel framework particles already containing high concentrations of matrix, and the first flood wave ($3.2\text{m}^3\text{s}^{-1}$) being of insufficient magnitude to rattle the armour layer to allow tracer to penetrate deeper void spaces. Infiltration was evident on the margins and tail of Riffle A, but was restricted to the surface 0-15cm. Cores A3, A4, A6, A7, A8 and A9 showed evidence of infiltration into the near surface 0-15cm of substrate, although closer visual inspection revealed a dark layer of tracer often only in the surface 5cm of substrate. In this investigation it was not possible to split cores to a vertical resolution finer than 15 cm due to coarse framework clasts straddling the boundary between layers. The presence of tracer was not as evident in the substrate of Riffle B, supporting basket trap and Bartington loop observations, which further suggests this to be a high energy riffle. Cores taken from the head of the Riffle B1, B2 and B3 recorded the highest susceptibility values for the near surface 0-15cm, which is also supported by basket trap data, whereas presence of tracer was marginal in cores B4 and B7 and non-existent in the other cores. This may reflect surface flushing due to higher shear stresses in this area. Tracer material does not appear to have infiltrated the substrate of Riffle C, with the exception of the near-surface 0-15 cm of core C7. Tracer was clearly detected in the surface 0-15cm of substrate of Pool 2, however, presence of tracer was marginal in Pool 3. A further freeze-core survey in March 1997 revealed that magnetic susceptibility had returned to background levels within the substrate matrix, and that no further vertical development had occurred.

7.5 Discussion and conclusions

A combination of basket trapping and magnetic tracing techniques may be used to describe Phase 1 sediment sorting and routing patterns in the Rede riffle-pool and shed light upon the observed low flow sedimentology shown in Chapter Three. The approach used here was to trap fine bedload in basket traps and to measure the movement of a magnetic tracer. It is useful to compare the fine sediment accumulation rates with other published research before concentrating on within-site spatial and temporal patterns.

7.5.1 Accumulation of fines within traps

Table 7.1 documents a selection of field studies which have monitored accumulation rates of fine sediments within traps similar to those used in the present investigation. Most of the studies in this Table were designed to monitor siltation rates in salmonid spawning grounds. The infiltration rates measured for the River Rede are comparable to those measured close to the Rede catchment in the adjacent North Tyne. Accumulation rates tend to be higher than some studies on chalk streams (e.g. Acornley and Sear, 1999; Welton, 1980), and other lowland streams (Thoms, 1987). It should be noted however that a much greater proportion of the fines collected in the traps situated in the lowland streams is derived from suspended sediments rather than bedload (Acornley and Sear, 1999; Thoms, 1987).

7.5.2 Fine bedload routing

Data concerning accumulation rates of fine bedload in basket traps set within the river bed provided information concerning routing of fines through the permanently wetted area of the channel. Strong spatial patterns of accumulation were evident, both down riffle, cross riffle and between riffles and pools. Highest accumulations tended to occur on the traps situated on areas of low form and grain roughness on the riffles, although one pool / glide situated on a straight section of channel registered higher values occasionally. As was shown in Chapter Four, low elevation areas exhibit the highest tractive force during periods of high flow, hence the high accumulation reflects the high rates of delivery to the traps. Grain roughness also appears to influence accumulation rates possibly due to sheltering / hiding effects. This

River	Reference	D ₅₀ (Framework) (mm)	Rate of accumulation Kg m ⁻² day ⁻¹)	Discharge conditions
Rede UK	This study	53	0.0013-1.527	Variable
Wallop Brook, UK	Acornley & Sear (1999)	36.5	0.0428-0.4071	Variable
River Test, UK	Acornley & Sear (1999)	21.6	0.0143-1.0	Variable
River Piddle, UK	Walling and Amos (1994)	22.6	0.0143-0.6429	Variable
North Tyne UK	Sear (1992)	54	0.005-0.086 0.004-0.064 0.013-1.574	Compensation Hydropower Flood
Caspar, Jacoby, & Prairie Creeks, US	Lisle (1989)	21-25	9-133	Flood
Black Brook UK	Thoms (1987)	13	0.614 0.26-2.49	Variable
River Blythe UK	Thoms (1987)	15	0.644 0.312-0.861	Variable
River Tame UK	Thoms (1987)	22	0.399 0.008-0.779	Variable
Turkey Brook UK	Frostick <i>et al.</i> (1984)	27	0.24 4.43	Baseflow Flood
Tadnoll Brook UK	Welton (1980)	22	0.37-0.93 5.00-10.00	Baseflow Flood
Great Eggleshope Beck UK	Carling and McMahon (1987)	20	0.008 0.29-2.5	Baseflow Flood
Harris Creek Canada	Church <i>et al.</i> (1991)	20	0.03 25.9	Baseflow Nival Flood
River Sanno Japan	Ebise <i>et al.</i> (1983)	-	0.401 0.03-1.469	Variable
Thompson River Australia	Davey <i>et al.</i> (1987)	<45	0.056-0.307 0.073-0.506	Upstream dam Downstream dam
Strawberry Creek California	Reiser <i>et al.</i> (1985)	-	1.20 0.876-4.56	Variable
East Creek Alaska	Meehan and Swanson (1977)	-	0.497 0.320-0.670	Variable
Centennial Creek	Slaney <i>et al.</i> (1977)	45	25.0	Flood

Table 7.1 Documented field studies describing accumulation rates of fines in gravel-bed rivers.

information may be of significance to spawning fish such as salmonids, as the location of the redd in relation to surrounding grain and form roughness may have a control upon siltation of the redd.

Cross riffle variation

The cross-riffle variation in accumulation rate is likely to be due to the location of the thalweg, which is strongly influenced by point bar morphology. The cross-riffle difference shown in this study again show some difference to the results of Thoms (1987), who found maximum infiltration to occur in the centre of the channel and almost equal minima on either channel margin. Maximum concentrations tended to be found in the channel centre along the line of the thalweg, supporting the findings of Frostick *et al.* (1984) who found maximum accumulation in high velocity zones. There were substantial differences in the amount of fine bedload which accumulated in the channel margin traps; the right bank sometimes showed greatest accumulations and left bank consistently showed the lowest accumulations.

Downstream variation

A surprising finding was that the lowest rates of accumulation were found at the head of the riffles, and for a gradual increase towards the tail of the riffles, opposite to that found by Thoms (1987). The larger accumulations at the riffle tails may be explained by a combination of factors, such as stage-dependent variation in hydraulics and sediment supply over the riffle. Deposition of fines occurs on the riffle at high stage where traps will begin to fill gravel voids. As the flood recedes, shear stresses on the riffle head are reduced whereas the riffle tail experiences the highest shear stresses allowing any available fines to be winnowed into the tail traps.

Although pool data was limited, the information obtained appeared to suggest that fines avoided settling in pools situated on channel bends (Pools 2 and 4). In contrast Pool 3, which was situated on a straight section of channel recorded greater accumulations in comparison to the adjacent riffles, indicating that fines were routed through this pool.

Fine bedload sorting

Down-riffle size sorting was also different to that of Thoms (1987) who found coarser fines at the head of riffles and finest accumulations at the riffle tail. On the Rede it is the riffle tails that collect the coarsest fine bedload material. The coarser sediments also tended to accumulate along the traps positioned along the channel centre. This may reflect local variations in both magnitude and duration of stream competence which may influence grain size and the quantity of accumulated fines in two ways. Firstly, greater shear stresses at riffle tails and centres may transport coarser grades of sand for longer than other areas of the riffle. Secondly, post depositional modification of infiltrated fines may occur in zones of high shear stress in the form of winnowing-out of silt and fine sand from near-surface interstitial spaces within traps (before sampling). This sorting pattern was also picked up in the fine matrix obtained from freeze-cores (see Figure 3.8, section 3.3.6).

7.5.3 Movement and storage of tracer

The basket trap survey provided information on the principal routing zones. A more detailed account of storage zones however was provided by the results from the tracer survey. Movement of the tracer centroid indicated that sub-2mm material was transported through the Rede riffle-pool sequence at a rate of 0.62 m day^{-1} between 20th April 1996 and 11th March 1997, when taking into consideration calendar time. The virtual rate of travel, which takes into consideration only the period when sub 2mm material was mobile (flows $> 0.35 \text{ m}^3 \text{s}^{-1}$), equated to a velocity of 2.28 m day^{-1} which is faster than 20-30mm gravel in pools, however slower than gravel on riffles (section 6.3.7). From magnetic measurements of surface sediments, infiltrated basket fines and freeze-cores, it is possible to present a morphologically-based summary of fine sediment storage sites (Figure 7.8) based on the percentage of tracer material deposited. The patterns displayed by the magnetic bedload tracer are different to those reported for other channels. Very little or no tracer was deposited in pools, with only a tiny fraction recorded in sub-surface sediments. Instead the greatest concentrations were found along riffle margins (particularly on the margins of the riffle crest), and bar tops where most of the material was located (44%). Winnowing of fines from riffles into pools at flows below the tractive force reversal threshold (Lisle and Hilton, 1992; 1999), does not appear to happen in the Rede channel. Pools do not operate as fine sediment storage zones, instead the morphological high points appear to act as

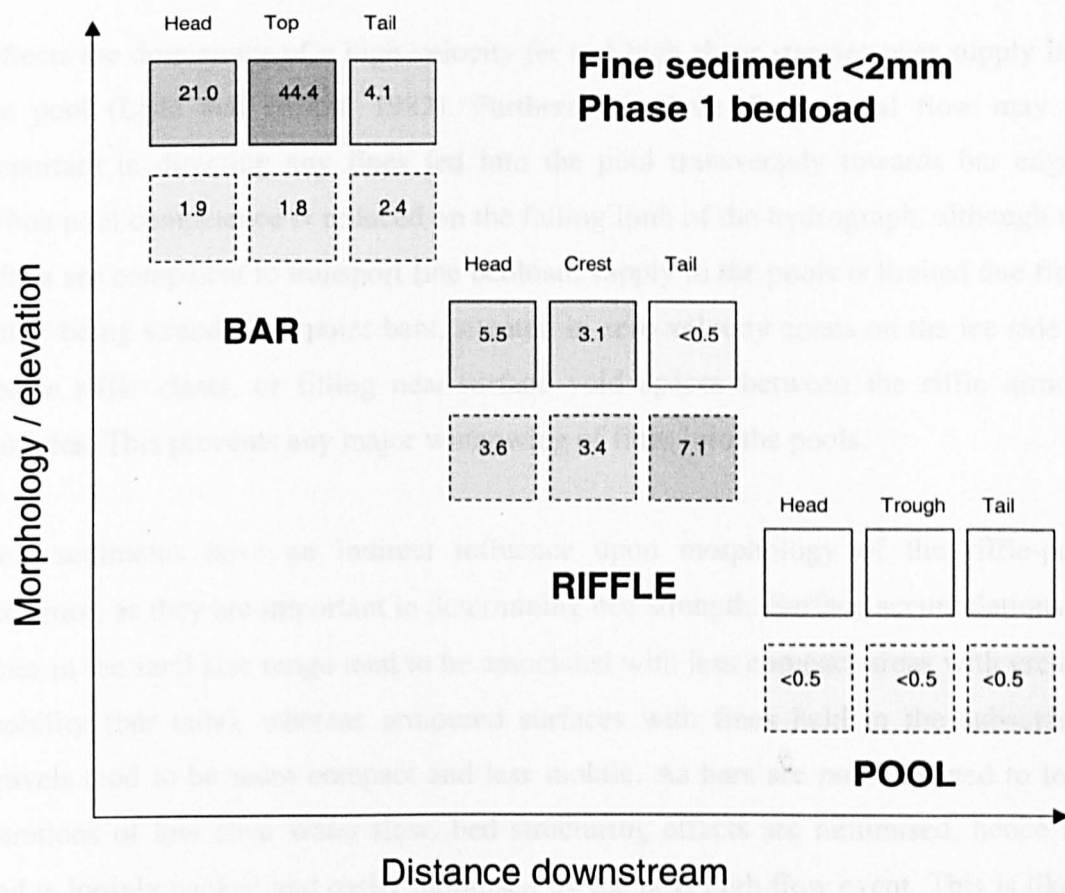


Figure 7.8 A morphologically-based summary of fine bedload storage through the Rede riffle-pool sequence. Units indicate percentage retrieval of tracer material.

stores (e.g. Mosely and Tindale, 1985; Larrouse and Duncan, 1992). Fine sediment transport is analogous to that of gravel with transport from riffle to riffle, rather than pool to pool which has been described for some rivers at high discharge (e.g. Wohl *et al.*, 1993; Clifford, 1993). Limited ingress of fine material into the subsurface void spaces suggests that the subsurface gravel and matrix which fills the voids remains stable. Sediment transport, in the range of flows studied in this investigation appears to be limited to movement of bedload over a stable bed.

Deposition reflects the spatial pattern of high flow competence, with the lowest shear stress areas (bars) collecting the greatest amounts of material. Notably, bar tops collect the most fines, and riffle heads collect the greatest concentrations in the permanently submerged part of the channel. Pools remain clean of fines which

reflects the dominance of a high velocity jet and high shear stresses over supply into the pool (Lisle and Hilton, 1982). Furthermore, three dimensional flow may be important in directing any fines fed into the pool transversely towards bar edges. When pool competence is reduced on the falling limb of the hydrograph, although the riffles are competent to transport fine bedload, supply to the pools is limited due fines either being stranded on point bars, situated in zero velocity zones on the lee side of coarse riffle clasts, or filling near-surface void spaces between the riffle armour particles. This prevents any major winnowing of fines into the pools.

Fine sediments have an indirect influence upon morphology of the riffle-pool sequence, as they are important in determining bed strength. Surface accumulations of fines in the sand size range tend to be associated with less compact areas with greater mobility (bar tails), whereas armoured surfaces with fines held in the subsurface gravels tend to be more compact and less mobile. As bars are not subjected to long durations of low clear water flow, bed structuring effects are minimised, hence the bed is loosely packed and easily mobilised by the next high flow event. This is likely to promote quasi-equilibrium in the riffle-pool sequence as it would prevent the bar elevation from increasing, which would otherwise have to be compensated for via a morphological response elsewhere in the system. Low surface accumulations and greatest ingress of fines occurs at the riffle tails, which reflects greater hydraulic energy in this zone, particularly during lower flows. This is likely to promote armouring and increase bed strength in this area, thus promoting riffle tail stability, preventing headward scour. Greater surface accumulations at the riffle head, are likely to be a temporary phenomenon, flushed rapidly by the next high flow event. Infiltration appears limited, hence bed structural effects are likely to be negligible.

7.5.4 Fine sediment storage in gravel interstices

Less storage of fine bedload in interstitial void spaces of channel bed occurred than had been expected at the outset of the study. Limiting factors controlling infiltration include (i) the existing vertical sediment structure; the size, shape and arrangement of coarse framework particles which influence the size and shape of void spaces (Meehan and Swanston, 1977; Frostick, *et al.*, 1984), (ii) size of the infiltrating fines in relation to the void size (Einstein, 1968, Beschta and Jackson, 1979, Carling,

1984), (iii) hydraulic jiggling of framework clasts (Schälchli, 1995), and (iv) near-bed hydraulics (Beschta and Jackson, 1979).

In light of the data obtained from the River Rede, it is thought that the controlling factor involved lack of void spaces and limited disruption of the armour layer and subsurface. As was shown in Section 3.3.5., the matrix concentration in near surface voids is consistently lower than that found beyond 15cm depth, with a mean of 12%. The sediment found between 30 and 45cm depth tends to have the greatest concentrations of matrix material with between 15 and 19% by weight. A reduction in the concentration of fines was again evident at the base of the freeze-cores. Visual inspection of freeze-cores also demonstrated that void spaces between gravel framework deeper than 15 cm depth, were full of matrix material (Plate 3.2 and 3.3). This vertical sediment structure suggests little bed disturbance over the study riffles during floods, a suggestion which was also corroborated with morphometric re-survey information over a 3 year period (Appendix 2.1).

7.6 Summary

- 1) Traps located in zones of low relative form roughness such as the riffle centre and tail appeared to act as preferential sediment routing zones and also tended to collect coarser material in comparison to traps located on higher elevation areas. Zones of low relative form roughness are (i) competent to transport fines for longer periods (greater time for flushing out of silt and fine sand), and (ii) zones of greater shear stress which are capable of mobilising coarser grades of sand,
- 2) The limited data obtained from pools situated on channel bends suggested lower rates of accumulation in comparison to riffles. However a pool / glide situated on a straight section occasionally tended to accumulate more fines than the riffles,
- 3) Areas of low relative grain (armour) roughness appeared to improve the delivery of fine bedload, resulting in greater accumulations in traps,
- 4) Tracer data indicate morphological high points; bars and riffle margins to act as fine sediment stores. Pools do not store fines. This is related mainly to sediment supply and the hydraulic character of the pool-riffle sequence,

- 5) Tracer data suggest that fine bedload moved through the riffle-pool sequence at a rate of 0.62 m day^{-1} over the study period. The virtual velocity of tracer, using mobilisation time only, equated to 2.28 m day^{-1} . Downstream movement is hindered by burial of material and subsequent re-exposure after disruption of the surface armour,
- 6) Fine bedload tends to be stored on dry bar surfaces rather than in the subsurface sediments. Infiltration was limited due to the lack of void space available beyond 5cm and by the stability of the armour layer. Some limited infiltration was found in Riffle A, close to the seeded zone in freeze-cores, supporting the possibility of burial / infiltration and subsequent re-exposure.

The next Chapter considers the routing and sorting of gravel (Phase 2 bedload) through the Rede riffle-pool sequence.

Chapter Eight

Phase 2 sediment sorting and routing through a riffle-pool sequence

8.1 Introduction

The existence of coarser pool sediments in comparison to the riffles on the Rede, demonstrated in Chapter Three, is contrary to the majority of published studies (Leopold *et al.*, 1964, Keller, 1971, Yang, 1971, Cherkauer, 1973, Bhowmik and Demissie, 1982, Teisseyre, 1984, Sear, 1996). The pattern of surface sediment grain size has been linked to the mechanism by which riffle-pool morphology is maintained; the reversal hypothesis (Keller, 1971); this however, has usually been used to explain why pools become finer than riffles, not coarser. However, some contend that pools should be coarser than the riffles if they represent zones of maximum tractive force (Gilbert, 1914; Bhowmik and Demissie, 1982, Thompson *et al.*, 1999). This view is supported by those studies which report coarser sediments in pools (Table 1.1). In situations where coarse pools exist it has often been unclear whether the coarse clasts have been supplied from upstream (Gilbert, 1914), or result from local bank erosion. The later would produce a less active/inactive lag deposit, which was suggested by Leopold *et al.* (1964) to explain some of Hack's (1957) data. The existence of coarse lag material complicates the issue as most models of riffle-pool sorting only account for inputs and outputs of material derived from the bed of morphological units.

Information on gravel routing through the Rede riffle-pool sequence would clarify the sorting mechanisms in operation and provide further information concerning morphological maintenance. Lisle (1979) and Jackson and Beschta (1982) suggest that Phase 2 (gravel) transport is initiated on riffles when the tractive force of the pools exceeds that of the adjacent riffles. Riffle sediments are routed into the pool downstream, where they are transferred to the next riffle downstream and deposited if competence is low. Thus the morphological highs and lows are maintained. Phase 2 bedload transport may be conceptualised as 'leap frogging' of bed material from riffle to riffle (Jackson and Beschta, 1982).

As equalisation and marginal reversal of tractive force is evident on the Rede riffle-pool sequence, it may be hypothesised that Jackson and Beschta's (1979) two-phase model of sediment sorting should apply. This chapter aims to investigate the sediment sorting mechanisms operating on the Rede by describing a series of sediment routing experiments using pebble tracers.

8.2 Approach

Field analysis

To provide information on Phase 2 sorting processes a coarse clast tracer survey was conducted, as described in Chapter Two (Section 2.4.2) and Chapter Six (section 6.2), whereby transport paths of individual clasts of coarse-grained material were measured directly by tracking 288 measured and weighed painted clasts, placed throughout the study reach. It should be noted that the coarse tracer study was conducted after the fine sediment work (Chapters Five and Seven) between 21 January 98 to 28 February 1999 inclusive, hence sequence and character of flow events are different. The hydrographs for each event were plotted in Figure 6.1.

Statistical analysis

A multiple comparisons Analysis of Variance was conducted to see if there were any significant differences in the size of tracer clasts depositing on different morphological sub-units. Clasts depositing on riffles should be coarser than those depositing in pools (based upon Keller's 1971 reversal hypothesis). The size distribution of tracer particles deposited on each morphological unit was also compared to the size of the surface material in each depositional morphological sub-unit, the details of which were presented in Figure 2.6. Unfortunately, bed size data was not available for bar edges or pool heads. Therefore, tracers deposited on pool heads were compared against size data obtained for the whole pool. Tracers deposited on bar apices were compared against size data for the middle of the bar. The rationale behind this test is that the size of the tracer clasts depositing in each morphological sub-unit should mirror the size of the bed material if these sediments are derived from contemporary fluvial deposition.

8.3 Results

8.3.1 Tracer paths and morphology

Tracer paths after five different events for riffles and pools draped over a channel morphology DEM are presented in Figure 8.1 – 8.5. From these data a morphologically based summary of Phase 2 sediment sorting has been produced in the form of a sequence of matrices (Appendices 8.1 – 8.5). Three sediment size classes; 20-40mm, 40-70mm and >70mm, were used to separate any size-specific sorting which may be in operation in the gravel range. In the matrices the open circles indicate minor re-distribution of tracer clasts (<5m) within the same morphological sub-unit e.g. staying within the riffle head. Half circles show movements <10m between units, whereas solid circles indicate larger movements >10m movement from one unit to another and those which straddle morphological units. The following section describes tracer movement over the sequence of five hydrographs described in Figure 6.1.

Overview

Movement at flows up to $2.71\text{m}^3\text{s}^{-1}$ was minor and restricted to a rattling of tracer grains and small movements within sub-units into more structurally stable positions. Flows close to 60% bankfull ($5.95\text{m}^3\text{s}^{-1}$), appear capable of transferring clasts between units with transfer from pool troughs to riffle heads and from riffle crests and tails to bar edges. Path lengths are in the order of 5-15m. After a further flood of $7.44\text{m}^3\text{s}^{-1}$ less activity is evident, possibly reflecting increased bed structuring or shorter mobilisation time related to the character of the preceding hydrograph(s). After this flow it appeared that the riffles had been more active in comparison to the pools, with some deposition on bar edges but relatively little movement from pools to riffles. As may be expected the largest flow ($9.92\text{m}^3\text{s}^{-1}$) appeared to be responsible for moving tracer clasts the greatest distance. Clasts located in Pool 2 appeared to be transported the furthest overall indicating this area to be the zone of greatest competence in the Rede riffle-pool sequence, a factor that was also substantiated by hydraulic data (see Chapter Four). It appears that clasts may skip over intervening riffle-pool units at these higher discharges instead of being transported from unit to unit, e.g. two medium sized clasts located around Pool 2 passed over three riffles and two pools, finally coming to rest on point Bar 3 (Figure 8.5b). It appears that, at flows

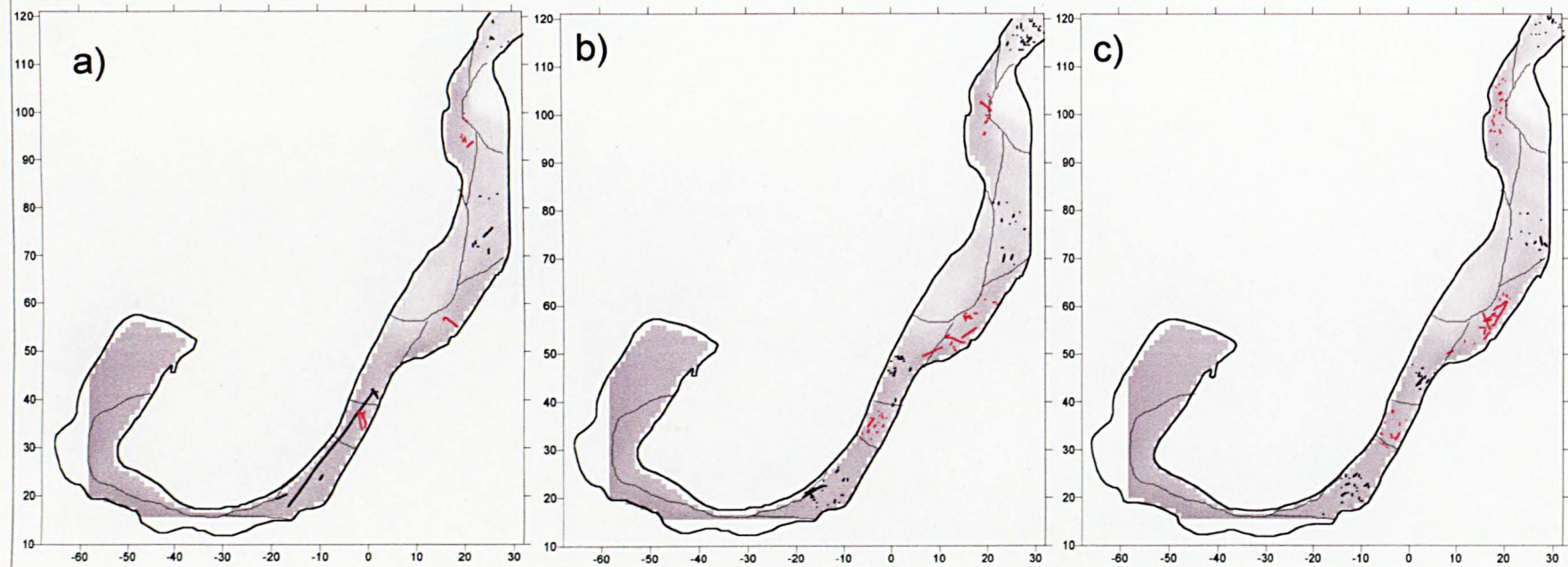


Figure 8.1 Tracer paths after a peak flow of $2.71 \text{ m}^3 \text{s}^{-1}$, a) 20-40mm, b) 40-70-mm, c) >70mm.

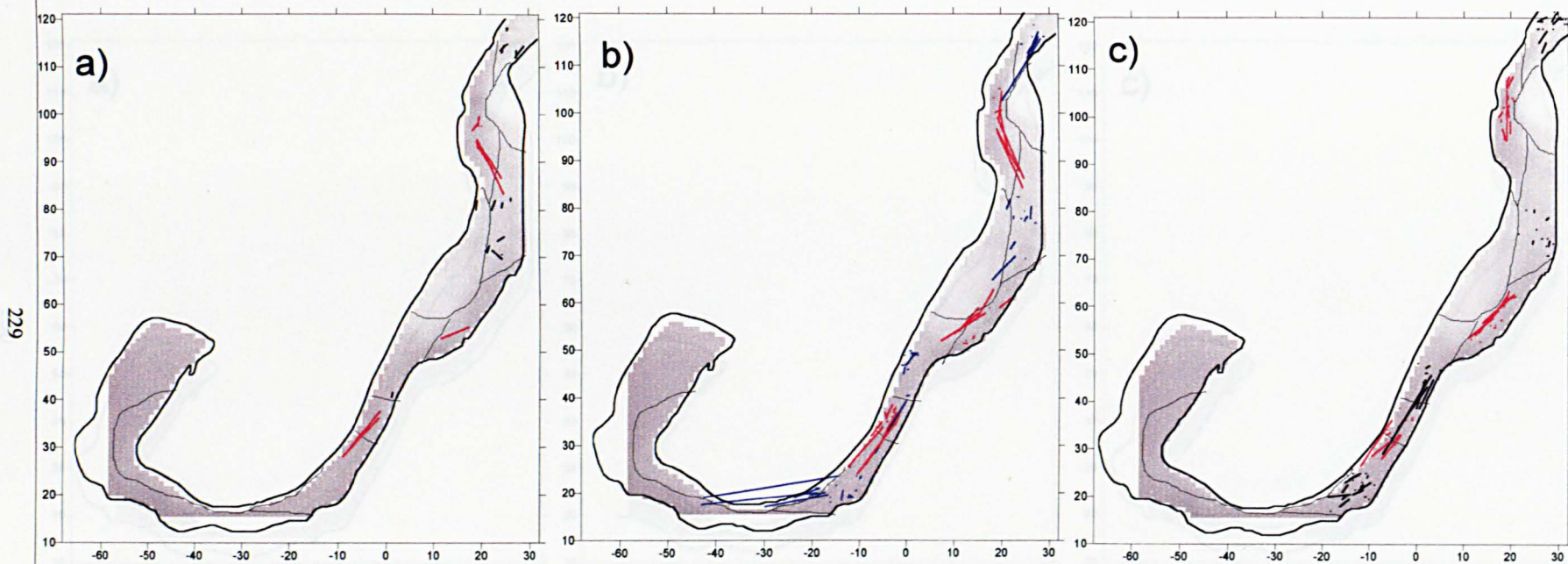


Figure 8.2 Tracer paths after a peak flow of $5.95\text{m}^3\text{s}^{-1}$, a) 20-40mm, b) 40-70-mm, c) >70mm.

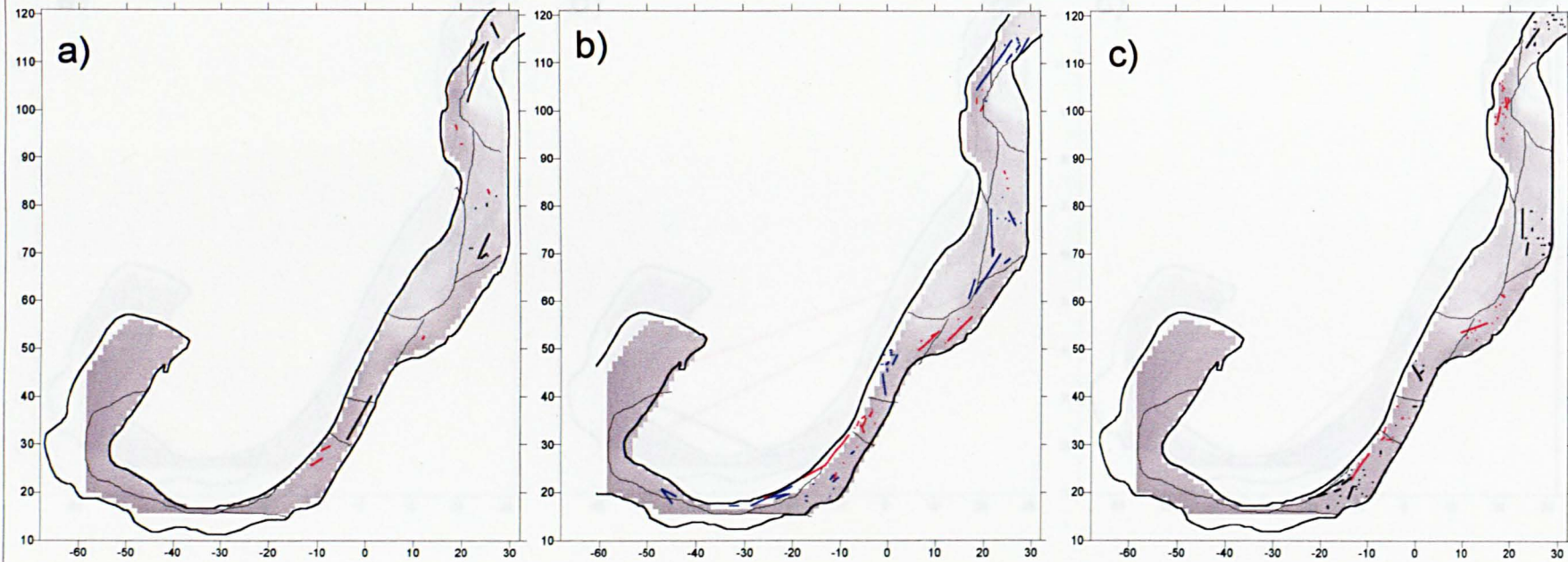


Figure 8.3 Tracer paths after a peak flow of $7.44\text{m}^3\text{s}^{-1}$, a) 20-40mm, b) 40-70-mm, c) >70mm.

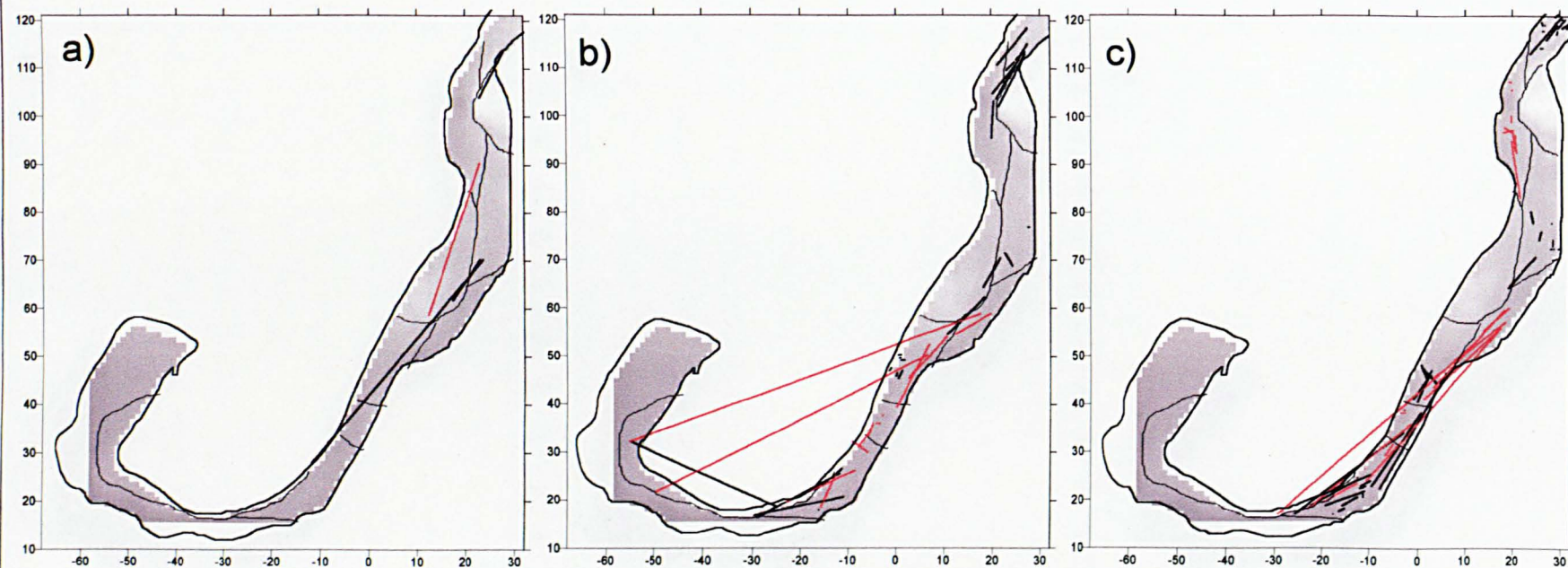


Figure 8.4 Tracer paths after a peak flow of $9.92\text{m}^3\text{s}^{-1}$, a) 20-40mm, b) 40-70-mm, c) >70mm.

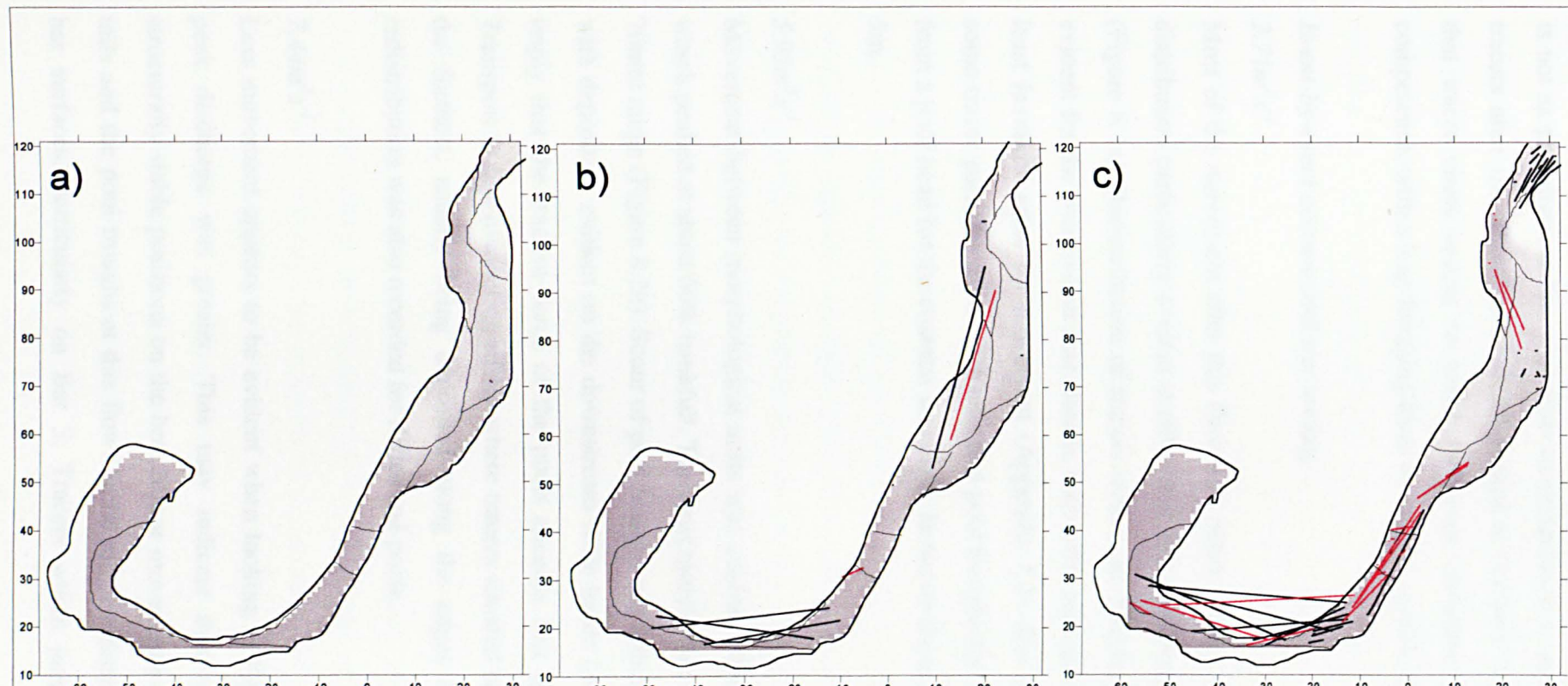


Figure 8.5 Tracer paths after a peak flow of $6.94 \text{ m}^3 \text{s}^{-1}$, a) 20-40mm, b) 40-70-mm, c) >70mm.

of bankfull and over, bars are the favoured zone of deposition for clasts originating from both riffles and pools. Deposition of sediments on riffles, originating from pools is not as prominent at this high flow in comparison to smaller floods. Movement of tracers after the final flood (which peaked at $6.94m^3s^{-1}$) quite clearly demonstrates that tracer clasts appear to avoid the lower elevation, deeper zones of greatest competence, with a leap-frogging from bar to bar, or riffle head to bar.

Event-by-event account and size sorting

$2.71m^3s^{-1}$

Most of the movement after this flow was minor (<5m) with a small amount of redistribution particularly evident at riffle tails and pool troughs for the 20-40mm class (Figure 8.1a). Redistribution of tracers within the morphological sub-units was also evident for the two coarser size classes, with riffle tails and crests appearing to be the least favoured areas for movement (Appendix 8.1). Bar edges appeared to receive some tracer particles from riffle tails and pool troughs for the medium size class and from a pool head for the coarsest size class. However these movements were less than 5m.

$5.95m^3s^{-1}$

Movement between morphological units was evident after this second higher flow, which peaked at about 60% bankfull. The most mobile size class appears to be the 40-70mm range (Figure 8.2b). Scour of pool troughs and tails is shown for all grain sizes with deposition evident on the downstream riffle heads (Appendix 8.2). This would imply that the tractive force of the pools exceeds that of the riffles at this flow. Transport is also evident on riffles where tracers situated on the crest and tail moved the furthest, usually being deposited along the edges of the bar heads. Minor redistribution was also recorded for riffles and pools.

$7.44m^3s^{-1}$

Less movement appears to be evident when looking at Figure 8.3, even though the peak discharge was greater. This may indicate that tracers have found more structurally stable positions on the bed. Minor movements are found for riffle crests, tails and the pool troughs at this flow. Some minor redistribution is also evident on bar surfaces, particularly on Bar 3. Tracers which jumped morphological units

followed a similar pattern as those shown after the previous flow, with clasts scoured from riffles being deposited on bar edges or apices, and pool tracers deposited on riffle heads. There were exceptions however; a medium sized clast scoured from the tail of Riffle 0 appears to have been deposited in the trough of Pool 1, contrary to the trend. It is possible that this clast may have been deposited on the bar apex on a steep shelf that slopes into the pool, and subsequently fallen into the pool. The sediments in this zone were very soft, and some material was observed falling down the steep slope at low flow.

$9.92m^3s^{-1}$

The largest recorded flood demonstrated the longest path lengths for tracer clasts. Path lengths in excess of 30m are shown in Appendix 8.4 as solid circles. Unfortunately by this stage, most of the finer tracers (<40mm) had been lost, probably due to burial. For all size classes it again appears that the favoured areas for deposition are bar edges, heads and apices. The source of clasts deposited on bar surfaces does not appear to be restricted to the riffles; pools also appear to be an important source, particularly of medium size sediments (40-70 mm). These would normally be deposited on riffle heads after smaller flood peaks (Figure 8.4). The coarsest size class in the pools appears to show some deposition on riffle crests and tails, behaving in a similar way to the medium size class after a smaller flood. There is also substantial redistribution on bar surfaces after this flow. Some pool tracers were found to skip units, particularly those which were seeded in Pool 2, which was demonstrated in Chapter Four as exhibiting the highest shear stresses throughout the reach.

$6.94m^3s^{-1}$

The final tracer survey did not record any of the finest size class. The pattern for the medium size class is for substantial movement (>30m) from riffle crests and tails to bar surfaces, and for pool sediment to be scoured from the trough and tail and deposited on bar surfaces (Figure 8.5). There is also some evidence of tracer movement from pool tails to riffle heads. For the coarsest size fraction there is some evidence of clasts being transported from riffle crest to crest. However, the dominant feature once more is for tracers scoured from riffles to be deposited on bar edges, and

for the tracers scoured from pool troughs and tails to be deposited on riffle heads and crests.

In summary there appear to be four types of tracer movement which are linked to flow magnitude;

- 1) intra sub-unit movement which occurs at flows below 30% bankfull,
- 2) secondly there is inter-unit movement which appears to occur at flows of around 70% bankfull, which is dominated by pool scour and exit slope deposition,
- 3) Transfer of gravel from riffle to riffle, with routing around bar edges occurs at 70-90% bankfull,
- 4) Bar to bar transport of gravel and sand, and inter-unit skipping occurs at flows close to bankfull and over.

Tracers show a strong tendency to be transported from morphological high point to high point i.e. riffles to bars, bar edges to bar tops at high flows and for pool tracers to be spat out onto riffle heads and crests at medium flows. There was very little evidence to suggest that clasts were deposited or fed into pools situated on the outside of bends. In fact the data strongly suggests that material is transported around the edges of point bars and over the tops of point bars on meander bends, rather than being fed through the pool centre, contrary to Jackson and Beschta's (1982) model. Even for pools located on straight sections (Pool 3), tracers appeared to follow the line of shallowest flow rather than the thalweg.

8.3.2 Grain size attributes of depositing tracers

To provide more detail on sediment sorting processes it is necessary to consider grain size in more detail in relation to depositional zones. The grain-size distribution and D_{50} values for the final recorded positions of tracers on each morphological sub unit are presented in Figure 8.6 alongside the grain size distribution of the surrounding surface layer. It is clear that the tracers located in the pools are the coarsest with D_{50} 's ranging from 60-73mm in comparison to 55-64 mm for riffles and 34-50 mm for bars. However as very few clasts were transported into pools (see section 8.3.1), it is likely that the coarseness is due to retention of coarse tracer particles within the seeded pool locations, and preferential export of finer tracer clasts.

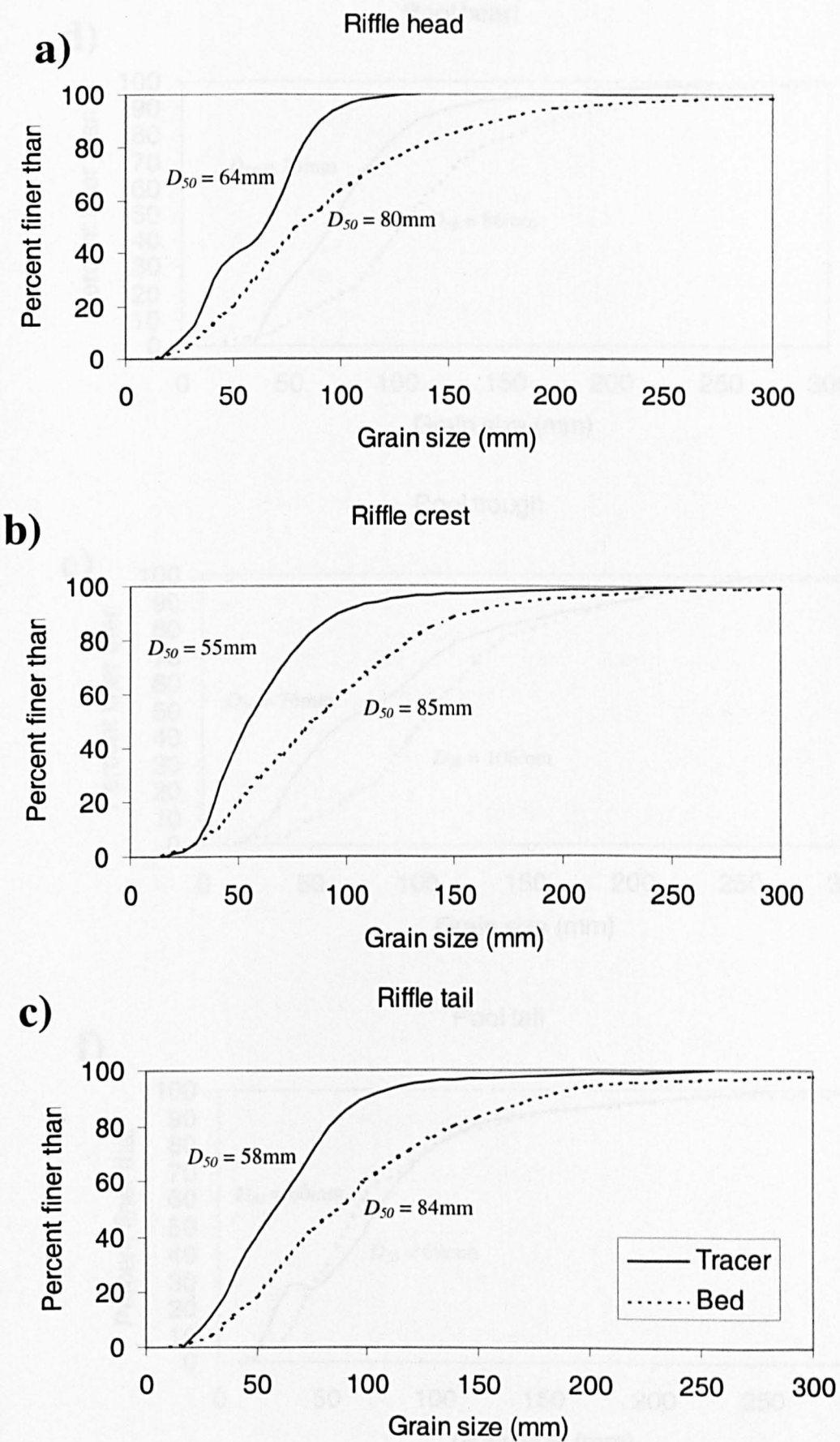


Figure 8.6 Comparison of grain size of deposited tracer clasts with surrounding morphological sub-unit, a) Riffle head, b) riffle crest, c) riffle tail. Tracer data is indicated by a solid line, whereas bed size data is indicated by a hatched line.

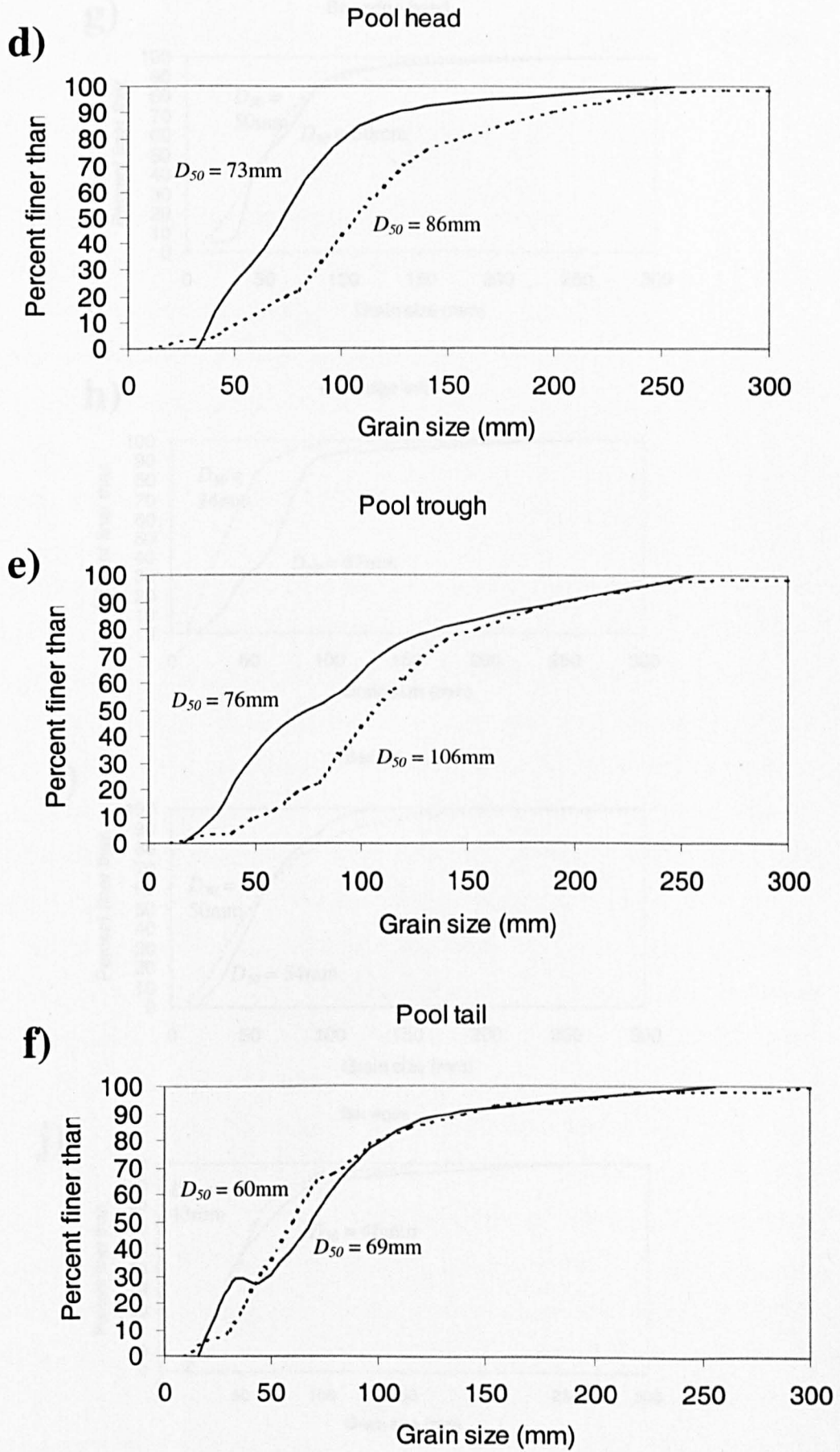


Figure 8.6 Comparison of grain size of deposited tracer clasts with surrounding morphological sub-unit, d) Pool head, e) Pool trough, f) pool tail. Tracer data is indicated by a solid line, whereas bed size data is indicated by a hatched line.

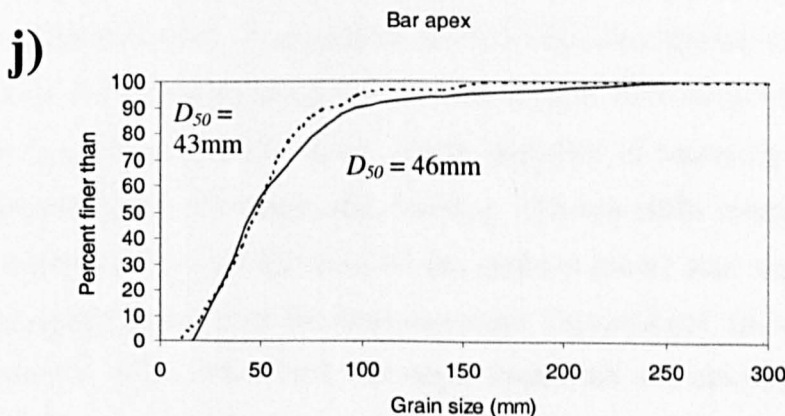
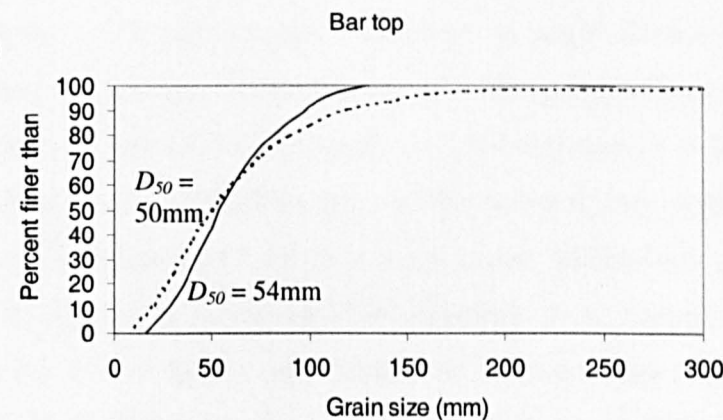
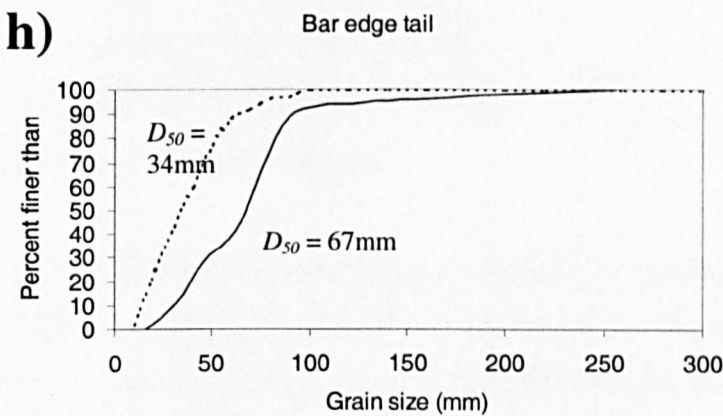
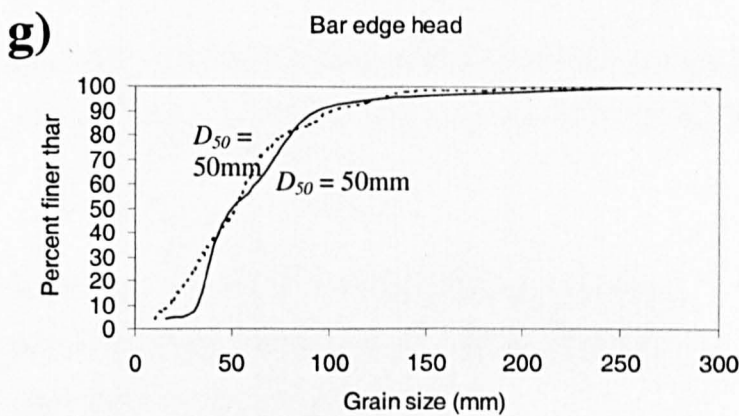


Figure 8.6 Comparison of grain size of deposited tracer clasts with surrounding morphological sub-unit, g) Bar head edge, h) Bar edge tail, i) Bar top, j) Bar apex. Tracer data is indicated by a solid line, whereas bed size data is indicated by a hatched line.

The multiple comparisons analysis of variance indicated highly significant ($p<0.0001$) overall differences in the sizes of tracers depositing on different morphological sub-units;

- riffle heads and crests were significantly finer than pool troughs,
- riffle tails significantly finer than pool heads, troughs and tails,
- riffle tails significantly coarser than bar tails,
- pool heads significantly coarser than bar heads,
- pool troughs significantly coarser than bar heads,
- pool tails significantly coarser than bar heads, and
- bar heads significantly finer than bar tops.

This suggests a strong size-based morphological selection. A summary of the sizes depositing in different morphological units is presented in Figure 8.7a which generally supports the findings of Section 8.3.1. Particles between 16 and 90mm are preferentially deposited on riffles, and to a lesser extent bars, and particles between 90 and 256mm appear to be preferentially deposited in pools. However, as stated in 8.2.1, it is unlikely that coarse material is actually fed into pools, as tracer evidence suggests that clasts are preferentially routed over bar surfaces. It is more likely that scour of finer tracers leaves behind the less mobile coarse tracers in the pool (as a lag deposit). At the morphological sub-unit scale some differences in depositional patterns may be identified which are not observed at a coarser morphological resolution (Figure 8.7b). Riffle tails appear to be important depositional sites, particularly for the 16-32mm fraction, which may reflect winnowing of fine gravel from riffle heads and crests. Pool tails act as secondary depositional sites for this fine gravel fraction, reflecting deposition of material scoured from the pool in this zone of reduced flow competence. Riffle heads appear important in capturing medium-coarse gravel, particularly the 64-90mm size fraction, whereas riffle crests and bar edge heads are important depositional sites for the medium gravel size range (32-64mm). Pool troughs again appear to be the most important 'depositional' site for 128-256mm material. Overall, riffle crests, tails, bar edges (head, tail and apices) all collected a disproportionately large number of tracers. Riffle heads and pools (Head, trough and tails), however, all collected a disproportionately small number of tracers relative

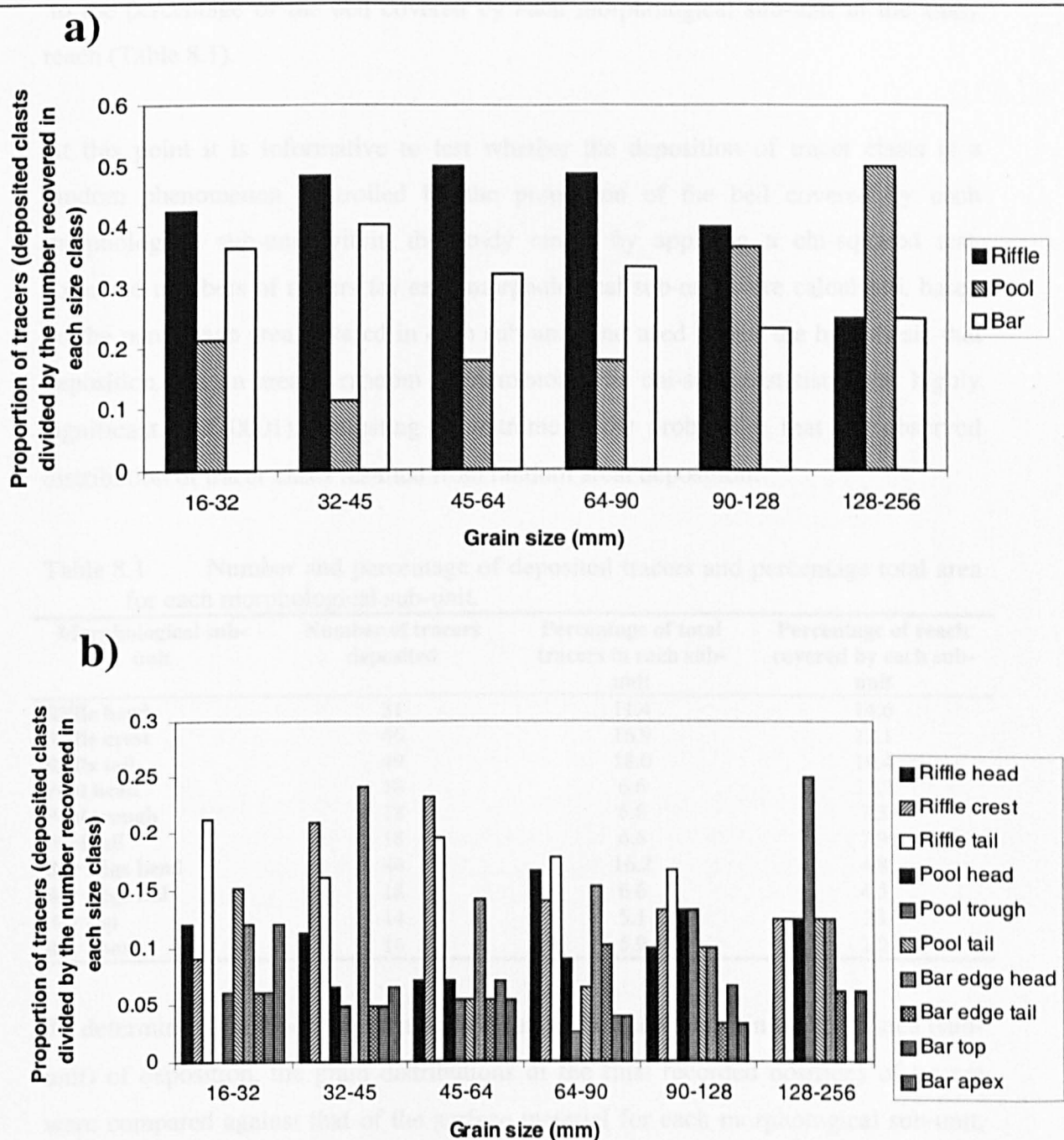


Figure 8.7 Summary of tracer grain-sizes deposited on different morphological a) units, b) sub-units.

to the percentage of the bed covered by each morphological sub-unit in the study reach (Table 8.1).

At this point it is informative to test whether the deposition of tracer clasts is a random phenomenon controlled by the proportion of the bed covered by each morphological sub-unit within the study reach, by applying a chi-squared test. Expected numbers of tracers for each morphological sub-unit were calculated, based on the percentage area covered in each sub-unit, and used to test the hypothesis that deposition was an areally random phenomenon. The chi-square statistic was highly significant ($p<0.0001$), indicating an extremely low probability that the observed distribution of tracer clasts resulted from random areal deposition.

Table 8.1 Number and percentage of deposited tracers and percentage total area for each morphological sub-unit.

Morphological sub-unit	Number of tracers deposited	Percentage of total tracers in each sub-unit	Percentage of reach covered by each sub-unit
Riffle head	31	11.4	14.6
Riffle crest	46	16.9	12.1
Riffle tail	49	18.0	10.4
Pool head	18	6.6	13.2
Pool trough	18	6.6	7.3
Pool tail	18	6.6	7.9
Bar edge head	44	16.2	4.8
Bar edge tail	18	6.6	4.5
Bar top	14	5.1	23
Bar apex	16	5.9	2.2

To determine if the tracer clasts mirrored natural bed sediments in the local area (sub-unit) of deposition, the grain distributions of the final recorded positions of tracers were compared against that of the surface material for each morphological sub-unit. Before discussing these differences, it is important to highlight initial differences which were evident between the size of the introduced tracers and the Rede bed surface sediments (Figure 8.8). It is clear that the introduced tracers were substantially finer ($D_{50}=60\text{mm}$) than the naturally occurring riffle and pool sediments with D_{50} 's of 85 and 110mm respectively, and slightly coarser than the naturally occurring bar sediments ($D_{50}=50\text{mm}$). The coarse nature of the Rede size distributions is partly a reflection of some very coarse immobile boulders ($D_{max}=700\text{mm}$) found in the bed, compared to a tracer D_{max} of 240mm. After re-distribution of tracer clasts these initial differences are still apparent (Figure 8.6a-j), with the tracers deposited on riffles, pool

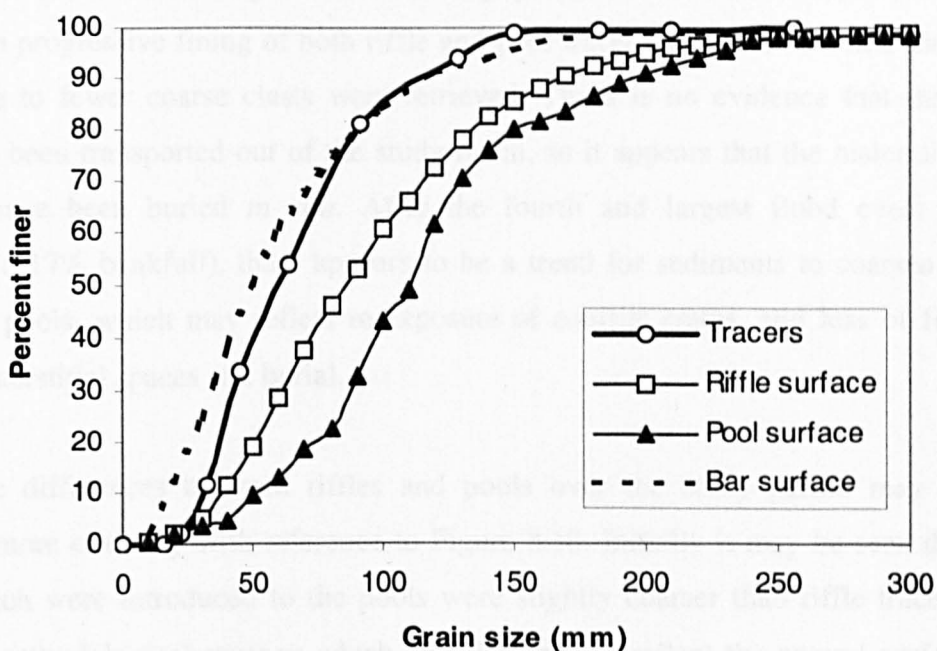


Figure 8.8 Comparison of cumulative grain size distributions for tracer clasts (all 288 grains) against riffle, pool and bar surface sediments sampled using a Wolman grid technique (see chapter 3 for further details).

heads and troughs being finer than the naturally occurring material, and tracers deposited on bar edge tails being coarser than the naturally occurring bed material. Tracers deposited on pool tails and bars (head edges, tops and apices) however reflected the natural size distribution much more closely, suggesting that the sorting patterns displayed by tracers deposited in these zones explain the naturally occurring sorting processes in the Rede channel. The data for riffles, pool heads and troughs does not reflect natural sorting patterns closely. This is probably due to the limited tracer size range used in the study; some coarser tracer clasts up to the Reach D_{max} should have been employed in the Rede channel.

Tracer size changes and sorting

Information concerning the grain size change of the retrieved tracers can give a further insight into sorting processes through riffles and pools. Figure 8.9 demonstrates grain size changes over the study period for both riffles and pools, indicating a progressive fining of both riffle and pool tracer clasts over the first three events, due to fewer coarse clasts were retrieved. There is no evidence that these clasts have been transported out of the study reach, so it appears that the material is likely to have been buried *in situ*. After the fourth and largest flood event of $9.92 \text{ m}^3 \text{s}^{-1}$ (117% bankfull), there appears to be a trend for sediments to coarsen in riffles and pools, which may reflect re-exposure of coarser grains, and loss of fine gravel to interstitial spaces and burial.

Tracer size differences between riffles and pools over the study period may be compared more critically with reference to Figure 8.10. Initially it may be seen that tracers which were introduced to the pools were slightly coarser than riffle tracers, reflecting methodological strategy which was designed to reflect the natural surface sedimentology (see Chapter Three). Over the first three floods it appears that grain size differences between riffles and pools are reduced gradually. After the largest flood ($9.2 \text{ m}^3 \text{s}^{-1}$), the pool tracers that were retrieved were finer, possibly reflecting the burial of coarse clasts with locally derived bank and bed material. After the final flood, there was little difference between the D_{50} of riffle and pool tracers, although pools contained slightly more 100-140mm clasts and fewer 60-mm clasts in comparison to the riffle tracers.

8.4 Discussion and conclusions

8.4.1 Sorting patterns

The tracer results help to explain the sediment sorting patterns in the Rede riffle-pool sequence described in Chapter Three. A similar budgeting procedure to that conducted for Phase 1 bedload (Chapter Seven) was conducted for the gravel tracing experiment, whereby the total percentage of clasts deposited in each morphological sub-unit, was calculated (Figure 8.11). The numbers in brackets indicate the percentage of clasts deposited on each morphological sub-unit, taking into consideration clasts which were not transported out of the unit where they were

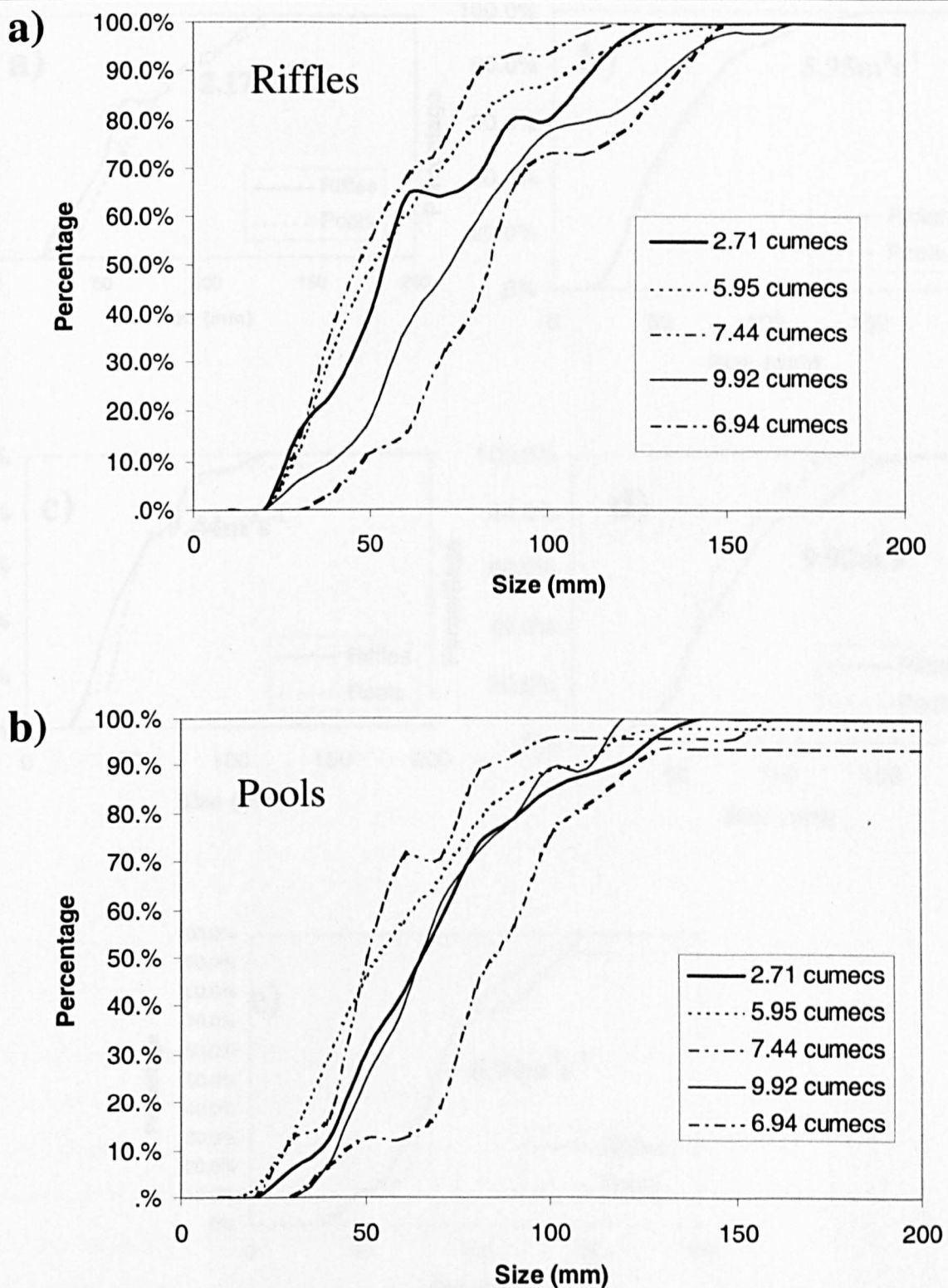


Figure 8.9 Change in the grain size distribution of tracer clasts located in a) riffles and b) pools. The size distribution appears to get finer after the first two flood events up to around 80% bankfull for both riffles and pools. In contrast the grain size distribution shows a distinct coarsening after the final two events, one of which was 117% bankfull.

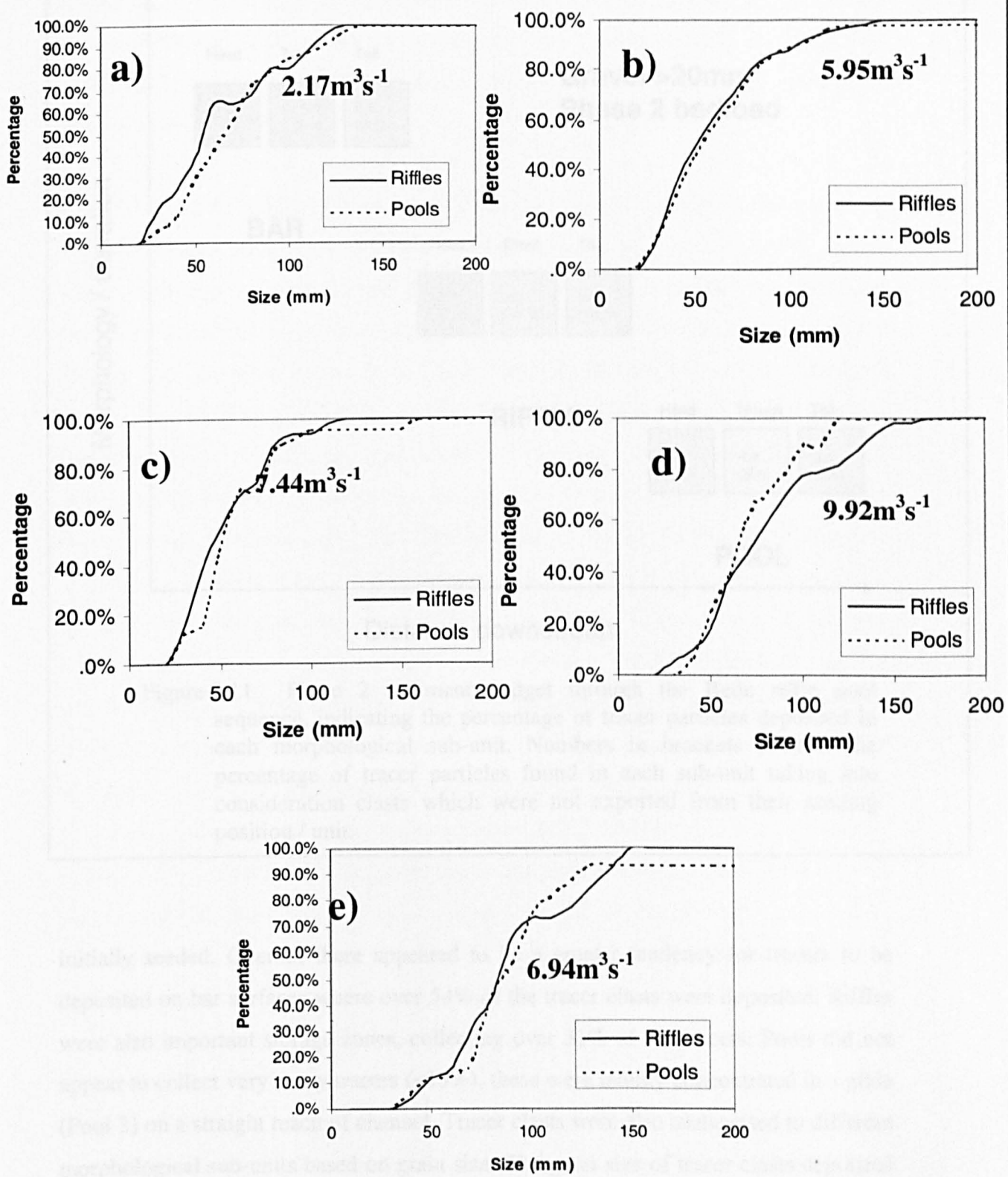


Figure 8.10 Grain size differences between riffles and pools after each recorded flood. Initially pool tracers are slightly coarser than riffle material, reflecting the natural grain size differences (see chapter 3). By the third flood, the grain size distributions of tracers from riffles and pools are very similar. After the final two flows, the riffles appear to have more coarse grains in the distribution, reflected in differences in the coarse tail.

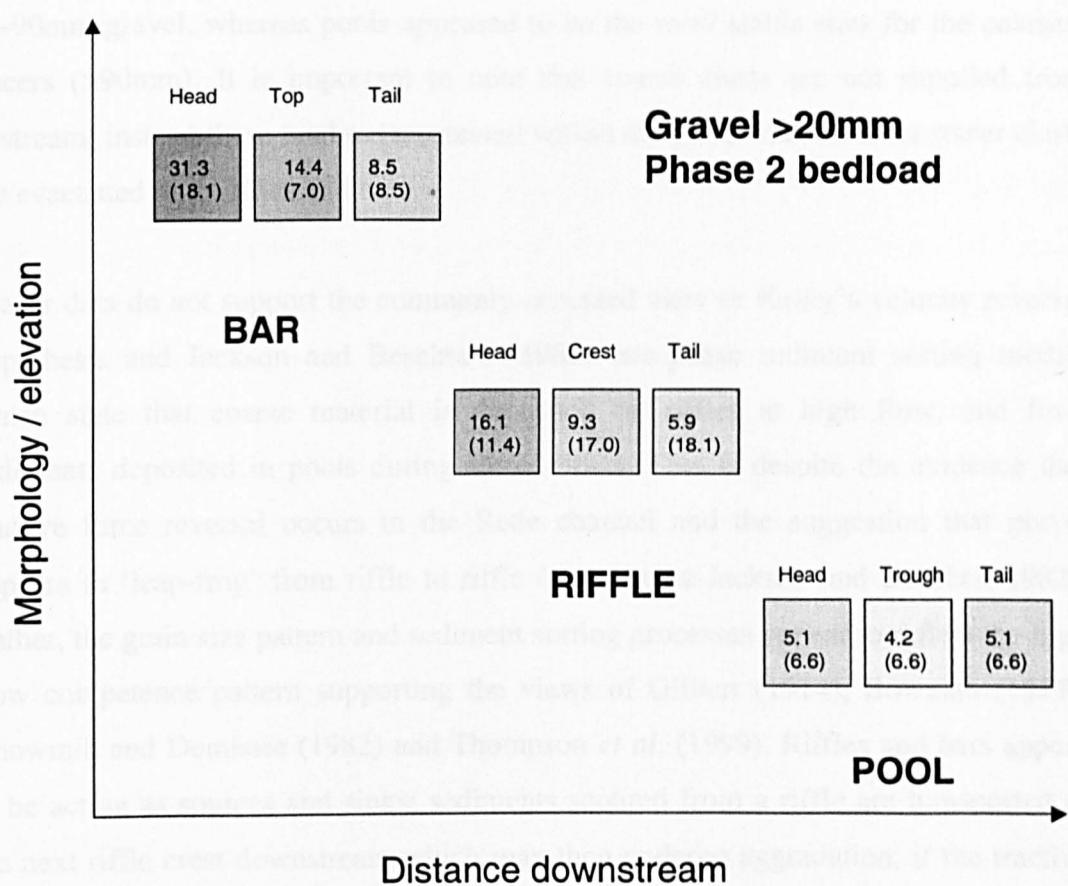


Figure 8.11 Phase 2 sediment budget through the Rede riffle pool sequence, indicating the percentage of tracer particles deposited in each morphological sub-unit. Numbers in brackets indicate the percentage of tracer particles found in each sub-unit taking into consideration clasts which were not exported from their seeding position / unit.

initially seeded. Overall, there appeared to be a greater tendency for tracers to be deposited on bar surfaces where over 54% of the tracer clasts were deposited. Riffles were also important storage zones, collecting over 31% of the tracers. Pools did not appear to collect very many tracers (<15%), these were mainly concentrated in a glide (Pool 3) on a straight reach of channel. Tracer clasts were also transported to different morphological sub-units based on grain size. The grain size of tracer clasts deposited on riffle heads and crests tended to be significantly finer than those left in pool troughs, and riffle tails were significantly finer than pool heads, troughs, and tails. Furthermore, riffle tails were found to be significantly coarser than bar tails, whilst pool heads, troughs and tails were significantly coarser than bar heads and tops. Data suggested that riffles and bars provide the most stable high-flow depositional sites for

16-90mm gravel, whereas pools appeared to be the most stable sites for the coarsest tracers (>90mm). It is important to note that coarse clasts are not supplied from upstream; instead these tend to be retained within the pool, whereas finer tracer clasts are evacuated onto riffles and bars.

Tracer data do not support the commonly accepted view of Keller's velocity reversal hypothesis and Jackson and Beschta's (1982) two-phase sediment sorting model, which state that coarse material is deposited on riffles at high flow, and finer sediments deposited in pools during lower flows. This is despite the evidence that tractive force reversal occurs in the Rede channel and the suggestion that gravel appears to 'leap-frog' from riffle to riffle / bar (*sensu* Jackson and Beschta, 1982). Rather, the grain size pattern and sediment sorting processes appear to reflect the high flow competence pattern supporting the views of Gilbert (1914), Bowman (1977), Bhowmik and Demissie (1982) and Thompson *et al.* (1999). Riffles and bars appear to be acting as sources and sinks; sediments scoured from a riffle are transported to the next riffle crest downstream which may then undergo aggradation, if the tractive force is below the critical threshold for mobilisation. Conversely, a riffle section which undergoes aggradation may result in a reduced supply of sediment to the next riffle downstream, with the consequence that the next riffle downstream undergoes scour. The Rede data also demonstrate scour of pools and deposition on riffle heads / pool exit slope, which is a feature supported by Sear's (1996) and Thompson *et al.*'s (1996) studies. This can be attributed to the upstream-sloping portion of the channel that controls the size of the bedload that leaves the pool (Petit, 1987; Thompson *et al.*, 1996). The exit slope merges into the riffle head and finishes at the riffle crest, creating strong flow divergence (Schmidt *et al.*, 1993; Thompson *et al.*, 1998), and areas of upwelling that increase the likelihood of sediment deposition (Petit, 1987; Thompson *et al.*, 1996). This feature may explain the downstream fining which has also been observed in pools by some workers (e.g. Sear, 1996), and why fine sediments are often reported as being deposited on the pool tail (Lisle and Hilton, 1992; 1999). The resolution of grain size measurement was not detailed enough to pick out down-pool size variation (within-unit) in this investigation (see Chapter Three).

Mean transport distances for tracer clasts suggest no major difference in hydraulic condition between riffles and pools, with distances of 8.35 m and 8.97 m respectively (see Figure 6.3). This is possibly due to the energy which is dissipated/expended whilst the particle is trying to hurdle the sloping pool exit. In this manner the pool exit slope controls further sediment transport. However maximum transport distances of 59.7m for riffles and 72.61m for pools suggest greater competence in pools in comparison to riffles, further supporting Keller's (1971) velocity reversal model and the hydraulic data presented in Chapter Four. It was also evident that the most stable tracer size, i.e. that which travelled the least distance, was equivalent to the reach D_{50} (see Chapter Six, Figure 6.4). This suggests that the present flow regime adjusts any introduced sediment (tracers) around a quasi-equilibrium condition, which is reflected in the D_{50} . A change in surface D_{50} may be found where there has been a disruption to this equilibrium linked to changing flow and sediment supply regime, for example below a recently constructed reservoir (Milan, 1994; 1996).

The observed tracer sorting pattern; selective scour of smaller tracers from pools and deposition on bars, appears to reflect the high-flow tractive force distribution. Tracers deposited on pool tails and bars (head edges, tops and apices) closely matched natural size distributions, however tracers deposited on riffles, pool heads and troughs tended to be finer than the naturally occurring material. This may reflect supply limitation of coarse tracer clasts from upstream pools, and the finer nature of the introduced tracers in comparison to the natural surface sediments. Tracers deposited on bar edge tails were also found to be coarser than naturally occurring material, which may suggest some low flow sorting in operation; selective removal of finer tracers under winnowing flow conditions.

The Rede tracer data highlights potential differences in riffle-pool sediment sorting dynamics to previous studies, as there is limited evidence of fine tracer (sand and gravel) deposition in pools, particularly the pools situated on bends. Previous models (e.g. Keller, 1971; Jackson and Beschta, 1982; Thompson *et al.*, 1996, 1999) suggest that the grain size of the pool reflects sediment sizes which are transported into the pool. Tracer clasts in the Rede appeared to avoid the deepest parts of the channel, and tended to be routed towards bar surface from riffles. The coarsening of the tracer clasts in the pool over the study duration reflects scour of finer tracers from the pool

and retention of coarser clasts. Tracer data indicate that the maximum grain size evacuated from the pool was never as coarse as the largest particle recorded in the pool (Table 8.2). This would suggest that some of this pool material may never move, or only very occasionally, and would explain the existence of a coarse lag deposit on the pool bed highlighted in Chapter Three. It is suggested therefore that this lag material does not comprise bedload fed from upstream, but are the products of bank (banks being composed of relic gravel which lies on boulder clay).

Table 8.2 Comparison of the sizes of tracers mobilised in pools compared with the largest bed particle measured in the pool.

Unit	Surface D_{max} (mm)	Tracer D_{max} (mm)
P1	310	160
P2	270	140
P3	380	240

Riffle-pool maintenance implications

Accumulation of gravel on riffles and bars would suggest a progressive increase in elevation of these features, whilst lack of accumulation in pools, yet some scour of finer locally derived finer grades may suggest either some lowering of the pool bed or bed stability. Other balancing factors must play a role in keeping the riffle-pool sequence relatively stable. As mentioned in Chapter Three, and section 7.5.3, although bar tops are accumulating sediment, deposits tend to be structureless, fine-grained, and have a high relative mobility. Thus, bar deposits tend to be transitional in that they are easily transported downstream by the next high flow event. The coarse nature of the pool bed effectively acts as an armour during high flow preventing further vertical scour and dis-equilibrium, rather than sediment being fed into the pool replacing that which has been scoured, which is an important difference to the previous ideas of maintenance (e.g. Keller, 1971; Clifford and Richards, 1992). The tendency for bars and riffles to aggrade must be balanced by lateral channel shift, which is evident on channel bends on the Rede. Pools on straight sections do collect some gravel (Pool 3), so the conventional model of scour and fill to maintain pool bed elevation should hold.

8.4.2 Influence of flow character upon tracer movements and implications for morphological change

Using the limited hydrograph data available for the Rede an analysis of the frequency and duration of events capable of achieving the types of spatial sediment transfer patterns recorded in the tracer survey, those capable of geomorphological work, may be presented. The implications of sediment transport and flow hydraulics upon riffle-pool maintenance are then considered in more detail. Data presented in Chapters Five and Seven demonstrated that Phase 1 (sand) sediment movement was initiated in the Rede channel at about 4% bankfull discharge ($0.34\text{m}^3\text{s}^{-1}$). From analysis of the Rede flow records in Figure 8.12, it may be seen that this situation was possible, assuming an unlimited supply of sediment, for around 45% of the time. Over a one-year period, between November 1996 and 1997, there were 103 occasions where flow was competent enough to transport sand in the Rede channel (Figure 8.13). Sand has very little influence upon morphology, and it is the movement of gravel (Phase 2) which is more pertinent when considering riffle-pool maintenance.

From the tracer evidence presented in this Chapter and in Chapter Six, gravel movement appeared to be initiated on riffles at flows of around 31% bankfull. Movement tended to be restricted to intra-unit transport and hence this flow would cause limited morphological change. Flows capable of jostling the riffle surface layer only appear to occur about 2.6% of the time, when reference is made to flow duration data given in Figure 8.12. Over a period of one year (November 1996-November 1997) this was found to occur on 35 occasions. At between 31% and 70% bankfull, the tractive force in some but not all of the pools exceeds adjacent riffles (Chapter Four, Milan *et al.*, 2001). These flows appear responsible for pool scour and exit slope deposition. This magnitude of flow appears to have an important influence on morphological change. Tracer evidence presented in this chapter and in Milan *et al* (in press) suggests that the sediments, which are evacuated onto pool exit slopes, are derived from the pool bed or outer bank, rather than from riffles, pools or bars upstream. Hence at these flows, sediments are not being translated from unit to unit, maintaining equilibrium form, rather a dis-equilibrium state where pool troughs are deepening and pool exit slopes / riffle heads are aggrading, through deposition of freshly-scoured *extrinsic* sediments, appears to operate. Flows of 70% bankfull occurred about 0.19% of the time on the Rede channel between November 1996 and

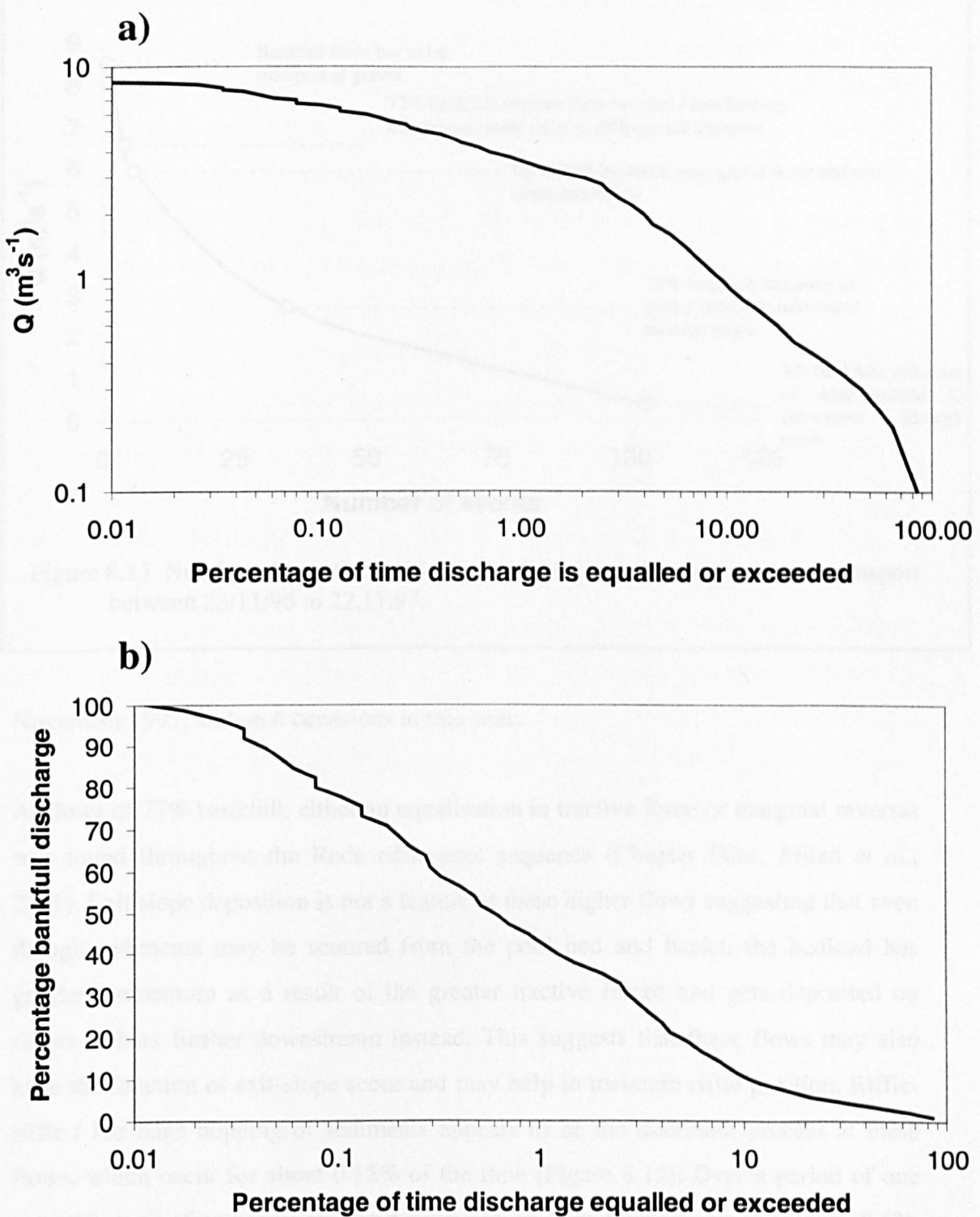


Figure 8.12 Duration curves for the River Rede, a) flow, b) percentage bankfull discharge.

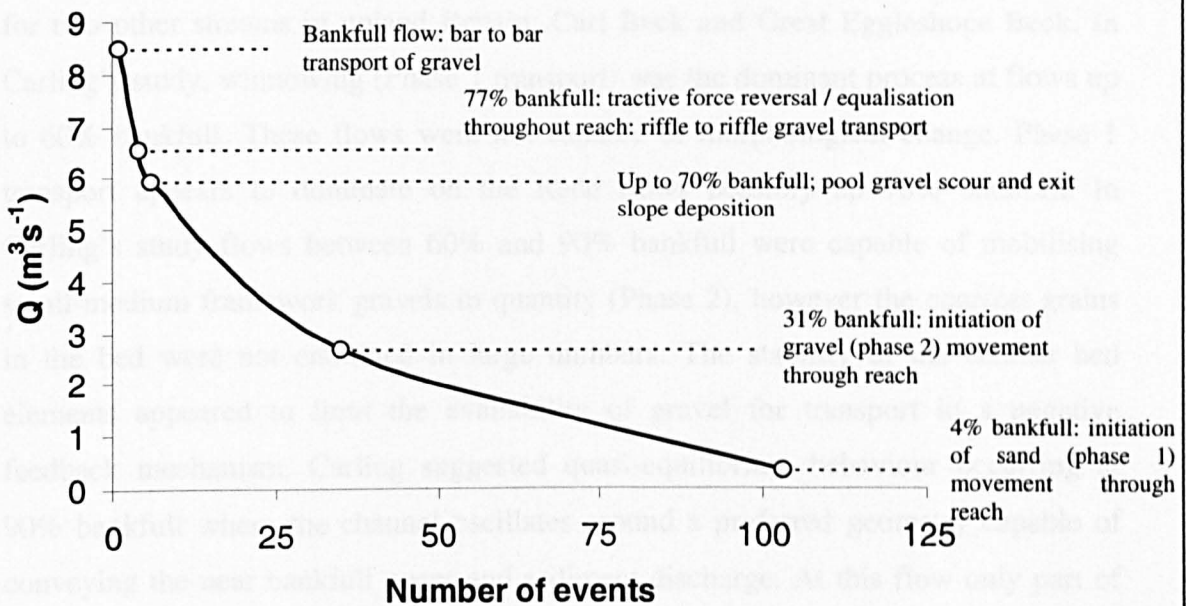


Figure 8.13 Number of events capable of morphological change / sediment transport between 23/11/96 to 22.11.97.

November 1997, and on 6 occasions in this year.

At flows of 77% bankfull, either an equalisation in tractive force or marginal reversal was found throughout the Rede riffle-pool sequence (Chapter Four, Milan *et al.*, 2001). Exit slope deposition is not a feature at these higher flows suggesting that even though sediments may be scoured from the pool bed and banks, the bedload has greater momentum as a result of the greater tractive forces and gets deposited on riffles or bars further downstream instead. This suggests that these flows may also have the function of exit-slope scour and may help to maintain riffle position. Riffle-riffle / bar edge hopping of sediments appears to be the dominant process at these flows, which occur for about 0.12% of the time (Figure 8.12). Over a period of one year this type of sediment transport occurred on only four occasions (Figure 8.13). Bankfull flow only appeared to occur 0.02% of the time over the study period (Figure 8.12), and between 23.11.96 and 22.11.97 only occurred once, however more bankfull floods did occur after this period (during the pebble tracer survey). These flows largely appear responsible for transferring sediments from bar to bar.

Similarities may be drawn between the Rede data and the findings of Carling (1988) for two other streams in upland Britain; Carl Beck and Great Eggleshope Beck. In Carling's study, winnowing (Phase 1 transport) was the dominant process at flows up to 60% bankfull. These flows were not capable of morphological change. Phase 1 transport appears to dominate on the Rede flows possibly up 70% bankfull. In Carling's study flows between 60% and 90% bankfull were capable of mobilising small-medium framework gravels in quantity (Phase 2), however the coarsest grains in the bed were not entrained in large numbers. The stability of the coarser bed elements appeared to limit the availability of gravel for transport in a negative feedback mechanism. Carling suggested quasi-equilibrium behaviour occurring at 90% bankfull where the channel oscillates around a preferred geometry capable of conveying the near bankfull water and sediment discharge. At this flow only part of the bed width and depth is mobile. This situation appears evident on the Rede at between 77% and bankfull condition. It is suggested by Carling (1988) that morphological adjustment (positive feedback) only occurs at flows above bankfull which are capable of mobilising the whole bed width (Phase 3 transport). Observations over four years on the Rede recorded one overbank flow of $9.92\text{m}^3\text{s}^{-1}$ (117%) bankfull, however this did not appear to be capable of transporting some of the D_{max} clasts within the Rede channel. Some morphological change was evident in the pools and point bars (see Chapter Nine).

Changes in the form of alluvial channels over moderate timescales oscillates around an equilibrium state unless the channel encounters different bank materials or has a different discharge regime imposed on it (Richards, 1982). Discharge regime may be altered by factors such as climate change, land-use alteration or flow regulation. There is strong evidence to suggest that the flashiness of spate rivers in upland Britain has changed in the last hundred years (Archer, 2000). The analysis described in this section could be developed further so that response of riffle-pool morphology to changes in flow / sediment transport regime may be predicted.

Keller's (1971) tractive force reversal and Thompson *et al*'s (1996, 1998, 1999) pool-exit-slope sediment sorting models can be shown to both influence sediment sorting patterns through the Rede riffle-pool sequence, and thus riffle-pool maintenance. However there is room for modification of the model to take into account the limited

supply of sediment into pools and development of coarse lag layers. This will be addressed in Chapter Nine.

8.5 Summary

- 1) Bar surfaces (particularly bar edges) and riffles act as gravel storage zones in the Rede riffle pool sequence;
- 2) For low magnitude (<30% bankfull), high frequency flows, movement of gravel is restricted to movement within morphological units;
- 3) For medium flows of around 70% bankfull sediments do appear to be transferred from one unit to the next, however the step lengths are usually quite short (<10m), with scour from pools and exit-slope deposition dominating. Some deposition on bar apices occurs;
- 4) For flows close to bankfull (82%), sediments may be transferred between units, with greater transport distances. Riffles – riffle / bar transfer dominates;
- 5) For flows of bankfull and over (117%) sediments are almost exclusively deposited on bars regardless of their source. Bar to bar transfer dominates;
- 6) Sediments are transported from riffle-riffle/bar rather than being fed through pools;
- 7) Pools act as zones of scour, there is little evidence of any deposition in pool troughs even at lower flows, sediment is supply limited to the pools;
- 8) Limited transport of very coarse tracers seeded in pools, yet evacuation of fine-medium gravel, demonstrates how lag coarse surface layers may develop in the Rede pools;
- 9) Multiple comparisons analysis of variance demonstrated highly significant differences in the sizes of tracer clasts deposited in different morphological sub-units;
- 10) Application of a chi-squared test indicated that random deposition could not account for the observed tracer clast deposition patterns;
- 11) The grain-size of tracers deposited on riffles and bars showed similarities to the natural bed sediments in the depositional sub-unit, however tracers located in scour zones (pools) tended to be much finer reflecting limited supply of tracers into the pools;

12) Analysis of flow records for the Rede in conjunction with tracer data may be used to assess the frequency of sediment transfer patterns, and to predict the influence of this upon channel morphology.

Chapter Nine

Discussion and conclusions: sand and gravel transport and the maintenance of the riffle-pool sequence

9.1 Tractive force reversal

This chapter summarises the sediment transport and hydraulic processes operating in the River Rede and discusses the implications for riffle-pool maintenance. As was shown in Chapter One, a diverse literature has addressed the mechanisms by which undulating bedforms (associated with spatial differences in flow strength and sediment sorting) are both formed and maintained. In terms of riffle-pool maintenance, the most widely accepted explanation is provided through the concept of tractive force reversal between the pool and riffle as discharge rises (Keller, 1971).

In this study reversal in mean section-averaged velocity was found at four out of six riffle-pool units (Figure 4.1), as a result of marginally smaller cross-section areas. Many workers contend that pool cross-section averaged velocity can only exceed that of the adjacent riffle if the pool cross-section area is smaller (e.g. Bhowmik and Demissie, 1982). Carling and Wood (1994) have demonstrated using computer simulation the increased potential for velocity reversal where riffles are in excess of 50% wider than the pools. However, numerous workers have presented field data that demonstrate larger cross-sectional areas for pools at high flow (e.g. Richards, 1978; Carling, 1991; Carling and Wood, 1994; Thompson *et al.*, 1996; 1999), thus providing support for an alternative explanation for riffle-pool maintenance.

9.1.1 Support for reversal from tracer data; limitations with cross-section average measures

Although the reversal in cross-section average velocity was only marginal in nature, and did not occur for every riffle-pool unit in the Rede study reach, gravel tracer data (Chapters Six and Eight) provide further support for its occurrence. Of particular interest was the behaviour shown by one of the riffle-pool units situated at the upstream end of the study reach (Pool 1-Riffle A), which did not show a reversal or equalisation from cross-section averaged velocity data. Tracer data showed this pool to scour at discharges below bankfull ($5.95 \text{ m}^3 \text{s}^{-1}$, 70% bankfull), with deposition of tracers (20-70 mm) on the pool exit slope / head of Riffle A. Even though section

average velocity data suggest otherwise, this has to imply that the pool had greater competence than the riffle head downstream, and that competence reversal occurred. Sediment sorting processes in this case provide support for tractive force reversal.

The reason for disparity between tracer and hydraulic data lie with the cross-section averaged nature of the velocity measure. Were point velocity values to be taken solely in the pool trough, above the roughness elevation of the bed surface sediments, at or near bankfull, higher values might be expected in the pool. Cross-section average velocity estimates are also influenced by the morphology of the cross-section. Pools situated on channel bends adjacent to point bars with asymmetric cross-section profiles have much narrower cross-sections than riffles at low flow. The flow is confined between the steeply shelving bank of the bar edge and the near-vertical outer bank. As discharges rises, mean section velocity within the pool increases at a faster rate compared with the adjacent riffles; cross-sectional areas are smaller and the continuity of mass principle is satisfied. However just before the discharge reaches bankfull (or equal to the elevation of the point bar), the bar surface begins to become flooded and becomes part of the pool-cross section (at approximately 70% bankfull). In this situation the cross-section area may increase sufficiently to exceed that of the adjacent riffles. This effect may be responsible for the deviation from the log-log relationship at the upper flow range evident in Figure 4.1.

A further reason for this disparity could be the existence of turbulent eddies associated with high velocity jets, in the region of downwelling flow close to the outer bank on bends (Bathurst, 1979), which may result in locally high velocities and shear stresses in the pool trough. This is discussed in more detail in sections 9.5.1 and 9.7.

9.1.2 Further support for reversal using point measures

Although some point velocity values were obtained, it was not possible to obtain measurements in pool trough at high flow. However more detailed tractive force information was obtained in the form of boundary shear stress using the Du Boys equation. Analysis of these results appear to indicate more clearly, reversals in point shear stress for all riffle-pool units studied throughout the reach. At high flow the tractive force maxima may be extremely localised in the pool trough, and understandably would not be represented well by a cross-section averaged measure

(see Pool 1 / Riffle A, Figure 4.8). Apparently therefore, boundary shear stress data support the occurrence of tractive force reversal but their interpretation should be approached with caution due to the possible influence of three dimensional flow effects and turbulence, which are not accounted for by the Du Boys equation (see section 9.5.1 and 9.7).

However, when hydraulic information is coupled with tracer data the evidence supporting a reversal in tractive force, is more convincing. The influence of the recorded hydraulic measurements and sediment transport upon riffle-pool maintenance may be assessed by employing a modified Shields approach to the data.

9.2 Implications of tractive force distribution for riffle-pool maintenance and sediment transport

Data for the critical dimensionless shear stress for entrainment (θ_c), obtained from tracer data (see Chapter Six) for riffles and pools, may be used in a predictive fashion to provide information on the direction of channel change and riffle-pool maintenance (Milan *et al.*, 2001). Data on surface grain size (D_{50}) may be entered into a modified Shields equation to yield the initial boundary shear stress (τ_c) required for mobilisation:

$$\tau_c = \theta_c(\rho_s - \rho_w) g D_{50} \quad (9.1)$$

Traditionally, values assumed for θ_c are 0.06 for well-sorted sediments and 0.047 for poorly sorted sediments (Miller *et al.*, 1977), although Buffington and Montgomery (1997) have highlighted that values may range from 0.052 to 0.086 for reference-based studies and 0.030 to 0.073 for visually-based studies. A range of factors including non-uniform grain size distribution and particle shape have been suggested to account for this range (e.g. Andrews, 1983). Here, θ_c is estimated from tracer data using Equations 6.2 and 6.3 rather than the Andrews (1983) equation which was used by Milan *et al.* (2001).

Equation 9.1 may then be used to derive a measure of entrainment potential by subtracting the critical boundary shear stress (τ_c) for the D_{50} from local boundary shear stress values (τ_o) calculated using hydraulic data for five flow events (see Chapter Four). The amount by which τ_o exceeds τ_c indicates the sediment transport potential. It is important to note that this measure of competence does not necessarily indicate areas of entrainment and fill as it does not take into account sediment flux. While this flux is likely to be an important factor in streams with a high sediment supply, where transport capacity is high and the competence threshold low (Lisle pers comm, 1998), this argument will not apply under the supply-limited conditions encountered in the River Rede (Milan *et al.*, 2001).

9.2.1 Predicted areas of potential morphological change

Positive values for τ_o minus τ_c were plotted to indicate areas of potential entrainment and channel change for four discharges (Figure. 9.1a to e). A very similar pattern of entrainment to that using Andrews (1983) value for θ_c (see Milan *et al*, 2001, Fig. 7). However, more entrainment appears to be predicted at bankfull discharge ($8.52 \text{ m}^3 \text{s}^{-1}$), where there is potential for entrainment of the D_{50} in Pool 1, the head of Riffle A and Bar 1. Very little entrainment is predicted for Bar 2 or the tail of Riffle A / head of Pool 2, hence deposition is likely to occur in these areas. Moderate entrainment is predicted from the trough of Pool 2 through to the crest of Riffle C. Greatest entrainment is predicted at the tail of Riffle C extending into Pool 3. At just below bankfull ($7.26 \text{ m}^3 \text{s}^{-1}$), Pool 1 still appears competent to entrain the D_{50} . A small patch of entrainment is evident at the tail of Riffle A, however most of Riffle A, Pool 2 and Bars 1 and 2 are not scoured at this flow. This would suggest that deposition may occur in these areas. Some localised entrainment is also predicted on Riffle B and Pool 3, however as Riffle C is incapable of transporting any material, sediments scoured from Pool 3 may be deposited here. Some potential entrainment is also predicted in at the tail of Riffle C and Pool 4.

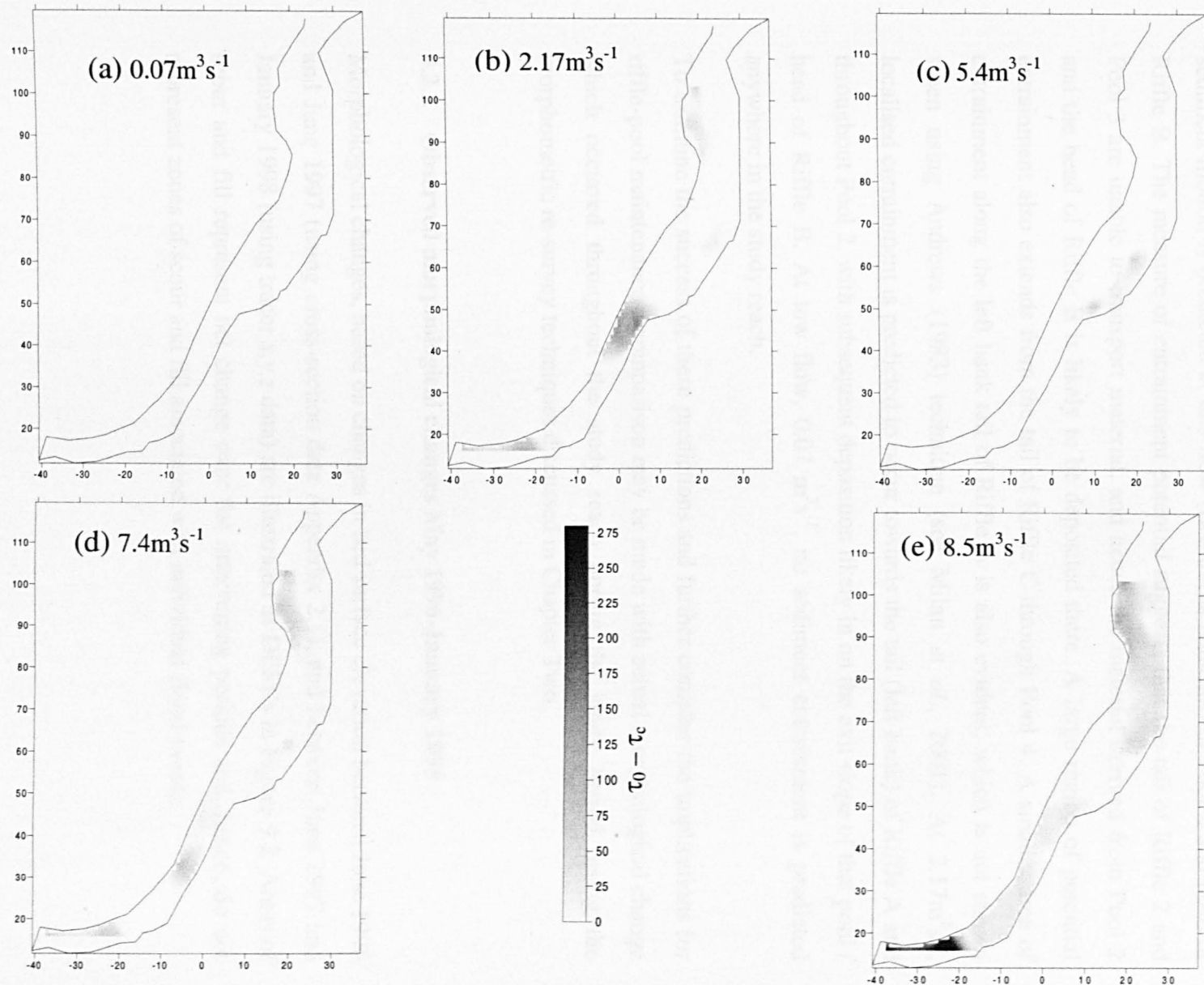


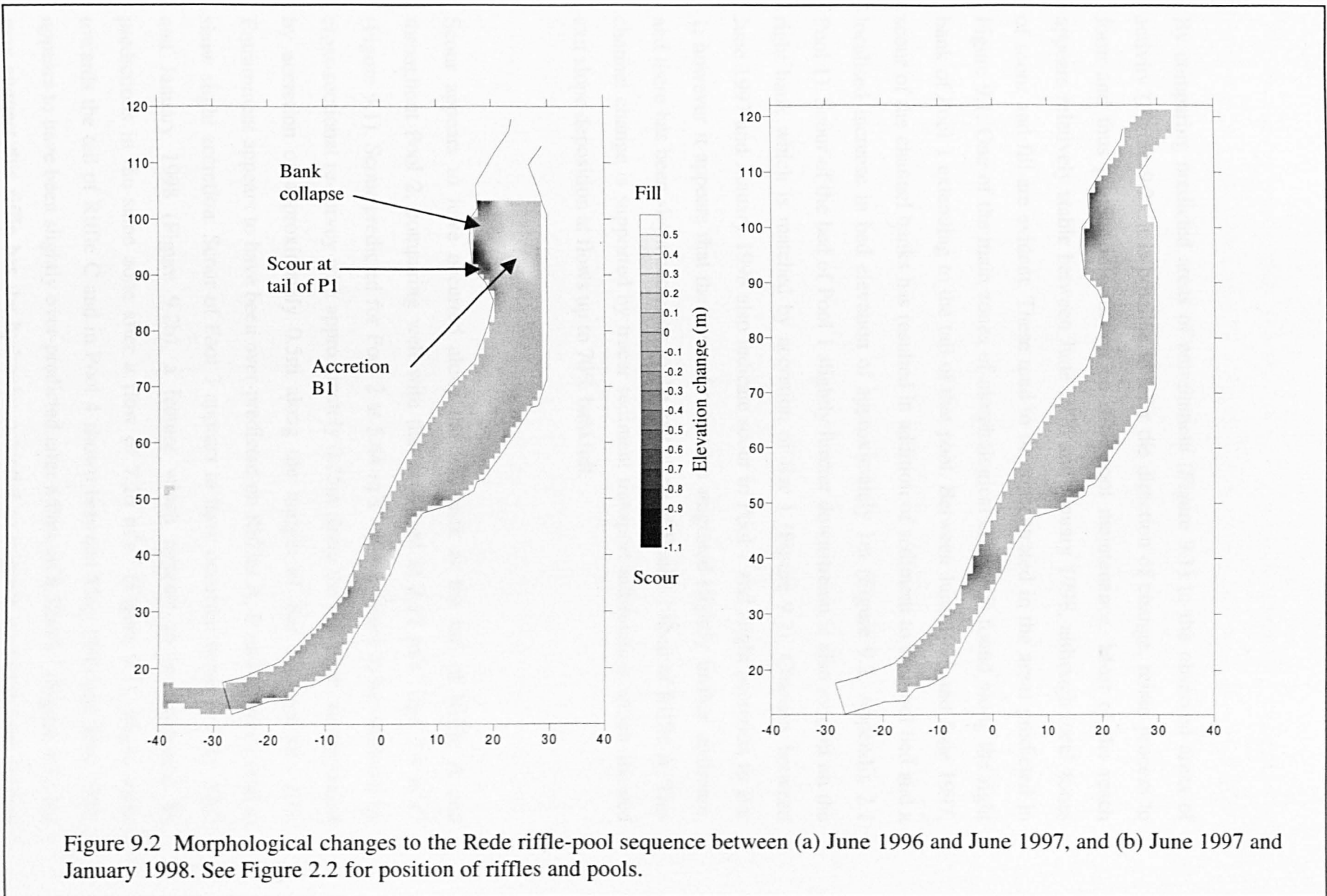
Figure 9.1 Grey-scale plots indicating the spatial pattern of scour ($\tau_0 - \tau_c$) at (a) $0.07\text{m}^3\text{s}^{-1}$, (b) $2.17\text{m}^3\text{s}^{-1}$, (c), $5.4\text{m}^3\text{s}^{-1}$ (d), $7.3\text{m}^3\text{s}^{-1}$ (e) $8.5\text{m}^3\text{s}^{-1}$. See Figure 2.2 for position of riffles and pools.

At $5.44 \text{ m}^3\text{s}^{-1}$ there is limited entrainment in Pool 1, again suggesting that some deposition might occur just downstream of this point. The most extensive area of sediment motion is predicted at this flow (two-thirds bankfull) in Pool 2 and head of Riffle B. The measure of entrainment potential suggests that the tail of Riffle 2 and Pool 3 are unable to transport material, and hence the material derived from Pool 2 and the head of Riffle B is likely to be deposited there. A large region of potential entrainment also extends from the tail of Riffle C through Pool 4. A smaller area of entrainment along the left bank tail of Riffle A is also evident, which is not shown when using Andrews (1983) technique (see Milan *et al.*, 2001). At $2.17 \text{ m}^3\text{s}^{-1}$, localised entrainment is predicted to occur towards the tail (left bank) of Riffle A and throughout Pool 2, with subsequent deposition likely in on the exit slope of that pool / head of Riffle B. At low flow, $0.07 \text{ m}^3\text{s}^{-1}$, no sediment entrainment is predicted anywhere in the study reach.

To examine the success of these predictions and further consider the implications for riffle-pool maintenance a comparison may be made with actual morphological change which occurred throughout the study reach during the study period, using the morphometric re-survey techniques discussed in Chapter Two.

9.2.2 Observed morphological changes May 1996-January 1998

Morphological changes, based on changes in bed surface elevation between June 1996 and June 1997 (using cross-section data Appendix 2.1), and between June 1997 and January 1998 (using tracer x,y,z data) are illustrated as DEM's in Figure 9.2. Areas of scour and fill represent net change over the intervening periods and, hence, do not represent zones of scour and fill associated with individual flood events.



By comparing predicted areas of entrainment (Figure 9.1) to the observed areas of activity (Figure 9.2), it is possible to infer the direction of change, relate process to form and thus provide information on riffle-pool maintenance. Most of the reach appears relatively stable between June 1996 and January 1998, although local zones of scour and fill are evident. These tend to be concentrated in the areas predicted in Figure 9.1. One of the main zones of morphological change is found along the right bank of Pool 1 extending to the tail of that pool. Between June 1996 and June 1997, scour of the channel banks has resulted in addition of sediment to the pool bed and a localised increase in bed elevation of approximately 1m (Figure 9.2, Appendix 2.1 Pool 1). Scour of the bed of Pool 1 slightly further downstream is also evident on the right bank which is matched by accretion of Bar 1 (Figure 9.2). Changes between June 1997 and January 1998 also indicate scour in Pool 1 and slight accretion to Bar 1; however it appears that the zone of scour has migrated slightly further upstream, and there has been slight accretion to the exit slope of Pool 1 / head of Riffle A. This channel change is supported by tracer sediment transport information which showed exit slope deposition at flows up to 70% bankfull.

Scour appears to have occurred along the left bank at the tail of Riffle A and throughout Pool 2, comparing well with that predicted at $2.17 \text{ m}^3 \text{s}^{-1}$ and $5.4 \text{ m}^3 \text{s}^{-1}$ (Figure 9.1). Scour predicted for Pool 2 at $5.44 \text{ m}^3 \text{s}^{-1}$ also appears to be validated by cross-sectional re-survey with approximately 0.25m along the left bank, accompanied by accretion of approximately 0.5m along the margin of Bar 2 (Appendix 2.1). Entrainment appears to have been over-predicted on Riffles A, B and C which tend to show slight accretion. Scour of Pool 3 appears to have occurred between May 1997 and January 1998 (Figure 9.2b), a feature which appears to be supported by predictions in the same zone after a flow of $7.26 \text{ m}^3 \text{s}^{-1}$ (Figure 9.1). Slight scour towards the tail of Riffle C and in Pool 4 shown between May 1996 and May 1997, appears to have been slightly over-predicted after a flow of $8.52 \text{ m}^3 \text{s}^{-1}$ (Figure 9.2), but may suggest this riffle has the hydraulic potential to migrate upstream (see section 9.3.3).

The measure of entrainment potential ($\tau_o - \tau_c$) appears reasonably successful at predicting zones of scour and fill. Observed changes suggest pool scour and bank erosion, some slight bar aggradation, and stable riffle surface elevations. However, slight upstream migration of riffle heads, and pool scour zones (Pool 1) is also suggested.

9.3 Sediment sorting patterns and tractive force reversal

If tractive force reversal is to be used to explain the maintenance of riffle-pool morphology on the Rede, then the sediment sorting patterns should reflect this stage-dependent hydraulic behaviour. The observed sediment sorting patterns through the Rede riffle-pool sequence strongly reflect high flow hydraulics and limited sediment supply. A lag layer of coarse sediment mantles the pool troughs at low flow. Tracer data suggest that this material is not transported into the pool from upstream; instead it appears to originate from the bed and banks, either from former alluvial deposits or till (Figure 9.3). Any finer material which is present is likely to be flushed out of the pool during high flow, leaving behind coarser clasts. This may set up a positive feedback mechanism which further promotes tractive force reversal (Figure 9.4). Carling and Wood (1994) have suggested that an increase in grain roughness increases the likelihood of tractive force reversal, thus Rede pools are more likely to show a reversal. Every time a reversal in tractive force occurs, new coarse material may be added to the bed from erosion of the outer banks. Unlike many streams (e.g. Lisle and Hilton, 1992; 1999), the Rede pools are not smothered with drapes of fines winnowed into the pools on the waning limb of the flood hydrograph. This probably reflects a combination of supply limitation, a steep falling limb to the hydrograph and hiding opportunities behind coarser riffle clasts. Fines that are fed into pools may be deflected towards bar edges by strong transverse secondary flow. Alternatively, fines may not be routed into the pools, instead following the path of riffles and bars (similar to the routing patterns shown for gravel tracers).

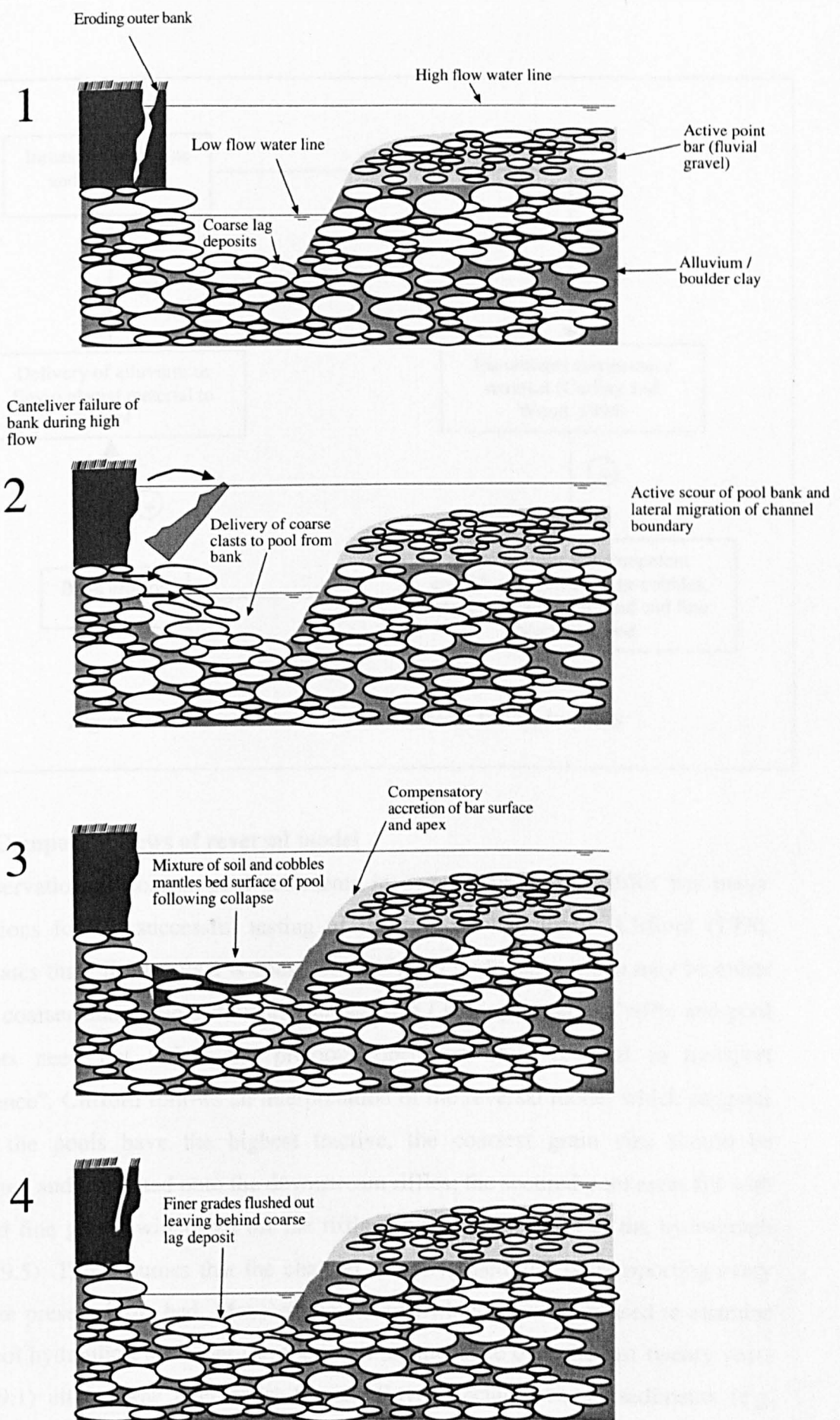
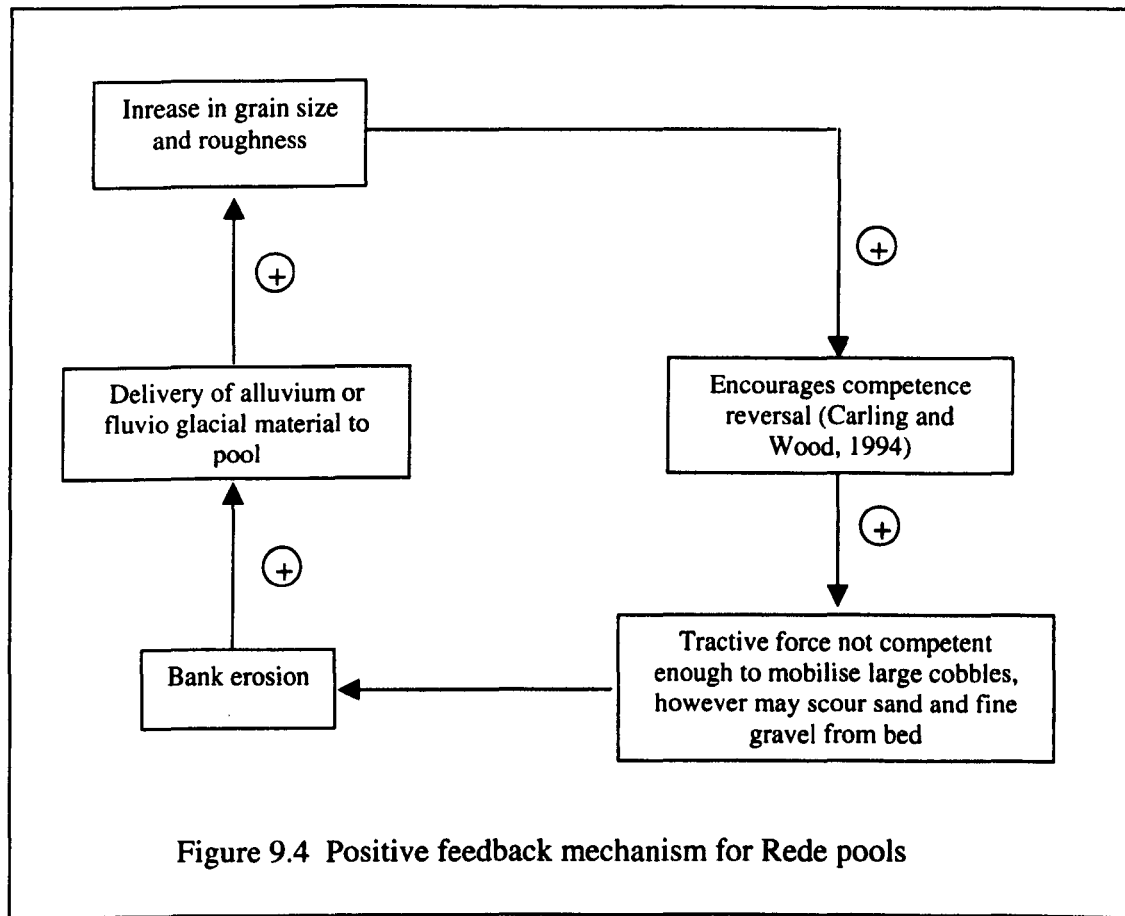


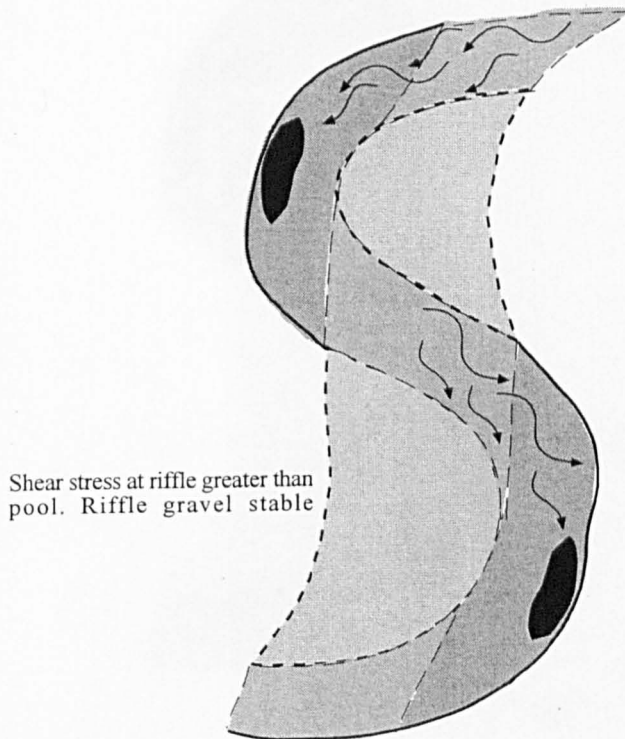
Figure 9.3 Coarse lag development and sustainability in pools



9.3.1 Competing views of reversal model

The observation of coarser pool sediments in comparison to the riffles has major implications for the successful testing of the reversal hypothesis. Clifford (1990, p195) states that "if a reversal is consistent with pool sediments which may be either finer or coarser than riffle sediments, surface size / sorting pattern of riffle and pool sediments need not reflect the previous operation of a reversal in transport competence". Clifford follows an interpretation of the reversal model which suggests that, if the pools have the highest tractive, the coarsest grain size should be transported and deposited onto the downstream riffles; the scoured pool areas fill with sand and fine gravel winnowed off the riffles on the falling limb of the hydrograph (Figure 9.5). This assumes that the channel is self-formed and is transporting every grain size present in its bed. Many of the streams which have been used to examine riffle-pool hydraulics, sediment transport and maintenance over the last twenty years (Table 9.1) either flow over relict fluvial, fluvio-glacial outwash sediments (e.g. Milne, 1982), or glacial materials such as till (e.g. Ashworth, 1987). These streams therefore may conceivably be re-working this material, some of which is too coarse to

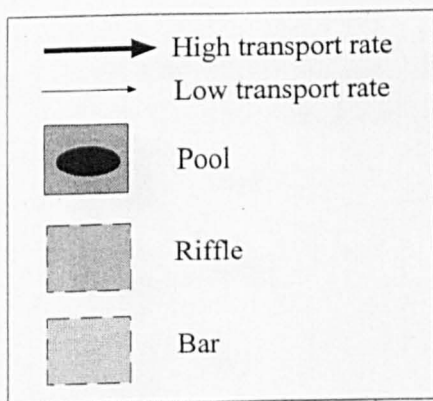
a) 5-30% bankfull, Sand transport



On the falling limb of hydrograph fines are winnowed into pools where they are stored on the pool tail until the next high flow. Flow and sediment directed into pool trough. Pool bed composed of finer sediments than the riffles

b) 30-70% bankfull, Gravel transport

Riffle shear stress rises high enough for patchy armour disruption, fine gravel fed into pool and stored as shear stress is lower than adjacent pools. Pool cross section begins to decrease promoting velocity to rise at a faster rate than the riffle.



Exit slope gravel deposition occurs. Fine sediment drapes on tails flushed

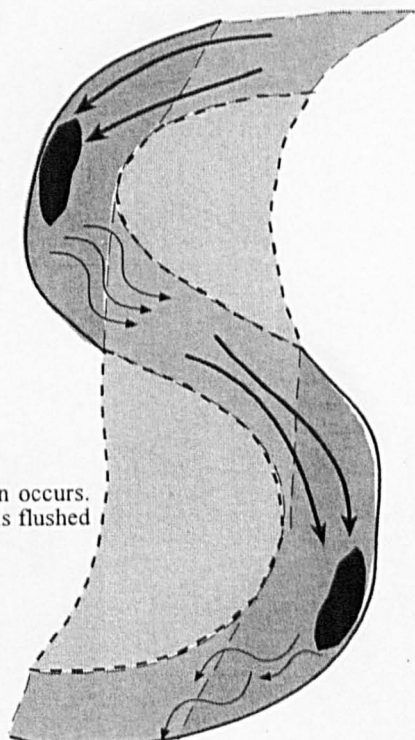
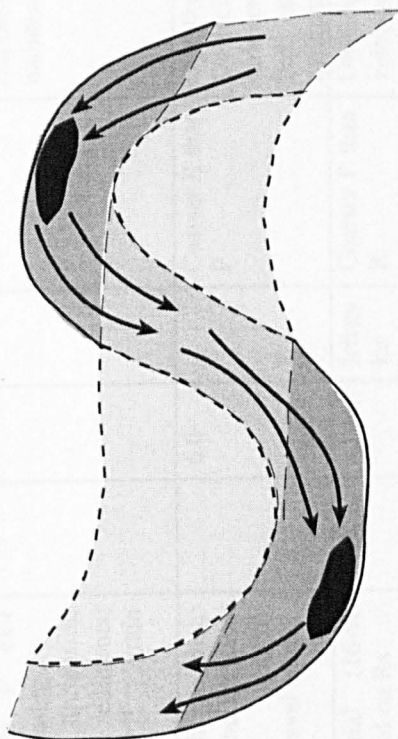


Figure 9.5 Reversal model in a riffle-pool sequence with finer pools than riffles.

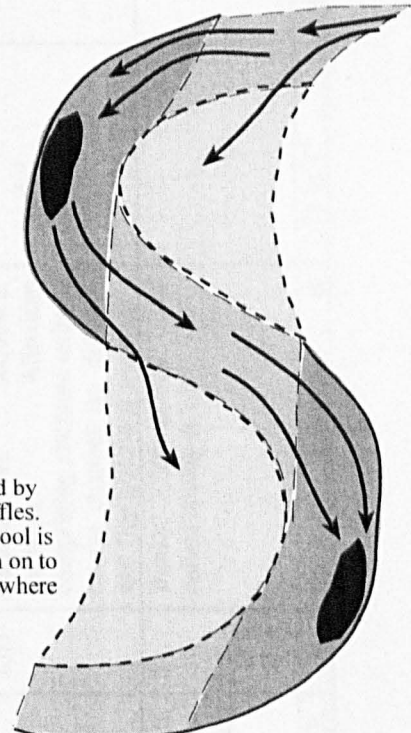
**c) 70-90% bankfull,
Gravel transport**



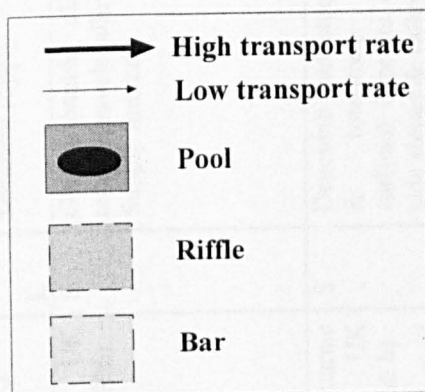
Tractive force equalisation. Riffle armour begins to break. Pools transport sediment at the same rate as the riffles

Coarse lag exposed, particularly if sediment supply is low

**d) 90% - 100%+ bankfull,
Gravel transport**



Tractive force reversal. Pools transporting sediment at a higher rate than the adjacent riffles. Coarse gravel queues up at riffles. Pools scour if competence exceeds supply. Low grain roughness



Coarsest grains mobilised by pool and deposited on riffles. Any gravel fed into the pool is ejected out of pool trough on to bar or riffle downstream where shear stress is lower

Figure 9.5 Reversal model in a riffle-pool sequence with finer pools than riffles.

Table 9.1 Studies on riffles and pools: site-specific characteristics

River & Author	L	Sediment supply	Hydrograph character	Role of fines	s (m/m ⁻¹)	w (m)	P-P space	D ₅₀ (mm)	Comments
North Tyne, UK (Sear (1992;1996))	S	Glacial boulder clay, peat, terrace gravels, alluvium Supply limited	Regulated flow 1.3-16 m ³ s ⁻¹ BF=167 m ³ s ⁻¹	Infiltration into R gravel voids, Surficial deposition on P exit slopes \Rightarrow decreasing compaction, decreasing θ_c of P sediments, decreasing P grain roughness	0.0018	31.0		R=60; P=43	Bed structure proposed as being major mechanisms responsible for R-P maintenance
River Quarne (Clifford, UK 1992; 1993 a & b)	S	Devonian sandstone, slates & limestone. Coarse surficial deposits to valley side slopes & valley floor		Fines thought to help increase θ_c , and fill voids between tightly interacting gravel clasts		6.0		Coarser R than P	D _g =50mm Obstacle-induced macro-turbulent flow structures and bed strength important in maintenance
North Saint Vrain Creek US (Thompson <i>et al.</i> , 1999)	S	Alluvial, coarse bed	SM 0.23-12.9 m ³ s ⁻¹ BF=5 m ³ s ⁻¹	Finer material (16-90 mm) deposited on Rs	0.01, 0.026	\approx 10.0	Irregular spacing	Coarser P than R	Obstacle clasts promote velocity and τ reversal, and produce re-circulating eddies fPR Supply limited
Treia River, Italy, (Cherkauer, 1973)	S 1.03	Pleistocene volcanics, Plio-Pleistocene marine transgressive sequence. Terraces. Alluvium comprising alternate units of coarse channel lag deposits and fine overbank material	Low flow only studied <1 m ³ s ⁻¹		\approx 0.006			R=Cobbles & boulders, little matrix P=Sand & fine gravel	Supported Langbein and Leopold's (1962) proposal that rivers adjust their flow so as to minimise total power expenditure
Steavenson River, Australia (Wilkinson <i>et al.</i> , 2000)	S	Banks composed of cohesive clay & silt			0.013	4.5		R=76; P=50	Model of sediment continuity applied to explain formation and maintenance. Reversal found only in parts of R-P sequence
Bambi Creek, S.E.	1.1	Silurian greywacke &	1.75 m ³ s ⁻¹	Fines dominant in	0.0082	3.6			Gravel transport only triggered

Alaska US (Campbell & Sidle, 1985 ; Sidle, 1988)		argillite, and Devonian limestone. Spodosol soils with organics. Numerous bogs. Debris jams control in-channel storage		bedload, higher on rising limb of floods					by 1/5yr floods. Transport of sediment controlled by log jams. Antecedent conditions important. Rs scour in winter and spring and fill in summer
Rede, UK (This study)	1.4	Glacial boulder clay / alluvium made available via erosion scars, slope-channel coupling important. Flavioglacial outwash / boulder clay made available via bank scour. Channel storage (point bars) Supply limited	RF, SM BF = 8.5 m ³ s ⁻¹	No fines winnowed into Ps. P subsurface sediments contains slightly less matrix in voids (10.7% compared with 12.8%). Matrix in Ps however contains more silt and clay which may act to increase θ_c of P clasts	0.007	HF= 14.0 LF= 8.7	HF= 3.6 LF= 5.7	R=101;P= 122	Tractive force reversal apparent in some R-P units. P sediments have higher θ_c , compared to Rs. sediments routed around P, Rs maintained without further downward scour of Ps. Rate of increase in v falls due to drowning of bar surfaces and bank roughness effects
Skirden Beck UK (Thompson (1986)	1.45	Composite silt over coarse gravel in banks	BF = 19.2 m ³ s ⁻¹		0.0048	12.0	5		
Flynn Creek US (Jackson & Beschta (1982)	≈1.6	Forested catchment. Deep soils, gravelly loams. Sandstone and siltstone BR. Sediment supply by soil creep and shallow mass movements of soil to channel.	Winter freshets most important for sediment transport BF = 1.2 m ³ s ⁻¹	Two phase sediment transport model proposed. Fines (Phase 1) transported for most of the time over a stable gravel surface	0.01	3.5	5.1	Reach D ₅₀ =36	Bed sediments dominated by sand 80%, gravel 20%. Two phase model requires tractive force reversal for gravel (Phase 2) transport to begin.
Kingledoors Burn, Tweed, Peeblesshire UK (Milne, 1982)	1.73	Silurian and Ordovician lithology. Bluffs comprised of fluvio-glacial valley fill. Erosion scars supply sediment to channel		Ps clean of fines <2mm. Very low fine sediment content related to geology	0.01	5.9	7.3*	R=43; P=36	Ps with more asymmetric cross-sections and tighter planform, curvature more likely to collect fines
East Fork River, Wyoming US (Andrews, 1979; Lisle, 1979)	1.8	Pleistocene outwash terraces. Low gravel supply, high sand supply.	SM	Coarse sand dominates bedload and fills Ps at low flow	S _c = 0.001	50-60		R coarser at low flow, P coarser at high flow	τ reversal occurs, however usually below θ_c to mobilise gravel. Gravel 25% of bed but only 8% of bedload

La Rulles, Ardenne, France (Petit, 1987)	1.86	Quartzite BR. Alluvial. Gravel in banks and bed.	RF BF=1.3 m^3s^{-1}	Fines may delay transport if present in voids. Fines winnowed into Ps.		3.8	2.8	R=15.2; P=50-100	Lag boulders in P prevent vertical scour Shear stress reversal occurs
Dry Creek, California (Keller, 1971)	S 2.4	Alluvial	Intermittent 4.5 m^3s^{-1}		0.0025	10.07	5.92	R=32; P=10	Velocity equalisation, velocity reversal hypothesis proposed. Fine sediment drapes in pools due to winnowing at low flow
Little Rouge River, Ontario, Canada (Robert 1997)	S	Alluvial	2.55-4.62 m^3s^{-1}		0.0008	9.0	≈5.6	36	τ equalisation at two-thirds BF
Boulder Creek, Utah, US (O'Conner <i>et al.</i> , 1986)		BR channel							Ω & S_c reversal
River Fowey UK (Richards, 1976a & b; 1978)	S&C	Banks 5-40% silt/clay Bed material derived from granite bedrock	RF		Reach1 0.0056 Reach3 0.0013	R = 8.2 P = 7.2		R=45-60 P= 7-52	Convergence in velocity at high flow but not reversal. Macro-scale flows thought responsible for formation. No reversal, however S_c increases at faster rate over P's with increasing Q compared to R
Bronte Creek, S. Ontario, Canada (Richards, 1978)									No reversal, however S_c increases at faster rate over P's with increasing Q compared to R
Kaskasia River, Illinois US (Bhowmik & Demissie, 1982 a&b; Yang, 1971)	S&C							R=46 P=0.034	Reversal was not found to occur

River Severn, Shropshire, UK (Carling, 1991; Carling & Orr, 2000)	S&C	Incised into Bentonitic clays. Sandy banks, gravel point bars and terrace gravel	RF BF = $250 \text{ m}^3 \text{s}^{-1}$		S = 0.0003-0.002 C = 0.0004-0.0005	80.0 ≈3.75	R=25; P=43	No reversal found to occur, only equalisation. Importance of macro-scale turbulent flow structures in formation and possibly maintenance emphasised. v begins to fall near bankfull in curved reaches
River Severn and Swale Bathurst (1979)	S&C	Severn banks composed of fine alluvium over gravel, Swale banks composed of sand and gravel	Measured Q ranges: Severn; 0.76-25.84 $\text{m}^3 \text{s}^{-1}$ Swale; 0.71-7.84 $\text{m}^3 \text{s}^{-1}$		Severn 8.8-31.9 Swale 18.2-19.6		Coarse gravel / cobble	τ in curved reaches strongly influenced by 3D flow, and shows wide variation with Q. 3D flow most active at medium Q, and is associated with a jet of high velocity which at low and high Q is situated towards the downstream end of the pool, and at medium Q is situated at the head or trough of pool. 3D flow poorly developed in straight pools, τ pattern varies little with Q.
River Bóbr Poland (Teisseyre, 1984)	S&C	Alluvial loams	Floods & Freshets	High suspended sediment load. P fine-sediment deposition reflects gradually varied flow, leading into the P, without a bottom zone of flow separation				Differences in three-dimensional flow structure in C and S reaches. Velocity reversal thought to occur. Observations suggested that turbulent flow structures were also very important in maintenance.
Allt Dubhaig (Ashworth, 1987; Ferguson and Ashworth, 1991)	1.2	BR-metamorphic granulites & mica schists, occasional granite erratics. Hummocky Pleistocene moraines mantle bases of hillsides. Valley floor moraines thought to be re-	Flashy hydrograph. Rainfall and some snowmelt hydrographs $10.0 \text{ m}^3 \text{s}^{-1}$	Ps clean of fines Low fine sediment supply	0.021 0.015 0.011	16 27 14	R=113; P=125 R=87; P=120 R=70; P=59	Shear stress reversal was found in most reaches. Lag gravel in some Ps; boulder clay

D	1.5	worked by meltwater erosion during deglaciation.			0.0083	24		R=78; P=64	
E	1.1				0.003	8		R=40; P=40	
F	1.1				0.001	9		Reach D ₅₀ =20	
Big Pine Creek US	(Keller & Meltzer, 1978)	1.18	Sandstone BR (Little alluvium)	Perrenial		0.0014	29.28	6.84	
Boone Fork US		1.25	Alluvial (little BR)	Perrenial (regulated)		0.0045	9.46	4.90	
Durkee Run Creek US		1.13	Alluvial	Intermittent		0.0023	4.27	5.56	
Little Bear Creek US		1.13	Metavolcanic (little alluvium)	Perrenial		0.0036	7.63	6.28	
Mc Alpine Creek US		1.01	Alluvial (little BR)	Perrenial (Channelised)		0.001	6.03	6.74	
Middle River US		2.05	Limestone (little alluvium)	Perrenial		0.0067	14.23	6.73	
Simms Creek US		1.31	Alluvial	Perrenial (regulated)		0.0049	3.66	5.52	
Ramsey Creek US		1.08	Metavolcanic	Perrenial		0.0089	4.58	7.00	
Wea Creek US		1.38	Alluvial	Perrenial		0.0015	20.44	5.25	
Wildcat Creek US		1.42	Alluvial	Perrenial		0.0014	25.01	5.01	
Cattaraugus Creek US (Hirsh & Abrahams, 1984)			Sediments arise from sandstone BR and non-sedimentary glacial erratics. Bank sloughing. Transport of sediment from upstream. Erosion of in-channel sediment		Fine sediments winnowed from Rs to Ps. Deposition below reversal threshold.		10.0		Rs coarser & better sorted
Feshie UK (Ashworth, 1987)	Braided			Flashy upland, RF & SM				R=62; P=70	Assumes possibility of tractive force reversal
Gaylor Creek N.California US (Keller & McDonald, 1987)					Ps clean of fines Low fine sediment supply			P coarser than R	Reversal in stream power, however gravel immobile. Bed a relict feature of the late Pleistocene, some elements too

unpublished)									coarse to mobilise
Washington US									
Tolt 1	Montgomery <i>et al.</i> (1995)	Tolt catchment underlain by Tertiary igneous & sedimentary BR and pre-Tertiary melange. Valley floors covered by Pleistocene recessional outwash & alpine glacial deposits. Other reaches in southeast Alaska, glaciated during the Pleistocene, underlain by limestone, granite, and metasediments		0.035	14.5	0.81			fPR
Tolt 2				0.034	24.9	0.21			fPR
Tolt 6				0.04	16.3	0.57			SP
Tolt 7				0.029	12.2	1.12			SP
Tolt 9				0.054	15.3	0.61			SP
Tolt 10				0.029	12.8	5.08			PB
Tolt 11				0.04	2.8	12.50			PB
Tolt 12				0.03	3	>13.2			PB
Tolt 13				0.03	2.7	3.70			PR
Tolt 14				0.021	5.4	1.34			fPR
Tolt 15				0.007	4.1	3.35			fPR
Tolt 16				0.014	4.4	1.14			fPR
Tolt 17				0.006	4.9	0.75			fPR
Tolt 18				0.012	4.5	0.70			fPR
Tolt 19				0.01	35	2.43			PR
Tolt 20				0.013	23.5	9.36			PB
Tolt 21				0.085	4.1	1.34			SP
Tolt 22				0.023	4.9	>12.2			PB
Tolt 23				0.006	4.2	3.27			fPR
Tolt 24				0.002	4.0	2.14			fPR
Tolt 25				0.007	4.4	1.23			fPR
Tolt 26				0.006	4.9	0.95			fPR
Tolt 27				0.005	4.5	1.18			fPR
Tolt 28				0.008	38.1	1.99			fPR
Trap 2				0.007	12.5	0.32			fPR
Trap 4				0.008	7.0	0.76			fPR
Alaska, US									
Trap 5				0.009	12.0	0.51			fPR
Trap 6				0.009	14.0	0.32			fPR
East Fork Trap				0.009	7.7	0.55			fPR
				0.025	8.2	0.86			fPR

				0.023	5.1	1.08		fPR
Muri 1				0.023	6.2	0.73		fPR
Muri 2				0.015	15.0	2.30		PB
Corner 1				0.027	9.1	0.82		fPR
Corner 2				0.03	5.4	0.79		fPR
Corner 4				0.016	4.9	1.36		Hole in the Wall 1
Bambi 1				0.009	14.7	0.26		Hole in the Wall 2
Bambi 2				0.006	4.0	2.63		Hole in the Wall 3
Bambi 3				0.016	4.0	2.67		PR
Kook 3				0.016	5.3	0.94		fPR
Kook 5				0.01	9.7	0.54		fPR
Kook 6				0.027	5.0	1.02		SP
Buckthorn				0.022	4.7	1.18		SP
Gold				0.005	11.5	0.50		fPR
Montanna				0.025	4.4	11.36		PB
				0.003	18.3	2.60		PB
Trinity river and other N.W. California streams (Lisle, 1982; Lisle & Hilton, 1992)	Bedload dominated by sand and influenced by logging activities within the catchment.		Fines winnowed into Ps on waning flows. Fine sediment drapes found on P tails, up to R crest.				R coarser at low flow; P coarser at high flow	Filling of Ps by fines implies lower τ in Ps on falling limb of hydrograph. In some extreme circumstances of very high fine sediment supply Ps were found to fill completely and become more 'R-like'. This situation is likely to strongly effect the continuity of mass principle, and thus mean velocity for a given discharge, as it is likely to effect reduce
Big French Creek US		$\approx 52 \text{ m}^3 \text{s}^{-1}$		0.019				
Bear Creek US		$\approx 8 \text{ m}^3 \text{s}^{-1}$		0.042				
Horse Linto Creek US		$\approx 66 \text{ m}^3 \text{s}^{-1}$		0.018				
Rattlesnake Creek US		$\approx 51 \text{ m}^3 \text{s}^{-1}$		0.013				
North Rattlesnake Creek US		$\approx 15 \text{ m}^3 \text{s}^{-1}$		0.044				
Three Creeks Creek US		$\approx 19 \text{ m}^3 \text{s}^{-1}$		0.016				

Grouse Creek US			$\approx 90 \text{ m}^3 \text{s}^{-1}$		0.016					cross-sectional are
Grass Valley Creek US			$\approx 37 \text{ m}^3 \text{s}^{-1}$		0.017					
Stanhope Burn UK (Milne, 1982)	1.26	RF, SM				7.4	10.3*			
Black Water, UK (Milne, 1982)	1.31					8.7	8.0*			
Black Water, UK (Milne, 1982)	1.28					8.2	10.8*			
Polmaddy Burn Loch UK (Milne, 1982)	1.39					14.1	7.8*			
Carsphairn Lane Loch UK (Milne, 1982)	1.1					11	4.1*			
Snaizeholme Beck UK (Milne, 1982)	1.1					8.4	8.9*			
River Ure UK (Milne, 1982)	1.71					9.0	5.7*			
River Rede, UK (Milne, 1982)	1.94					8.1	10.9*			
Bowmont Water UK (Milne, 1982)	1.06					15.5	3.0*			
Halter Burn UK (Milne, 1982)	1.18					2.5	10.0*			

s – bed slope, S_e water surface slope; w -Bankfull width; L – sinuosity BF: bankfull discharge; BR: bedrock; R-Rs, P-Ps; fPR – forced P-R; PR – P-R; PB-plane bed; SP-step-P; * estimated from maps in paper; RF-rainfall; SM-snowmelt; S- straight; C-curved; HF-high flow; LF-low flow

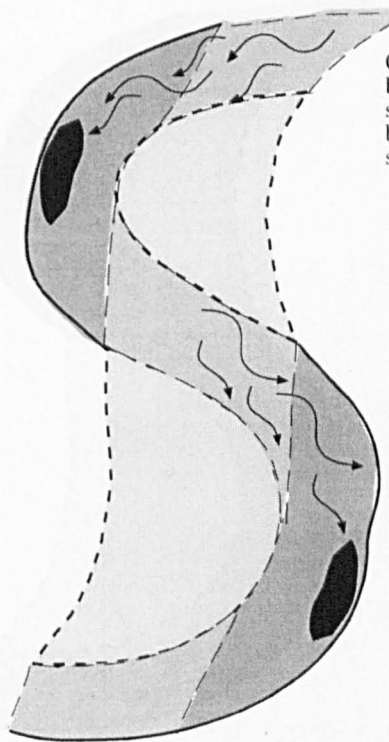
mobilise under the contemporary hydraulic regimes. This concept is further substantiated by other workers. Firstly, Lisle (1979), who worked on the East Fork River (which has a stable channel and a high sand load) found that although shear stress reversal happened, it occurred at a discharge lower than that required to initiate any substantial gravel movement, which he attributed to armouring and low gravel supply. Secondly, Keller and McDonald (Keller, unpublished), working on Gaylor Creek, Northern California showed that the gravel bed material was immobile, despite the existence of a reversal in stream power. Keller and McDonald suggested that the bed was a relict feature of the late Pleistocene (Table 9.1), when greater runoff from upstream glaciers may have been responsible for sculpting the bed.

With this in mind, an alternative interpretation of the reversal model (shown in Figure 9.6), which is followed by Keller (1971), Bhowmik and Demissie (1982) and Thompson *et al.* (1999), is that progressively coarser bed material is found in areas with a progressively greater tractive force, similar to that reported by Bowman (1977). Hence pools should have the coarsest sediments if they are zones of maximum tractive force at high flow. In this situation the reversal persists for long enough to evacuate all available material, of a competent size, onto the riffle. This situation allows for the development of a coarse lag layer at the pool bed. In this model the source of the coarse lag material arises from scour of the bed or banks, and not from upstream. The lag cobbles which are left in pools at low flow indicate the upper boundary of the pool's competence, with all smaller sizes susceptible to scour. Scoured material from the pool source area is deposited on topographic highs downstream (initially the pool-exit slope / riffle head), as Jackson and Beschta (1982) suggested. If a sufficient supply of fine bedload is available then this may cover the coarse immobile lag, similar to the situation reported by Lisle (1979) for the East Fork River, Colorado, US. This alternative interpretation appears to apply to the Rede channel.

9.3.2 Modification of reversal model

Sediment tracer data in conjunction with information on flow hydraulics have provided further insight into riffle-pool maintenance processes on the river Rede. The data presented in this thesis may be used to devise a modification of existing riffle-pool maintenance theory, which predicts coarser pool sediments. It appears feasible

**a) 5-30% bankfull,
Sand transport**



On the falling limb of hydrograph most fines have been stranded on bar tops. Those that remain find stable sites in the wake of coarse riffle clasts or may be winnowed into the downstream pool. Flow and sediment routed from riffles into pools

Pools are composed of coarse lag cobbles, visible at low flow if fines are supply limited. Fines may cover coarse lag at low flow in high supply scenarios

**b) 30-70% bankfull,
Gravel transport**

Phase 1 sediment transport over a stable gravel bed. Riffles transport Phase 1 material at faster rate than pools. If supply is high pools may fill, reducing cross-section area. Exit slope deposition may occur

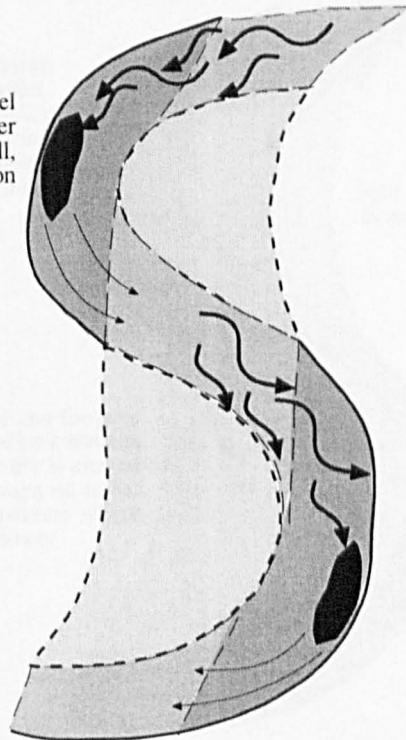
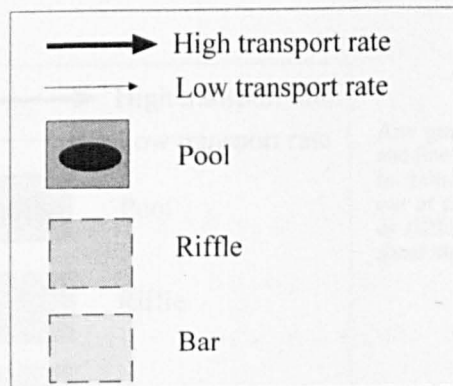
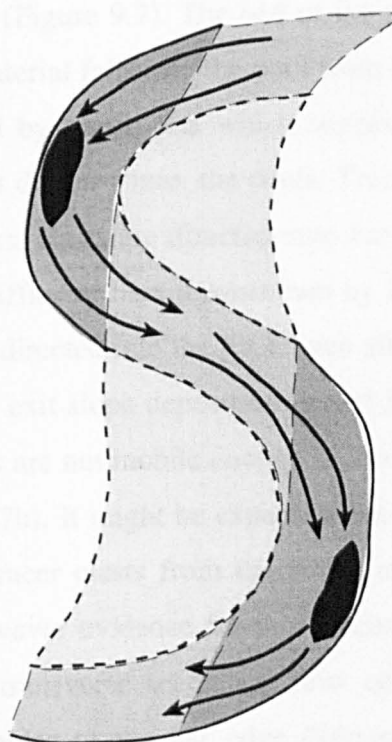


Figure 9.6 Reversal model in a riffle-pool sequence with coarser pools than riffles.

**c) 70-90% bankfull,
Gravel transport**



Tractive force equalisation. Flow converges into pool, and diverges onto riffle. Riffle armour begins to break. Pools transport sediment at the same rate as the riffles. Pool lag stable

Coarse lag exposed. May be covered if sediment supply is exceptionally high

**d) 90% - 100%+ bankfull,
Gravel transport**

Tractive force reversal. Pools transporting sediment at a higher rate than the adjacent riffles. Bed and bank scoured. Coarse cobbles introduced from bank to pool bed, increasing grain roughness. Coarse lag material left reflects upper competence limit of the pool

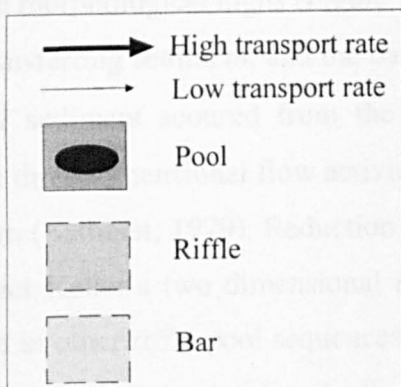
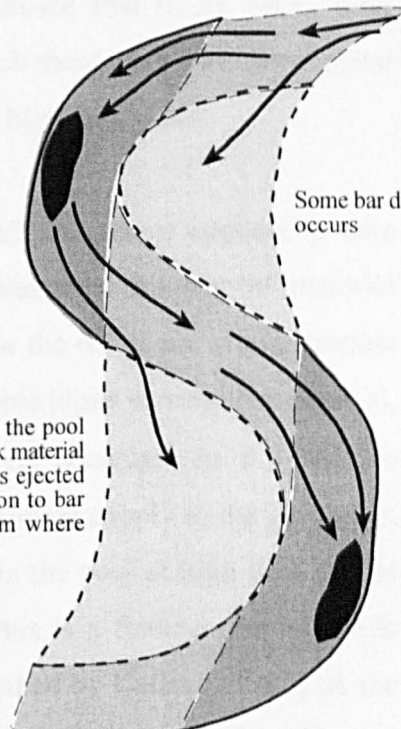


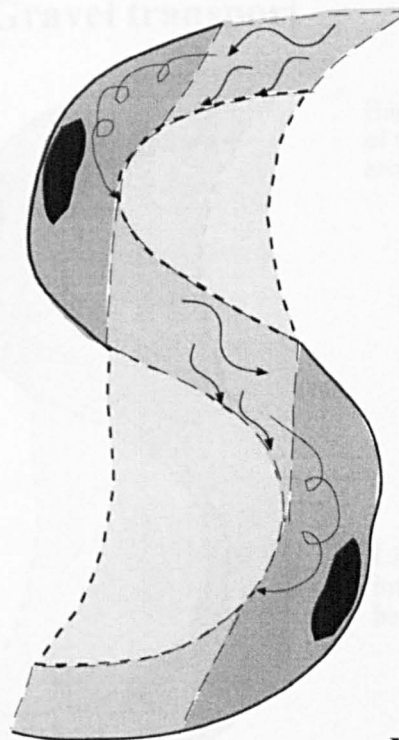
Figure 9.6 Reversal model in a riffle-pool sequence with coarser pools than riffles.

that on the Rede, pools act as scour zones only and never store any sediment derived from upstream (Figure 9.7). The bed of the pool is a product of bed and bank scour only, unless material falls into the pool from the adjacent point bar slope. This notion is substantiated by tracer data which suggest that gravel and sand may be scoured from, but is not directed into, the pools. Tracer data also indicate that under medium magnitude flows, clasts are directed onto bar surfaces and edges, whereafter they are transferred to riffles or bars downstream by larger discharges. There is no indication that tracers are directed into the pool, even after smaller (intra-unit movement) floods. Pool scour and exit slope deposition occurs for floods up to 70% bankfull; however, riffle sediments are not mobile enough at this flow to be transported down to the next pool (Figure 9.7b). It might be expected that larger floods (Figure 9.7 c and d) result in routing of tracer clasts from the riffle into the pool, with subsequent exit slope deposition, however evidence for this mechanism is non-existent. If sediment is fed into the pool, transverse secondary flow cells must be strong enough to transport gravel and cobbles to the bar edge (Teisseyre, 1984), as there is no evidence in support of deposition in the line of the primary flow direction. Although Figure 9.7c is developed from limited data, there appears to be evidence that tracer clasts were preferentially routed around bar edges. When clasts reach these positions, they appear to be more easily transported to the next bar by the next high flow event.

Tracer data indicate that sediment transport at bankfull and above appears to take place over bars and riffles only, with a general downstream transfer of material between morphological highs (Figure 9.7d). At high flow the riffles act as topographic lows transferring sediment, and the bars act as topographic highs storing this material. Lack of sediment scoured from the pools may suggest decreases in τ related to reduced three-dimensional flow activity, and lack of sediment supply to the pool from upstream (Bathurst, 1979). Reduction in tractive force in the pool at high flow would contradict Keller's two dimensional model, however this is a feature that has been reported in other riffle pool sequences such as those studied by Carling (1991) on the River Severn. In terms of fine bedload, riffle basket trap data presented in Chapter Seven, suggest greater rates of transport over areas of relatively lower bed elevation, which implies that the pools should have the greatest transport rates.

a)

5-30% bankfull, Sand transport



On the falling limb of hydrograph most fines have been stranded on bar tops. Those that remain find stable sites in the wake of coarse riffle clasts or may be winnowed into the downstream pool.

b)

30-70% bankfull, Gravel transport

Scour of pool bed and banks, with deposition on pool exit slope / riffle head

Intra-riffle movement of gravel clasts towards bar edges and bar heads

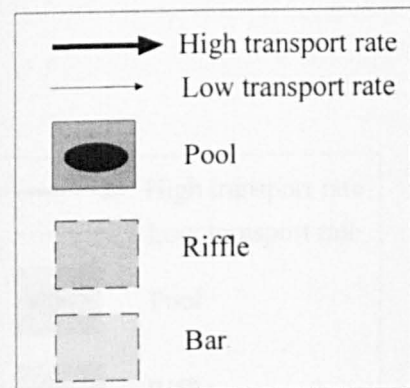
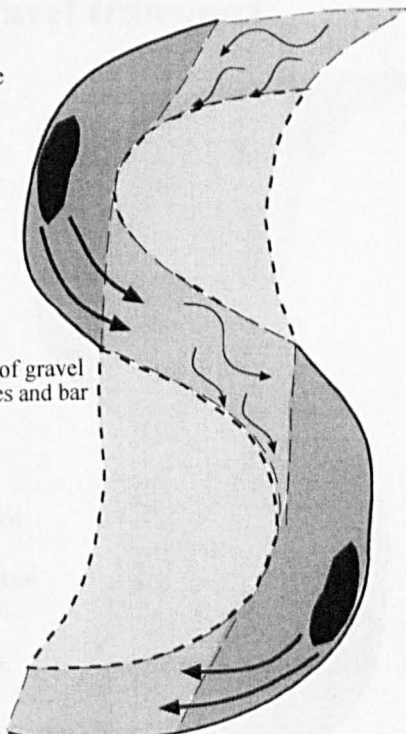
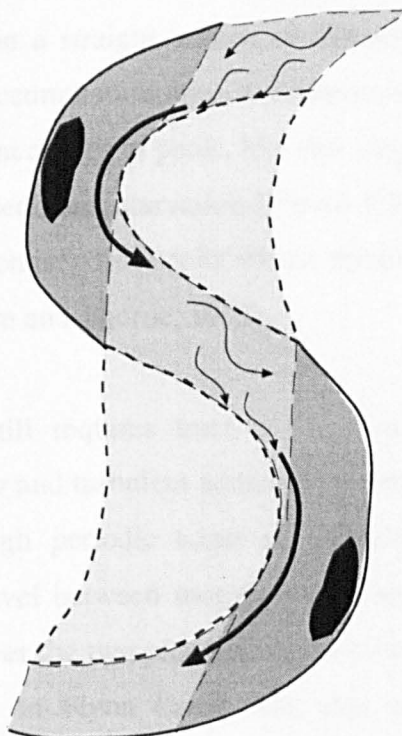


Figure 9.7 Modification of reversal model, detailing sediment transport routing through the Rede riffle-pool sequence

**c) 70-90% bankfull,
Gravel transport**

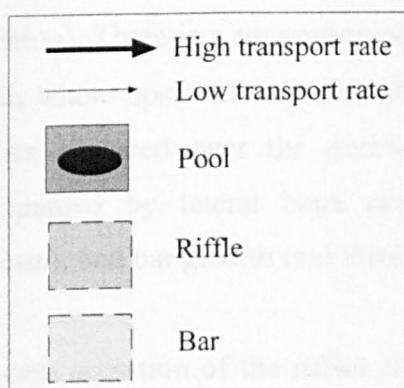


Bar surfaces still above water surface. Bulk of sediment transport appears to take place around bar margins

Little evidence to show routing of clasts into pools - particularly those situated on bends

**d) 90% - 100+% bankfull,
Gravel transport**

Riffle-bar-riffle leap-frogging
of gravel clasts



Little evidence of pool scour and exit slope deposition. Any material scoured from pools at these flows must be deposited on bar tops.

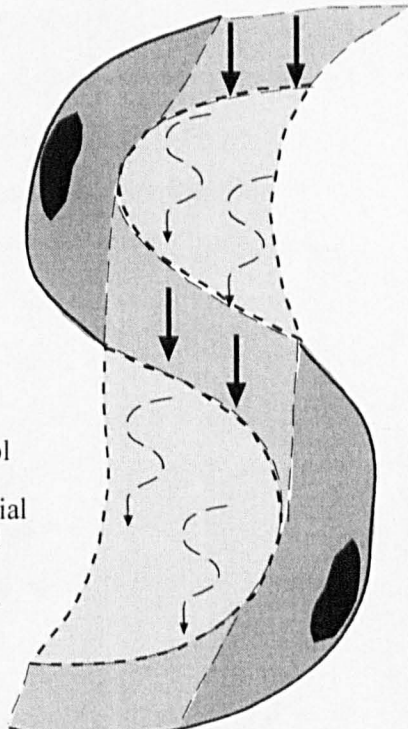


Figure 9.7 Modification of reversal model, detailing sediment transport routing through the Riffle-pool sequence

However, the limited data available from pools suggests this may only apply to pools on straight sections, as those situated on sinuous sections of channel (Pools 2 and 4) tend to have lower rates of accumulation in comparison to the riffles. Pool 3, which was situated on a straight section of channel, supports this notion and appeared to have greater accumulation rates in comparison to riffles (see section 7.3.1). The lack of fine sediment drapes in pools, like that suggested by Lisle and Hilton (1992; 1999), would imply sediment starvation (Figure 9.7a), and further support the existence of transverse secondary flow cells which drive fines laterally onto the bars (Teisseyre, 1984; Markham and Thorne, 1992).

This model still requires tractive force reversal (incorporating the influence of secondary flow and turbulent eddies) to maintain the position of riffle heads and pool troughs, through periodic scour of deposited sediments, and would involve the transfer of gravel between morphological highs as evoked by Jackson and Beschta (1982). However the two phase nature of transport on the Rede may not be as distinct as that found on Flynn Creek, US, due to lower sand loadings and a gradual, incomplete break-up of the surface layer on riffles. Sediment transport on the Rede is essentially a stage dependent continuum of grain size transported versus discharge. Although Jackson and Beschta do not discuss flow-sediment interaction in intervening pools in any detail, the implication is that sediments are passed through the pool, whereas in the revised model sediments are transferred from riffle to bar to riffle. The morphological implication is that new sediment scoured from the pool bed and banks and deposited on pool exit slopes by medium discharges may lead to headward growth of the downstream riffle, particularly if associated with a decrease in larger flood events that may remove this material (such as that resulting from flow regulation). There is a suggestion of this on the Rede study reach at the Pool 1-Riffle A unit, where upstream accretion of the riffle head and lateral accretion of the point bar has occurred over the duration of this study (Figure 9.3). This has been accompanied by lateral bank erosion (which has also been migrating slowly upstream), and bar growth (see Pool 1 Appendix 2.1).

Upstream accretion of the riffles is often balanced by down-riffle scour in order to counteract the tendency for riffles to progressively lengthen (although this has not been observed on the River Rede within the timescale of this investigation). For

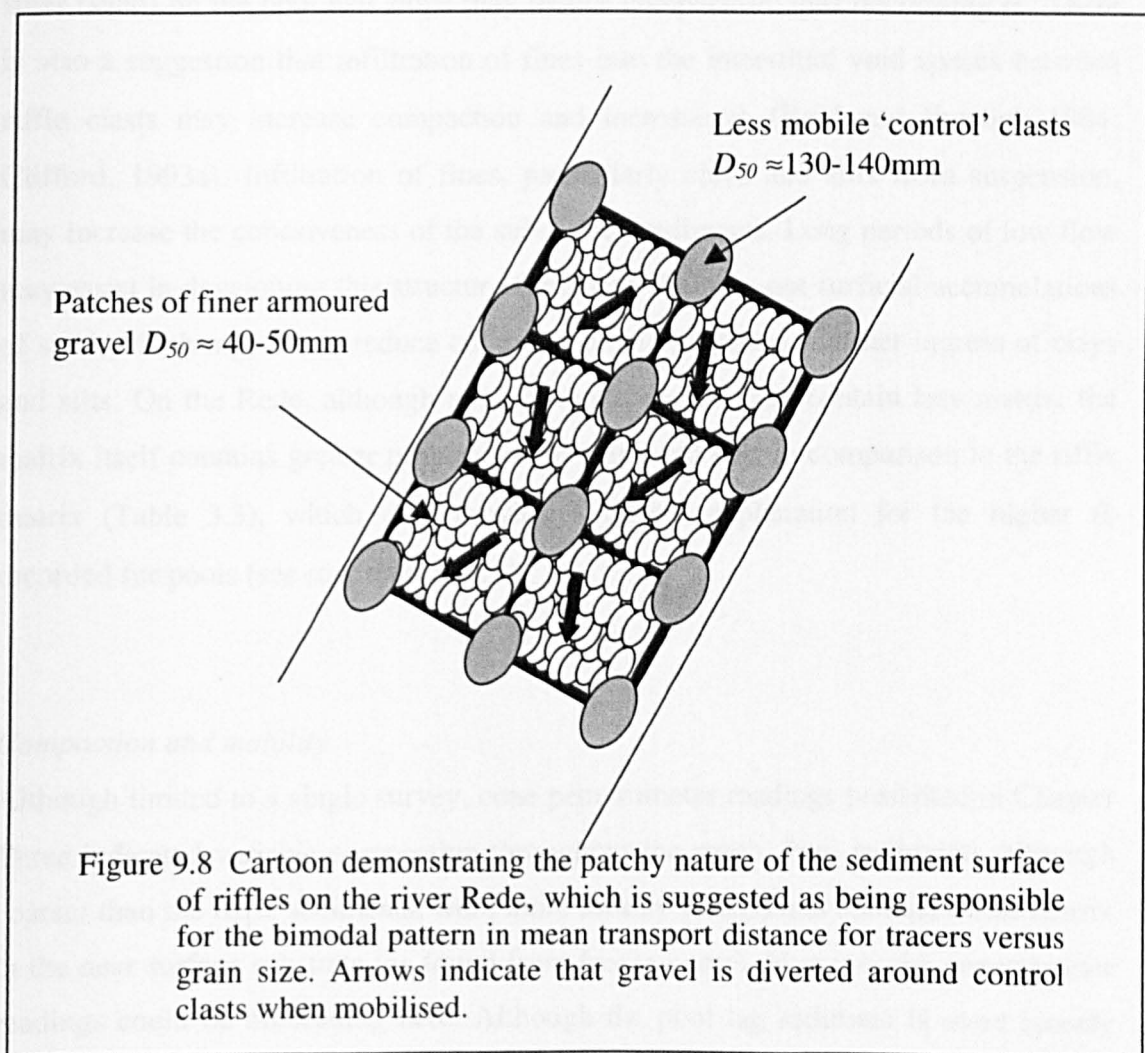
example, Teisseyre (1984) has observed headward growth and riffle tail scour on a seasonal cycle, whilst Lisle (1982) has commented upon headward erosion of finer gravel material from riffle tails at falling stages. Thompson *et al.* (1999) also comment on the likelihood of headward growth of riffles as a result of exit slope deposition; however they suggest that scour of riffle heads must occur at some stage in order to maintain the riffle at its particular location. Indeed, some tracer clasts that had been deposited on pool exit slopes / riffle heads on the Rede were scoured during larger floods (Chapter Eight). This observation would support stability within the riffle-pool sequence.

9.4 Influence of sediment structure upon riffle-pool maintenance

Sediment structure also plays an important role in determining sediment mobility and thus riffle-pool maintenance. As was discussed in Chapter One (section 1.4.2), surface structuring can exist at a variety of scales in situations where transport rates are low, ranging from macro-scale armouring phenomenon, where finer grades have been winnowed away (Parker and Klingeman, 1982; Sutherland, 1987), to micro-scale pebble clusters (Brayshaw *et al.*, 1983), transverse ribs, and patches Larronne *et al.* (2000). These all play a significant role in regulating bedload transport through increasing θ_c for initial motion. All these features have most commonly been reported on riffle surfaces, implying that riffles are more highly structured forms with greater stability in comparison to pools.

The findings of this investigation also suggest that sediment structuring on the Rede influences sediment transport. Tracer data revealed evidence of hiding factors on two scales, both of which are related to the surface structure of the bed. Riffle surfaces on the Rede exhibit an arrangement of armoured gravel patches or ribbons, interspersed with coarser 'control' clasts, possibly of glacial origin, which freeze-core evidence suggests are embedded to a substantial depth (c 400mm) in the bed (Figure 9.8). Medium gravel and sand transport is likely to occur in the region of the patches at between 30 and 70% bankfull. Mean transport distance versus grain size plots as a bimodal distribution for data both originating from riffles and pools (Figure 6.4). The transport of sand and fine gravel, up to 50mm on the riffles, and 90mm in the pools, appears to be limited by the sheltering effects of the coarser gravel in the patches on

the riffles and lag gravel in the pools. Increases in travel distance with progressive increases in grain size (rising limb) represent hiding effects, whereas the decreases in travel distance with progressive increases in grain size (falling limb) represent selective transport. The first rising limb demonstrates that as the grain size of the tracer increases it is likely to be transported further due to increased protrusion effects until a point roughly correlating to the D_{50} of the patches on the riffles (50mm) and just below the overall D_{50} for the pools (90mm) is reached, after which size selective entrainment predominates. The grain size which moves the smallest distance (110 mm) is not the coarsest, as might be expected, but is slightly coarser than the reach D_{50} . For grains between 110mm and 140mm, protrusion effects again appear to become important, as indicated by a second rising limb; 140mm



grains are transported around 20m further on average in comparison to 110mm grains. It is possible that coarser 'control' clasts in the Rede bed are responsible for these

hiding effects, which are found lodged in riffles and which occur occasionally in pools (Figure 9.8). Selective transport appears to operate once more for the coarsest tracer grains between 140 and 240mm. The pool data in Figure 6.4 demonstrate that hiding effects are more extensive in the finer grain size classes, between 20-90mm, compared with 30-50mm for the riffles. This may be explained by the coarser grain sizes found in the pool and may partly explain the greater θ_c values found for pool tracer data in Chapter Six.

Role of fines

Most investigations have not discussed the role of fines in riffle-pool maintenance (Table 9.1). However Sear (1992) suggests that surficial deposition of non-cohesive fines (sand) on the pool exit slope may reduce compaction, thus decreasing θ_c . There is also a suggestion that infiltration of fines into the interstitial void spaces between riffle clasts may increase compaction and increase θ_c (Reid and Frostick 1984; Clifford, 1993a). Infiltration of fines, particularly clays and silts from suspension, may increase the cohesiveness of the subsurface sediments. Long periods of low flow may assist in developing this structure further by flushing out surficial accumulations of sand, which may act to reduce compaction, and promoting further ingress of clays and silts. On the Rede, although pool subsurface sediments contain less matrix, the matrix itself contains greater proportions of clays and silts in comparison to the riffle matrix (Table 3.3), which may provide a further explanation for the higher θ_c recorded for pools (see section 6.3.5).

Compaction and mobility

Although limited to a single survey, cone penetrometer readings presented in Chapter Three indicated variable compaction throughout the reach. Pool sediments, although coarser than the riffle sediments, were more loosely packed and contained less matrix in the near surface substrate (as found from freeze-cores). However the penetrometer readings could be misleading here. Although the pool lag sediment is more loosely packed at the surface, the clasts are too large to be mobilised and be transported over the negative slope of the pool tail. Critical dimensionless shear stress values for bedload sediment (θ_c) between riffles and pools were significantly different

($p<0.001$), tending to be higher on average for pool sediments (section 6.3.5), due to hiding effects. This has potentially important implications for riffle-pool maintenance, as lower θ_c for riffles would imply that riffles are more easily scoured in comparison to pools (the opposite to that required for riffle maintenance and pool scour). These findings contrast with the empirical data of Sear (1992; 1996) for the North Tyne, and the views of Clifford (1990; 1993b), and would suggest that bed structure differences between riffles and pools do not explain their maintenance on the River Rede. However some of Clifford's (1990) data for the River Quarne support the Rede findings. Clifford suggested that if pool sediments of a given grain size were relatively more easy to entrain than riffle sediments, a larger difference between the grain size curves describing surface and subsurface sediments should occur at pool locations than at riffles. Clifford found this to be the case for only one out of four instances, suggesting that riffle sediments on the Quarne had a lower θ_c in comparison to the pools. Data for the Rede presented in Chapter Three also indicate greater differences between surface and subsurface grain size curves for riffle data (Figure 3.9), supporting the θ_c data obtained from sediment tracing. Some caution must however be given to this interpretation as the Shields criterion (θ_c) calculated using Equation 1.1, only takes into consideration grain size as the resistive force variable, with ρ_s , ρ_w and g being parameters. The effects of bed structure on the resistive force are not considered in the equation itself.

9.4.1 Sediment structure and turbulent flow

Clifford (1993a) claims that turbulent flow maintains riffle-pool morphology through its influence upon differential particle organisation. Clifford suggested that spatial differences in the near-bed turbulence field, arising from incipient riffle-pool topography, create differences in surface sediment entrainment which enhance and maintain the sequence in a form-process feedback mechanism. Clifford (1993a) and Clifford *et al.* (1993) have demonstrated that zones of higher relative form roughness (riffles) possess greater turbulent intensities and flow spectra which are multi-peaked with high frequency components. Zones of lower relative roughness (pools), possess lower turbulent intensities and flow spectra with more dominant low frequency components. These differences in turbulence characteristics are related to sediment transport primarily through surface sediment organisation in a variety of micro-

topographical bedforms (Clifford *et al.*, 1992), and consequently exert a strong influence upon local sediment supply. Buffin-Bélanger and Roy (1998) have shown that pebble clusters may enhance the presence of large-scale flow structures by inducing eddy shedding and the ejection of low-speed fluid into the flow from the separation zone in the lee of the clast. Buffin-Bélanger *et al.* (2000) has further demonstrated the existence of high- and low-speed regions which develop in the flow in the absence of protruding clasts. These wedges have a tendency to self-organise and interact with larger features on the bed such as pebble clusters.

9.5 Site-specificity in riffle-pool sequences and riffle-pool maintenance

It is clear from the literature that a single general model of riffle-pool maintenance does not exist. Several site-specific factors could have an influence on previous workers findings and subsequent model formulation. Table 9.1 lists a range of field studies that have focussed upon riffles and pools, and identifies the characteristics of those sites e.g. channel sinuosity, sediment supply and source, bed slope etc. The model of maintenance, if suggested in the relevant research article, is given in the column labelled 'comments'.

9.5.1 Sinuosity

A number of studies including this investigation, indicate differences in the character of straight and curved riffle-pool reaches. In this study the pool situated on the most sharply curved bend did not show a reversal in mean section velocity, even though tracer data suggested this to occur. Instead pool velocities, as discharge reaches that capable of drowning bar surfaces, either begin to fall, or increase at a lesser rate. This is also a feature noted by Carling (1991) on the River Severn, the effects of which may be attributed to the effects of increased bank roughness. Highest transport rates of fine-grained sediments on the Rede appeared to occur in a pool located on a straight section of channel, suggesting more material was supplied to the straight pool in comparison to the curved pool. This observation may also provide further support for the existence of well developed secondary flow cells and turbulent eddies in curved pools, and suggest more poorly developed three-dimensional flow in straight pools with transport of fines dominated by the primary flow direction. Milne (1982) in contrast has shown pools with a high curvature to collect more fines in comparison to

straighter pools, however it should be noted that this reflects low flow accumulation, and not high flow throughput, as measured on the Rede.

From the information compiled in Table 9.1 it is unclear whether sinuosity has a direct influence upon the occurrence of tractive force reversal. Reversal appears to occur in some straight and sinuous reaches, however is not a universal phenomenon. Keller's (1971) hypothesis of velocity reversal was devised on a straight section of Dry Creek, however he was only able to show equalisation in his data. Both Carling (1991) and Bhowmik and Demissie (1982) were unable to demonstrate a reversal in tractive force for both curved and straight sections. However, Ashworth (1987) and Wilkinson *et al.* (2000) report reversal for straight sections, whilst Andrews (1984) and Petit (1987) report reversal for sinuous reaches. Carling (1991) reported strong three-dimensional flow structures in the meandering reach at Leighton on the River Severn, which masked any trends between shear velocity and discharge. His straight reaches in contrast demonstrated clear trends, with the shear velocity in pools increasing at a faster rate in pools than in riffles.

Three dimensional flow structure

Distinct differences are evident between the three-dimensional flow structure of curved and straight pools (Bathurst, 1979; Teisseyre, 1984). Bathurst (1979) found straight pool cross-sections to be characterised by peaks and troughs in τ that resulted from alternate regions of upwelling and downwelling flow associated with multi-cell, secondary circulations, and for this cross-section pattern to change little with discharge. Teisseyre (1984) describes flow in straight pools with symmetrical cross-sections as either being (i) gradually varied (without a zone of flow separation), or (ii) rapidly varied (with a bottom zone of flow separation). In the first case, graded fine sediment deposits result (possibly explaining the high accumulation in Pool 3). In the second case, the riffle ends with a steep face dipping into the pool. A large bottom zone of flow separation is evident at the front of the slip face. During high flows, downward and backward erosion is dominant. At mean and low flows, the pool fills with gravel eroded from the riffle tail / pool head.

Flow through asymmetrical pools located on bends is always three-dimensional comprising at high flow; (i) spiral vortices (bottom and surficial), (ii) transverse secondary flows, induced by the bottom spiral vortex, (iii) mushroom-like eddies and whirlpools or descending vortices with vertical axis of rotation (Teisseyre, 1984). Spiral vortices are responsible for erosion of the bank and bed, and important agents of transverse sediment transport directed from the outer erosional bank to the inner depositional bank (bar). Skew induced secondary circulation is strongest at medium discharges and can be 10-70% of the primary flow strength, thus capable of substantial sediment mobilisation (Teisseyre, 1984), however at high discharges the primary flow is more dominant (Bhowmik and Stal!, 1978; Bathurst, 1979). Along the inner bank, a zone of flow separation with backflow circulation and independent zones of microturbulence may be present. The positions and the relative magnitudes of τ peaks on bends, change markedly with discharge. τ peaks at bends are associated with a core of maximum velocity and downwelling near the outer bank. Downwelling occurs at the junction between two transverse counter rotating eddies; a main skew induced eddy that rotates towards the point bar, and a smaller eddy that rotates towards the outer bank. The region of highest shear stress tends to be located near to the inner bank/bar at the bend entrance and then crosses towards the outer bank, at or just downstream of the bend apex (e.g. Hooke, 1975; Bridge and Jarvis, 1976). The position of the shear stress peak associated with the core of maximum velocity is influenced by the strength of secondary circulations and the bend arc angle (Bathurst, 1979). When secondary circulations are at their weakest, at low and high flow, the crossover region tends to be located further downstream. Conversely, at medium discharges, the crossover region of high shear stress lies further upstream and closer to the outer bank, due to the increased strength of skew-induced secondary circulation.

Teisseyre (1984) suggests that three dimensional flow strongly influences sediment sorting in pools located on bends. Sediment may be sorted into four fractions; 1) fines may be transported longitudinally in suspension, 2) flat clasts are transported longitudinally via saltation-load on to the pool exit slope, 3) large flat pebbles and cobbles are transported by secondary flow towards the inner bank/bar, via creeping

and saltation, 4) coarsest and spherical clasts are left as a lag, although some large spherical clasts may be transported downstream via rolling.

9.5.2 Sediment supply and source

The relative differences between riffle and pool grain size is determined by supply of sediment from upstream, local supply and hydraulic character (Table 9.1). Grain size can alter local roughness, thus influencing velocity (Carling and Wood, 1994). The supply of sediment has implications for riffle-pool maintenance. In high supply scenarios, where transport capacity of the pools is exceeded, there is a tendency for pools to fill with sediments, and for a reduction in the amplitude of the riffle-pool sequence. This can also lead to a reduction in the cross-sectional area, with implications for mean_velocity and the continuity of mass principle (Clifford and Richards, 1992). Conversely, low supply conditions are more suited to maintaining riffle-pool morphology.

In catchments with a high supply of fine sediment pools tend to fill with fine sediment drapes during waning flows. This is a particular feature of catchments in California, many of which have been disturbed by logging activities (e.g. Keller, 1971; Lisle, 1982; Jackson and Beschta, 1982; Lisle and Hilton, 1992). Streams with a lower fine sediment supply such as the Rede in this investigation, tend to exhibit coarser pools at low discharge (e.g. Petit, 1987; Ashworth, 1987; Keller and McDonald, unpublished; Thompson *et al.*, 1999). The coarse lag gravel is often covered by a drape of fines that accumulates during low flows (e.g. Andrews, 1984) which often leads to pools being reported as being finer than adjacent riffles.

Most studies, including the present investigation, that report coarse lag material suggest that this originates from local input from scoured banks, and not from upstream (e.g. Gilbert, 1914; Hack, 1957; Keller, 1982; Ashworth, 1987; Keller and McDonald, unpublished). These studies also report that the coarse material being re-worked is non-fluvial in origin, e.g. often a relict deposit of the Pleistocene such as boulder clay, or fluvio-glacial outwash (Table 9.1). Studies do exist however, which have shown that coarse clasts can be fed into pools and deposited from upstream sources (e.g. Haschenburger and Church, 1998). Further work is needed to identify

the possible causes of these differences in sediment routing and implications to riffle-pool maintenance.

9.5.3 Mode of pool formation / influence of channel obstructions

Both the formation and maintenance of pools is strongly influenced by three dimensional flow structures initiated by obstructions in the channel such as boulders and log jams (Table 9.1). Clifford (1993b) describes their role in the formation of the riffle-pool unit, whilst Thompson *et al.* (1999) describes their role in the maintenance of the unit. Obstructions to the flow are very common in heavily forested catchments, where the riparian zone is not managed or cleared. In Washington, US, for example, Montgomery *et al.* (1995) separated reaches where pools had been formed without constrictions (PR) from those which had been 'forced' by an obstruction such as a log jam (fPR). They found that the normal spacing of $2\pi w$ commonly reported for pool-pool spacing was not applicable to river reaches where pools have been forced, where instead the spacing tends to be much shorter (Table 9.1). A smaller pool-pool spacing also appears evident in channels with large boulders in the bed, where pools are also spaced at irregular intervals (e.g. Thompson *et al.*, 1999).

Pool-riffle morphology can be formed and maintained where channel obstructions initiate turbulent flow structures, and alter cross-section areas sufficiently to cause stage-dependent variations in tractive force between pools and riffles (Thompson *et al.*, 1999). However, many streams do not have large obstructions available (Table 9.1), and therefore their formation and maintenance must in part be due to the natural formation of macro-scale eddies in open channel flow (Yalin, 1971; Richards, 1976; Thompson *et al.*, 1999). Whether obstructions influence formation and maintenance of riffle-pool morphology on the Rede is however questionable.

9.6 Riffle-pool maintenance; the Rede and other sites

For the Rede, riffle-pool maintenance is largely explained by tractive force reversal. The model shown in Figure 9.9 does however include bed structure effects, which although were not dominant on the Rede, may operate in different situations depending upon the site specific variables discussed in section 9.5. For the Rede one

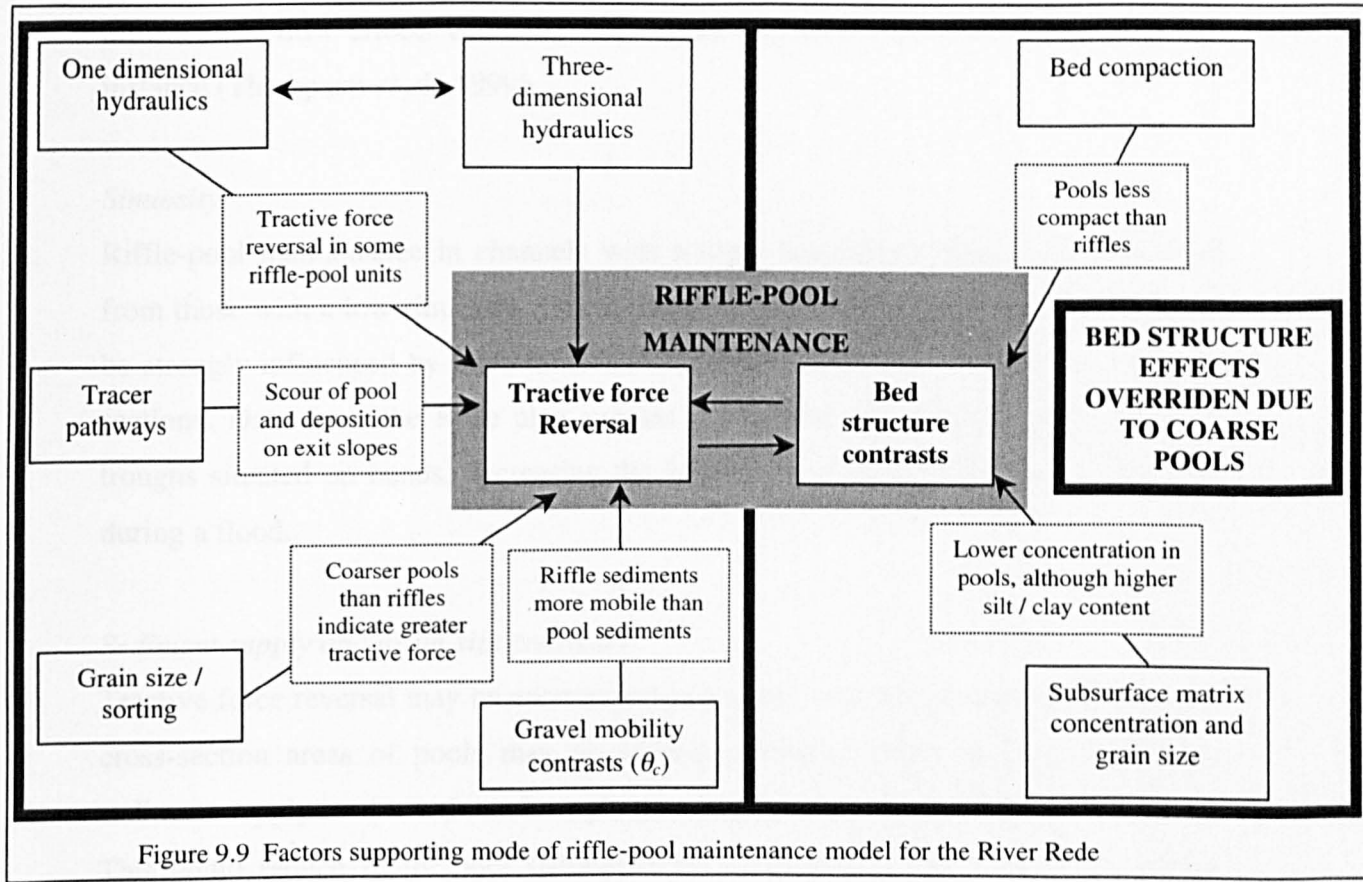


Figure 9.9 Factors supporting mode of riffle-pool maintenance model for the River Rede

dimensional hydraulic data in the form of boundary shear stress and mean section velocity provide support for reversal, although this does not happen for every riffle-pool sequence, and for the ones that it does it tends to be marginal in nature. Pools situated on straight sections of channel may experience enhanced reversal due to a reduction in cross-section area, as sediment passes through the section. However pools on bends do not appear to have gravel fed in to them. Pools with smaller cross-section areas are therefore less likely at high flow, hence a reversal in tractive force may be dependent upon the existence and strength of three dimensional flow structures (not quantified in this investigation). Although deposition of tracers on pool exit slopes may also provide evidence of local velocity reversal in pools situated on bends, one dimensional hydraulic data fail to support this in some instances. Even though pools are less compact than riffles, pool scour in these situations is unlikely to reflect bed structure and mobility contrasts between riffle and pool sediments. This is due to strong shielding effects induced by the coarse immobile lag clasts in the pools, which results in pool bedload sediment being less mobile than riffle bedload. The occurrence of coarser pools than riffles alone provide further support for tractive force

reversal, and may even be a contributory factor (Carling and Wood, 1994). Three dimensional flow effects could be responsible for reversal in tractive force in this instance (Thompson *et al.*, 1999).

Sinuosity

Riffle-pool maintenance in channels with a high sinuosity is likely to be different from those with a low sinuosity. Tractive force in pools situated on bends is likely to be strongly influenced by three-dimensional flow in comparison to pools on straight sections. Data from the Rede also suggest a tendency for sediment to avoid pool troughs situated on bends, decreasing the likelihood of cross-section area reduction during a flood.

Sediment supply and grain size contrasts

Tractive force reversal may be encouraged in streams with a high sediment supply as cross-section areas of pools may be reduced during a flood. Streams with high sediment supply tend to exhibit finer pools with low compaction and grain roughness. This could reduce θ_c for pool sediments, hence increasing the importance of bed structure contrasts in riffle-pool maintenance. However, structural contrasts between riffle and pools may not be as well defined in conditions of high supply, unless there are long periods of low flow, to re-distribute fines. Local inputs, like those shown on the Rede may have a significant influence upon riffle-pool maintenance. Bed structure contrasts may also be more significant in maintaining riffle-pool morphology in streams which can transport every grain in their bed, rather than re-working non-fluvial deposits. In this situation pools are likely to be finer and less compact than riffle sediments. Grain size contrasts between riffles and pools influence grain roughness. Coarser pools may encourage tractive force reversal. This situation is likely to be found in supply limited streams which are re-working coarse bank deposits (e.g. Pleistocene boulder clays).

Flow regime

The magnitude and frequency of discharge is critical in maintaining the riffle-pool unit. Riffles and pools are quasi-equilibrium bedforms reflecting the magnitude and frequency of hydraulic events capable of sediment transport. A change in hydraulic

regime is likely to result in disturbance to the riffle-pool unit. Bankfull floods are responsible tractive force reversal, and transport the most sediment from riffle to riffle. However the Rede data suggests medium flows may be important in scouring pools and depositing sediment on exit slopes, possibly due to well developed three-dimensional flow effects. The length of time between flows is also important in developing bed structure. Insufficient periods of low flow between flood peaks is likely to result in a homogenous structure between riffles and pools; maintenance in this instance is likely to rely more on tractive force reversal than bed structure contrasts.

9.6 Summary and fulfilment of study objectives

This study has provided a detailed set of data concerning the morphology, hydraulics, sedimentology and sediment transport processes operating through a riffle-pool sequence. The interrelationship between these various elements and their influence upon riffle-pool maintenance has been investigated. This study initially set out to improve current understanding of riffle-pool maintenance and sediment sorting processes in upland gravel bed rivers. Surface sediments of the pools tended to be coarser than those found on the riffles, which was contrary to the majority of published studies (see Table 1.1). An examination of Keller's reversal hypothesis provided convincing support for a reversal in tractive force on the Rede, which suggests that the observed coarseness of the pools may reflect both sediment supply and hydraulic character at high discharge. Tracer data provided further clues to the reasons behind the observed sorting patterns. Sediment traps located on areas of low relative form roughness on straight sections of channel consistently recorded greater accumulations of coarser fines in comparison to zones of higher form roughness. Although few data were available for pools, the implication was that pools should have the greatest transport rates of fine bedload at high flow. As the pool beds are clean of fines at low flow, it appears that transport capacity exceeds supply in the later stages of flood events, or transverse secondary flow directs fines towards bar edges. Gravel showed little evidence of being routed into pool troughs, and showed a preference for deposition on bar edges and tops. Fresh material was introduced to the channel through scour of the pool banks and bed. Riffle to riffle / bar hopping of sediments appears to operate at flows close to bankfull, supporting Jackson and Beschta's (1982) model of Phase 2 transport, however the gravel does not appear to

be routed through the trough of the pools as their model suggests, possibly due to the effects of three dimensional flow structures which are most well developed at medium discharges (Bathurst, 1979; Teisseyre, 1984). The bank materials on the Rede are composed of boulder clay / alluvium, some of which appears too coarse for the contemporary flows to mobilise. After bank collapse, the finer material is flushed away leaving behind a coarse lag deposit. Sand tracing and trapping demonstrate a large sand throughput in the Rede channel, but also show that majority of this material is stored on bar surfaces rather than being winnowed into pools during low flow.

Tracer data also provided useful information regarding initial motion criteria. Pools tended to have higher θ_c in comparison to riffles, suggesting that sediments are more difficult to mobilise in the pools. This reflects greater hiding effects caused by the coarser nature of the pool lag sediments in comparison to the riffle surface, and higher silt and clay concentrations in the pool matrices. Pool tracer clasts tended not to be transported as far as those situated on riffles, further supporting this finding. However, compaction readings taken in the pools using a penetrometer suggested the coarse pool lag to be more loosely packed in comparison to the riffles. Although this may act to reduce θ_c the lag grains are too coarse to be transported up the steep negative pool exit slope. Any smaller clasts that do find their way into the pool, e.g. through bank collapse may be sheltered by the coarse lag grains.

Hydrograph character and riffle-pool maintenance

Hydrograph character is likely to be very important to the maintenance of riffle-pool morphology. An analysis of tracer pebble movement through the Rede riffle-pool sequence revealed the importance of flood magnitude and duration in determining scour and deposition loci, and thus morphological change. The slight upstream migration of riffles in the Rede study reach between June 1996 and January 1998 may reflect the contemporary flow and sediment supply regime (Chapter Eight). An increase in the frequency and/or duration of half to two-thirds bankfull flows, would provide conditions of enhanced secondary flow and scour towards the head of the pool (Bathurst, 1979) and would result in exit slope deposition. If this was accompanied by a reduced frequency and/or duration of bankfull and overbank flows (required to scour riffle heads), headward migration of the riffle-pool unit may result.

The stability of the riffle-pool morphology would therefore be sensitive to any changes in flow character, for example those induced by flow regulation, land-use change or climate change.

9.7 Macro-scale turbulent flow structures and riffle-pool maintenance: Future and ongoing research

This study has provided a one-dimensional analysis of flow and sediment transport through riffle-pool morphology, due to restrictions on equipment and funding. The data presented does therefore have some limitations. Future studies should aim to identify the significance of macro-scale turbulent flow structures upon riffle-pool formation and maintenance. Thompson *et al.* (1996; 1999) has recently revised the velocity reversal hypothesis to include the effects of re-circulating eddies caused by an obstruction in the pool. Clifford (1993a) has also extended the Yalin-Richards macro-scale flow structure model of pool formation to include the influence of large obstacles on the bed. Macro-scale turbulent flow structures such as these may explain locally high velocities and scour, in situations where pool cross-section section average velocity does not exceed the riffle, for example in Pool 1 on the Rede. Bathurst (1979) has described stage variation in the position of maxima associated with secondary flow cells and a high velocity vortex. It is uncertain what effects a change to flood hydrograph character would have upon three-dimensional flow structure, sediment sorting, and riffle-pool maintenance. Some recent field studies have demonstrated the existence of macro-scale flow structures that scale on multiples of channel width (e.g. Clifford, 1993a; Carling and Orr, 2000, see section 1.3.3). However measurements undertaken thus far have only been limited to flows up to around half-bankfull, and hence macro-scale flow structure which may be responsible for riffle-pool formation has not yet been effectively measured in natural channels; the flow structures which have been measured may therefore relate more to maintenance processes.

Data presented in this investigation has argued in support of Keller's reversal hypothesis as a mechanism of riffle-pool maintenance. A modification of existing riffle-pool maintenance theory may be presented in the light of the data presented in this thesis. Reversal in tractive force is necessary for the development of pools, as is the periodic scour of riffle heads, in order to prevent significant upstream migration.

Scour and deposition patterns are shown to be sensitive to flow character and thus the quasi-equilibrium riffle-pool form may potentially be disrupted by a change in flow or sediment supply. The revision of the riffle-pool maintenance model provided in section 9.3.2 still requires testing more fully, possibly by using active tracing techniques (e.g. McEwan and Habersack, 2000), in conjunction with a thorough assessment of the influence of three-dimensional flow structures upon riffle-pool maintenance. This would prove whether material is preferentially routed over bars or through pools. Further work should also concentrate on validation of alternative hypotheses such as Wilkinson *et al's.* (2000) sediment continuity mechanism (see section 1.3.4). This is part of continuing research on the River Rede.

References

Acornley, R.M. and Sear, D.A. 1999. Sediment transport and siltation of brown trout (*Salmo trutta* L.) spawning gravels in chalk streams. *Hydrological Processes*, **13**, 447-458.

Agrawal, Y. C., McCave, I. N. and Riley, J. B. (1991) Laser diffraction analysis, in Syvitski, J. P. M. *Principles, methods, and application of particle size analysis*, Chapter 9, 119-128.

Allan, A.F. and Frostick, L.E. 1999. Framework dilation, winnowing, and matrix particle size distribution: the behaviour of some sand-gravel mixtures in a laboratory flume. *Journal of Sedimentary Research*, **69**, 20-26.

Allen, J.R.L. 1983. Gravel overpassing on humpback bars supplied with mixed sediment: examples from the lower Old Red Sandstone, Southern Britain. *Sedimentology*, **30**, 285-294.

Andrews, E. D. 1983. Entrainment of gravel from naturally sorted riverbed material. *Geological Society of America Bulletin*, **95**, 371-378.

Andrews, E. D. and Parker, G. 1987 Formation of a coarse surface layer as the response to gravel mobility. In C.R. Thorne, J.C. Bathurst, and R.D. Hey (eds.), *Sediment Transport in Gravel Bed Rivers*. John Wiley and Sons, Chichester, 269-300.

Andrews, E.D. 1979. Scour and fill in a stream channel: East Fork River, Western Wyoming, *United States Geological Survey Professional Paper*, **1117**.

Andrews, E.D. and Erman, D.C. 1986. Persistence in the size distribution of surficial bed material during an extreme snowmelt flood. *Water Resources Research*, **22**(2), 191-197.

Archer, D. 2000. Indices of flow variability and their use in identifying the impact of land use changes, *BHS 7th National Hydrology Symposium*, Newcastle, 2000.

Arkell, B. 1985. Magnetic tracing of river bedload. Unpublished PhD thesis. University of Liverpool.

Arkell, B., Leeks, G., Newson, M. and Oldfield, F. 1983. Trapping and tracing: some recent observations of supply and transport of coarse sediment from upland Wales. In Collinson, J.D and Lewin, J. (eds) *Modern and Ancient Fluvial Systems*, Special Publication of the International Association of Sedimentologists, **6**, 117-129.

Ashworth, P.A. and Ferguson, R.L. 1989. Size-selective entrainment of bed load in gravel bed streams. *Water Resources Research*, **25**, 627-634.

Ashworth, P.J. 1987. Bedload transport and channel change in gravel-bed rivers, PhD thesis, University of Stirling.

Bathurst, J. C. 1982. Theoretical aspects of flow resistance. In Hey, R.D., Bathurst, J. C. and Thorne, C. R. (eds), *Gravel Bed Rivers: Fluvial Processes, Engineering and Management*, Wiley, Chichester, 83-107.

Bathurst, J.C. 1979. Distribution of boundary shear stress in rivers. In Rhodes, D.D. & Williams, G.P. (eds) *Adjustments to the fluvial system*, Dubuque, Iowa, Kendall Hunt, pp 95-116.

Beschta, R.L. and Jackson, W.L. 1979. The intrusion of fine sediment into a stable gravel bed. *Journal of the Fisheries Research Board of Canada*, **36**, 204-210.

Bhowmik, N.G. and Demissie, M. 1982a, Bed material sorting in pools and riffles. *Journal of Hydraulic Engineering, American Society of Civil Engineers*, **108**, 1227-1231.

Bhowmik, N.J. and Stall, J.B. 1978. Hydraulics of flow in the Kaskasia River. In American Society of Civil Engineers Proceedings, Special conference on Verification of Mathematical and Physical models in Hydraulic Engineering, University of Maryland, August 9-11, p 79-86.

Bjornn, T. C., Brusven, M. A., Molanau, M. P., Millagan, J., Klamt, R., Chaco, E. and Schaye, C. 1977. Transport of granitic sediment in streams and its effects on insects and fish. *University of Idaho Forest Wild Range Experimental Station Bulletin*, **12**, 43pp.

Blatt, H., Middleton, G. and Murray, R. 1980. Origins of sedimentary rocks (2nd ed). Englewood Cliffs, N. J., Prentice Hall, 782p.

Bloomfield, P. 1976. *Fourier analysis of time-series: an introduction*, John Wiley and Sons, New York, 258pp.

Bowman, D., 1977. Stepped-bed morphology in arid gravelly channels. *Geological Society of America Bulletin*, **83**, 291-298.

Box, G.E.M. and Jenkins, G.M. 1976. *Time-series analysis-forecasting and control*, Holden-Day, San Francisco, 553pp.

Bray, D. I. and Church, M. 1980. Armoured versus paved gravel beds. *Journal of the Hydraulics Division of the American Society of Civil Engineering*, **106**, 1937-1940.

Bray, D.I. 1980. Evaluation of effective boundary roughness for gravel bedded rivers. *Canadian Journal of Civil Engineering*, **7**, 392-397.

Brayshaw, A.C., Frostick, L.E. and Reid, I., 1983. The hydrodynamics of particle clusters and sediment entrainment in coarse alluvial channels. *Sedimentology*, **30**, 137-143.

Bridge, J.S. and Jarvis, J. 1976. Flow and sedimentary processes in the meandering River South Esk, Glen Cova, Scotland. *Earth Surface Processes and Landforms*, **1**, 303-336.

Brookes, A. 1990. Restoration and enhancement of engineered British river channels: some European experiences. *Regulated Rivers Research and Management*, **5**, 45-56.

Brookes, A. 1992. Recovery and restoration of some engineered British river channels. In Boon, P.J., Calow, P. and Petts, G.E. (eds) *River Conservation and Management*, John Wiley and Sons, Chichester, 337-352

Brush, L.C. 1961. Drainage basins and flow characteristics of selected streams in central Pennsylvania. *US Geological Survey Professional Paper*, **282-F**, 17pp.

Buffin-Bélanger, T. and Roy, A.G. 1998. The effects of a pebble cluster on the turbulence structure of a depth-limited flow in a gravel-bed river. *Geomorphology*, **249-267**.

Buffin-Bélanger, T., Roy, A.G. and Kirkbride, A.D. 2000. On large-scale flow structures in a gravel-bed river. *Geomorphology*, **32**, 417-435.

Buffington, J.M. and Montgomery, D.R. 1997. A systematic analysis of eight decades of incipient motion studies, with special reference to gravel-bedded rivers, *Water Resources Research*, **33**, 1993-2029.

Buffington, J.M. and Montgomery, D.R. 1999. Effects of sediment supply on surface textures of gravel-bed rivers. *Water Resources Research*, **35**, 3523-3530.

Buffington, J.M., Dietrich, W.E. and Kirchner, J.W. 1992. Friction angle measurements on a naturally formed gravel streambed: implication for critical boundary shear stress. *Water Resources Research*, **28**, 411-425.

Burner, C. J. 1951. Characteristics of spawning nests of Columbia River salmon. *U.S. Fish and Wildlife Service Bulletin*, **61**, 97-110.

Butler, P.R. 1977. Movement of cobbles in a gravel-bed stream during a flood season. *Geological Society of America Bulletin*, **88**, 1072-1074.

Campbell, A.J. and Sidle, R.C. 1985. Bedload transport in a pool-riffle sequence of a coastal Alaska stream. *Water Resources Bulletin*, **21**, 579-590.

Carling P.A. and Reader N.A. 1981. A freeze-sampling technique for coarse river bed material. *Sedimentary Geology*, **29**, 233-239.

Carling P.A. and Reader, N.A. 1982. Structure, Composition and bulk properties of upland stream gravels. *Earth Surface Processes and Landforms*, **7**, 349-365.

Carling, P.A. 1981. Armoured versus paved gravel beds, Proceedings of the American Society of Civil Engineers. *Journal of the Hydraulics Division*, **107**, 1117-1118.

Carling, P.A. 1983b. Threshold of coarse sediment transport in broad and narrow rivers. *Earth Surface Processes and Landforms*, **8**, 1-18.

Carling, P.A. 1984. Deposition of fine and coarse sand in an open-work gravel bed. *Canadian Journal of Fisheries and Aquatic Sciences*, **41**, 263-270.

Carling, P.A. 1987. Bed stability in gravel streams with reference to stream regulation and ecology. In Richards, K (ed), *River Channels: environment and process*, Basil Blackwell Ltd.

Carling, P.A. 1988. The concept of dominant discharge applied to two gravel-bed streams in relation to channel stability thresholds. *Earth Surface Processes and Landforms*, **13**, 355-367.

Carling, P.A. 1991. An appraisal of the velocity-reversal hypothesis for stable pool-riffle sequences in the river Severn, England. *Earth Surface Processes and Landforms*, **16**, 19-31.

Carling, P.A. and Glaister, M.S. 1987. Rapid deposition of sand and gravel mixtures downstream of a negative step: the role of matrix infilling and particle-overpassing in the process of bar accretion. *Journal of the Geological Society, London*, **144**, 543-551.

Carling, P.A. and MacCahon, C. P. 1987. Natural siltation of brown trout (*Salmo trutta* L.) spawning gravels during low-flow conditions. In Craig, J.F. and Kemper, T.B. (eds), *Regulated Streams*, Plenum, 229-224.

Carling, P.A. and Orr, H. 2000. Morphology of riffle-pool sequences in the river Severn, England. *Earth Surface Processes and Landforms*, **25**, 369-384.

Carling, P.A. and Wood, N. 1994. Simulation of flow over pool-riffle topography: a consideration of the velocity reversal hypothesis. *Earth Surface Processes and Landforms*, **19**, 319-332.

Carling, P.A. Kelsey, A. and Glaister, M.S. 1992. Effect of bed roughness, particle shape and orientation on initial motion criteria. In Thorne, C.R., Bathurst, J.C. and Hey, R.D. (eds) *Sediment transport in Gravel-bed rivers*, Chichester, Wiley, 23-37.

Carling, P.A., Orr, H. and Kelsey, A. unpublished. The dispersion of magnetite bedload tracer across a gravel point-bar and the development of heavy-mineral placers.

Cherkauer, D.S. 1973. Minimisation of power expenditure in a riffle-pool alluvial channel. *Water Resources Research*, **9**, 1613-1628.

Church, M. 1972. Baffin Island Sandurs: A study of Arctic fluvial processes. *Canada Geological Survey Bulletin*, **216**, 89-93.

Church, M.A. and Hassan, M.A. 1992 Size and distance of ravel of unconstrained clasts on a streambed. *Water Resources Research*, **28**, 299-303.

Church, M.A., Hassan, M.A. and Wolcott, J.F. 1998. Stabilising, self organised structures in gravel-bed stream channels: field and experimental observations. *Water Resources Research*, **34**, 3169-3179.

Church, M.A., McClean, D.G. & Wolcott, J.F. 1987. River bed gravels: Sampling and analysis. In C.R. Thorne, J.C. Bathurst and R.D. Hey (Editors), *Sediment Transport in Gravel-bed Rivers*. John Wiley & Sons Ltd., Chichester, pp. 43-79.

Church, M.A., Wolcott, J.F. and Fletcher, W.K. 1991. A test of equal mobility in fluvial sediment transport: behaviour of the sand fraction. *Water Resources Research*, **27**, 2941-2951.

Clifford, N.J. 1990. The formation, nature and maintenance of riffle-pool sequences in gravel-bedded rivers, *Unpublished PhD thesis*, University of Cambridge.

Clifford, N.J. 1993a. Formation of riffle-pool sequences: field evidence for an autogenetic process. *Sedimentary Geology*, **85**, 39-51.

Clifford, N.J. 1993b. Differential bed sedimentology and the maintenance of riffle-pool sequences. *Catena*, **20**, 447-468.

Clifford, N.J. and Richards, K.S. 1992. The reversal hypothesis and the maintenance of riffle-pool sequences: a review and field appraisal, in Carling, P.A. and Petts, G.E. (eds), *Lowland Floodplain Rivers: Geomorphological Perspectives*, John Wiley and Sons Ltd, 43-70.

Clifford, N.J. Hardisty, J., French, J.R. and Hart, S. 1993. Downstream variation in bed material characteristics: a turbulence controlled form-process feedback mechanism. In Bristow, C. and Best, J. (eds) Braided Rivers: form. Process and economic significance. Geological Society Special Publication.

Clifford, N.J., Richards, K.S. and Robert, A. 1992. The influence of microform bed roughness elements on flow and sediment transport in gravel-bed rivers- comment. *Earth Surface Processes and Landforms*, **17**, 529-534.

Crickmore, M. J. 1967. Measurement of sand transport in rivers with special reference to tracer methods. *Sedimentology*, **8**, 175-228.

Davey, G.W., Doeg, T.J. and Blythe, J.D. 1987. Change in benthic sediment in the Thompson River, Victoria during construction of the Thompson Dam. *Regulated Rivers Research and Management*, **1**, 71-84.

Dietrich, W.E., Kirchner, J.W., Ikeda, H. and Iseya, F. 1989. Sediment supply and the development of the coarse surface layer in gravel-bed rivers. *Nature*, **340**, 215-217.

Dietrich, W.E. and Whiting, P. 1989. Boundary shears tress and sediment transport in river meanders of sand and gravel. In Ikeda, H. and Parke, G. (eds) *River Meandering*. *Water Resources Monograph*, **12**, Washington DC: American Geophysical Union, 1-50.

Diplas, P 1987. Bedload transport in gravel-bed streams. Proceedings of the American Society of Civil Engineers. *Journal of Hydraulic Engineering*, **113**, 277-293

Dolling, R. K. 1968. Occurrence of pools and riffles: an element in the quasi-equilibrium state of river channels. *Ontario Geography*, **2**, 3-11.

Drake, T.G., Shreve, R.L., Dietrich, W.E., Whiting, P.J. and Leopold, L.B. 1988. Bedload transport of fine gravel observed by motion-picture photography. *Journal of Fluid Mechanics*, **192**, 193-217.

Dury, G.H. 1970. A re-survey of part of the Hawkesbury River, New South Wales, after one hundred years. *Australian Geographical Studies*, **8**, 121-132.

Einstein, H. A. 1968. Deposition of suspended particles in a gravel bed. *Journal of the Hydraulics Division, ASCE*, **94**, 1197-1205.

Einstein, H.A. 1937. Bedload transport as a probability problem (in German), PhD. Dissertation. Eidgenoess. Tech. Hochsch., Zurich, Switzerland. (English translation by Sayre, W.W., Sedimentation, Shen, H.W. (ed), Appendix C, Shen, H.W., Fort Collins, Colorado, 1972)

Ergenzinger, P. and Conrady, J. 1982. A new tracer technique for measuring bedload in natural channels. *Catena*, **9**, 77-80.

Everts, C.H. 1973. Particle overpassing on flat granular boundaries. *Journal of Waterways, Harbours & Coastal Engineering Division ASCE*, **99**, 425-438.

Fenton, J.D. and Abbott, J.E. 1977. Initial movement of grains on a streambed: the effect of relative protrusion. *Proceedings of the Royal Society*, **352A**, 523-537.

Ferguson, R.I. 1986. River loads underestimated by rating curve. *Water Resources Research*, **22**, 74-76.

Ferguson, R.I. and Wathen, S.J. 1998. Tracer-pebble movement along a concave river profile: virtual velocity in relation to grain-size and shear stress. *Water Resources Research*, **34**, 2031-2038.

Folk, R.L. 1974. Petrology of sedimentary rocks. Hemphill, London.

Fordham, C. E. 1989. The influence of sedimentary structures and facies on the fluid flow (permeability) in the Fell Sandstones, Northumberland. Unpublished M.Phil thesis, dept of Geology, University of Newcastle upon Tyne.

Frost, D.V. and Holliday, D.W. 1980. Geology of the country around Bellingham. Memoir for 1:50 000 Geological Sheet 19. HMSO, London, 112p.

Frostick, L.E. Lucas, P.M. and Reid, I. 1984. The infiltration of fine matrices into coarse-grained alluvial sediments and its implications for stratigraphic interpretation. *Journal of the Geological Society of London*, **141**, 955-965.

Garde, R.J. and Ranga Raju, K.G. 1977. *Mechanics of sediment transportation and alluvial stream problems*, Wiley Eastern Ltd, 483pp.

Gessler, J. 1971. Beginning and ceasing sediment motion. In Shen, H.W. (ed) *River Mechanics*, Fort Collins, CO, Colorado State University, 7: 1-7:22.

Gilbert, G.K. 1914. Transportation of debris by running water. *U.S. Geological Survey Professional Paper*, **294-B**.

Gomez, B. 1983a. Temporal variations in bedload transport rates: the effect of progressive bed armouring, *Earth Surface Processes and Landforms*, **8**, 41-54.

Gomez, B. 1984. Typology of segregated (armoured/paved) surfaces: some comments, *Earth Surface Processes and Landforms*, **9**, 19-24.

Gomez, B. 1995. Bedload transport and changing grain size distributions. In Gurnell, A. and Petts, G.E. (eds), *Changing river channels*, Chichester, Wiley, 177-199.

Gordon, N.D., McMahon, T.A. and Finlayson, B.L. 1992. *Stream hydrology: an introduction for ecologists*, Chichester, Wiley.

Gottesfeld, A.S. 1997. Bedload transport during salmon spawning and floods, Stuart-Takla experimental watersheds, British Columbia, Canada. *Supplementi di geografia fisica dinamica quaternaria - Supplemento III* (1997), Fourth International conference on Geomorphology, p185.

Grass, A.J. 1971. Structural features of turbulent flow over smooth and rough boundaries. *Journal of Fluid Mechanics*, **50**, 233-255.

Greenwood, M. and Richardo-Coulet, 1996. Aquatic invertebrates, in Petts, G. E. & Amoros, C. (eds) *Fluvial Hydrosystems*, Chapman and Hall, London, 137-166.

Hack, J.T. 1957. Studies in longitudinal stream profiles in Virginia and Maryland. USGS Prof Paper 294B.

Hammond, F.D.C., Heathershaw, A.D. and Langhorne, D.N. 1984. A comparison between Shield's threshold and the movement of loosely packed gravel in a tidal channel. *Sedimentology*, **31**, 51-62.

Haschenburger, J. K. and Church, M.A. 1998. Bed material transport estimated from the virtual velocity of sediment. *Earth Surface Processes and Landforms*, **23**, 791-808.

Hassan, M. A. and Church, M. 1992. The movement of individual grains on the streambed. In Billi, P., Hey, R.D., Thorne, C.R. and Tacconi, P. (eds), *Dynamics of gravel bed rivers*, John Wiley and Sons, Chichester.

Hassan, M. A. and Church, M. 1994. Vertical mixing of coarse particles in gravel bed rivers: a kinematic model. *Water Resources Research*, **30**, 1173-1185.

Hassan, M.A. 1988. Bed material and bedload movement in two ephemeral streams and its relationship to the transport mechanism of the scour layer, Ph.D. thesis, The Hebrew University of Jerusalem, 203pp.

Hassan, M.A. Schick, A.P. and Laronne, J.B. 1984. The recovery of flood dispersed coarse sediment particles. A three dimensional magnetic tracing method. *Catena supplement*, **5**, Braunschweig, 153-162.

Hassan, M.A., Church, M. and Ashworth, P.J. 1992. Virtual rate and mean distance of travel of individual clasts in gravel-bed streams. *Water Resources Research*, **27**, 503-511.

Hey, R.D. 1975. Design discharges for natural channels, in Hey, R.D. and Davies, J.D. (eds) *Science and Technology in Environmental Management*, Farnborough, Saxon House, 73-88.

Hey, R.D. 1976. Geometry of River meanders, *Nature*, **262**, 482-484.

Hey, R.D. and Thorne, C.R. 1983. Accuracy of surface samples from gravel bed material. *Proceedings of the American Society of Civil Engineers, Journal of Hydraulic Engineering*, **106**, 842-851.

Hirsch, P. J. and Abrahams, A. D. 1984. The properties of bed sediments in pools and riffles. *Journal of Sedimentary Petrology*, **51**, 757-760.

Hooke, J. 1975. Distribution of sediment transport and shear stress in a meander bend. *Journal of Geology*, **83**, 543-565.

Hooke, J. 1977. The distribution and nature of changes in river channel patterns: the example of Devon. In Gregory, K.J. (ed) *River Channel Changes*, Chichester, Wiley, pp 265-280.

Hughes, N. 1992. Heavy mineral distribution in upland gravel-bed rivers. *Unpublished PhD Thesis*, Department of Geography, Loughborough University.

Hughes, N., Coats, J.S. and Petts, G.E. 1995. Local variability of gold in active stream sediments. *Journal of Geochemical Exploration*, **54**, 137-148.

Institute of Hydology 1998. Provision of flow data for the River Rede at Rede Bridge.

Jackson, W.L and Beschta, R.L 1982. A model of two-phase bedload transport in an Oregon Coast Range stream. *Earth Surface Processes and Landforms*, **7**, 517-527.

Johnston, C.E., Andrews, E.D. and Pitlick, J. 1998. In situ determinaton of particle friction angles of fluvial gravels. *Water Resources Research*, **34**, 2017-2030.

Keller, E. A. 1971a. Areal sorting of bed-load material: the hypothesis of velocity reversal. *Geological Society of America Bulletin*, **82**, 753-756.

Keller, E. A. 1972. Areal sorting of bed-load material: the hypothesis of velocity reversal. A reply. *Geological Society of America Bulletin*, **83**, 915-918.

Keller, E. A. 1978. Pools, riffles and channelisation. *Environmental Geology*, **2**, 119-127.

Keller, E.A. 1970. Bedload movement experiments, Dry Creek, California. *Journal of Sedimentary Petrology*, **40**, 1339-1344.

Keller, E.A. 1982. Bed material sorting in pools and riffles. *Journal of the Hydraulics Division, American Society of Civil Engineers*, **109**, 1243-1245.

Keller, E.A. and Florsheim, J.L. 1993. Velocity-reversal hypothesis: a model approach, *Earth Surface Processes and Landforms*, **18**, 733-740.

Keller, E.A. and Melhorn, W.N. 1978. Rhythmic spacing and origin of pools and riffles. *Geological Society of America Bulletin*, **89**, 723-730.

Kellerhals, R. and Bray, D.I. 1971. Sampling procedures for coarse fluvial sediments. *Journal of the Hydraulics Division*, **97 HY8**, 1165-1180.

Kirchener, J.W., Dietrich, W.E. Iseya, F. and Ikeda, H. 1990. The variability of critical stress, friction angle and grain protrusion in water-worked sediments. *Sedimentology*, **37**, 647-672.

Klingeman, P.C. and Emmett, W.W. 1982. Gravel bedload transport processes. In: R.D. Hey, J.C. Bathurst and C.R. Thorne (Editors), *Gravel-bed Rivers*. John Wiley and Sons, Chichester, pp. 141-179..

Komar, P.D. 1987. Selective grain entrainment by a current from a bed of mixed sizes: a reanalysis. *Journal of Sedimentary Petrology*, **57**, 203-211.

Komar, P.D. 1989. Flow competence evaluations of hydraulic parameters of floods: an assessment of the technique. In Bevan, K. and Carling, P.A., (eds) *Floods: hydrological, sedimentological and geomorphological implications*, Chichester, Wiley, 107-134.

Komar, P.D. 1996. Entrainment of sediments from deposits of mixed grain sizes and densities. In Carling, P.A. and Dawson, M.R. (eds) *Advances in fluvial dynamics and stratigraphy*, Chichester, Wiley, 128-181.

Komar, P.D. and Carling, P.A. 1991. Grain sorting in gravel bed streams and the choice of particle sizes for flow competence evaluatons, *Sedimentology*, **38**, 489-502.

Komar, P.D. and Shih, S.M. 1992. Equal mobility versus changing bedload grain sizes in gravel-bed streams. In Billi, P. Hey, R.D., Thorne, C.R. and Tacconi, P. (eds) *Dynamics of gravel bed rivers*, Chichester, Wiley, 73-93.

Komar, P.D. and Wang, C. 1984. Processes of selective grain transport and the formation of placers on beaches, *Journal of Geology*, **92**, 637-655.

Kondolf, G.M. and Micheli, E.R. 1995. Evaluating stream restoration projects, *Environmental Management*, **19**, 1-15.

Kuhnle, R.A. 1993a. Incipient motion of sand-gravel sediment mixtures. *Journal of Hydraulic Engineering*, **119**, 1400-1415.

Kuhnle, R.A. 1993b. Fluvial transport of sand and gravel mixtures with bimodal size distributions. *Sedimentary Geology*, **85**, 17-24.

Langbein, W.B. and Leopold, L.B. 1968. *River channel bars and dunes – theory of kinematic waves*. USGS Professional Paper, **422-L**.

Langbein, W.B. and Leopold, L.B. 1966. River meanders – theory of minimum variance, *Professional Paper. United States Geological Survey*, **422H**.

Laronne, J.B. and Duncan, M.J. 1992. Bedload transport paths and gravel bar formation. In Billi, P., Hey, R.D., Thorne, C.R. and Tacconi, P. (eds) *Dynamics of gravel-bed rivers*, Wiley, Chichester, 49-50.

Laronne, J.B., Garcia, C. and Reid, I. 2000. Mobility of patch sediment in gravel-bed streams: patch character and its implications for bedload. *Paper presented at Gravel-bed Rivers, 2000, Christchurch and Franz Joseph, New Zealand, August, 2000*.

Laronne, J.B. and Carson, M.A. 1976. Inter-relationships between bed morphology and bed material transport for a small gravel-bed channel. *Sedimentology*, **23**, 67-85.

Leopold, L.B., Wolman, M.G. and Miller, J.P. 1964. *Fluvial processes in geomorphology*, W.H. Freeman and Co., San Francisco, California.

Leopold, L.M. and Wolman, M.G. 1960. River Meanders. *Bulletin of the Geological Society of America*, **71**, 769-94.

Lewin, J. 1981. British Rivers.

Li, Z. and Komar, P.D. 1986. Laboratory measurements of pivoting angles for applications to selective entrainment of gravels in a current. *Sedimentology*, **33**, 413-423.

Lisle, T. E. 1979a. A sorting mechanism for a riffle-pool sequence: Summary, *Geological Society of America Bulletin*, Part I, **90**, 616-617.

Lisle, T. E. 1979b. A sorting mechanism for a riffle-pool sequence. *Geological Society of America Bulletin*, Part II, **90**, 1142-1157.

Lisle, T. E. 1989. Sediment transport and resulting deposition in spawning gravels, North Coastal California. *Water Resources Research*, **25** (6), 1303-1319.

Lisle, T. E. and Hilton, S. 1992. The volume of fine sediment in pools: an index of sediment supply in gravel-bed streams. *Water Resources Bulletin*, **28** (2), 371-383.

Lisle, T.E. 1982. Effects of aggradation and degradation on riffle-pool morphology in natural gravel channels, Northwest California. *Water Resources Research*, **18**, 1643-1651.

Lisle, T.E. 1986. Stabilisation of a gravel channel by large streamside obstructions and bedrock bends, Jacoby Creek, Northwest California. *Geological Society of America Bulletin*, **97**, 999-1011.

Lisle, T.E. 1995. Particle size variations between bedload and bed material in natural gravel bed channels. *Water Resources Research*, **31**, 1107-1118.

Lisle, T.E. and Eads, R.E. 1991. Methods to measure sedimentation of spawning gravels. USDA Forest Service Research Note PSW-411.

Lisle, T.E. and Hilton, S. 1999. Fine bed material in pools of natural gravel bed channels. *Water Resources Research*, **35**, 1291-1304.

Lisle, T.E. and Madej, M.A. 1992. Spatial variation in armouring in a channel with high sediment supply. In P. Billi, R.D. Hey, C.R. Thorne and Tacconi, P. (eds) *Dynamics of gravel-bed rivers*. John Wiley and Sons, Chichester, UK, pp277-296

Livesey, R.H. 1965. Channel armouring below Fort Randall Dam, *USDA Miscellaneous Publication, 1970*, 461-470.

Lotspeich, F.B. and Reid, B.H. 1980. Tri-tube freeze-core procedure for sampling stream gravels. *The progressive fish culturalist, 42*, 96-99.

Mather, P.M. (ed) 1993. Geographical information handling – research and applications. John Wiley & Sons Ltd.

Matheron, G. 1971. The theory of regionalised variables and its applications. *Les Cahiers du Centre de Morphologie Mathematique de Fontainbleau*, no. 5.

McEwan, I.K., Habersack, H.M. and Heald, J.G.C. 2000. Discrete particle modelling and active tracers: new techniques for studying sediment transport as a lagrangian phenomenon. *Paper presented at Gravel-bed Rivers, 2000, Christchurch and Franz Joseph, New Zealand, August, 2000.*

McNeil, W. and Ahnell, W. 1964. *Success of pink salmon spawning relative to size of spawning bed materials*, US fish and Wildlife service special scientific report, *Fisheries 469*.

Meehan, W.R. and Swanston, D.N. 1977. Effects of gravel morphology on fine sediment accumulation and survival of incubating salmon eggs. *Research Paper US Forest Service INT-156*, 14pp.

Milan, D. J. 1994. Sediment quality characteristics of salmonid spawning grounds. *Unpublished M.Phil thesis, University of Technology, Loughborough*, 204pp.

Milan, D. J. and Petts, G. E. 1998. Sediment quality of salmonid spawning grounds in a stream suffering from low flows; River Glen, UK. In G. Bretschko & Helesic, J. (eds) *Advances in River Bottom Ecology*. Backhuys, Netherlands, pp 277-299.

Milan, D.J. 1996. The application of freeze-coring for siltation assessment in a recently regulated stream. In Merot, P. & Jigorel, A. (eds) *Hydrologie dans les pays celtiques*. Actes du 1er Colloque interceltique d'Hydrologie et de Gestion des Eaux. Organise par CEMAGREF, DIREN, IFREMER, INRA, INSA. Rennes France, 8-11 juillet 1996, Les Colloques no 79, 253-266.

Milan, D.J. Heritage, G.L., Large, A.R.G. and Brunsdon, C.F. 1999. Influence of particle shape and sorting upon sample size estimates for a coarse-grained upland stream, *Sedimentary Geology, 128*, 85-100

Milan, D.J., Heritage, G.L. and Large, A.R.G. in press. Tracer pebble entrainment and deposition loci: influence of flow character and implications for riffle-pool maintenance. In Jones, S. and Frostick, L. (eds) *Sediment flux to basins: causes, controls and consequences*, Geological Society of London Special Issue.

Milan, D.J., Heritage, G.L., Large, A.R.G. & Charlton, M.E. 2001. Stage-dependent variability in shear stress distribution through a riffle-pool sequences. *Catena, 44*, 85-109.

Milan, D.J., Petts, G.E. and Sambrook, H. 2000. Regional variations in sediment structure of trout streams in southern England. *Aquatic Conservation, 10*, 407-420

Milhous, R. T. 1973. Sediment transport in a gravel-bottomed stream. Unpublished Ph. D dissertation, Oregon State University, 232pp.

Milhous, R. T. 1981. Armoured versus paved gravel beds. Discussion. Proceedings of the American Society of Civil Engineers. *Journal of the Hydraulics Division, 107*, 1119-1120.

Milhous, R.T. 1996. Numerical modelling of flushing flow needs in gravel bed rivers, Paper presented at Gravel bed rivers IV, Victoria Falls, Zimbabwe, 1996.

Miller, A.J. 1994. Debris-fan constrictions and flood hydraulics in river canyons: some implications from two-dimensional flow modelling. *Earth Surface Process and Landforms*, **9**, 681-697.

Miller, H. 1887. The geology of the Country around Otterburn and Elsdon. Explanation of the quarter Sheet 108SE (New Series Sheet 8). Memoir of the Geological Survey of England and Wales. HMSO, London, 147pp.

Miller, M.C., McCave, I.N. and Komar, P.D. 1977. Threshold of sediment motion under unidirectional currents. *Sedimentology*, **24**, 507-527.

Miller, R.L. and Byrne, R.J. 1966. The angle of repose for a single grain on a fixed rough bed, *Sedimentology*, **24**, 507-527.

Milne, J. A. 1982. Bed material size and the riffle/pool sequence. *Sedimentology*, **29**, 267-278.

Montgomery, D.R., Buffington, J.M., Smith, R.D., Schmidt, K.M. and Pess, G. 1995. Pool spacing in forest channels. *Water Resources Research*, **31**, 1097-1105.

Mosely, M. P. 1978. Bed material transport in the Tamaki River near Dannevirke, North Island, New Zealand. *New Zealand Journal of Science*, **21**, 619-626.

Mosely, M. P. and Tindale, R. S. 1985. Sediment variability and bed material sampling in gravel-bed rivers. *Earth Surface Processes and Landforms*, **10**, 465-482.

Newbury, R. 1995. Rivers and the art of stream restoration, in *Natural and Anthropogenic influences in Fluvial Geomorphology*, Geophysical Monograph, **89**, American Geophysical Union.

Newson, M., Thorne, C. and Brookes, A. 2000. The management of gravel-bed rivers in England and Wales: from geomorphological research to strategy and operations. *Paper presented at Gravel-bed Rivers, 2000, Christchurch and Franz Joseph, New Zealand, August, 2000*.

Nordin, C.F. 1971. Statistical properties of dune profiles. *US Geological Survey Professional Paper 56-F*, 41pp.

O'Connor, J.E., Webb, R.H. and Baker, V.R. 1986. Paleohydrology of pool-riffle pattern development: Boulder Creek, Utah, *Geological Society of America Bulletin*, **97**, 410-420.

O'Neill, M.P. and Abrahams, A.D. 1984. Objective identification of pools and riffles. *Water Resources Research*, **20**, 921-926.

Oldfield, F., Thompson, R., and Dicson, D.P.E. (1981) Artificial enhancement of stream bedload: a hydrological application of supermagnetism. *Physics of the Earth and Planetary Interiors*, **26**, 107-124.

Olea, R.A. 1975. Optimum mapping techniques using regionalised variable theory. Series on spatial analysis, no. 2., Kansas Geological Survey, Lawrence, Kansas, USA.

Padmore, C.L. 1998. The role of physical biotopes in determining the conservation status and flow requirements of British rivers. *Aquatic Ecosystem Health and Management*, **1**, 25-35.

Paintal, A.S. 1971. A stochastic model for bedload transport. *Journal of Hydraulic Research*, **9**, 527-553.

Paola, C. and Seal, R. 1995. Grain size patchiness as a cause of selective deposition and downstream fining. *Water Resources Research*, **31**, 1395-1407.

Parker, G. 1981. Armoured versus paved gravel beds. *Proceedings of the American Society of Civil Engineers. Journal of the Hydraulics Division*, **107**, 112s0-1121.

Parker, R. T. G. and Klingeman, P. C. 1982. On why gravel bed streams are paved. *Water Resources Research*, **18**, 1409-1423.

Parker, R. T. G. and Sutherland, A.J. 1990. Fluvial armour. *Journal of Hydraulic Research*, **28**, 529-544.

Parker, R. T. G., Dhamotheran, P.C. and Stefan, H. 1982b. Model experiments on mobile, paved gravel-bed streams. *Proceedings of the American Society of Civil Engineers, Journal of the Hydraulics Division*, **107**, 1395-1408.

Parker, R. T. G., Klingeman, P. C. and McClean, D. G. 1982a. Bedload and size distribution in gravel-bed streams. *Journal of Hydraulics Division*, **108**, 544-571.

Petit, F. 1987. The relationship between shear stress and the shaping of a pebble-loaded river La Rulles-Ardenne. *Catena*, **14**, 453-468.

Petit, F. 1989. The evaluation of grain shear stresses from experiments in a pebble-bedded flume. *Earth Surface Processes and Landforms*, **14**, 499-508.

Petit, F. 1990. Evaluation of grain shear stresses required to initiate movement. *Earth Surface Processes and Landforms*, **15**, 135-148.

Petts, G. E., Thoms, M. C., Brittan, K. and Atkin, B. 1989. A freeze-coring technique applied to pollution by fine-grained sediments in gravel-bed rivers, *The Science of the Total Environment*, **84**, 259-272.

Petts, G.E. 1984a. *Impounded Rivers*, Wiley, Chichester.

Petts, G.E. 1984b. Sedimentation in regulated rivers. *Earth Surface Processes and Landforms*, **9**, 125-134.

Petts, G.E. 1987 to 1992. Sediment sampling in fish spawning grounds in the upper Tamar catchment. Roadford Environmental Investigation. *Internal reports to Water Research Centre/National Rivers Authority South West Region*.

Petts, G.E. and Thoms, M.C. 1986. Channel aggradation below Chew Valley Lake, Somerset, UK., *Catena*, **13**, 305-320.

Powell, D.M. 1998. Patterns and processes of sediment sorting in gravel-bed rivers. *Progress in Physical Geography*, **22**, 1-32.

Rathburn, R.E. and Kennedy, V.C. 1978. Transport and dispersion of fluorescent tracer particles for the dune-bed condition, Atrisco Feeder Canal near Bernalillo, New Mexico. *US Geological Survey Professional Paper 1037*.

Raudkivi, A. J. and Ettema, R. 1982. Stability of armour layers in rivers. *Journal of Hydraulics Division, ACSE*, **108**, 1047-1057.

Rayner, D.H. 1981. The stratigraphy of the British Isles (second edition). Cambridge University Press, 460pp.

Reid, I., Brayshaw, A.C. and Frostick, L.E. 1984. An electromagnetic device for automatic detection of bedload motion and its field applications. *Sedimentology*, **31**, 269-276.

Reid, I.. and Frostick, L.E. 1984. Particle interaction and its effect on the thresholds of initial and final bedload motion in coarse grained alluvial channels. In Koster, E.H. and Steel, R.J. (Eds), *Sedimentology of gravels and conglomerates*. Canadian Society of Petroleum Geologists Memoir, **10**, 61-68.

Reiser, D.W. Ramay, M.P. and Lambert, T.R. 1985. Review of flushing flow requirements in regulated streams. *Pacific gas and electric company, Department of Engineering Research San Ramon, California*, **94583**, 97pp.

Rice, S. and Church, M. 1996. Sampling surficial fluvial gravels: the precision of size distribution percentile estimates. *Journal of Sedimentary Research*, **66**, 654-665.

Richards, K. S. 1976a. The morphology of riffle-pool sequences. *Earth Surface Processes and Landforms*, **1**, 71-88.

Richards, K. S. 1976b. Channel width and the riffle-pool sequence. *Geological Society of America Bulletin*, **87**, 883-890.

Richards, K. S. 1978. Simulation of flow geometry in a riffle-pool stream. *Earth Surface Processes and Landforms*, **3**, 345-354.

Richards, K. S. 1990. Fluvial Geomorphology: initial motion of bed material in gravel-bed rivers. *Earth Surface Processes and Landforms*, **15**, 395-415.

Richards, K.S. 1982. *Rivers: fluvial form and process*. Methuen, London.

Richards, K.S. and Clifford, N. 1991. Fluvial geomorphology: structured beds in gravelly rivers. *Progress in Physical Geography*, **15**, 407-422.

Robert, A. 1997. Characteristics of velocity profiles along riffle-pool sequences and estimates of bed shear stress. *Geomorphology*, **19**, 89-98.

Rood, K. and Church, M. 1994. Modified freeze-core technique for sampling the permanently wetted stream bed. *North American Journal of Fisheries Management*, **14**: 852-861.

Rummery, T.A., Oldfield, F., Thompson, R. and Newson, M. 1979. Magnetic tracing of stream bedload. *Geophysical Journal of the Royal Astrological Society*, **57**, 278-279.

Russel, R. J. 1968. Where most grains of very coarse sand and fine gravel are deposited. *Sedimentology*, **11**, 31-38.

Sangerlat, G. 1979 *The penetrometer and soil exploration*, Elsevier, Amsterdam.

Sargent, R. J. 1979. Variation in Manning's n roughness coefficient with flow in open river channels, *Journal of the Institution of Water Engineers and Scientists*, **33**, 290-294.

Sawada, T. Ashida, K. and Takahashi, T. 1985. Sediment transport in mountain basins, in *Proceedings, International Symposium on Erosion, Debris flow, and disaster prevention*, pp.139-144, University of Tsukuba, Tsukuba, Japan.

Schälchli, U. 1992. The clogging of coarse gravel river beds by fine sediment. *Hydrobiologia*, **235/236**, 189-187.

Schälchli, U. 1995. Basic equations for siltation of riverbeds. *Journal of Hydraulic Engineering*, **121**(3), 274-287.

Schmidt, J.C., Rubin, D.M., Ikeda, H. 1993. Flume simulation of recirculating flow and sedimentation. *Water Resources Research*, **29**, 2925-2939.

Schmidt, K. and Ergenzer, P. 1992. Bedload entrainment, travel lengths, step lengths, rest periods-studied with passive (iron, magnetic) and active (radio) tracer techniques,. *Earth Surface Processes and Landforms*, **17**, 147-165.

Scullion, J., Parish,C.A., Morgan,N. and Edwards, W. 1982. Comparison of benthic macroinvertebrate fauna and substratum composition in riffles and pools in the impounded River Elan and the unregulated River Wye, mid-Wales. *Freshwater Biology*, **12**, 579-595.

Sear, D. A. 1992a. Sediment transport processes in riffle-pool sequences and the effects of river regulation for hydroelectric power in the River North Tyne, *Unpublished PhD thesis*, University of Newcastle upon Tyne.

Sear, D. A. 1992b. Sediment transport processes in riffle-pool sequences in a river experiencing hydropower regulation,. In Hey, R. D., Billi, P., Thorne, C. R.

and Tacconi, P. (Eds), *Dynamics of Gravel-bed Rivers*, John Wiley, Chichester, 629-650.

Sear, D. A. 1996. Sediment transport processes in pool-riffle sequences. *Earth Surface Processes and Landforms*, **21**, 241-262.

Sear, D.A. 1992c. Discussion, in Hey, R.D., Billi, P., Thorne, C.R. and Tacconi, P. (Eds), *Dynamics of Gravel-bed Rivers*, John Wiley, Chichester, p292.

Sear, D.A. 1993. Fine sediment infiltration into gravel spawning beds within a regulated river experiencing floods: ecological implications for salmonids, *Regulated Rivers Research and Management*, **8**, 373-390.

Sear, D.A. 1994. River restoration and geomorphology. *Aquatic Conservation: Marine and Freshwater Ecosystems*, **4**, 169-177.

Shen, H.W. and Cheong, H.F. 1977. Statistical properties of sediment bed profiles, *Journal of the Hydraulics Division, ASCE*, **103**(HY11), 1303-1321.

Shields,, A. 1936. *Anwendung der annlichkeitsmechanik und der turbulenzforschung auf die geschiebebewegung. Mitteilung der Preussischen versuchsanstalt fuer Wasserbau und Schiffbau* Heft 26, Berlin (trans. Ott, W.P. and van Uchlen, J.C., Pasadena, CA: USDA, Soil Conservation service, Coop Lab., California, Institute of Technology)

Sidle, R.C. 1988. Bed load transport regime of a small forest stream. *Water Resources Research*, **24**, 207-218.

Sidorchuk, A.K. 1996. The structure of river bed relief, in Ashworth, P.J., Bennett, S.J., Best, J.L. and McLelland, S.J. (eds), *Coherent Flow Structures in Open Channels*, John Wiley & Sons, Chichester, 397-421.

Slaney, P.A. Halsey, T.G. and Tautz, A.F. 1977. Effects of forest harvesting practices on spawning habitat of stream salmonids in the Centennial Creek watershed, British Columbia, *Fish Management Report*, **73**, 45pp. Province of British Columbia, Mineral, Recreation and Conservation.

Stelczer, K. 1981. *Bed load transport – theory and practice*, Water Resources Publications, Littleton, 296pp.

Strahler, A.N. 1952 Hyposometric (area-altitude) analysis of erosional topography. *Bulletin of the Geological Society of America*, **63**, 1117-11142.

Stuart, T.A. 1953. Water currents through permeable gravels and their significance to spawning salmonids. *Nature*, **52**, 821-828.

Stunell, J.M. and Younger, P.L. 1995. Hydrogeology of upland peat: hydrological and chemical processes in Redesdale, N. England. *Proceedings of the BHS 5th National Symposium*, Edinburgh, Institute of Hydrology.

Sundborg, A. 1956. The river Klaralven: a study of fluvial processes. *Geografiska Annaler*, **38**, 127-316.

Sutherland, A.J. 1987. Static armour layers by selective erosion. IN Thorne, C.R., Bathurst, J.C. and Hey, R.D. (eds): *Sediment Transport in Gravel-bed Rivers*. Wiley, Chichester, 243-267.

Tanner, W.F. 1964. Modification of sediment size distributions. *Journal of Sedimentary Petrology*, **34**, 156-164.

Teisseyre, A.K. 1984. The River Bobr in the Blazkowa study reach (central Sudetes): a case study in fluvial processes and fluvial sedimentology. *Geological Sudetica*, **19**, 7-71.

Thompson, A. 1986. Secondary flows and the pool-riffle unit: a case study of the processes of meander development. *Earth Surface Processes and Landforms*, **11**, 631-641.

Thompson, D.M., Nelson, J.N., and Wohl, E.E. 1998. Interactions between pool geometry and hydraulics. *Water Resources Research*, **12**, 3673-3681.

Thompson, D.M., Wohl, E.E. and Jarrett, R.D. 1996. A revised velocity-reversal and sediment-sorting model for a high gradient, pool-riffle stream. *Physical Geography*, **17**, 142-156.

Thompson, D.M., Wohl, E.E. and Jarrett, R.D. 1999 Velocity reversals and sediment sorting in pools and riffles controlled by channel constrictions. *Geomorphology*, **27**, 229-241.

Thompson, R. and Oldfield, F. 1986. *Environmental Magnetism*. London: Unwin and Allen.

Thoms, M. C. 1987. Channel sedimentation in urban gravel-bed rivers. PhD thesis, University of Technology, Loughborough.

Thoms, M.C., 1992. A comparison of grab- and freeze-sampling techniques in the collection of gravel-bed river sediments. *Sedimentary Geology*, **78**: 191-200.

Thorne, C.R. and Lewin, J. 1979. Bank processes, bed material movement and planform development in a meandering river. In Rhodes, D.D. and Williams, G.P. (eds) *Adjustments of the fluvial system*. Binghampton, SUNY, 117-137.

van der Post, K.D., Oldfield, F. and Voulgaris, G. 1994. Magnetic tracing of beach sand: preliminary results, Proceedings Coastal Dynamics '94, approved for publication by the Waterway, Port, Coastal and Ocean Division/ASCE, February 21-25, 1994, Barcelona, Spain.

Walling, D.E. and Amos, C.M. 1994. Rivers Piddle action plan, *Unpublished report to Southern Region NRA*, University of Exeter, 88p.

Walling, D.E. and Webb, B.W. 1987. Suspended load in gravel bed rivers: UK experience. In Thorne, C.R., Bathurst, J.C. and Hey, R.D. (eds) *Sediment transport in Gravel-bed rivers*, Wiley, Chichester, 691-732.

Wathen, S.J., Ferguson, R.I., Hoey, T.B. and Werrity, A. 1995. Unequal mobility of gravel and sand in weakly bimodal river sediments, *Water Resources Research*, **31**, 2087-2096.

Webber, N.B. 1971. *Fluid mechanics for civil engineers*. Chapman and Hall, 340pp.

Welton, J.S. 1980. Dynamics of sediment and organic detritus in a small chalk stream. *Archive für Hydrobiologia*, **90**, 162-181.

Whittaker, J. G. and Jaeggi, M. N. R. 1982. Origin of step-pool systems in mountain streams. *Journal of Hydraulics Division, American Society of Civil Engineers*, **108**, 758-773.

Wiele, S.M., Graf, J.B. and Smith, J.D. 1996. Sand deposition on the Colorado River in the Grand Canyon from flooding of the Colorado River. *Water Resources Research*, **32**, 3579-3596.

Wilcock, P.R. 1988. Methods for estimating the critical shear stress for motion of uniform and heterogenous sediments. *Water Resources Research*, **23**, 1471-1480.

Wilcock, P.R. 1989. Bedload transport of mixed size sediment: fractional transport rates, bed forms and the development of a coarse surface layer. *Water Resources Research*, **25**, 1629-1641.

Wilcock, P.R. 1992. Experimental investigation of the effect of mixture properties on transport dynamics. In Billi, P., Hey, R.D., Thorne, C.R. and Tacconi, P., (eds) *Dynamics of Gravel bed Rivers*, Chichester, Wiley, 109-130.

Wilcock, P.R. 1993. Critical shear stress of natural sediments. *Journal of Hydraulic Engineering*, **119**, 491-505.

Wilcock, P.R. 1997. Entrainment, displacement and transport of tracer gravels. *Earth Surface Processes and Landforms*, **22**, 1125-1138.

Wilcock, P.R. and McArdell, B.W. 1997. Partial transport of a sand/gravel mixture. *Water Resources Research*, **33**, 235-245.

Wilcock, P.R. and Southard, J.B. 1988. Experimental study of incipient motion in mixed-size sediment. *Water Resources Research*, **24**, 1137-1151.

Wilcock, P.R. and Southard, J.B. 1989. Bedload transport of mixed-sized sediment: fractional transport rates, bedforms and the development of a coarse surface layer. *Water Resources Research*, **25**, 1629-1641.

Wilkinson, S.N., Keller, R.J. and Rutherford, I.D. 2000. Predicting the behaviour of riffle-pool sequences in natural rivers: a conceptual approach, in Maione, Majone Lehto and Monti (eds) *New trends in Water and Environmental Engineering and Life*. Balkema, Rotterdam.

Wohl, E.E., Anthony, D.J., Madsen, S.W. and Thompson, D.M. 1996. A comparison of surface sampling methods for coarse fluvial sediments. *Water Resources Research*, **32**, 3219-3226.

Wohl, E.E., Vincent, K.R. and Merritts, D.J. 1993. Pool and riffle characteristics in relation to channel gradient. *Geomorphology*, **6**, 99-110.

Wolcott, J. 1988. Nonfluvial control of bimodal distributions in river-bed gravels. *Journal of Sedimentary Petrology*, **58** (6), 979-984.

Wolcott, J. and Church, M. 1991. Strategies for sampling spatially heterogeneous phenomena: the example of river gravels. *Journal of Sedimentary Petrology*, **61**: 534-543.

Wolman, M. G. 1954. A method of sampling coarse river gravels. *Transactions of the American Geophysical Union*, **35**, 951-956.

Wolman, M.G. 1955. The natural channel of Brandywine Creek, Pennsylvania. *USGS Professional Paper*, **271**.

Yalin, M.S. 1971. On the formation of dunes and meanders, *International Association of Hydraulic research, 14th Congress, Paris, Proc. 3*, paper C13, 1-8.

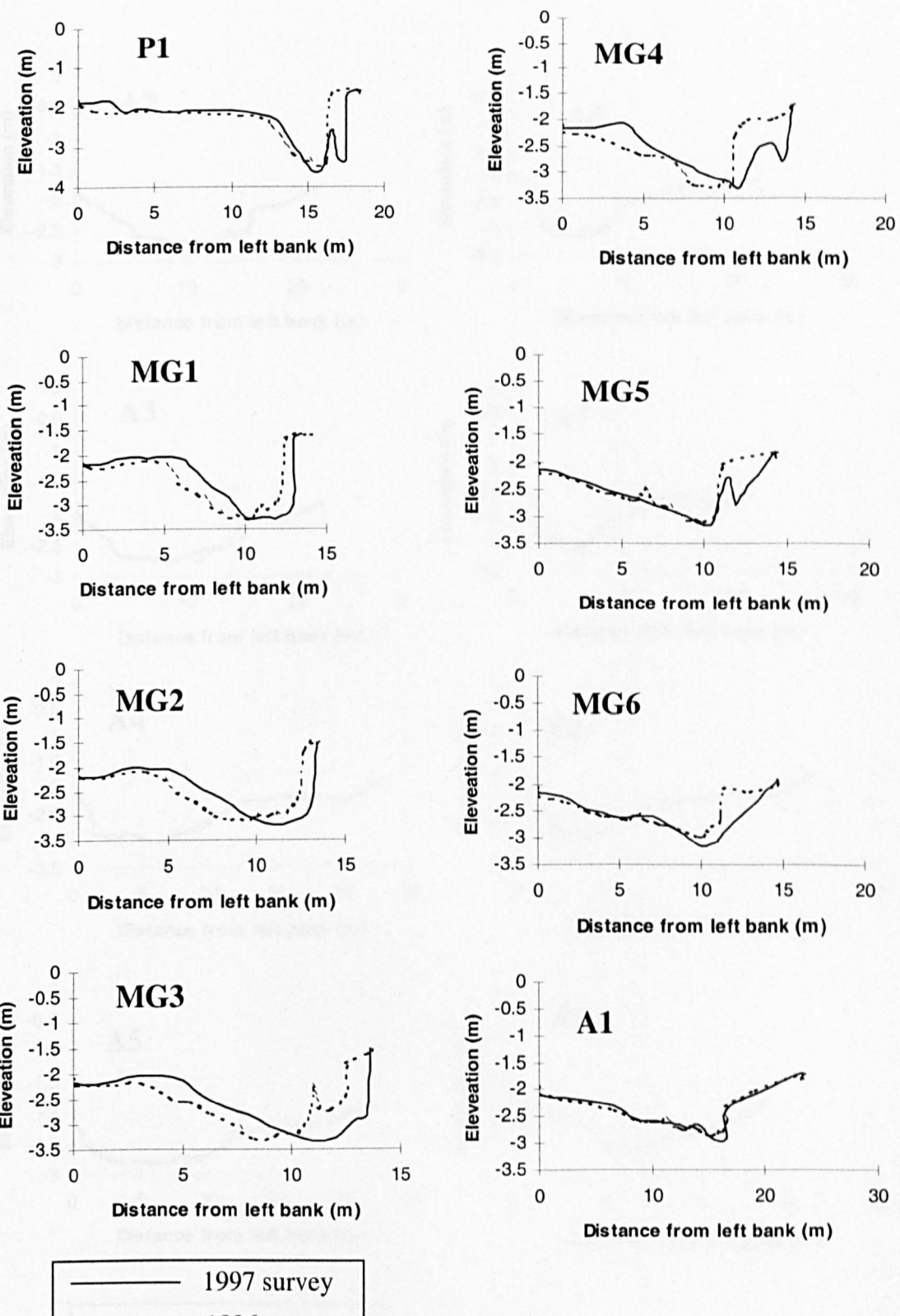
Yalin, M.S. 1977. *Mechanisms of sediment transport*, 2nd edtn, Permagon Press, Oxford, 298pp.

Yalin, M.S. 1992. *River Mechanics*, Permagon Press, Oxford, 219pp.

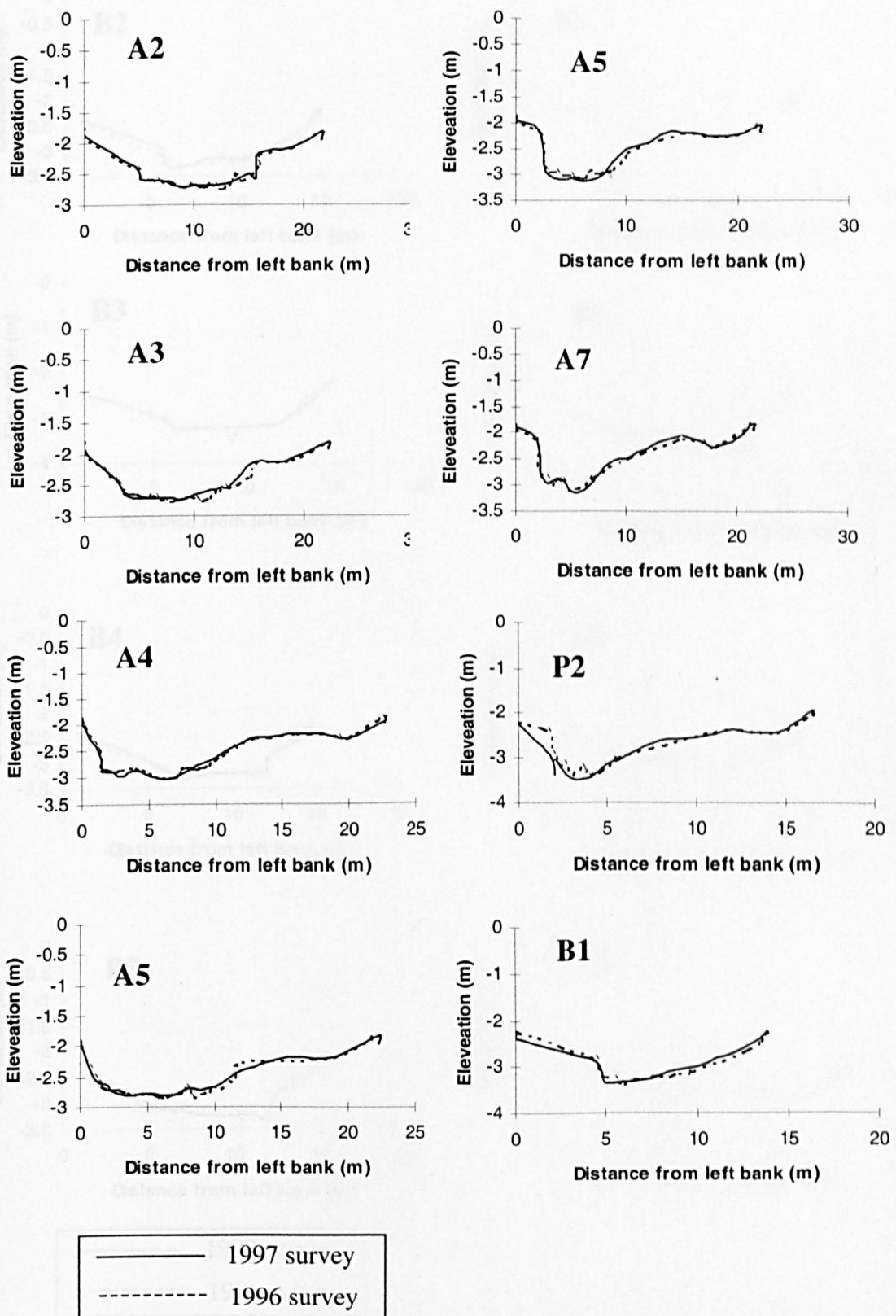
Yang, C.T. 1971. Formation of riffles and pools. *Water Resources Research*, **7**, 1567-1574.

Younger, P. L. 1991. A hydrogeological reconnaissance of Redesdale. Research report prepared for CLUWRR, University of Newcastle upon Tyne, 97pp.

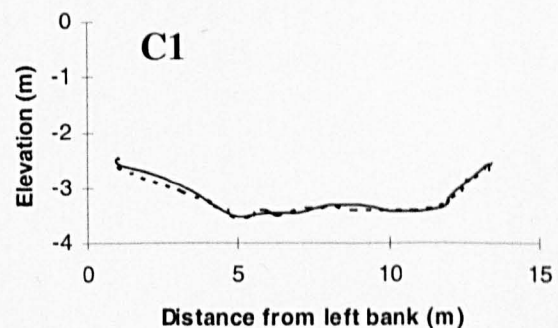
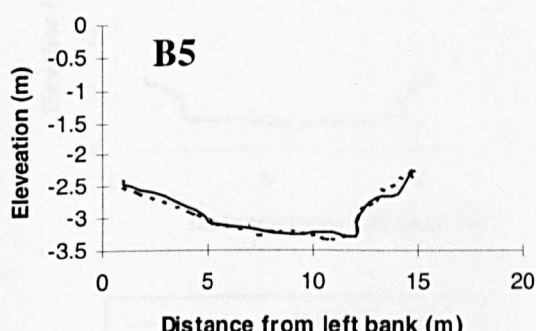
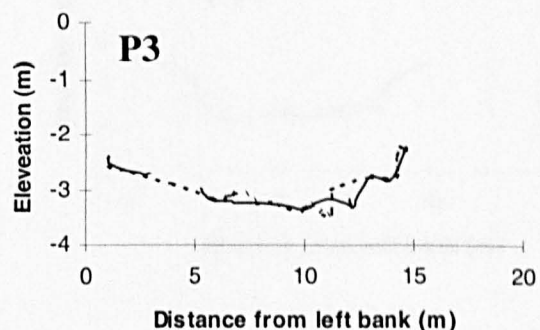
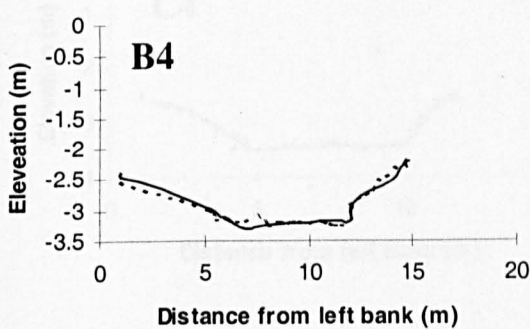
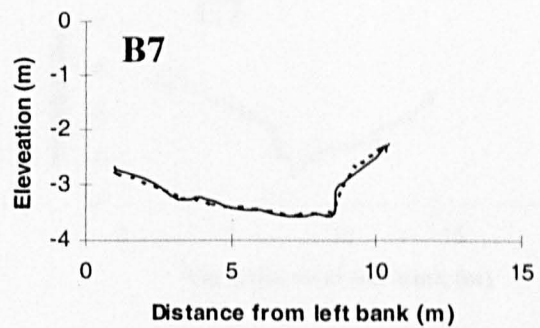
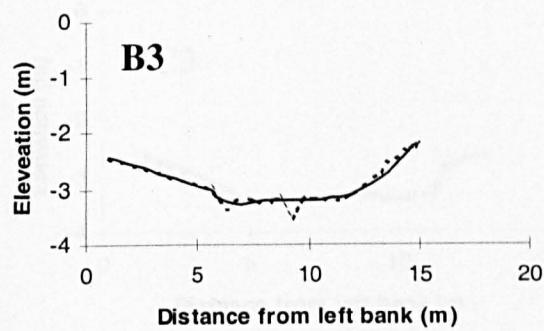
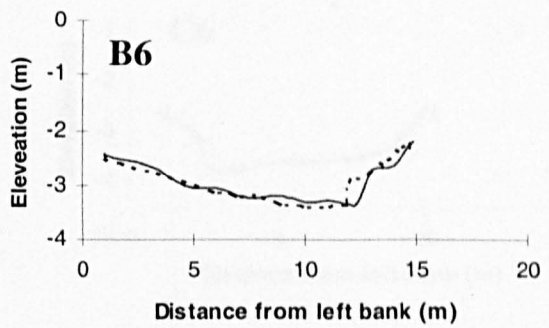
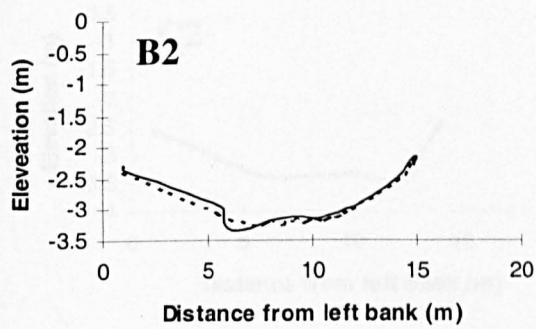
Zingg, T. 1935. Beitrag zur Schotteranalyse. *Schweizerische Mineralogische und Petrographische Mitteilungen*, **15**: 39-140.



Appendix 2.1 Cross-section profiles for the study reach for June 1997 (solid line) and June 1996 (hatched line). Cross section codes correspond to the monumented cross-section positions presented in Figure 2.2. Peg MG7 unfortunately was eaten by a sheep, therefore no re-survey data are presented.

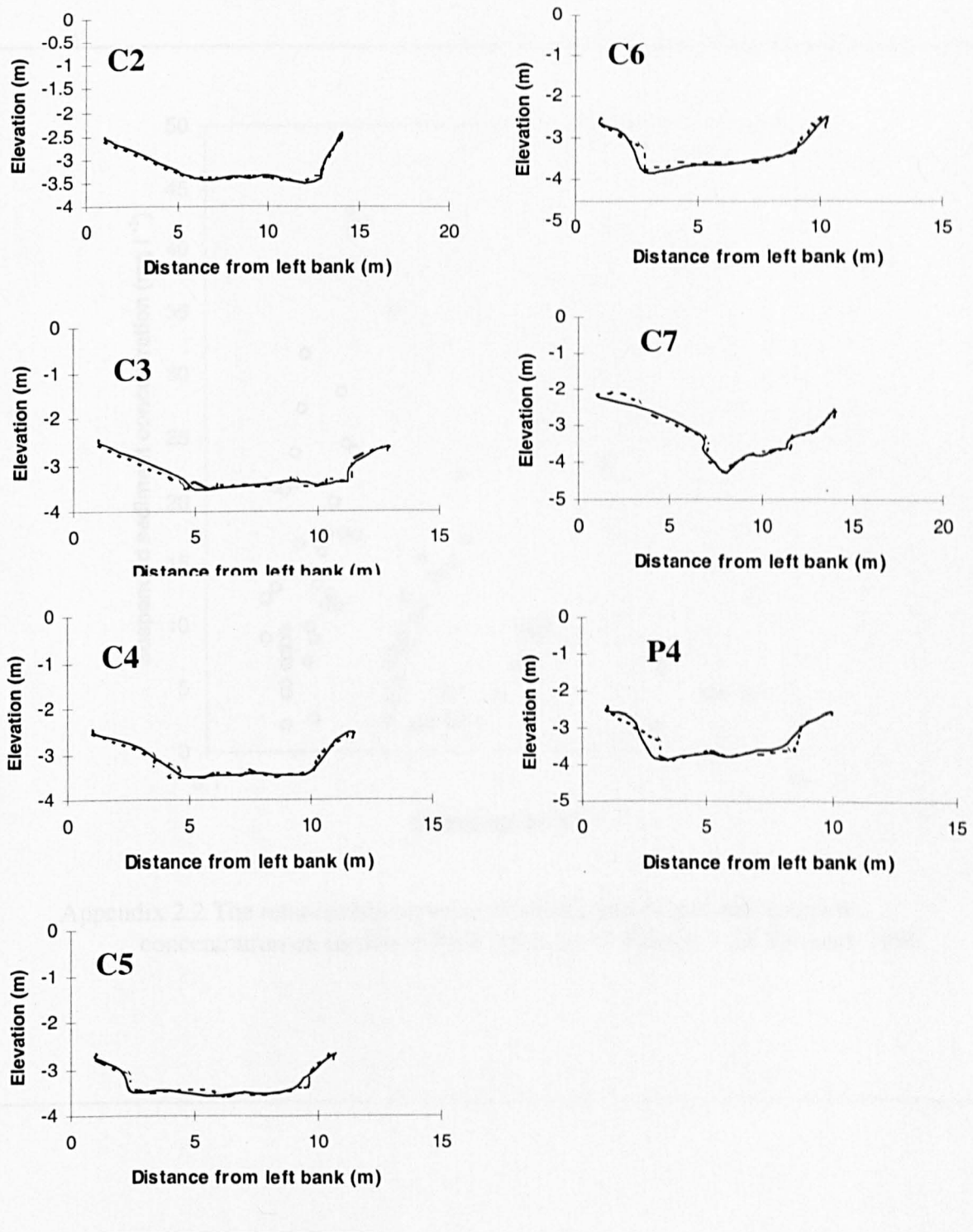


Appendix 2.1 Cross-section profiles for the study reach for June 1997 (solid line) and June 1996 (hatched line). Cross section codes correspond to the monumented cross-section positions presented in Figure 2.2.

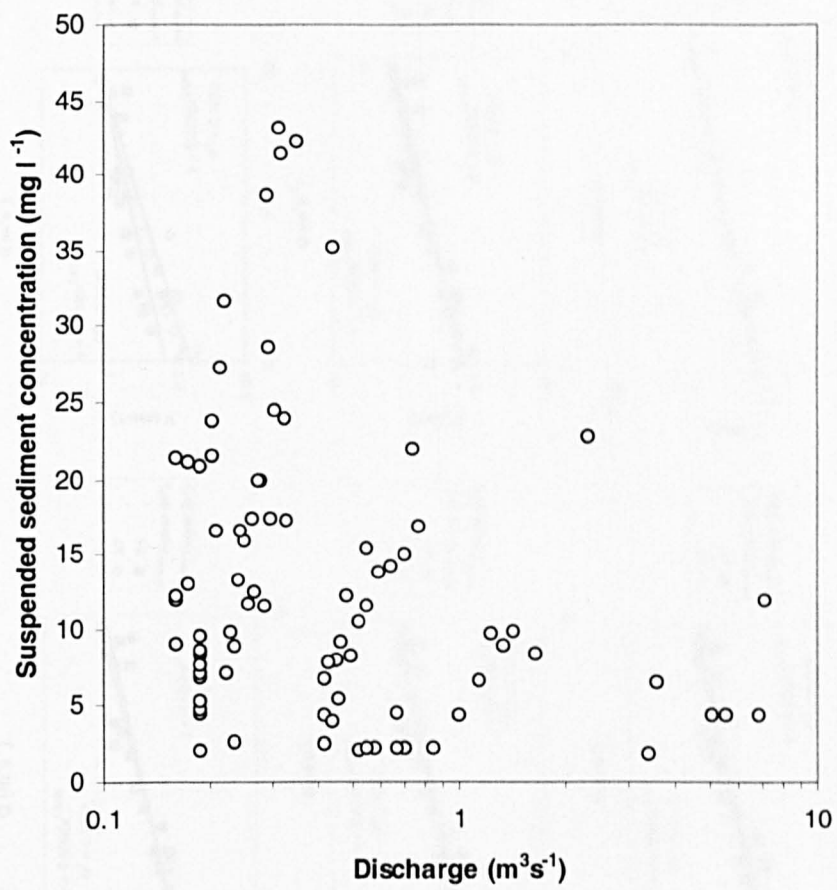


— 1997 survey
- - - 1996 survey

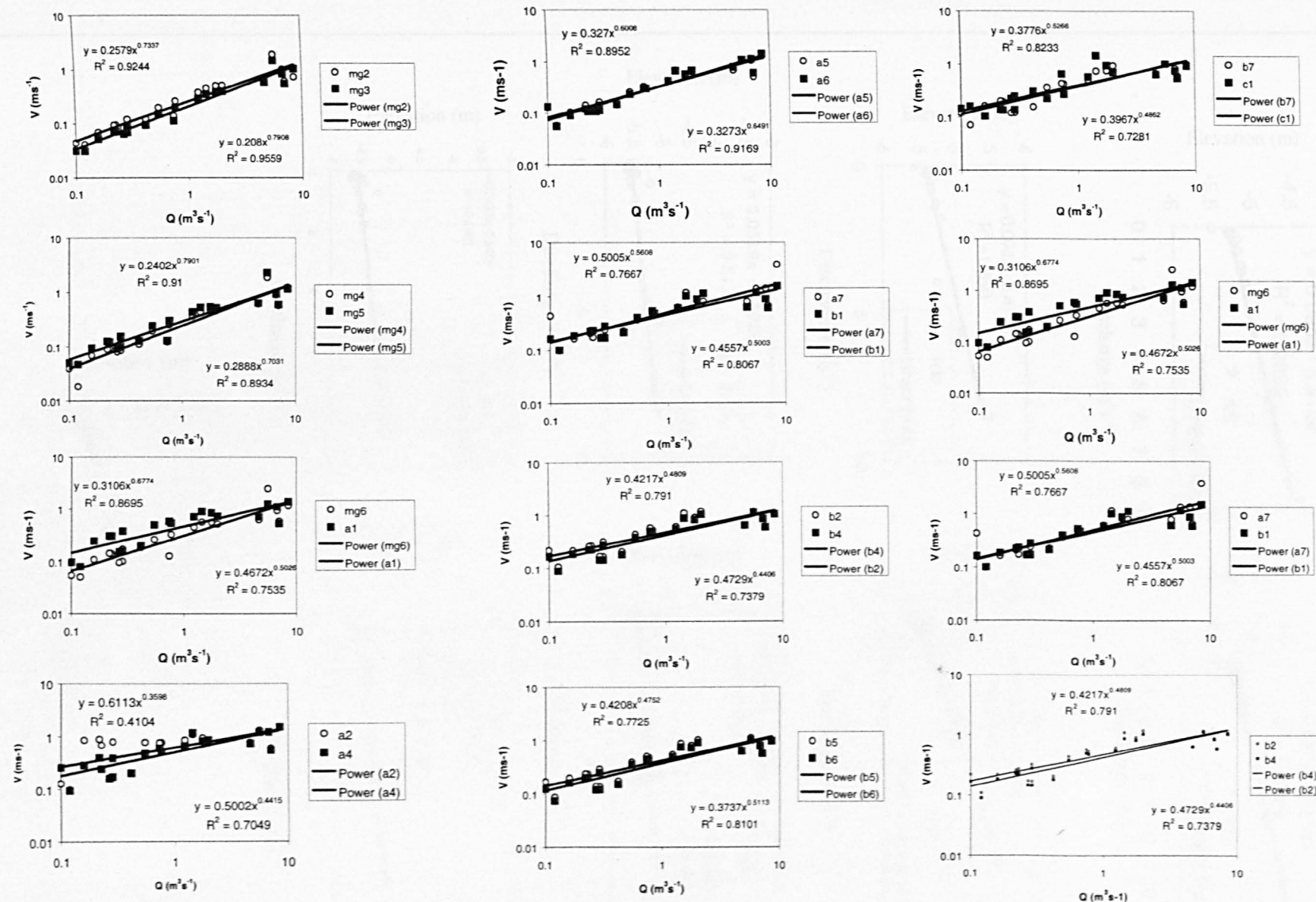
Appendix 2.1 Cross-section profiles for the study reach for June 1997 (solid line) and June 1996 (hatched line). Cross section codes correspond to the monumented cross-section positions presented in Figure 2.2.



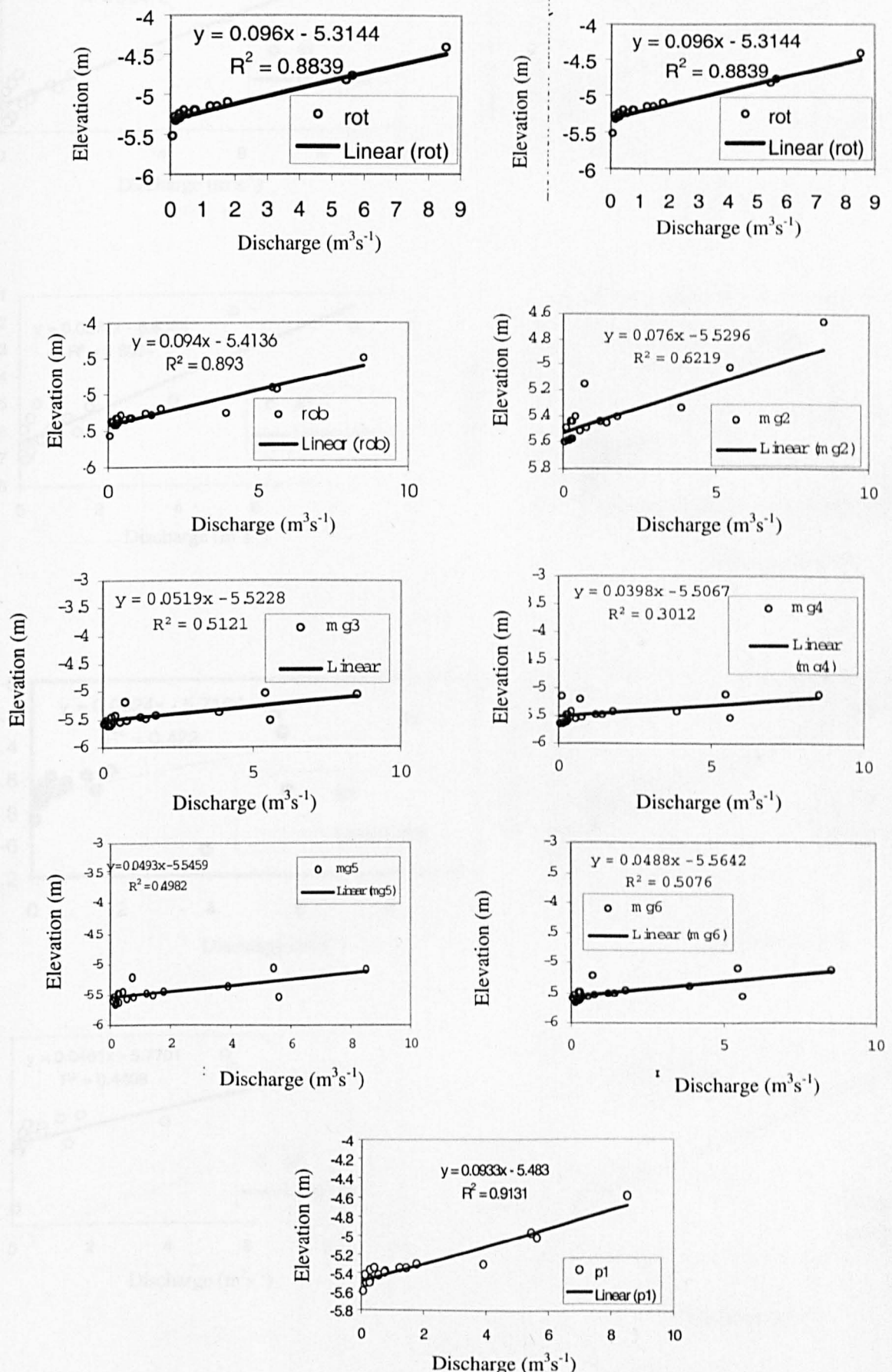
Appendix 2.1 Cross-section profiles for the study reach for June 1997 (solid line) and June 1996 (hatched line). Cross section codes correspond to the monumented cross-section positions presented in Figure 2.2.



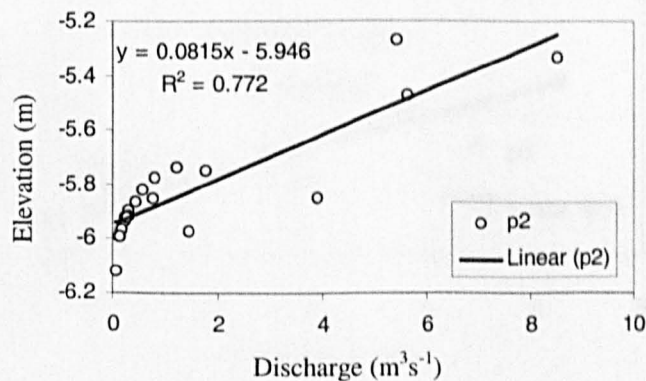
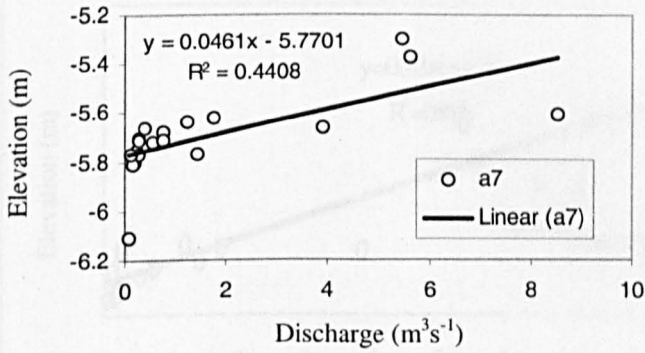
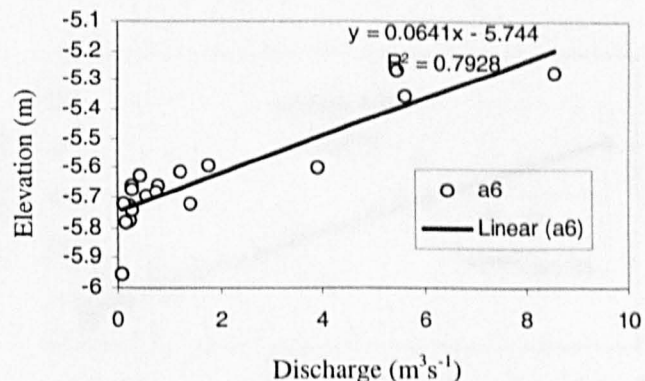
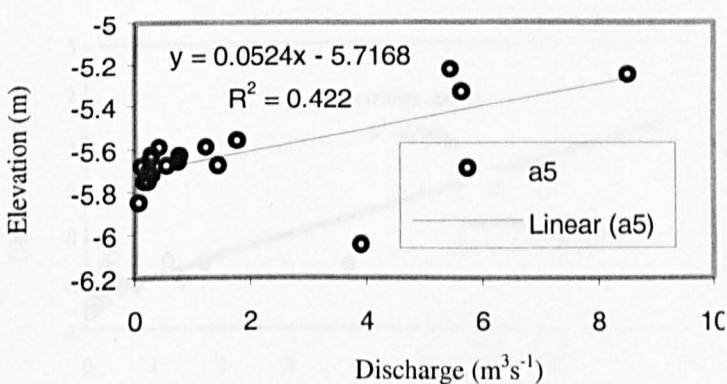
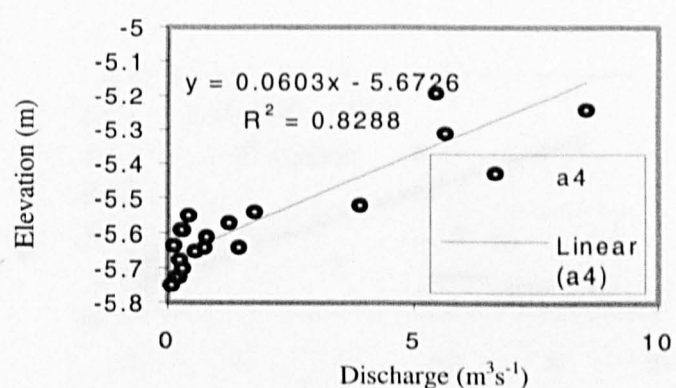
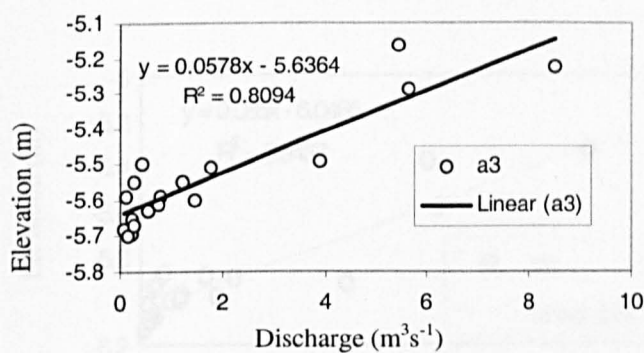
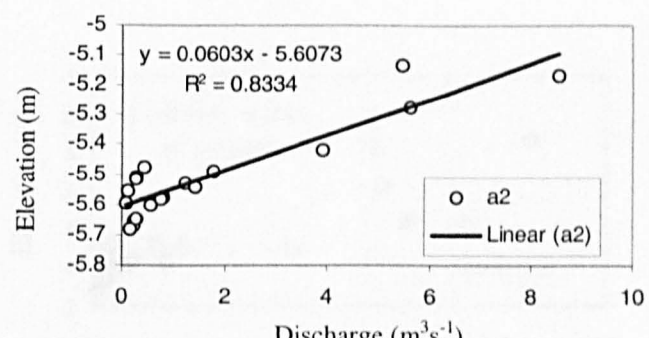
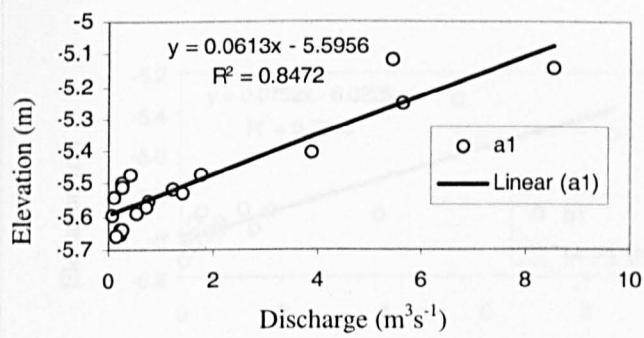
Appendix 2.2 The relationship between discharge and suspended sediment concentration on the River Rede between 17 January – 26 February 1996.



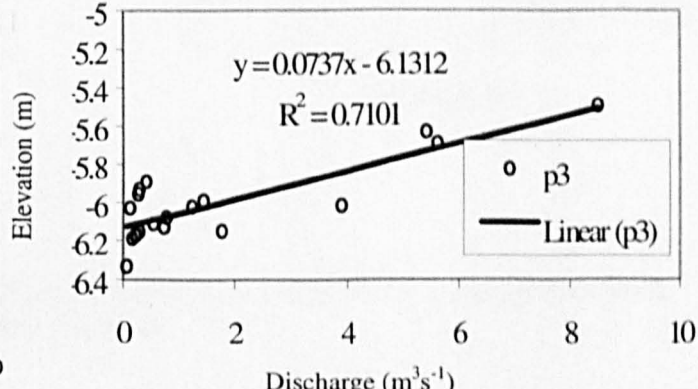
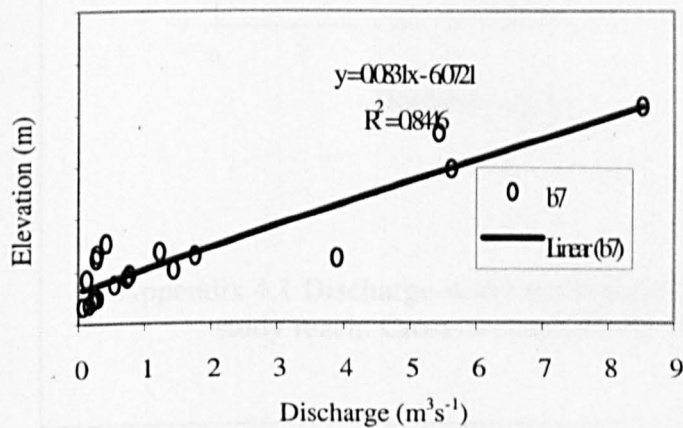
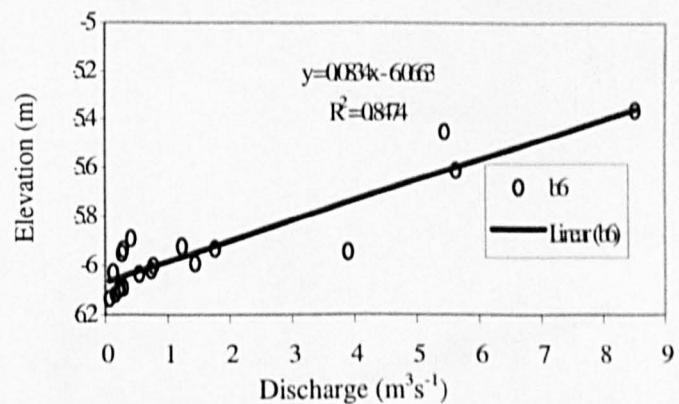
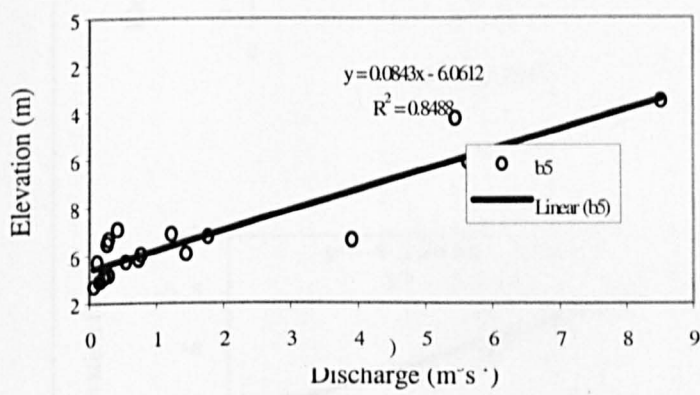
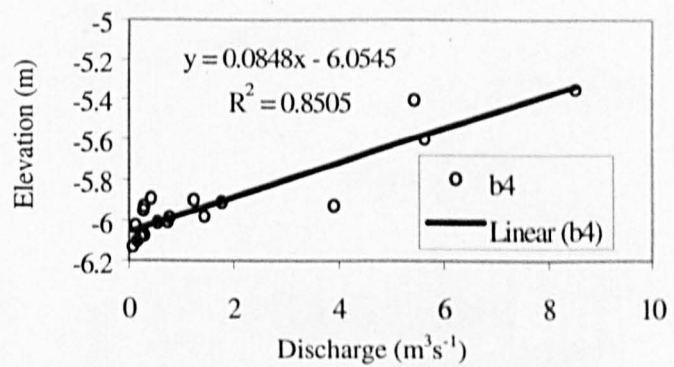
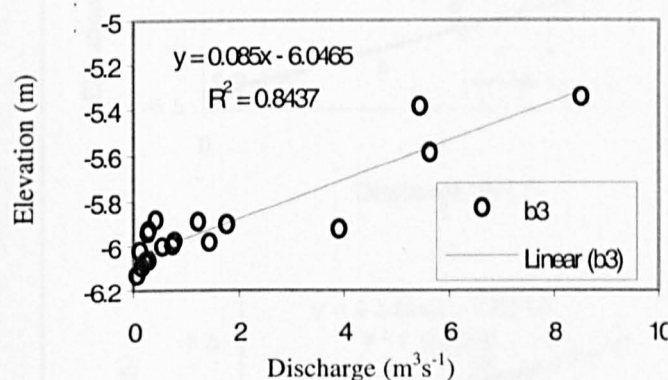
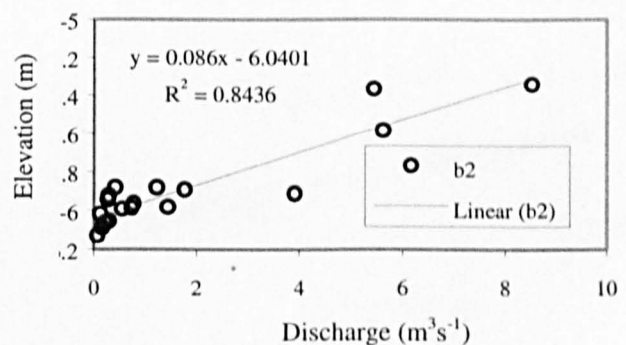
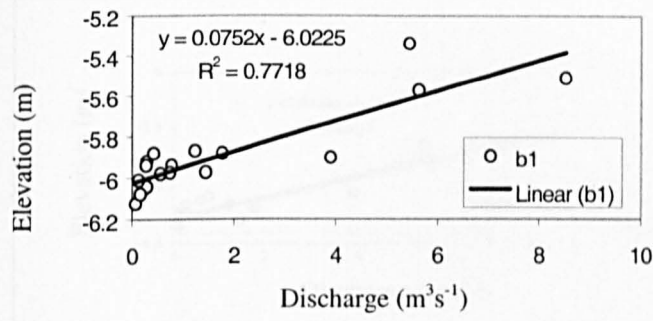
Appendix 4.1 Velocity discharge relationships for the Rede cross-sections not included in Figure 4.1.



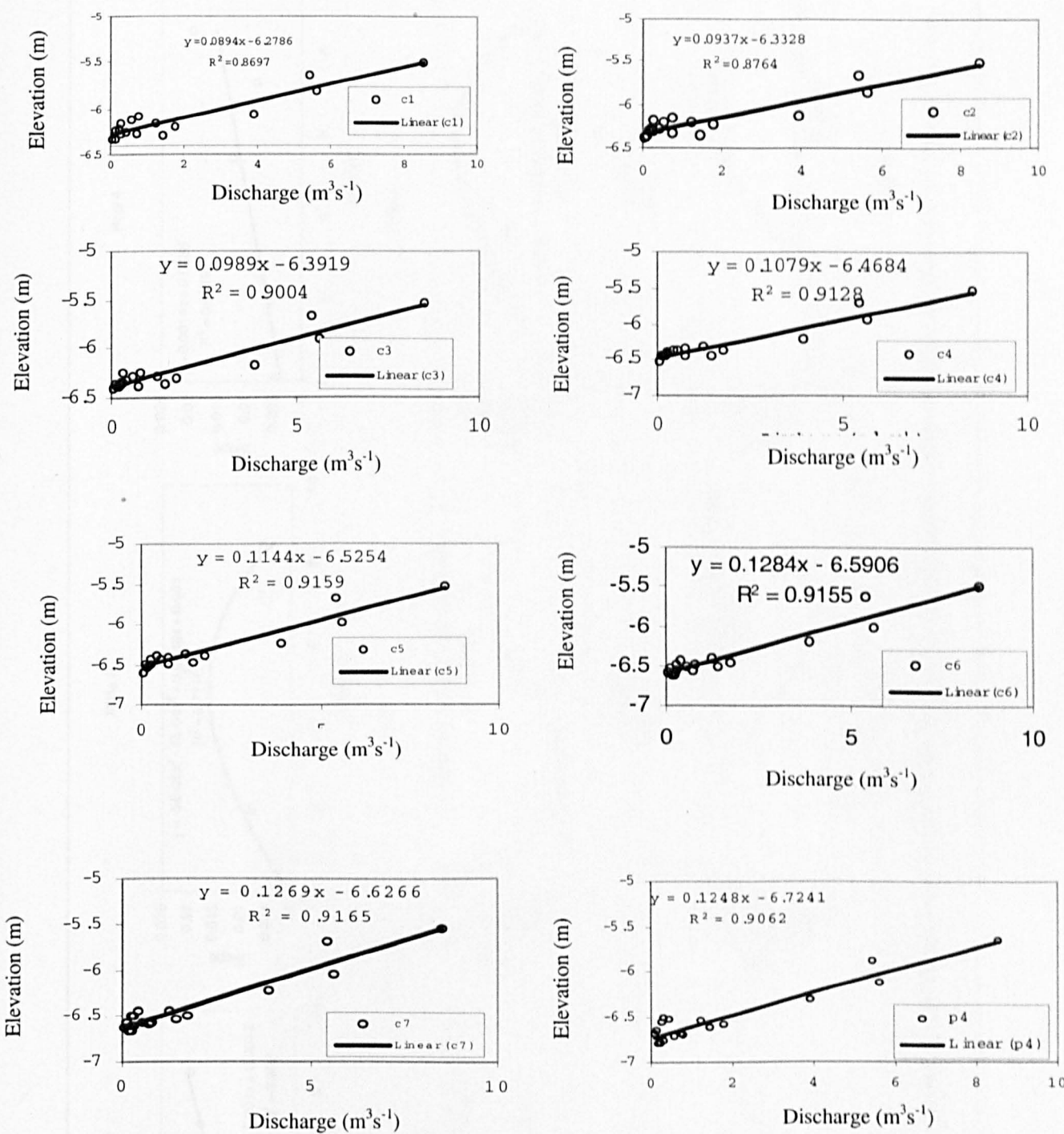
Appendix 4.1 Discharge-water surface elevation (*d*) rating curves for 30 cross-sections in Rede study reach. Cross-section id indicated in legend.



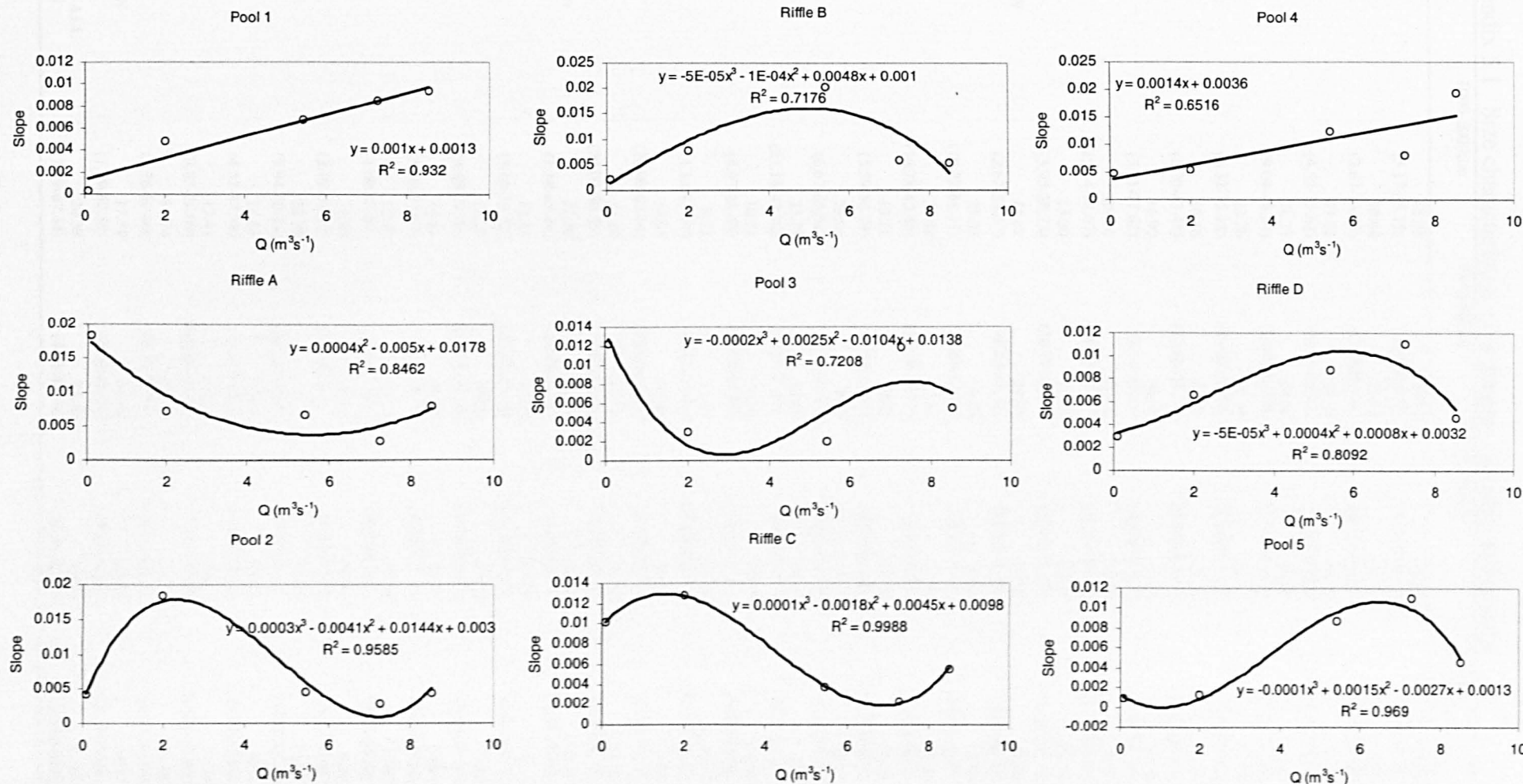
Appendix 4.1 Discharge-water surface elevation (d) rating curves for 30 cross-sections in Rede study reach. Cross-section id indicated in legend.



Appendix 4.1 Discharge-water surface elevation (d) rating curves for 30 cross-sections in Rede study reach. Cross-section id indicated in legend.



Appendix 4.1 Discharge-water surface elevation (*d*) rating curves for 30 cross-sections in Rede study reach. Cross-section id indicated in legend.



Appendix 4.3 Slope discharge rating relations. P1 and P4 are linear regression. RA is a second order polynomial, whilst the others are third order polynomial functions.

Appendix 5.1 Size characteristics of sediments entering basket traps.

	1000-2000µm	500-1000µm	250-500µm	125-250µm
A1	18.05 (5.17-43.75)	18.57 (6.25-26.79)	44.89 (31.25-58.57)	18.48 (9.84-41.38)
A2	10.64 (2.67-23.53)	22.87 (11.76-29.41)	51.47 (42.35-63.41)	15.02 (2.33-29.60)
A3	17.22 (4.52-35.62)	28.39 (13.70-38.33)	40.79 (25.56-63.28)	13.59 (7.79-23.49)
A4	21.23 (9.04-40.24)	29.04 (15.91-41.30)	38.40 (27.27-60.23)	11.33 (2.44-21.99)
A5	22.26 (6.32-35.38)	27.34 (19.42-36.57)	38.47 (23.08-57.47)	11.93 (5.14-26.62)
A6	16.48 (5.20-43.48)	21.94 (13.04-28.74)	44.24 (23.91-61.27)	17.34 (9.09-34.19)
A7	16.90 (5.11-27.62)	28.57 (8.51-38.71)	39.54 (28.95-63.07)	14.98 (8.60-34.04)
A8	29.56 (15.34-58.67)	32.78 (18.67-47.31)	30.68 (17.33-52.91)	6.97 (1.69-18.89)
A9	13.30 (3.95-29.73)	23.40 (10.17-38.58)	48.41 (35.14-71.19)	14.89 (4.57-26.52)
A MEAN	18.41 (2.67-58.67)	25.88 (6.25-47.31)	41.88 (17.33-71.19)	13.84 (1.69-41.38)
B1	25.03 (16.22-61.11)	34.28 (25.81-42.16)	35.19 (26.32-43.01)	7.90 (3.41-10.75)
B2	32.99 (16.78-45.45)	17.13 (12.50-24.31)	35.58 (13.89-53.69)	12.06 (3.17-26.16)
B3	18.11 (5.59-54.79)	10.82 (5.59-15.57)	49.76 (22.73-64.25)	22.34 (13.79-38.18)
B4	25.06 (6.67-65.91)	9.67 (6.06-13.33)	44.83 (16.44-63.03)	22.28 (7.41-39.55)
B5	33.77 (21.18-47.70)	26.99 (18.89-39.55)	27.05 (9.09-42.22)	7.72 (2.27-15.38)
B6	10.55 (4.97-24.69)	31.54 (22.35-40.88)	46.56 (32.94-61.36)	11.70 (4.55-22.60)
B7	8.71 (1.14-47.54)	17.13 (9.78-29.21)	56.30 (33.33-68.72)	20.72 (11.24-29.55)
B8	39.05 (20.00-67.44)	34.49 (28.65-43.96)	23.27 (14.21-35.56)	5.67 (2.26-10.99)
B9	34.10 (24.02-50.56)	17.26 (7.82-28.81)	31.81 (11.63-49.16)	13.50 (5.43-26.32)
B MEAN	25.26 (1.14-67.44)	22.15 (5.59-43.96)	38.93 (9.09-68.72)	13.77 (2.26-39.55)
C1	18.13 (3.16-33.52)	27.30 (16.47-34.74)	42.88 (31.46-64.29)	10.50 (5.46-19.57)
C2	18.29 (4.40-29.05)	28.09 (16.09-34.59)	48.89 (40.00-56.82)	9.62 (5.03-24.39)
C3	15.33 (5.68-33.33)	20.75 (7.41-35.15)	50.19 (26.67-67.76)	19.86 (7.41-42.86)
C4	12.44 (1.09-52.94)	18.57 (4.00-26.83)	39.90 (20.59-74.47)	19.80 (9.76-44.00)
C5	22.87 (3.19-62.50)	29.28 (10.64-38.15)	36.00 (6.25-61.88)	9.60 (6.21-14.04)
C6	22.30 (9.94-40.43)	23.61 (14.71-28.65)	42.18 (23.89-61.58)	11.08 (6.25-20.71)
C7	18.63 (4.52-37.78)	29.44 (23.50-39.31)	40.91 (24.46-62.30)	9.57 (2.53-20.00)
C8	17.41 (3.83-26.09)	30.29 (18.03-46.20)	48.61 (37.78-60.00)	12.58 (3.26-41.67)
C9	14.74 (4.76-38.40)	15.54 (10.71-19.77)	41.73 (24.13-62.15)	24.66 (6.67-38.46)
C MEAN	17.79 (1.09-62.50)	24.76 (4.00-46.20)	43.48 (6.25-74.47)	14.14 (2.53-44.00)
MEAN ALL TRAPS	20.38 (1.09-67.44)	24.43 (4.00-47.31)	24.43 (4.00-47.31)	13.92 (1.69-44.00)

	A1	A2	A3	A4	A5	A6	A7	A8	A9	B1	B2	B3	B4	B5	B6	B7	B8	B9	C1	C2	C3	C4	C5	C6	C7	C8	C9
A1	1.00																										
A2	0.95	1.00																									
A3	0.92	0.78	1.00																								
A4	0.86	0.95	0.78	1.00																							
A5	0.94	0.91	0.94	0.84	1.00																						
A6	0.98	0.96	0.99	0.82	0.97	1.00																					
A7	0.83	0.78	0.86	0.88	0.94	0.92	1.00																				
A8	0.72	0.53	0.89	0.78	0.89	0.86	0.71	1.00																			
A9	0.03	0.68	0.31	0.67	0.43	0.25	0.57	0.67	1.00																		
B1	0.80	0.99	0.81	0.94	0.83	0.80	0.97	0.77	0.50	1.00																	
B2	0.93	0.93	0.96	0.87	0.82	0.74	0.87	0.74	0.88	0.90	1.00																
B3	0.69	0.76	0.80	0.84	0.86	0.77	0.75	0.76	0.70	0.58	0.77	1.00															
B4	0.97	0.97	0.93	0.99	0.90	0.98	1.00	0.76	0.82	0.72	0.86	0.95	1.00														
B5	0.99	0.62	1.00	0.75	0.95	0.92	0.83	0.80	0.21	0.81	0.63	0.54	0.95	1.00													
B6	0.85	0.87	0.86	0.90	0.90	0.88	0.86	0.91	0.67	0.75	0.66	0.55	0.58	0.75	1.00												
B7	0.53	0.87	0.58	0.94	0.59	0.56	0.84	0.60	0.61	0.49	0.66	0.82	0.97	0.42	0.34	1.00											
B8	0.39	0.57	0.50	0.98	0.83	0.80	0.74	0.81	0.81	0.87	0.76	0.15	0.91	0.85	0.91	0.70	1.00										
B9	0.93	0.84	0.97	0.74	0.92	0.80	0.91	0.86	0.44	0.90	0.94	0.58	0.70	0.94	0.73	0.34	0.88	1.00									
C1	0.78	0.75	0.95	0.58	0.93	0.91	0.86	0.84	0.33	0.99	0.92	0.90	0.99	0.95	0.72	0.65	0.41	1.00	1.00								
C2	0.96	0.92	0.99	0.83	0.99	0.98	0.81	0.81	0.31	0.97	0.70	0.43	0.32	0.92	0.84	0.13	0.43	0.99	1.00	1.00							
C3	0.83	1.00	0.66	0.94	0.71	0.74	0.71	0.56	0.16	0.97	0.82	0.48	0.61	0.95	0.84	0.21	0.76	0.97	0.43	0.98	1.00						
C4	1.00	0.95	1.00	0.64	0.90	0.82	0.96	0.96	0.95	0.97	0.24	0.43	0.78	0.92	0.63	0.15	0.74	0.99	1.00	1.00	1.00	1.00					
C5	1.00	0.98	1.00	0.81	0.99	0.95	0.87	0.91	0.95	0.98	0.35	0.46	0.98	0.95	0.82	0.19	0.77	0.97	1.00	0.99	1.00	0.95	1.00				
C6	0.70	1.00	0.87	0.44	0.83	0.81	0.81	0.84	0.94	0.99	0.96	0.51	1.00	0.99	0.55	0.24	0.86	0.99	0.97	1.00	0.23	0.97	1.00	1.00			
C7	1.00	0.93	1.00	0.86	0.99	0.99	0.65	0.98	0.94	0.98	0.38	0.46	1.00	0.84	0.91	0.19	0.76	0.89	1.00	0.89	1.00	1.00	0.93	1.00	1.00		
C8	0.76	0.51	0.90	0.68	0.92	0.91	0.95	0.96	0.96	0.92	0.04	0.20	0.33	0.95	0.76	0.19	0.74	0.98	0.86	0.86	0.47	0.92	0.94	0.94	0.93	1.00	
C9	0.99	1.00	0.95	0.92	0.99	0.99	0.87	0.83	0.95	0.98	1.00	0.48	0.97	0.98	0.97	0.23	0.32	1.00	0.85	0.99	0.84	1.00	1.00	0.74	1.00	0.75	1.00

Appendix 5.2 Correlation coefficient between sediment sample sequences at different traps for 1-2mm.

A1	A2	A3	A4	A5	A6	A7	A8	A9	B1	B2	B3	B4	B5	B6	B7	B8	B9	C1	C2	C3	C4	C5	C6	C7	C8	C9	
A1	1.00																										
A2	0.82	1.00																									
A3	0.88	0.87	1.00																								
A4	0.95	0.76	0.80	1.00																							
A5	0.93	0.78	0.98	0.83	0.98	1.00																					
A6	0.95	0.82	0.98	0.83	0.98	1.00																					
A7	0.95	0.82	0.97	0.89	0.98	0.98	1.00																				
A8	0.43	0.31	0.58	0.91	0.79	0.89	0.38	1.00																			
A9	0.84	0.93	0.73	0.97	0.65	0.80	0.78	0.91	1.00																		
B1	0.97	0.87	0.90	0.96	0.85	0.92	0.94	0.90	0.93	1.00																	
B2	0.99	0.97	0.95	0.81	0.95	0.90	0.89	0.69	0.96	0.94	1.00																
B3	0.86	0.94	0.76	0.89	0.70	0.81	0.80	0.39	0.99	0.93	0.99	1.00															
B4	0.85	0.95	0.74	0.66	0.82	0.66	0.86	0.47	0.75	0.84	0.89	0.84	1.00														
B5	0.72	0.62	0.96	0.61	0.90	0.90	0.87	0.41	0.57	0.83	0.68	0.64	0.57	1.00													
B6	0.69	0.43	0.77	0.95	0.76	0.86	0.79	0.91	0.84	0.87	0.58	0.72	0.43	0.68	1.00												
B7	0.92	0.55	0.89	0.97	0.77	0.86	0.87	0.97	0.91	0.93	0.70	0.79	0.60	0.81	0.97	1.00											
B8	0.96	0.61	0.88	0.97	0.85	0.90	0.67	0.85	0.97	0.99	0.94	0.76	1.00	0.80	0.85	0.90	1.00										
B9	0.61	0.72	0.81	0.68	0.69	0.81	0.72	0.40	0.94	0.97	0.91	0.94	0.64	0.81	0.73	0.99	0.98	1.00									
C1	1.00	0.77	0.99	0.90	0.97	1.00	0.95	0.61	0.85	0.98	0.93	0.90	0.99	0.98	0.76	0.89	0.83	0.94	1.00								
C2	0.78	0.70	0.98	0.73	0.92	0.96	0.83	0.68	0.85	0.97	0.97	0.86	0.68	0.97	0.86	0.86	0.89	0.93	0.99	1.00							
C3	0.97	0.45	0.99	0.78	0.99	0.95	0.99	0.76	0.67	0.91	0.55	0.75	0.94	0.99	0.89	0.80	0.99	0.82	0.65	0.95	1.00						
C4	0.99	0.59	0.99	0.93	1.00	1.00	0.97	0.47	1.00	0.99	0.37	0.96	0.44	1.00	0.70	0.89	0.98	1.00	1.00	0.99	1.00						
C5	0.90	0.89	1.00	0.85	0.99	0.99	0.99	0.61	0.99	0.99	0.23	0.95	0.50	0.94	0.81	0.91	0.98	0.94	1.00	0.98	1.00	0.98	1.00				
C6	0.99	0.90	0.99	1.00	1.00	1.00	1.00	0.67	0.99	1.00	1.00	0.97	0.79	0.96	0.62	0.98	0.99	0.96	0.96	1.00	0.51	0.97	1.00	1.00	1.00		
C7	1.00	0.94	0.92	0.95	0.97	0.97	0.98	0.37	0.99	0.98	0.22	0.95	0.69	0.79	0.88	0.87	0.65	0.80	0.96	0.79	0.99	1.00	0.94	1.00	1.00		
C8	1.00	0.35	1.00	0.99	0.94	0.95	0.71	0.91	1.00	0.99	0.22	0.72	0.25	0.97	0.84	0.97	0.98	1.00	0.87	0.90	0.74	0.96	0.98	0.94	0.71	1.00	
C9	1.00	0.44	1.00	1.00	1.00	1.00	0.91	0.72	0.99	1.00	0.79	0.93	0.98	1.00	0.99	0.98	0.90	1.00	0.85	1.00	0.97	1.00	1.00	0.72	0.92	0.82	1.00

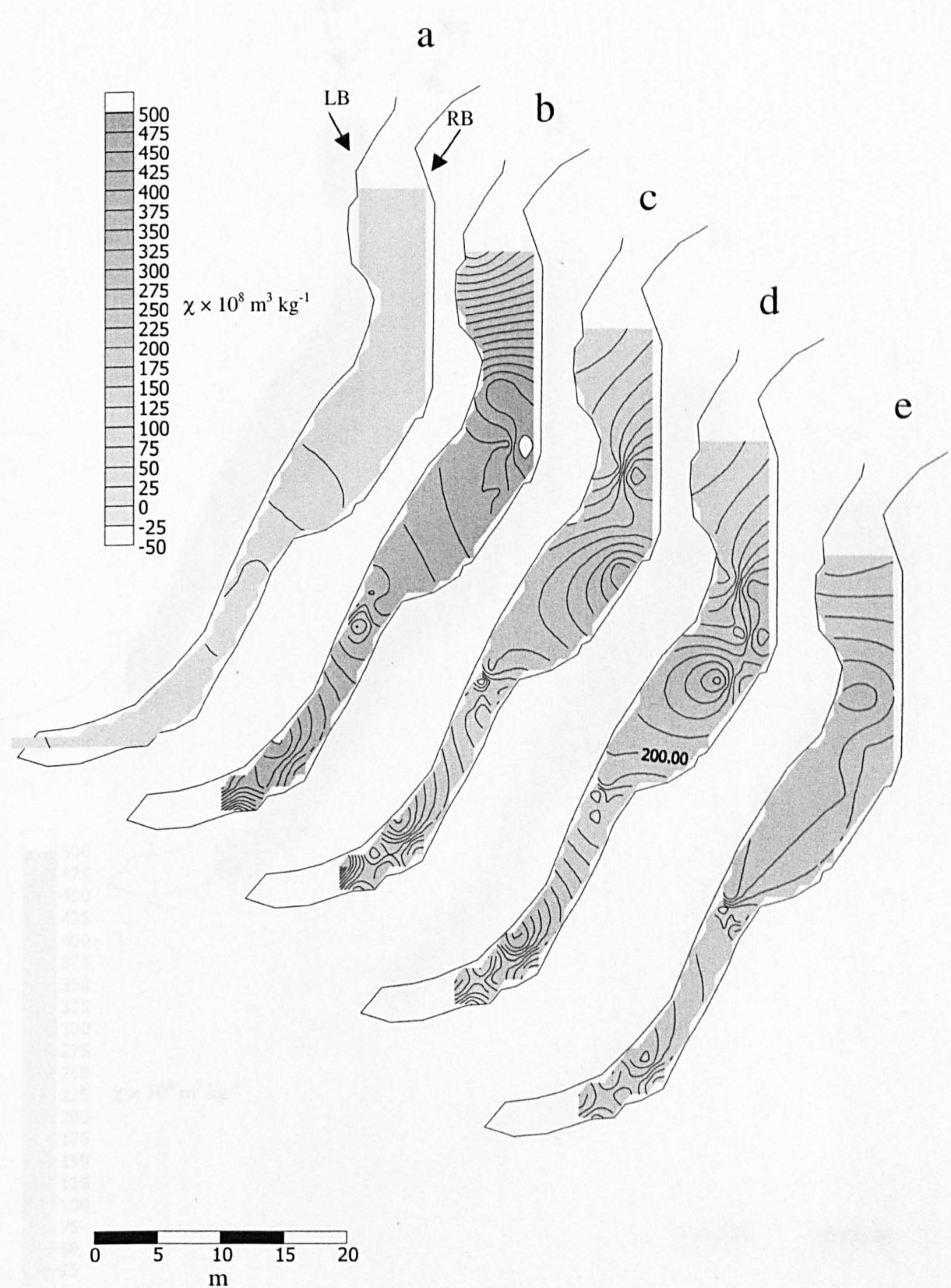
Appendix 5.3 Correlation coefficient between sediment sample sequences at different traps for 500-1000μm.

	A1	A2	A3	A4	A5	A6	A7	A8	A9	B1	B2	B3	B4	B5	B6	B7	B8	B9	C1	C2	C3	C4	C5	C6	C7	C8	C9	
A1	1.00																											
A2	0.91	1.00																										
A3	0.85	0.86	1.00																									
A4	0.82	0.90	0.97	1.00																								
A5	0.86	0.82	0.94	0.96	1.00																							
A6	0.84	0.94	0.99	0.97	0.95	1.00																						
A7	0.89	0.86	0.98	0.99	0.97	0.99	1.00																					
A8	0.74	0.63	0.90	0.88	0.81	0.94	0.77	1.00																				
A9	0.90	0.78	0.94	0.89	0.82	0.97	0.92	0.96	1.00																			
B1	0.95	0.82	0.98	0.93	0.87	0.96	0.96	0.95	1.00	1.00																		
B2	0.99	0.98	0.84	0.94	0.99	0.91	0.90	0.68	0.88	0.83	1.00																	
B3	0.87	0.94	0.65	0.62	0.54	0.69	0.65	0.59	0.77	0.78	0.99	1.00																
B4	0.95	0.95	0.70	0.92	0.98	0.83	0.85	0.52	0.75	0.81	0.97	0.95	1.00															
B5	0.72	0.65	0.93	0.91	0.95	0.92	0.92	0.74	0.80	0.84	0.73	0.42	0.68	1.00														
B6	0.86	0.60	0.90	0.84	0.83	0.79	0.90	0.87	0.91	0.93	0.46	0.50	0.55	0.93	1.00	1.00	1.00											
B7	0.79	0.44	0.99	0.93	0.89	0.92	0.94	0.90	0.91	0.93	0.46	0.50	0.55	0.93	1.00	1.00	1.00											
B8	0.85	0.82	0.98	1.00	0.99	0.99	0.99	0.95	0.94	0.95	0.92	0.59	0.99	0.97	0.96	0.95	1.00											
B9	0.93	0.94	0.83	0.71	0.65	0.83	0.81	0.81	0.93	0.93	0.93	0.94	0.83	0.61	0.62	0.76	0.81	1.00										
C1	0.80	0.88	1.00	0.97	0.92	0.99	0.97	0.90	0.99	0.97	0.95	0.92	0.97	0.96	0.88	0.95	0.99	0.92	1.00									
C2	0.99	0.89	0.98	0.96	0.93	0.99	0.94	0.91	0.99	0.97	0.95	0.89	0.97	0.94	0.96	0.95	1.00	0.94	0.98	1.00								
C3	0.97	0.85	0.85	0.87	0.94	0.85	0.91	0.77	0.88	0.91	0.47	0.74	0.98	1.00	0.96	0.94	1.00	0.76	0.81	0.93	1.00							
C4	1.00	0.20	1.00	0.96	0.99	0.99	1.00	0.99	1.00	0.97	0.01	1.00	0.82	0.99	0.80	0.96	1.00	0.98	1.00	1.00	1.00	1.00						
C5	1.00	0.64	1.00	0.97	0.98	0.99	0.88	0.98	1.00	0.99	0.10	0.98	0.34	0.92	0.86	0.99	0.99	0.98	0.99	0.97	1.00	0.99	1.00					
C6	0.68	0.96	0.95	0.97	0.90	0.95	0.92	0.91	1.00	1.00	0.90	0.99	0.30	0.94	0.78	1.00	1.00	1.00	0.96	1.00	0.74	0.97	0.99	1.00				
C7	1.00	0.71	1.00	1.00	1.00	1.00	0.84	0.99	1.00	0.97	0.06	0.99	0.46	0.91	0.97	0.96	1.00	0.98	1.00	0.96	1.00	1.00	0.99	1.00	1.00			
C8	0.81	0.78	0.99	0.98	0.94	0.98	0.97	0.91	1.00	0.99	0.02	0.97	0.35	0.98	0.89	0.99	0.97	1.00	0.98	0.97	0.85	0.98	1.00	0.98	0.99	1.00		
C9	1.00	0.95	0.87	0.82	0.90	0.84	0.89	0.84	1.00	1.00	0.57	0.97	0.79	1.00	0.99	1.00	1.00	1.00	0.81	1.00	0.99	1.00	1.00	0.68	1.00	0.82	1.00	

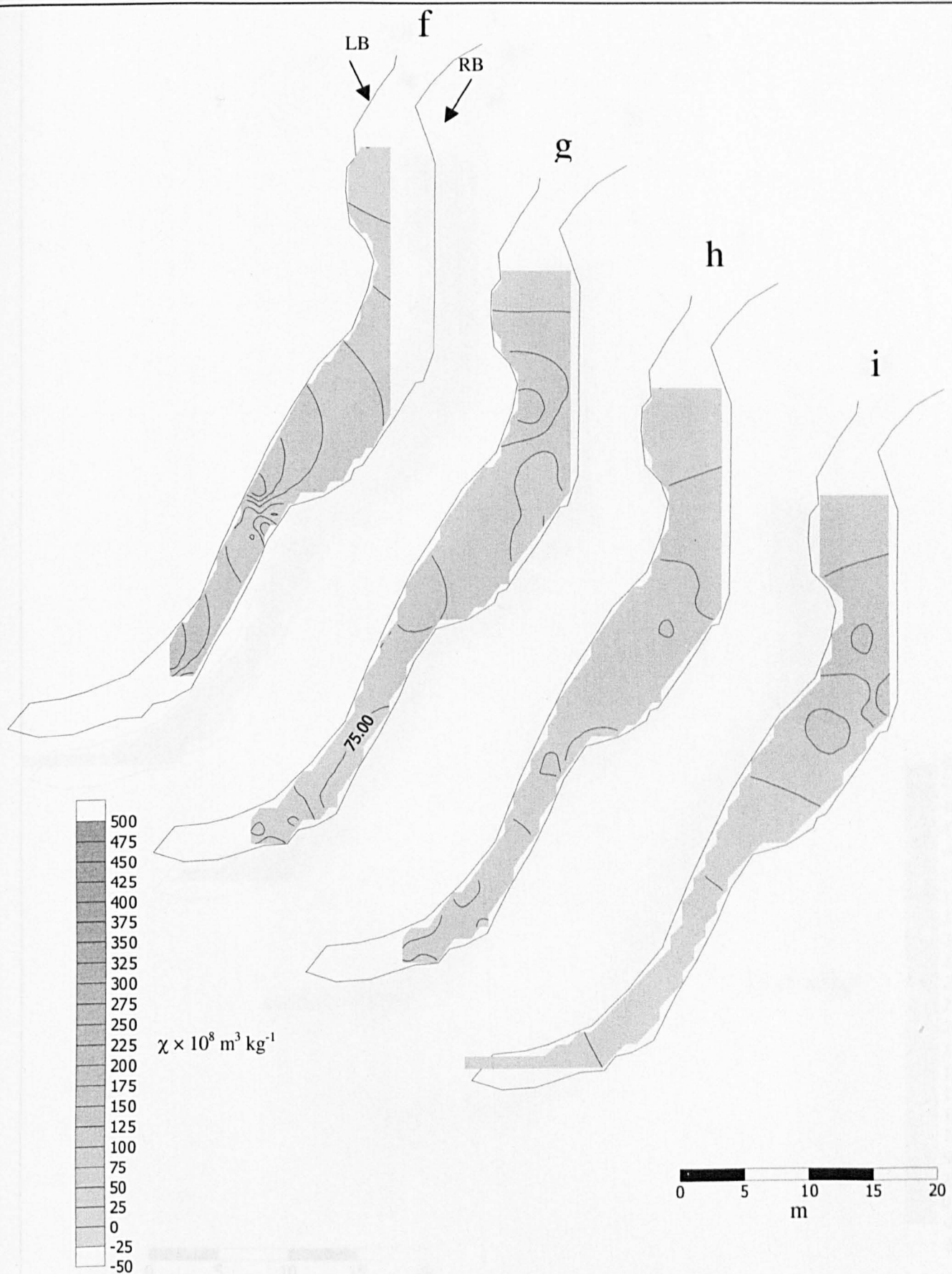
Appendix 5.4 Correlation coefficient between sediment sample sequences at different traps for 250-500µm.

	A1	A2	A3	A4	A5	A6	A7	A8	A9	B1	B2	B3	B4	B5	B6	B7	B8	B9	C1	C2	C3	C4	C5	C6	C7	C8	C9
A1	1.00																										
A2	0.98	1.00																									
A3	0.82	0.90	1.00																								
A4	0.88	0.96	0.98	1.00																							
A5	0.88	0.82	0.90	0.91	1.00																						
A6	0.96	0.97	0.95	0.96	0.93	1.00																					
A7	0.92	0.95	0.90	0.92	0.83	0.97	1.00																				
A8	0.84	0.85	0.91	0.95	0.87	0.98	0.95	1.00																			
A9	0.95	0.97	0.84	0.86	0.86	0.95	0.99	0.97	1.00																		
B1	0.95	0.95	0.95	0.96	0.97	0.99	0.95	0.95	0.94	1.00																	
B2	1.00	1.00	0.96	0.99	0.97	0.98	0.96	0.94	0.97	0.93	1.00																
B3	0.94	1.00	0.65	0.64	0.70	0.82	0.90	0.83	0.93	0.81	1.00	1.00															
B4	1.00	0.99	0.92	0.99	1.00	0.98	0.92	0.90	0.93	0.98	0.99	0.99	1.00														
B5	0.64	0.97	0.94	0.94	0.92	0.83	0.72	0.77	0.61	0.82	0.98	0.44	0.98	1.00													
B6	0.63	0.27	0.91	0.86	0.81	0.92	0.52	0.70	0.59	0.93	0.87	0.57	0.92	0.85	1.00												
B7	0.58	0.75	0.95	0.90	0.88	0.80	0.71	0.79	0.59	0.83	0.73	0.38	0.86	0.98	0.97	1.00											
B8	0.98	0.99	0.92	0.92	0.96	0.99	1.00	0.99	0.99	0.98	0.98	0.88	1.00	0.78	0.88	0.75	1.00										
B9	0.86	0.95	0.58	0.60	0.61	0.77	0.84	0.72	0.89	0.77	0.97	0.97	0.94	0.33	0.49	0.32	0.86	1.00									
C1	0.87	0.97	0.99	0.99	0.85	0.96	0.90	0.85	0.88	0.94	0.93	0.89	0.83	0.99	0.98	0.98	0.98	0.47	1.00								
C2	0.97	0.90	1.00	0.98	0.95	0.99	0.96	0.92	0.94	0.94	0.91	0.91	0.74	0.96	0.73	0.97	0.99	0.61	0.98	1.00							
C3	0.96	0.93	0.78	0.82	0.98	0.88	0.75	0.78	0.84	0.96	0.30	0.79	0.98	0.99	0.98	0.99	1.00	0.40	0.74	0.96	1.00						
C4	1.00	0.84	1.00	0.90	0.96	0.94	0.99	1.00	1.00	0.92	0.80	0.99	0.96	0.96	0.94	0.95	0.94	0.98	1.00	0.98	0.97	1.00					
C5	1.00	0.42	1.00	0.98	1.00	1.00	0.92	0.99	1.00	0.97	0.28	0.90	0.89	0.99	0.94	0.99	1.00	0.99	0.99	0.93	1.00	0.94	1.00				
C6	0.81	0.99	0.96	0.97	0.75	0.89	0.93	0.93	1.00	1.00	0.96	0.79	0.91	1.00	1.00	1.00	0.97	0.99	0.99	1.00	0.63	0.84	0.97	1.00			
C7	1.00	0.50	1.00	1.00	1.00	1.00	0.95	1.00	1.00	0.97	0.39	0.89	0.84	0.99	0.91	1.00	0.99	0.99	0.99	0.95	1.00	0.95	0.99	1.00	1.00		
C8	0.98	0.93	0.98	0.98	0.96	1.00	0.95	0.89	1.00	0.99	0.06	0.89	0.78	0.97	1.00	1.00	0.99	0.97	0.95	0.97	0.89	0.95	0.99	0.91	0.99	1.00	
C9	0.85	0.95	0.64	0.64	0.89	0.75	0.68	0.65	1.00	0.99	0.90	0.98	0.98	0.94	0.98	0.98	1.00	1.00	0.52	0.99	0.96	1.00	0.99	0.43	0.97	0.75	1.00

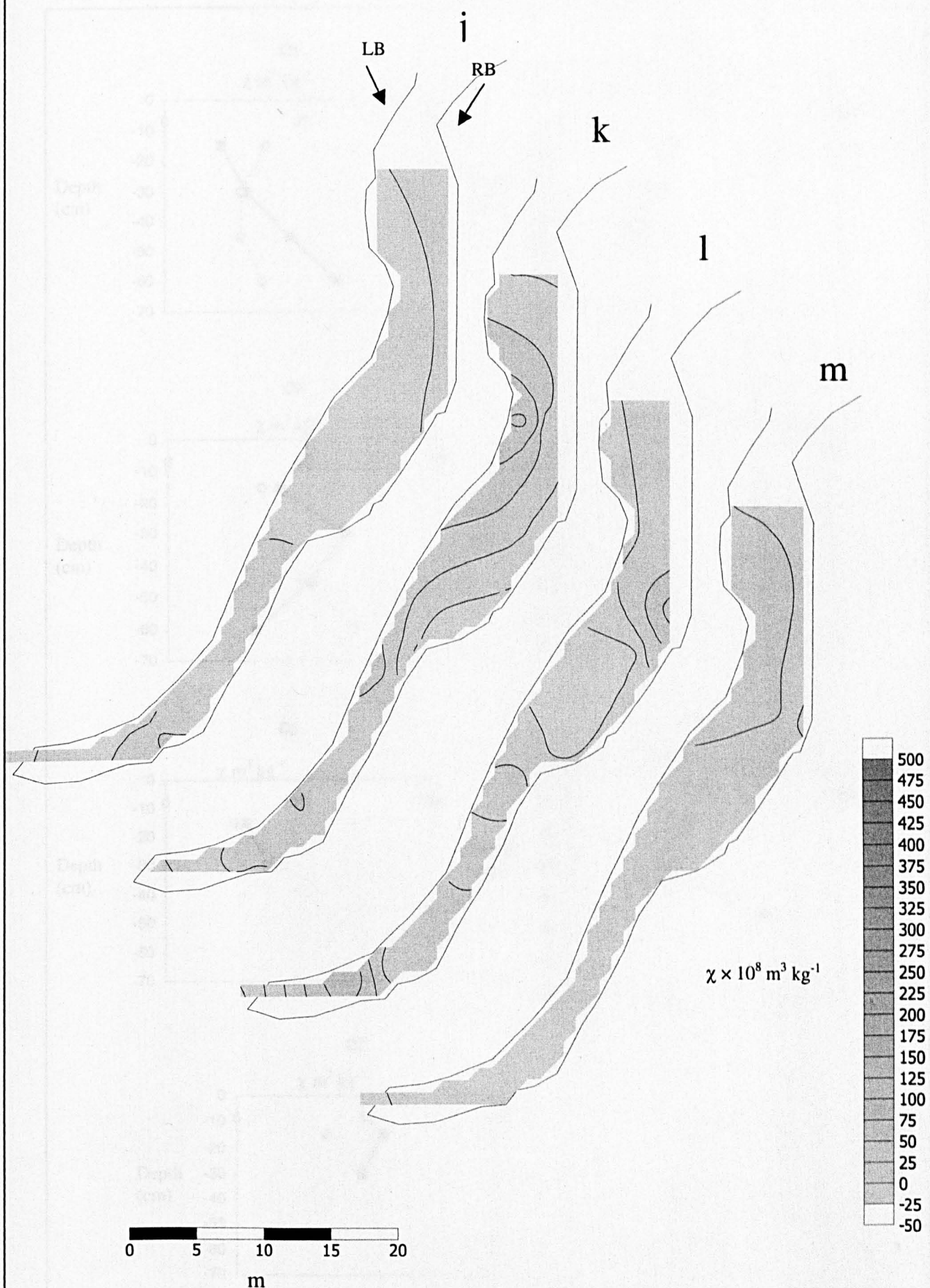
Appendix 5.5 Correlation coefficient between sediment sample sequences at different traps for 125-250µm.



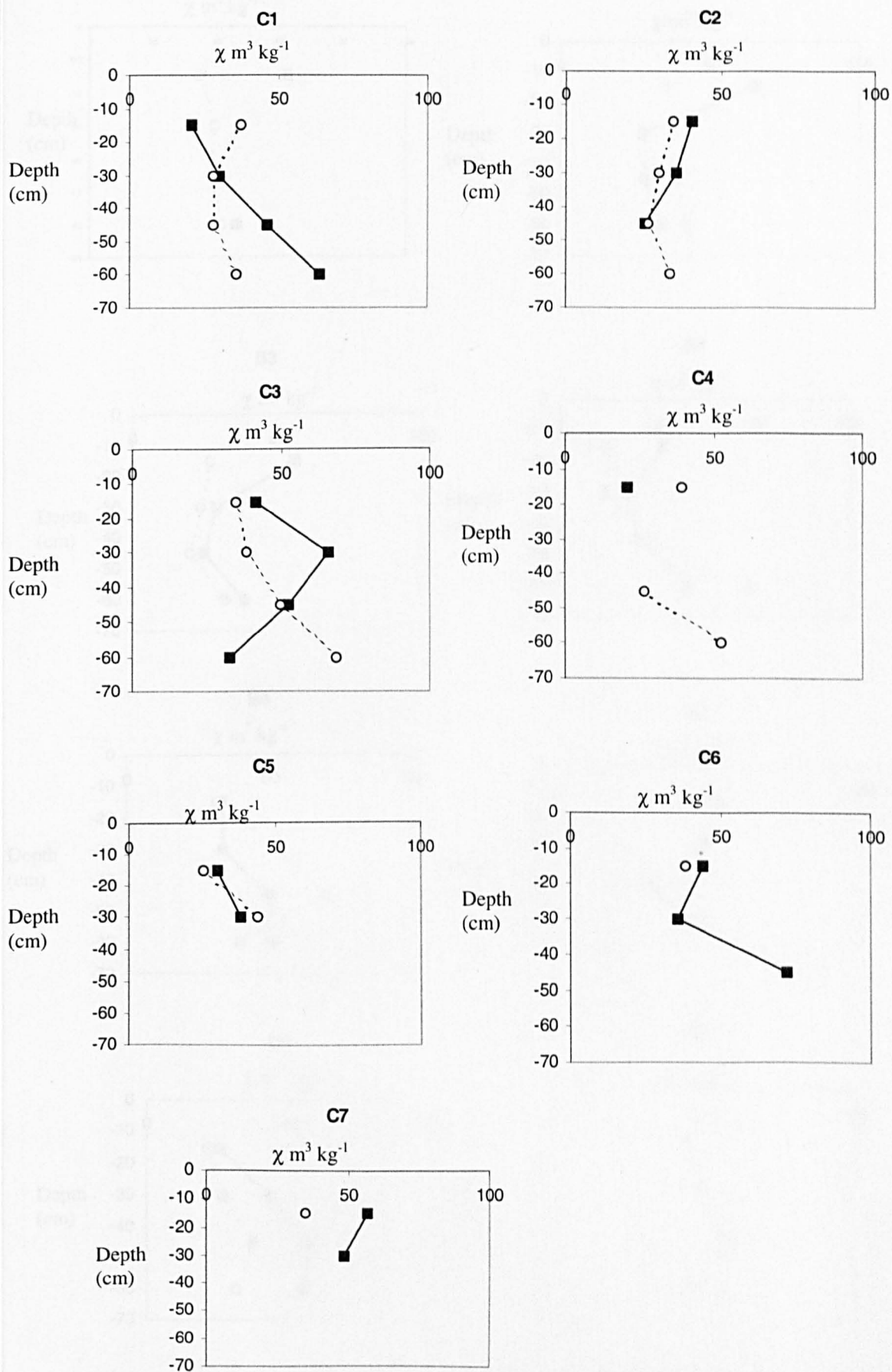
Appendix 7.1 Spatial variability in magnetic susceptibility of Phase 1 bedload accumulating in basket traps; a) background 20.4.96, b) $3.2 \text{ m}^3 \text{s}^{-1}$ 22.5.95, c) $0.54 \text{ m}^3 \text{s}^{-1}$ 6.6.96, d) $2.08 \text{ m}^3 \text{s}^{-1}$ 10.9.96, e) $3.39 \text{ m}^3 \text{s}^{-1}$ 14.10.96. LB – left bank, RB – right bank.



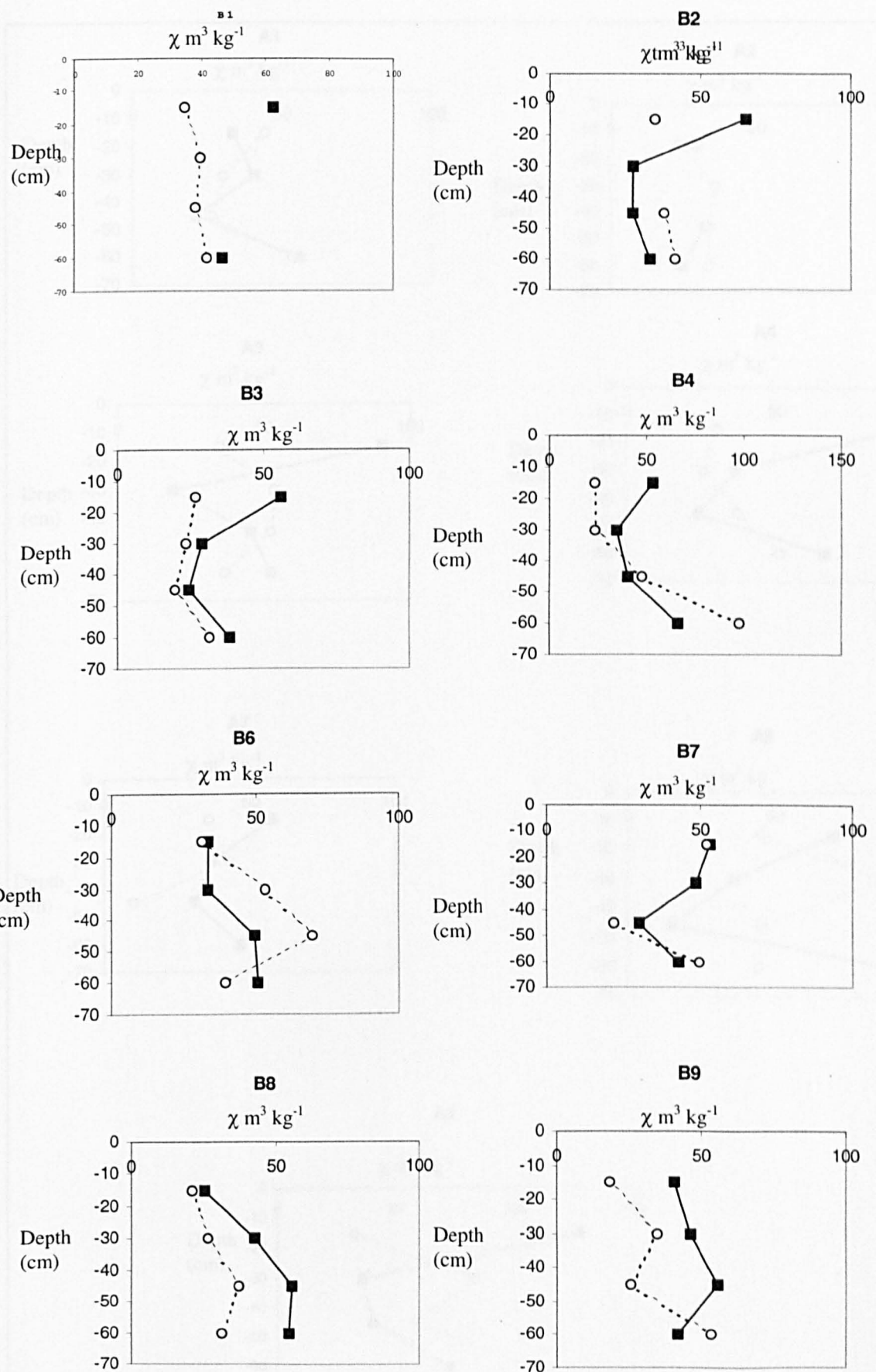
Appendix 7.1 Spatial variability in magnetic susceptibility of phase 1 bedload accumulating in basket traps; f) $5.44 \text{ m}^3 \text{s}^{-1}$ 2.11.96, g) $7.12 \text{ m}^3 \text{s}^{-1}$ 17.11.96, h) $4.13 \text{ m}^3 \text{s}^{-1}$ 10.12.96, i) $4.09 \text{ m}^3 \text{s}^{-1}$ 22.12.96



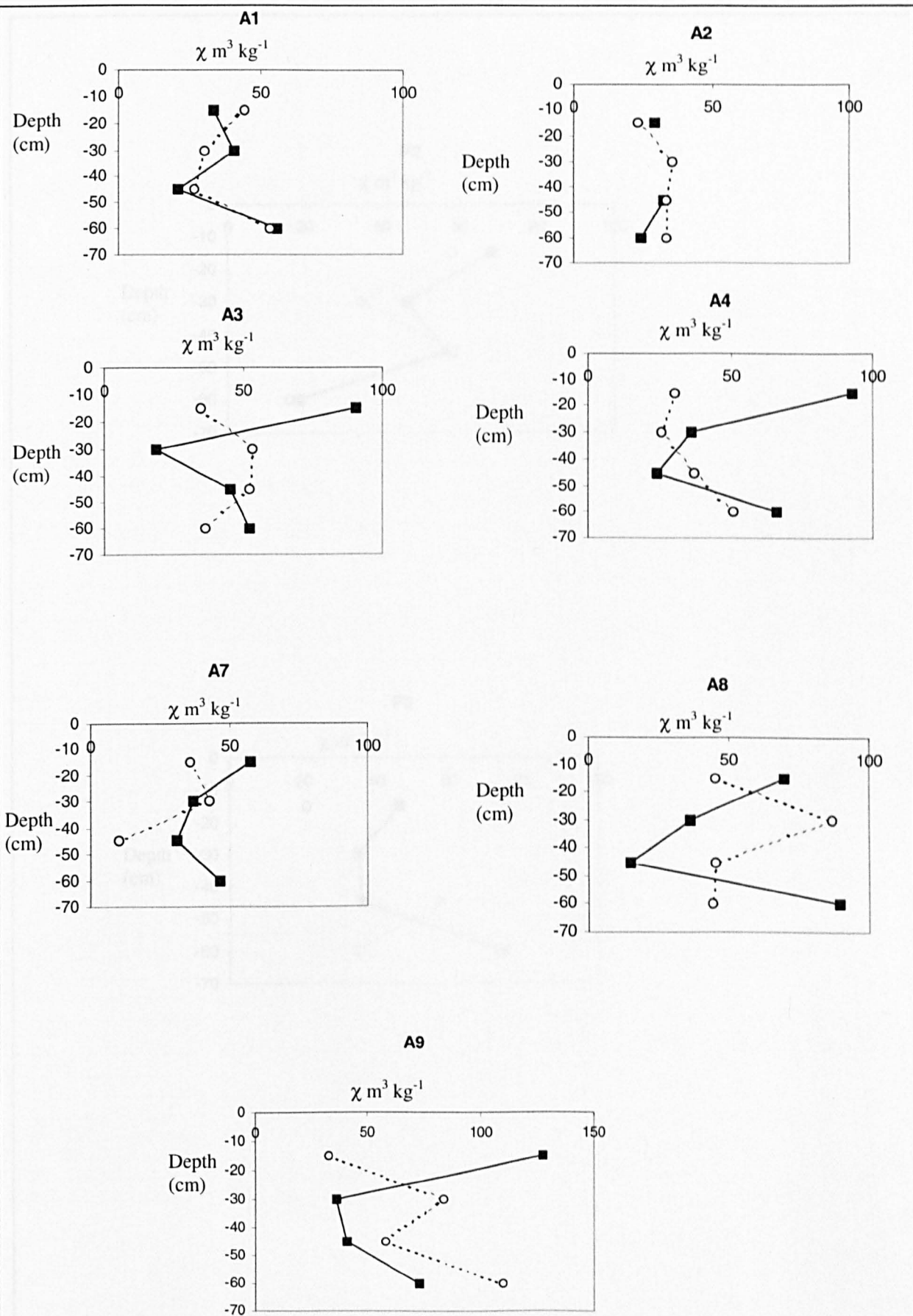
Appendix 7.1 Spatial variability in magnetic susceptibility of phase 1 bedload accumulating in basket traps; j) $1.23 \text{ m}^3 \text{s}^{-1}$ 15.1.97, k) $3.81 \text{ m}^3 \text{s}^{-1}$ 31.1.97, l) $3.99 \text{ m}^3 \text{s}^{-1}$ 8.2.97, m) $8.62 \text{ m}^3 \text{s}^{-1}$ 11.3.97



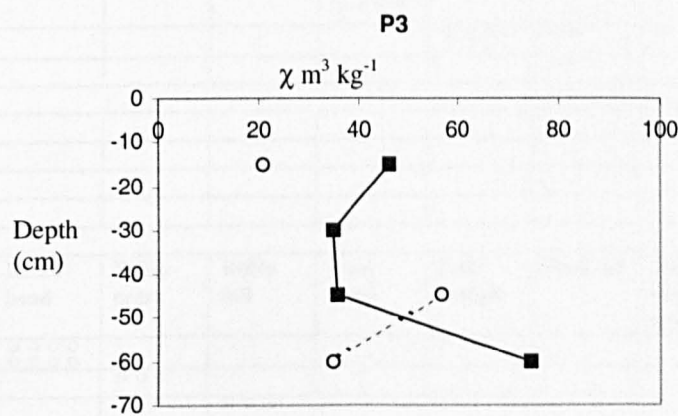
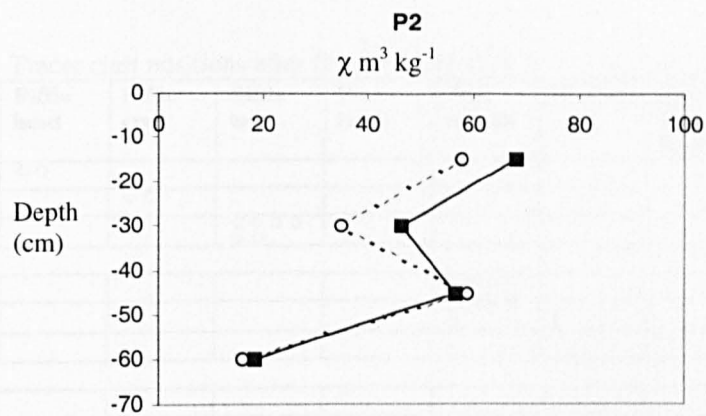
Appendix 7.2 Depth variation in magnetic susceptibility of matrix sediments sampled using freeze-coring. Circles and dashed lines indicate background variability, solid squares and solid lines indicate survey undertaken in July 1997 after tracer emplacement



Appendix 7.2 Depth variation in magnetic susceptibility of matrix sediments sampled using freeze-coring. Circles and dashed lines indicate background variability, solid squares and solid lines indicate survey undertaken in July 1997 after tracer emplacement



Appendix 7.2 Depth variation in magnetic susceptibility of matrix sediments sampled using freeze-coring. Circles and dashed lines indicate background variability, solid squares and solid lines indicate survey undertaken in July 1997 after tracer emplacement



Appendix 7.2 Depth variation in magnetic susceptibility of matrix sediments sampled using freeze-coring. Circles and dashed lines indicate background variability, solid squares and solid lines indicate survey undertaken in July 1997 after tracer emplacement

Appendix 8.1 Tracer clast positions after flood 1 ($2.71 \text{ m}^3 \text{ s}^{-1}$)

FINE	Riffle head	Riffle crest	Riffle tail	Pool head	Pool trough	Pool tail	Bar edge head	Bar edge tail	Bar top	Bar apex
Riffle head	○○									
Riffle Crest		○○								
Riffle tail		●	○○○○							
Pool head					○○○○					
Pool trough					○○○○	○				
Pool tail										
Bar edge head										
Bar edge tail										
Bar top										
Bar apex										

MEDIUM	Riffle head	Riffle crest	Riffle tail	Pool head	Pool trough	Pool tail	Bar edge head	Bar edge tail	Bar top	Bar apex
Riffle head	○○○○ ○○○○ ○○									
Riffle Crest		○○○○								
Riffle tail			○○○○				○○○			
Pool head				○○○○						
Pool trough					○○○○	○○	○	○		
Pool tail						○○				
Bar edge head										
Bar edge tail										
Bar top										
Bar apex										

COARSE	Riffle head	Riffle crest	Riffle tail	Pool head	Pool trough	Pool tail	Bar edge head	Bar edge tail	Bar top	Bar apex
Riffle head	○○○○ ○○○○									
Riffle Crest		○○○								
Riffle tail			○○○							
Pool head				○○○○ ○○	○			○		
Pool trough					○○○○	○				
Pool tail						○○				
Bar edge head										
Bar edge tail										
Bar top										
Bar apex										

Appendix 8.2 Tracer clast positions after flood 2 ($5.95 \text{ m}^3 \text{ s}^{-1}$)

FINE	Riffle head	Riffle crest	Riffle tail	Pool head	Pool trough	Pool tail	Bar edge head	Bar edge tail	Bar top	Bar apex
Riffle head	○ ○ ○									
Riffle Crest			○ ○							
Riffle tail			○ ○ ○ ○							
Pool head	○							○		
Pool trough	○ ○ ○			○						
Pool tail					○ ○					
Bar edge head										
Bar edge tail										
Bar top										
Bar apex										
MEDIUM	Riffle head	Riffle crest	Riffle tail	Pool head	Pool trough	Pool tail	Bar edge head	Bar edge tail	Bar top	Bar apex
Riffle head	○ ○ ○ ○	○					○			
Riffle Crest		○ ○ ○ ○	○ ○				○ ○			○
Riffle tail	○		○				○ ○ ○			
Pool head					○ ○ ○					
Pool trough	○ ○ ○ ○			○ ○ ○		○				
Pool tail	○	○			○					
Bar edge head							○ ○ ○			
Bar edge tail	○									
Bar top										
Bar apex										
COARSE	Riffle head	Riffle crest	Riffle tail	Pool head	Pool trough	Pool tail	Bar edge head	Bar edge tail	Bar top	Bar apex
Riffle head	○ ○ ○ ○	○ ○ ○ ○	○ ○							
Riffle Crest		○ ○	○ ○	○ ○	○ ○	○				
Riffle tail			○ ○ ○ ○							
Pool head				○ ○ ○ ○		○		○		
Pool trough	○				○ ○ ○	○ ○				
Pool tail	○ ○				○ ○ ○	○ ○ ○				
Bar edge head							○			
Bar edge tail										
Bar top										
Bar apex										

Appendix 8.3 Tracer clast positions after flood 3 ($7.4 \text{ m}^3 \text{ s}^{-1}$)

FINE	Riffle head	Riffle crest	Riffle tail	Pool head	Pool trough	Pool tail	Bar edge head	Bar edge tail	Bar top	Bar apex
Riffle head	○ ○ ○									
Riffle Crest		○ ○ ○	○							
Riffle tail			○	○		○				○
Pool head										
Pool trough			○							
Pool tail										
Bar edge head								○		
Bar edge tail										
Bar top										
Bar apex										

MEDIUM	Riffle head	Riffle crest	Riffle tail	Pool head	Pool trough	Pool tail	Bar edge head	Bar edge tail	Bar top	Bar apex
Riffle head	○ ○						○			
Riffle Crest		○ ○ ○	○ ○				○			
Riffle tail			○ ○ ○		○					○ ○
Pool head					○	○				
Pool trough					○ ○ ○ ○					
Pool tail	○					○ ○				
Bar edge head							○ ○	○		
Bar edge tail										○ ○ ○ ○
Bar top										○ ○
Bar apex										

COARSE	Riffle head	Riffle crest	Riffle tail	Pool head	Pool trough	Pool tail	Bar edge head	Bar edge tail	Bar top	Bar apex
Riffle head		○ ○								
Riffle Crest		○ ○	○ ○				○			
Riffle tail			○ ○ ○ ○				○			
Pool head								○		
Pool trough						○ ○ ○ ○				
Pool tail										
Bar edge head										
Bar edge tail										
Bar top										
Bar apex										

Appendix 8.4 Tracer clast positions after flood 4 ($9.92 \text{ m}^3 \text{ s}^{-1}$)

FINE	Riffle head	Riffle crest	Riffle tail	Pool head	Pool trough	Pool tail	Bar edge head	Bar edge tail	Bar top	Bar apex
Riffle head										
Riffle Crest							•			
Riffle tail							•			•
Pool head										
Pool trough								•		
Pool tail								•		
Bar edge head							•			
Bar edge tail										
Bar top										
Bar apex										

MEDIUM	Riffle head	Riffle crest	Riffle tail	Pool head	Pool trough	Pool tail	Bar edge head	Bar edge tail	Bar top	Bar apex
Riffle head							•			
Riffle Crest		○○○○		•						
Riffle tail			○○				•			•
Pool head										
Pool trough					○			○		
Pool tail	○						•			
Bar edge head		○					○	•	•	○○
Bar edge tail		○	○					•		
Bar top										
Bar apex										

COARSE	Riffle head	Riffle crest	Riffle tail	Pool head	Pool trough	Pool tail	Bar edge head	Bar edge tail	Bar top	Bar apex
Riffle head	○○○○○	○	○				○			
Riffle Crest	○	○○○○○	○○				○○			
Riffle tail			○							○
Pool head		○○○	○	○			○			
Pool trough					○○○		○○			
Pool tail							○			
Bar edge head										
Bar edge tail		○				○				
Bar top										
Bar apex										○

Appendix 8.5 Tracer clast positions after flood 5 ($6.9 \text{ m}^3 \text{ s}^{-1}$)

FINE	Riffle head	Riffle crest	Riffle tail	Pool head	Pool trough	Pool tail	Bar edge head	Bar edge tail	Bar top	Bar apex
Riffle head										
Riffle Crest										
Riffle tail										
Pool head										
Pool trough										
Pool tail										
Bar edge head										
Bar edge tail										
Bar top										
Bar apex										

MEDIUM	Riffle head	Riffle crest	Riffle tail	Pool head	Pool trough	Pool tail	Bar edge head	Bar edge tail	Bar top	Bar apex
Riffle head										
Riffle Crest							•			
Riffle tail								•		
Pool head										
Pool trough								•		
Pool tail	○							•		
Bar edge head							•			
Bar edge tail										
Bar top										
Bar apex										

COARSE	Riffle head	Riffle crest	Riffle tail	Pool head	Pool trough	Pool tail	Bar edge head	Bar edge tail	Bar top	Bar apex
Riffle head	○									
Riffle Crest		• • •	○ ○ ○				○ ○ ○ ○			
Riffle tail			○ ○ ○	○				○		
Pool head										
Pool trough		○			○					
Pool tail	○	○								
Bar edge head							○ ○	•	• •	• •
Bar edge tail		○				○			○	
Bar top									○	
Bar apex										